Title
A Unified, [2+2+n] Cycloaddition Platform for Synthesis of Diverse Conjugated Nanocarbons

Author
Kiel, Gavin Ray

Publication Date
2019

Peer reviewed|Thesis/dissertation

A Unified, [2+2+n] Cycloaddition Platform for Synthesis of Diverse Conjugated Nanocarbons

By

Gavin R. Kiel

A dissertation submitted in partial satisfaction of the

requirements for the degree of

Doctor of Philosophy

in

Chemistry

in the

Graduate Division

of the

University of California, Berkeley

Committee in charge:

Professor T. Don Tilley, Chair
Professor K. Peter C. Vollhardt
Professor Alexis T. Bell

Summer 2019

Abstract

A Unified, [2+2+n] Cycloaddition Platform for Synthesis of
Diverse Conjugated Nanocarbons

by

Gavin R. Kiel

Doctor of Philosophy in Chemistry

University of California, Berkeley

Professor T. Don Tilley, Chair

Future developments in molecular carbon nanoscience will hinge on the availability of versatile synthetic strategies that enable rational control of properties. Since the majority of nanocarbons are comprised of fused rings, polycyclic aromatic hydrocarbons (PAHs) can be viewed both as the smallest nanocarbons and as building blocks for their macromolecular congeners (e.g. graphene nanoribbons and carbon nanotubes). The major synthetic challenge is the fusion of many rings, which requires regioselective formation of many C–C bonds. Very few methods have found general use in this regard, and most provide unfunctionalized products or cannot easily produce analogues. This thesis develops an efficient and versatile ring-fusion platform, based on a final-step [2+2+n] cycloaddition, which also enables divergent production of functionalized analogues. The work presented herein not only puts the large number of known [2+2+n] cycloadditions into a unified conceptual framework for strategic application to conjugated nanocarbons, but also contributes new reactions to the toolbox.

Chapter 1 introduces the general features of the synthetic platform, which can be conceptually broken up into three steps: 1) modular synthesis of an oligo-diyne or -dinitrile precursor; 2) ring-fusion via metal-mediated cyclization; and 3) divergent, "post-fusion" functionalization. Steps 2 and 3, which together make up a formal [2+2+n] reaction, can usually be performed in the one pot or make up part of a catalytic cycle. Chapters 2–7 chronicle the development of the synthetic strategy via its target-driven application to synthetically challenging nanocarbons. Some targets have a storied history (e.g. arylene ethynylene macrocycles and cycloarenes) and others are previously unknown (e.g. expanded helicenes and their macrocyclic derivatives), but all are inaccessible using previous approaches.

Table of Contents

Acknowledgements

In 2008, as a 23-year old, second-year corporate banking analyst, I thought I had life figured out. The following year, while pursuing a master's degree in financial economics at Oxford University, that view gradually changed. I did not grow to dislike finance; rather, I became captivated by chemistry, which was borne from an interest in energy finance. Primarily out of curiosity, this path of discovery eventually led me to enroll in a chemistry course at a local community college, and the rest is history. Since this was my first serious science course, the journey to become PhD chemist has been a long one. I could not have done this without a tremendous support system. Thus, the first people to thank are those who have shown unwavering support in this change.

Charlene, Kyle, and Risa, my amazing family, never questioned my career change with a negative tone and provided me with the emotional, and on a few occasions financial, safety net that kept me going when things got hard. Even though I am terrible at keeping in touch, you guys have always been there for me and I am extremely lucky to have you. I love you!

Many teachers and mentors aided my transition. At the beginning of my change, Professor John Davison believed in me enough to permit me to take his organic chemistry course concurrently with general chemistry, which was essential to meet my strict timeline that was imposed by financial difficulty. He also provided the introduction to the intellectual love of my life, organic chemistry, with a jovial, passionate delivery. Dr. Yi Liu at the Molecular Foundry provided me with my first research experience, and I was extremely fortunate to be personally trained by him. Even though I was with Yi only 5 months, it was a transformative experience. Prior to this, my interest in chemistry was more of a curiosity.

Professor T. Don Tilley is, of course, the mentor to whom I owe the most. Without him, I wouldn't have had the opportunity to stay in the best chemistry department in the world for my PhD studies. He is extremely supportive and open-minded, and allowed me the intellectual freedom to pursue literally any idea. I have learned a great deal from Don, not only about how to approach chemical research, but also about how to conduct myself in a professional environment. Professor K. Peter C. Vollhardt, the pioneer of the field that made this thesis possible, was also an encouraging, supportive mentor throughout my PhD studies. Rarely do you come across such a positive person, but such positivity is highly motivating for a young researcher.

The real learning of my PhD took place when I began to formally mentor younger students. Thus, I am deeply indebted to Sajan Patal, Adrian Samkian, Hanh Nguyen, Alejandro Cuellar De Lucio, and Harry Bergman. I hope they learned as much from me as I did from them. The additions of Harry and Adrian to the group were especially critical to my continued happiness.

I owe a lot to my best friend, Andy I. Nguyen. It was from him that I initially learned to constantly interrogate my research from a broader perspective. We overlapped for my first 3 years in the Tilley group and then for my last 3 years while he carried out his Postdoc at the Molecular Foundry. Never have I had such a selfless friend. I overlapped with many other great people during my time in the Tilley group and made a lot of friends along the way. Raul Huerta, with whom I lived for a little over a year, is the most positive person I have ever met and really knows how to bring people together. Other people with whom I had particularly meaningful interactions include Rosemary Tilley, Nicolas Schüwer (my initial mentor in the group), Pascual Ona Burgos, Truman Wambach, Patrick Smith, Ben Suslick ("Sussels"), Daniel Levine ("Levinsky"), Lukas Rochlitz ("Spooky Lukey"), Micah Ziegler, Jom

("Jombie") Amtawong, and Yuyang Dong. This list is not comprehensive, but rather a few names at the top of my mind.

Last, but certainly not least, I'd like to acknowledge someone who has profoundly influenced my personal life. I met Angela Chen about a year before the end of my PhD and she has been my faithful confidant and best friend (sorry, Andy) since that time. She gives me something to look forward to each day. Our time together has not always been easy – but when have great things ever come easy? I love you, Angela, and I look forward to seeing what the future holds.

Chapter 1: Introduction to the Unified Synthetic Strategy

Purpose of this Introductory Chapter

Chapters 2–6 of this thesis were written for individual journal articles and thus are self-contained. This chapter unites them by providing 1) general motivation and background, 2) a description of the unified synthetic strategy featured in every chapter, and 3) a summary of each subsequent chapter in a continuous narrative.

The Quest for Atomic Precision in Conjugated Nanocarbons: A Ring Fusion Challenge

The isolation of graphene and the elucidation of its extraordinary properties (e.g. ballistic charge transport, mechanical strength, transparency, and flexibility) incited a renaissance in the field of conjugated nanocarbons.[1,2] In the context of electronics, graphene has been considered a possible solution to limits on device miniaturization.[3] Numerous other applications have been proposed, for example in optoelectronics,[4] sensing,[5] catalysis,[6–8] and energy storage.[8] These possibilities have motivated considerable research, including the European Union's "The Graphene Flagship", a $1 billion commitment to graphene.[9] Tremendous challenges remain, especially in the area of molecular electronics, which is hindered not only by the inherent lack of a bandgap in this material but also by the difficulties associated with device fabrication on the molecular scale (which is ultimately a molecular self-assembly problem). While much current attention focuses on graphene and related graphene nanostructures, older conjugated nanocarbons such as fullerenes and carbon nanotubes remain vibrant areas of research, and many new classes of nanocarbons have emerged.[10,11]

Since structure dictates properties, a means to fabricate nanocarbons of arbitrary complexity, in an atomically precise fashion, might be considered the holy grail in the field. Not only would this enable bandgap engineering by the rational incorporation of defects (e.g. heteroatoms, strain, or holes), but it is essential for the more challenging task of device fabrication via programmed assembly of nanocarbons. Since atomically precise nanocarbons are simply large organic molecules (or polymers for those with a molecular weight distribution), organic chemists are uniquely suited for this challenge. Indeed, much progress has been made in employment of organic synthesis in pursuit of atomic precision, and the conceptual framework has been firmly established;[12,13] however, tremendous challenges remain.

Since many conjugated nanocarbons are comprised of fused rings, polycyclic aromatic hydrocarbons (PAHs) can be viewed as their building blocks.[12–17] Thus, significant attention has focused on PAHs as molecular models for, or synthetic precursors to, diverse nanocarbons.[18–20] Importantly, large PAHs are also attractive in their own right, for example as potential replacements for inorganic components of in the active layers of electronic and optoelectronic devices.[21–23] Their suitability for this purpose is due not only to their unique electronic and photophysical properties, which result from their extended conjugation and rigidity,[24] but also their tendency to assemble into highly ordered structures in the solid state.[25] This ordering promotes intermolecular π-overlap and thus high charge carrier

mobilities.[26,27] While PAHs have been studied since the early days of organic chemistry,[28] there has recently been spectacular growth in their structural diversity and applications. This has been driven by continued advances in organic synthesis, which has enabled the discovery of new, exceptional properties.

The large number of fused rings in conjugated nanocarbons renders their syntheses difficult, as many C–C bonds must be simultaneously and regioselectively formed. Versatile strategies that enable such ring fusions are scarce, but in high demand. The most widely employed is intramolecular cyclodehydrogenation, promoted by a Lewis acid (Scholl reaction) or light (Mallory reaction).[29,30] This strategy owes its success to its operational simplicity and readily available precursors. More importantly, it often provides near-quantitative yields for each C–C bond formation (a strict requirement for larger nanocarbons given the large number of bonds that must be formed). However, there are severe limitations, including a lack of functional group tolerance and low regioselectivities. Variations on cyclodehydrogenation that involve a leaving group (i.e. loss of H-X instead of H_2) can mitigate these difficulties and are valuable additions to the ring-fusion toolkit.[31–33]

Organometallic methods might be considered the best chance at realization of "the perfect nanocarbon synthesis" since the number of conceivable transition metal catalysts is limitless (the only limitation is the speed with which catalyst variations can be screened). Importantly, this ideal will not be comprised of one method or strategy, but rather a toolbox of many. The organometallic ring-fusion toolbox is rapidly expanding[34] and includes (but is certainly not limited to) ring-closing alkene metathesis,[35,36] carbometallation cascades,[37] C-H functionalization,[38] and [2+2+2] cycloadditions.[39–48]

Metal-Mediated Cycloadditions in the Synthesis of Large PAHs and Conjugated Nanocarbons

Popularized by Vollhardt in the 1970s, transition metal promoted cycloadditions are powerful synthetic methods for the construction of aromatic rings.[49–53] The most developed of these reactions, the [2+2+2] cycloaddition of three alkynes, has proven invaluable for the synthesis of PAHs.[39–48] This reaction can be broken up into three categories, based on the number of alkyne-containing reactants, as demonstrated in Scheme 1: 1) "fully-intramolecular" – all three alkynes are tethered onto the same substrate (e.g. **1**, Scheme 1a);[39–41] 2) "partially-intramolecular" – a tethered diyne (e.g. **2**, Scheme 1b) unites with a monoyne;[41–46] 3) "fully-intermolecular" – three separate alkynes unite (Scheme 1c).[47,48] Category 1 is a powerful strategy for formation of a PAH from a non-PAH precursor, and has found the most use for syntheses of helical PAHs (e.g. heliphenes like compound **3**,[39] and helicenes[40]). Category 2 has proven valuable both for annulation of an existing PAH[41–43] and formation of a PAH from a non-PAH precursor.[41,44–46] The former is demonstrated by Siegel's divergent elaboration of di(alkynyl)corannulenes (**2**) into substituted indenocorannulenes (**4**).[42] Category 3 is represented by the Pd-catalyzed cyclotrimerization of arynes (e.g. **5**) to form π-extended triphenylenes (e.g. **6**).[47,48] The direct formation of a PAH with this strategy requires at least one polycyclic aryne as a reaction partner. Fully-intermolecular [2+2+2] reactions that do not involve arynes have long been employed as an expedient route to highly symmetrical nanographene precursors, but a subsequent Scholl reaction is required for PAH formation.[54] As an interesting aside, Tanaka and coworkers have constructed some remarkable, "non-fused" nanocarbons (e.g. nanohoops and nanocages) using their highly regioselective, fully-intermolecular [2+2+2] reaction.[55,56]

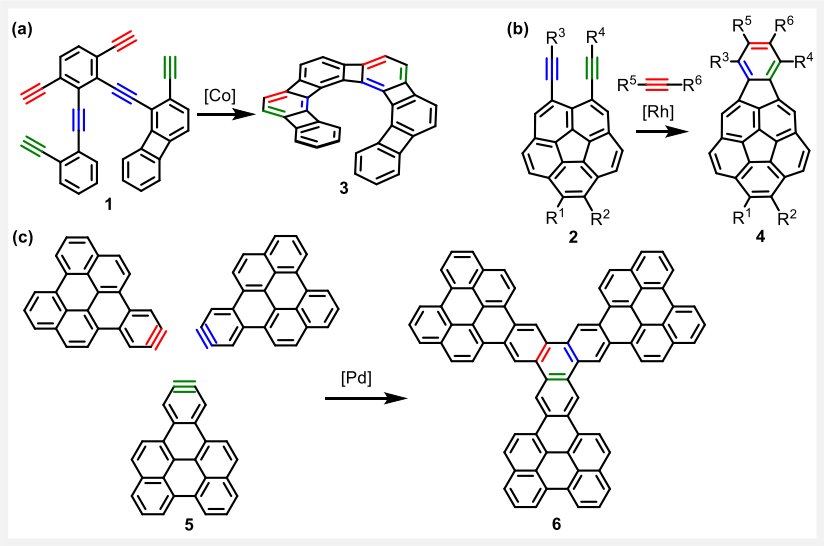

Scheme 1. Examples of PAH syntheses via [2+2+2] reactions: **(a)** fully-*intra*molecular; **(b)** partially-intramolecular; **(c)** fully-*inter*molecular.

While most attention in the context of PAH synthesis has focused on [2+2+2] reactions, the conceptual framework of metal-mediated cycloadditions is much broader.[49,53,57] Simply by variation of the third reaction component (i.e. a [2+2+n] reaction), accessible chemical space is significantly expanded. More than 45 years ago, in some of the earliest work on synthetic applications of metal-mediated cycloadditions, Müller and coworkers showed that diynes with π-conjugated tethers (e.g. **7** in Scheme 2a) can be subjected to a formal [2+2+1] reaction with a Rh reagent to form a PAH appended by a synthetically versatile rhodacyclopentadiene fragment (e.g. **8**).[58] There are two compelling features of this chemistry: 1) it provides a divergent pathway for *direct* installation of functionality into a PAH, including heterocycles (e.g., thiophenes or selenophenes), 6-membered aromatic rings, and cyclopentadienones; 2) it furnishes a PAH from a non-PAH precursor. Notably, the minimal loss of entropy upon cyclization of **7** contributes to high yields. Surprisingly, however, this ring-fusion strategy has been employed only sparingly and, before this work, for relatively small PAHs via an intermediate containing one metallacyclopentadiene synthon.[58–63] Perhaps the most

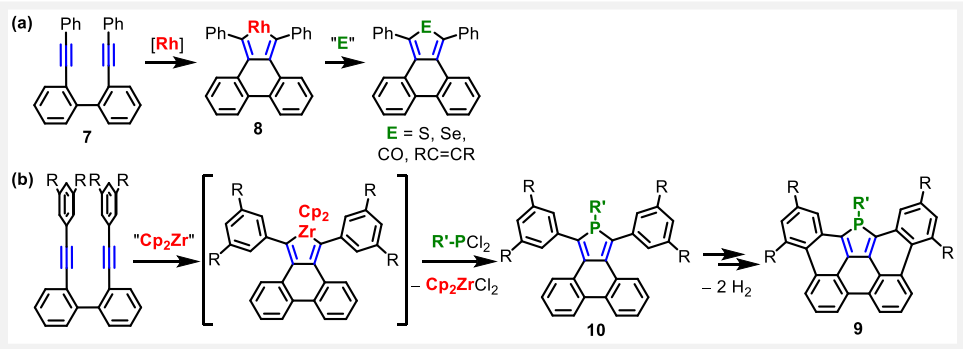

Scheme 2. (a) Müller's pioneering work on divergent use [2+2+n] reactions for PAH synthesis; **(b)** Construction of a P-containing nanographene using a sequential [2+2+1]/cyclodehydrogenation strategy.

notable example, from Hissler, Réau, and coworkers, is the construction of phosphorus-containing nanographene **9** (Scheme 2b) using a sequential [2+2+1]/cyclodehydrogenation strategy.[59] The first step, a zirconocene-mediated [2+2+1] reaction, is a direct extension of Müller's work; however, critically, it employed a more versatile and economical zirconacyclopentadiene intermediate (**10**).

Zirconacyclopentadienes are highly versatile intermediates and have been used in related PAH synthetic strategies. The earliest work is by Takahashi and coworkers, who developed an iterative approach to functionalized acenes **11** (Scheme 3a), but this requires a post-ring-fusion aromatization step.[64,65] Using chemistry that was previously developed by Takahashi,[66,67] Wang and coworkers demonstrated that zirconacyclopentadienes (**12**, Scheme 3b) can be used as annulation reagents to *directly* extend the π-system of naphthalene diimide **13** to form a tetracene diimide **14**.[68] The same group also showed that benzannulated zirconacyclopentene **15** (a partially saturated analogue of a zirconacyclopentadiene) can be used for *direct* extension of **13** to the longer hexacene diimide **16**.[69] This is a remarkable result since the expected product is a saturated analogue **17**, but it is unclear if the dehydrogenation occurred during the workup (performed under ambient conditions) or under the reaction conditions.

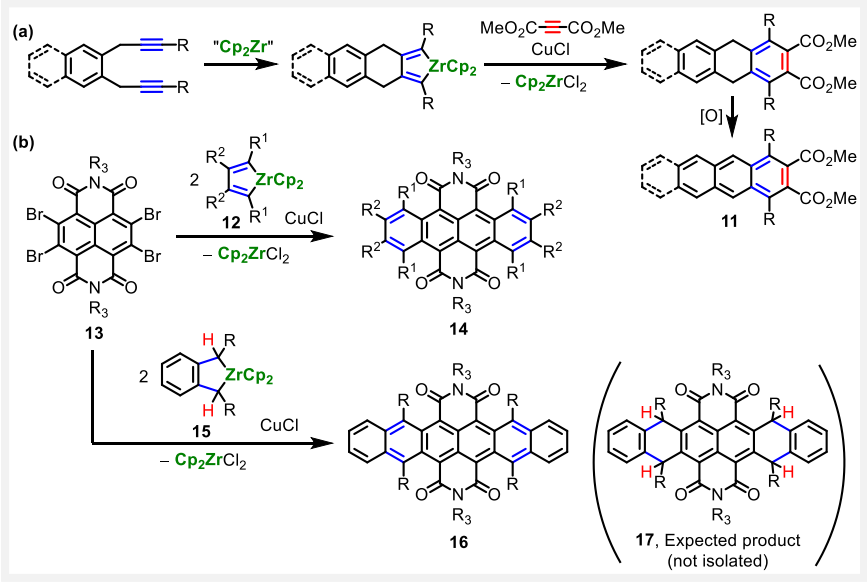

Scheme 3. (a) Takahashi's iterative acene synthesis; **(b)** Wang's annulation of naphthalene diimide with a zirconacyclopentadiene and zirconacyclopentene.

Introduction to the Synthetic Platform Developed in this Thesis

This thesis presents the development of a unified strategy to synthesize conjugated nanocarbons via the employment of metal-mediated [2+2+n] cycloadditions. Inspiration is drawn both from the early work of Müller and the significant developments in [2+2+2] and zirconacyclopentadiene chemistry since that time. The strategy can be conceptually broken up into the two steps shown in Scheme 4. First is cyclization of a precursor (**18**) containing one or more tethered diyne (or dinitrile) units to give a large, polyaromatic system containing one or more appended metallacyclopentadiene rings (**19**).

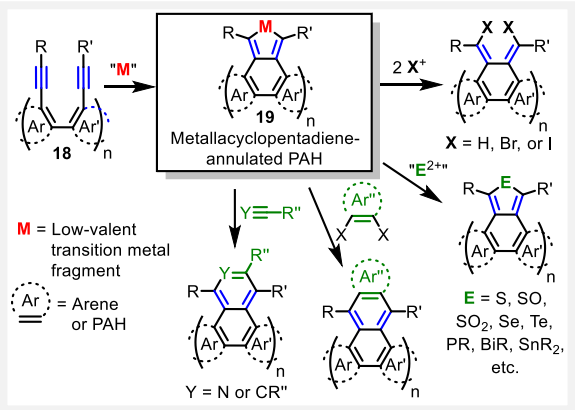

Scheme 4. Unified synthetic strategy developed in this thesis.

Intermediate **19** can be either isolable or part of a catalytic cycle. Importantly, **18** can be assembled in a modular fashion using standard C–C bond-forming reactions. Second is a *divergent* "post-fusion" functionalization, which enables a final step utilization of the *full arsenal of [2+2+n] chemistry*. This is made possible in part by the synthetic versatility of metallacyclopentadienes, which are effective precursors to 5-, 6-, or even 8-membered rings,[70–76] dienes,[77,78] and more extended π-systems.[66,67]

As a proof of concept, the strategy was applied to the synthesis of several different types of conjugated nanocarbons, including expanded helicenes (a new class of chiral nanocarbons), two types of chiral macrocyclic nanocarbons (bridged expanded helicenes and a macrocycle with "figure-8" topology), and large, PAH-containing arylene ethynylene macrocycles. Additionally, although only a few highlights are given here, it has been applied to cycloarenes, which are fully fused macrocyclic arrays of arene rings. Importantly, highly functionalized versions of all new nanocarbons can now be targeted using this strategy, which will greatly aid in future investigations of their properties and applications. The framework is also shown to accommodate the isoelectronic dinitrile precursors, which enables general access to nitrogen-containing PAHs. Below, a summary is provided of the major results in each chapter.

Extended Summary of Subsequent Chapters

Zirconacyclopentadiene-Annulated Polycyclic Aromatic Hydrocarbons (Chapter 2).[79] This project was the first demonstration of the unified synthetic strategy. It addressed the ring-fusion challenge discussed above by exploiting the ability of low-valent zirconocene to effect high-yielding cyclization of alkynes. Precursors like **20** (Scheme 5), which contain several tethered diyne units and can be assembled using well-established C–C bond forming reactions, were shown to cyclize *quantitatively* with a zirconocene reagent to give very large PAHs. The example of Scheme 5 shows the synthesis of a system containing sixteen fused rings (**21**), from a precursor with zero fused rings (**20**), in excellent yield. The generality was demonstrated with a total of seven PAH topologies that are annulated by one or more zirconacyclopentadiene rings (a "ZrPAH"). The synthetic versatility of these ZrPAHs is a defining feature of this strategy, as they can potentially undergo any of the transformations shown in Scheme 4. Here, they were employed (via protodemetallation) as a conceptually new means of generating *o*-quinodimethanes (*o*-QDMs), which are ubiquitous reactive intermediates in organic synthesis. These *o*-QDM-containing PAHs (e.g. **22** in Scheme 5) were unexpectedly persistent, which allowed isolation and full characterization of eight examples, nearly

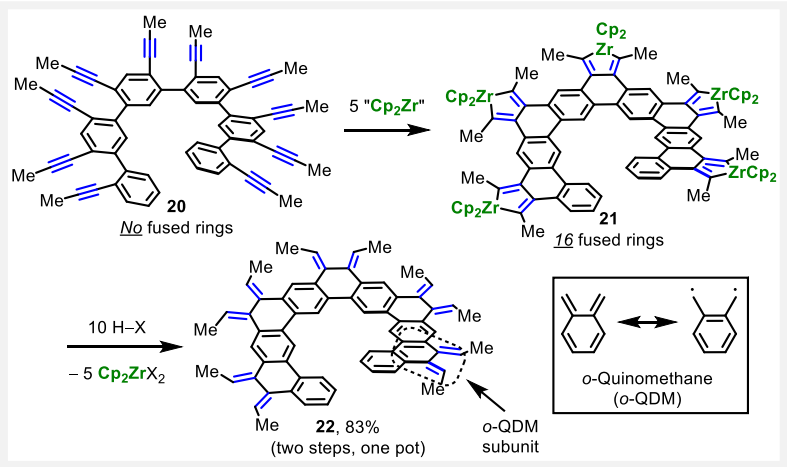

Scheme 5.

doubling the number of known isolable *o*-QDMs. The stability of these compounds allowed an unprecedented *o*-QDM transformation, 1,4-hydrogenation, to give heavily alkylated PAHs that are inaccessible using other synthetic technology.

Expanded Helicenes: General Synthetic Strategy and Remarkable Self-Assembly (Chapter 3).[80] Compounds **21** and **22** (Scheme 5) were the first members of a fascinating new class of compounds, which were called "expanded helicenes" (**23**, Figure 1) since they are conceptually related to the well-studied carbohelicenes (**24**). Helicenes are currently under intense investigation for exceptional properties that result from their non-planarity and chirality (e.g. non-linear optical responses, circular dichroism, circularly polarized emission, and complex supramolecular chemistry). This project was the first study of this broad new class of helicenes. The effort was aided by identification of a *quantitative*, Ir-catalyzed [2+2+2] cycloaddition to access a series of benzannulated expanded helicenes (**25**, Scheme 6). This [2+2+2] reaction is complementary to the zirconocene-mediated [2+2+1] reactions used to access helicenes **26** and **27**. This was the first demonstration of the divergence inherent in the [2+2+n] strategy, which provides a rapid means to manipulate properties. The new helicenes display remarkable supramolecular and solid-state behavior, which is heavily influenced by the annulated ring introduced in the final synthetic step. Benzannulated expanded 13-helicene **25** forms an unusual π-stacked double helix **28**, both in solution and in the solid state, while selenophene-annulated **26** exhibits long-range π-stacking. The presence of diastereotopic Cp rings in **27** allowed the determination of its very low racemization barrier (~11 kcal/mol) by

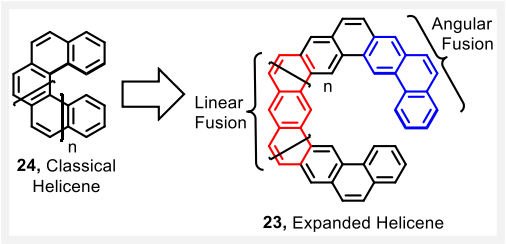

Figure 1.

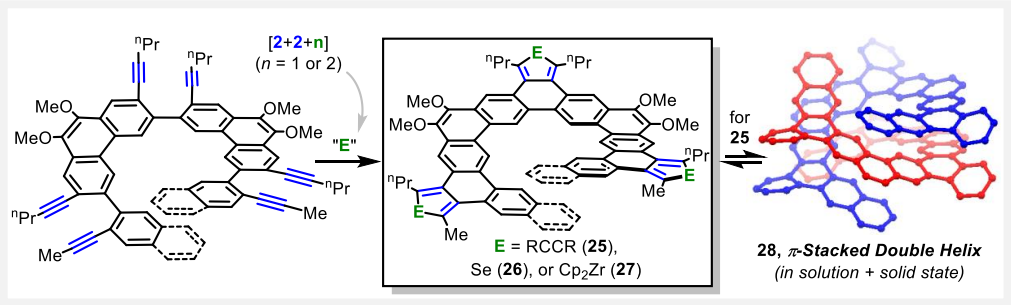

Scheme 6.

dynamic ^{1}H NMR spectroscopy, demonstrating that expanded helicenes are much more flexible than all-angularly-fused helicenes.

A Site-Selective [2+2+2] Cycloaddition and its Orthogonality to Alkyne Metathesis: Rapid, General Synthesis of Macrocyclic Nanocarbons (Chapter 4).[81] Polycyclic aromatic hydrocarbons (PAHs) are ideal building blocks for arylene ethynylene macrocycles (AEMs) due to their rigidity, structural diversity, and exceptional supramolecular, electronic, and photophysical properties. These hybrid nanocarbons are difficult to access because of challenges associated with syntheses of appropriately functionalized PAH precursors. Here, a general [2+2+2] cycloaddition strategy was developed to synthesize such PAHs. It was applied to six structurally diverse PAH ring systems (twelve new alkynylated PAHs in total). The strategy is enabled by the identification of a site-selective, Ir-catalyzed [2+2+2] cycloaddition, which preferentially cyclizes tethered diyne units with preservation of peripheral alkynyl groups. This allows a subsequent macrocyclization via alkyne metathesis, a scalable and high-yielding method for AEM synthesis. As a proof of concept, the [2+2+2]/metathesis sequence is employed to access four structurally complex, PAH-containing AEM frameworks, including an elliptical dimer (**29**, Scheme 7) and a series of three trimers (**30**–**32**) with rationally modified cavity sizes. Three of these AEMs are based on previously unknown PAH ring systems. More generally, this work demonstrates how site-selective reactions can be harnessed to rapidly build up complexity in conjugated nanocarbons.

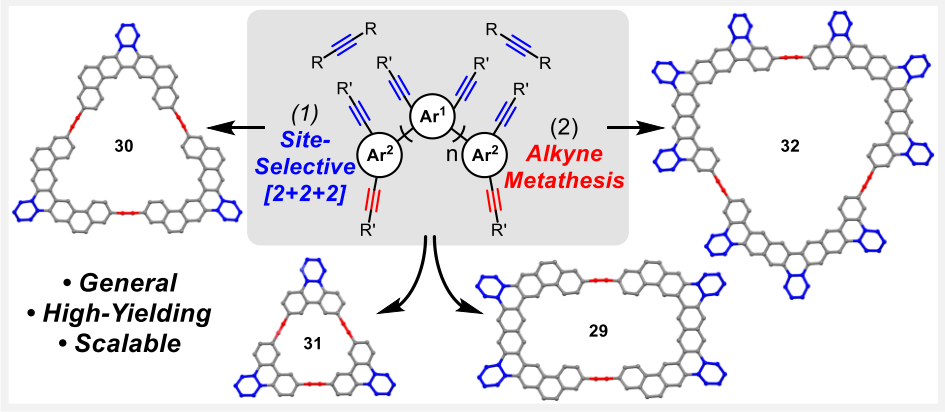

Scheme 7.

Expanded Helicenes as Synthons for Chiral Macrocyclic Nanocarbons (Chapter 5). In this project, expanded helicenes were used as building blocks for more complex chiral nanocarbons. This required appreciable quantities of an alkyne-functionalized precursor helicene (**33**, Scheme 8), which was accomplished (on gram scale) using the site selective [2+2+2] cycloaddition that was introduced in Chapter 4. As a proof of concept, two distinct types of chiral macrocyclic nanocarbons were synthesized via single-step transformations involving the alkynyl groups on the helicene: 1) a "figure-8" dimer (**34**) via alkyne metathesis and 2) two arylene-bridged expanded helicenes (**35**) via Zr-mediated, formal [2+2+n] cycloadditions. The phenylene-bridged helicene displays substantially higher enantiomerization barrier (>20 kcal/mol) than its precursor **33** (<12 kcal/mol), which makes this a promising strategy to access configurationally stable expanded helicenes. In contrast, the topologically distinct "figure-8" retains the configurational lability of the helicene precursor. Despite its remarkable flexibility, crystallization of this compound enabled resolution of its enantiomers in the solid-state via the formation of conglomerates. Here, the enantiomers are stabilized by an intricate network of two unique yet interconnected helical superstructures.

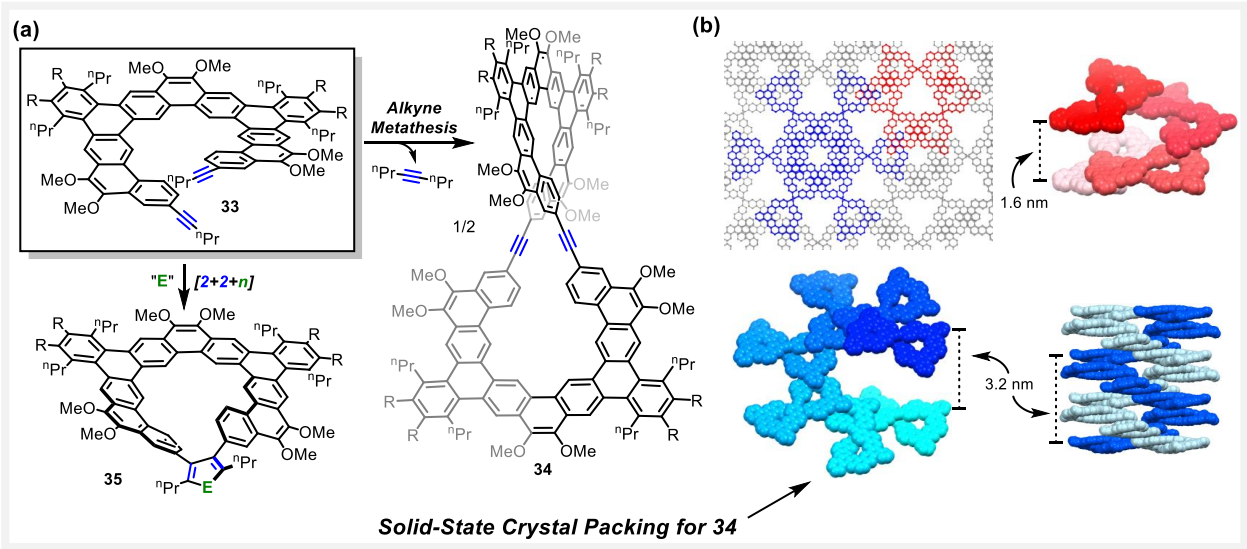

Scheme 8.

Titanocene-Mediated Dinitrile Coupling: A Divergent Route to Nitrogen-Containing Polycyclic Aromatic Hydrocarbons (Chapter 6).[82] The goal of this project was to generalize the strategy described above to include isoelectronic dinitriles (**36**, Scheme 9), which would allow rational incorporation of a variety of nitrogen-based heterocycles into PAHs. The greatest challenge was that [2+2+n] reactions involving dinitrile substrates had very little literature precedent, probably because this requires an "umpolung" bond formation between the two electrophilic carbons. A key discovery was that a readily-available reagent, $Cp_2Ti(Me_3SiC{\equiv}CSiMe_3)$, can be employed for the cyclization of tethered dinitrile substrates **36**. Like the analogous diynes, the substrates are nearly ideal from an entropic perspective (only one conformational degree of freedom must be frozen out on cyclization). Furthermore, the resulting di(aza)titanacyclopentadienes (**37**) are versatile synthons for further transformations, providing *divergent* access to PAHs containing one or more pyrazines (**38**), quinones (**39**), and diazoles (**40**). This was the first productive use of di(aza)metallacyclopentadiene

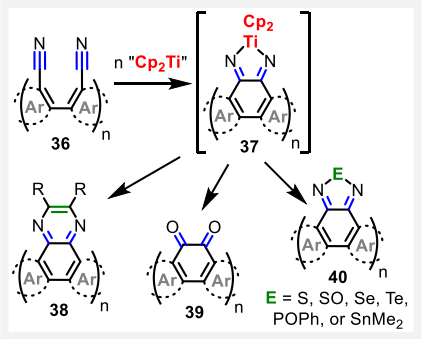

Scheme 9.

intermediates in organic synthesis, including the first formal [2+2+2] reaction to form a pyrazine ring. The new methodology enables rational, late-stage control of HOMO and LUMO energy levels and thus photophysical and electrochemical properties, as was demonstrated on a series of compounds by UV/vis and fluorescence spectroscopy, cyclic voltammetry, and DFT calculations.

Future Directions as Illustrated by Two Preliminary Results (Chapter 7). The synthetic platform developed in Chapters 2–6 will allow in-depth studies of the nanocarbons presented in those chapters via the construction of highly functionalized analogues. More importantly, it is applicable to other nanocarbons. This chapter presents two preliminary results along these lines. The first result demonstrates how this strategy is currently being applied to a synthetically challenging and highly-sought-after class of macrocyclic nanocarbons, the cycloarenes (Figure 2a). The second is the isolation of a *configurationally stable* expanded 23-helicene (Figure 2b), which is 7 rings longer than any known carbohelicene. Importantly, both demonstrate the sequential application of [2+2+n] reactions to rapidly build up complexity. This is enabled in part by the site-selectivity of the [2+2+2] reaction (developed in Chapter 4), which furnishes alkynylated PAHs that are poised for further [2+2+n] reactions. Since these stories are a work-in-progress and are being completed during my last few months at Berkeley, only a few highlights are presented.

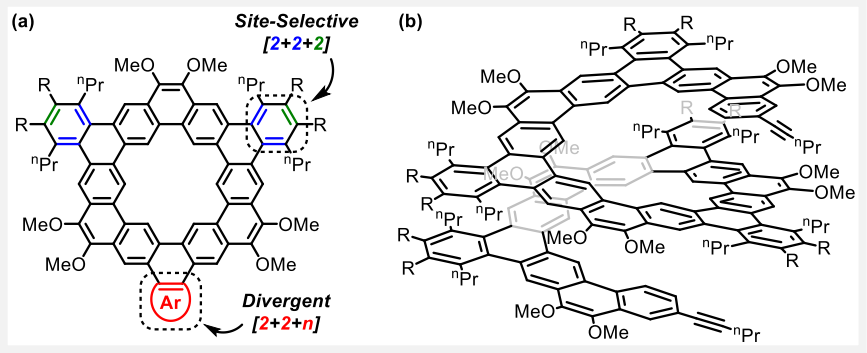

Figure 2. (a) Annulated cycloarene; **(b)** Expanded 23-helicene.

References for Chapter 1

(1) Novoselov, K. S.; Geim, A. K.; Morozov, S. V.; Jiang, D.; Zhang, Y.; Dubonos, S. V.; Grigorieva, I. V.; Firsov, A. A. *Science* **2004**, *306* (5696), 666–669.
(2) Geim, A. K. *Science* **2009**, *324* (5934), 1530–1534.
(3) Schwierz, F. *Nat. Nanotechnol.* **2010**, *5* (7), 487–496.
(4) Bonaccorso, F.; Sun, Z.; Hasan, T.; Ferrari, A. C. *Nat. Photonics* **2010**, *4* (9), 611–622.
(5) Hill, E. W.; Vijayaragahvan, A.; Novoselov, K. *IEEE Sens. J.* **2011**, *11* (12), 3161–3170.
(6) Huang, C.; Li, C.; Shi, G. *Energy Environ. Sci.* **2012**, *5* (10), 8848–8868.
(7) Xiang, Q.; Yu, J.; Jaroniec, M. *Chem Soc Rev* **2012**, *41* (2), 782–796.
(8) Zhang, J.; Xia, Z.; Dai, L. *Sci. Adv.* **2015**, *1* (7), e1500564.
(9) Johnson, D. Europe Invests €1 Billion to Become "Graphene Valley" http://spectrum.ieee.org/nanoclast/semiconductors/nanotechnology/europe-invests-1-billion-to-become-graphene-valley (accessed August 12, 2019).
(10) Luis Delgado, J.; Ángeles Herranz, M.; Martín, N. *J. Mater. Chem.* **2008**, *18* (13), 1417–1426.
(11) Guldi, D. M.; Martín, N. *Carbon Nanotubes and Related Structures: Synthesis, Characterization, Functionalization, and Applications*; John Wiley & Sons, 2010.
(12) Müllen, K. Graphene as a Target for Polymer Synthesis. In *Hierarchical Macromolecular Structures: 60 Years after the Staudinger Nobel Prize II*; Percec, V., Ed.; Advances in Polymer Science; Springer International Publishing, 2013; pp 61–92.
(13) Segawa, Y.; Ito, H.; Itami, K. *Nat. Rev. Mater.* **2016**, *1* (1), 15002.
(14) Narita, A.; Wang, X.-Y.; Feng, X.; Müllen, K. *Chem. Soc. Rev.* **2015**, *44*, 6616–6643.
(15) Stępień, M.; Gońka, E.; Żyła, M.; Sprutta, N. *Chem. Rev.* **2017**, *117* (4), 3479–3716.
(16) Ball, M.; Zhong, Y.; Wu, Y.; Schenck, C.; Ng, F.; Steigerwald, M.; Xiao, S.; Nuckolls, C. *Acc. Chem. Res.* **2015**, *48* (2), 267–276.
(17) Pun, S. H.; Miao, Q. *Acc. Chem. Res.* **2018**, *51* (7), 1630–1642.
(18) Konishi, A.; Hirao, Y.; Matsumoto, K.; Kurata, H.; Kishi, R.; Shigeta, Y.; Nakano, M.; Tokunaga, K.; Kamada, K.; Kubo, T. *J. Am. Chem. Soc.* **2013**, *135* (4), 1430–1437.
(19) Fogel, Y.; Zhi, L.; Rouhanipour, A.; Andrienko, D.; Räder, H. J.; Müllen, K. *Macromolecules* **2009**, *42* (18), 6878–6884.
(20) Ruffieux, P.; Wang, S.; Yang, B.; Sánchez-Sánchez, C.; Liu, J.; Dienel, T.; Talirz, L.; Shinde, P.; Pignedoli, C. A.; Passerone, D.; Dumslaff, T.; Feng, X.; Müllen, K.; Fasel, R. *Nature* **2016**, *531* (7595), 489–492.
(21) Wu, J.; Pisula, W.; Müllen, K. *Chem. Rev.* **2007**, *107* (3), 718–747.
(22) Jiang, W.; Li, Y.; Wang, Z. *Chem. Soc. Rev.* **2013**, *42* (14), 6113–6127.
(23) Sun, Z.; Ye, Q.; Chi, C.; Wu, J. *Chem. Soc. Rev.* **2012**, *41*, 7857–7889.
(24) Rieger, R.; Müllen, K. *J. Phys. Org. Chem.* **2010**, *23* (4), 315–325.
(25) Sergeyev, S.; Pisula, W.; Geerts, Y. H. *Chem. Soc. Rev.* **2007**, *36* (12), 1902–1929.
(26) Reese, C.; Bao, Z. *Mater. Today* **2007**, *10* (3), 20–27.
(27) Wang, C.; Dong, H.; Hu, W.; Liu, Y.; Zhu, D. *Chem. Rev.* **2012**, *112* (4), 2208–2267.
(28) Clar, E. *Polycyclic Hydrocarbons: Volume 1*; Springer-Verlag: Berlin Heidelberg, 1964.
(29) Kivala, M.; Wu, D.; Feng, X.; Li, C.; Müllen, K. Cyclodehydrogenation in the Synthesis of Graphene-Type Molecules. In *Materials Science and Technology*; Wiley-VCH Verlag GmbH & Co. KGaA, 2006.
(30) Mallory, F. B.; Mallory, C. W. Photocyclization of Stilbenes and Related Molecules. In *Organic Reactions*; John Wiley & Sons, Inc., 2004.

(31) Allemann, O.; Duttwyler, S.; Romanato, P.; Baldridge, K. K.; Siegel, J. S. *Science* **2011**, *332* (6029), 574–577.
(32) Papaianina, O.; Akhmetov, V. A.; Goryunkov, A. A.; Hampel, F.; Heinemann, F. W.; Amsharov, K. Y. *Angew. Chem. Int. Ed.* **2017**, *56* (17), 4834–4838.
(33) Daigle, M.; Picard-Lafond, A.; Soligo, E.; Morin, J.-F. *Angew. Chem. Int. Ed.* **2016**, *55* (6), 2042–2047.
(34) Jin, T.; Zhao, J.; Asao, N.; Yamamoto, Y. *Chem. – Eur. J.* **2014**, *20* (13), 3554–3576.
(35) Bonifacio, M. C.; Robertson, C. R.; Jung, J.-Y.; King, B. T. *J. Org. Chem.* **2005**, *70* (21), 8522–8526.
(36) Lee, J.; Li, H.; Kalin, A. J.; Yuan, T.; Wang, C.; Olson, T.; Li, H.; Fang, L. *Angew. Chem. Int. Ed.* **2017**, *56* (44), 13727–13731.
(37) Luo, Y.; Pan, X.; Yu, X.; Wu, J. *Chem Soc Rev* **2014**, *43* (3), 834–846.
(38) Ito, H.; Segawa, Y.; Murakami, K.; Itami, K. *J. Am. Chem. Soc.* **2019**, *141* (1), 3–10.
(39) Han, S.; Bond, A. D.; Disch, R. L.; Holmes, D.; Schulman, J. M.; Teat, S. J.; Vollhardt, K. P. C.; Whitener, G. D. *Angew. Chem. Int. Ed.* **2002**, *41* (17), 3223–3227.
(40) Teplý, F.; Stará, I. G.; Starý, I.; Kollárovič, A.; Šaman, D.; Rulíšek, L.; Fiedler, P. *J. Am. Chem. Soc.* **2002**, *124* (31), 9175–9180.
(41) Miljanić, O. Š.; Vollhardt, K. P. C. [N]Phenylenes: A Novel Class of Cyclohexatrienoid Hydrocarbon. In *Carbon-Rich Compounds*; Haley, M. M., Tykwinski, R. R., Eds.; Wiley-VCH Verlag GmbH & Co. KGaA, 2006; pp 140–197.
(42) Wu, Y.-T.; Hayama, T.; Baldridge, K. K.; Linden, A.; Siegel, J. S. *J. Am. Chem. Soc.* **2006**, *128* (21), 6870–6884.
(43) Kumar, B.; King, B. T. *J. Org. Chem.* **2012**, *77* (23), 10617–10622.
(44) McIver, A.; Young, D. D.; Deiters, A. *Chem. Commun.* **2008**, No. 39, 4750–4752.
(45) Sawada, Y.; Furumi, S.; Takai, A.; Takeuchi, M.; Noguchi, K.; Tanaka, K. *J. Am. Chem. Soc.* **2012**, *134* (9), 4080–4083.
(46) Murayama, K.; Sawada, Y.; Noguchi, K.; Tanaka, K. *J. Org. Chem.* **2013**, *78* (12), 6202–6210.
(47) Schuler, B.; Collazos, S.; Gross, L.; Meyer, G.; Pérez, D.; Guitián, E.; Peña, D. *Angew. Chem. Int. Ed.* **2014**, *53* (34), 9004–9006.
(48) Alonso, J. M.; Díaz-Álvarez, A. E.; Criado, A.; Pérez, D.; Peña, D.; Guitián, E. *Angew. Chem. Int. Ed.* **2012**, *51* (1), 173–177.
(49) Vollhardt, K. P. C. *Acc. Chem. Res.* **1977**, *10* (1), 1–8.
(50) Varela, J. A.; Saá, C. *Chem. Rev.* **2003**, *103* (9), 3787–3802.
(51) Agenet, N.; Buisine, O.; Slowinski, F.; Gandon, V.; Aubert, C.; Malacria, M. Cotrimerizations of Acetylenic Compounds. In *Organic Reactions*; John Wiley & Sons, Inc., 2004.
(52) Chopade, P. R.; Louie, J. *Adv. Synth. Catal.* **2006**, *348* (16–17), 2307–2327.
(53) *Transition-Metal-Mediated Aromatic Ring Construction*; Tanaka, K., Ed.; John Wiley & Sons, Inc.: Hoboken, NJ, 2013.
(54) Iyer, V. S.; Wehmeier, M.; Brand, J. D.; Keegstra, M. A.; Müllen, K. *Angew. Chem. Int. Ed. Engl.* **1997**, *36* (15), 1604–1607.
(55) Miyauchi, Y.; Johmoto, K.; Yasuda, N.; Uekusa, H.; Fujii, S.; Kiguchi, M.; Ito, H.; Itami, K.; Tanaka, K. *Chem. – Eur. J.* **2015**, *21* (52), 18900–18904.
(56) Hayase, N.; Nogami, J.; Shibata, Y.; Tanaka, K. *Angew. Chem.* **2019**, *131* (28), 9539–9542.
(57) Lautens, M.; Klute, W.; Tam, W. *Chem. Rev.* **1996**, *96* (1), 49–92.
(58) Müller, E. *Synthesis* **1974**, *1974* (11), 761–774.

(59) Bouit, P.-A.; Escande, A.; Szűcs, R.; Szieberth, D.; Lescop, C.; Nyulászi, L.; Hissler, M.; Réau, R. *J. Am. Chem. Soc.* **2012**, *134* (15), 6524–6527.
(60) Guo, X.; Wang, S.; Enkelmann, V.; Baumgarten, M.; Müllen, K. *Org. Lett.* **2011**, *13* (22), 6062–6065.
(61) Miyajima, T.; Matano, Y.; Imahori, H. *Eur. J. Org. Chem.* **2008**, *2008* (2), 255–259.
(62) Matano, Y.; Miyajima, T.; Fukushima, T.; Kaji, H.; Kimura, Y.; Imahori, H. *Chem. – Eur. J.* **2008**, *14* (27), 8102–8115.
(63) Dahlmann, U.; Neidlein, R. *Helv. Chim. Acta* **1997**, *80* (1), 111–120.
(64) Takahashi, T.; Kitamura, M.; Shen, B.; Nakajima, K. *J. Am. Chem. Soc.* **2000**, *122* (51), 12876–12877.
(65) Takahashi, T.; Li, S.; Huang, W.; Kong, F.; Nakajima, K.; Shen, B.; Ohe, T.; Kanno, K. *J. Org. Chem.* **2006**, *71* (21), 7967–7977.
(66) Takahashi, T.; Hara, R.; Nishihara, Y.; Kotora, M. *J. Am. Chem. Soc.* **1996**, *118* (21), 5154–5155.
(67) Takahashi, T.; Li, Y.; Stepnicka, P.; Kitamura, M.; Liu, Y.; Nakajima, K.; Kotora, M. *J. Am. Chem. Soc.* **2002**, *124* (4), 576–582.
(68) Yue, W.; Gao, J.; Li, Y.; Jiang, W.; Di Motta, S.; Negri, F.; Wang, Z. *J. Am. Chem. Soc.* **2011**, *133* (45), 18054–18057.
(69) Cui, X.; Xiao, C.; Winands, T.; Koch, T.; Li, Y.; Zhang, L.; Doltsinis, N. L.; Wang, Z. *J. Am. Chem. Soc.* **2018**, *140* (38), 12175–12180.
(70) Jiang, B.; Tilley, T. D. *J. Am. Chem. Soc.* **1999**, *121* (41), 9744–9745.
(71) Fagan, P. J.; Nugent, W. A.; Calabrese, J. C. *J. Am. Chem. Soc.* **1994**, *116* (5), 1880–1889.
(72) Yan, X.; Xi, C. *Acc. Chem. Res.* **2015**, *48* (4), 935–946.
(73) Yamashita, K.; Yamamoto, Y.; Nishiyama, H. *J. Am. Chem. Soc.* **2012**, *134* (18), 7660–7663.
(74) Tamao, K.; Kobayashi, K.; Ito, Y. *J. Org. Chem.* **1989**, *54* (15), 3517–3519.
(75) Shibata, T.; Yamashita, K.; Ishida, H.; Takagi, K. *Org. Lett.* **2001**, *3* (8), 1217–1219.
(76) Wender, P. A.; Christy, J. P.; Lesser, A. B.; Gieseler, M. T. *Angew. Chem. Int. Ed.* **2009**, *48* (41), 7687–7690.
(77) Nugent, W. A.; Thorn, D. L.; Harlow, R. L. *J. Am. Chem. Soc.* **1987**, *109* (9), 2788–2796.
(78) Buchwald, S. L.; Nielsen, R. B. *J. Am. Chem. Soc.* **1989**, *111* (8), 2870–2874.
(79) Kiel, G. R.; Ziegler, M. S.; Tilley, T. D. *Angew. Chem. Int. Ed.* **2017**, *56* (17), 4839–4844.
(80) Kiel, G. R.; Patel, S. C.; Smith, P. W.; Levine, D. S.; Tilley, T. D. *J. Am. Chem. Soc.* **2017**, *139* (51), 18456–18459.
(81) Kiel, G. R.; Tilley, T. D. A Site-Selective [2+2+2] Cycloaddition and Its Orthogonality to Alkyne Metathesis: Rapid, General Synthesis of Macrocyclic Nanocarbons. *Submitted.*
(82) Kiel, G. R.; Samkian, A. E.; Nicolay, A.; Witzke, R. J.; Tilley, T. D. *J. Am. Chem. Soc.* **2018**, *140* (7), 2450–2454.

Chapter 2: Zirconacyclopentadiene-Annulated Polycyclic Aromatic Hydrocarbons

This chapter was adapted with permission from: Kiel, G. R.; Ziegler, M. S.; Tilley, T. D., *Angew. Chem. Int. Ed.*, **2017**, 56, 4839–4844.

The Tilley group previously reported the synthesis of π-conjugated oligomers,[1] polymers,[2] and macrocycles[3] *via* the reductive coupling of alkynes with a low-valent zirconocene reagent. Given its ability to form new rings in high yield, this reaction should be well-suited for syntheses of large polycyclic aromatic hydrocarbons (PAHs). The Takahashi group demonstrated its application to the iterative elongation of an acene (Scheme 1a); however, the strategy is lengthy and requires a post-ring-fusion oxidation step.[4] Wang *et al.* employed zirconacyclopentadienes in the annulation of naphthalene diimides, but alkyne coupling was not involved in the ring fusion event (Scheme 1b).[5] A related and potentially far-reaching approach was indicated more than 40 years ago by Müller,[6] who used diynes with π-conjugated tethers to access several fully-unsaturated fused-ring systems *via* a rhodacyclopentadiene synthon (e.g., **A**, Scheme 1c). Two promising features of this chemistry are: 1) a PAH is *directly* obtained from the precursor (e.g., no subsequent oxidation is required) and 2) functionality can be divergently introduced using metal transfer reactions. Surprisingly, this approach has been employed for only a limited number of PAHs *via* an organometallic intermediate containing a single annulated metallacyclopentadiene.[7,8]

Here, a generalization of Müller's approach is developed, enabled by the high efficiency of zirconocene coupling. Specifically, the quantitative intramolecular reductive cyclization of an oligo(diyne) (**B**,

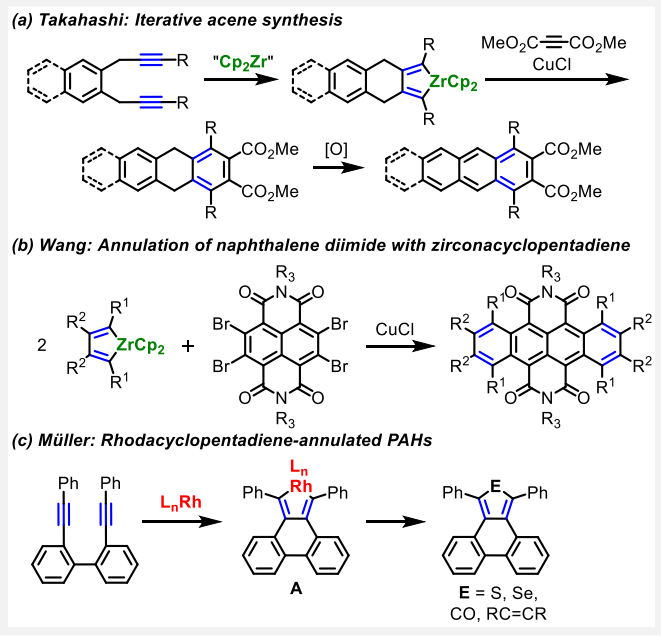

Scheme 1. Previously reported approaches for the synthesis of PAHs with zirconacyclopentadiene and rhodacyclopentadiene synthons.

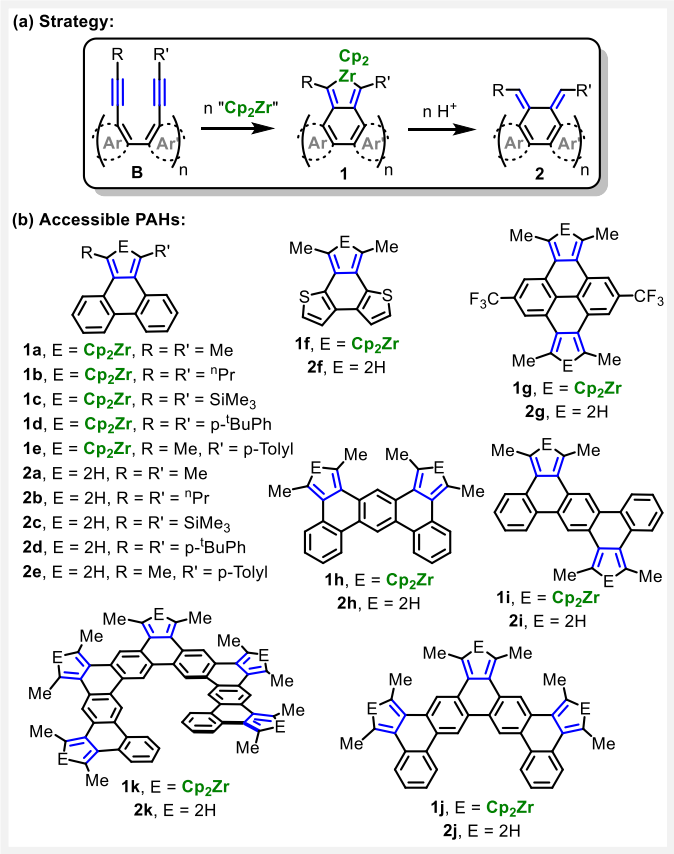

Scheme 2. Synthetic strategy explored in this work and accessible PAHs.

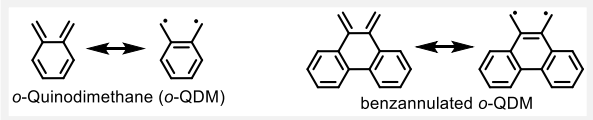

Figure 1. Resonance structures of o-QDM and a benzannulated o-QDM.

Scheme 2a) with a low-valent zirconocene reagent gives a zirconacyclopentadiene-annulated PAH ("ZrPAH", **1**). Eleven ZrPAHs (**1a–k**, Scheme 2b), representing seven different PAH topologies, are presented, including one with *sixteen* fused rings and five appended zirconacyclopentadiene rings (**1k**). Importantly, these ZrPAHs result from precursors that have no fused rings and could thus be easily assembled using established C–C bond forming reactions. Furthermore, the high yielding and stereoselective protodemetallation of **1a–k** was exploited as a novel entry to several PAHs with exocyclic diene functionality (**2a–k**). Such compounds might be expected to exhibit high reactivity, as is typically the case for dienes with the *o*-quinodimethane (*o*-QDM, Figure 1) structure.[9] However, they are remarkably stable when incorporated into a PAH framework (with certain R substituents), which allowed the isolation and full characterization of eight rare examples (**2a–c** and **2g–k**). Not only are these isolable *o*-QDMs interesting from a fundamental perspective, they also can be selectively hydrogenated using a simple procedure to produce highly alkylated PAHs.

Investigations began with the model system of Scheme 3, which involves the reductive coupling of a diyne (**3–7**) to form a phenanthrene annulated with a single zirconacyclopentadiene (ZrPAHs **1a–e**). There were two initial goals: 1) establish efficient conditions for the zirconocene coupling, which needs to be very high-yielding to be applied in multifold coupling reactions, and 2) determine the suitability of these ZrPAHs as precursors to *o*-QDMs, which might then be employed in Diels-Alder reactions for fusion of additional rings. Toward this end, ZrPAH **1a** was isolated in 92% yield by treatment of diyne **3** with 1.1 equiv of $Cp_2Zr(pyr)(Me_3SiC{\equiv}CSiMe_3)$,[10] a convenient, well-defined source of "Cp_2Zr".[11] Monitoring by ^{1}H NMR spectroscopy revealed that this reaction is rapid (complete in <5 min) and quantitative.

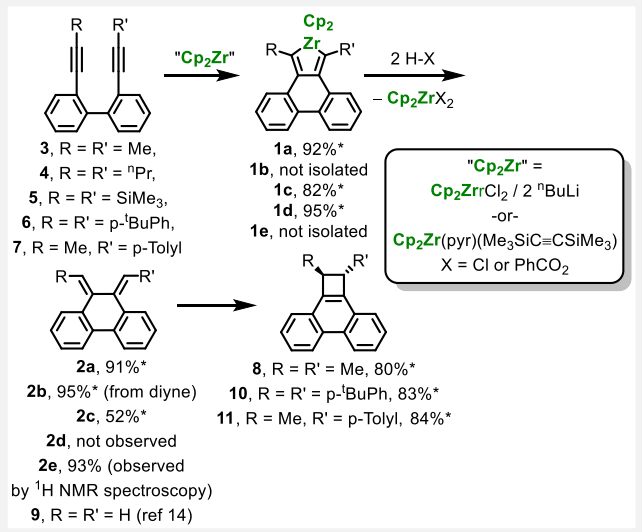

Scheme 3. Investigations on a model system. *Yields of isolated products. ZrPAHs 1a and 1c–1e were formed quantitatively according to 1H NMR spectroscopy (the formation of 1b was not monitored).

Treatment of **1a** with excess HCl (5 equiv) produced a surprisingly persistent species consistent with **2a** (as judged by a characteristic quartet at 5.7 ppm and corresponding doublet at 1.8 ppm for the vinyl and methyl protons, respectively) in nearly quantitative yield. Observation of this species despite the presence of excess strong acid is remarkable; however, 70% of **2a** decomposed to an unidentified product within 6 h. Replacement of HCl with benzoic acid produced **2a** in similarly high yield, and there were no signs of its decomposition after one week in benzene-d_6 solution.

The stability of **2a** in solution motivated its isolation, as examples of isolable *o*-QDMs are very rare and invariably involve substitution patterns that preclude their use as synthetic intermediates.[12,13] Treatment of **1a** with excess benzoic acid afforded pure **2a** as a colorless crystalline solid after a simple filtration of the hexanes-diluted reaction mixture through a plug of silica gel. The stability of **2a** permitted its full characterization, including by X-ray crystallography, which revealed its "twisted" nature in the solid state (Figure 2a). This twist can be quantified by two angles: 1) the torsion angle of the exocyclic diene unit (51.3°) and 2) the twist angle of the biphenyl backbone (19.8°). Compound **2a** can be handled for a few hours in air (in solution or as a solid) without detectable decomposition, but prolonged exposure to air at ambient temperature (ca. 21 °C) leads to slow decomposition, probably by oligomerization catalyzed by O_2. The solid can be stored indefinitely under nitrogen at ambient temperature. In the absence of O_2, ring-closure to cyclobutarene **8** (Scheme 3) is the major

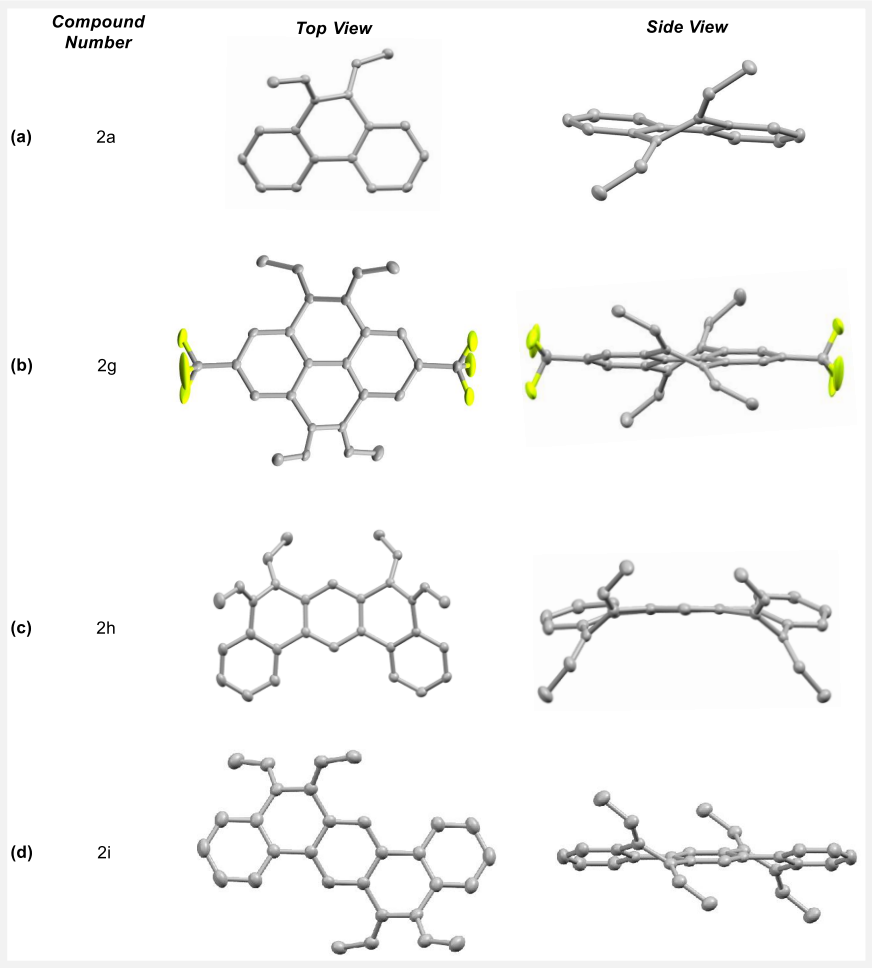

Figure 2. Crystal structures of **2a**, **2g**, **2h**, and **2i**. Thermal ellipsoids set at 50% probability.

decomposition pathway, but heating to 100 °C for 24 h was required for complete conversion. In contrast, the unsubstituted analogue **9** could not be isolated and was reported to rapidly decompose *via* [4+2] dimerization.[14]

The analogous n-propyl-substituted *o*-QDM **2b** was prepared in 95% yield by *in situ* generation of **1b** using Negishi's Cp_2ZrCl_2/^{n}BuLi reagent,[15] followed by treatment with aqueous HCl. This high yield was possible despite the use of excess strong acid, but short reaction times (<10 min) are required. Successful isolation of $SiMe_3$-substituted *o*-QDM **2c** required stoichiometric HCl, as this compound rapidly reacted with excess HCl to form an unidentified product. Employment of benzoic acid gave a mixture containing only a small amount of **2c** (~10%).

An attempt to isolate diaryl-substituted *o*-QDM **2d** led, instead, to cyclobutarene **10** as the sole product upon protodemetallation of **1d** with HCl, likely through electrocyclic ring-closing of **2d**. Treatment with benzoic acid gave a complex mixture. An intermediate case was mono-aryl-substituted *o*-QDM **2e**, which cyclized to **11** with a half-life of ~2 days at 19 °C upon protodemetallation of **1e** with HCl (and subsequent neutralization to prevent HCl-promoted side reactions). The intermediate **2e** was

identified by ^{1}H NMR spectroscopy in 93% yield and attempts were not made to isolate pure product. It is well known that aryl groups lower the barrier for this reversible ring-closing reaction.[16]

Thiophene-annulated *o*-QDM **2f** (Scheme 4) was predicted to be more reactive than its benzannulated analogue **2a** for two reasons: 1) a diminished steric interaction between the methyl groups and annulated rings and 2) lower aromaticity of the annulated thiophene rings. Indeed, generation of ZrPAH **1f** from diyne **12** followed by its *in situ* protodemetallation led to a rapid (< 5 min) 1,4-addition of HCl to yield **13** as the major product. The intermediacy of **2f** is supported by the isolation of Diels-Alder adduct **14** in 76% yield (in one pot, from **12**) upon protodemetallation in the presence of *N*-ethylmaleimide at 21 °C. In contrast, the analogous Diels-Alder reaction with **2a** (Scheme 4) required elevated temperature to proceed at a reasonable rate (70 °C for 15 h). The low reactivity of **2a** in the presence of a good dienophile is surprising, but the adduct **15** forms quantitatively and was isolated in high yield (90%). Compound **13** is not a precursor to **14**, as addition of *N*-ethylmaleimide *after* generation of **2f** resulted only in isolation of **13**. Importantly, the efficient one-pot reaction to form **14** from **12** suggests that this method should also be of value for more traditional, reactive *o*-QDM chemistry.

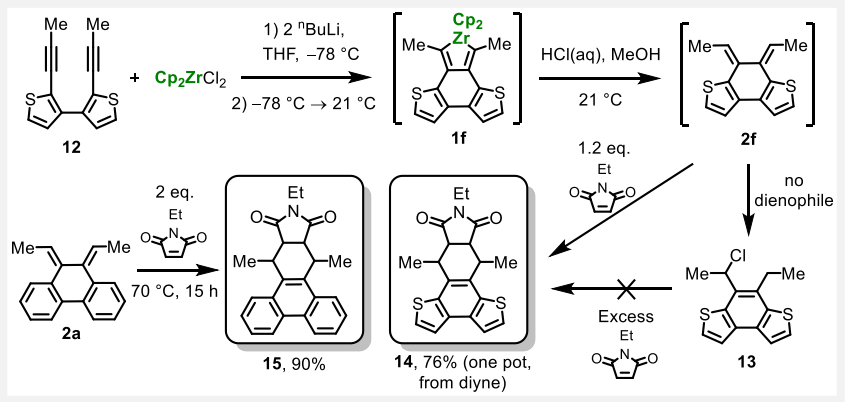

Scheme 4. Diels–Alder reactivity of the thiophene-annulated o-QDM **2f** and comparison with its benzannulated analogue **2a**.

The extension of this approach to larger polyaromatic systems *via* multifold coupling reactions began with precursor bis(diynes) **16–18** (Scheme 5). These compounds were easily accessible *via* Suzuki coupling (see SI). Methyl substituents were chosen to simplify structural analysis and promote crystallinity of the target bis(*o*-QDMs). Upon treatment of **16–18** with 2.2 equiv of $Cp_2Zr(pyr)(Me_3SiC{\equiv}CSiMe_3)$ followed by excess benzoic acid, bis(*o*-QDMs) **2g–i** were isolated in high yields. The intermediate ZrPAHs **1g–i** were isolated as crude solids, re-suspended in benzene or toluene, and then treated with benzoic acid, but isolation of the ZrPAH is optional. Preparation of these compounds was simple, efficient, and required minimal purification. While $Cp_2Zr(pyr)(Me_3SiC{\equiv}CSiMe_3)$ is an extremely convenient reagent (especially on a small scale), the Negishi protocol (*vide supra*) is often preferred. Thus, to demonstrate both the scalability and applicability of this protocol, it was employed to isolate 1.5 g of **2g** (89% yield). The structures of **2g–i** were elucidated by X-ray crystallography (Figure 2b–d). Each diene unit was determined to possess a similar amount of distortion as **2a**, as determined by their diene torsion and biphenyl twist angles.

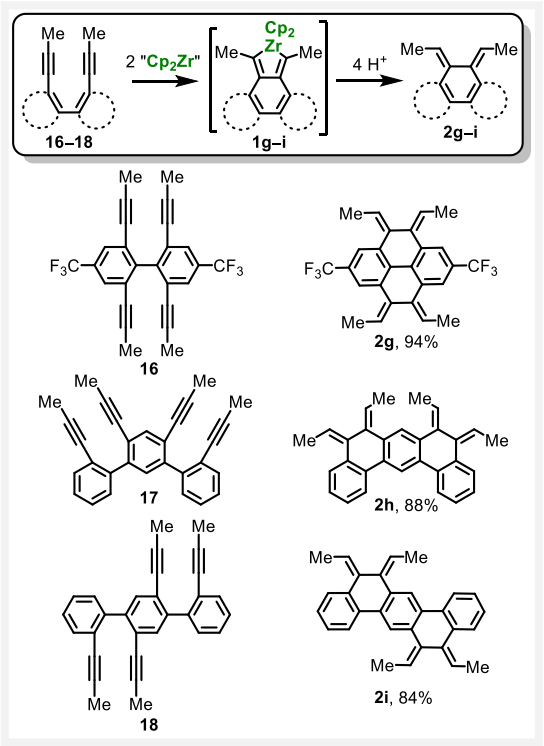

Scheme 5. Twofold couplings for the synthesis of compounds **2g**–**2i**.

They also have qualitatively similar stabilities. To the best of our knowledge, these are the first examples of isolable compounds with more than one *o*-QDM subunit.

The isolable *o*-QDMs are structurally fascinating, but their promise for post-coupling functionalization is perhaps of greater interest. Diels-Alder reactions are the obvious choice; however, initial difficulties with the aromatization of **15** prompted the establishment of an alternative route to valuable functionality. A 1,4-addition of H_2 across the diene is potentially the simplest transformation and would give unique PAHs decorated with alkyl groups. Such functionality, which is currently difficult to install, improves solubility and often promotes liquid crystallinity, with minimal perturbation of electronic properties. A selective 1,4-addition was observed upon exposure of **2a–b** and **2g–i** to 1 atm of H_2 over Pd/C to furnish alkylated PAHs **19–23** in good to very high yields (Scheme 6). A wide range of alkylated PAHs are now within reach using this approach.

As a test for applicability of the method to more demanding multifold couplings, PAHs containing three and five *o*-QDM units were targeted (**2j** and **2k**; Scheme 7). Remarkably, treatment of tris(diyne) **24** and pentakis(diyne) **25** with $Cp_2Zr(pyr)(Me_3SiC{\equiv}CSiMe_3$ (3.3 and 5.5 equiv), followed by excess benzoic acid, furnished **2j** and **2k** in excellent isolated yields (89 and 83%). Structural proof is provided by the characteristic ^{1}H NMR spectra of these isolable *o*-QDMs (*vide supra*). Synthesis of helical PAH **2k** not only demonstrates the high efficiency of the method, this compound is also the first member of a new class of helicenes, then with alternating angular and linear fusion ("expanded helicenes"). Hydrogenation of **2j** furnished the angular PAH **26** (Scheme 6) in 66% yield.

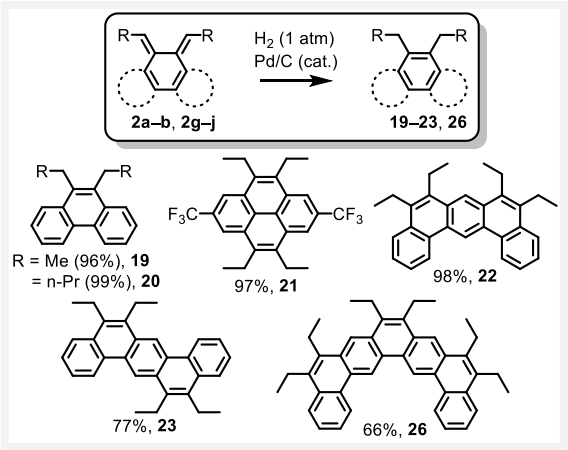

Scheme 6. Hydrogenation of **2a**, **2b**, and **2g**–**2j**.

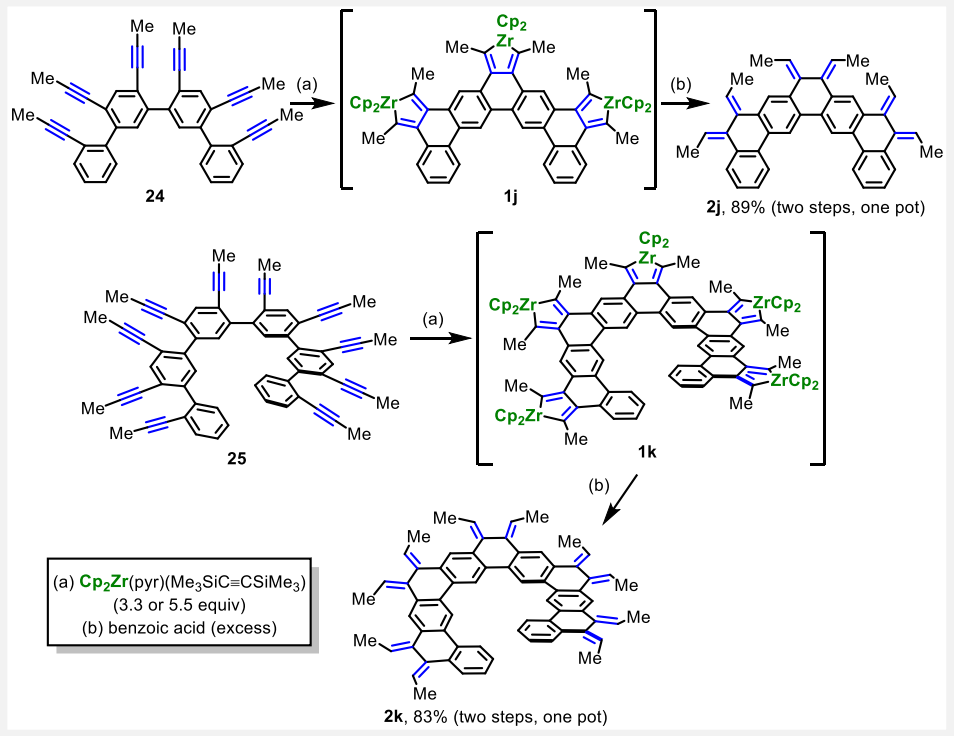

Scheme 7. Threefold and fivefold couplings.

The method presented above is a highly efficient means to fuse multiple rings into a PAH that contains the valuable zirconacyclopentadiene functionality (ZrPAH). Protodemetallation of these ZrPAHs gives a new entry to PAHs containing embedded *o*-QDMs. The high yield of these reactions suggests their suitability for the synthesis of even larger PAHs and graphene nanostructures. The discovery of a general class of isolable *o*-QDMs, which are usually generated as fleeting intermediates, opens new possibilities, including reaction with other reactive intermediates (e.g., arynes) or precise control of stoichiometry (e.g., for a Diels-Alder polymerization). Finally, and perhaps most importantly, these ZrPAHs are poised for use in any of the known zirconocene transfer reactions and should provide direct access to large heteroatom-functionalized PAHs and carbon-rich nanostructures.[17]

References for Main Text of Chapter 2

(1) M. C. Suh, B. Jiang, T. D. Tilley, *Angew. Chem.* **2000**, *112*, 2992–2995.
(2) B. L. Lucht, S. S. H. Mao, T. D. Tilley, *J. Am. Chem. Soc.* **1998**, *120*, 4354–4365.
(3) V. H. Gessner, J. F. Tannaci, A. D. Miller, T. D. Tilley, *Acc. Chem. Res.* **2011**, *44*, 435–446.
(4) T. Takahashi, S. Li, W. Huang, F. Kong, K. Nakajima, B. Shen, T. Ohe, K. Kanno, *J. Org. Chem.* **2006**, *71*, 7967–7977.
(5) W. Yue, J. Gao, Y. Li, W. Jiang, S. Di Motta, F. Negri, Z. Wang, *J. Am. Chem. Soc.* **2011**, *133*, 18054–18057.
(6) E. Müller, *Synthesis* **1974**, *1974*, 761–774.
(7) Example based on: a) zirconacylopentadiene intermediate: P.-A. Bouit, A. Escande, R. Szűcs, D. Szieberth, C. Lescop, L. Nyulászi, M. Hissler, R. Réau, *J. Am. Chem. Soc.* **2012**, 134, 6524–6527; (b) rhodacylopentadiene intermediate: X. Guo, S. Wang, V. Enkelmann, M. Baumgarten, K. Müllen, *Org. Lett.* **2011**, 13, 6062–6065.
(8) There are several reports based on the catalytic [2+2+2] reaction that are conceptually analogous to this approach. For example: a) Y.-T. Wu; T. Hayama; K. K. Baldridge; A. Linden; J. S. Siegel, *J. Am. Chem. Soc.* **2006**, *128*, 6870–6884; b) A. McIver; D. D. Young; A. Deiters, *Chem. Commun.*, **2008**, 4750-4752.
(9) J. L. Segura, N. Martín, *Chem. Rev.* **1999**, *99*, 3199–3246.
(10) U. Rosenthal, A. Ohff, W. Baumann, A. Tillack, H. Görls, V. V. Burlakov, V. B. Shur, *Z. Für Anorg. Allg. Chem.* **1995**, *621*, 77–83.
(11) J. R. Nitschke, S. Zürcher, T. D. Tilley, *J. Am. Chem. Soc.* **2000**, *122*, 10345–10352.
(12) a) F. Toda, K. Tanaka, M. Matsui, *Tetrahedron Lett.* **1982**, *23*, 217–220; b) T. Suzuki, Y. Sakano, T. Iwai, S. Iwashita, Y. Miura, R. Katoono, H. Kawai, K. Fujiwara, Y. Tsuji, T. Fukushima, *Chem. – Eur. J.* **2013**, *19*, 117–123..
(13) The annulated aromatic rings are one reason that **2a** exhibits higher stability than non-annulated o-QDMs. This can be explained by invoking Clar's rules, which predict that the diradical resonance structure (Figure 1) is much less important in describing the electronic structure of **2a** compared to an analogous non-benzannulated *o*-QDM.
(14) J. P. Anhalt, E. W. Friend, E. H. White, *J. Org. Chem.* **1972**, *37*, 1015–1019.
(15) E. Negishi, F. E. Cederbaum, T. Takahashi, *Tetrahedron Lett.* **1986**, *27*, 2829–2832.
(16) A. K. Sadana, R. K. Saini, W. E. Billups, *Chem. Rev.* **2003**, *103*, 1539–1602.
(17) X. Yan, C. Xi, *Acc. Chem. Res.* **2015**, *48*, 935–946.

Supporting Information for Chapter 2

General Details

Unless otherwise stated, all manipulations of organometallic compounds were carried out in dry solvents under an atmosphere of nitrogen, using either standard Schlenk techniques or a glovebox. Pentane, toluene, tetrahydrofuran, and diethyl ether were dried using a JC Meyers Phoenix SDS solvent purification system. Benzene was dried using a Vacuum Atmosphere solvent purification system. 1-Bromo-2-(pent-1-ynyl)benzene (**S2**),[1] 1-bromo-2-(4-*tert*-butylphenylethynyl)benzene (**S4**),[2] 2-(prop-1-ynyl)phenylboronic acid,[3] 3-bromo-2-iodothiophene,[4] 2-bromo-1,3-diiodo-5-(trifluoromethyl)benzene,[2] 2,5-dibromo-1,4-diiodobenzene,[5] and 2,4-dibromo-1,5-diiodobenzene[6] were prepared by literature procedures or slight modifications thereof. 1,4-Benzoquinone was purified by sublimation. Organolithium reagents (*n*-butyllithium and *tert*-butyllithium) were titrated by ^{1}H NMR spectroscopy immediately prior to use.[7] All other reagents and solvents were purchased from commercial suppliers and used as received. Melting points were determined on an SRS OptiMelt and are uncorrected. Mass spectrometry was performed by the QB3/Chemistry Mass Spectrometry Facility at the University of California, Berkeley. Elemental analyses were performed by the Microanalytical Laboratory in the College of Chemistry at the University of California, Berkeley. Column chromatography was carried out using Fischer Chemical 40–63μm, 230–400 mesh silica gel. NMR spectra were acquired at ambient temperature (ca. 22 °C) using Bruker AV-600, AV-500, DRX-500, AV-400, and AV-300 spectrometers. Chemical shifts (δ) are given in ppm and referenced to residual solvent peaks for ^{1}H NMR spectra (δ = 7.26 ppm for chloroform-*d*, δ = 7.16 for benzene-d_6, δ = 5.32 for dichloromethane-d_2, and δ = 2.09 for toluene-d_8) and for ^{13}C{^{1}H} NMR spectra (δ = 77.16 ppm for chloroform-*d*, δ = 128.06 for benzene-d_6, and δ = 54.00 for dichloromethane-d_2). For ^{19}F NMR spectra, chemical shifts are referenced to a C_6F_6 internal standard (δ = –162.2 ppm) and are reported relative to $CFCl_3$ at 0 ppm.

Comments About Purity and Storage of $Cp_2Zr(pyr)(Me_3SiC{\equiv}CSiMe_3)$

This compound undergoes some decomposition on storage at ambient temperature; thus, it was stored at –35 °C (in an N_2-filled glovebox). In the procedures below, the reagent's purity was typically 90–95%, as determined by ^{1}H NMR spectroscopy in benzene-d_6 (using hexamethylbenzene as internal standard). The masses reported below reflect the quantity of active species and the impurities do not noticeably affect results.

Synthesis of Oligo(Diyne) Precursors

Precursor diynes **3–7** and **12** and bis(diynes) **16–18** (Table S1) were accessed by a general two step procedure analogous to that reported by Swager and coworkers.[8] The first step was a high-yielding, chemoselective Sonogashira reaction[9] using readily available starting materials to give (*o*-bromoalkynyl)arenes **S1–S9**. The second step was either a Cu-mediated homocoupling to give **3-6**, **12** and **16** or a Pd-catalyzed cross-coupling under standard Suzuki conditions[10] to give **7**, **17** and **18**.

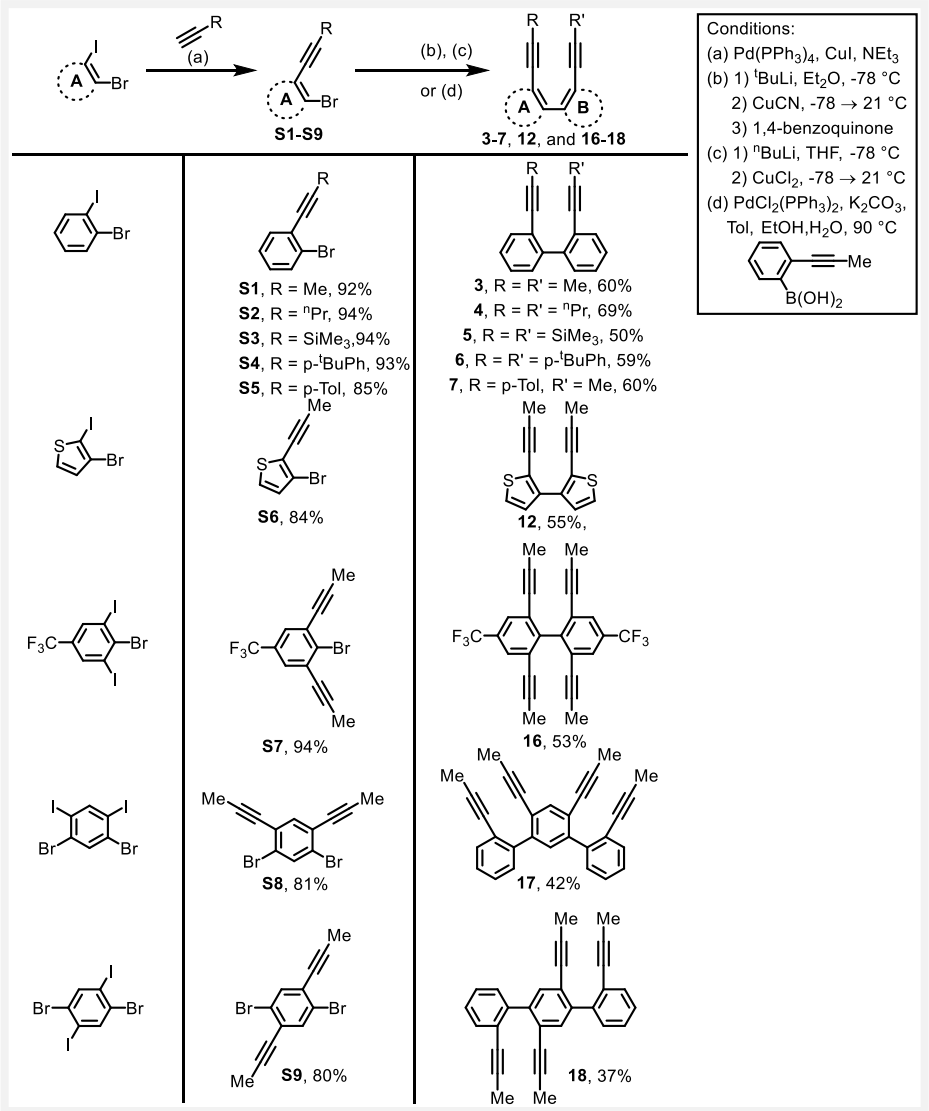

Table S1. Synthesis of diyne and bis(diyne) precursors

The more complex tris(diyne) **24** and pentakis(diyne) **25** were rapidly accessed (Scheme S1), although yields for the final step (26 and 24%, respectively) were low. This was partly due to a difficult separation, as ^{1}H NMR analysis of the crude reaction mixtures revealed formation of **24** and **25** in 46 and 53% yield, respectively. Critical to the synthesis of **25** was the iteration of the copper-mediated

homocoupling to furnish dibromide **S11** from intermediate dibromide **S10**. In principle, very large structures are accessible by this route since the number of alkynes is doubled in each step; however, a statistical mixture of mono- and dilithiated intermediates is expected upon another iteration of the current procedure (dilithiated intermediates give rise to side products that are difficult to separate, as is already apparent in the lower yield of **S11**).

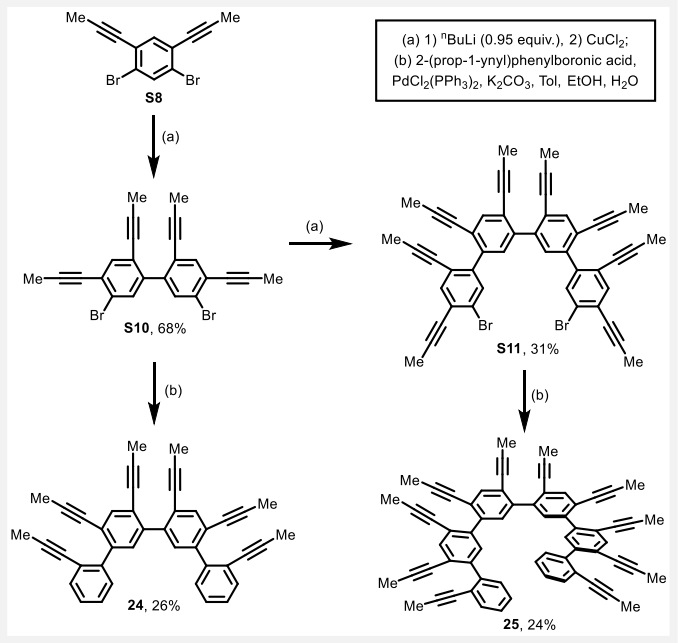

Scheme S1. Synthesis of tris(diyne) and pentakis(diyne) precursors

General Synthetic Procedures

General Procedure A: *Sonogashira Coupling with Propyne Gas*

1-Bromo-2-(prop-1-ynyl)benzene (S1). A 350 mL flask with Teflon stopper and side arm was connected to a 225 mL gas addition apparatus and charged with $Pd(PPh_3)_4$ (0.49 g, 0.42 mmol) and CuI (0.24 g, 1.27 mmol). The apparatus was degassed, then charged with a degassed solution of 2-bromoiodobenzene (11.97 g, 42.3 mmol), tetrahydrofuran (60 mL), and triethylamine (60 mL) *via* cannula transfer. The mixture was frozen with liquid N_2, the apparatus was evacuated, and propyne (1.86 g, 46.5 mmol) was sequentially added in five portions (225 mL each, at 1 atm) by condensation of the gas onto the frozen reaction mixture. The flask was sealed and the solution was warmed to 21 °C and stirred for 24 h. The mixture was then filtered through a short plug of silica gel and washed through with an additional 200 mL diethyl ether. The filtrate was washed with aqueous HCl (1 M, 3 x 200 mL) and saturated aqueous NaCl (100 mL), dried with $MgSO_4$, and filtered. Solvents were removed from the filtrate by rotary evaporation and the crude material was purified by Kugelrohr distillation under vacuum to afford **S1** (7.60 g, 92%) as a pale yellow liquid.

General Procedure B: *Isolation of zirconacyclopentadiene-annulated polycyclic aromatic hydrocarbon (ZrPAH)*

ZrPAH (1a). To a stirred solution of $Cp_2Zr(pyr)(Me_3SiC{\equiv}CSiMe_3)$ (1.49 g, 3.14 mmol) in benzene (6 mL) was added a solution of **3** (0.688 g, 2.99 mmol) in benzene (10 mL). The reaction mixture was stirred for 1 h, concentrated to ca. 6 mL *in vacuo*, and diluted with pentane (12 mL). The precipitate was collected on a fritted funnel, washed with pentane (2 x 5 mL), and dried under vacuum to yield **1a** (1.24 g, 92%) as a red/maroon powder.

General Procedure C: *Protodemetallation of an Isolated ZrPAH*

(9Z,10Z)-9,10-Diethylidene-9,10-dihydrophenanthrene (2a). To a stirred, heterogeneous mixture of ZrPAH **1a** (0.204 g, 0.452 mmol) in benzene (4 mL) was added benzoic acid (0.130 g, 1.06 mmol). The mixture quickly turned from red to bright yellow and homogeneous. After 5 min, the solution was exposed to air, diluted with hexanes (40 mL), filtered through a plug of silica gel, and the plug was eluted with excess hexanes. Removal of solvents under reduced pressure furnished **2a** (0.096 g, 91%) as a colorless, crystalline solid.

General Procedure D: *Negishi Protocol for Generation of ZrPAH and in situ Protodemetallation*

(9Z,10Z)-9,10-Diethylidene-9,10-dihydrophenanthrene (2a). A 150 mL Schlenk tube was charged with Cp_2ZrCl_2 (0.839 g, 2.87 mmol) and tetrahydrofuran (20 mL), and the solution was cooled to –78 °C. To this solution was added *n*-butyllithium (1.60 M in hexanes, 3.6 mL) dropwise over 5 min and the resulting mixture was stirred for 30 min at –78 °C. A solution of **3** (0.600 g, 2.61 mmol) in tetrahydrofuran (6 mL) was added dropwise via syringe, the cold bath was removed, then the reaction mixture was allowed to warm to 21 °C and stirred for an additional 3 h. Aqueous HCl (3.0 M, 3.5 mL) was then added via syringe. After 3 min, the reaction mixture was quenched with saturated aqueous $NaHCO_3$ (40 mL) and extracted with hexanes (40 mL). The extract was washed with saturated aqueous NaCl (20 mL), dried over Na_2SO_4, filtered, and concentrated by rotary evaporation. The resulting crude product was purified by filtration through a plug of silica gel with excess hexanes to afford **2a** (0.545 g, 90%) as a colorless, crystalline solid.

General Procedure E: *$CuCl_2$-Mediated Homocoupling*

2,2'-Di(prop-1-ynyl)biphenyl (3). A 350 mL Schlenk flask was charged with **S1** (5.28 g, 27.1 mmol) and tetrahydrofuran (90 mL), and the solution was cooled to –78 °C. To this solution was added *n*-butyllithium (1.48 M in hexanes, 20.1 mL, 29.8 mmol) dropwise over 5–10 min and the resulting mixture was stirred for 1 h at –78 °C. Copper(II) chloride (4.73 g, 35.2 mmol) was then added in one portion, the cold bath was removed, and the reaction mixture was allowed to warm to 21 °C and stirred for 11 h at this temperature. The reaction mixture was quenched with 10% aqueous NH_4OH (100 mL) and extracted with ethyl acetate (100 mL). The organic layer was washed with saturated aqueous NaCl (50 mL) and dried with Na_2SO_4. Filtration and removal of solvents from the filtrate by rotary evaporation gave a crude solid that was purified by recrystallization from boiling methanol to afford **3** (1.88 g, 60%) as colorless needles.

General Procedure F: *CuCN-Mediated Homocoupling*

2,2'-Di(pent-1-ynyl)biphenyl (4). This procedure was adapted from methodology published by Iyoda et. al.[11] A 1000 mL Schlenk flask was charged with **S2** (5.00 g, 22.4 mmol) and diethyl ether (300 mL), and the solution was cooled to –78 °C with a dry ice / acetone bath. To this solution was added *tert*-butyllithium (1.55 M in pentane, 17 mL) dropwise over 5 min and the resulting mixture was stirred for 2 h at –78 °C. Copper(I) cyanide (1.00 g, 11.2 mmol) was added and the heterogeneous solution was stirred at –78 °C for 30 min, then left to warm to 21 °C over ~1 h. Finally, 1,4-benzoquinone (3.9 g, 36 mmol) was added, then the reaction mixture was stirred for 3 h and quenched with aqueous HCl (2 M, 200 mL). The layers were separated and the organic layer was washed with saturated aqueous NaCl (100 mL) and dried with $MgSO_4$. Solvents were removed by rotary evaporation and the residue was eluted through a plug of silica gel with excess CH_2Cl_2. The crude product was purified by column chromatography (0–10% $CHCl_3$ in hexanes) to afford **4** (2.20 g, 69%) as a viscous, pale yellow oil.

General Procedure G: *Suzuki Cross-Coupling*

2-(Prop-1-ynyl)-2'-(4-tolylethynyl)biphenyl (7). A 150 mL flask with Teflon stopper was charged with **S5** (0.532 g, 1.96 mmol), 2-(prop-1-ynyl)phenylboronic acid (0.408 g, 2.55 mmol), $Pd(PPh_3)_2Cl_2$ (0.016 g, 0.023 mmol), K_2CO_3 (0.352 g, 2.55 mmol), toluene (8 mL), absolute ethanol (8 mL), and water (2 mL). The solution was degassed by the freeze-pump-thaw method, then the flask was backfilled with nitrogen and sealed. The stirred reaction mixture was heated for 3 h at 90 °C, then cooled to 21 °C, diluted with ethyl acetate (25 mL), and washed with aqueous HCl (3 M, 20 mL) and saturated aqueous NaCl (20 mL). The organic layer was dried with Na_2SO_4, filtered, and the filtrate was concentrated under reduced pressure. The yield of **7** was determined to be 78% by ^{1}H NMR spectroscopy using 1,5-cyclooctadiene as internal standard. The crude product was purified by column chromatography (0–10% CH_2Cl_2 in hexanes), followed by recrystallization from hexanes to afford **7** (0.361 g, 60%) as yellow crystals.

General Procedure H: *Hydrogenation of o-QDMs*

9,10-Diethylphenanthrene (19). A 100 mL flask with Teflon stopper was charged with *o*-QDM **2a** (57.5 mg, 0.248 mmol), 10% palladium on carbon (5.8 mg), tetrahydrofuran (1.5 mL), and ethanol (1.5 mL), and degassed by the freeze-pump-thaw method. Hydrogen gas (1 atm at 21 °C) was added, the flask was sealed, and the reaction mixture was stirred vigorously for 5 h. The reaction mixture was filtered and the flask and filter cake were rinsed with CH_2Cl_2 (2 x 2 mL). Solvents were removed from the filtrate to afford **19** (55.6 mg, 96%) as a colorless, crystalline solid.

Preparation and Characterization of New Compounds

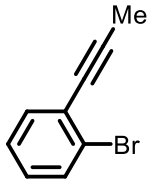

S1

1-Bromo-2-(prop-1-ynyl)benzene (S1). The preparation of this compound (including yield) is described as General Procedure A. ^{1}H NMR (benzene-d_6, 500 MHz): δ = 7.29 – 7.33 (m, 2 H), 6.72 (td, J = 7.6 Hz, 1.2 Hz, 1H), 6.56 (td, J = 7.8 Hz, 1.7 Hz, 1H), 1.65 (s, 3H). ^{1}H NMR data in chloroform-d match the reported values.[12]

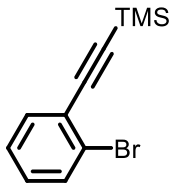

S3

1-Bromo-2-(2-trimethylsilylethynyl)benzene (S3). A 1000 mL Schlenk flask equipped with Teflon stopper was charged with $Pd(PPh_3)_4$ (0.92 g, 0.80 mmol) and CuI (0.93 g, 4.9 mmol), then the flask was put under an atmosphere of N_2 after three vacuum/N_2 cycles. An N_2-sparged solution of 1-bromo-2-iodobbenzene (39.4 g, 139 mmol), tetrahydrofuran (120 mL), and triethylamine (120 mL) was added via cannula, the mixture was stirred for 10 min, then deaerated trimethylsilylacetylene (15.3 g, 156 mmol) was added via syringe. The flask was sealed and the reaction mixture was stirred for 4 days at r.t. (~21 °C), after which time the solution was filtered and solvents were removed from the filtrate via rotary evaporation. The residue was purified by elution through a plug of silica gel with 100% hexanes to afford **S3** (33.0 g, 94%) as a pale yellow oil. ^{1}H NMR data match that reported in the literature.[3]

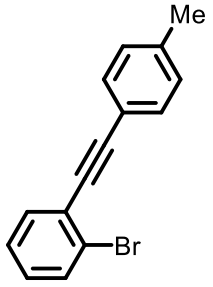

S5

1-Bromo-2-(4-tolylethynyl)benzene (S5). A 500 mL round-bottomed flask equipped with Teflon stopper was charged with 1-bromo-2-iodobenzene (40.0 g, 141 mmol), $Pd(PPh_3)_2Cl_2$ (0.20 g, 0.28 mmol), PPh_3 (0.15 g, 0.56 mmol), and CuI (0.11 g, 0.56 mmol), and the flask put under an N_2-atmosphere with three vacuum/N_2 cycles. To this flask was added triethylamine (240 mL) followed by 4-ethynyltoluene (17.2 g, 148 mmol) (both of which were sparged with N_2 prior to addition). The

flask was sealed and the stirred mixture was heated at 90 °C for 5 h. The mixture was cooled to r.t., filtered, the salt was washed with hexanes (2 x 100 mL), and the filtrate was concentrated dryness via rotary evaporation. The residue was purified by elution through a plug of silica gel with hexanes followed by recrystallization from hexanes to afford **S5** (32.6 g, 85%) as an off-white, crystalline solid. ^{1}H NMR data match that reported in the literature.[13]

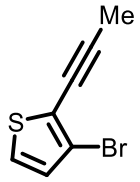

S6

3-Bromo-2-(prop-1-ynyl)thiophene (S6). General procedure A was employed with the following quantities: 3-bromo-2-iodothophene (4.66 g, 16.1 mmol), propyne (0.745 g, 18.6 mmol), $Pd(PPh_3)_4$ (0.37 g, 0.32 mmol), CuI (0.15 g, 0.81 mmol), triethylamine (20 mL), and tetrahydrofuran (20 mL). The reaction time was 12 h. The crude product was purified by column chromatography (100% hexanes) to afford **S6** (2.71 g, 84%) as a colorless liquid. ^{1}H NMR (chloroform-*d*, 400 MHz): δ = 7.11 (d, *J* = 5.4 Hz, 1H), 6.92 (d, *J* = 5.4 Hz, 1H), 2.12 (s, 3H); ^{13}C{^{1}H} NMR (chloroform-*d*, 101 MHz): δ = 129.9, 125.9, 121.7, 114.8, 94.6, 71.5, 5.1; HRMS-EI (m/z): $[M]^+$ calcd. for C_7H_5BrS, 199.9295; found, 199.9298.

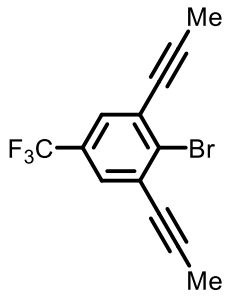

S7

4-Bromo-3,5-di(prop-1-ynyl)benzotrifluoride (S7). General procedure A was employed, except that the bromide was initially added to the flask with the other solids. Amounts used were as follows: 2-bromo-1,3-diiodo-5-(trifluoromethyl)benzene (9.63 g, 20.2 mmol), propyne (1.86 g, 46.5 mmol), $Pd(PPh_3)_4$ (0.47 g, 0.40 mmol), CuI (0.19 g, 1.01 mmol), triethylamine (45 mL), and tetrahydrofuran (75 mL). The reaction time was 2 days. The crude product was purified by filtration through a plug of silica gel with 100% hexanes to give **S7** (5.69 g, 94%) as a light yellow solid. mp 87.6–89.1 °C. ^{1}H NMR (chloroform-*d*, 400 MHz): δ = 7.54 (s, 2 H), 2.13 (s, 6 H); ^{13}C{^{1}H} NMR (chloroform-*d*, 101 MHz): δ = 131.9, 129.6 (q, *J* = 33.4 Hz), 128.4 (q, *J* = 3.7 Hz), 127.9, 123.4 (q, *J* = 272.5 Hz), 93.1, 77.9, 4.6; ^{19}F NMR (chloroform-*d*, 376 MHz): δ = –63.7; HRMS-EI (m/z): $[M]^+$ calcd. for $C_{13}H_8F_3Br$, 299.9761; found, 299.9759.

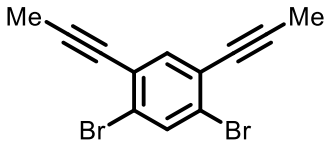

S8

1,5-Dibromo-2,4-di(prop-1-ynyl)benzene (S8). General procedure A was employed, except that the bromide was initially added to the flask with the other solids. Amounts used were as follows: 2,4-dibromo-1,5-diiodobenzene (10.3 g, 21.1 mmol), propyne (1.86 g, 46.5 mmol), $Pd(PPh_3)_4$ (0.45 g, 0.39 mmol), CuI (0.18 g, 0.96 mmol), triethylamine (45 mL), and tetrahydrofuran (75 mL). The reaction time was 32 h. The crude product was purified by recrystallization from CH_2Cl_2/methanol to yield **S8** (5.30 g, 81%) as pale yellow needles. mp 88.5–89.9 °C. ^{1}H NMR (chloroform-*d*, 500 MHz): δ = 7.76 (s, 2 H), 7.45 (s, 2 H), 2.09 (s, 6 H); ^{13}C{^{1}H} NMR (chloroform-*d*, 126 MHz): δ = 137.1, 135.4, 125.3, 124.5, 92.5, 77.3, 4.8; HRMS-EI (m/z): $[M]^+$ calcd. for $C_{12}H_8Br_2$, 309.8993; found, 309.8988.

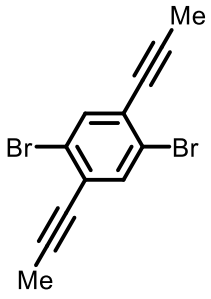

S9

1,4-Dibromo-2,5-di(prop-1-ynyl)benzene (S9). General procedure A was employed, except that the bromide was initially added to the flask with the other solids. Amounts used were as follows: 2,5-dibromo-1,4-diiodobenzene (10.3 g, 21.1 mmol), propyne (1.86 g, 46.5 mmol), $Pd(PPh_3)_4$ (0.45 g, 0.39 mmol), CuI (0.18 g, 0.96 mmol), triethylamine (45 mL), and tetrahydrofuran (75 mL). The reaction time was 36 h. The crude product was purified by column chromatography (100% hexanes) to afford **S9** (5.25 g, 80%) as a white solid. mp 144–147 °C. ^{1}H NMR (chloroform-*d*, 400 MHz): δ = 7.59 (s, 2H), 2.11 (s, 6H); ^{13}C{^{1}H} NMR (chloroform-*d*, 126 MHz): δ 136.2, 126.6, 123.5, 93.7, 77.5, 4.8; HRMS-EI (m/z): $[M]^+$ calcd. for $C_{12}H_8Br_2$, 309.8993; found, 309.8997.

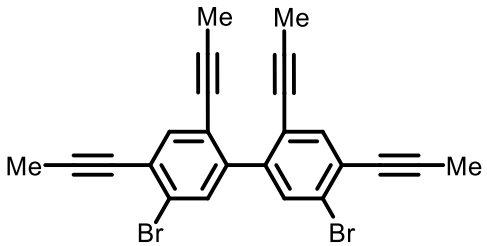

S10

2,2',4,4'-Tetra(prop-1-ynyl)-5,5'-dibromobiphenyl (S10). General procedure E was employed with the following quantities: **S8** (2.85 g, 9.13 mmol), tetrahydrofuran (45 mL), *n*-butyllithium (1.60 M in hexanes, 5.4 mL, 8.7 mmol), and $CuCl_2$ (1.60 g, 11.9 mmol). The crude solid was purified by recrystallization from dichloromethane (~35 mL) at –80 °C to afford **S10** (1.45 g, 72%) as a white

solid. mp 189.5–191.1 °C. ^{1}H NMR (chloroform-*d*, 400 MHz): δ = 7.63 (s, 2H), 7.52 (s, 2H), 2.13 (s, 6H), 1.88 (s, 6H); ^{13}C{^{1}H} NMR (chloroform-*d*, 101 MHz): δ = 141.0, 136.9, 133.8, 125.5, 123.5, 122.5, 91.9, 91.2, 77.9, 77.3, 4.8, 4.5; HRMS-EI (m/z): $[M]^+$ calcd. for $C_{24}H_{16}Br_2$, 461.9619; found, 461.9618.

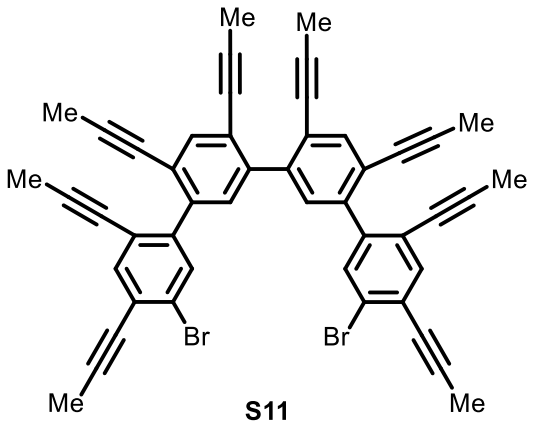

S11

5,5'''-dibromo-2,2''',4,4',4'',4''',6',6''-octa(prop-1-ynyl)-1,1':3',1'':3'',1'''-quaterphenyl (S11). General procedure E was employed with the following quantities (and with noted differences): **S10** (0.216 g, 0.465 mmol), tetrahydrofuran (4 mL), *n*-butyllithium (1.60 M in hexanes, 0.28 mL, 0.44 mmol), and $CuCl_2$ (0.081 g, 0.605 mmol). After addition of $CuCl_2$, the reaction mixture was kept at –78 °C for 1 h before the cold bath was removed. The crude product was purified by column chromatography (0–33% CH_2Cl_2 in hexanes) to afford **S11** (0.055 g, 32%) as a colorless solid. ^{1}H NMR (chloroform-*d*, 300 MHz): δ = 7.68 (s, 2H), 7.58 (s, 2H), 7.51 (s, 2H), 7.40 (s, 2H), 2.12 (s, 6H), 1.92 (s, 12H), 1.78 (s, 6H); ^{13}C{^{1}H} NMR (chloroform-*d*, 101 MHz): δ = 142.6, 140.9, 139.4, 136.8, 136.1, 133.9, 131.8, 125.0, 123.4, 123.2, 122.7, 122.43, 91.5, 90.7, 90.4, 89.9, 78.3, 78.02, 77.97, 77.6, 4.7, 4.6, 4.52, 4.47; HRMS-EI (m/z): $[M]^+$ calcd. for $C_{48}H_{32}Br_2$, 766.0871; found, 766.0858.

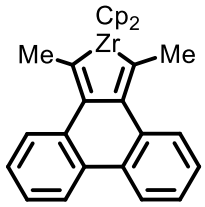

1a

ZrPAH (1a). The preparation of this compound (including yield) is described as General Procedure B. Single crystals were grown by layering hexanes onto a saturated benzene solution of **1a**, which was drawn directly from a smaller scale reaction, and the proposed structure was elucidated by X-ray crystallography (see Figure S88 and Table S3). ^{1}H NMR (benzene-d_6, 600 MHz): δ = 7.76 (d, *J* = 7.7 Hz, 2 H), 7.50 (d, *J* = 7.7 Hz, 2 H), 7.21 (t, *J* = 7.3 Hz, 2 H), 7.16 (t, *J* = 7.3 Hz, 2 H), 5.78 (s, 10 H), 2.28 (s, 6 H); ^{13}C{^{1}H} NMR (benzene-d_6, 101 MHz): δ = 191.4, 134.8, 133.9, 129.4, 127.0, 126.8, 124.9, 124.6, 109.9, 25.7; Anal. Calcd for $C_{28}H_{24}Zr$: C, 74.5; H, 5.4. Found: C, 73.9; H, 5.2.

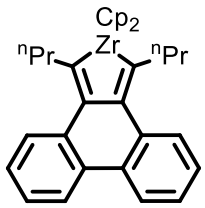

1b

ZrPAH (1b). The generation of this intermediate is described below in the synthesis of *o*-QDM **2b**.

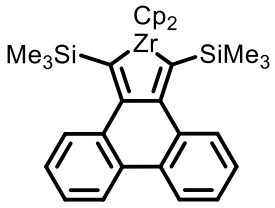

1c

ZrPAH (1c). To a solution of $Cp_2Zr(pyr)(Me_3SiC{\equiv}CSiMe_3)$ (0.626 g, 1.33 mmol) in pentane (10 mL) was added a solution of **5** (0.420 g, 1.21 mmol) in pentane (5 mL). After 12 h, the volume was reduced to 6-7 mL *in vacuo*. The precipitate was collected on a fritted funnel, washed with pentane (3 x 1.5 mL), and residual solvent was removed under vacuum to yield **1c** (0.56 g, 82%) as a bright red powder. ^{1}H NMR (benzene-d_6, 600 MHz): δ = 7.60 (d, J = 7.7 Hz, 2H), 7.51 (d, J = 7.7 Hz, 2H), 7.14 (t, J = 7.5 Hz, 2H), 7.07 (t, J = 7.5 Hz, 2H), 5.95 (s, 10H), 0.21 (s, 18H); ^{13}C{^{1}H} NMR (benzene-d_6, 151 MHz): δ = 208.9, 137.5, 136.2, 133.7, 129.7, 128.8, 126.9, 123.7, 110.2, 3.8; Anal. Calcd for $C_{32}H_{36}Si_2Zr$: C, 67.7; H, 6.4. Found: C, 67.5; H, 6.3.

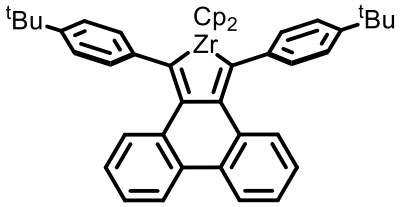

1d

ZrPAH (1d). General Procedure B was employed, except benzene was removed *in vacuo* before the addition of pentane. The following quantities were used: **6** (0.839 g, 1.80 mmol), $Cp_2Zr(pyr)(Me_3SiC{\equiv}CSiMe_3)$ (0.933 g, 1.98 mmol), and benzene (12 mL). ZrPAH **1d** (1.18 g, 95%) was isolated as a dark purple powder that was used (without further purification) for synthesis of compound **10**. ^{1}H NMR (benzene-d_6, 400 MHz): δ = 7.79 – 7.81 (m, 2 H), 7.65 – 7.67 (m, 2 H), 7.23 – 7.26 (m, 4 H), 6.96 – 7.00 (m, 2 H), 6.75 – 6.79 (m, 6 H), 5.99 (s, 10 H), 1.30 (s, 18 H); ^{13}C{^{1}H} NMR (benzene-d_6, 101 MHz): δ = 197.2, 146.3, 146.0, 139.2, 133.8, 133.7, 132.2, 127.0, 126.6, 126.4, 126.1, 124.3, 112.1, 34.4, 31.7.

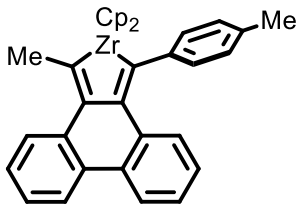

1e

ZrPAH (1e). The generation of this intermediate is described below in the synthesis of cyclobutarene **11**.

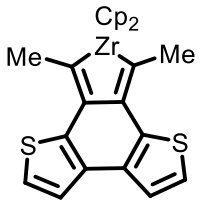

1f

ZrPAH (1f). The generation of this intermediate is described below in the syntheses of compound **13** and Diels-Alder adduct **14**.

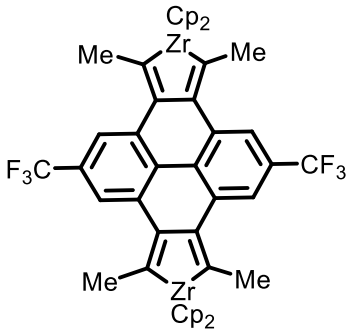

1g

ZrPAH (1g). General Procedure B was employed with the following quantities: bis(diyne) **16** (0.612 g, 1.38 mmol), $Cp_2Zr(pyr)(Me_3SiC{\equiv}CSiMe_3)$ (1.37 g, 2.90 mmol), and benzene (16 mL). The bright red precipitate was collected on a fritted funnel (without concentration and dilution with pentane as in General Procedure B), washed with pentane (2 x 5 mL), and dried under dynamic vacuum to afford ZrPAH **1g** (1.20 g, 98%) as a bright red solid that was used (without purification) for synthesis of bis(*o*-QDM) **2g**. ^{1}H NMR (benzene-d_6, 400 MHz): δ = 7.86 (s, 4H), 5.76 (s, 20H), 1.92 (s, 12H); Solubility was too low to acquire a ^{13}C NMR spectrum with suitable solvents.

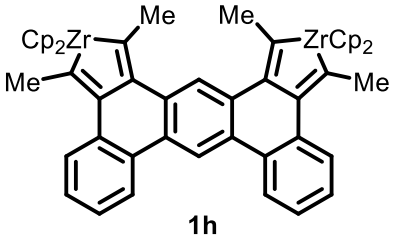

1h

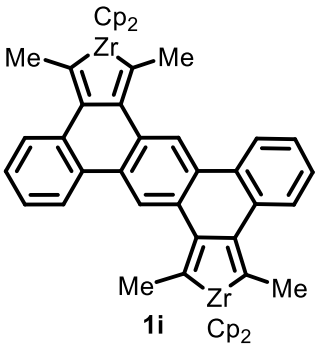

1i

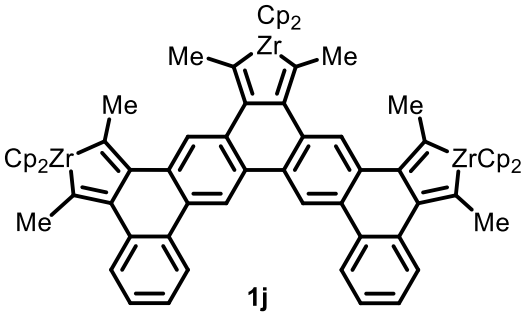

1j

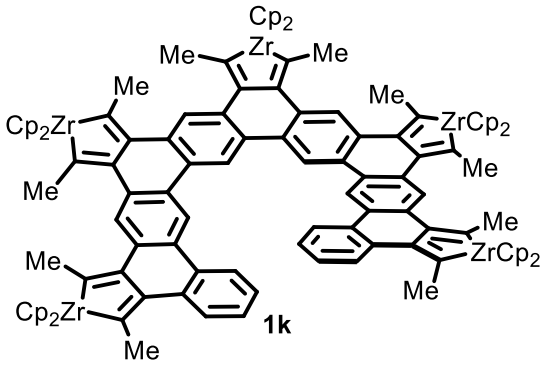

1k

ZrPAHs (1h–k). The generation of these intermediates is described below in the syntheses of *o*-QDMs **2h–k**.

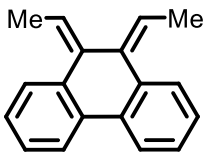

2a

(9Z,10Z)-9,10-Diethylidene-9,10-dihydrophenanthrene (2a). This compound was prepared in two different ways, which are described (including yield) as General Procedures C and D. Single crystals were grown by slow evaporation of a hexanes solution of **2a**, and the structure was confirmed by X-ray crystallography (see Figure S89 and Table S4). mp 117–121 °C, dec.* ^{1}H NMR (benzene-d_6, 600 MHz): δ = 7.69 (dd, *J* = 7.6 Hz, 1.5 Hz, 2 H), 7.46 (dd, *J* = 7.5 Hz, 1.6 Hz, 2 H), 7.10 – 7.16 (m, 4 H), 5.70 (q, J = 7.3 Hz, 2 H), 1.79 (d, J = 7.3, 6 H); ^{13}C{^{1}H} NMR (benzene-d_6, 126 MHz): δ = 140.2, 134.9, 134.5, 127.8, 127.7, 127.0, 124.4, 122.8, 15.2; HRMS-EI (m/z): $[M]^+$ calcd. for $C_{18}H_{16}$, 232.1252; found, 232.1253. *^{1}H NMR analysis after the melting point was obtained indicated ~5% formation of cyclobutarene **8**. This decomposition was a general observation for the isolated *o*-QDMs and was especially pronounced for those of higher molecular weight.

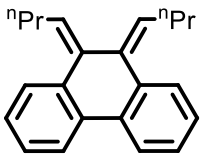

2b

(9Z,10Z)-9,10-Dibutylidene-9,10-dihydrophenanthrene (2b). General procedure D was employed with the following quantities: Cp_2ZrCl_2 (0.602 g, 2.06 mmol), *n*-butyllithium (1.60 M in hexanes, 2.6 mL), **4** (0.535 g, 1.87 mmol), aqueous HCl (3.0 M, 2.5 mL), and tetrahydrofuran (20 mL). Diyne **4** was added neat via syringe. *o*-QDM **2b** was isolated as a viscous, colorless oil (0.510 g, 95%). ^{1}H NMR (chloroform-*d*, 400 MHz): δ = 7.84 (dd, *J* = 7.7, 1.4 Hz, 2H), 7.46 (dd, *J* = 7.6, 1.5 Hz, 2H), 7.34 (td, *J* = 7.5, 1.5 Hz, 2H), 7.29 (td, *J* = 7.5, 1.5 Hz, 2H), 5.64 (t, *J* = 7.3 Hz, 2H), 2.37 (q, *J* = 7.4 Hz, 4H), 1.56 – 1.47 (m, 4H), 0.95 (t, *J* = 7.4 Hz, 6H); ^{13}C{^{1}H} NMR (dichloromethane-d_2, 151 MHz): δ = 139.0, 135.3, 134.3, 129.9, 128.0, 127.9, 127.4, 124.5, 31.9, 24.1, 14.3; HRMS-EI (m/z): $[M]^+$ calcd. for $C_{22}H_{24}$, 288.1878; found, 288.1880.

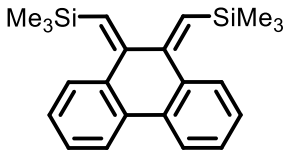

2c

(9E,10E)-9,10-bis((trimethylsilyl)methylene)-9,10-dihydrophenanthrene (2c). A solution of **1c** (0.100 g, 0.176 mmol) in toluene (4 mL) was cooled to –78 °C with a dry ice / acetone bath. To the stirred solution was added HCl (2.9 M in dioxane, 0.13 mL, 0.38 mmol), immediately producing a nearly colorless solution. The solution was warmed to ~21 °C with a water bath, then quenched with saturated aqueous $NaHCO_3$ (4 mL). In air, the mixture was extracted with hexanes (20 mL), then the extract was washed with saturated aqueous NaCl (10 mL), dried with $MgSO_4$, filtered, and the filtrate was concentrated *via* rotary evaporation. The residue was purified by elution through a plug of silica gel with 100% hexanes, followed by recrystallization from EtOH (~1 mL) at –25 °C to afford *o*-QDM **2c** as colorless needles (0.032 g, 52%). mp 93.8–96.4 °C, dec.* ^{1}H NMR (benzene-d_6, 400 MHz): δ = 7.71 (dd, *J* = 7.6, 1.4 Hz, 2H), 7.60 (dd, *J* = 7.9, 1.2 Hz, 2H), 7.13 (td, *J* = 7.6, 1.3 Hz, 2H), 7.03 (td, *J* = 7.5, 1.3 Hz, 2H), 6.23 (s, 2H), 0.13 (s, 18H); ^{13}C{^{1}H} NMR (benzene-d_6, 151 MHz): δ = 159.3, 136.4, 134.0, 129.4, 129.2, 127.8, 127.1, 124.1, 0.7; HRMS-EI (m/z): $[M]^+$ calcd. for $C_{22}H_{28}Si_2$, 348.1730; found, 348.1736. *A post-melt ^{1}H NMR melt showed a small amt (2-3%) of a species is hypothesized to be cyclobutarene (identified by a singlet at 3.06 ppm in benzene-d_6). The amount of this species will depend on specific melting conditions. Here, heating was started at 90 °C and ended at 98 °C (1.5 °C/min ramp rate).

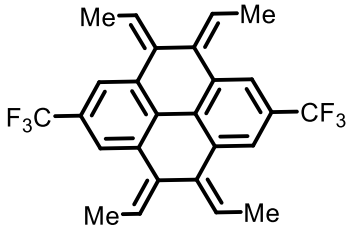

2g

(4Z,5Z,9Z,10Z)-4,5,9,10-Tetraethylidene-2,7-bis(trifluoromethyl)-4,5,9,10-tetrahydropyrene (2g). This compound was prepared using two different procedures. *General Procedure C*: the following quantities were used: ZrPAH **1g** (0.177 g, 0.200 mmol), benzoic acid (0.110 g, 0.901 mmol), and benzene (3 mL). Compound **2g** (0.084 g, 94%) was isolated as a colorless, crystalline solid. *General Procedure D*: the following quantities were used: Cp_2ZrCl_2 (2.28 g, 7.80 mmol), *n*-butyllithium (1.60 M

in hexanes, 9.7 mL), bis(diyne) **16** (1.57 g, 3.55 mmol), aqueous HCl (3.0 M, 9.3 mL), and tetrahydrofuran (total = 60 mL; 35 mL for initial generation of "Cp_2Zr" and 25 mL for addition of bis(diyne) **16**). Compound **2g** (1.40 g, 89%) was isolated as a colorless, crystalline solid. mp 136–151 °C, dec.* Single crystals were grown by slow evaporation of a hexanes solution of **2g**, and the structure was confirmed by X-ray crystallography (see Figure S90 and Table S5). ^{1}H NMR (benzene-d_6, 500 MHz): δ = 7.69 (s, 4 H), 5.63 (q, J = 7.4 Hz, 4 H), 1.66 (d, J = 7.3 Hz, 12 H); ^{13}C{^{1}H} NMR (chloroform-*d*, 151 MHz): δ = 137.5, 134.5, 131.5, 128.8 (q, *J* = 32 Hz), 126.2, 124.4 (q, *J* = 273 Hz), 122.4 (q, *J* = 4 Hz), 15.2; HRMS-EI (m/z): $[M]^+$ calcd. for $C_{26}H_{20}F_6$, 446.1469; found, 446.1476. *See comment for o-QDM **2a**.

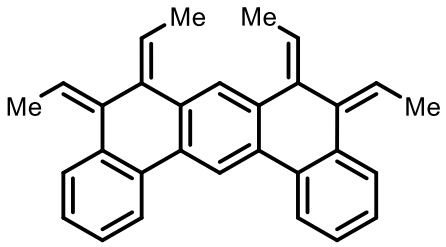

2h

(5Z,6Z,8Z,9Z)-5,6,8,9-Tetraethylidene-5,6,8,9-tetrahydrobenzo[m]tetraphene (2h). A 20 mL vial was charged with bis(diyne) **17** (0.102 g, 0.267 mmol) and $Cp_2Zr(pyr)(Me_3SiC{\equiv}CSiMe_3)$ (0.276 g, 0.587 mmol), followed by toluene (4 mL), and the resulting brown, homogeneous reaction mixture was stirred for 3 h. Volatile materials were then removed *in vacuo* and pentane (4 mL) was added to the vial to give a heterogeneous mixture which was stirred vigorously for 1 h. Crude ZrPAH **1h**, a light brown solid, was collected on a fritted funnel and re-dissolved in toluene (8 mL). Benzoic acid (0.164 g, 1.34 mmol) was added to the solution, which was then stirred for 15 min. Finally, in air, triethylamine (40 mg) was added to consume the excess benzoic acid and the solution was concentrated to 4 mL, diluted with hexanes (16 mL), and filtered through a plug of silica gel. The plug was eluted with excess 4:1 hexanes:toluene and solvents were removed from the filtrate to give bis(*o*-QDM) **2h** as a foamy, off-white solid. The solid was ground to a powder and residual solvents were removed under high vacuum. Yield: 0.091 g (88%) Characterization of intermediate ZrPAH **1h**: ^{1}H NMR (benzene-d_6, 400 MHz): δ = 8.30 (s, 1H), 7.83 (dd, *J* = 7.4, 1.6 Hz, 2H), 7.73 (s, 1H), 7.52 (dd, *J* = 7.7, 1.5 Hz, 2H), 7.25 (td, *J* = 7.4, 1.6 Hz, 2H), 7.20 (td, *J* = 7.4, 1.6 Hz, 2H), 5.89 (s, 20H), 2.64 (s, 6H), 2.38 (s, 6H). Characterization of bis(*o*-QDM) **2h**: Single crystals were grown by slow evaporation of a toluene solution of **2h**, and the structure was elucidated by X-ray crystallography (see Figure S91 and Table S6). ^{1}H NMR (benzene-d_6, 400 MHz): δ = 8.29 (s, 1H), 7.82 (dd, *J* = 7.6, 1.6 Hz, 2H), 7.72 (s, 1H), 7.50 (dd, *J* = 7.4, 1.6 Hz, 2H), 7.22 (td, *J* = 7.5, 1.6 Hz, 2H), 7.17 (td, *J* = 7.4, 1.6 Hz, 2H), 5.78 (q, *J* = 7.2 Hz, 2H), 5.77 (q, *J* = 7.2 Hz, 2H), 1.87 (d, *J* = 7.3 Hz, 6H), 1.85 (d, *J* = 7.4 Hz, 6H); ^{13}C{^{1}H} NMR (chloroform-*d*, 151 MHz): δ = 139.8, 139.6, 134.7, 134.2, 133.3, 133.1, 127.6, 127.6, 126.9, 126.6, 124.2, 123.0, 122.9, 120.0, 15.5, 15.3; HRMS-EI (m/z): $[M]^+$ calcd. for $C_{30}H_{26}$, 386.2035; found, 386.2033.

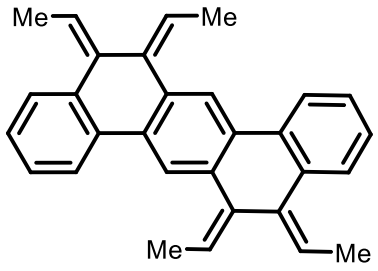

2i

(5Z,6Z,12Z,13Z)-5,6,12,13-Tetraethylidene-5,6,12,13-tetrahydrobenzo[k]tetraphene (2i). A 20 mL vial was charged with bis(diyne) **18** (0.100 g, 0.261 mmol) and $Cp_2Zr(pyr)(Me_3SiC{\equiv}CSiMe_3)$ (0.270 g, 0.574 mmol), followed by toluene (5 mL), and the resulting heterogeneous reaction mixture was stirred vigorously for 12 h. Crude ZrPAH **1i**, a red solid, was collected on a fritted funnel, washed with pentane (2 x 2 mL), and re-suspended in toluene (5 mL). Benzoic acid (0.192 g, 1.57 mmol) was added to the solution, which became yellow and homogeneous over 20–30 sec. After 20 min, in air, triethylamine (0.10 g) was added to consume the excess benzoic acid, then the solution was diluted with hexanes (10 mL) and filtered through a plug of silica gel. The plug was eluted with excess 2:1 hexanes:toluene and solvents were removed from the filtrate to give bis(*o*-QDM) **2i** (0.085 g, 84%) as a colorless, crystalline solid. Single crystals were grown by slow evaporation of a toluene solution of **2i**, and the structure was elucidated by X-ray crystallography (see Figure S92 and Table S7). ^{1}H NMR (chloroform-*d*, 400 MHz): δ = 7.96 (s, 2H), 7.85 (dd, *J* = 7.7, 1.5 Hz, 2H), 7.51 (dd, *J* = 7.5, 1.6 Hz, 2H), 7.36 (td, *J* = 7.5, 1.6 Hz, 2H), 7.31 (td, *J* = 7.4, 1.5 Hz, 2H), 5.82 (q, *J* = 7.3 Hz, 2H), 5.79 (q, *J* = 7.3 Hz, 2H), 2.09 (d, *J* = 7.3 Hz, 6H), 1.99 (d, *J* = 7.3 Hz, 6H); ^{13}C{^{1}H} NMR (chloroform-*d*, 101 MHz): δ = 139.7, 139.6, 134.7, 134.0, 133.6, 132.6, 127.6, 127.6, 126.9, 124.1, 123.2, 123.1, 122.9, 15.5, 15.4; HRMS-EI (m/z): $[M]^+$ calcd. for $C_{30}H_{26}$, 386.2035; found, 386.2032.

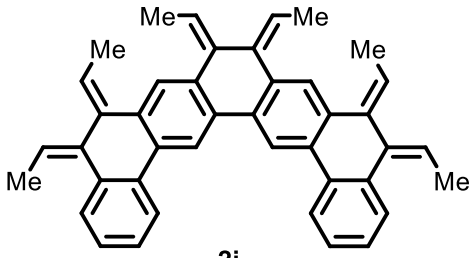

2j

(5Z,6Z,8Z,9Z,11Z,12Z)-5,6,8,9,11,12-Hexaethylidene-5,6,8,9,11,12-hexahydrodibenzo[a,o]pentaphene (2j). To a vial containing $Cp_2Zr(pyr)(Me_3SiC{\equiv}CSiMe_3)$ (230 mg, 0.488 mmol) was added a solution of tris(diyne) **24** (79.0 mg, 0.148 mmol) in benzene (8 mL). A maroon, crystalline solid (ZrPAH **1j**) gradually precipitated from the (initially homogeneous) reaction mixture over ~5 min. After 1 h, the precipitate was collected on a fritted funnel, washed with pentane (2 x 2 mL), and re-suspended in benzene (8 mL). Benzoic acid (162 mg, 1.33 mmol) was added to the solution, which quickly (~5 sec) became yellow and homogeneous. After 1 h, in air, triethylamine (0.10 g) was added to consume the excess benzoic acid, then the solution was diluted with hexanes (10 mL) and filtered through a plug of silica gel. The plug was eluted with excess 1:1 hexanes:toluene and solvents were removed from the filtrate to give tris(*o*-QDM) **2j** (71 mg, 89%) as a pale yellow (nearly colorless) solid. The above procedure was performed on a smaller scale (10%) in benzene-d_6 (without

isolation of the intermediate ZrPAH) and ^{1}H NMR spectroscopy indicated that **2j** formed in >95% yield (as determined by integration against hexamethylbenzene as internal standard). ^{1}H NMR (benzene-d_6, 400 MHz): δ = 8.50 (s, 2H), 7.92 (dd, *J* = 6.8, 2.1 Hz, 2H), 7.79 (s, 2H), 7.52 (dd, *J* = 6.7, 2.1 Hz, 2H), 7.23 – 7.15 (m, 4H), 5.87 (q, *J* = 7.3 Hz, 2H), 5.82 (q, *J* = 7.3 Hz, 2H), 5.81 (q, *J* = 7.3 Hz, 2H), 1.95 (d, *J* = 7.3 Hz, 3H), 1.91 (d, *J* = 7.3 Hz, 3H), 1.87 (d, *J* = 7.3 Hz, 3H); 139.87, 139.86, 139.67, 134.73, 134.17, 133.50, 133.41, 133.28, 133.19, 127.61, 127.60, 127.00, 126.60, 124.25, 123.07, 122.90, 122.89, 119.92, 15.55, 15.52, 15.36; HRMS-EI (m/z): $[M]^+$ calcd. for $C_{42}H_{36}$, 540.2817; found, 540.2808.

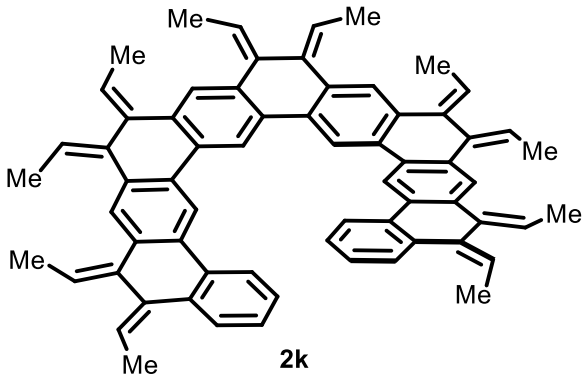

2k

Pentakis(*o*-QDM) (2k). A J-Young tube fitted with Teflon stopper was loaded with pentakis(diyne) **2k** (18.0 mg, 0.0215 mmol), hexamethylbenzene (~1.5 mg), and benzene-d_6 (1.2 mL), and a baseline ^{1}H NMR spectrum was acquired. The solution was poured into a vial containing a stirred solution of $Cp_2Zr(pyr)(Me_3SiC{\equiv}CSiMe_3)$ (56 mg, 0.118 mmol) in benzene-d_6 (0.8 mL), forming an initially homogeneous solution. A precipitate (ZrPAH **1k**) formed over the course of 2-3 min. After 30 min, benzoic acid (53 mg, 0.43 mmol) was added to the stirred mixture, which quickly became light yellow and homogeneous. After 25 min, in air, the solution was added to a vial containing triethylamine (35 mg) to consume excess benzoic acid, and the resulting mixture was diluted with hexanes (10 mL) and filtered through a plug of silica gel (5 g). The plug was eluted with a 1:1 hexanes/benzene mixture (40 mL) and solvents were removed by rotary evaporation to afford a pale yellow (nearly colorless) residue which was re-dissolved in benzene-d_6 and analyzed by ^{1}H NMR spectroscopy. Compound **2k** was observed in 85% yield (as determined by integration against hexamethylbenzene as internal standard), with no observable side products. The procedure was repeated without hexamethylbenzene and the desired compound was isolated as a pale yellow solid (15.2 mg, 83%). Note: this solid was obtained after dissolution of the initial residue in hexanes, then removal of the hexanes under vacuum (which is necessary to fully remove the benzene). ^{1}H NMR (benzene-d_6, 400 MHz): δ = 8.56 (s, 2H), 8.51 (s, 2H), 8.05 (d, *J* = 7.8 Hz, 2H), 7.87 (s, 2H), 7.83 (s, 2H), 7.59 (dd, *J* = 7.7, 1.3 Hz, 2H), 7.41 (t, *J* = 7.7 Hz, 2H), 7.27 (td, *J* = 7.5, 1.2 Hz, 2H), 5.92 (q, *J* = 7.3 Hz, 2H), 5.91 (q, *J* = 7.3 Hz, 2H), 5.91 (q, *J* = 7.3 Hz, 2H), 5.86 (q, *J* = 7.3 Hz, 2H), 5.85 (q, *J* = 7.3 Hz, 2H), 2.00 (d, *J* = 7.3 Hz, 6H), 2.00 (d, *J* = 7.3 Hz, 6H), 1.99 (d, *J* = 7.4 Hz, 6H), 1.96 (d, *J* = 7.3 Hz, 6H), 1.91 (d, *J* = 7.3 Hz, 6H); ^{13}C{^{1}H} NMR (chloroform-*d*, 151 MHz): δ = 139.93, 139.91, 139.85, 139.80, 139.67, 134.76, 134.26, 133.65, 133.58, 133.48, 133.42, 133.36, 133.36, 133.36, 133.31, 128.13, 127.69, 126.96, 126.70, 126.61, 123.81, 123.13, 123.10, 123.02, 123.02, 122.91, 120.04, 119.84, 15.60, 15.57, 15.53, 15.53, 15.40; HRMS-ESI (m/z): $[M]^+$ calcd. for $C_{66}H_{56}$, 848.4377; found, 848.4371.

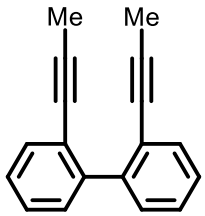

3

2,2'-Di(prop-1-ynyl)biphenyl (3). The preparation of this compound (including yield) is described as General Procedure E. mp 126–127 °C (lit.[14] mp 124–125 °C); ^{1}H NMR (benzene-d_6, 500 MHz,): δ = 7.64 (dd, *J* = 7.7 Hz, 1.4 Hz, 2 H), 7.47 (dd, *J* = 7.6 Hz, 1.3 Hz, 2 H), 7.09 (td, *J* = 7.6 Hz, 1.6 Hz, 2 H), 7.03 (td, *J* = 7.5 Hz, 1.4 Hz, 2 H), 1.46 (s, 6 H); ^{13}C{^{1}H} NMR (chloroform-*d*, 126 MHz): δ = 142.9, 132.3, 130.2, 127.0, 126.7, 123.2, 88.7, 78.9, 4.3; HRMS-EI (m/z): $[M]^+$ calcd. for $C_{18}H_{14}$, 230.1096; found, 230.1092.

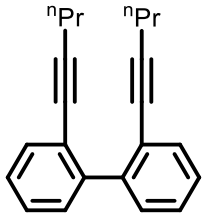

4

2,2'-Di(pent-1-ynyl)biphenyl (4). The preparation of this compound (including yield) is described as General Procedure F. ^{1}H NMR (benzene-d_6, 400 MHz): δ 7.63 (dd, *J* = 7.4, 1.6 Hz, 2H), 7.42 (dd, *J* = 7.4, 1.6 Hz, 2H), 7.08 (td, *J* = 7.5, 1.7 Hz, 2H), 7.03 (td, *J* = 7/.5, 1.6 Hz, 2H), 1.99 (t, *J* = 6.9 Hz, 4H), 1.25 (h, *J* = 7.2 Hz, 4H), 0.73 (t, *J* = 7.3 Hz, 6H); ^{13}C{^{1}H} NMR (chloroform-*d*, 101 MHz): δ = 143.3, 132.1, 130.2, 127.1, 126.8, 123.5, 93.3, 80.2, 22.1, 21.6, 13.4; HRMS-EI (m/z): $[M]^+$ calcd. for $C_{22}H_{22}$, 286.1722; found, 286.1725.

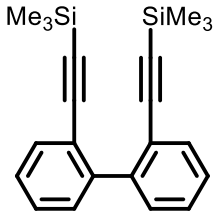

5

2,2'-Bis((trimethylsilyl)ethynyl)biphenyl (5). General procedure E was employed with the following quantities: **S3** (1.20 g, 4.74 mmol), tetrahydrofuran (24 mL), *n*-butyllithium (1.6 M in hexanes, 3.3 mL, 5.2 mmol), and copper(II) chloride (0.88 g, 6.5 mmol). Purification was carried out by column chromatography (100% hexanes) to afford **5** (0.414 g, 50%) as a viscous, pale yellow oil. ^{1}H NMR (chloroform-*d*, 400 MHz): δ = 7.54 (dd, *J* = 7.5, 1.2 Hz, 2H), 7.44 – 7.41 (m, 2H), 7.33 (td, *J* = 7.5, 1.6 Hz, 2H), 7.29 (td, *J* = 7.5, 1.5 Hz, 2H), 0.06 (s, 18H); ^{1}H NMR (chloroform-*d*, 400 MHz): δ = 7.54 (dd, *J* = 7.5, 1.2 Hz, 2H), 7.44 – 7.41 (m, 2H), 7.33 (td, *J* = 7.5, 1.6 Hz, 2H), 7.29 (td, *J* = 7.5, 1.5 Hz, 2H), 0.06 (s, 18H); ^{13}C{^{1}H} NMR (chloroform-*d*, 101 MHz): δ 143.6, 132.2, 130.2, 127.9, 127.2, 122.7, 104.7, 97.4, –0.2; HRMS-EI (m/z): $[M]^+$ calcd. for $C_{22}H_{26}Si_2$, 346.1573; found, 346.1579.

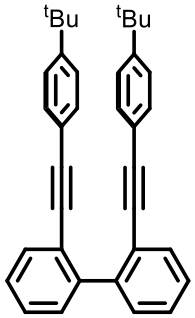

6

2,2'-Di(4-*tert*-butylphenylethynyl)biphenyl (6). General procedure F was employed with the following quantities: **S4** (6.68 g, 21.3 mmol), diethyl ether (200 mL), *tert*-butyllithium (1.7 M in pentane, 25 mL), CuCN (0.944 g, 10.5 mmol), 1,4-benzoquinone (3.70 g, 34.2 mmol). For work-up, the reaction was instead quenched with aqueous HCl (1 M, 250 mL) and allowed to stir for 10 min. The mixture was then extracted with ethyl acetate (3 x 100 mL) and the combined organics were washed with saturated aqueous NaCl (100 mL), dried with Na_2SO_4, then filtered. After removal of solvent by rotary evaporation, the crude mixture was run through a plug of silica gel with CH_2Cl_2 as eluant, then purified by column chromatography (100% hexanes) to afford **6** (2.89 g, 59%) as a colorless solid. mp 114–115 °C. ^{1}H NMR (benzene-d_6, 600 MHz): δ = 7.74 – 7.75 (m, 2 H), 7.53 – 7.54 (m, 2 H), 7.34 – 7.36 (m, 4 H), 7.10 – 7.13 (m, 2 H), 7.06 – 7.08 (m, 2 H), 7.00 – 7.03 (m, 4 H), 1.07 (s, 18 H); ^{13}C{^{1}H} NMR (chloroform-*d*, 151 MHz): δ = 151.3, 143.3, 132. 0, 131.2, 130.4, 127.5, 127.5, 125.3, 123.2, 120.6, 92.7, 88.6, 34.8, 31.3; HRMS-EI (m/z): $[M]^+$ calcd. for $C_{36}H_{34}$, 466.2661; found, 466.2671.

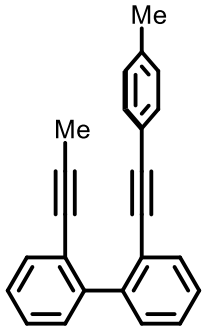

7

2-(Prop-1-ynyl)-2'-(4-tolylethynyl)biphenyl (7). The preparation of this compound (including yield) is described as General Procedure G. mp 68.5–71.0 °C; ^{1}H NMR (chloroform-*d*, 400 MHz): δ = 7.64 – 7.60 (m, 1H), 7.55 – 7.51 (m, 1H), 7.50 – 7.45 (m, 2H), 7.39 – 7.27 (m, 4H), 7.12 (d, J = 8.0 Hz, 2H), 7.05 (d, J = 8.0 Hz, 2H), 2.32 (s, 3H), 1.86 (s, 3H); ^{13}C{^{1}H} NMR (chloroform-*d*, 101 MHz): δ = 143.4, 142.9, 138.1, 132.5, 132.0, 131.3, 130.5, 130.3, 129.0, 127.5, 127.33, 127.27, 126.9, 123.6, 122.9, 120.6, 92.6, 89.0, 88.7, 79.1, 21.6, 4.5; HRMS-EI (m/z): $[M]^+$ calcd. for $C_{24}H_{18}$, 306.1409; found, 306.1408.

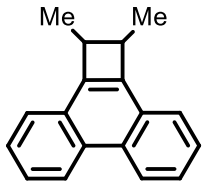

8

1,2-Dimethylcyclobuta[l]phenanthrene (8). An NMR tube fitted with Teflon stopper was charged with *o*-QDM **2a** (37.6 mg, 0.162 mmol), 1,3,5-trimethoxybenzene (17.5 mg), and toluene-d_8 (1.7 mL). The tube was degassed by three freeze-pump-thaw cycles and backfilled with N_2, then placed on a 100 °C oil bath for 24 h. ^{1}H NMR analysis with 1,3,5-trimethoxybenzene as internal standard indicated that **8** formed in 95% yield. Solvent was removed and the crude solid was recrystallized from EtOH at –25 °C to afford pure cyclobutarene **8** (30 mg, 80%) as colorless needles. mp 106–107 °C; ^{1}H NMR (benzene-d_6, 400 MHz): δ = 8.61 – 8.57 (m, 2H), 7.73 – 7.68 (m, 2H), 7.46 – 7.39 (m, 4H), 3.14 (q, *J* = 6.8 Hz, 2H), 1.43 (d, *J* = 6.8 Hz, 6H); ^{13}C{^{1}H} NMR (benzene-d_6, 101 MHz): δ = 142.2, 131.4, 129.4, 126.8, 125.7, 124.4, 123.1, 46.2, 18.0; HRMS-EI (m/z): $[M]^+$ calcd. for $C_{18}H_{16}$, 232.1252; found, 232.1255.

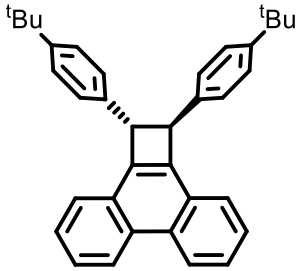

10

***trans*-1,2-Bis(4-tert-butylphenyl)cyclobuta[l]phenanthrene (10).** To a stirred solution of ZrPAH **1d** (0.380 g, 0.552 mmol) in benzene (15 mL) was added HCl (3.6 M in dioxane, 0.48 mL) via syringe. After 5 min, the reaction mixture was quenched with saturated aqueous $NaHCO_3$ (25 mL) and stirred for an additional 10 min. The solution was then extracted with ethyl acetate (50 mL) and the organic layer was washed with saturated aqueous NaCl (20 mL), dried with Na_2SO_4, then filtered. Solvents were removed from the filtrate under reduced pressure and the crude product was purified by filtration though a plug of silica gel with 4:1 hexanes:CH_2Cl_2 followed by recrystallization from boiling hexanes to afford **10** (0.215 g, 83%) as colorless crystals, some of which were X-ray quality. mp 202–203 °C, dec. The structure of **10** was elucidated by X-ray crystallography (see Figure S93 and Table S8). Monitoring of this reaction by ^{1}H NMR spectroscopy indicated formation of **10** in 95% yield. ^{1}H NMR (benzene-d_6, 400 MHz,): δ = 8.65 (d, *J* = 8.5 Hz, 2 H), 7.60 (dd, *J* = 7.9 Hz, 1.0 Hz, 2 H), 7.40 – 7.44 (m, 2 H), 7.24 – 7.28 (m, 6 H), 7.19 – 7.22 (m, 4 H), 4.66 (s, 2 H), 1.23 (s, 18 H); ^{13}C{^{1}H} NMR (chloroform-*d*, 101 MHz): δ = 149.6, 140.2, 138.6, 131.4, 128.7, 126.9, 126.9, 126.1, 125.6, 124.1, 123.7, 58.0, 34.6, 31.6; HRMS-EI (m/z): $[M]^+$ calcd. for $C_{36}H_{36}$, 468.2817; found, 468.2817.

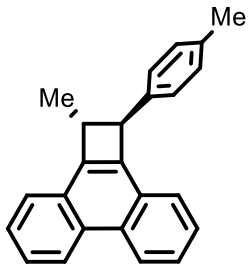

11

***trans*-1-methyl-2-(4-tolyl)-1,2-dihydrocyclobuta[l]phenanthrene (11).** To a vial containing $Cp_2Zr(pyr)(Me_3SiC{\equiv}CSiMe_3)$ (0.029 g, 0.062 mmol) was added a solution of **7** (0.019 g, 0.062 mmol) and 1,3,5-trimethoxybenzene (~8 mg; internal standard) in benzene-d_6 (1.6 mL). The solution was then transferred to an NMR tube fitted with Teflon stopper and analyzed by ^{1}H NMR spectroscopy 10 min after mixing. Integration against 1,3,5-trimethoxybenzene as internal standard revealed quantitative formation of ZrPAH **1e**. The tube was fitted with a rubber septum and HCl (3.6 M in dioxane, 0.10 mL) was added via syringe. ^{1}H NMR analysis 5 min after addition of HCl was consistent with *o*-QDM **2e** in 93% yield. In air, the solution was diluted with hexanes (4 mL), washed with saturated aqueous $NaHCO_3$ (2 x 5 mL) and saturated aqueous NaCl (5 mL), and dried with $MgSO_4$. The solution was filtered and solvents were removed from the filtrate to give an oily yellow solid. In a glovebox, this solid was re-dissolved in benzene-d_6 (1.0 mL) and added to a new NMR tube fitted with Teflon stopper. The solution was left to stand at 19 °C and periodically analyzed by ^{1}H NMR spectroscopy. After 10 days, cyclobutarene **11** formed in 97% yield. This yield was calculated from the amount of *o*-QDM **2e** present after aqueous work-up, which was in turn determined by integration against 1,3,5-trimethoxybenzene as internal standard. The half-life was ~2 days. For full characterization of compound **11**, the above procedure scaled up by a factor of 6. The reaction mixture was heated to 70 °C for 15 h (instead of 19 °C for 10 days). The crude product was eluted though a plug of silica gel with hexanes to afford **11** (0.103 g, 84%) as a pale yellow oil. Characterization of Intermediate *o*-QDM **2e**: ^{1}H NMR (benzene-d_6, 400 MHz): δ = 7.74 (dd, *J* = 7.6, 1.6 Hz, 1H), 7.64 (d, *J* = 7.8 Hz, 1H), 7.60 (dd, *J* = 7.8, 1.4 Hz, 1H), 7.46 (dd, *J* = 7.4, 1.6 Hz, 1H), 7.25 (d, *J* = 7.9 Hz, 2H), 7.19 (td, *J* = 7.6, 1.6 Hz, 1H), 7.15 (td, *J* = 7.5, 1.3 Hz), 7.05 (td, *J* = 7.6, 1.3 Hz, 1H), 6.87 (d, *J* = 7.9 Hz, 2H), 6.81 (td, *J* = 7.5, 1.3 Hz, 1H), 6.71 (s, 1H), 5.91 (q, *J* = 7.3 Hz, 1H), 2.05 (s, 3H), 1.79 (d, *J* = 7.3 Hz, 3H). Characterization of Cyclobutarene **11**: ^{1}H NMR (benzene-*d*6, 500 MHz): δ = 8.64 – 8.61 (m, 1H), 8.59 (d, *J* = 8.4 Hz, 1H), 7.71 – 7.68 (m, 1H), 7.63 (dd, *J* = 7.9, 1.3 Hz, 1H), 7.48 – 7.42 (m, 2H), 7.39 (ddd, *J* = 8.3, 6.8, 1.4 Hz, 1H), 7.29 (t, *J* = 7.5 Hz, 1H), 7.15 (d, *J* = 7.8 Hz), 6.99 (d, *J* = 7.8 Hz, 2H), 4.23 (d, *J* = 1.7 Hz, 1H), 3.52 (qd, *J* = 7.0, 1.7 Hz, 1H), 2.13 (s, 3H), 1.53 (d, *J* = 7.0 Hz, 3H); ^{13}C{^{1}H} NMR (benzene-*d*6, 101 MHz): δ = 143.5, 139.45, 139.41, 136.2, 131.8, 131.6, 129.6, 129.22, 129.18, 127.5, 127.0, 126.9, 126.1, 126.0, 124.5, 124.3, 123.5, 123.4, 55.8, 49.6, 21.1, 18.3; HRMS-EI (m/z): $[M]^+$ calcd for $C_{24}H_{20}$, 308.1565; found, 308.1563. The trans configuration was determined by NOESY.

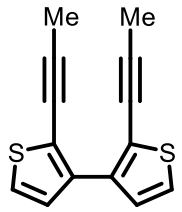

12

2,2'-Di(prop-1-ynyl)-3,3'-bithiophene (12). General procedure E was employed with the following quantities: **S6** (5.06 g, 25.2 mmol), tetrahydrofuran (90 mL), *n*-butyllithium (1.6 M in hexanes, 17.3 mL), and $CuCl_2$ (4.41 g, 32.8 mmol). The crude solid was purified by column chromatography (0–11% CH_2Cl_2 in hexanes), followed by recrystallization from hexanes to afford **12** (1.67 g, 55%) as colorless needles. mp 90.2–91.9 °C. ^{1}H NMR (chloroform-*d*, 400 MHz): δ = 7.60 (d, *J* = 5.3 Hz, 2H), 7.15 (d, *J* = 5.3 Hz, 2H), 2.09 (s, 6H); ^{13}C{^{1}H} NMR (chloroform-*d*, 101 MHz): δ = 138.0, 128.2, 124.6, 120.3, 93.4, 73.5, 5.0; HRMS-EI (m/z): $[M]^+$ calcd. for $C_{14}H_{10}S_2$, 242.0224; found, 242.0230.

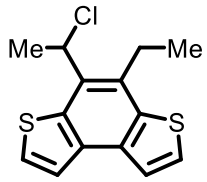

13

4-(1-chloroethyl)-5-ethylbenzo[1,2-b:4,3-b']dithiophene (13). To a 100 mL Schlenk flask containing **12** (0.150 g, 0.619 mmol) and $Cp_2Zr(pyr)(Me_3SiC{\equiv}CSiMe_3)$ (0.321 g, 0.681 mmol) was added benzene (10 mL) and the resulting homogeneous, brown reaction mixture was stirred for 1.5 h at 21 °C. A solution of HCl (3.6 M in dioxane, 1.4 mL) was then added via syringe to produce a light orange solution that was stirred for an additional 2 h. The solution was diluted with hexanes (20 mL), washed with saturated aqueous $NaHCO_3$ (20 mL) and saturated aqueous NaCl (25 mL), and dried with Na_2SO_4. After filtration and removal of solvents from the filtrate, compound **13** (0.070 g, 40%) was isolated by recrystallization from hexanes/CH_2Cl_2 at –25 °C as an off-white crystalline solid. mp 105–116 °C, dec. Notes: 1) only one crop of crystals was isolated, but ^{1}H NMR spectroscopy indicated that the product formed in ~95% yield; 2) compound **13** was also the major decomposition product when the procedure for **14** (below) was employed without a N-ethylmaleimide. ^{1}H NMR (benzene-d_6, 400 MHz): δ = 7.29 (d, *J* = 5.5 Hz, 1H), 7.27 (d, *J* = 5.4 Hz, 1H), 7.05 (d, *J* = 5.5 Hz, 1H), 7.03 (d, *J* = 5.4 Hz, 1H), 5.63 (q, *J* = 7.0 Hz, 1H), 2.87 – 2.67 (m, 2H), 1.92 (d, *J* = 7.1 Hz, 3H), 1.10 (t, *J* = 7.6 Hz, 3H); ^{13}C{^{1}H} NMR (chloroform-*d*, 101 MHz): δ = 138.2, 134.9, 134.7, 134.3, 131.4, 129.4, 127.1, 126.4, 122.8, 121.6, 55.3, 26.3, 24.5, 14.7; HRMS-EI (m/z): $[M]^+$ calcd. for $C_{14}H_{13}ClS_2$, 280.0147; found, 280.0147; Anal. Calcd for $C_{14}H_{13}ClS_2$: C, 59.9; H, 4.7. Found: C, 59.6; H, 4.6.

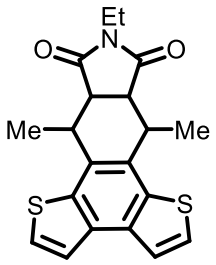

14

Diels-Alder Adduct (14). A 100 mL Schlenk tube was charged with Cp_2ZrCl_2 (0.300 g, 1.03 mmol) and tetrahydrofuran (9 mL) and the solution was cooled to –78 °C with a dry ice /acetone bath. To this solution was added *n*-butyllithium (1.63 M in hexanes, 1.3 mL) dropwise over 5 min and the reaction mixture was stirred for 30 min at –78 °C. A solution of **12** (0.227 g, 0.936 mmol) in tetrahydrofuran (3 mL) was added dropwise and the flask was removed from the cold bath. The reaction mixture was allowed to warm to 21 °C and stirred for an additional 3 h at this temperature. A solution of *N*-ethylmaleimide (0.140 g, 1.12 mmol), aqueous HCl (12 M, 0.5 mL), and methanol (1.4 mL) was then added quickly *via* syringe. After 1 h, the reaction mixture was diluted with ethyl acetate (15 mL), washed with saturated aqueous $NaHCO_3$ (15 mL) and brine (10 mL), dried over Na_2SO_4, filtered, and concentrated under reduced pressure. The residue was subjected to column chromatography (0–17% ethyl acetate in hexanes) to give a pale yellow powder as the desired product with small impurities. This powder was dissolved in CH_2Cl_2 (~1 mL) and hexanes (5 mL) was added to the solution to produce a colorless, crystalline precipitate that was collected by filtration and identified as the pure product. Yield: 0.262 g (76%). mp 215–216 °C. ^{1}H NMR (chloroform-*d*, 400 MHz): δ = 7.74 (d, *J* = 5.4 Hz, 2H), 7.56 (d, *J* = 5.4 Hz, 2H), 4.06 – 3.97 (m, 2H), 3.70 (q, *J* = 7.2 Hz, 2H), 3.51 – 3.45 (m, 2H), 1.47 (d, *J* = 7.4 Hz, 6H), 1.26 (t, *J* = 7.2 Hz, 3H); ^{13}C{^{1}H} NMR (chloroform-*d*, 101 MHz): δ = 178.0, 137.1, 133.5, 130.2, 125.9, 122.7, 42.8, 33.8, 32.1, 18.0, 13.4; HRMS-EI (m/z): $[M]^+$ calcd. for $C_{20}H_{19}NO_2S_2$, 369.0857; found, 369.0859.

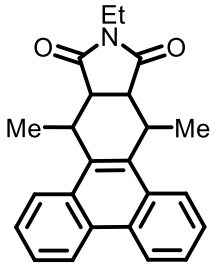

15

Diels-Alder Adduct (15). A 30 mL flask with Teflon stopper was charged with *o*-QDM **2a** (0.293 g, 1.26 mmol), *N*-ethylmaleimide (0.315 g, 2.52 mmol), $CHCl_3$ (8.0 mL), and dimethyl sulfoxide (4.0 mL). The flask was degassed by three freeze-pump-thaw cycles, backfilled with N_2, and submersed in a 70 °C oil bath for 15 h. The mixture was then brought to 21 °C, diluted with CH_2Cl_2 (20 mL), washed with water (30 mL) and saturated aqueous NaCl (30 mL), dried with $MgSO_4$, filtered, and concentrated under reduced pressure. Residual volatile materials (including most of the excess *N*-ethylmaleimide) were removed under high vacuum. The crude solid was dissolved in $CHCl_3$ (~1.5 mL) and to this solution was added methanol (7 mL), which rapidly give a precipitate. This precipitate was collected by filtration, washed with methanol (5 mL), and dried under vacuum to afford **15** (0.405 g, 90%) as a

colorless, crystalline solid. mp 241–242 °C. Monitoring of this reaction by ^{1}H NMR spectroscopy on a smaller scale (10%) indicated formation of **15** in quantitative yield. ^{1}H NMR (chloroform-*d*, 500 MHz): δ = 8.79 – 8.75 (m, 2H), 8.16 – 8.12 (m, 2H), 7.71 – 7.65 (m, 4H), 4.58 – 4.50 (m, 2H), 3.72 (q, *J* = 7.2 Hz, 2H), 3.43 – 3.37 (m, 2H), 1.44 (d, *J* = 7.5 Hz, 6H), 1.28 (t, *J* = 7.2 Hz, 3H); ^{13}C{^{1}H} NMR (dichloromethane-d_2, 101 MHz): δ = 178.9, 134.7, 130.6, 130.3, 127.7, 126.8, 123.9, 123.7, 43.0, 34.1, 28.3, 18.7, 13.6; HRMS–EI (m/z): $[M]^+$ calcd for $C_{24}H_{23}NO_2$, 357.1729; found, 357.1726.

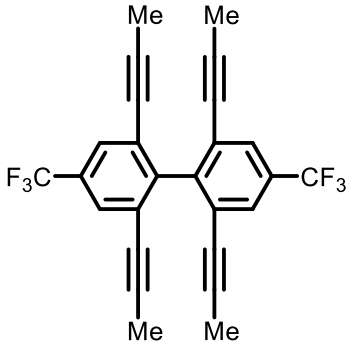

16

2,2',6,6'-Tetra(prop-1-ynyl)-4,4'-bis(trifluoromethyl)biphenyl (16). General procedure E was employed with the following quantities: **S7** (3.08 g, 10.2 mmol), tetrahydrofuran (50 mL), *n*-butyllithium (1.6 M in hexanes, 7.0 mL), and $CuCl_2$ (1.79 g, 13.3 mmol). The crude solid was recrystallized two times from CH_2Cl_2 at –80 °C to yield colorless crystals which contained a large amount of CH_2Cl_2. To remove the CH_2Cl_2 (important for the next step), the crystals were dissolved in hot toluene which was then removed under vacuum to afford pure **16** (1.19 g, 53%) as a colorless solid. mp 176–178 °C. ^{1}H NMR (chloroform-*d*, 500 MHz): δ = 7.63 (s, 4 H), 1.80 (s, 12 H); ^{13}C{^{1}H} NMR (benzene-d_6, 101 MHz): δ = 147.6, 130.7 (q, *J* = 33 Hz), 128.2 (q*, *J* = 4 Hz), 126.3, 124.3 (q, *J* = 273 Hz), 92.0, 77.5, 4.0; ^{19}F NMR (chloroform-*d*, 376 MHz): δ = -63.5; HRMS-EI (m/z): $[M]^+$ calcd. for $C_{26}H_{16}F_6$, 442.1156; found, 442.1165.

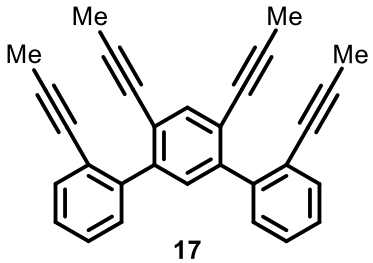

17

2,2'',4',6'-Tetra(prop-1-ynyl)-1,1':3',1''-terphenyl (17). General Procedure G was employed with the following quantities: **S8** (0.636 g, 2.04 mmol), 2-(prop-1-ynyl)phenylboronic acid (0.980 g, 6.13 mmol), $Pd(PPh_3)_2Cl_2$ (0.086 g, 0.12 mmol) and K_2CO_3 (0.847 g, 6.13 mmol), toluene (25 mL), absolute ethanol (25 mL), and deionized water (6 mL). The crude solid was purified by column chromatography (0–30% CH_2Cl_2 in hexanes) followed by trituration with hexanes (2 mL) to yield **17** (0.325 g, 42%) as a pale yellow powder. mp 167–169 °C; ^{1}H NMR (chloroform-*d*, 400 MHz): δ = 7.62 (s, 1H), 7.46 (dd, *J* = 7.3, 1.7 Hz, 2H), 7.43 – 7.38 (m, 3H), 7.32 – 7.23 (m, 4H*), 1.88 (s, 6H), 1.86 (s, 6H); ^{13}C{^{1}H} NMR (chloroform-*d*, 126 MHz): δ = 142.6, 141.5, 136.1, 132.3, 132.2, 130.1, 127.2, 126.9, 123.5, 122.4,

89.1, 89.0, 79.0, 78.5, 4.54, 4.46; HRMS-EI (m/z): $[M]^+$ calcd. for $C_{30}H_{22}$, 382.1722; found, 382.1721. *Overlaps w/ solvent peak, so integration was assumed.

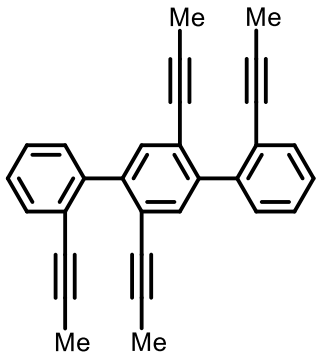

18

2,2',2'',5'-Tetra(prop-1-ynyl)-1,1':4',1''-terphenyl (18). General Procedure G was employed with the following quantities: **S9** (0.636 g, 2.04 mmol), 2-(prop-1-ynyl)phenylboronic acid (0.979 g, 6.12 mmol), $Pd(PPh_3)_2Cl_2$ (0.086 g, 0.12 mmol) and K_2CO_3 (0.846 g, 6.12 mmol), toluene (25 mL), absolute ethanol (25 mL), and deionized water (6 mL). At the completion of the reaction, the precipitated light gray solid was collected by filtration. The filtrate was then subjected to the workup outlined in General Procedure G to give a viscous oil. To this oil was added tetrahydrofuran (5 mL) and the resulting suspension was sonicated to produce a light brown solid which was also collected by filtration. The two crude solids were combined and stirred in boiling toluene (15 mL) until the solution became transparent, then the solution was filtered while hot. The filtrate was concentrated to 2 mL and diluted with hexanes (10 mL). Finally, the precipitated white solid was collected by filtration, washed with hexanes (2 x 3 mL), and dried under vacuum. Yield of **18**: 0.290 g (37%). mp 232–236 °C. ^{1}H NMR (benzene-d_6, 400 MHz): δ 7.92 (s, 2H), 7.63 (dd, J = 7.5, 1.6 Hz, 2H), 7.43 (dd, J = 7.5, 1.6 Hz, 2H), 7.06 (td, J = 7.5, 1.7 Hz, 2H), 7.01 (td, J = 7.5, 1.6 Hz, 2H), 1.54 (s, 6H), 1.43 (s, 6H); Solubility considerations precluded acquisition of a ^{13}C NMR spectrum; HRMS-EI (m/z): $[M]^+$ calcd. for $C_{30}H_{22}$, 382.1722.

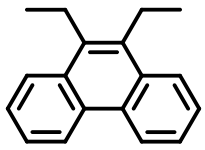

20

9,10-Diethylphenanthrene (19). A The preparation of this compound (including yield) is described as General Procedure H. mp 102–104 °C (lit.[15] mp 105–106 °C). ^{1}H NMR data match the literature values.[16]

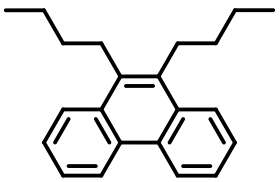

20

9,10-Di(n-butyl)phenanthrene (20). General Procedure H was employed to yield compound **20** (49.8 mg, 99%) as a colorless crystalline solid. mp 73.3–75.0 °C. ^{1}H NMR (chloroform-*d*, 500 MHz): δ = 8.76 – 8.68 (m, 2H), 8.15 – 8.06 (m, 2H), 7.66 – 7.55 (m, 4H), 3.19 – 3.11 (m, 4H), 1.75 – 1.67 (m, 4H), 1.61 (h, *J* = 7.2 Hz, 4H), 1.06 (t, *J* = 7.3 Hz, 6H); ^{13}C{^{1}H} NMR (chloroform-*d*, 101 MHz): δ = 134.0, 131.5, 129.9, 126.7, 125.5, 124.8, 123.1, 33.0, 29.2, 23.6, 14.2; HRMS-EI (m/z): $[M]^+$ calcd. for $C_{22}H_{26}$, 290.2035.

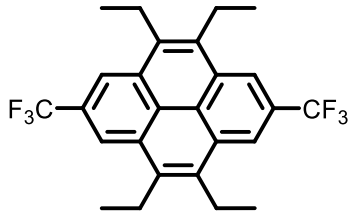

21

2,7-Bis(trifluoromethyl)-4,5,9,10-tetraethylpyrene (21). General Procedure H was followed, but the relative quantities were adjusted: *o*-QDM **2g** (33.1 mg, 0.0741 mmol), 10% palladium on carbon (9.9 mg), tetrahydrofuran (1 mL), and ethanol (1 mL). Compound **21** (32.5 mg, 97%) was isolated as a white solid. Single crystals were grown by slow evaporation of a chloroform-*d* solution of **21**, and the structure was elucidated by X-ray crystallography (see Figure S94 and Table S9). mp 260–261 °C; ^{1}H NMR (chloroform-*d*, 500 MHz): δ = 8.63 (s, 4H), 3.42 (q, *J* = 7.6 Hz, 8H), 1.48 (t, *J* = 7.6 Hz, 12H); ^{13}C{^{1}H} NMR (chloroform-*d*, 101 MHz): δ = 137.1, 131.5, 128.5 (q, *J* = 32 Hz), 125.2 (q, *J* = 273 Hz), 124.6, 117.8 (q, *J* = 3.7 Hz), 22.6, 15.4; ^{19}F NMR (chloroform-*d*, 376 MHz): δ = –61.3; HRMS-EI (m/z): $[M]^+$ calcd. for $C_{26}H_{24}F_6$, 450.1782; found, 450.1787.

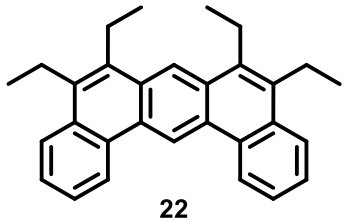

22

5,6,8,9-Tetraethylbenzo[m]tetraphene (22). General procedure H was employed with the following quantities: *o*-QDM **2h** (16.5 mg, 0.0427 mmol), 10% palladium on carbon (4.0 mg), and tetrahydrofuran (2 mL) (note that ethanol was not used). The crude product was eluted though a plug of silica gel with 6:1 hexanes:CH_2Cl_2. Removal of solvents afforded compound **22** (16.3 mg, 98%) as a white solid. ^{1}H NMR (chloroform-*d*, 400 MHz): δ = 10.08 (s, 1H), 9.04 (dd, *J* = 7.2, 2.1 Hz, 2H), 8.83 (s, 1H), 8.16 (dd, *J* = 7.8, 1.8 Hz, 2H), 7.73 – 7.62 (m, 4H), 3.37 (q, *J* = 7.6 Hz, 4H), 3.25 (q, *J* = 7.6 Hz, 4H), 1.50 (t, *J* = 7.6 Hz, 6H), 1.43 (t, *J* = 7.5 Hz, 6H); ^{13}C{^{1}H} NMR (chloroform-*d*, 151 MHz): δ = 134.90, 134.90, 131.45, 130.39, 129.88, 127.77, 126.90, 125.75, 124.91, 123.16, 120.00, 116.99, 22.52, 22.45, 15.17, 15.14; HRMS-EI (m/z): $[M]^+$ calcd. for $C_{30}H_{30}$, 390.2348; found, 390.2351.

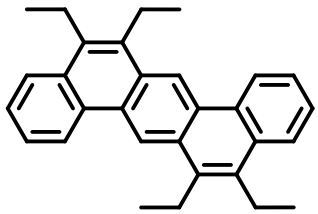

23

5,6,12,13-Tetraethylbenzo[k]tetraphene (23). General Procedure H was employed with the following quantities: *o*-QDM **2i** (14.1 mg, 0.0365 mmol), 10% palladium on carbon (7.5 mg), tetrahydrofuran (1 mL), and ethanol (1 mL). The reaction time was 18 h. The crude solid was dissolved in CH_2Cl_2 (4 mL) and EtOH (2 mL) and the resulting solution was concentrated to 2 mL to afford compound **23** (11.0 mg, 77%) as small colorless needles. ^{1}H NMR (chloroform-*d*, 500 MHz): δ = 9.45 (s, 2H), 8.95 – 8.91 (m, 2H), 8.18 – 8.15 (m, 2H), 7.70 – 7.63 (m, 4H), 3.43 (q, *J* = 7.6 Hz, 4H), 3.26 (q, *J* = 7.6 Hz, 4H), 1.53 (t, *J* = 7.6 Hz, 6H), 1.43 (t, *J* = 7.6 Hz, 6H); ^{13}C{^{1}H} NMR (chloroform-*d*, 151 MHz): δ = 135.0, 134.8, 131.6, 130.4, 128.9, 128.9, 127.0, 125.8, 125.0, 123.1, 118.5, 22.5, 22.4, 15.3, 15.2; HRMS-EI (m/z): $[M]^+$ calcd. for $C_{30}H_{30}$, 390.2348; found, 390.2346.

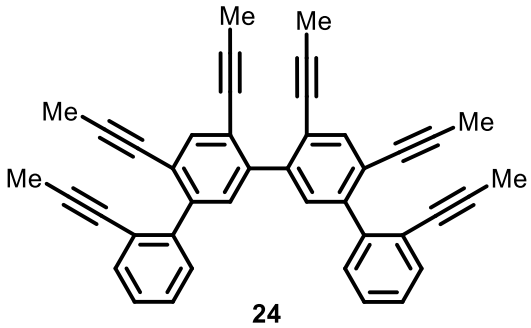

24

2,2''',4',4'',6',6''-Hexa(prop-1-ynyl)-1,1':3',1'':3'',1'''-quaterphenyl (24). General Procedure G was employed with the following quantities: **S10** (0.150 g, 0.323 mmol), 2-(prop-1-ynyl)phenylboronic acid (0.170 g, 1.06 mmol), $Pd(PPh_3)_2Cl_2$ (0.003 g, 0.004 mmol), K_2CO_3 (0.150 g, 1.09 mmol), toluene (1.4 mL), absolute ethanol (1.2 mL), and deionized water (0.4 mL). Analysis of the crude reaction product by ^{1}H NMR spectroscopy indicated that compound **24** formed in 46% yield (as determined by integration against 1,5-cyclooctadiene as internal standard). The crude solid was purified by column chromatography (0–50% CH_2Cl_2 in hexanes) followed by trituration with hexanes (2 x 2 mL) to yield **24** (0.045 g, 26%) as a pale yellow powder. ^{1}H NMR (benzene-d_6, 600 MHz): δ = 8.11 (s, 2H), 7.75 (s, 2H), 7.58 (dd, *J* = 7.7, 1.3 Hz, 2H), 7.46 (dd, *J* = 7.7, 1.3 Hz, 2H), 7.06 (td, *J* = 7.6, 1.4 Hz, 2H), 7.00 (td, *J* = 7.6, 1.4 Hz, 2H), 1.54 (s, 6H), 1.54 (s, 6H), 1.44 (s, 6H); ^{13}C{^{1}H} NMR (benzene-d_6, 101 MHz): δ = 143.22, 142.32, 142.06, 136.75, 133.00, 132.70, 130.67, 127.56, 127.07, 124.33, 123.80, 123.51, 89.79, 89.77, 89.69, 79.70, 79.22, 79.13, 4.27, 4.19, 4.16; HRMS-EI (m/z): $[M]^+$ calcd. for $C_{42}H_{30}$, 534.2348; found, 534.2339.

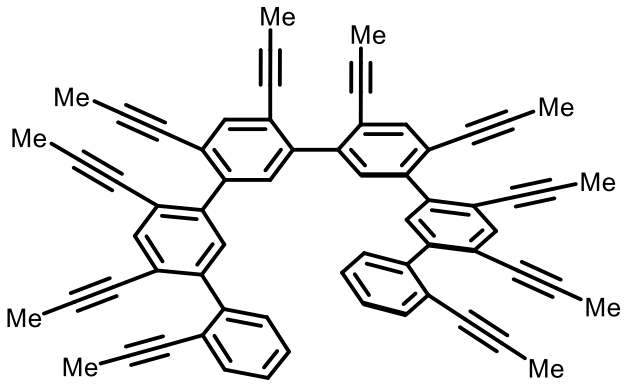

25

2,2'''',4',4'',4''',4'''',6',6'',6''',6''''-deca(prop-1-ynyl)-1,1':3',1'':3'',1''':3''',1'''':3'''',1''''-sexiphenyl (25). General Procedure G was employed with the following quantities: **S11** (49.6 mg, 0.0645 mmol), 2-(prop-1-ynyl)phenylboronic acid (35 mg, 0.22 mmol), $Pd(PPh_3)_2Cl_2$ (0.9 mg, 0.001 mmol), K_2CO_3 (30 mg, 0.22 mmol), toluene (0.6 mL), absolute ethanol (0.6 mL), and deionized water (0.2 mL). Analysis of the crude reaction product by ^{1}H NMR spectroscopy indicated that compound **25** formed in 53% yield (as determined by integration against 1,5-cyclooctadiene as internal standard). The crude solid was purified by column chromatography (0–50% CH_2Cl_2 in hexanes) followed by trituration with hexanes (2 x 2 mL) to yield **25** (12.8 mg, 24%) as a pale yellow powder. ^{1}H NMR (benzene-d_6, 500 MHz): δ = 8.08 (s, 2H), 8.06 (s, 2H), 7.70 (s, 2H), 7.68 (s, 2H), 7.58 (dd, J = 7.7, 1.4 Hz, 2H), 7.43 (dd, J = 7.6, 1.4 Hz, 2H), 7.05 (td, J = 7.5, 1.5 Hz, 2H), 7.00 (td, J = 7.5, 1.5 Hz, 2H), 1.57 (s, 6H), 1.55 (s, 6H), 1.52 (s, 6H), 1.52 (s, 6H), 1.44 (s, 6H); ^{13}C{^{1}H} NMR (dichloromethane-d_2, 151 MHz): δ = 142.82, 141.95, 141.61, 141.51, 141.42, 136.47, 136.37, 132.83, 132.69, 132.63, 130.56, 127.89, 127.45, 123.87, 123.28, 123.16, 123.07, 123.00, 90.47, 90.22, 90.18, 90.03, 89.87, 79.26, 78.65, 78.65, 78.65, 78.59, 4.63, 4.60, 4.58, 4.56, 4.49; HRMS-ESI (m/z): $[M]^+$ calcd. for $C_{66}H_{46}$, 838.3594; found, 838.3589.

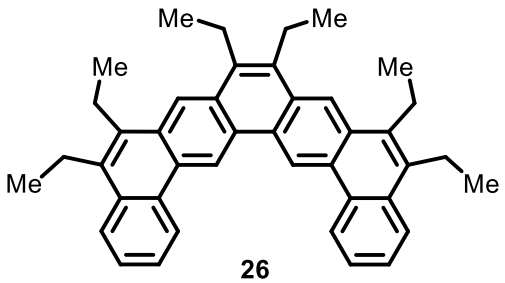

26

5,6,8,9,11,12-Hexaethyldibenzo[a,o]pentaphene (26). General Procedure H was employed, but the relative quantities were adjusted as follows: *o*-QDM **2j** (18.8 mg, 0.0348 mmol), 10% palladium on carbon (9.4 mg), and tetrahydrofuran (2.1 mL) (note that ethanol was not used). The reaction temperature was 50 °C and the reaction time was 3 h. Purification was carried out as follows. The crude solid was dissolved in CH_2Cl_2 (1 mL) and methanol (2 mL) was added to this solution to produce a pale yellow precipitate which was collected on a fritted funnel, washed with methanol, dried under vacuum, and identified to be compound **26**. Yield: 12.5 mg (66%). ^{1}H NMR (benzene-d_6, 400 MHz): δ = 10.52 (s, 2H), 9.14 – 9.06 (m, 2H), 8.99 (s, 2H), 8.13 – 8.06 (m, 2H), 7.60 – 7.51 (m, 4H), 3.33 (q, J = 7.6 Hz, 4H), 3.30 (q, J = 7.6 Hz, 4H), 3.11 (q, J = 7.6 Hz, 4H), 1.51 (t, J = 7.5 Hz, 6H), 1.47 (t, J

= 7.5 Hz, 6H), 1.33 (t, *J* = 7.5 Hz, 6H); $^{13}C\{^{1}H\}$ NMR (chloroform-*d*, 151 MHz): δ = 135.00, 134.98, 134.98, 131.53, 130.37, 130.15, 130.02, 128.14, 127.91, 126.95, 125.81, 124.98, 123.29, 120.28, 116.95, 22.71, 22.56, 22.48, 15.23, 15.20, 15.12; HRMS-EI (m/z): $[M]^+$ calcd for $C_{42}H_{42}$, 546.3287; found, 546.3282.

NMR Spectra

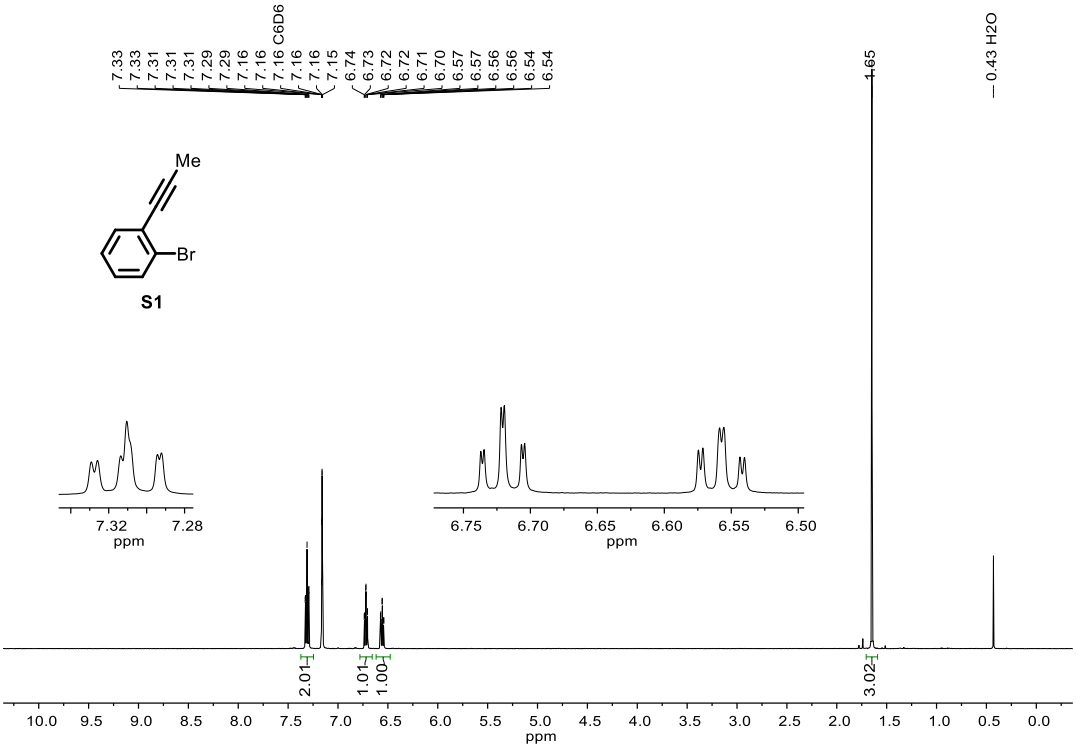

Figure S1. ^{1}H NMR Spectrum (500 MHz, Benzene-d_6) of **S1**.

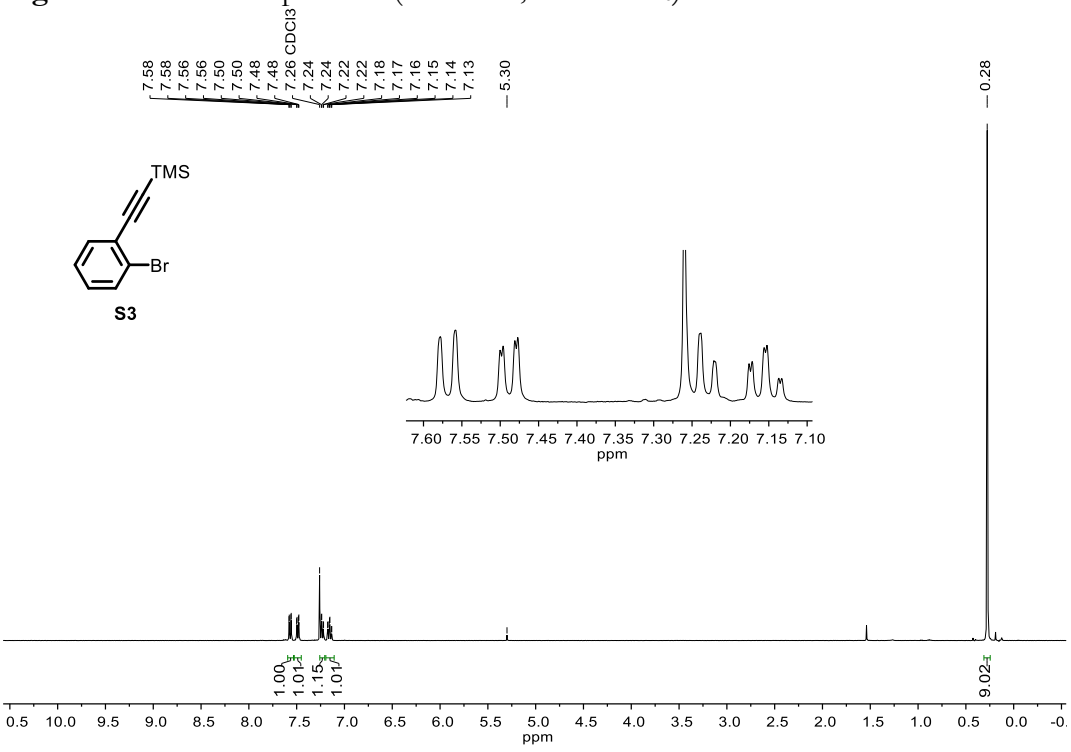

Figure S2. ^{1}H NMR Spectrum (400 MHz, Chloroform-*d*) of **S3**.

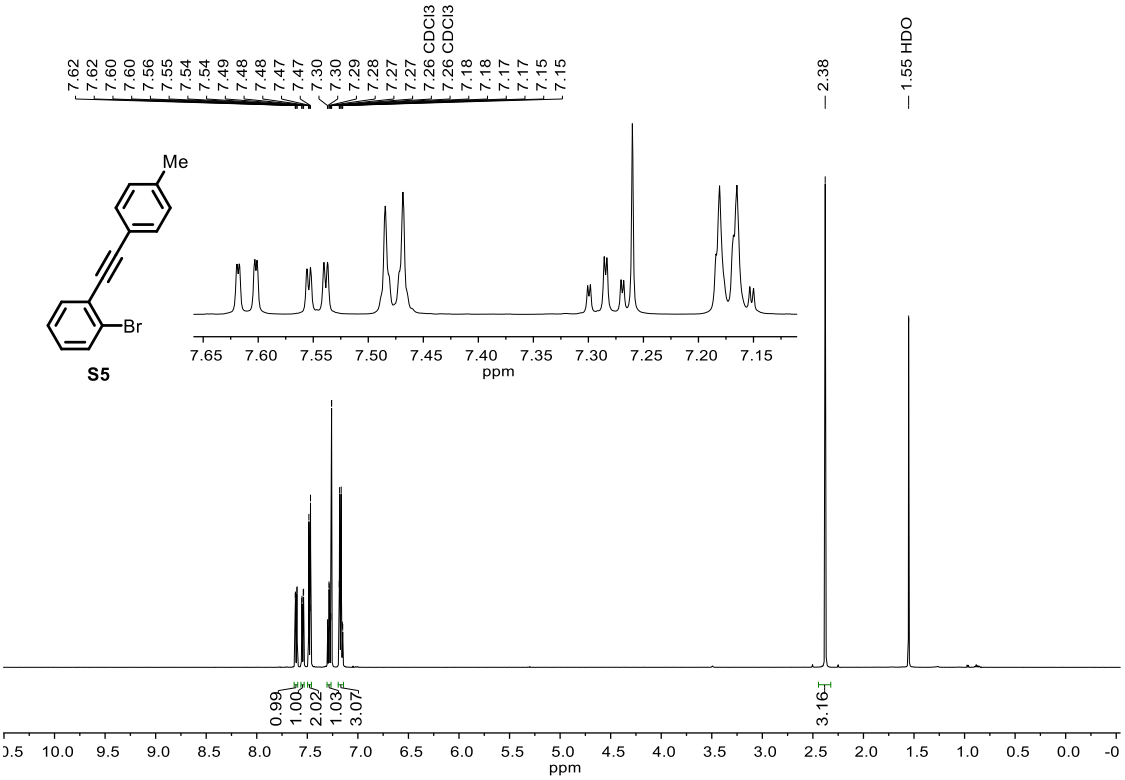

Figure S3. ^{1}H NMR Spectrum (500 MHz, Chloroform-*d*) of **S5**.

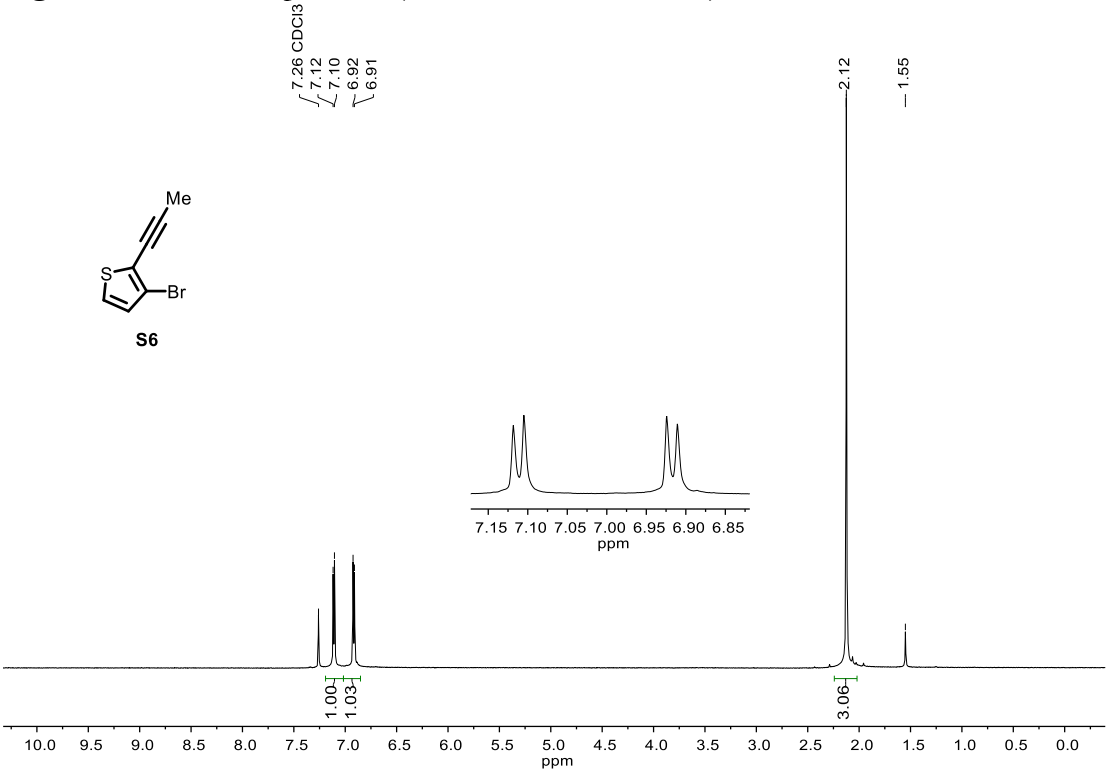

Figure S4. ^{1}H NMR Spectrum (400 MHz, Chloroform-*d*) of **S6**.

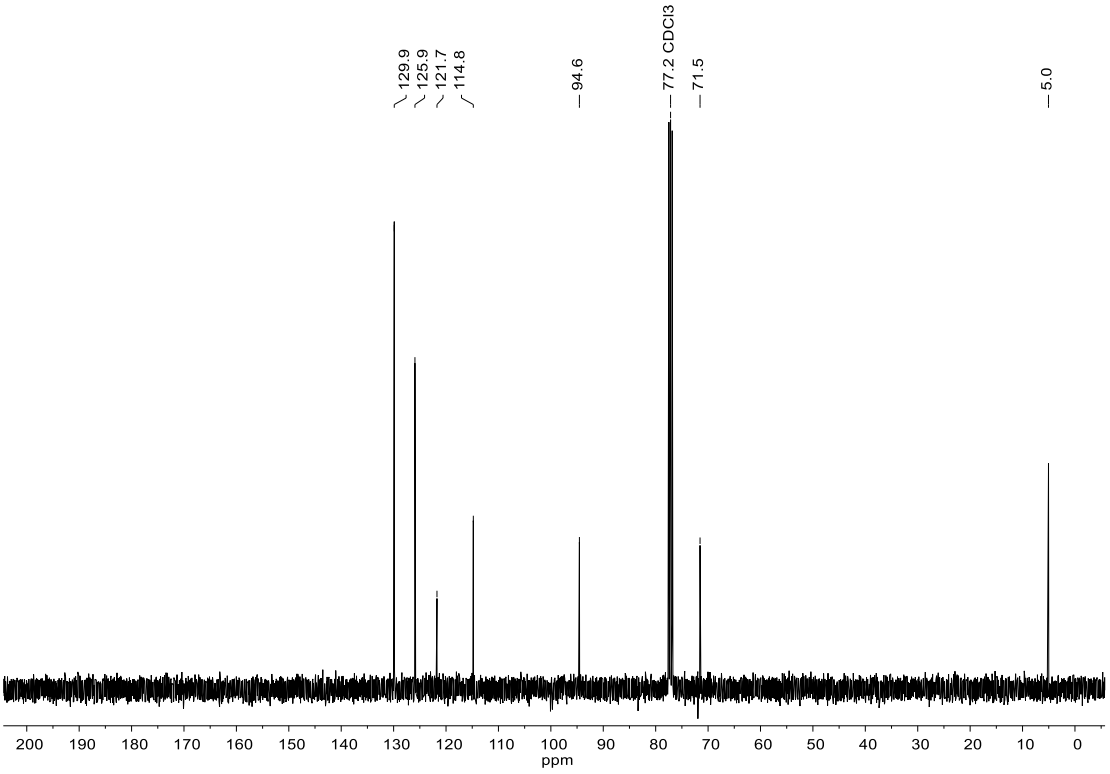

Figure S5. ^{13}C NMR Spectrum (101 MHz, Chloroform-*d*) of **S6**.

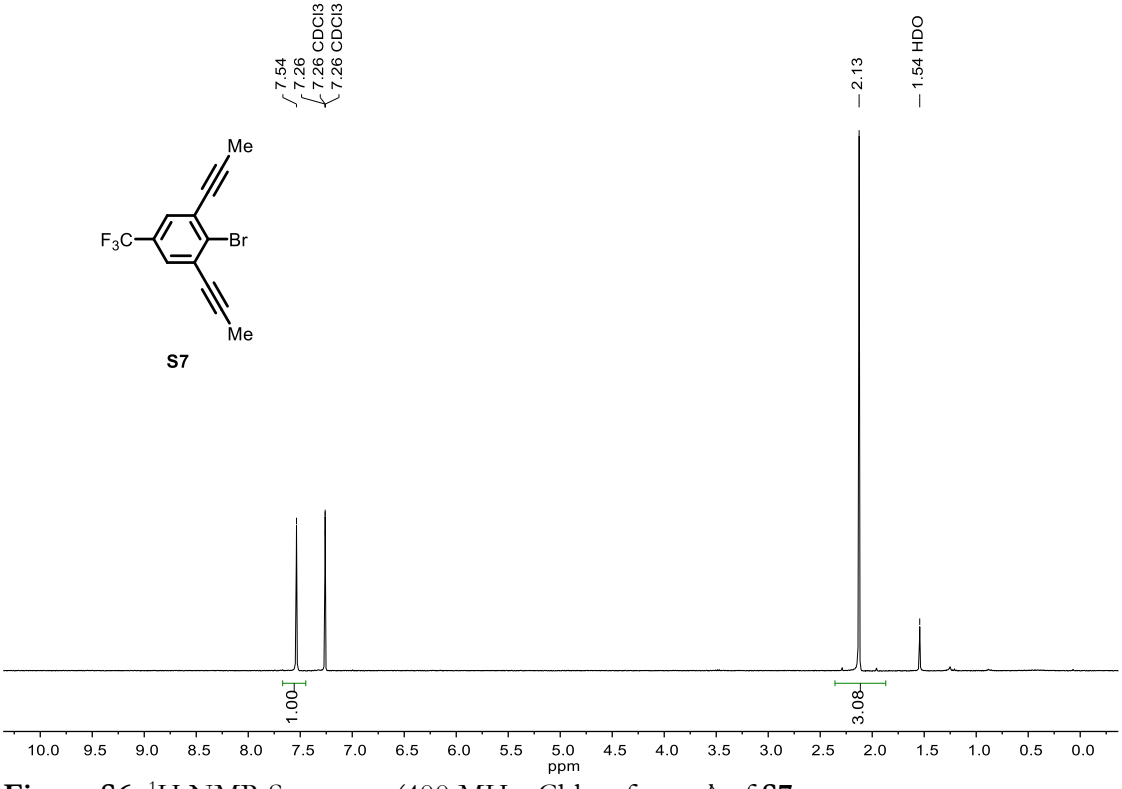

Figure S6. ^{1}H NMR Spectrum (400 MHz, Chloroform-*d*) of **S7**.

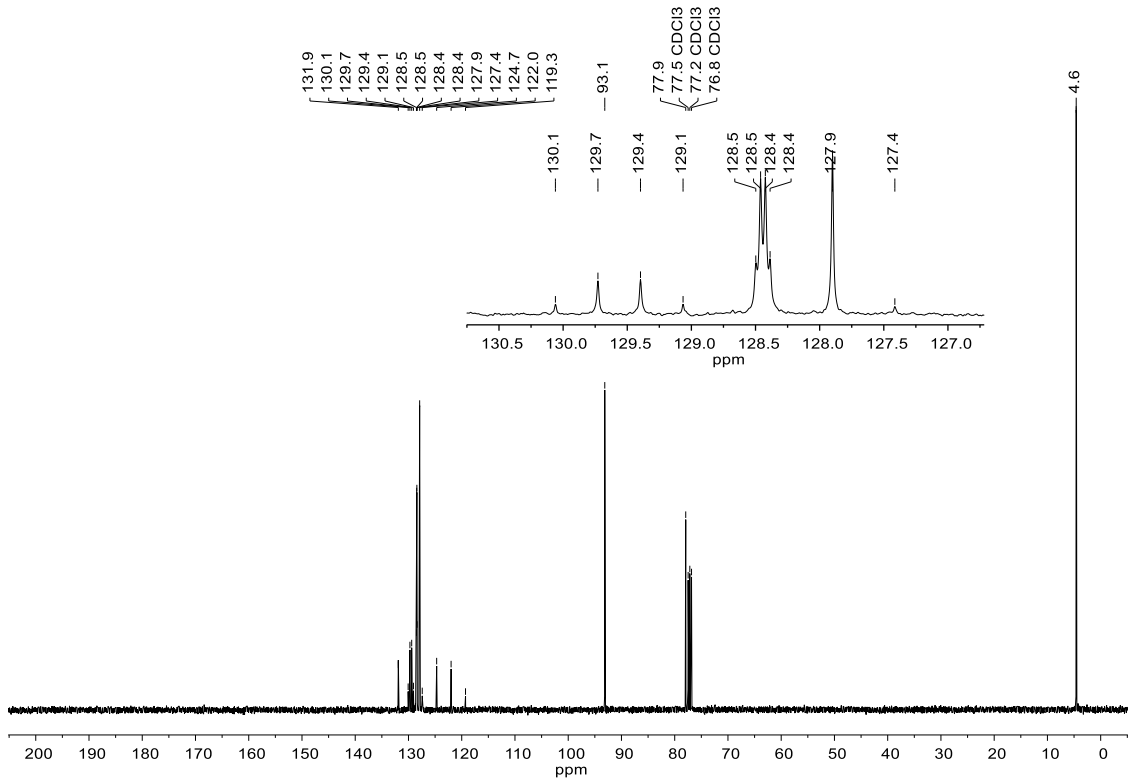

Figure S7. ^{13}C NMR Spectrum (101 MHz, Chloroform-*d*) of **S7**.

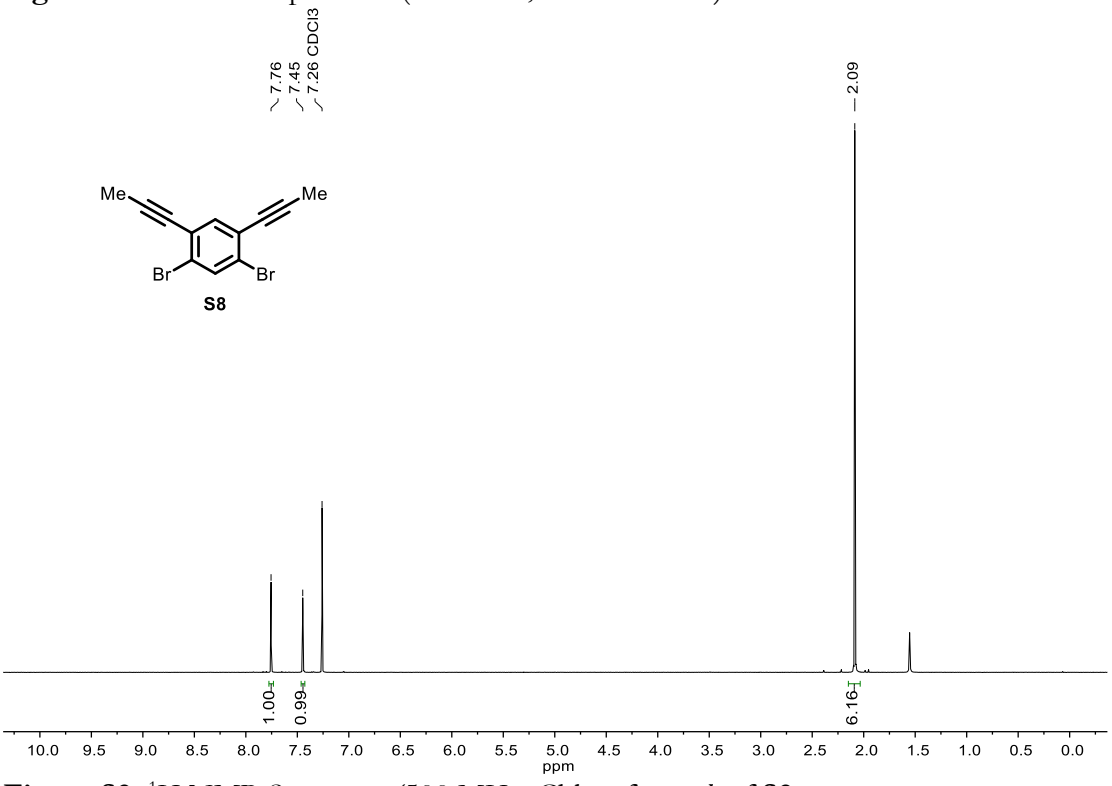

Figure S8. ^{1}H NMR Spectrum (500 MHz, Chloroform-*d*) of **S8**.

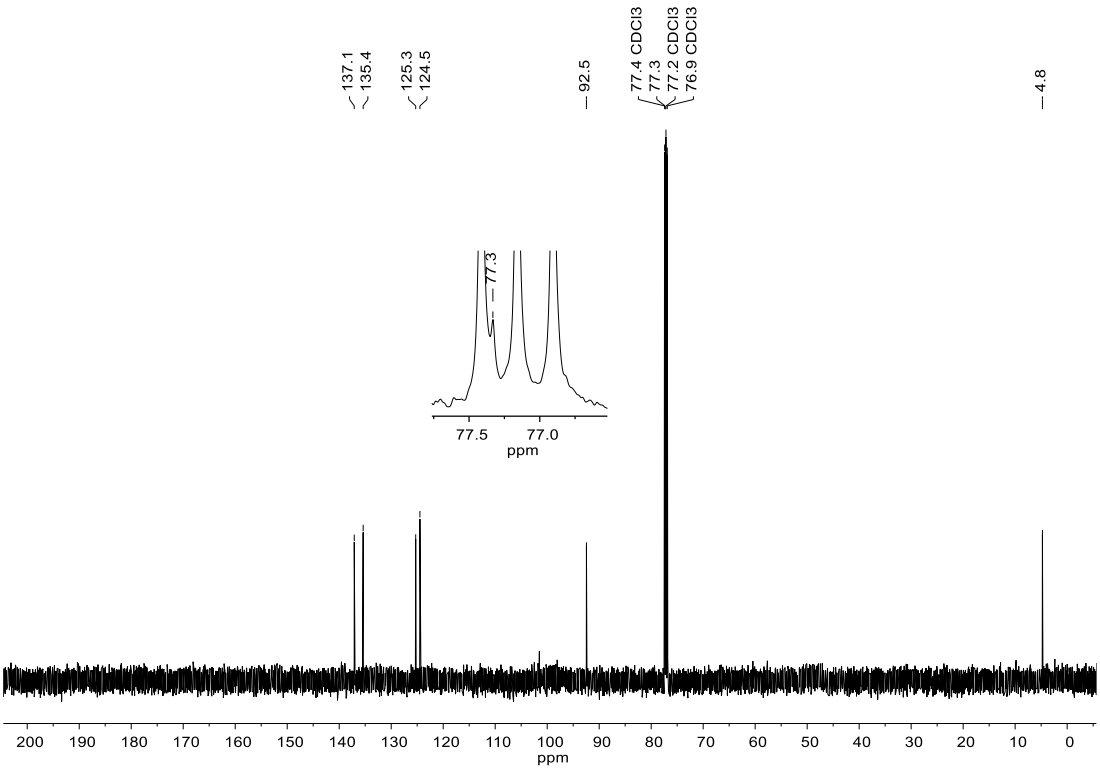

Figure S9. ^{13}C NMR Spectrum (126 MHz, Chloroform-*d*) of **S8**.

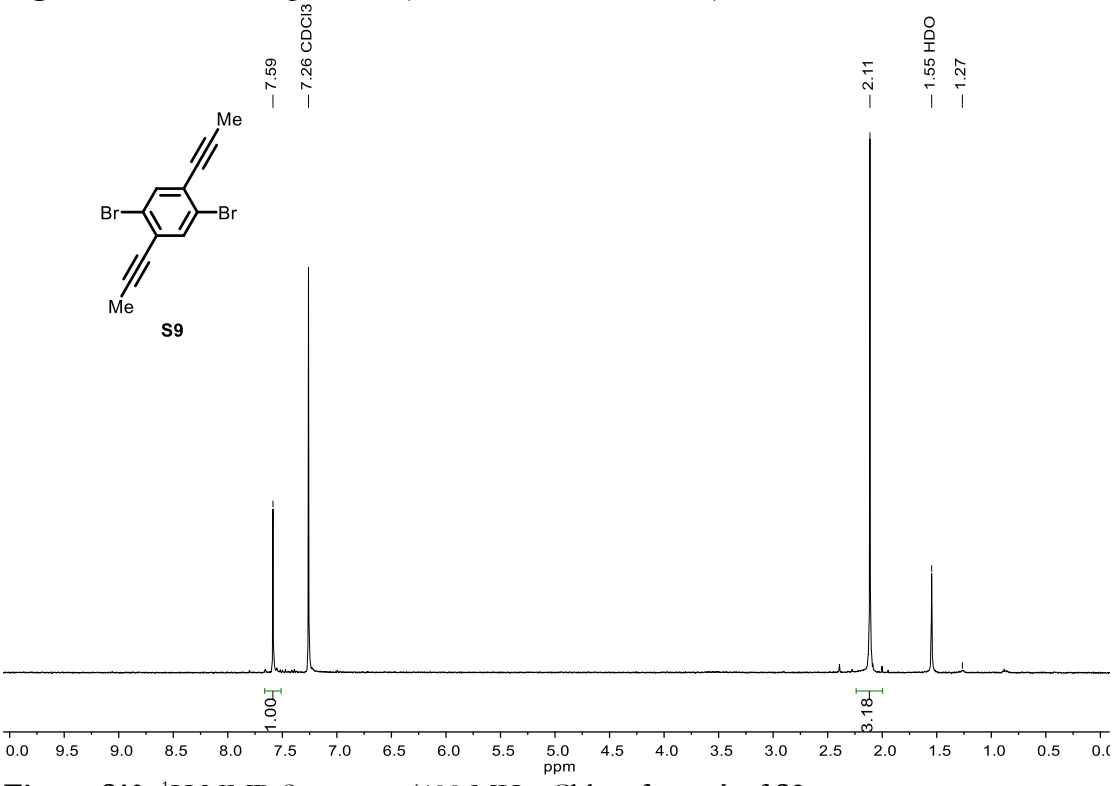

Figure S10. ^{1}H NMR Spectrum (400 MHz, Chloroform-*d*) of **S9**.

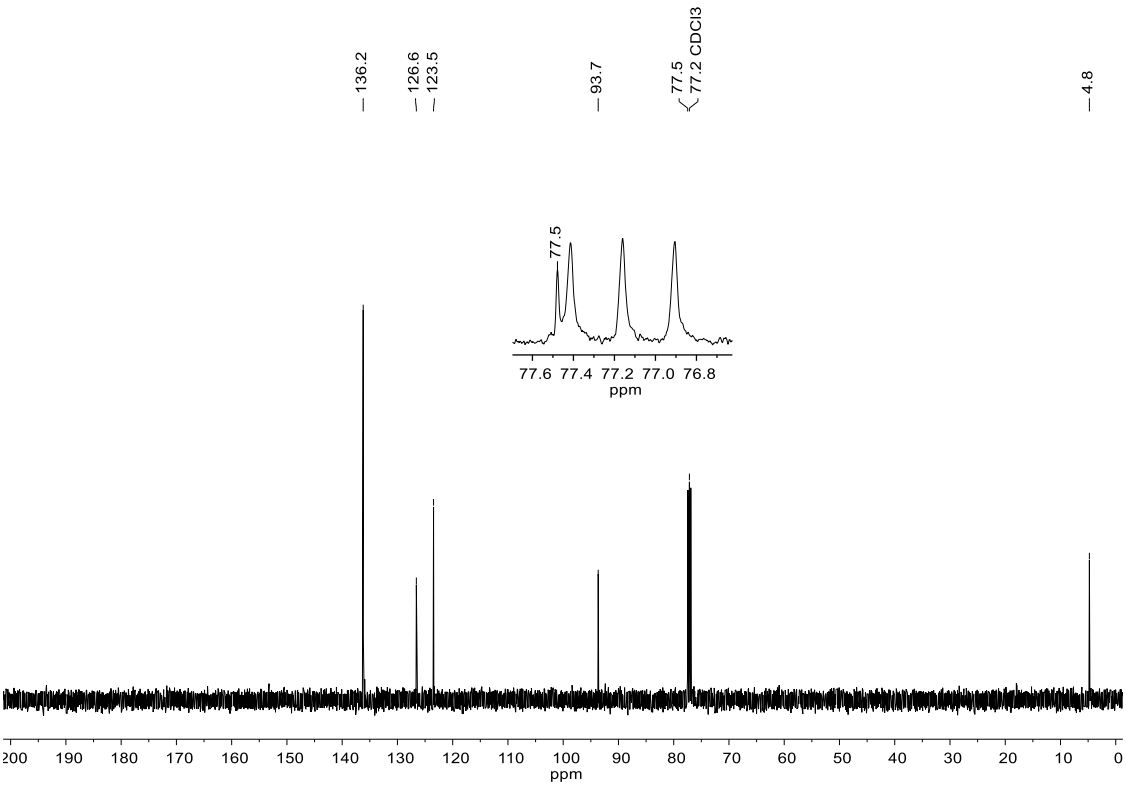

Figure S11. ^{13}C NMR Spectrum (126 MHz, Chloroform-*d*) of **S9**.

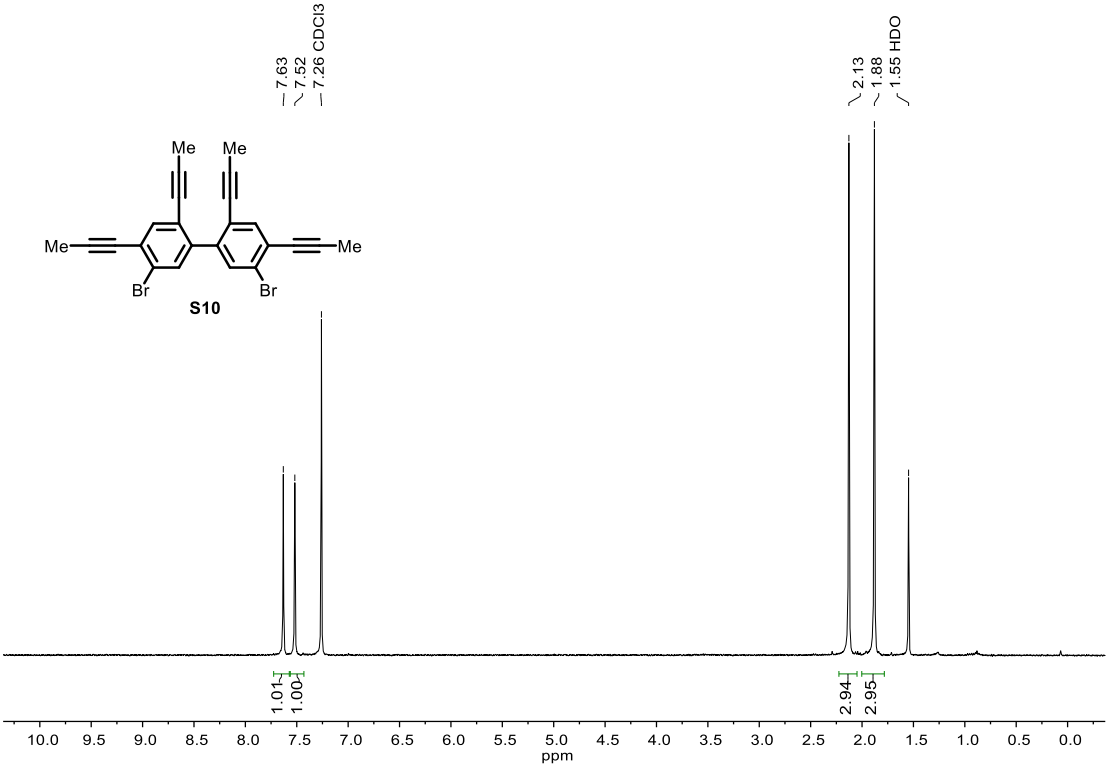

Figure S12. ^{1}H NMR Spectrum (400 MHz, Chloroform-*d*) of **S10**.

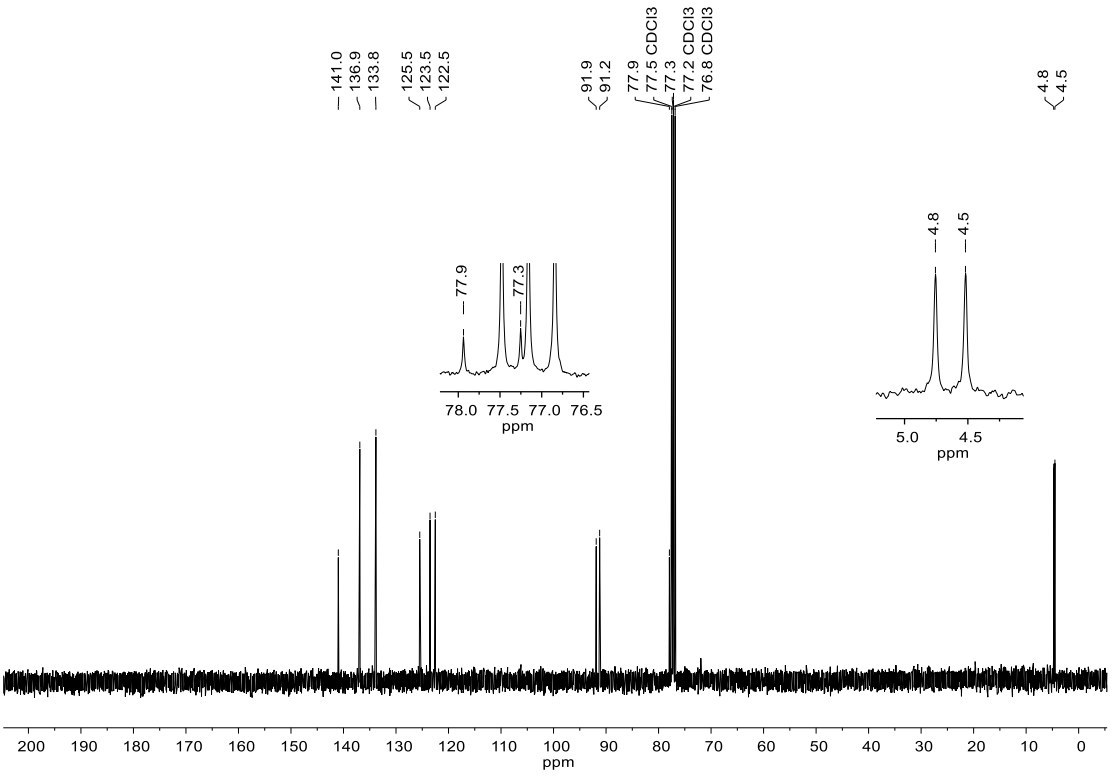

Figure S13. ^{13}C NMR Spectrum (101 MHz, Chloroform-*d*) of **S10**.

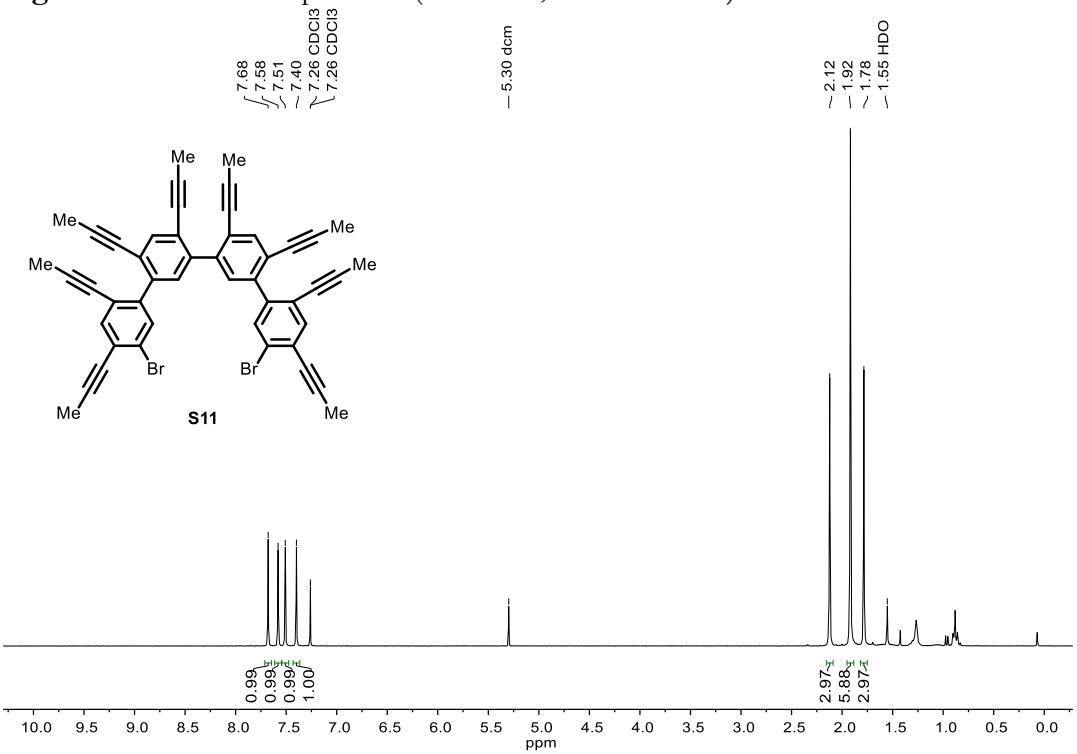

Figure S14. ^{1}H NMR Spectrum (300 MHz, Chloroform-*d*) of **S11**.

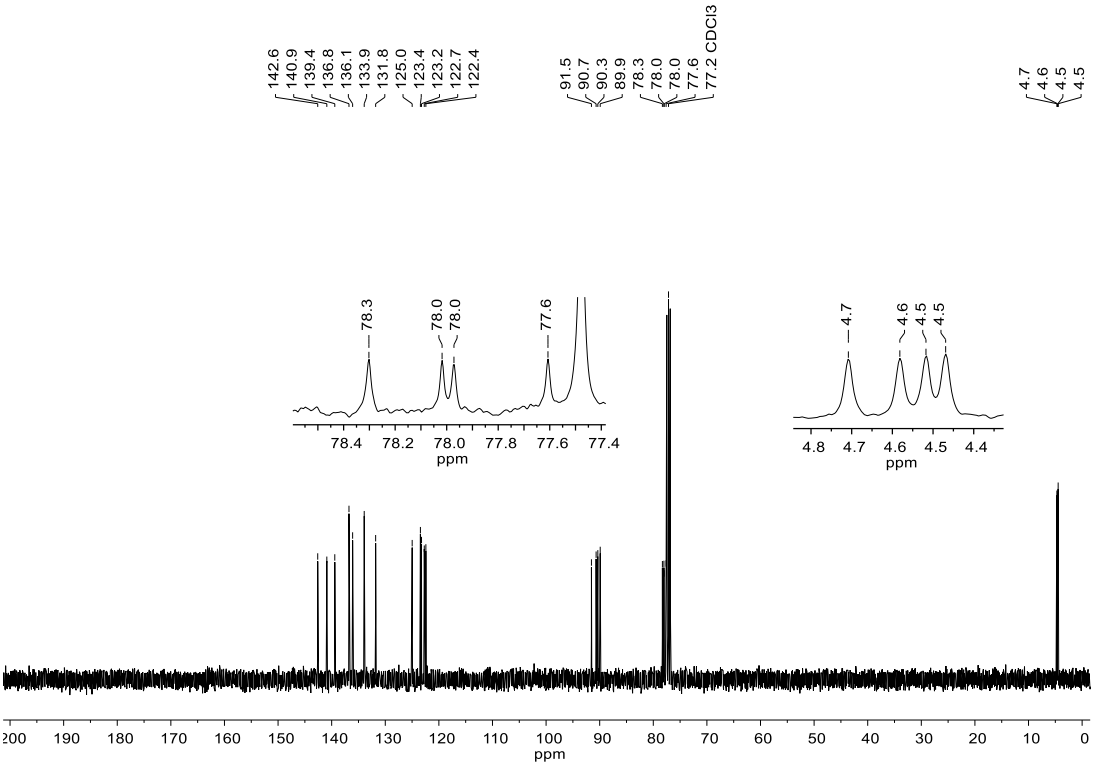

Figure S15. ^{13}C NMR Spectrum (101 MHz, Chloroform-*d*) of **S11**.

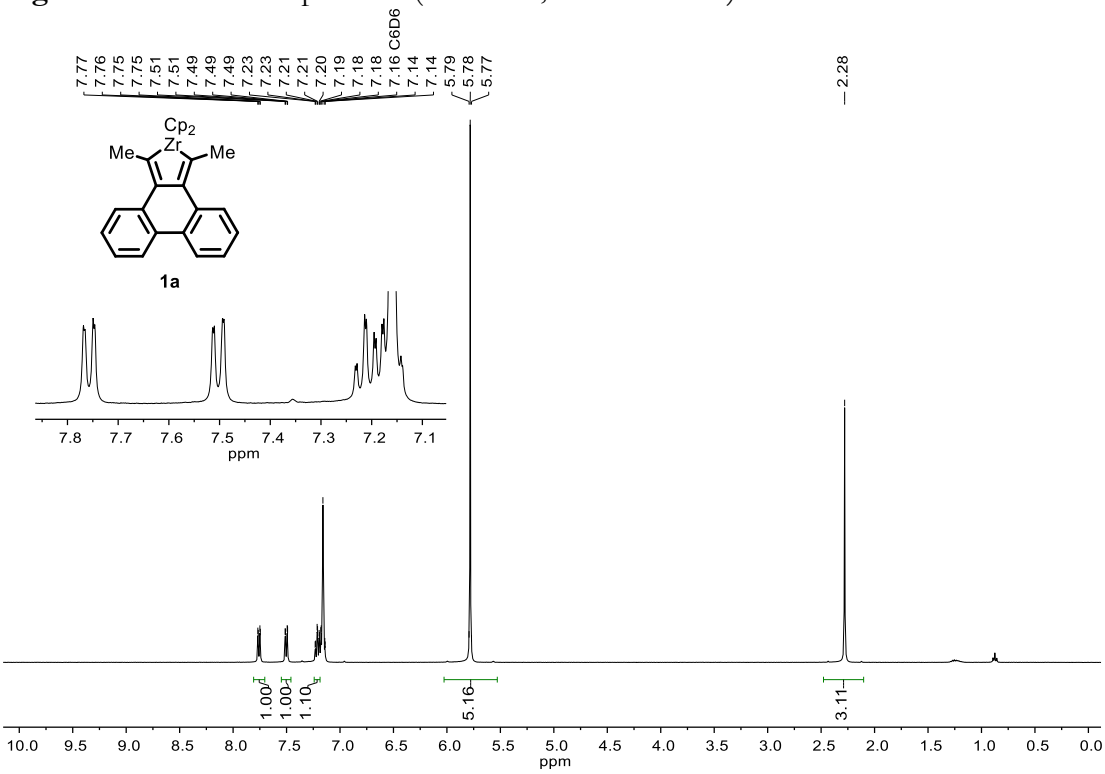

Figure S16. ^{1}H NMR Spectrum (400 MHz, Benzene-d_6) of **1a**.

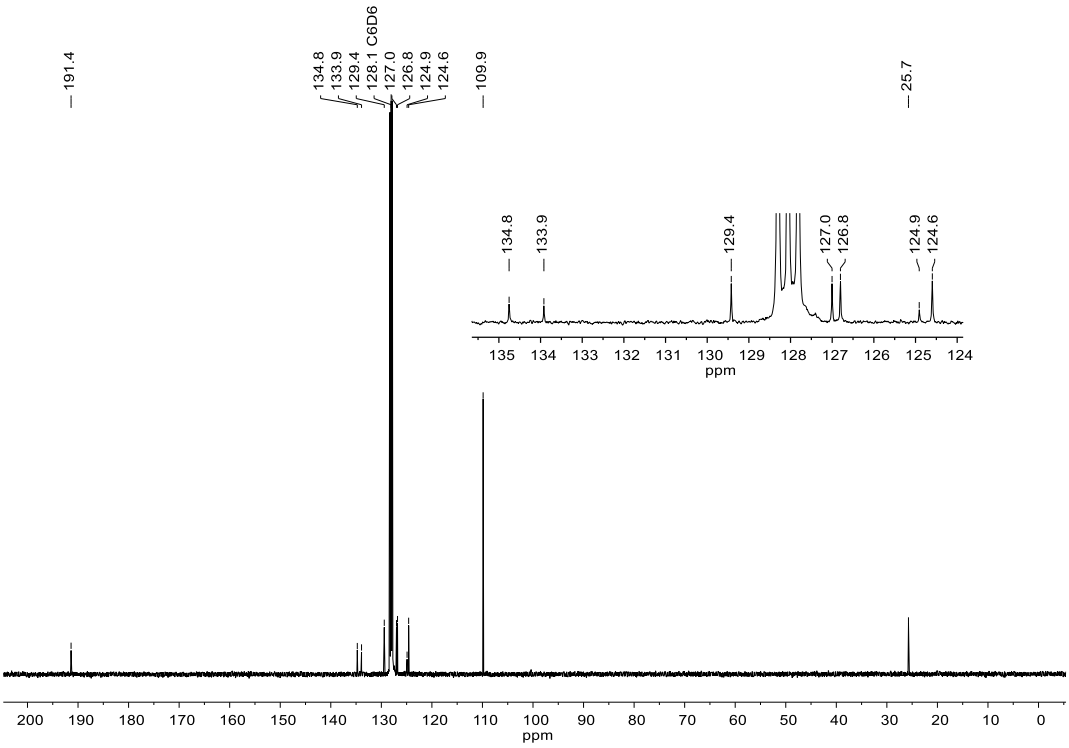

Figure S17. ^{13}C NMR Spectrum (151 MHz, Benzene-d_6) of **1a**.

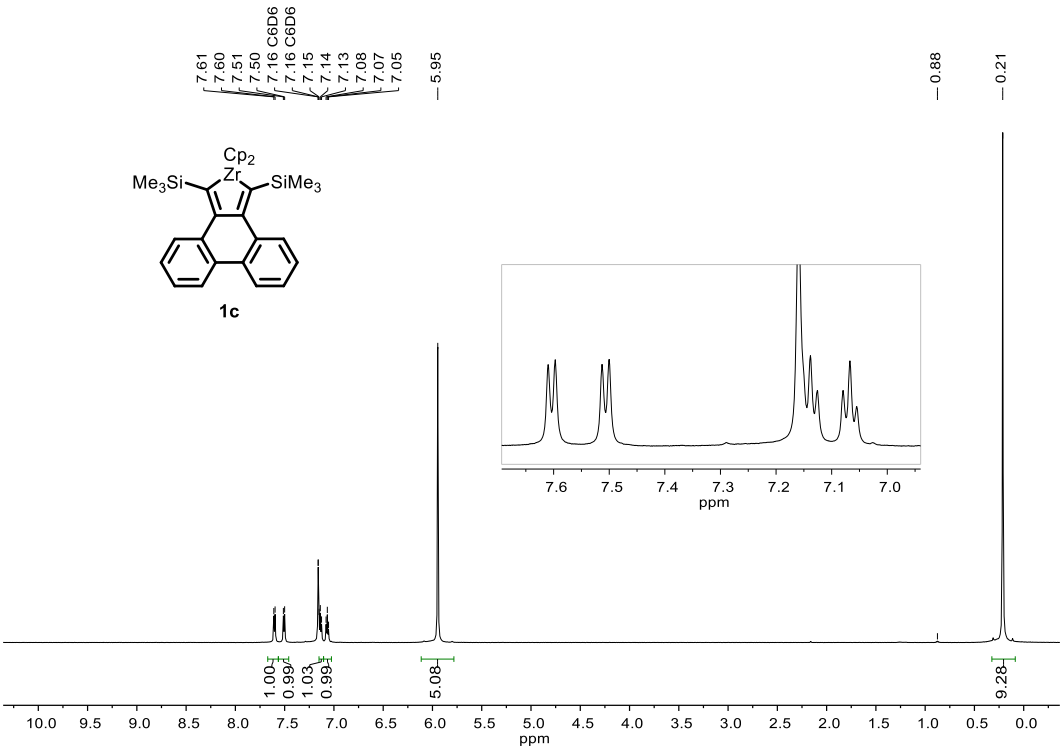

Figure S18. ^{1}H NMR Spectrum (600 MHz, Benzene-d_6) of **1c**.

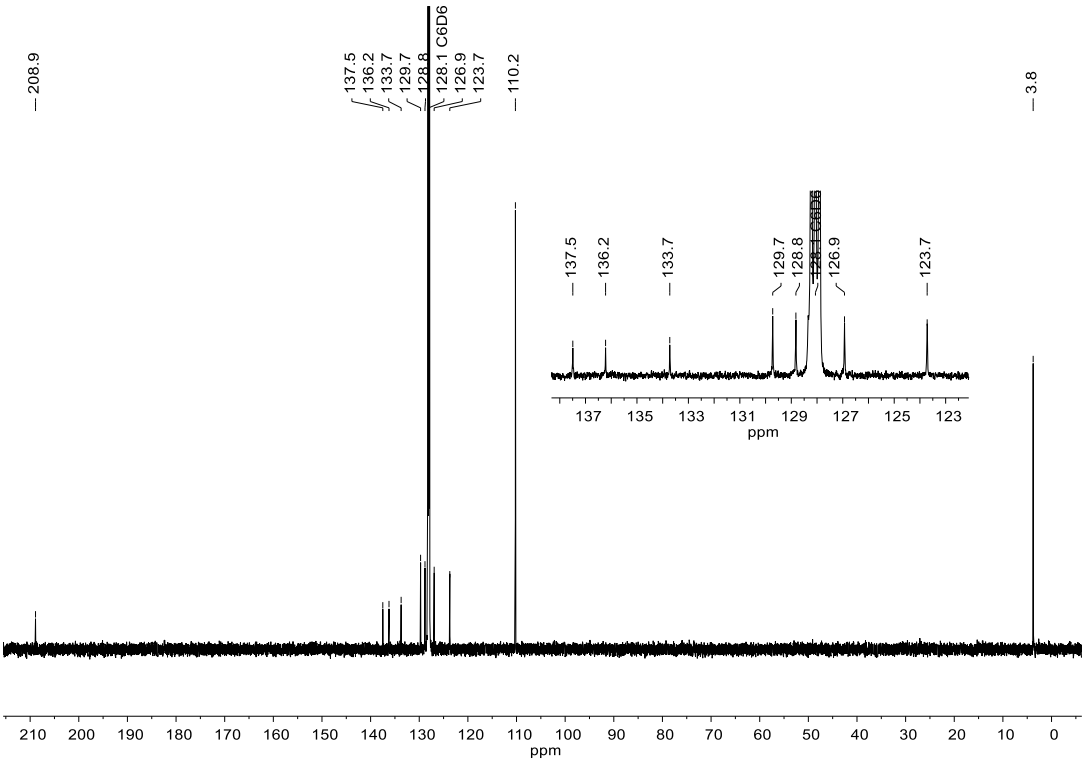

Figure S19. ^{13}C NMR Spectrum (151 MHz, Benzene-d_6) of **1c**.

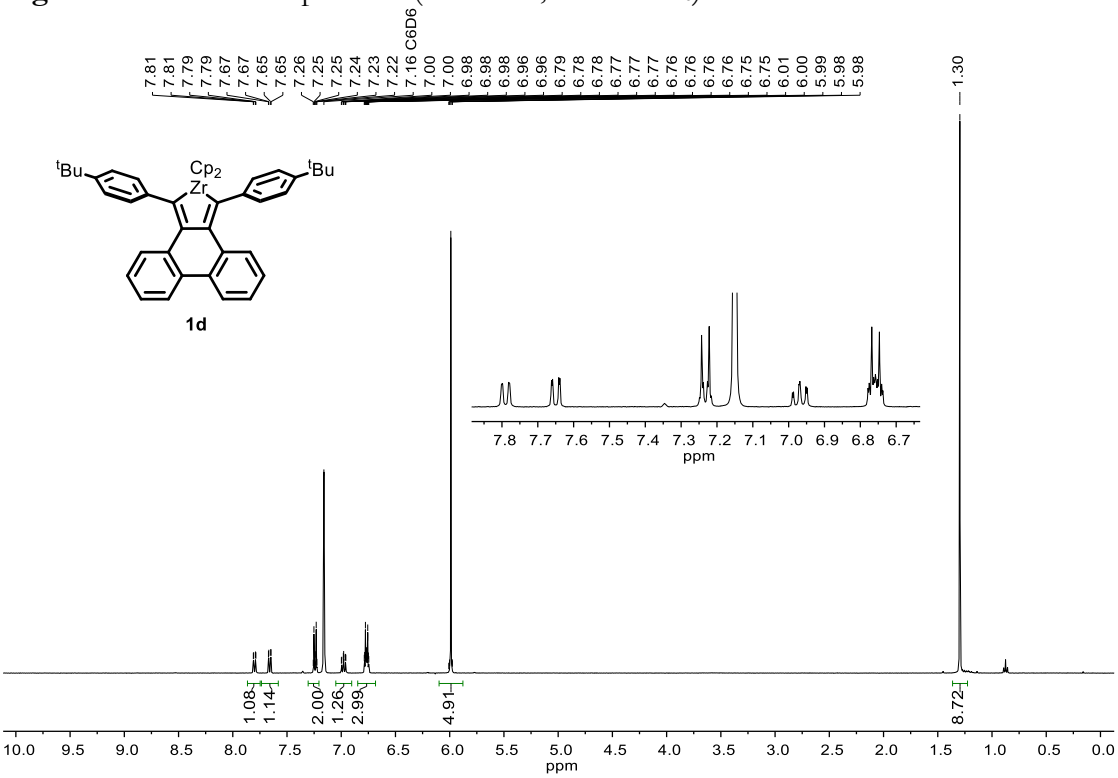

Figure S20. ^{1}H NMR Spectrum (400 MHz, Benzene-d_6) of **1d**.

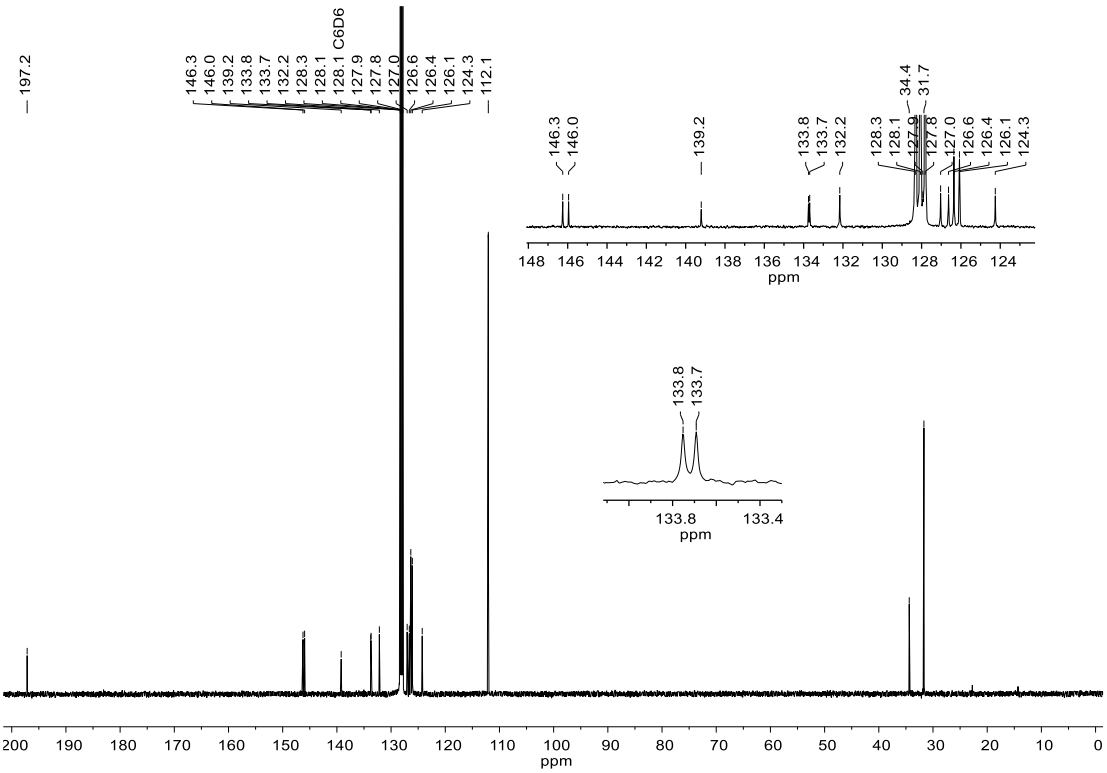

Figure S21. ^{13}C NMR Spectrum (101 MHz, Benzene-d_6) of **1d**.

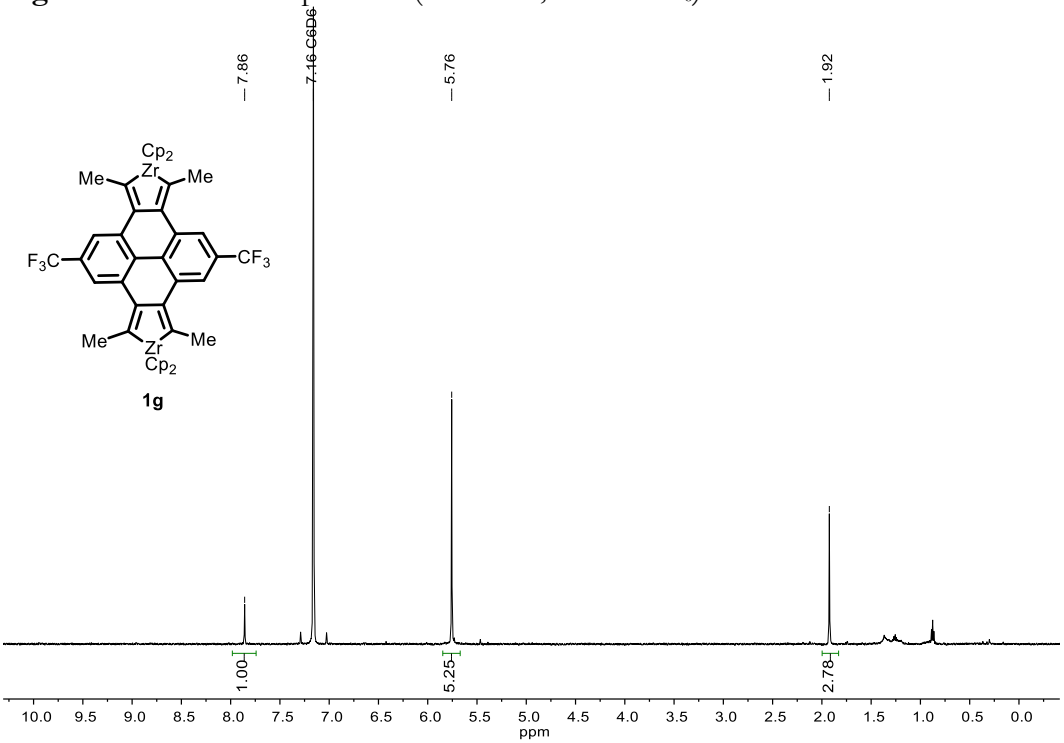

Figure S22. ^{1}H NMR Spectrum (600 MHz, Benzene-d_6) of **1g**.

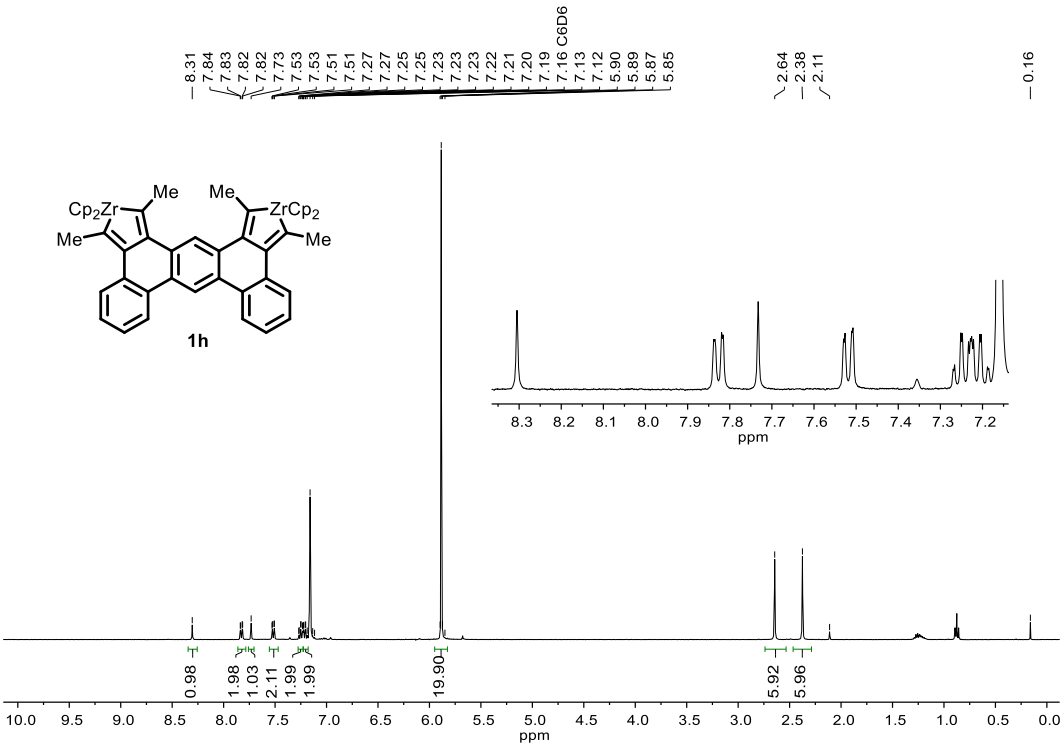

Figure S23. ^{1}H NMR Spectrum (400 MHz, Benzene-d_6) of **1h**.

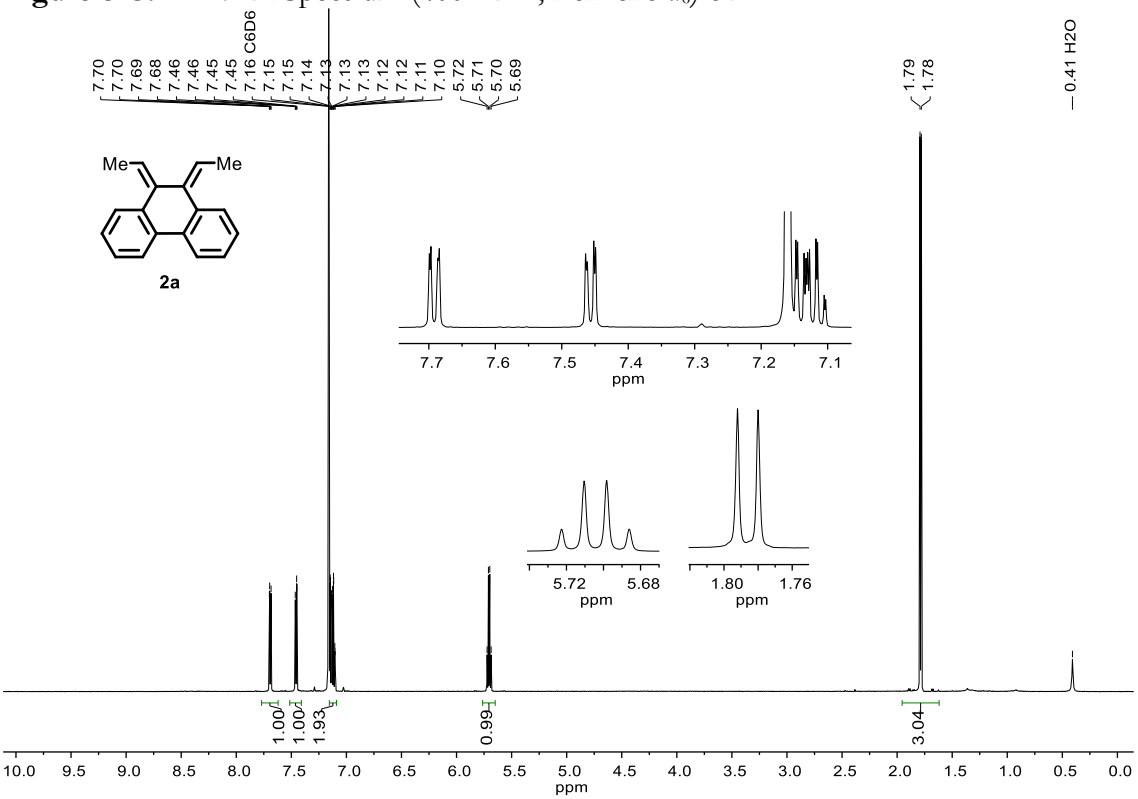

Figure S24. ^{1}H NMR Spectrum (600 MHz, Benzene-d_6) of **2a**.

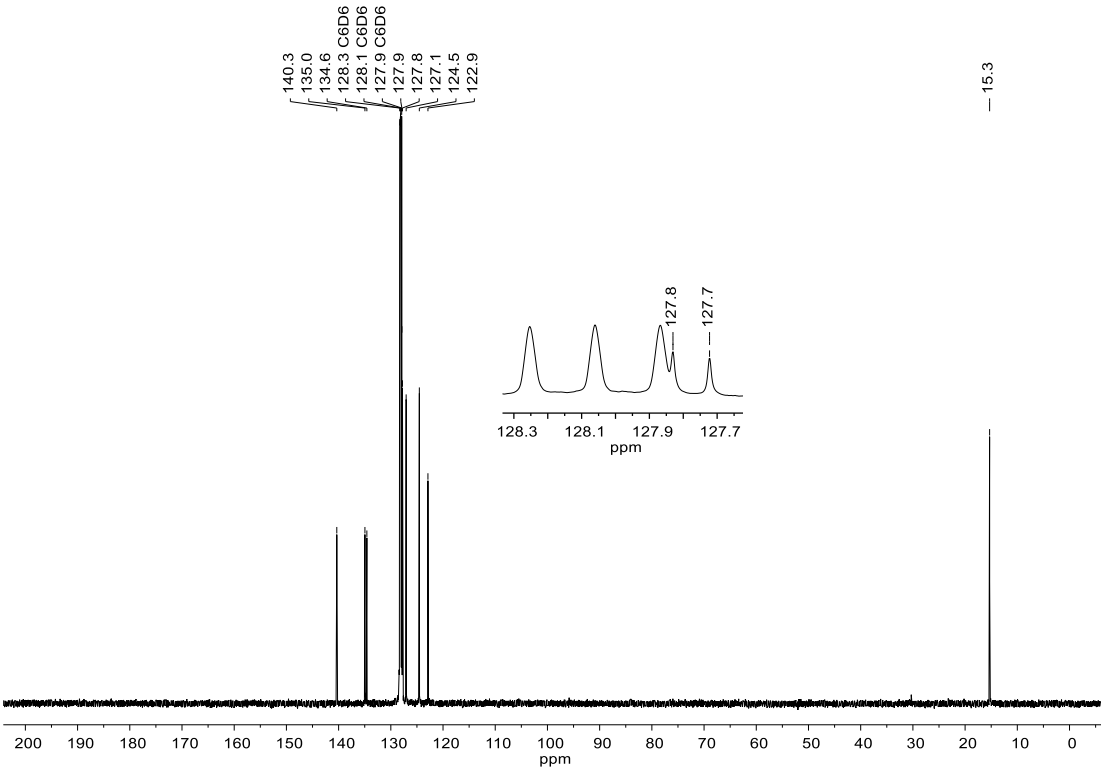

Figure S25. ^{13}C NMR Spectrum (151 MHz, Benzene-d_6) of **2a**.

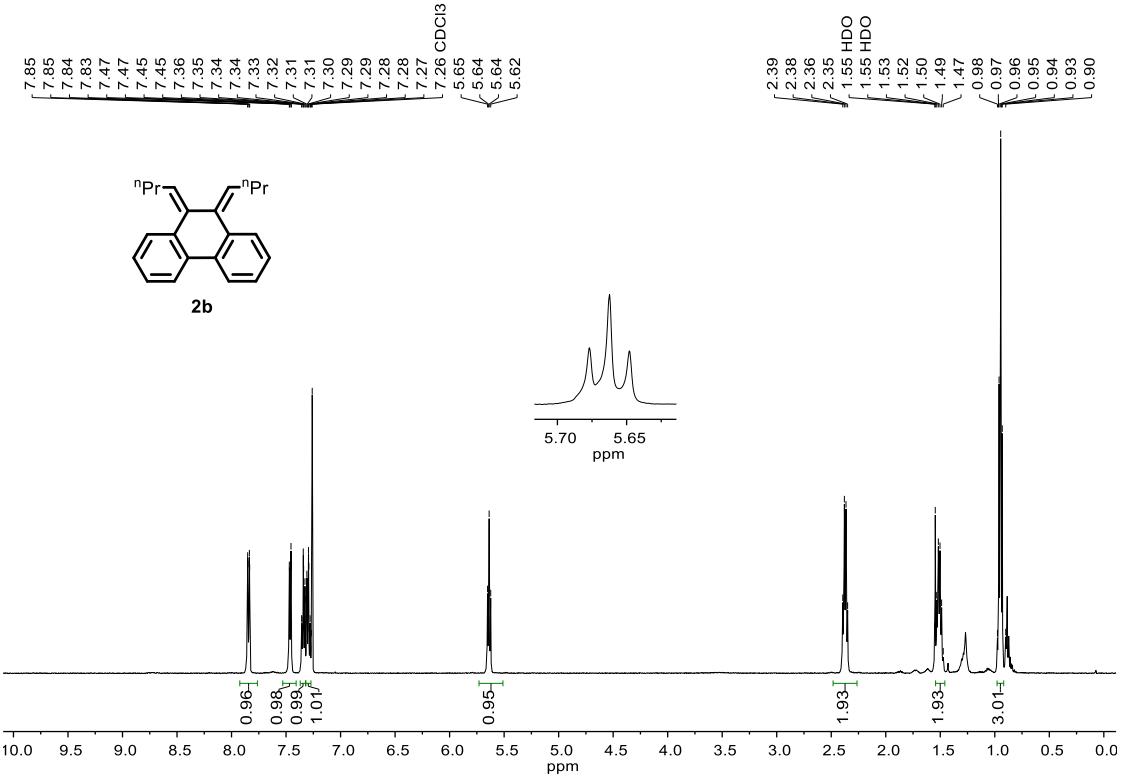

Figure S26. ^{1}H NMR Spectrum (400 MHz, Chloroform-*d*) of **2b**.

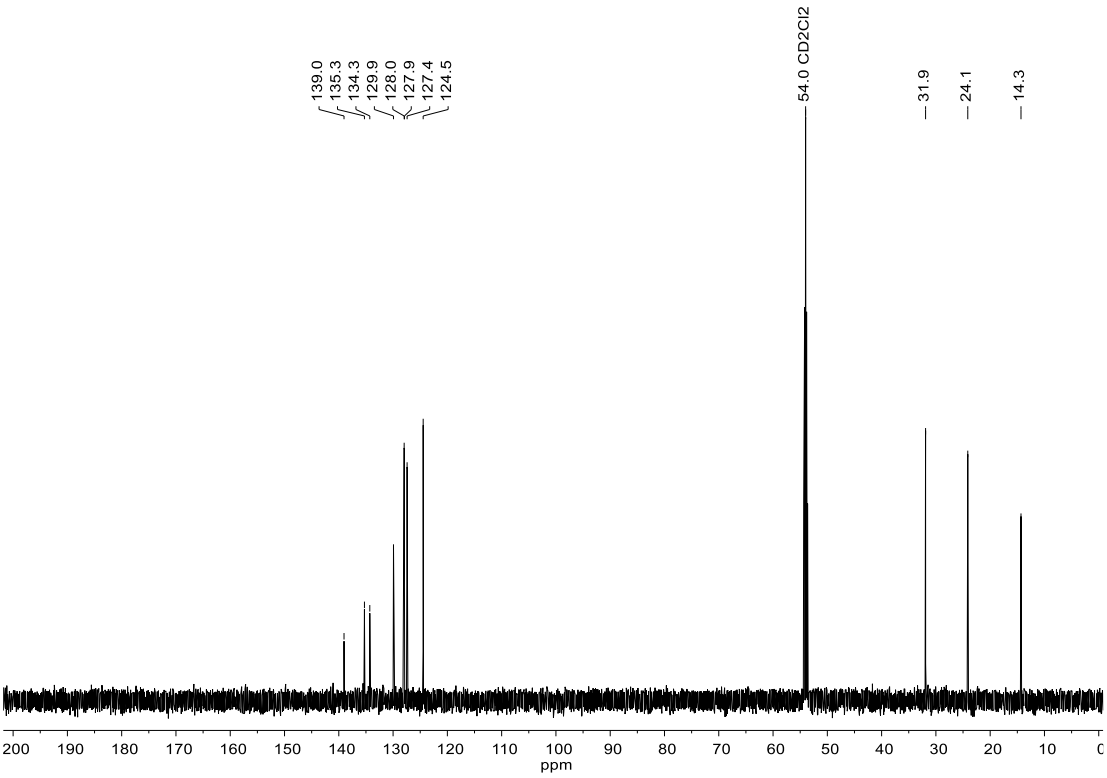

Figure S27. ^{13}C NMR Spectrum (151 MHz, Dichloromethane-d_2) of **2b**.

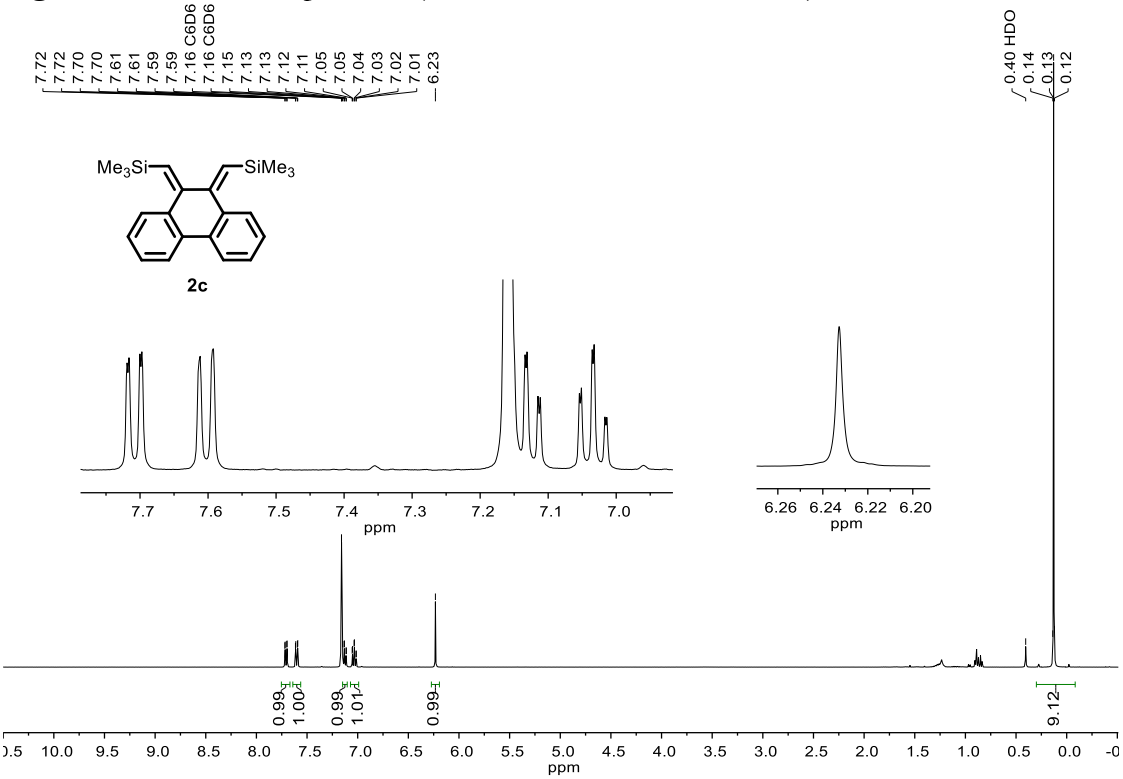

Figure S28. ^{1}H NMR Spectrum (400 MHz, Benzene-d_6) of **2c**.

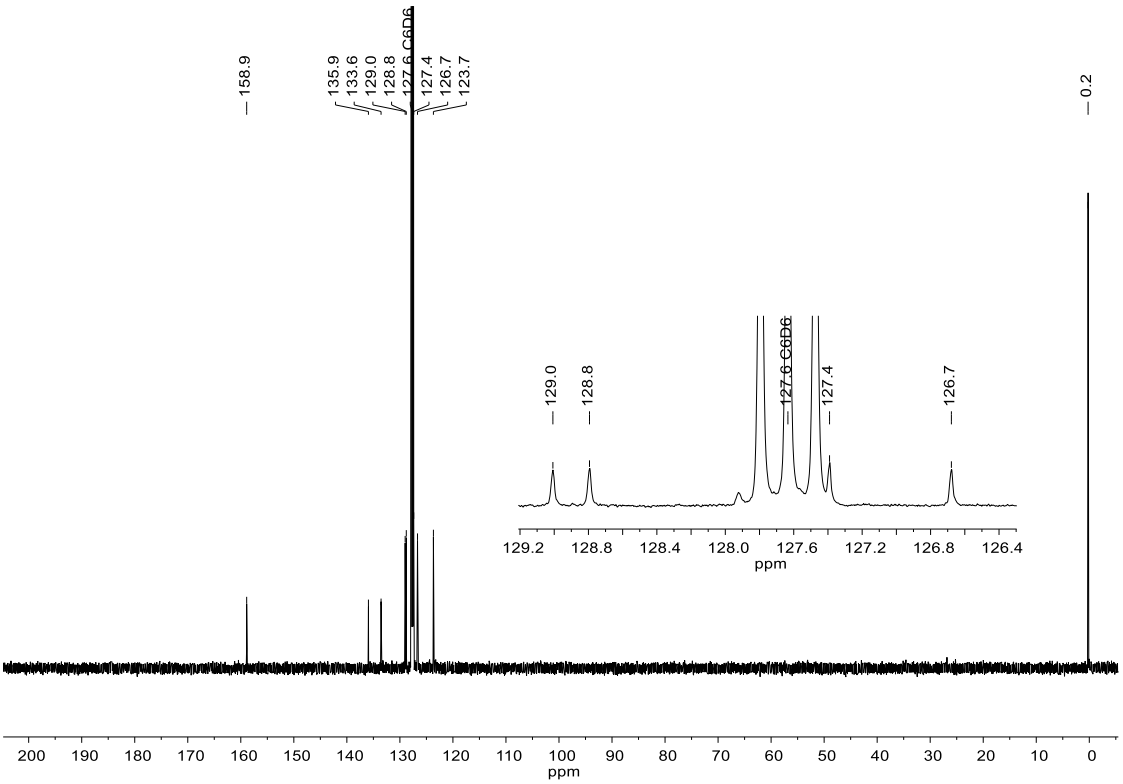

Figure S29. ^{13}C NMR Spectrum (151 MHz, Benzene-d_6) of **2c**.

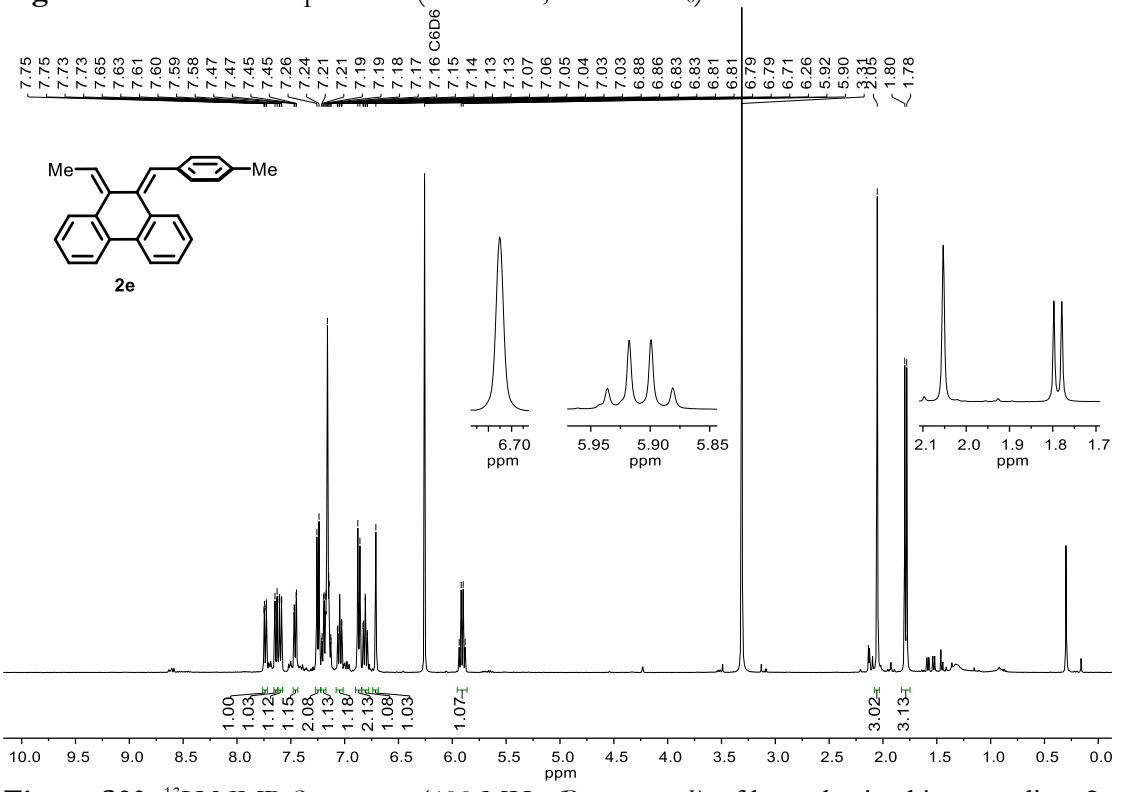

Figure S30. ^{13}H NMR Spectrum (400 MHz, Benzene-d_6) of hypothesized intermediate **2e**.

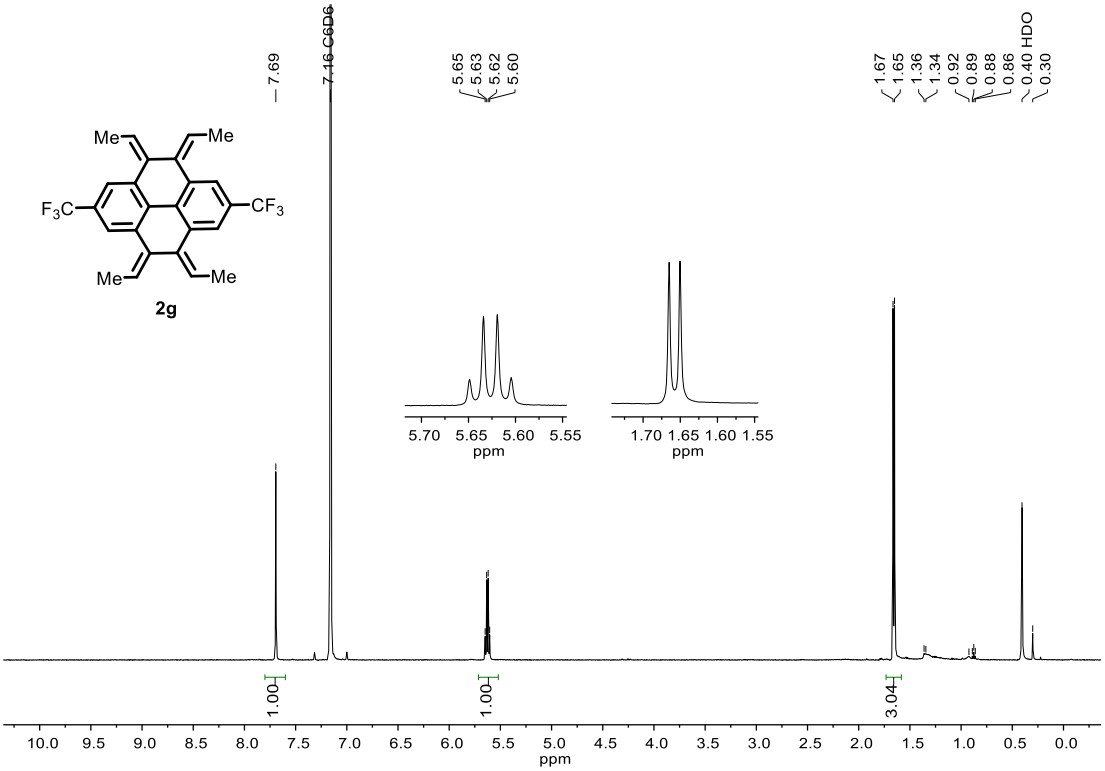

Figure S31. ^{1}H NMR Spectrum (600 MHz, Benzene-d_6) of **2g**.

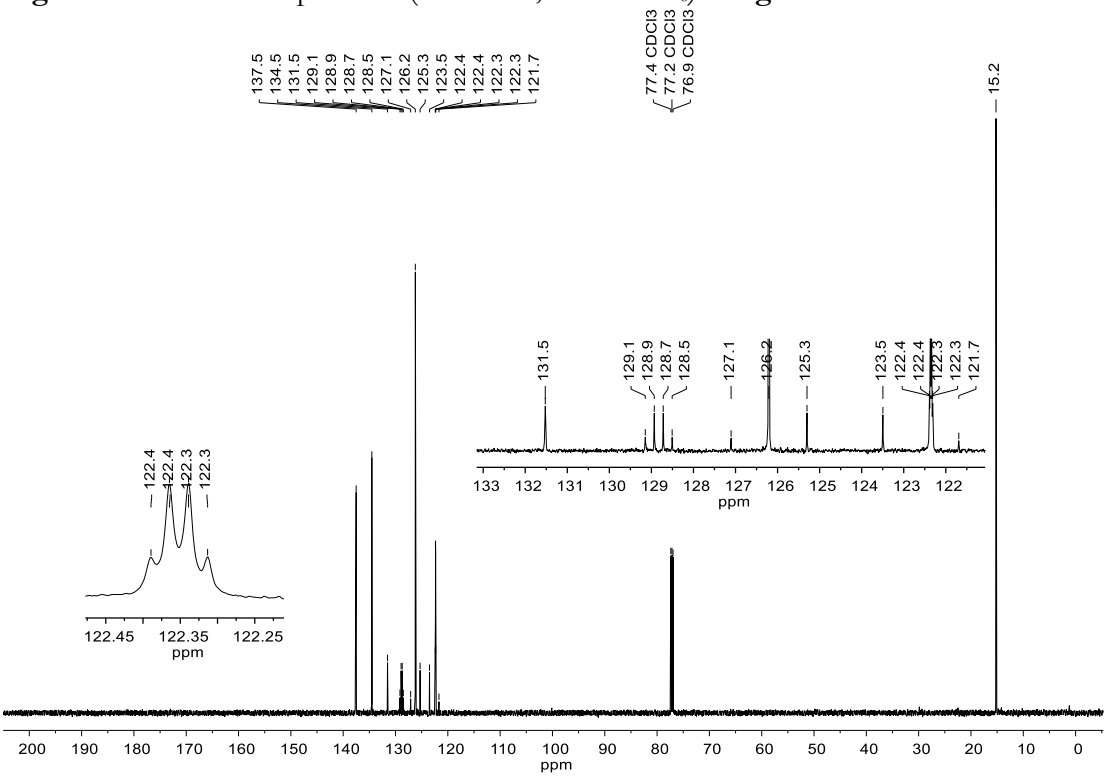

Figure S32. ^{13}C NMR Spectrum (151 MHz, Chloroform-*d*) of **2g**.

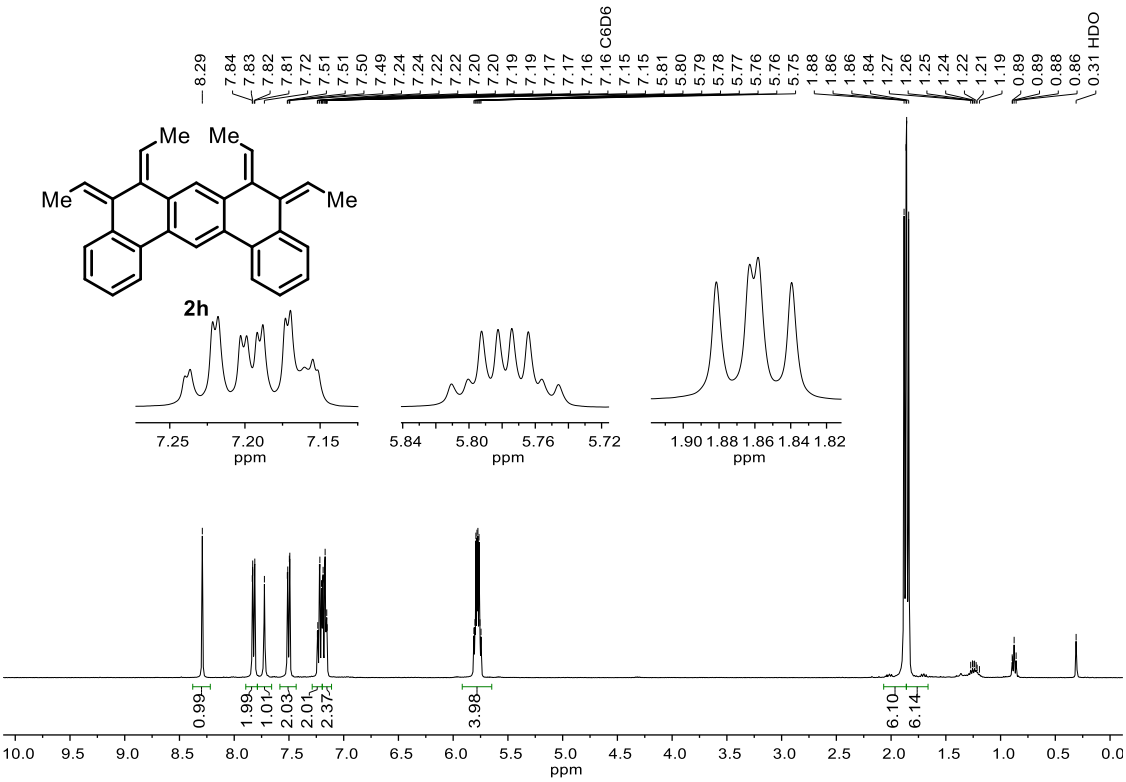

Figure S33. ^{1}H NMR Spectrum (400 MHz, Benzene-d_6) of **2h**.

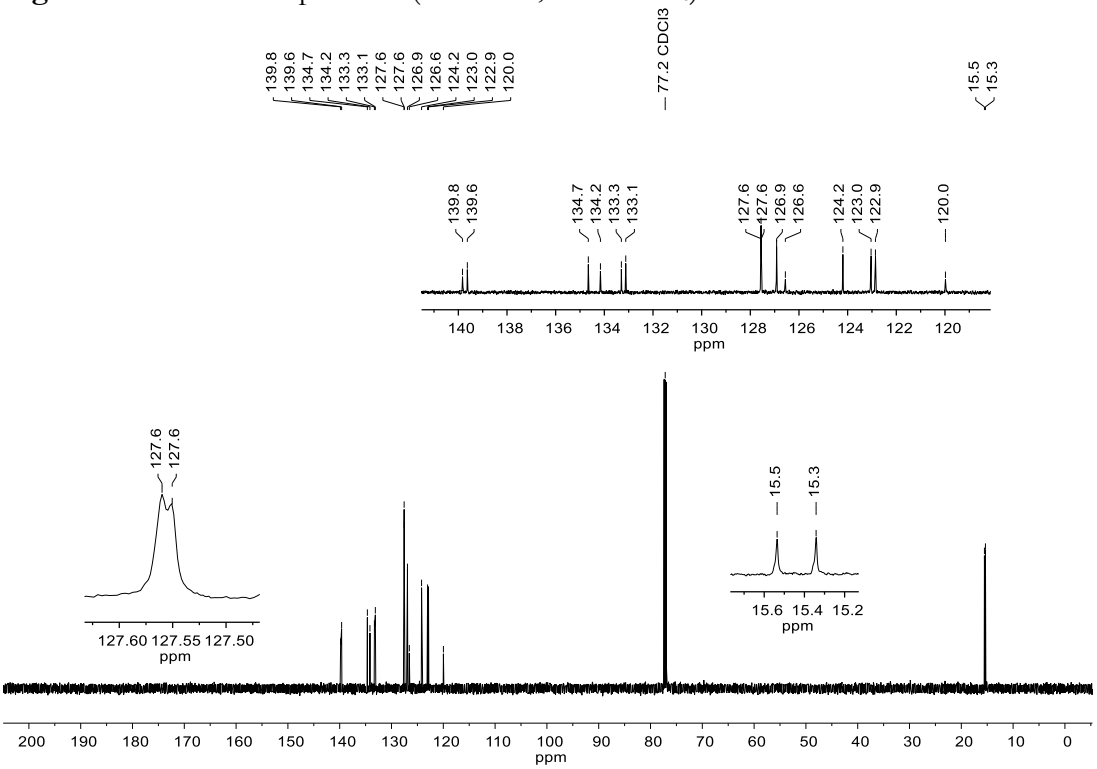

Figure S34. ^{13}C NMR Spectrum (151 MHz, Chloroform-*d*) of **2h**.

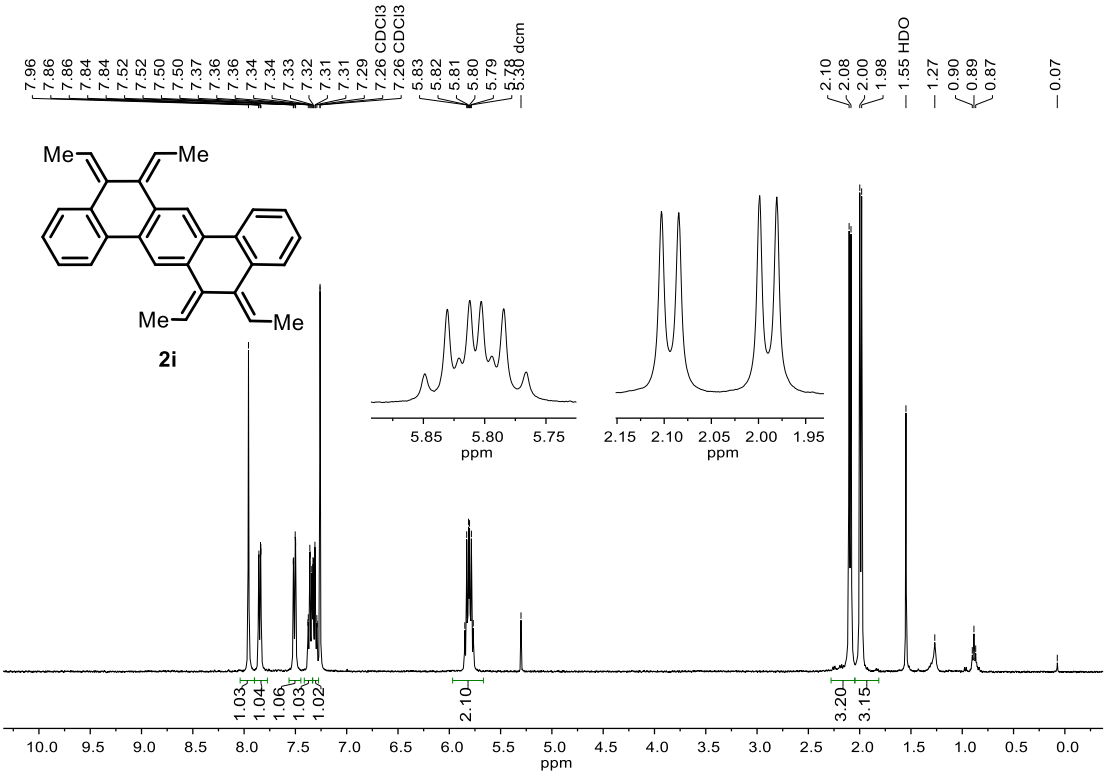

Figure S35. ^{1}H NMR Spectrum (400 MHz, Chloroform-*d*) of **2i**.

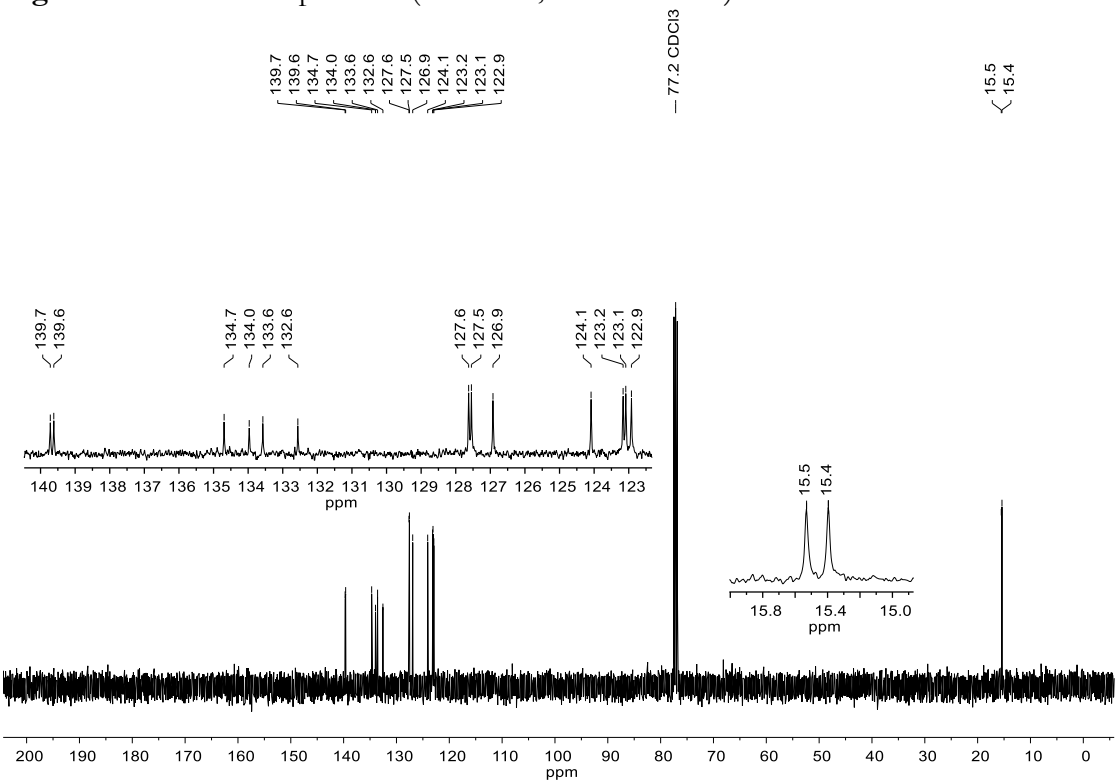

Figure S36. ^{13}C NMR Spectrum (101 MHz, Chloroform-*d*) of **2i**.

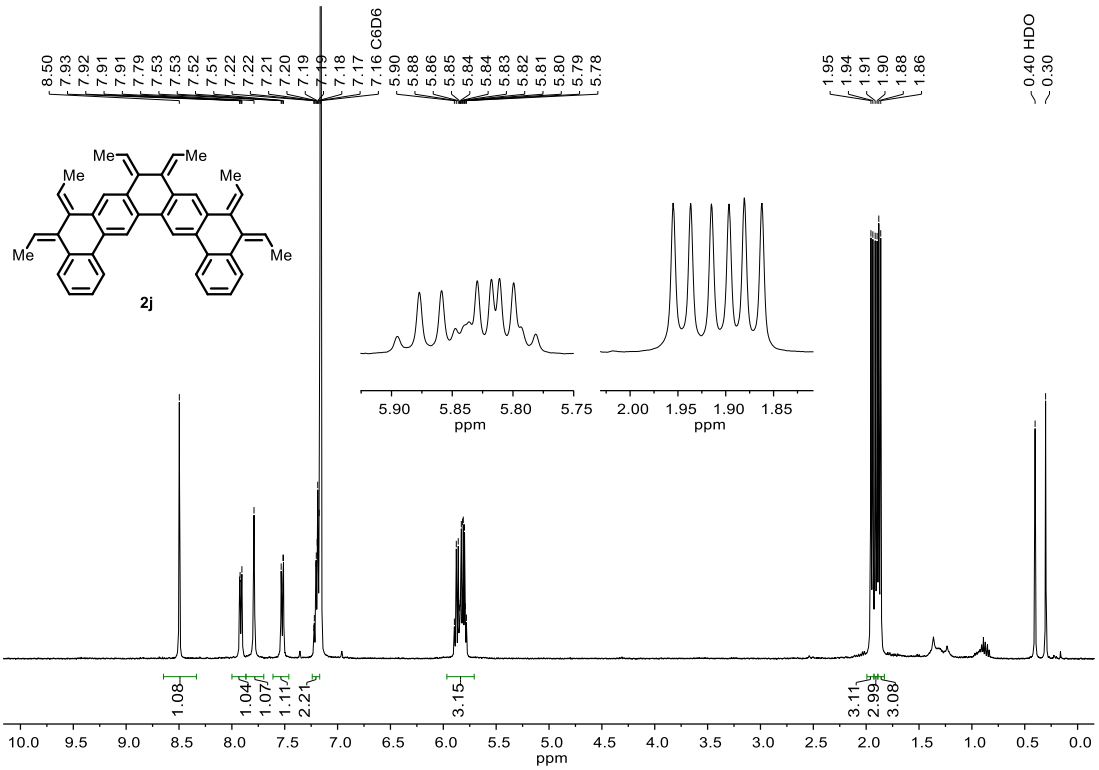

Figure S37. ^{1}H NMR Spectrum (400 MHz, Benzene-d_6) of **2j**.

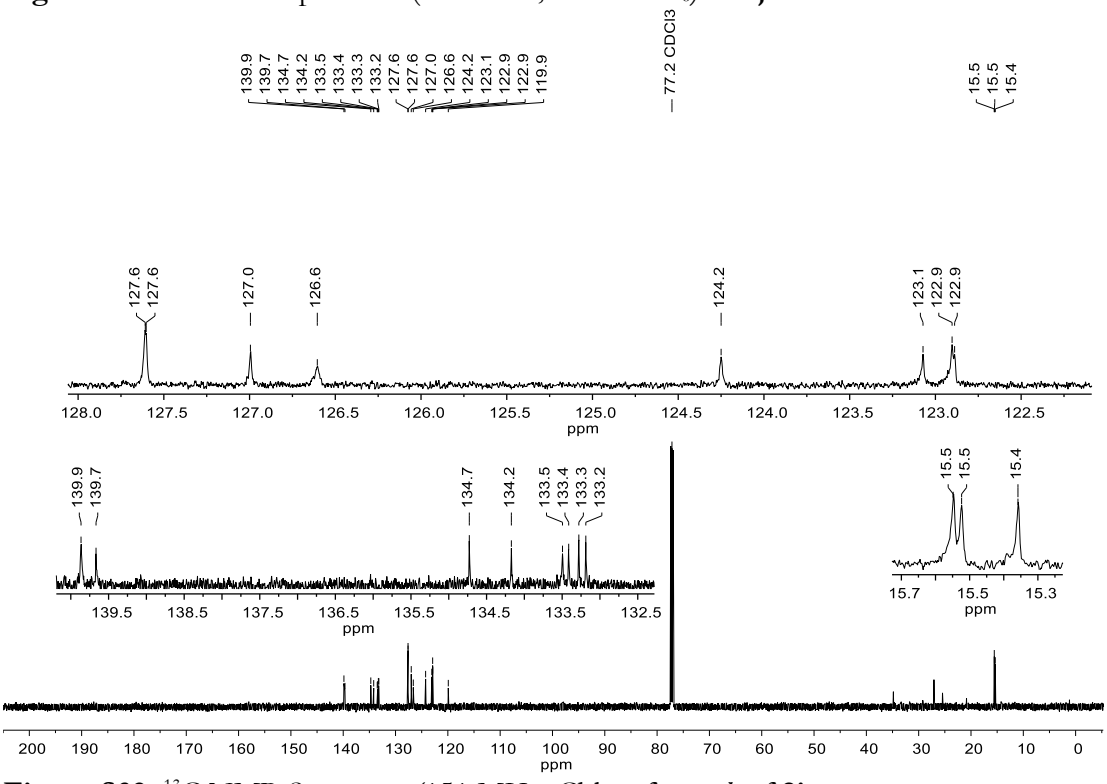

Figure S38. ^{13}C NMR Spectrum (151 MHz, Chloroform-*d*) of **2j**.

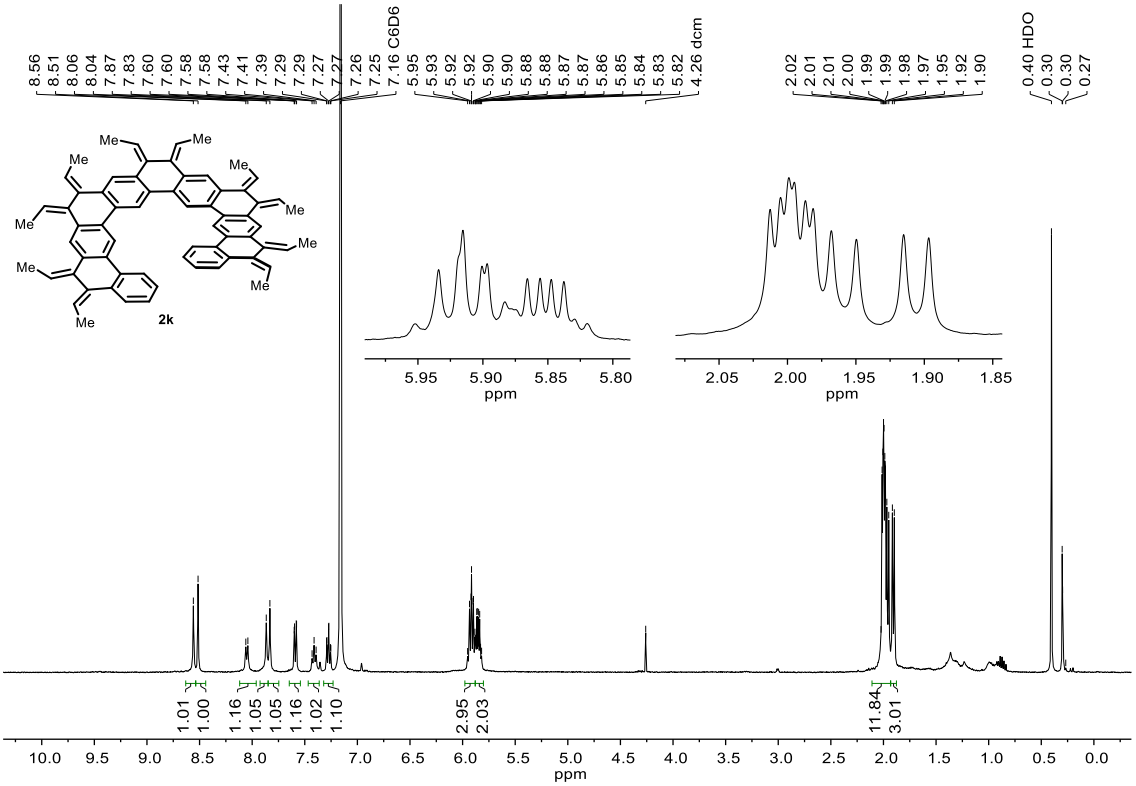

Figure S39. ^{13}H NMR Spectrum (400 MHz, Benzene-d_6) of **2k**.

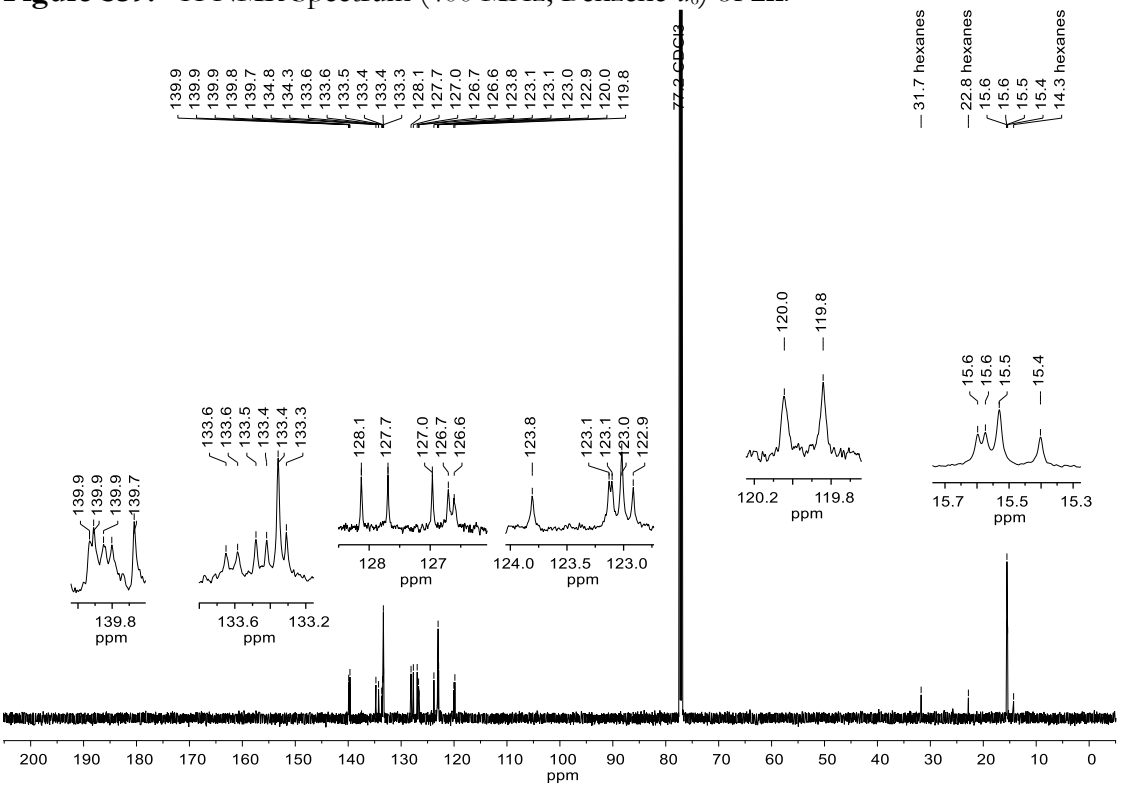

Figure S40. ^{13}C NMR Spectrum (151 MHz, Chloroform-*d*) of **2k**.

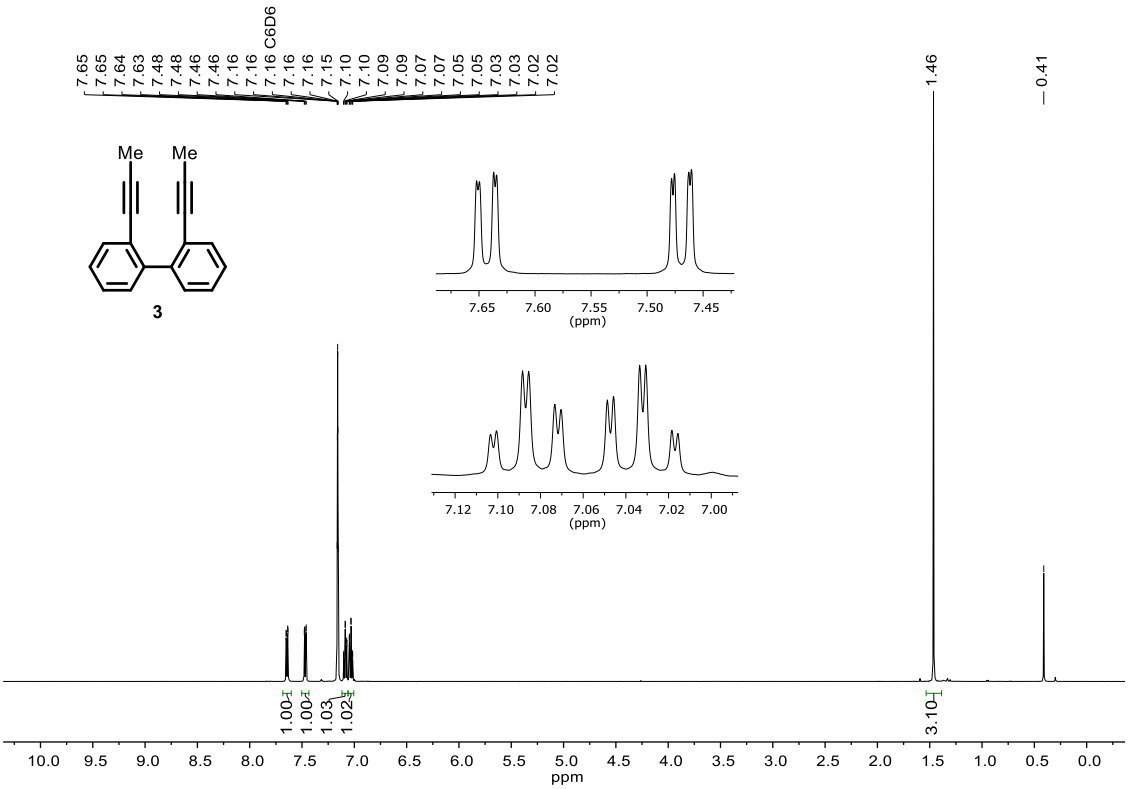

Figure S41. ^{1}H NMR Spectrum (500 MHz, Benzene-d_6) of **3**.

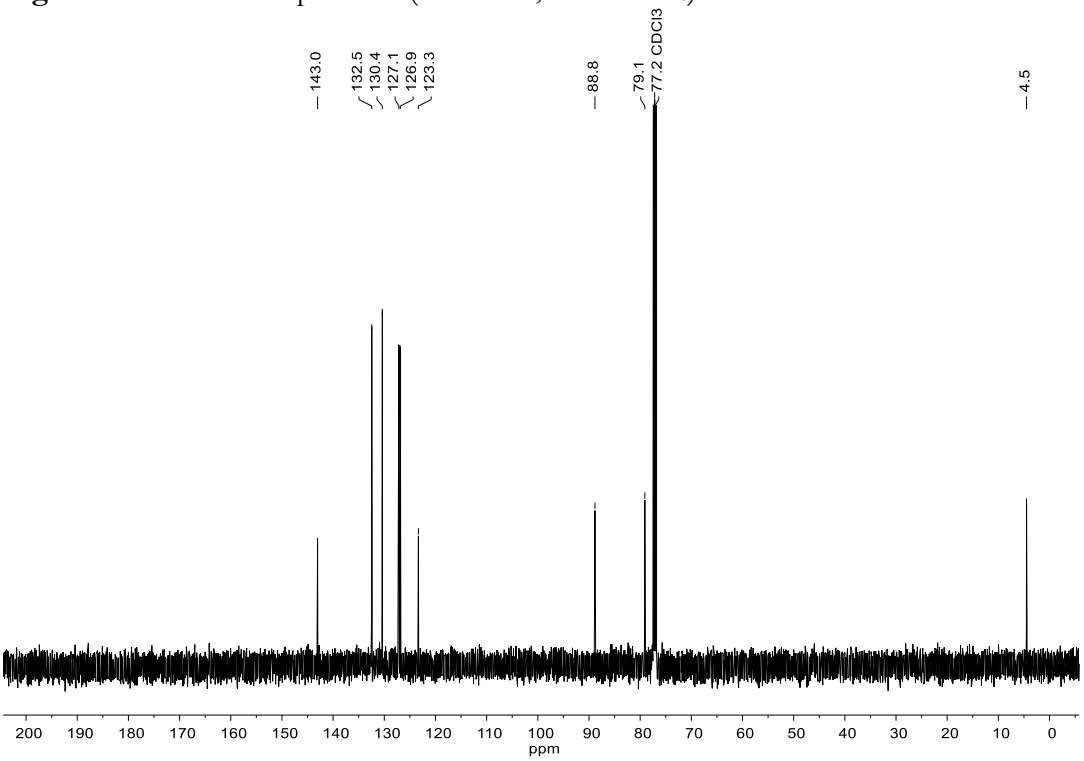

Figure S42. ^{13}C NMR Spectrum (126 MHz, Chloroform-*d*) of **3**.

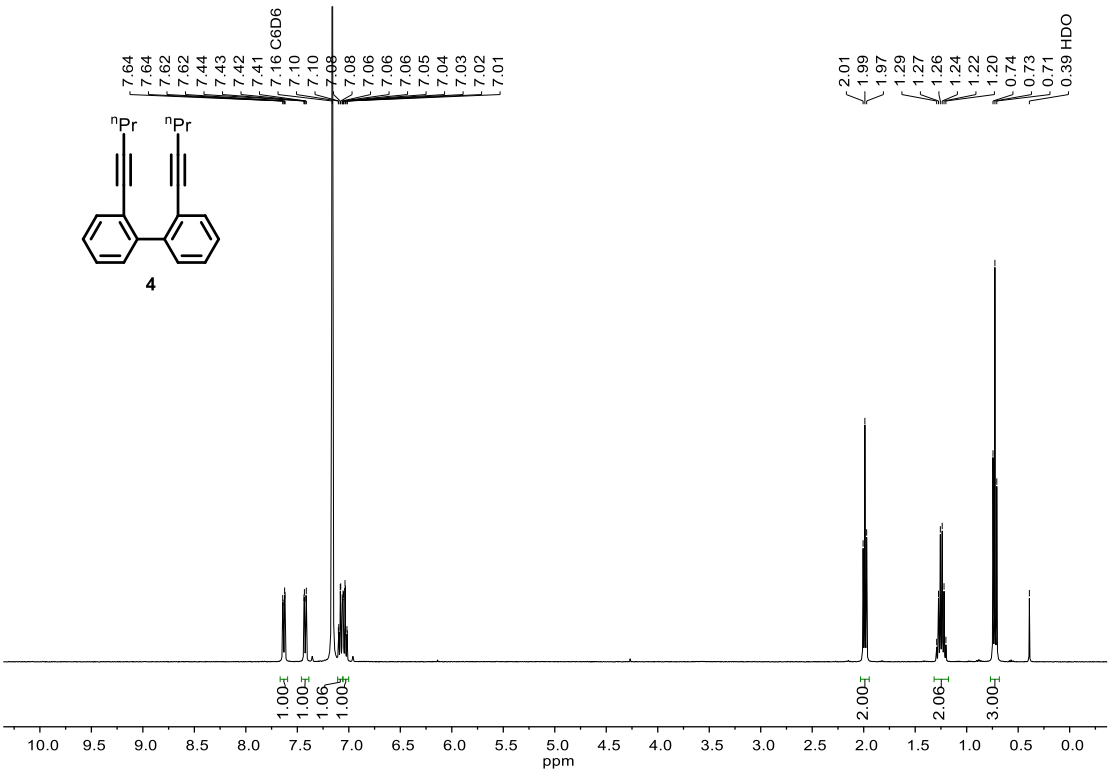

Figure S43. ^{1}H NMR Spectrum (400 MHz, Benzene-d_6) of **4**.

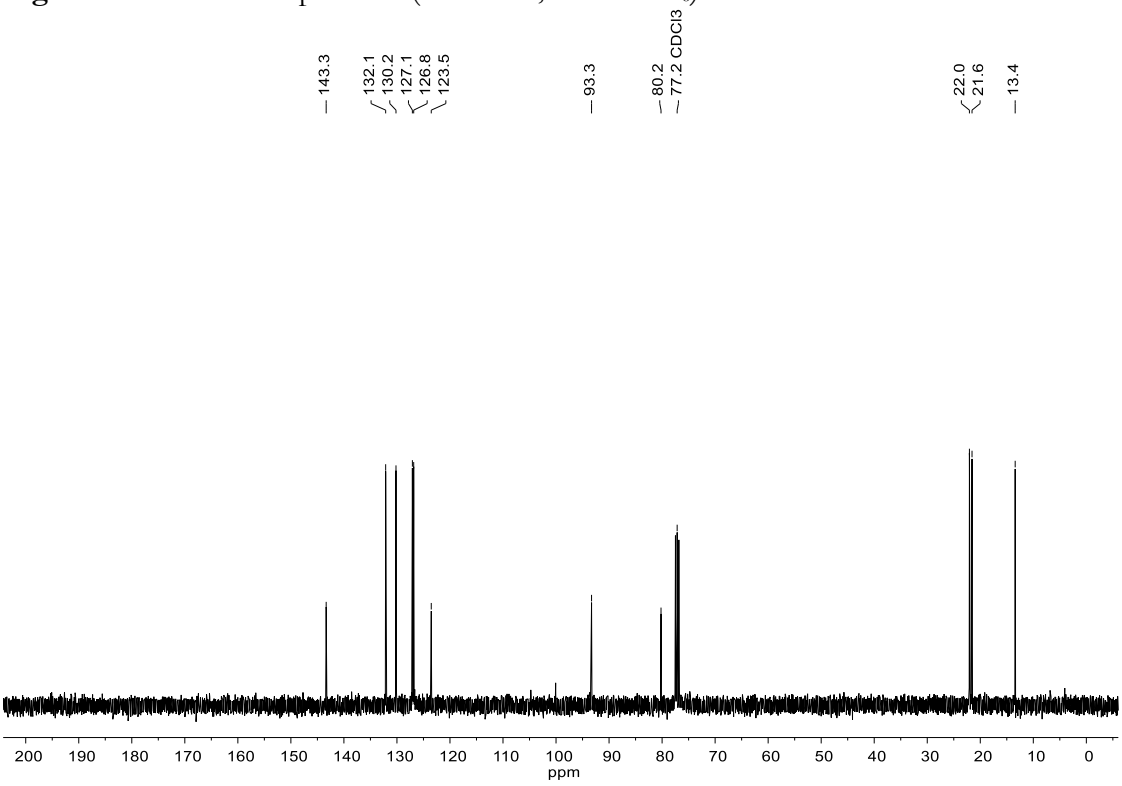

Figure S44. ^{13}C NMR Spectrum (101 MHz, Chloroform-*d*) of **4**.

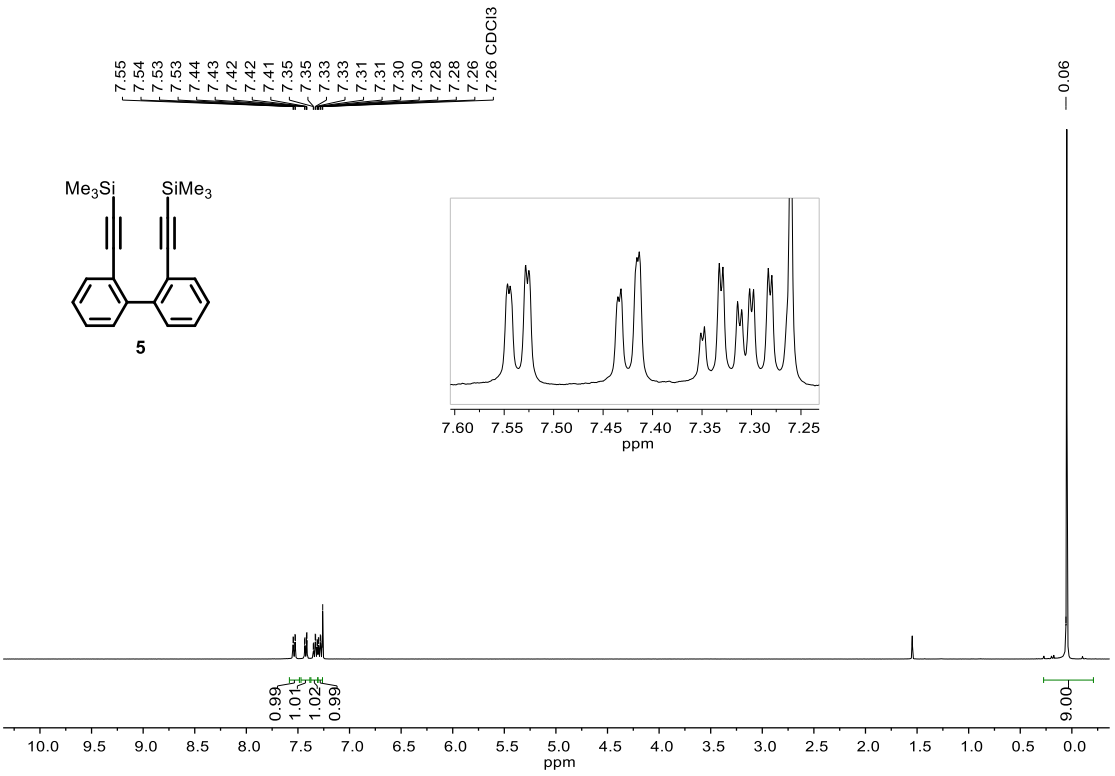

Figure S45. ^{1}H NMR Spectrum (400 MHz, Chloroform-*d*) of **5**.

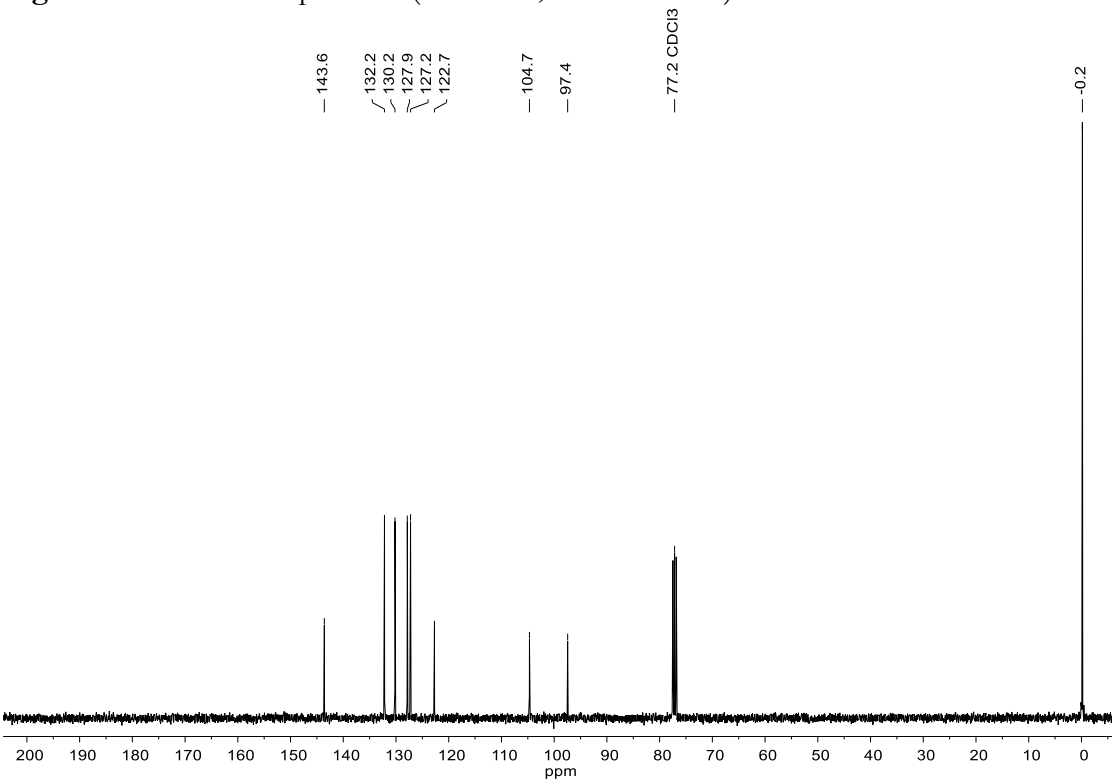

Figure S46. ^{13}C NMR Spectrum (101 MHz, Chloroform-*d*) of **5**.

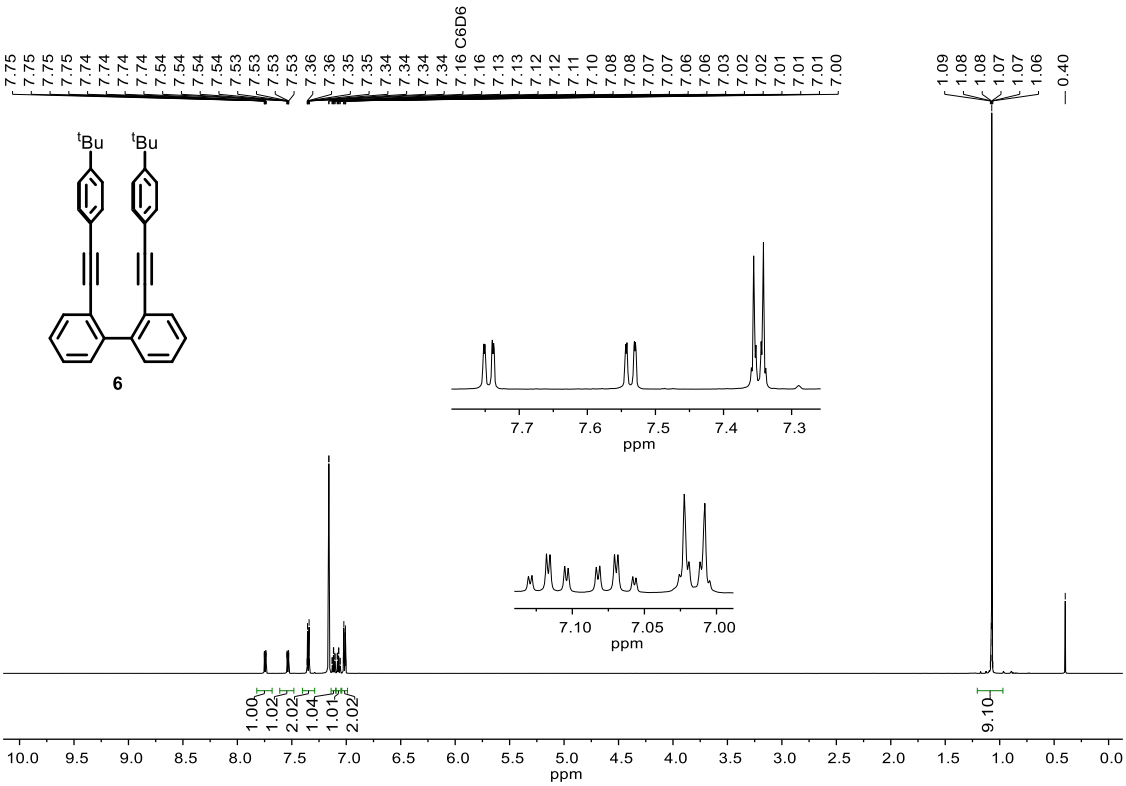

Figure S47. ^{1}H NMR Spectrum (600 MHz, Benzene-d_6) of **6**.

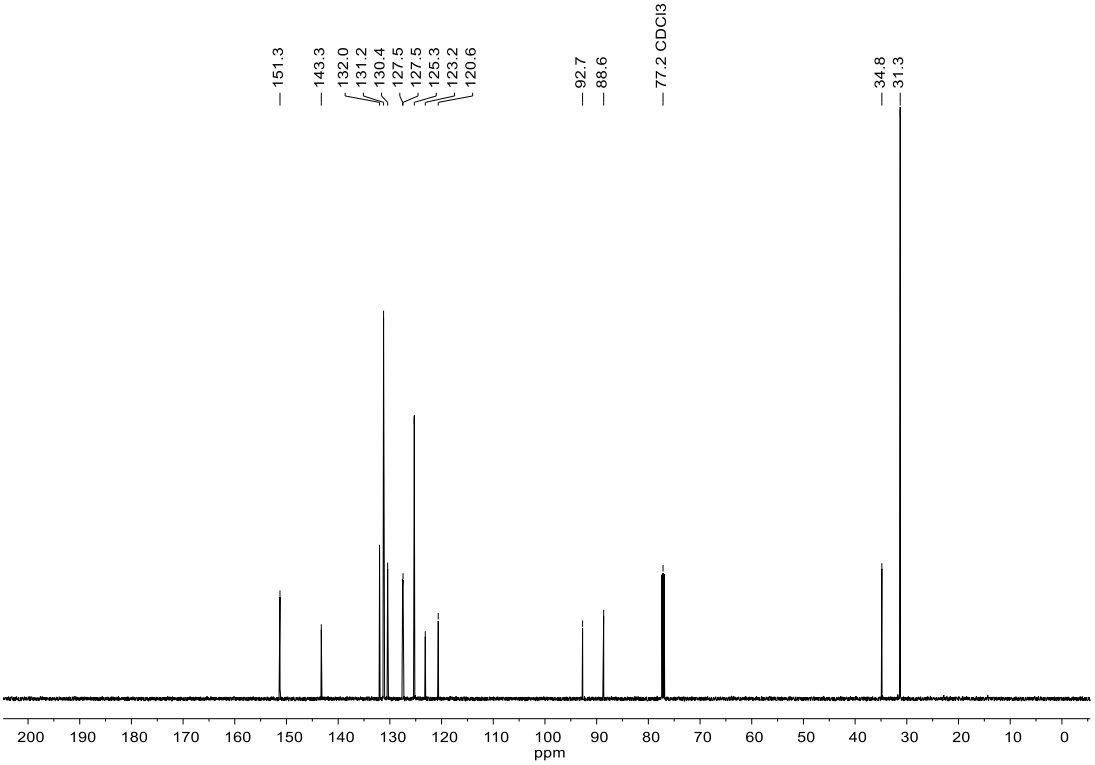

Figure S48. ^{13}C NMR Spectrum (151 MHz, Chloroform-*d*) of **6**.

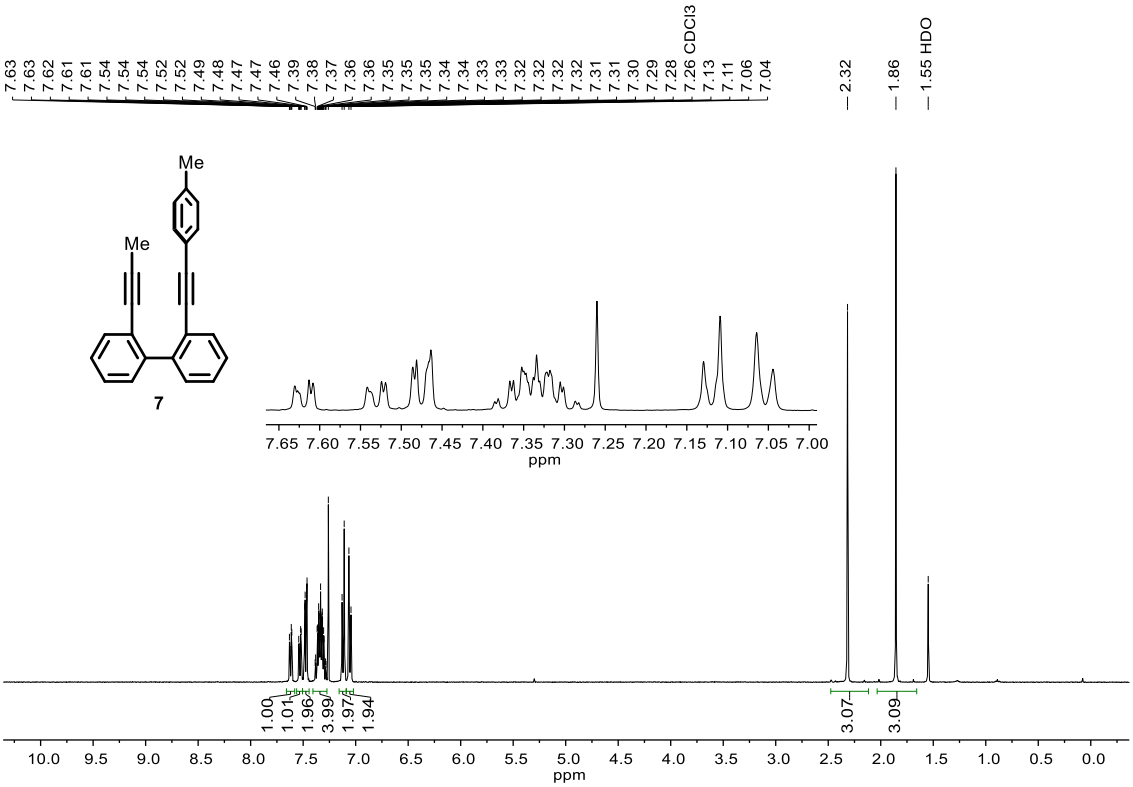

Figure S49. ^{1}H NMR Spectrum (400 MHz, Chloroform-*d*) of **7**.

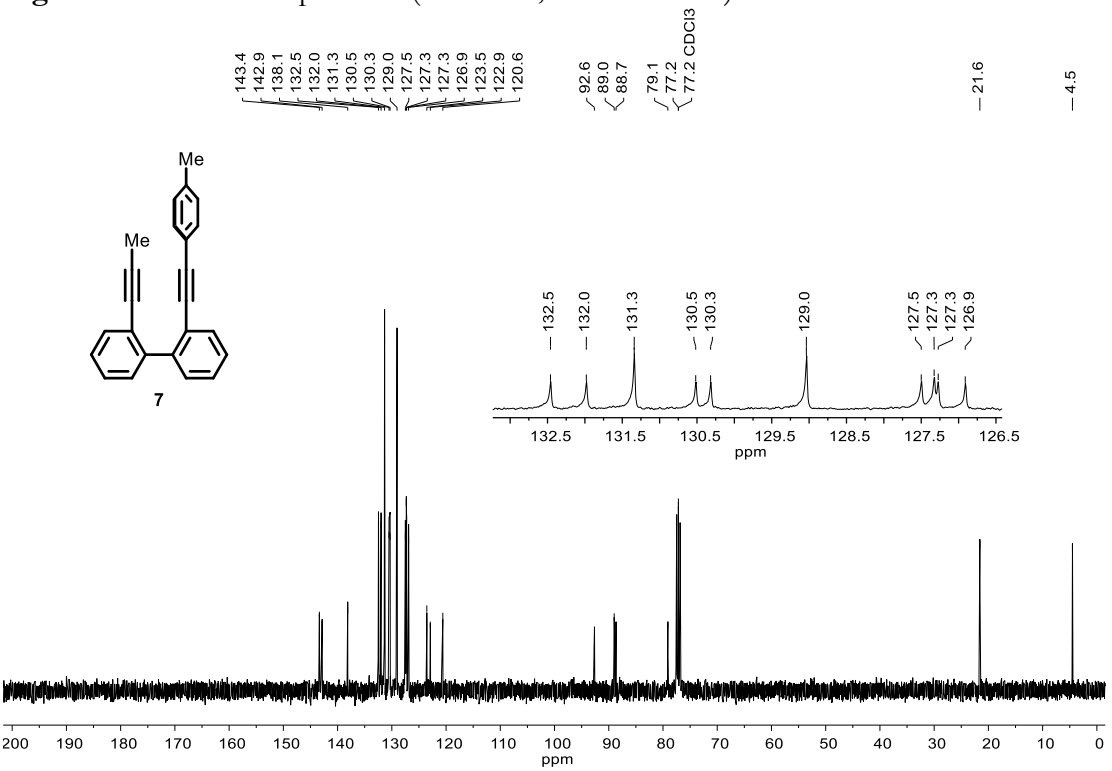

Figure S50. ^{13}C NMR Spectrum (101 MHz, Chloroform-*d*) of **7**.

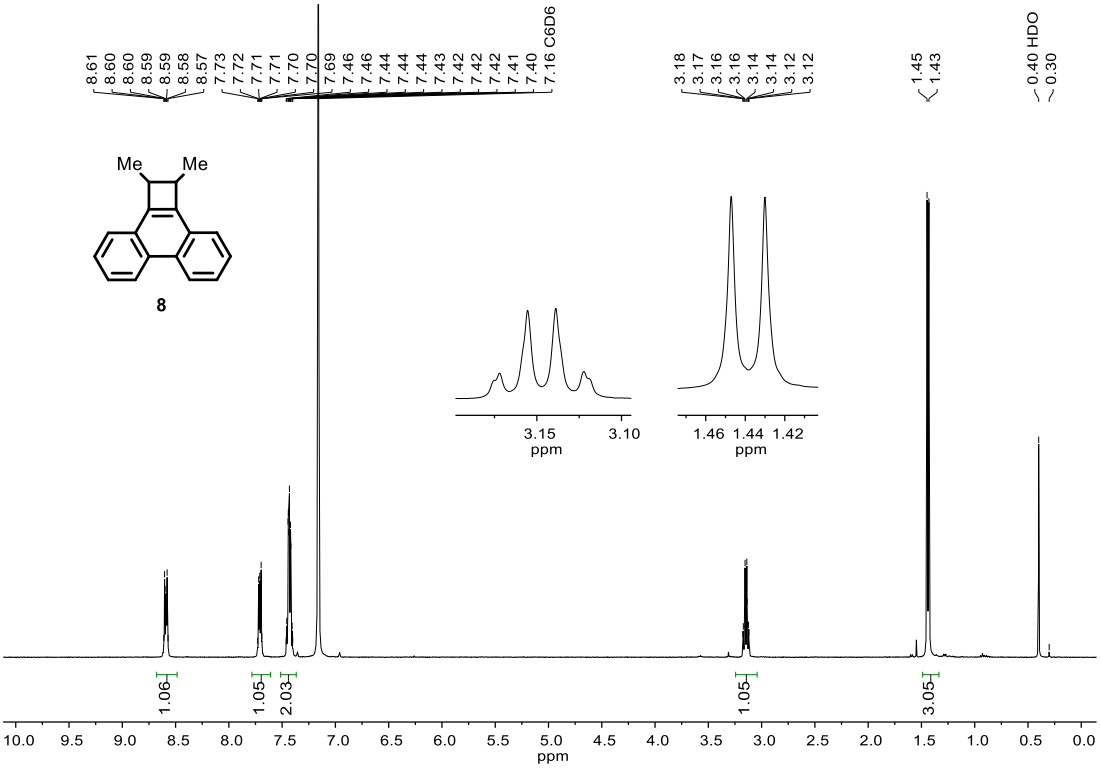

Figure S51. ^{1}H NMR Spectrum (400 MHz, Benzene-d_6) of **8**.

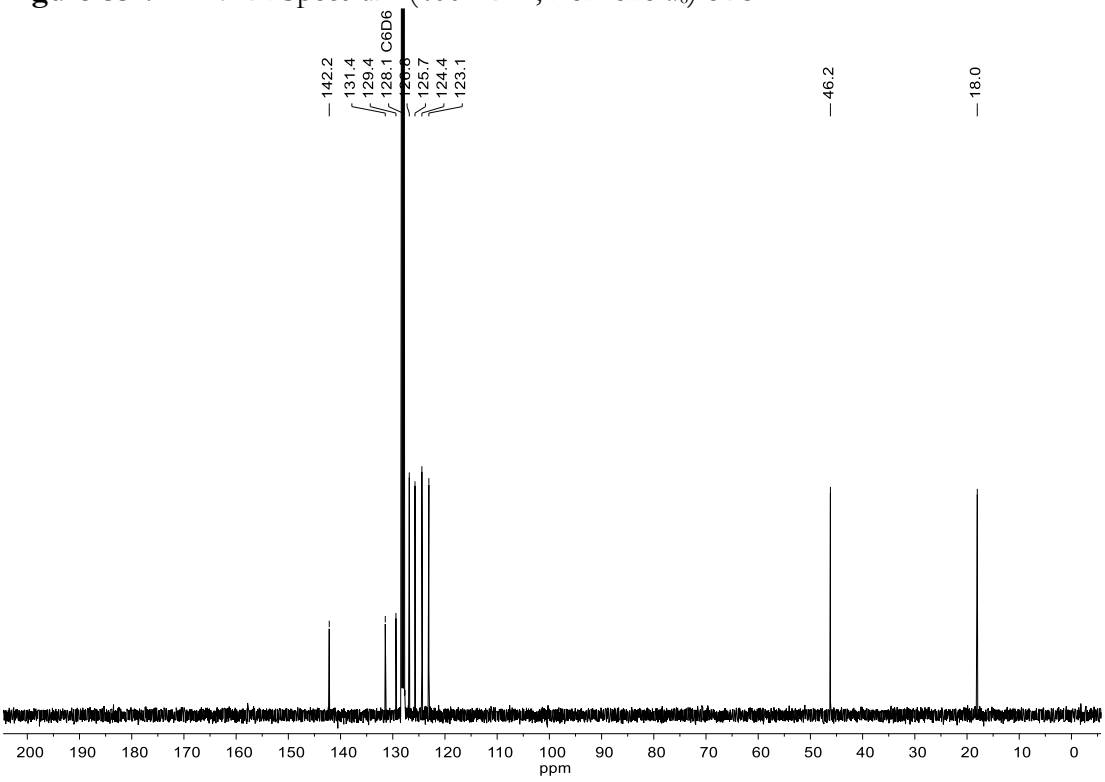

Figure S52. ^{13}C NMR Spectrum (101 MHz, Benzene-d_6) of **8**.

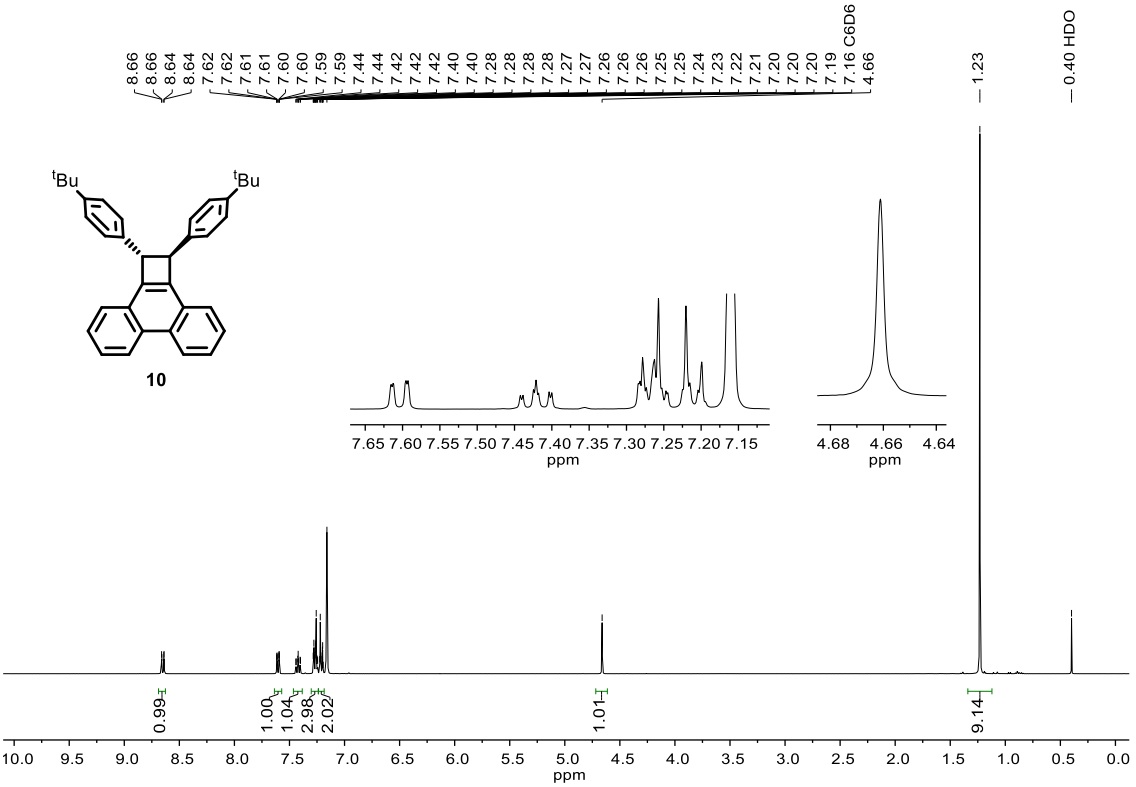

Figure S53. ^{1}H NMR Spectrum (400 MHz, Benzene-d_6) of **10**.

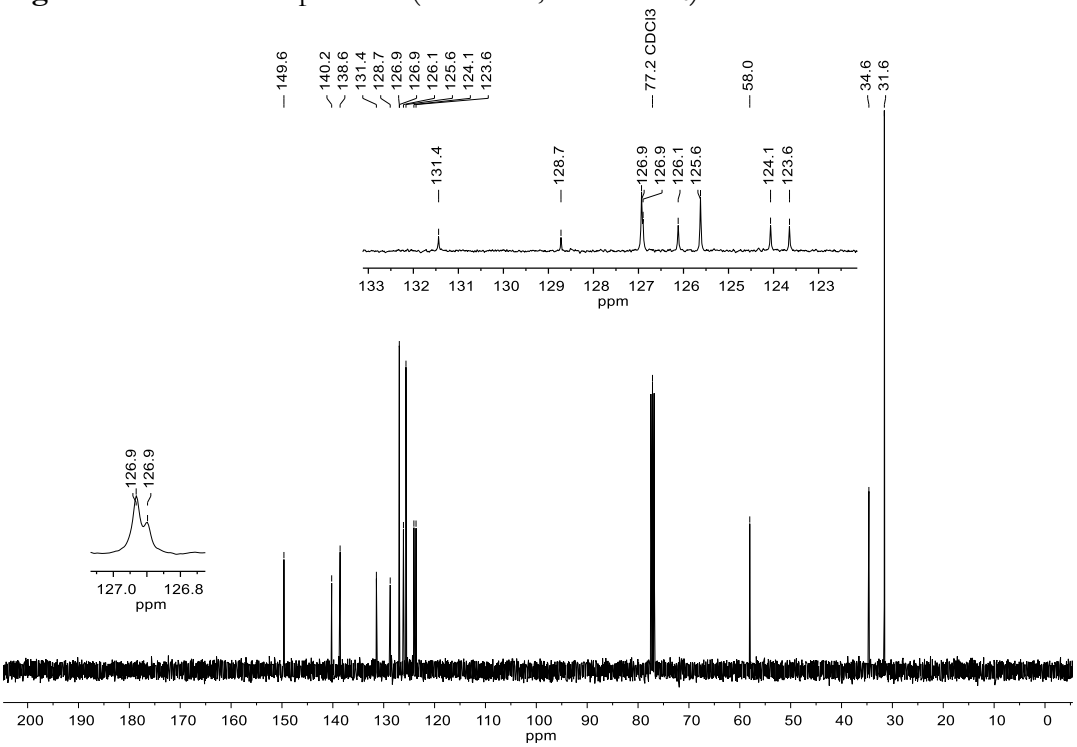

Figure S54. ^{13}C NMR Spectrum (101 MHz, Chloroform-d) of **10**.

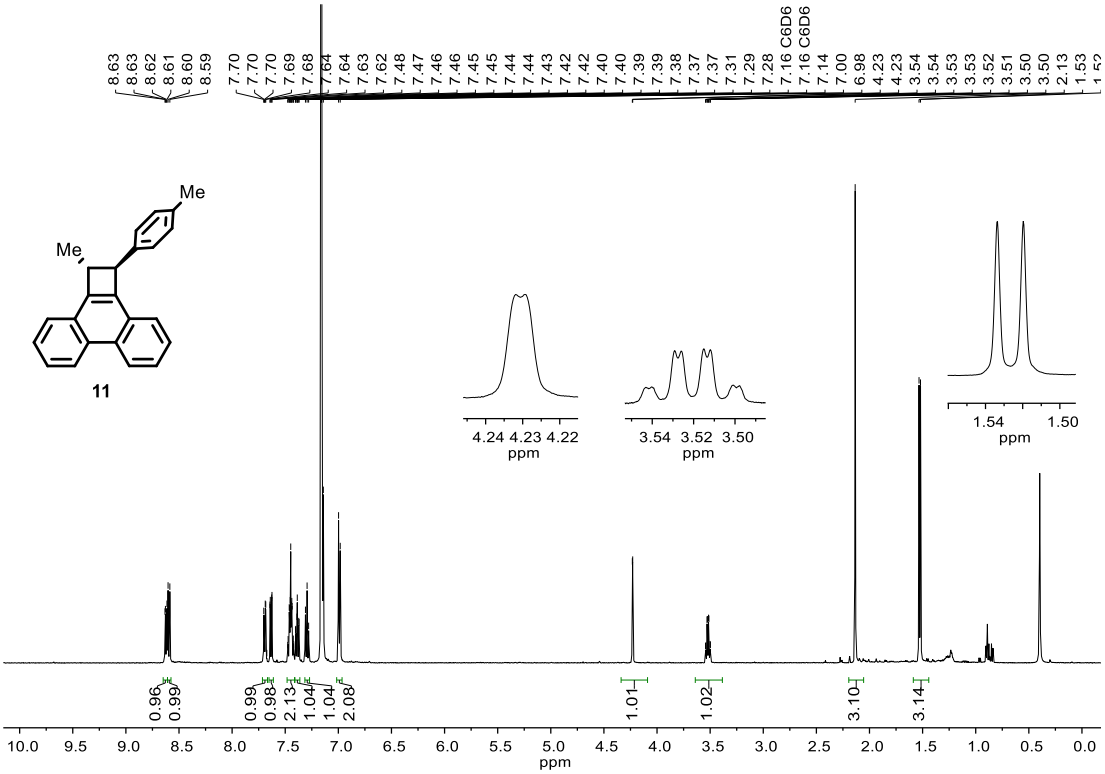

Figure S55. ^{13}H NMR Spectrum (500 MHz, Benzene-d_6) of **11**.

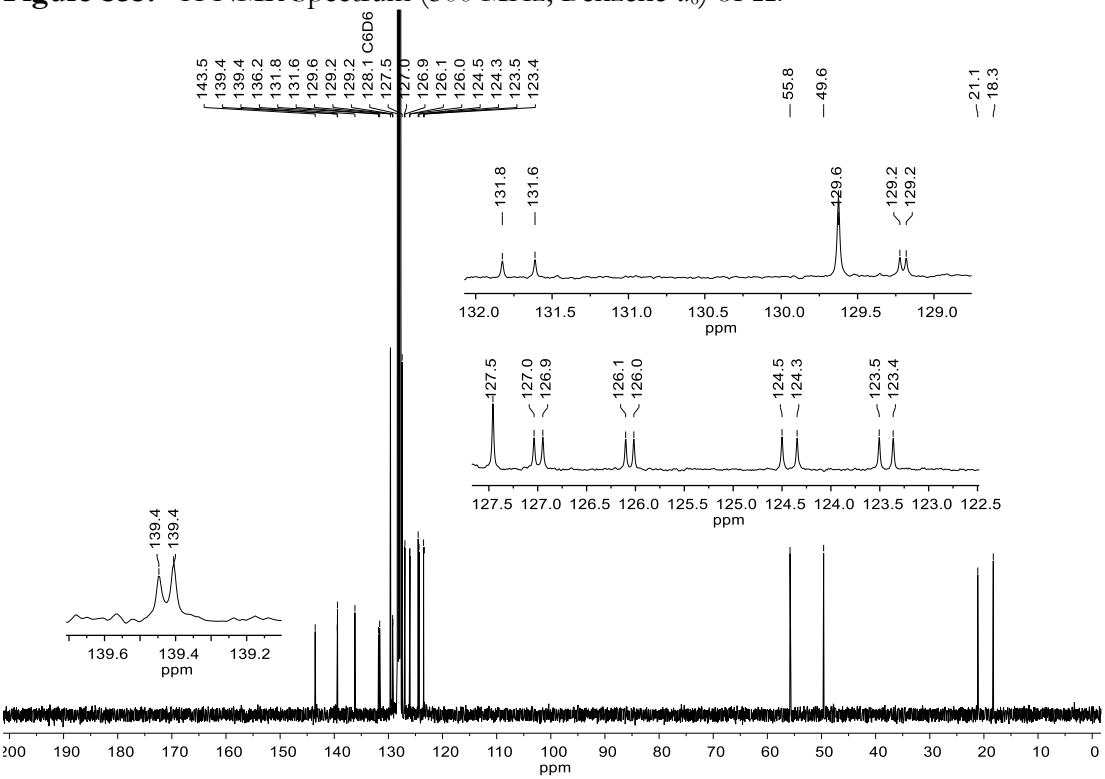

Figure S56. ^{13}C NMR Spectrum (101 MHz, Benzene-d_6) of **11**.

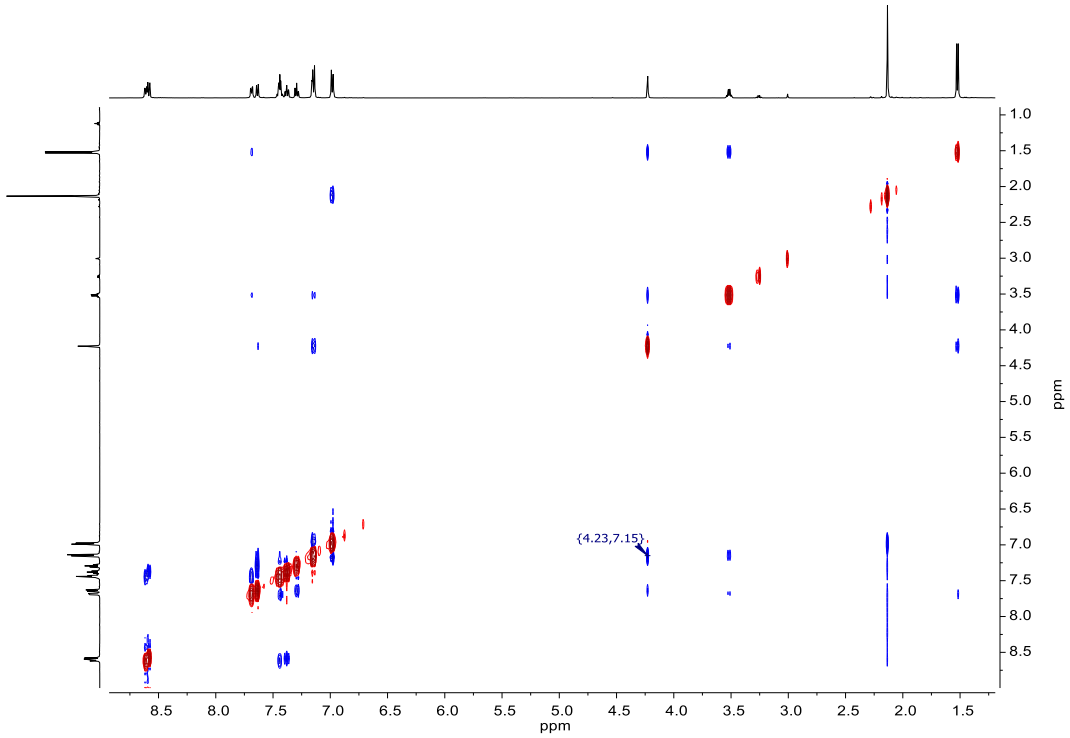

Figure S57. 2D NOESY Spectrum (500 MHz, Benzene-d_6) of **11**.

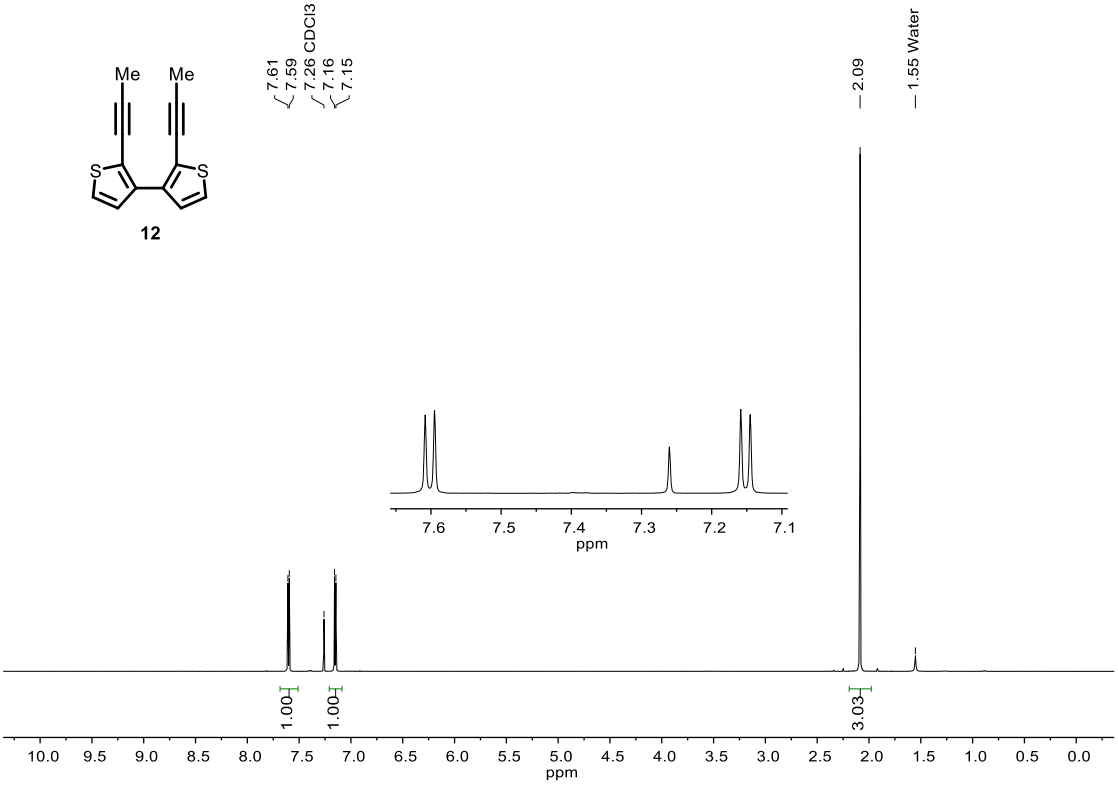

Figure S58. ^{1}H NMR Spectrum (400 MHz, Chloroform-*d*) of **12**.

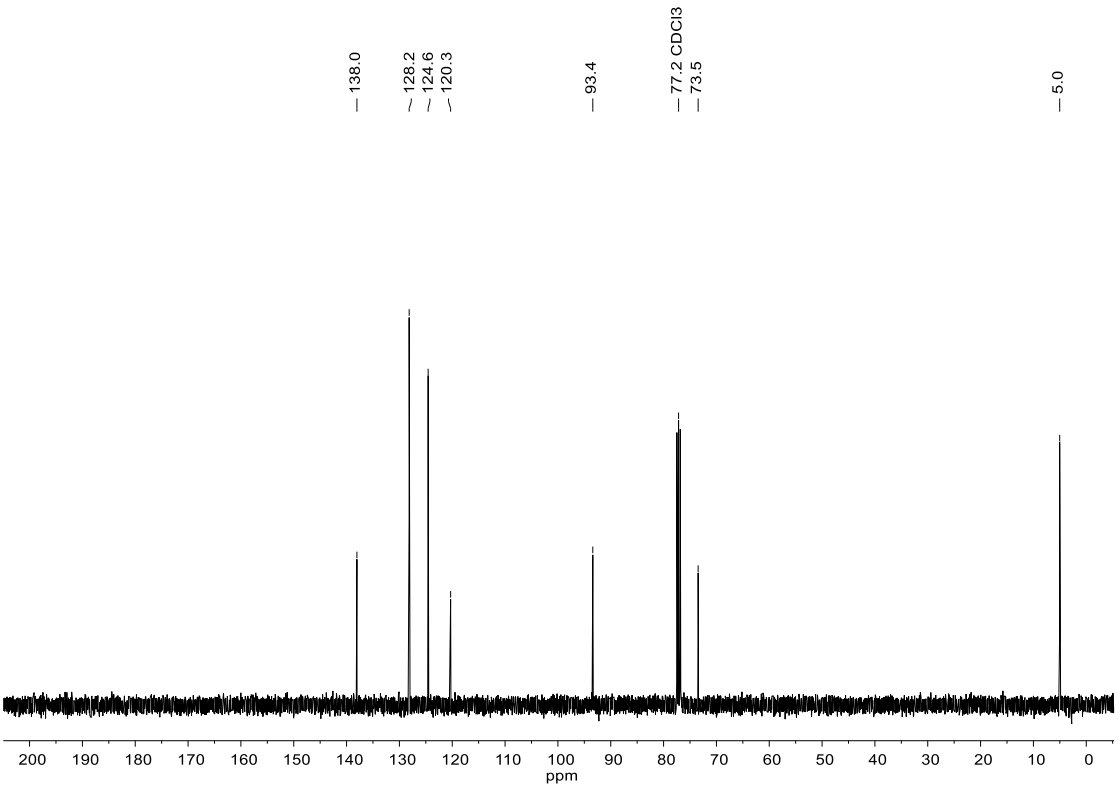

Figure S59. ^{13}C NMR Spectrum (101 MHz, Chloroform-*d*) of **12**.

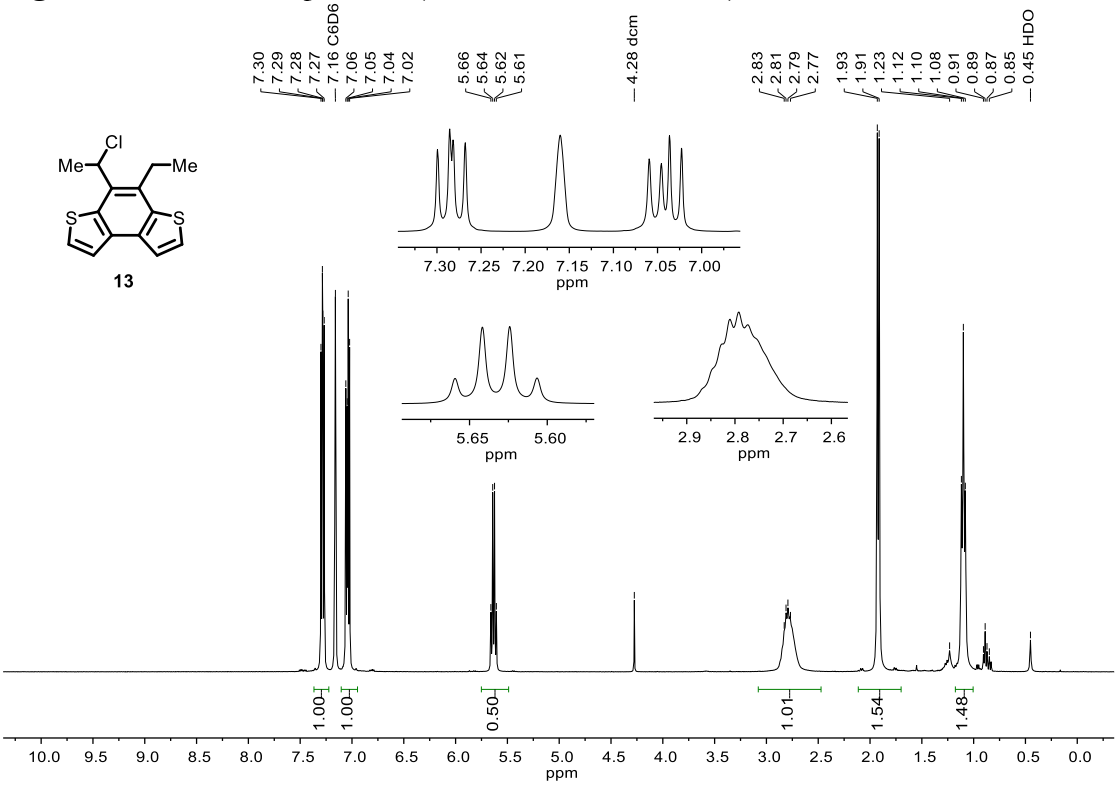

Figure S60. ^{1}H NMR Spectrum (400 MHz, Benzene-d_6) of **13**.

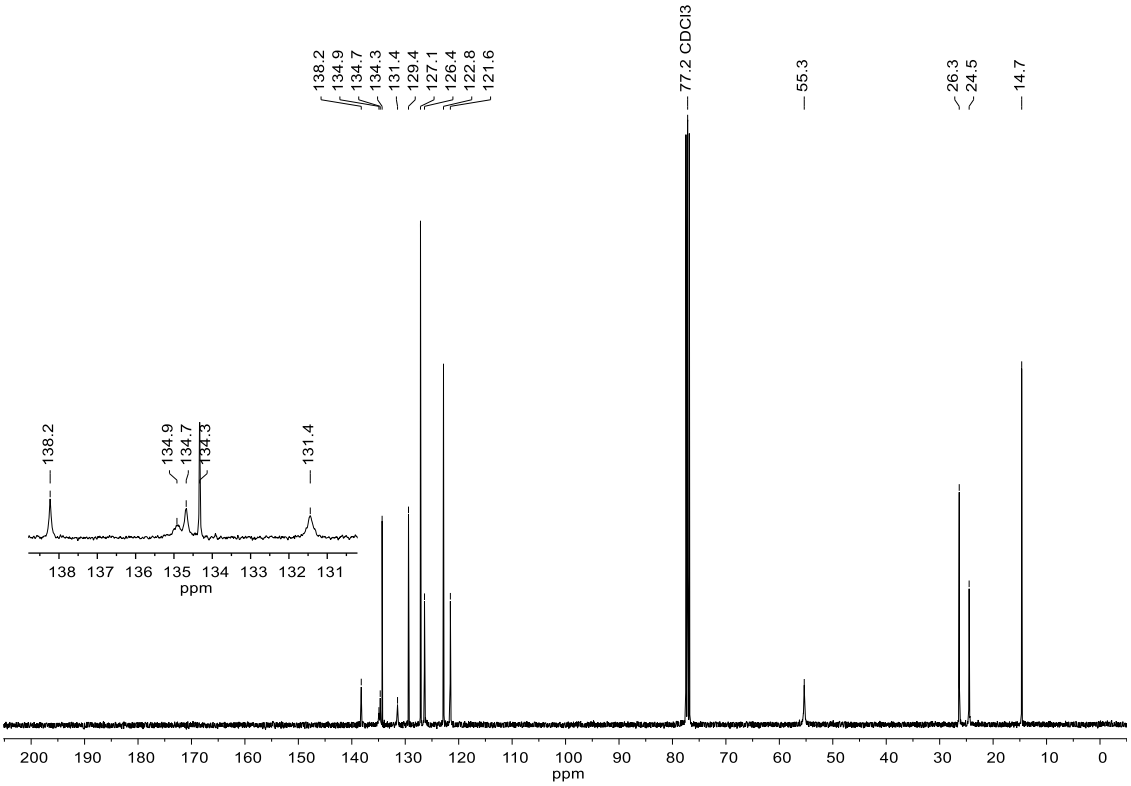

Figure S61. ^{13}C NMR Spectrum (101 MHz, Chloroform-*d*) of **13**.

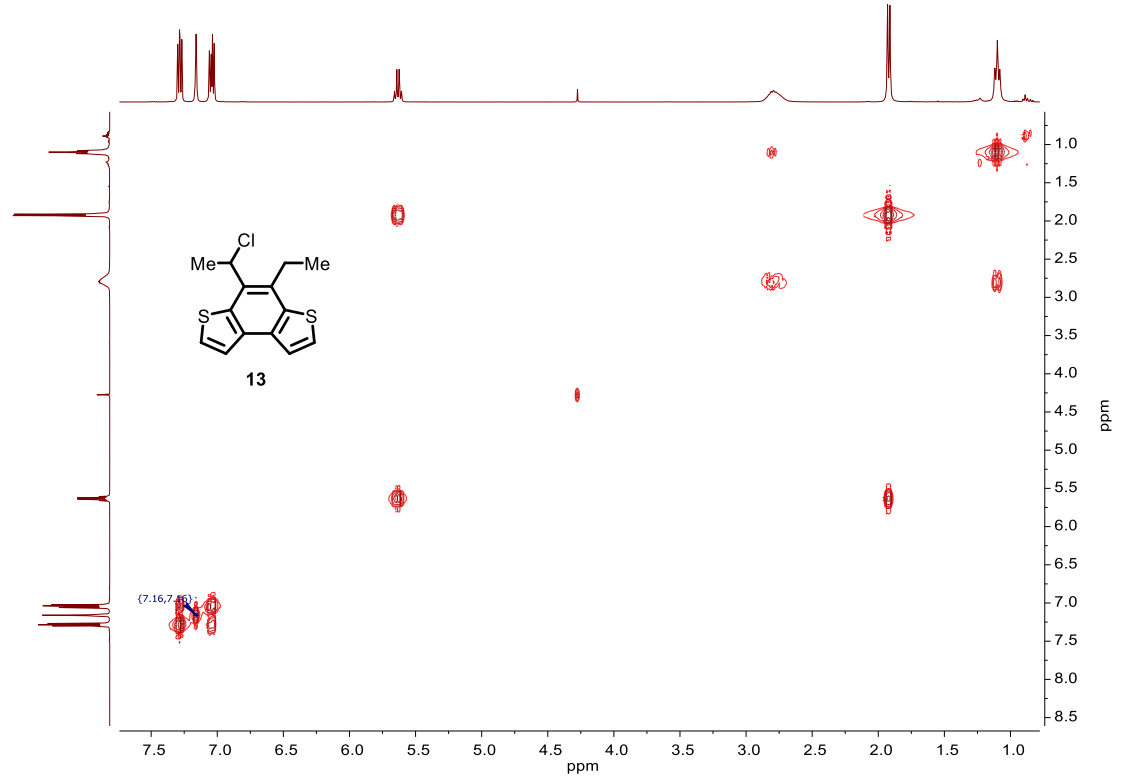

Figure S62. 2D COSY Spectrum (400 MHz, Benzene-d_6) of **13**.

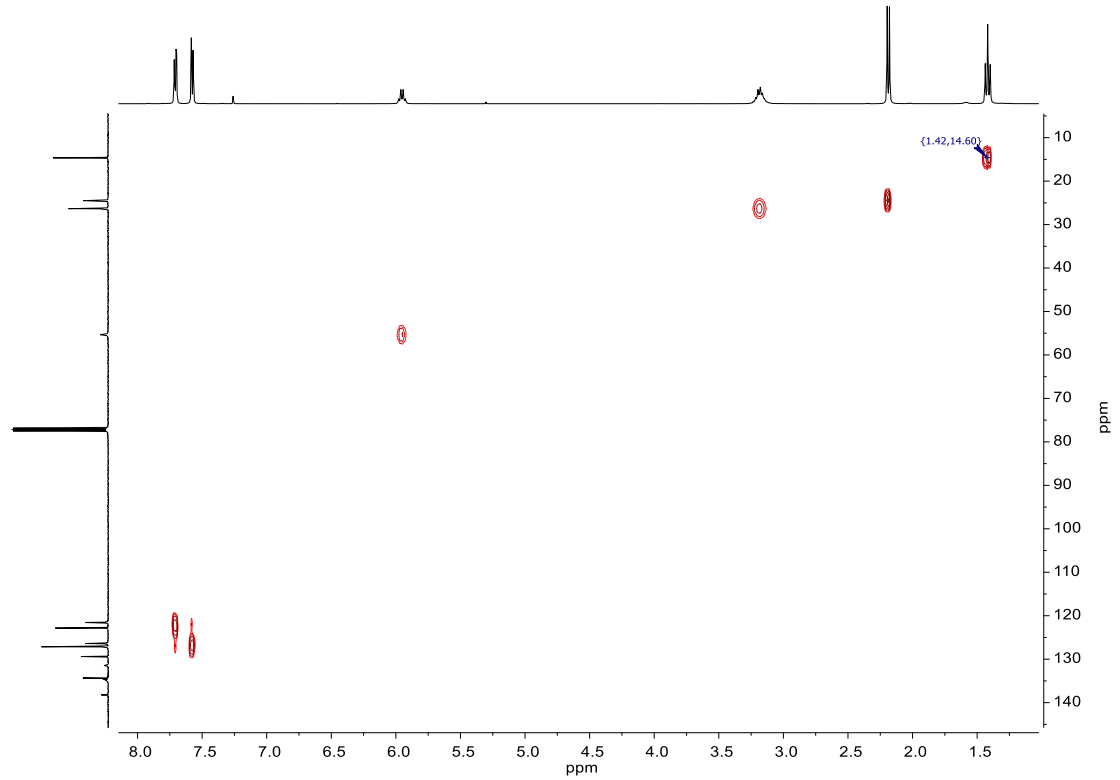

Figure S63. 2D HSQC Spectrum (400 MHz, Chloroform-*d*) of **13**.

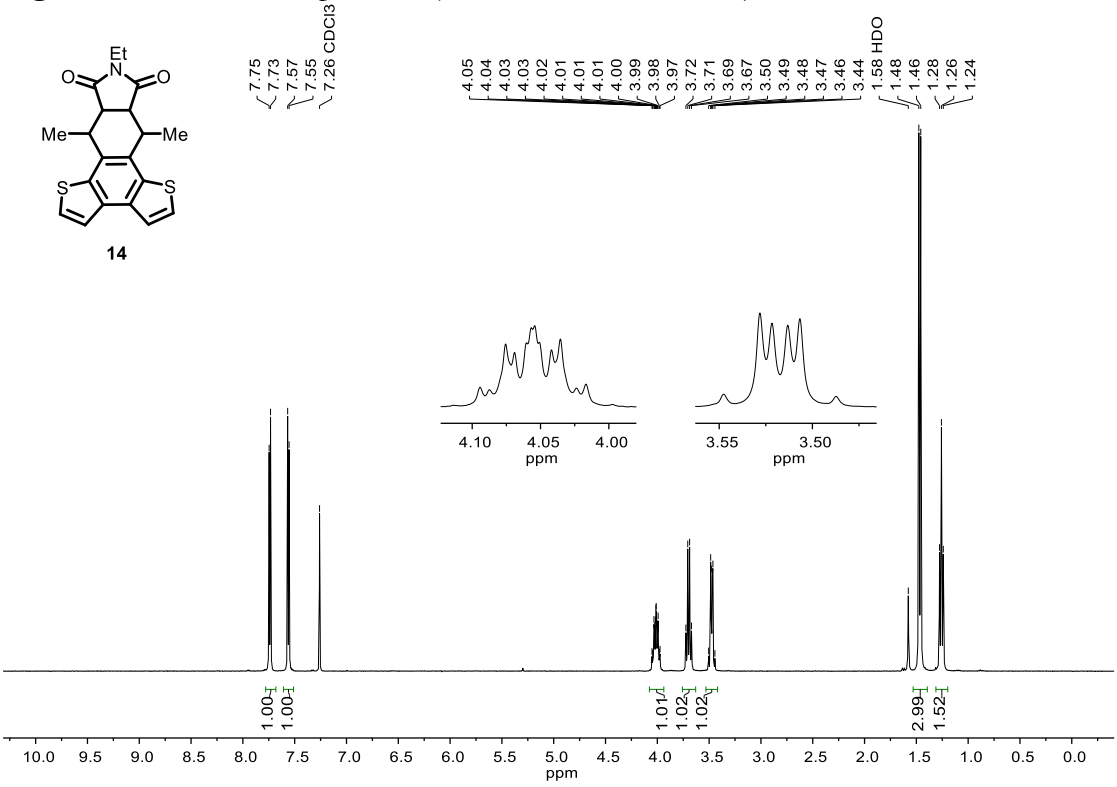

Figure S64. ^{1}H NMR Spectrum (400 MHz, Chloroform-*d*) of **14**.

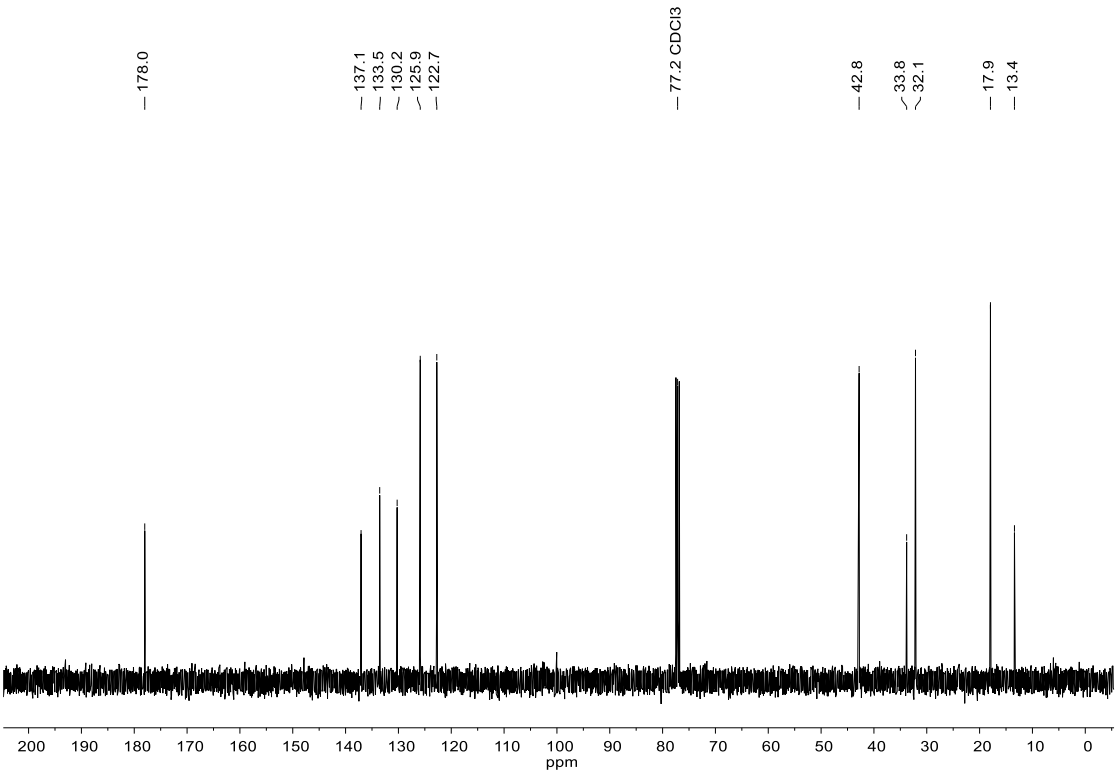

Figure S65. ^{13}C NMR Spectrum (101 MHz, Chloroform-*d*) of **14**.

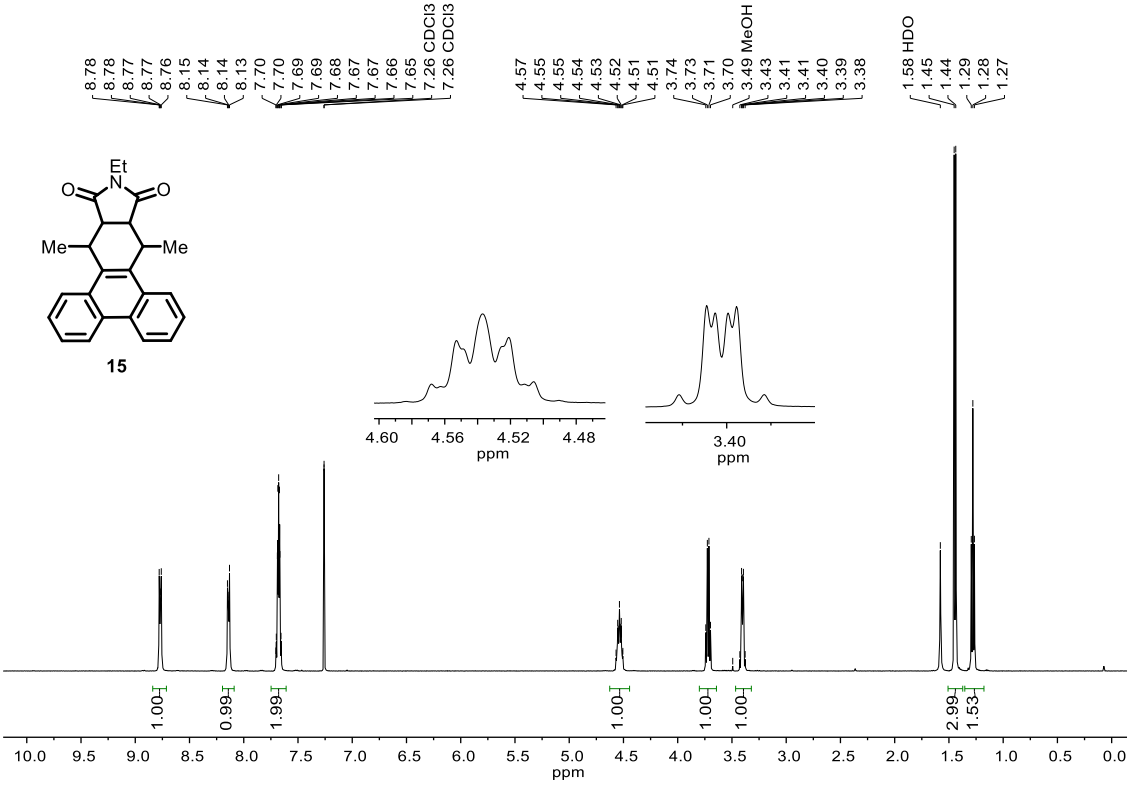

Figure S66. ^{1}H NMR Spectrum (500 MHz, Chloroform-*d*) of **15**.

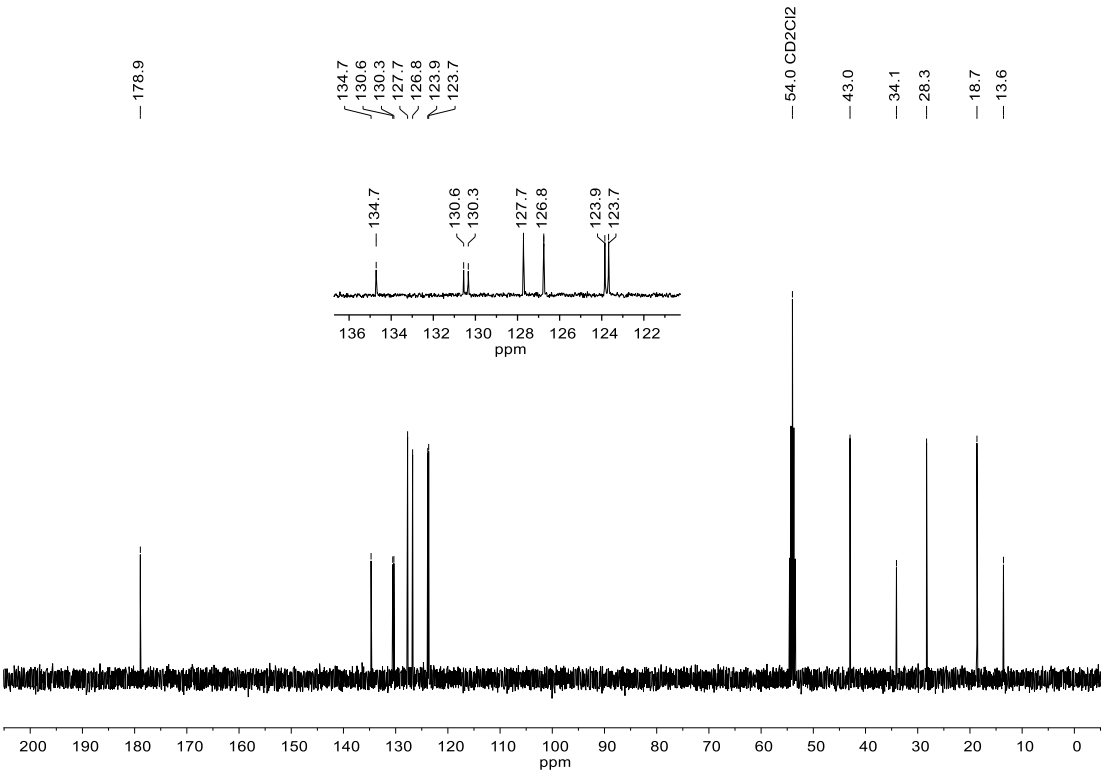

Figure S67. ^{13}C NMR Spectrum (101 MHz, Dichloromethane-d_2) of **15**.

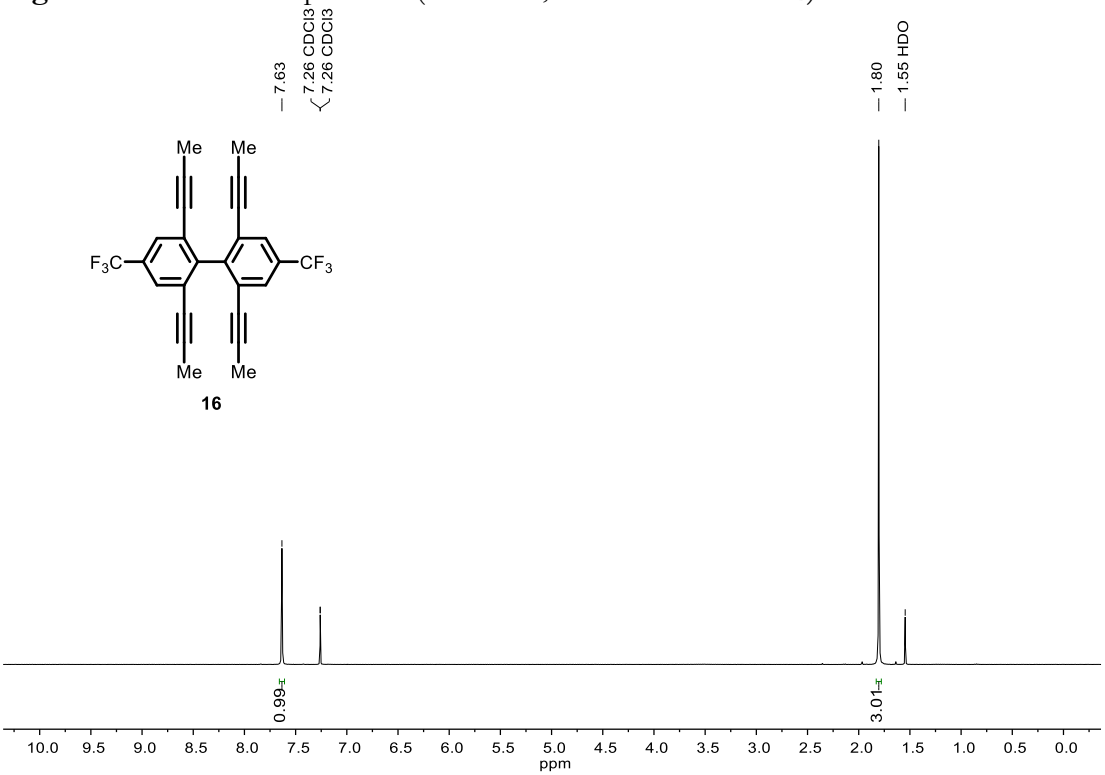

Figure S68. ^{1}H NMR Spectrum (400 MHz, Chloroform-*d*) of **16**.

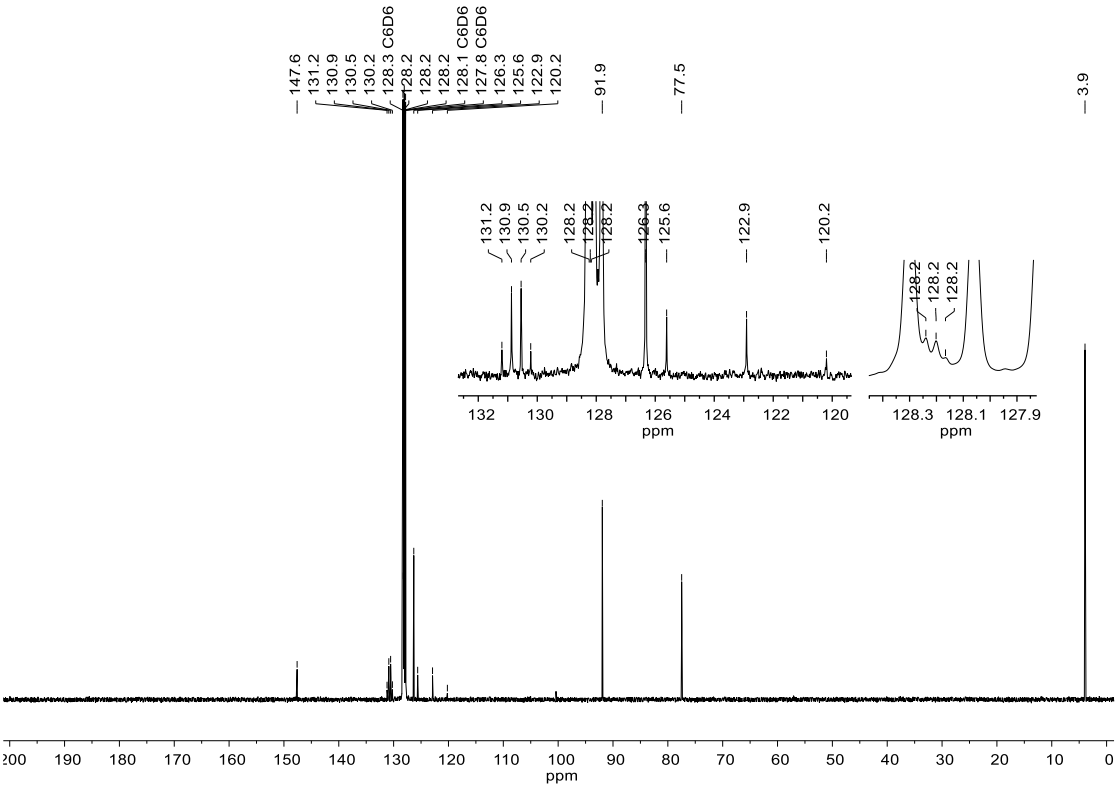

Figure S69. ^{13}C NMR Spectrum (101 MHz, Benzene-d_6) of **16**.

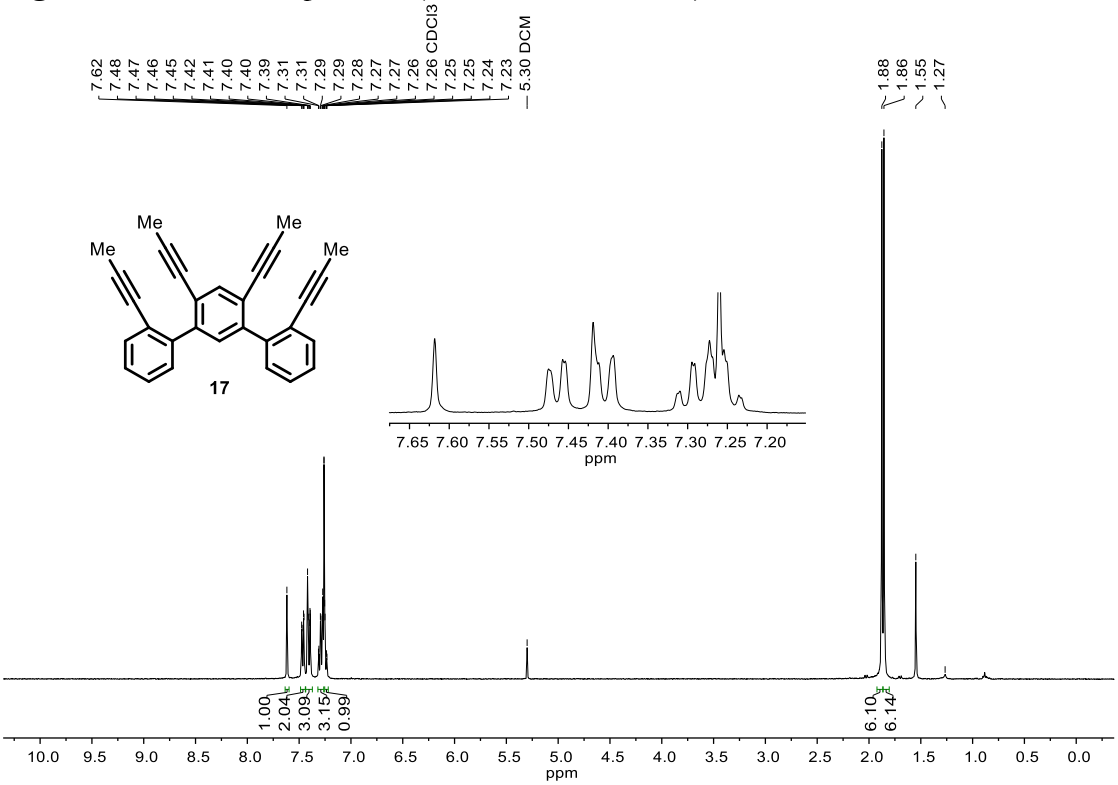

Figure S70. ^{1}H NMR Spectrum (400 MHz, Chloroform-*d*) of **17**.

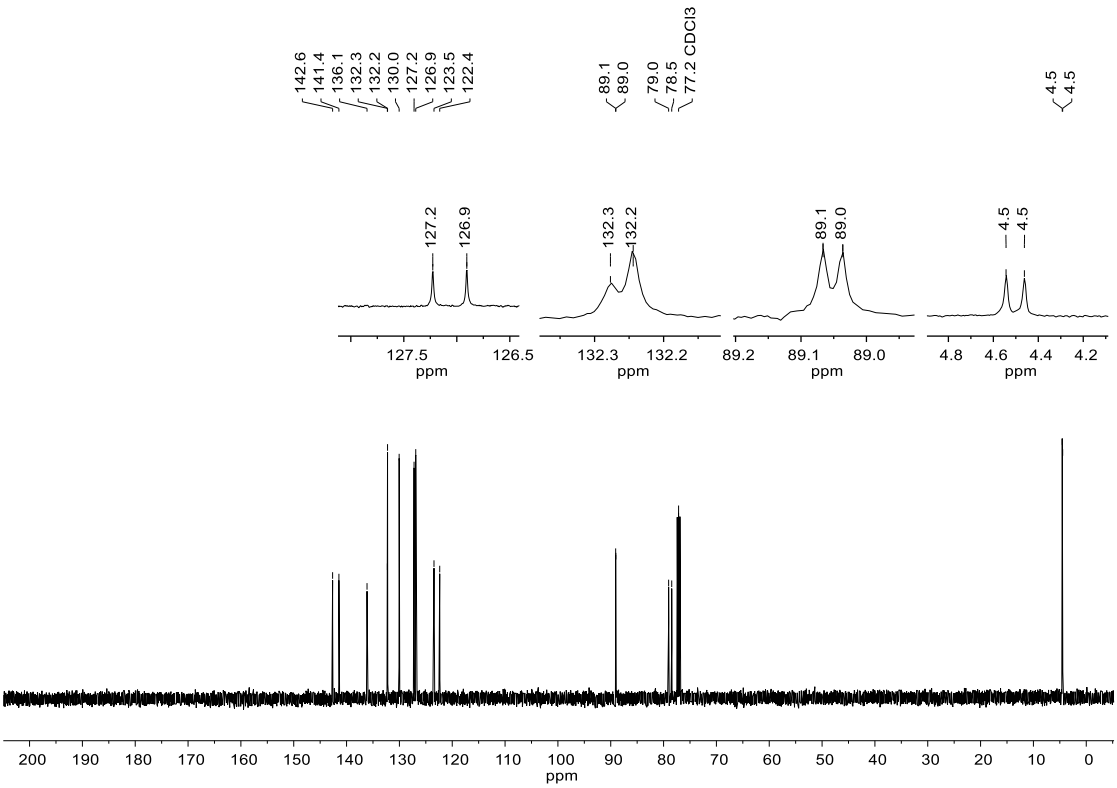

Figure S71. ^{13}C NMR Spectrum (126 MHz, Chloroform-*d*) of **17**.

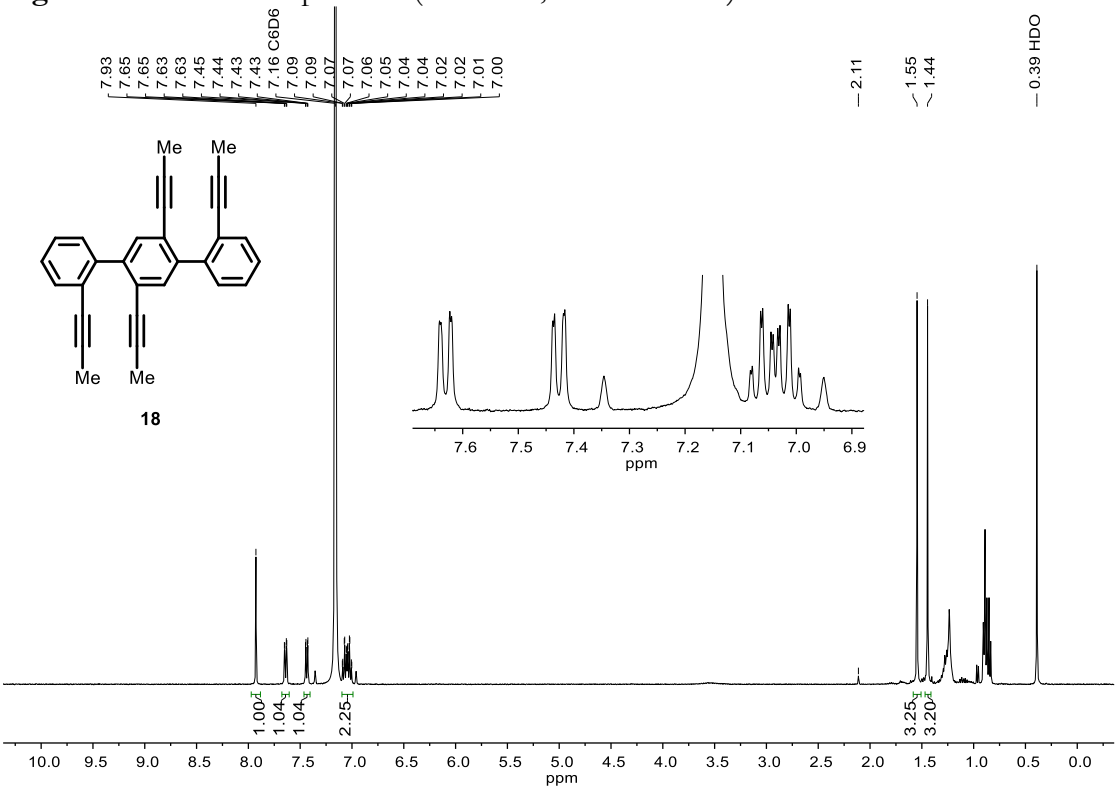

Figure S72. ^{1}H NMR Spectrum (400 MHz, Benzene-d_6) of **18**.

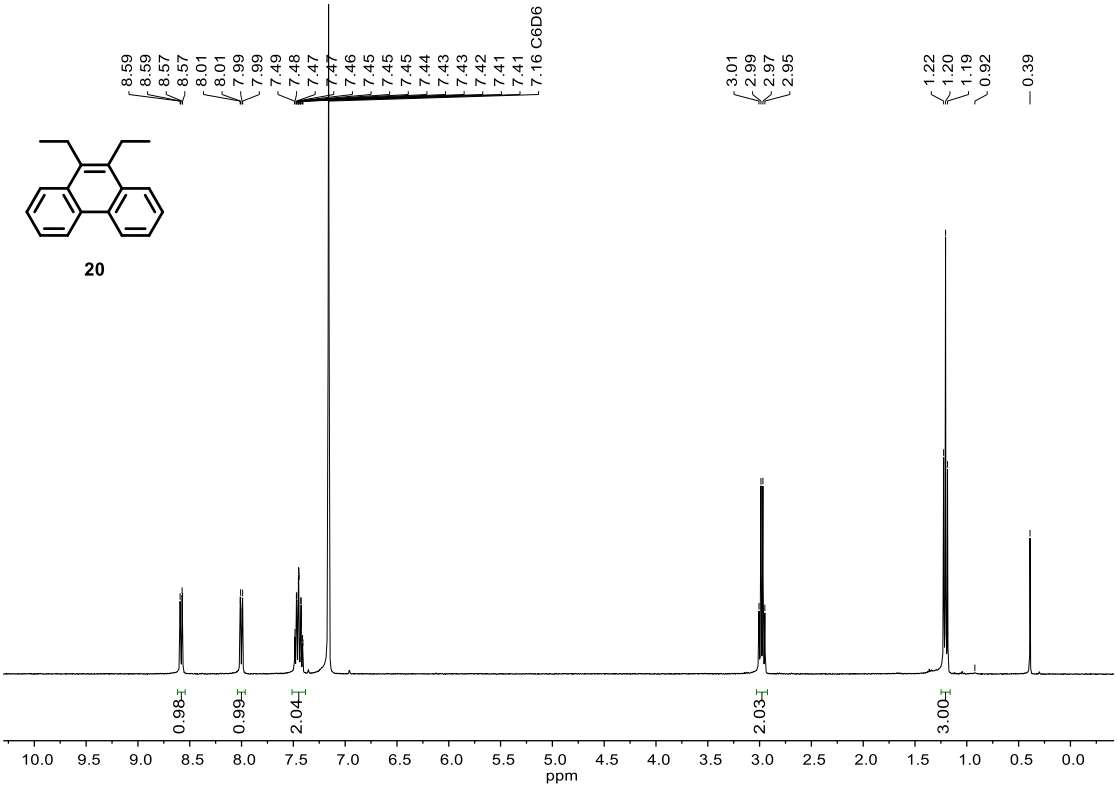

Figure S73. ^{1}H NMR Spectrum (400 MHz, Benzene-d_6) of **19**.

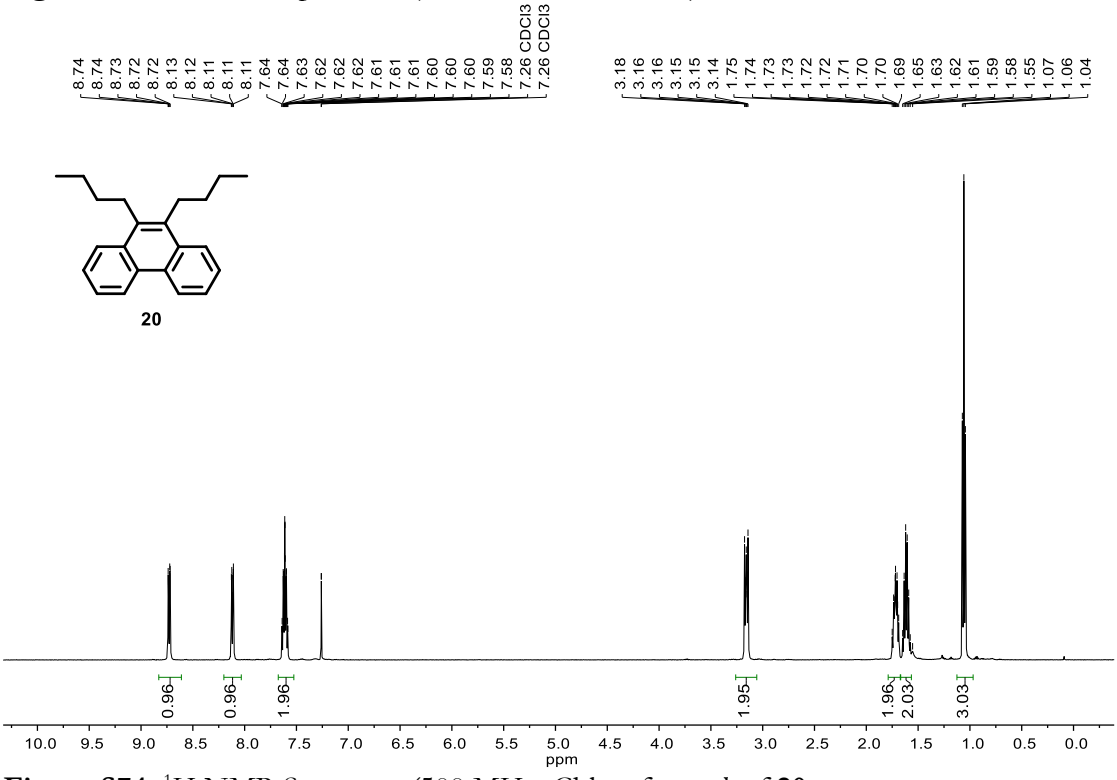

Figure S74. ^{1}H NMR Spectrum (500 MHz, Chloroform-*d*) of **20**.

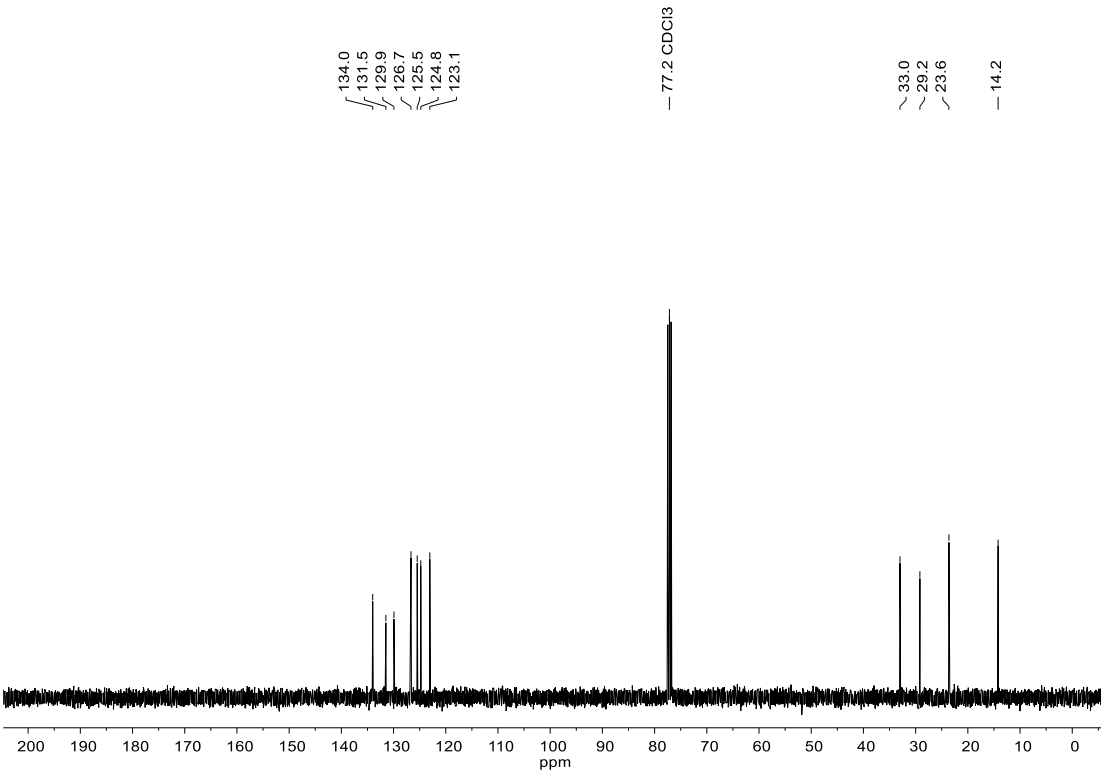

Figure S75. ^{13}C NMR Spectrum (101 MHz, Chloroform-*d*) of **20**.

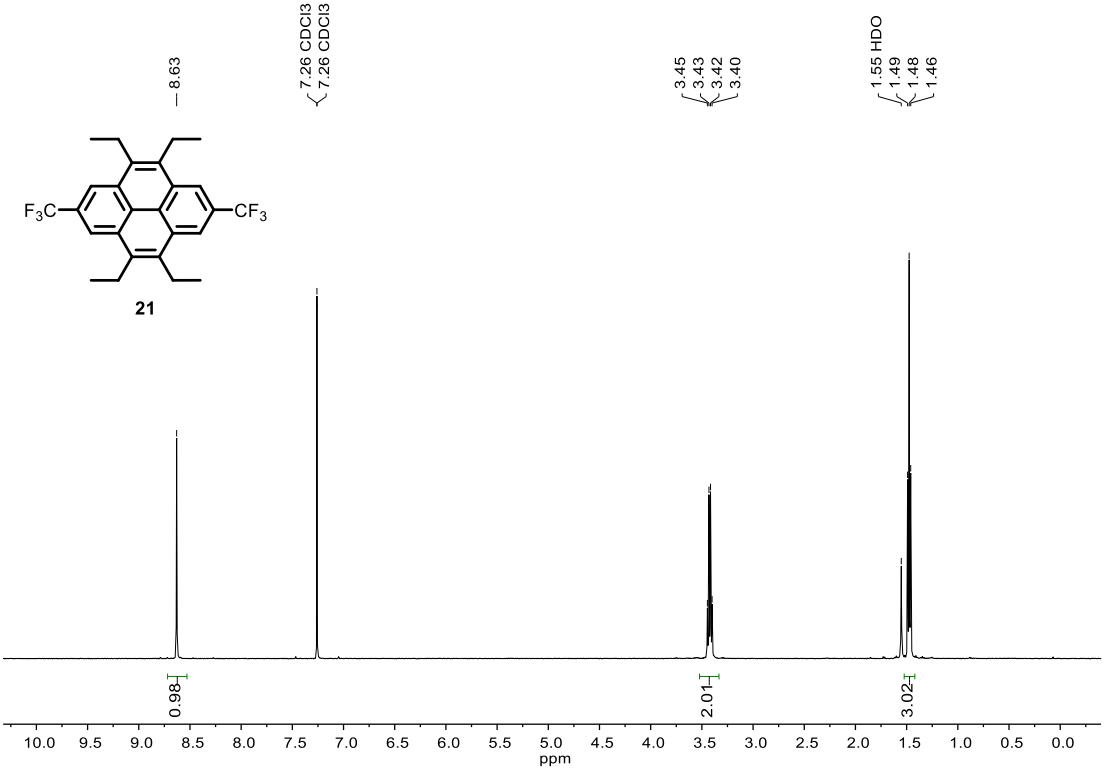

Figure S76. ^{1}H NMR Spectrum (500 MHz, Chloroform-*d*) of **21**.

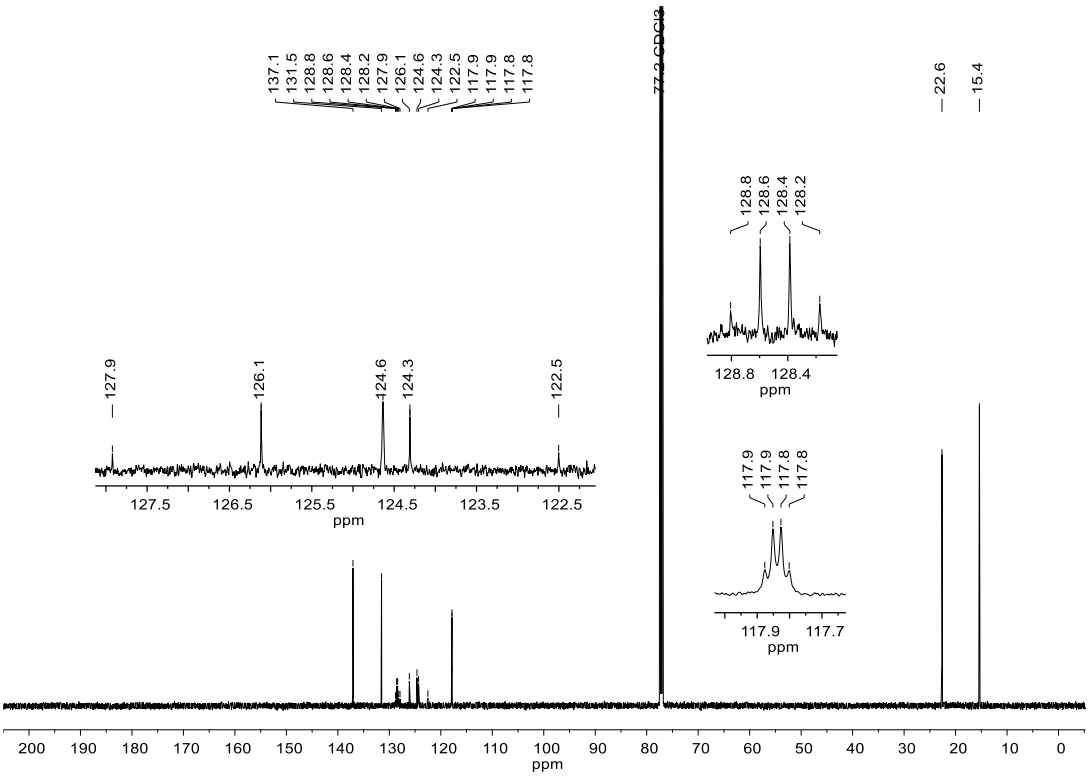

Figure S77. ^{13}C NMR Spectrum (151 MHz, Chloroform-*d*) of **21**.

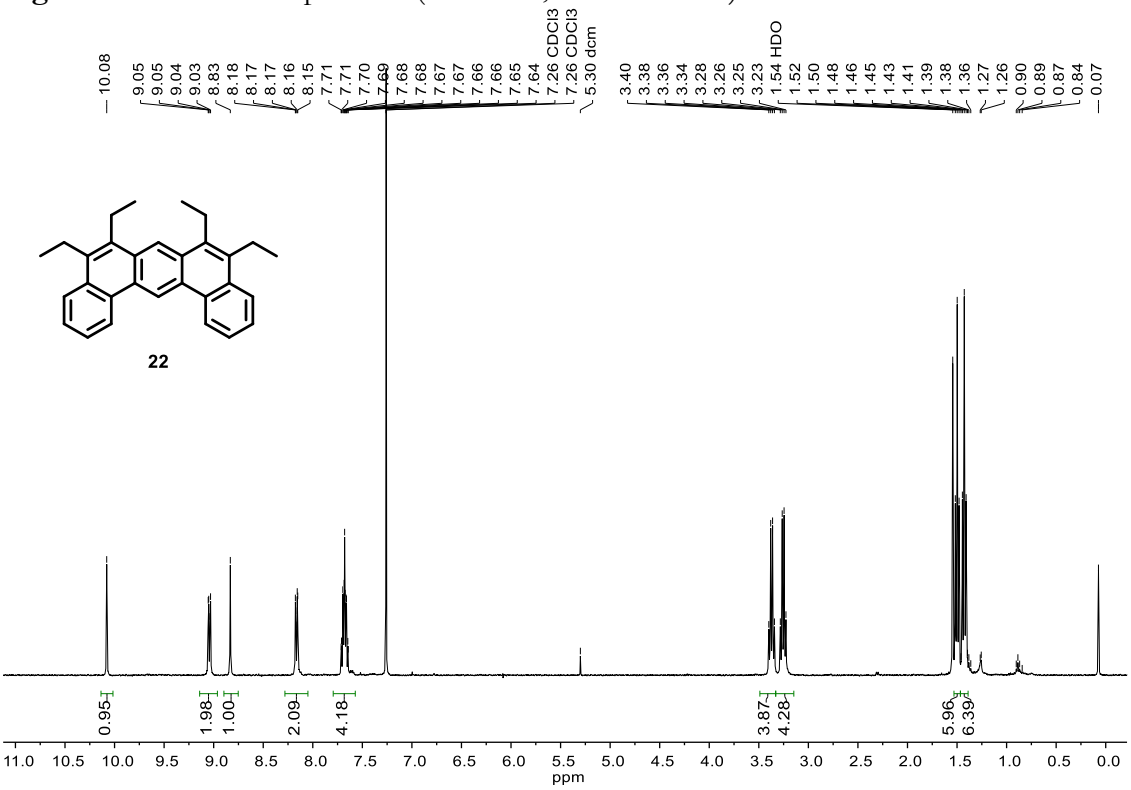

Figure S78. ^{1}H NMR Spectrum (400 MHz, Chloroform-*d*) of **22**.

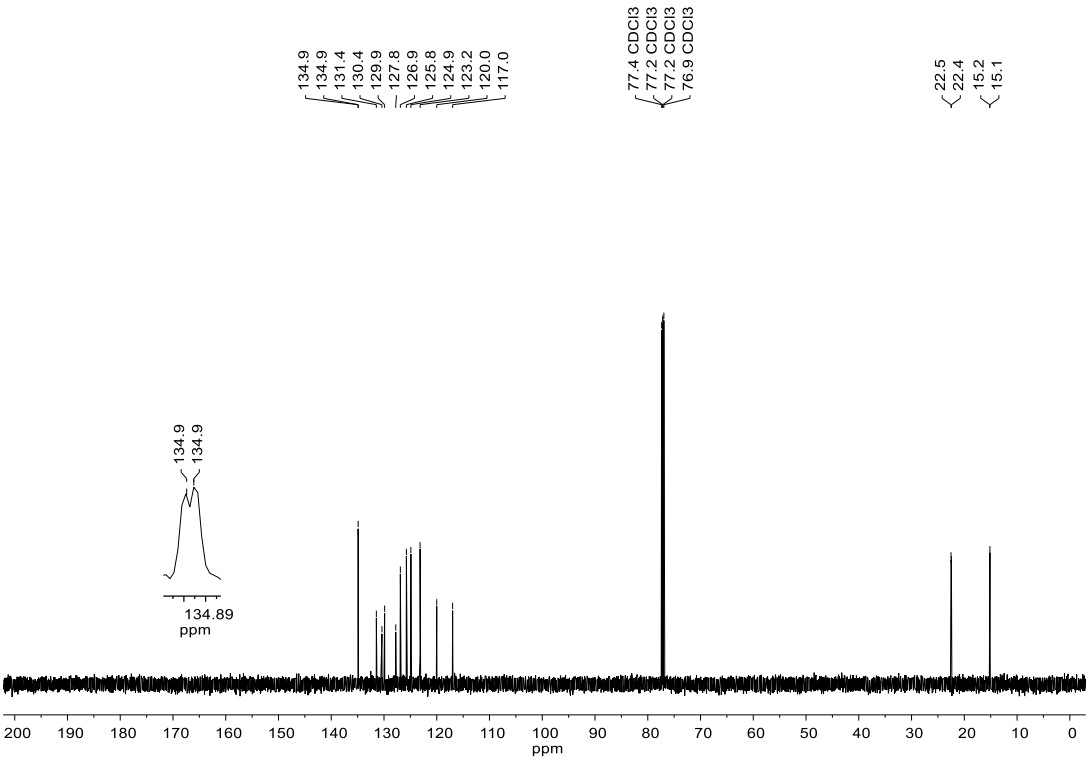

Figure S79. ^{13}C NMR Spectrum (151 MHz, Chloroform-*d*) of **22**.

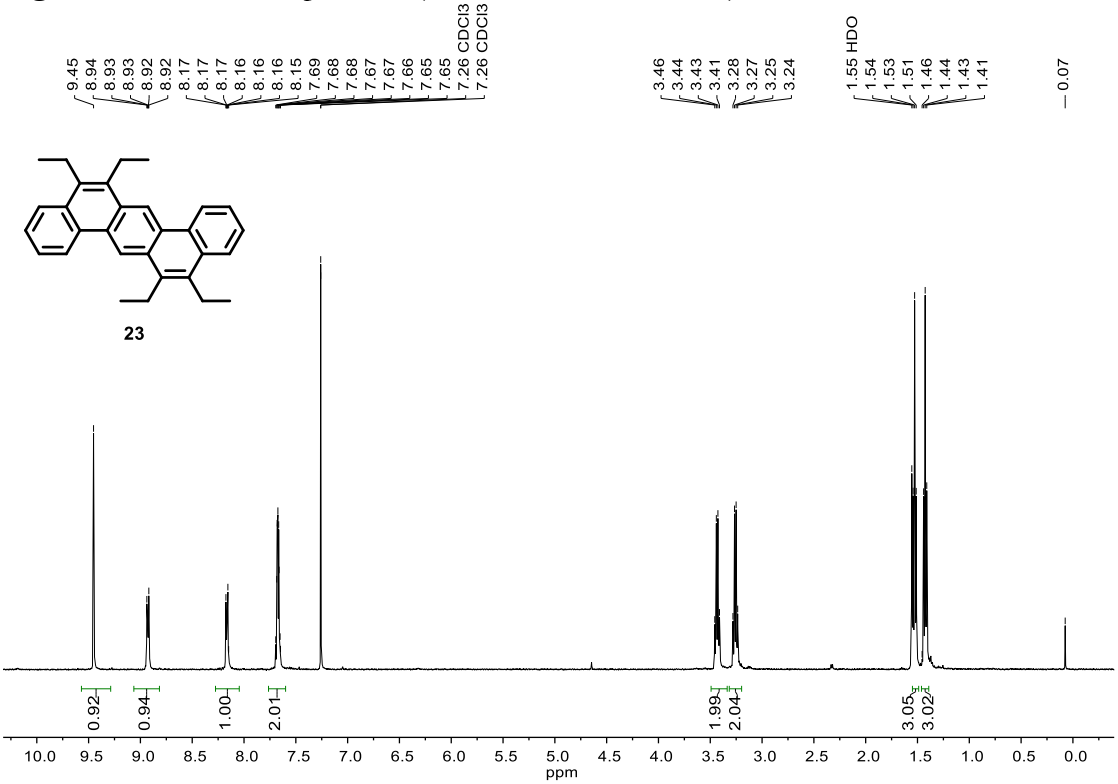

Figure S80. ^{1}H NMR Spectrum (400 MHz, Chloroform-*d*) of **23**.

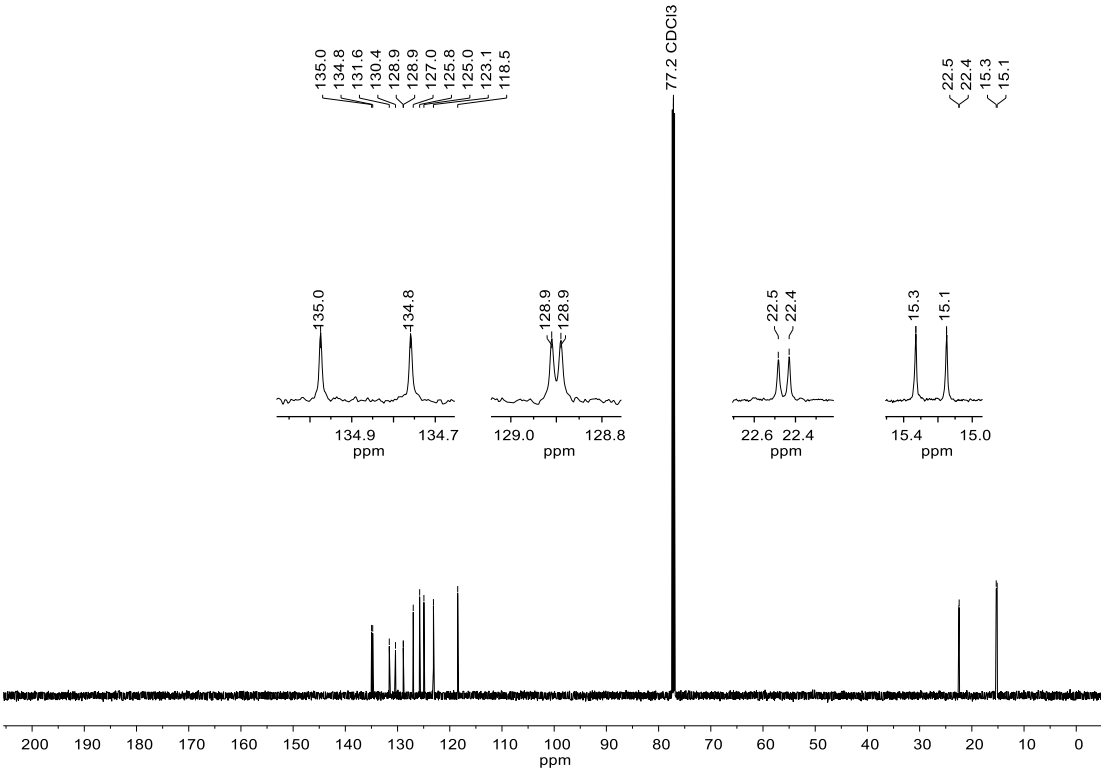

Figure S81. ^{13}C NMR Spectrum (151 MHz, Chloroform-*d*) of **23**.

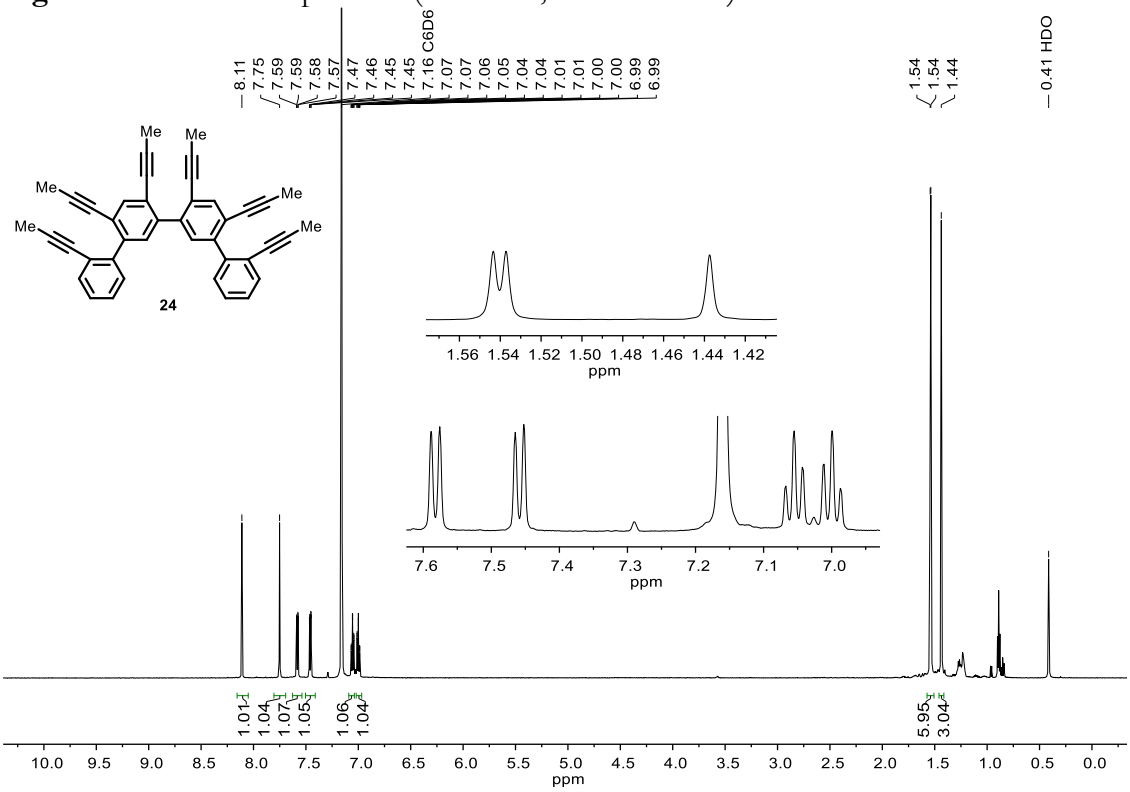

Figure S82. ^{1}H NMR Spectrum (600 MHz, Benzene-d_6) of **24**.

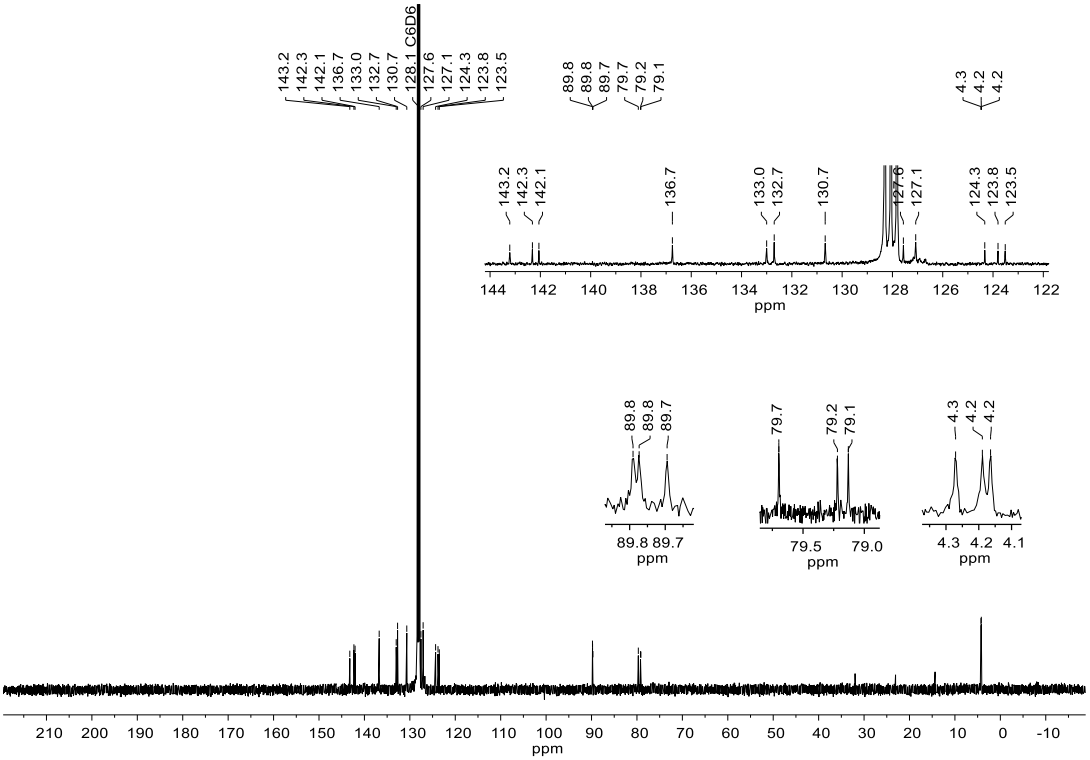

Figure S83. ^{13}C NMR Spectrum (101 MHz, Benzene-d_6) of **24**.

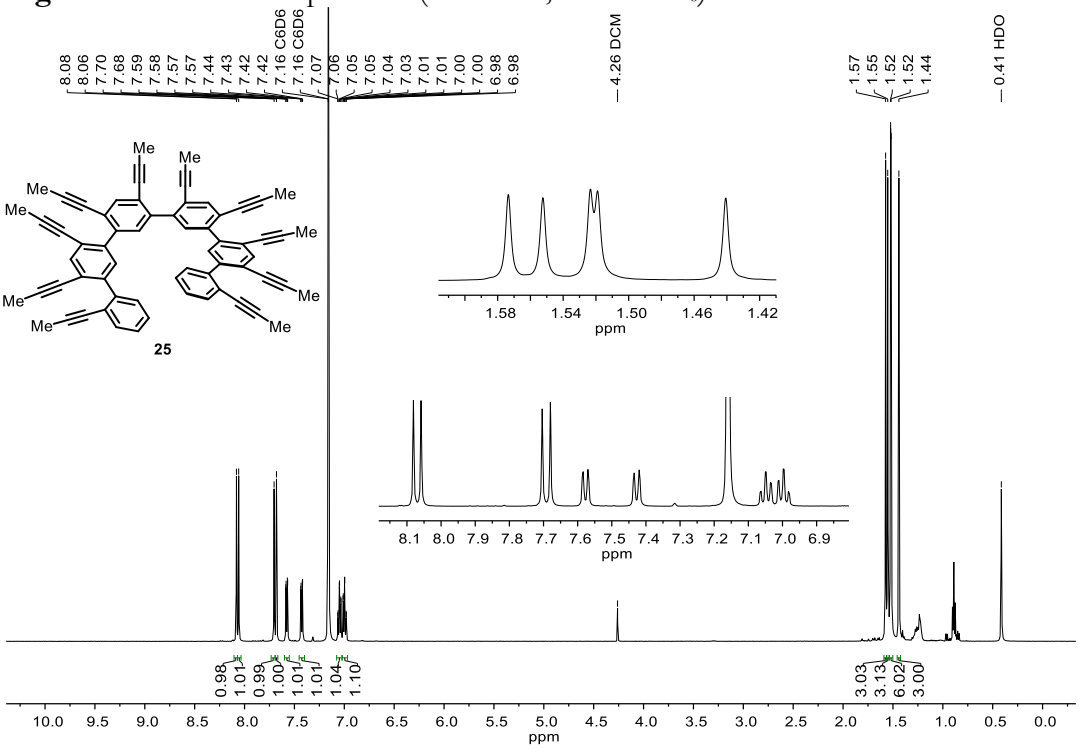

Figure S84. ^{1}H NMR Spectrum (500 MHz, Benzene-d_6) of **25**.

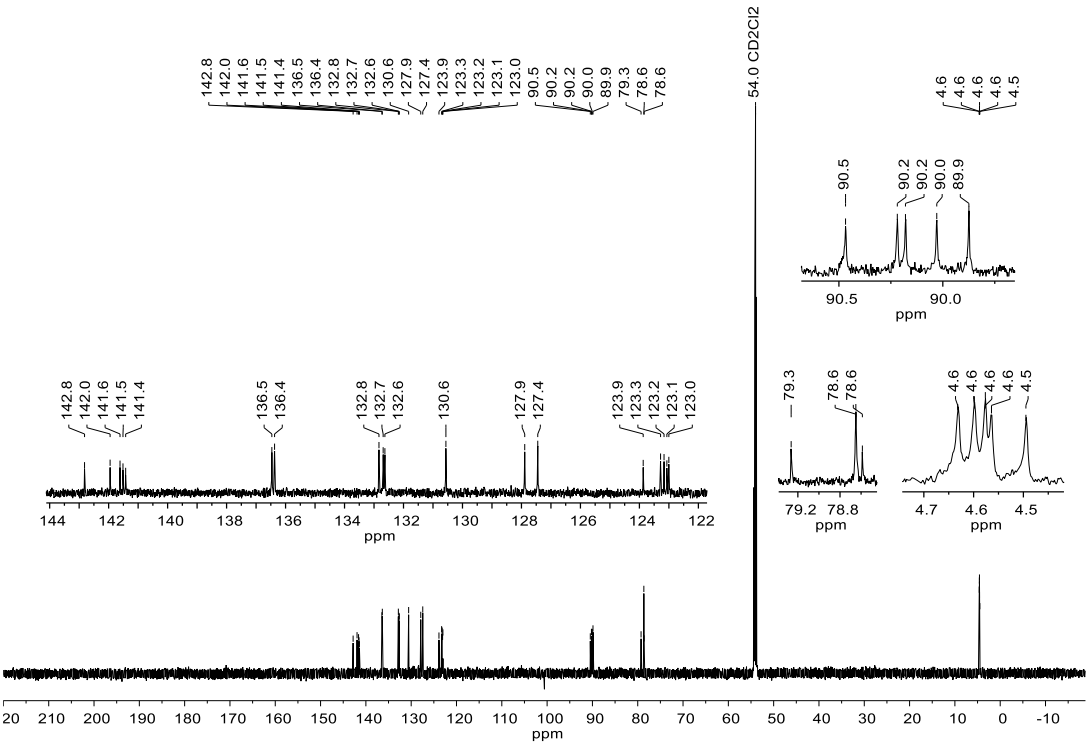

Figure S85. ^{13}C NMR Spectrum (151 MHz, Dichloromethane-d_2) of **25**.

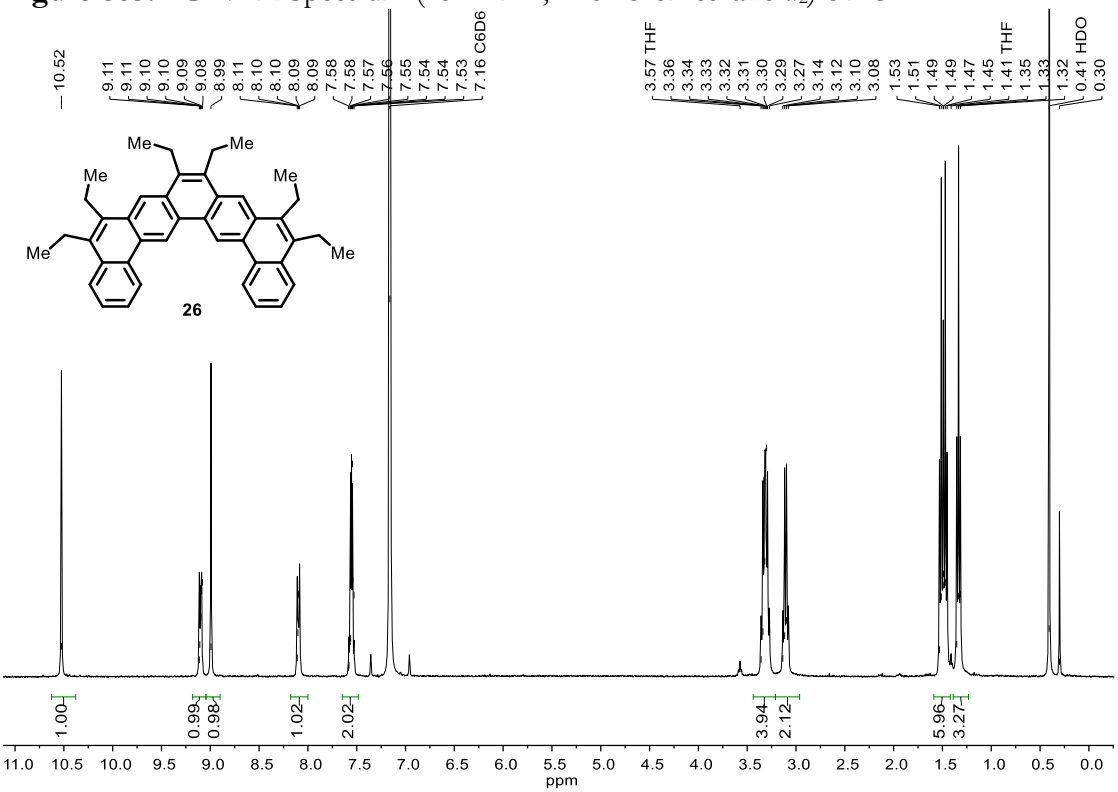

Figure S86. ^{1}H NMR Spectrum (600 MHz, Benzene-d_6) of **26**.

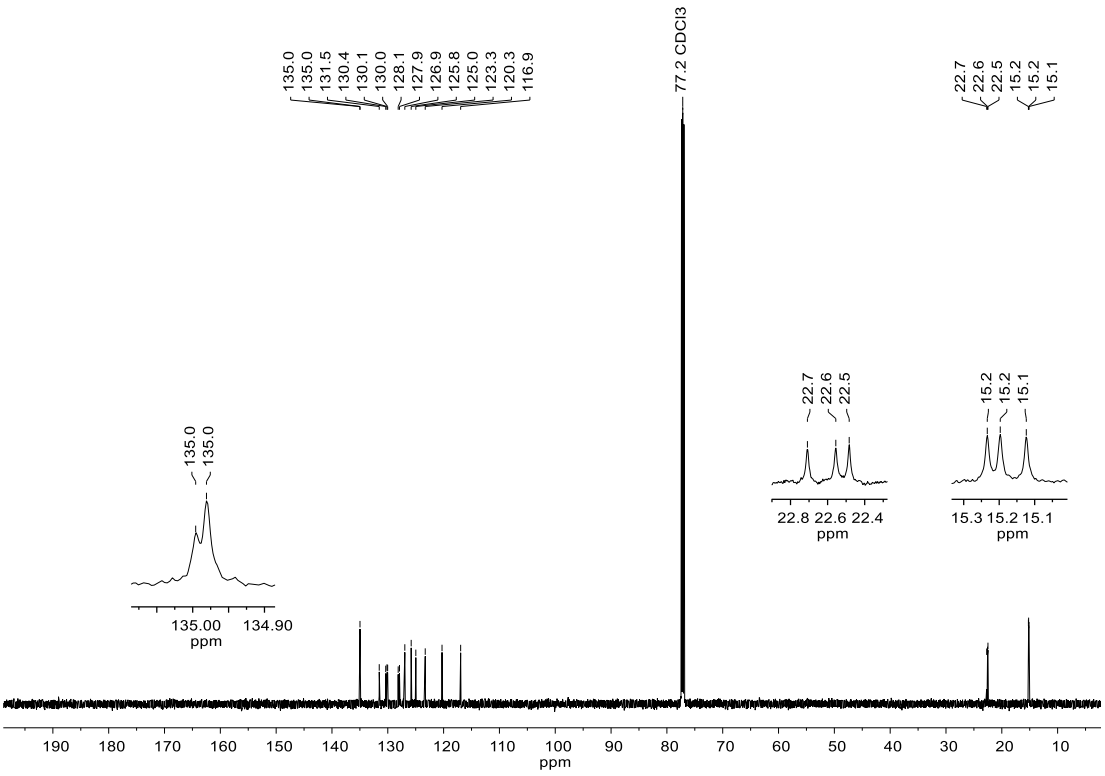

Figure S87. ^{13}C NMR Spectrum (151 MHz, Chloroform-*d*) of **26**.

X-Ray Crystallography

X-ray diffraction data for compound **1a** were collected on a Bruker AXS diffractometer with a fixed-chi, three-circle geometry goniostat coupled to an APEX-I CCD detector with Mo Kα (λ = 0.71073 Å) radiation generated by a fine-focus sealed tube and monochromated by graphite. X-ray diffraction data for compounds **2a**, **2g**, and **2h** were collected using a Bruker AXS diffractometer with a Kappa geometry goniostat coupled to an APEX-II CCD detector with Mo Kα (λ = 0.71073 Å) radiation generated by a microfocus sealed tube and monochromated by a system of QUAZAR multilayer mirrors. X-ray diffraction data for compounds **2i**, **10**, and **21** were collected using a Bruker AXS diffractometer with a Kappa geometry goniostat coupled to an APEX-II CCD detector with Cu Kα (λ = 1.5418 Å) radiation generated by a microfocus rotating anode and monochromated by a system of HELIOS multilayer mirrors.

Unless otherwise noted, crystals were kept at 100(2) K throughout collection. Data collection strategy determination, integration, scaling, and space group determination were performed with Bruker APEX2 (v. 2014.1-1, v. 2014.11-0) or APEX3 (v. 2016.5-0) software. Structures were solved by SHELXS-97, SHELXS-2013, SHELXT-2014, or Superflip (v. 04/17/13) and refined with SHELXL-2014, with refinement of F^2 on all data by full-matrix least squares.[17–20] The 3D molecular structure figures were visualized with Mercury 3.7.[21]

Compound #	Detector Distance (mm)	Image Width (°)	Exposure Time (seconds)
1a	60	0.3	10
2a	40	0.4	20
2g	40	0.4	20
2h	40	0.4	20
2i	60	1.0	3, 4, 5, 10 (depending on angle)
10	60	2.0	3, 4, 5, 10 (depending on angle)
21	60	2.0	3, 4, 5, 10 (depending on angle)

Table S2. X-Ray Crystallography Experimental Details

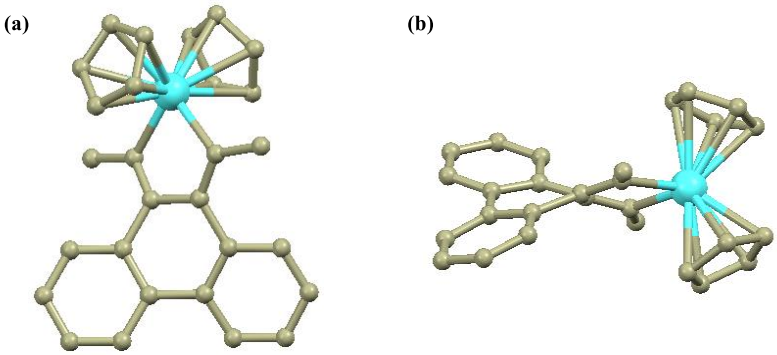

Figure S88. Solid state structure of **1a** as determined by single-crystal X-ray diffraction: (a) top view; (b) side view.

Empirical formula	$C_{28}H_{24}Zr$	
Formula weight	451.69	
Temperature	100(2) K	
Wavelength	0.71073 Å	
Crystal system	Orthorhombic	
Space group	P b c a	
Unit cell dimensions	a = 18.3434(9) Å	□□ = 90°.
	b = 11.2939(5) Å	□□ = 90°.
	c = 19.8851(9) Å	□ = 90°.
Volume	4119.6(3) $Å^3$	
Z	8	
Density (calculated)	1.457 Mg/m^3	
Absorption coefficient	0.545 mm^{-1}	
F(000)	1856	
Crystal size	0.20 x 0.20 x 0.06 mm^3	
Theta range for data collection	2.048 to 25.367°.	
Index ranges	-22<=h<=22, -13<=k<=13, -23<=l<=23	
Reflections collected	50785	
Independent reflections	3782 [R(int) = 0.0276]	
Completeness to theta = 25.000°	100.0 %	
Absorption correction	Semi-empirical from equivalents	
Max. and min. transmission	0.8747 and 0.7744	
Refinement method	Full-matrix least-squares on F^2	
Data / restraints / parameters	3782 / 0 / 264	
Goodness-of-fit on F^2	1.046	
Final R indices [I>2sigma(I)]	R1 = 0.0232, wR2 = 0.0576	
R indices (all data)	R1 = 0.0260, wR2 = 0.0601	
Extinction coefficient	n/a	
Largest diff. peak and hole	0.492 and -0.540 $e.Å^{-3}$	

Table S3. Crystal data and structure refinement for **1a**.

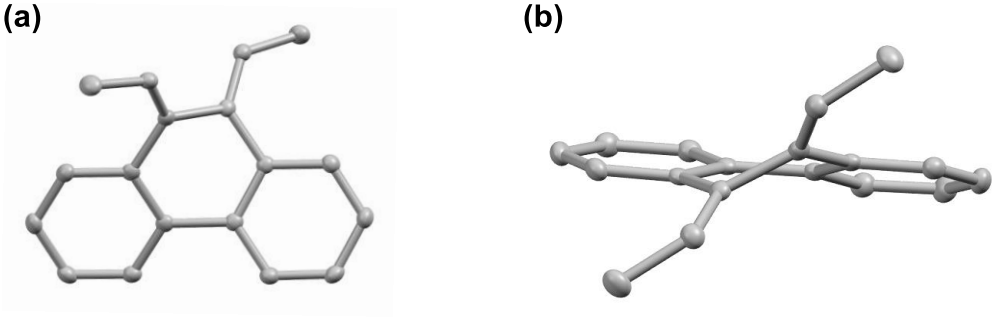

Figure S89. Solid state structure of **2a** as determined by single-crystal X-ray diffraction: (a) top view; (b) side view.

Empirical formula	$C_{18}H_{16}$	
Formula weight	232.31	
Temperature	103(2) K	
Wavelength	0.71073 Å	
Crystal system	Orthorhombic	
Space group	P b c a	
Unit cell dimensions	a = 17.6714(4) Å	□□ = 90°.
	b = 7.7601(2) Å	□□ = 90°.
	c = 18.6180(5) Å	□ = 90°.
Volume	2553.12(11) $Å^3$	
Z	8	
Density (calculated)	1.209 Mg/m^3	
Absorption coefficient	0.068 mm^{-1}	
F(000)	992	
Crystal size	0.120 x 0.100 x 0.050 mm^3	
Theta range for data collection	2.188 to 25.383°.	
Index ranges	-19<=h<=21, -9<=k<=9, -22<=l<=19	
Reflections collected	38868	
Independent reflections	2344 [R(int) = 0.0289]	
Completeness to theta = 25.000°	99.9 %	
Absorption correction	Semi-empirical from equivalents	
Max. and min. transmission	0.9801 and 0.9295	
Refinement method	Full-matrix least-squares on F^2	
Data / restraints / parameters	2344 / 0 / 165	
Goodness-of-fit on F^2	1.060	
Final R indices [I>2sigma(I)]	R1 = 0.0346, wR2 = 0.0872	
R indices (all data)	R1 = 0.0372, wR2 = 0.0897	
Extinction coefficient	n/a	
Largest diff. peak and hole	0.218 and -0.179 $e.Å^{-3}$	

Table S4. Crystal data and structure refinement for **2a**.

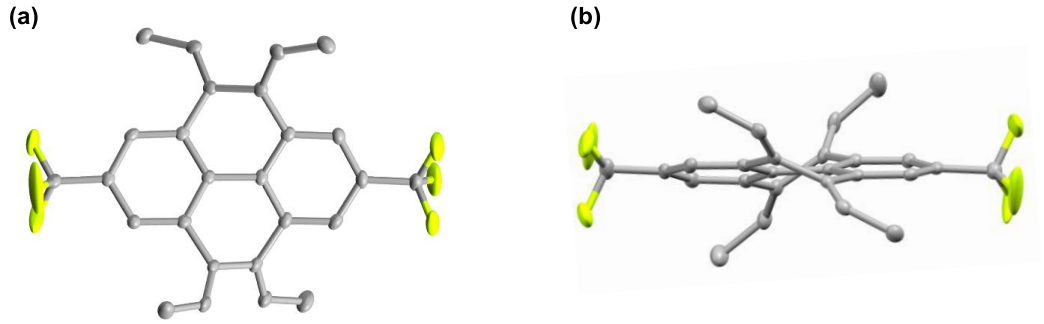

Figure S90. Solid state structure of **2g** as determined by single-crystal X-ray diffraction: (a) top view; (b) side view.

Empirical formula	$C_{26}H_{20}F_6$
Formula weight	446.42
Temperature	100(2) K
Wavelength	0.71073 Å
Crystal system	Orthorhombic
Space group	P 21 21 21
Unit cell dimensions	a = 7.9885(2) Å □□ = 90°. b = 12.0771(4) Å □□ = 90°. c = 21.3587(6) Å □ = 90°.
Volume	2060.64(10) $Å^3$
Z	4
Density (calculated)	1.439 Mg/m^3
Absorption coefficient	0.120 mm^{-1}
F(000)	920
Crystal size	0.100 x 0.080 x 0.070 mm^3
Theta range for data collection	1.907 to 25.370°.
Index ranges	-9<=h<=9, -12<=k<=14, -25<=l<=25
Reflections collected	31813
Independent reflections	3792 [R(int) = 0.0281]
Completeness to theta = 25.000°	100.0 %
Absorption correction	Semi-empirical from equivalents
Max. and min. transmission	0.9703 and 0.9329
Refinement method	Full-matrix least-squares on F^2
Data / restraints / parameters	3792 / 0 / 350
Goodness-of-fit on F^2	1.091
Final R indices [I>2sigma(I)]	R1 = 0.0273, wR2 = 0.0686
R indices (all data)	R1 = 0.0283, wR2 = 0.0694
Absolute structure parameter	0.1(7)
Extinction coefficient	n/a
Largest diff. peak and hole	0.145 and -0.186 $e.Å^{-3}$

Table S5. Crystal data and structure refinement for **2g**.

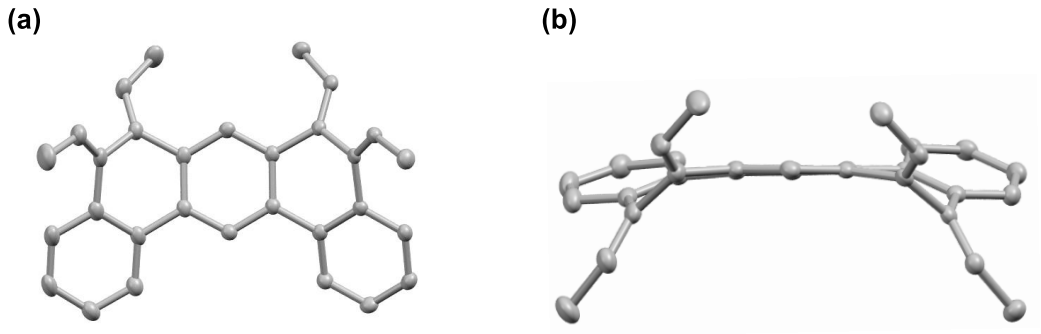

Figure S91. Solid state structure of **2h** as determined by single-crystal X-ray diffraction: (a) top view; (b) side view.

Empirical formula	$C_{30}H_{26}$	
Formula weight	386.51	
Temperature	100(2) K	
Wavelength	0.71073 Å	
Crystal system	Monoclinic	
Space group	P 21/n	
Unit cell dimensions	a = 8.4811(4) Å	□□ = 90°.
	b = 30.5399(13) Å	□□ = 114.107(2)°.
	c = 9.0917(4) Å	□ = 90°.
Volume	2149.48(17) $Å^3$	
Z	4	
Density (calculated)	1.194 Mg/m^3	
Absorption coefficient	0.067 mm^{-1}	
F(000)	824	
Crystal size	0.110 x 0.090 x 0.030 mm^3	
Theta range for data collection	1.334 to 25.421°.	
Index ranges	-10<=h<=10, -36<=k<=36, -10<=l<=10	
Reflections collected	24864	
Independent reflections	3955 [R(int) = 0.0387]	
Completeness to theta = 25.000°	100.0 %	
Absorption correction	Semi-empirical from equivalents	
Max. and min. transmission	0.9801 and 0.9118	
Refinement method	Full-matrix least-squares on F^2	
Data / restraints / parameters	3955 / 0 / 291	
Goodness-of-fit on F^2	1.120	
Final R indices [I>2sigma(I)]	R1 = 0.0445, wR2 = 0.1004	
R indices (all data)	R1 = 0.0498, wR2 = 0.1028	
Extinction coefficient	n/a	
Largest diff. peak and hole	0.184 and -0.188 $e.Å^{-3}$	

Table S6. Crystal data and structure refinement for **2h**.

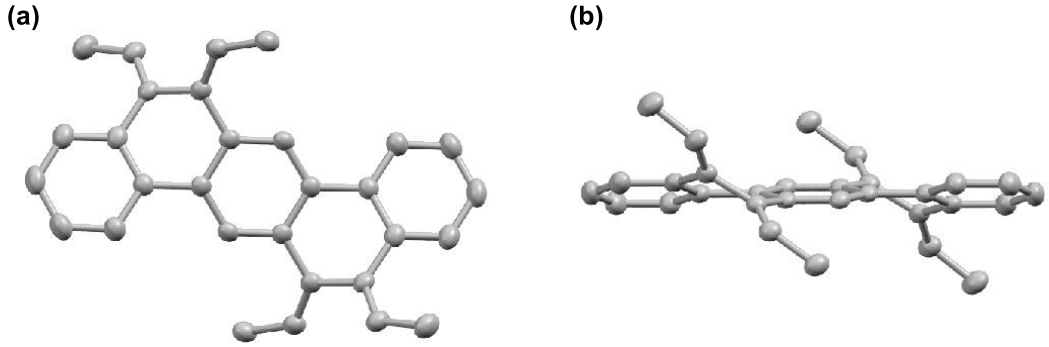

Figure S92. Solid state structure of **2i** as determined by single-crystal X-ray diffraction: (a) top view; (b) side view.

Empirical formula	$C_{30}H_{26}$
Formula weight	386.51
Temperature	100(2) K
Wavelength	1.54178 Å
Crystal system	Monoclinic
Space group	P 21/c
Unit cell dimensions	a = 13.4098(11) Å □□ = 90°. b = 7.7772(6) Å □□ = 95.267(3)°. c = 10.2459(8) Å □ = 90°.
Volume	1064.04(15) $Å^3$
Z	2
Density (calculated)	1.206 Mg/m^3
Absorption coefficient	0.510 mm^{-1}
F(000)	412
Crystal size	0.140 x 0.080 x 0.020 mm^3
Theta range for data collection	6.587 to 68.279°.
Index ranges	-16<=h<=16, -8<=k<=9, -12<=l<=9
Reflections collected	13035
Independent reflections	1951 [R(int) = 0.0423]
Completeness to theta = 25.000°	98.4 %
Absorption correction	Semi-empirical from equivalents
Max. and min. transmission	0.8893 and 0.8006
Refinement method	Full-matrix least-squares on F^2
Data / restraints / parameters	1951 / 0 / 146
Goodness-of-fit on F^2	1.052
Final R indices [I>2sigma(I)]	R1 = 0.0533, wR2 = 0.1432
R indices (all data)	R1 = 0.0549, wR2 = 0.1450
Extinction coefficient	n/a
Largest diff. peak and hole	0.279 and -0.147 $e.Å^{-3}$

Table S7. Crystal data and structure refinement for **2i**.

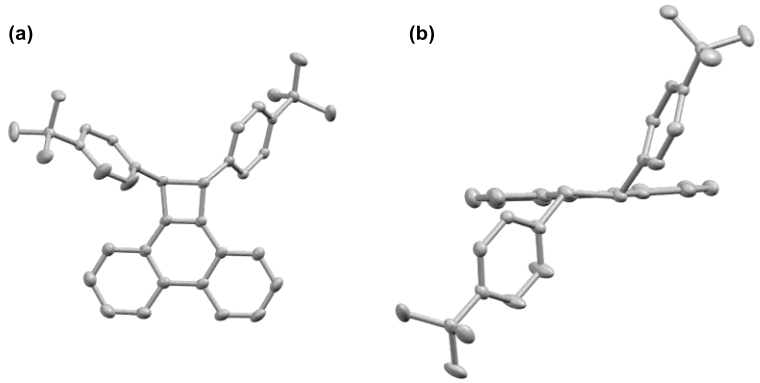

Figure S93. Solid state structure of **10** as determined by single-crystal X-ray diffraction: (a) top view; (b) side view.

Empirical formula	$C_{36}H_{36}$
Formula weight	468.65
Temperature	100(2) K
Wavelength	1.54178 Å
Crystal system	Monoclinic
Space group	P 21/n
Unit cell dimensions	a = 10.9938(4) Å □□ = 90°.
	b = 18.2907(7) Å □□ = 93.404(2)°.
	c = 13.4820(5) Å □ = 90°.
Volume	2706.24(17) $Å^3$
Z	4
Density (calculated)	1.150 Mg/m^3
Absorption coefficient	0.482 mm^{-1}
F(000)	1008
Crystal size	0.150 x 0.130 x 0.080 mm^3
Theta range for data collection	4.078 to 68.278°.
Index ranges	-12<=h<=9, -22<=k<=22, -16<=l<=16
Reflections collected	95058
Independent reflections	4920 [R(int) = 0.0312]
Completeness to theta = 67.000°	99.4 %
Absorption correction	Semi-empirical from equivalents
Max. and min. transmission	0.9022 and 0.8026
Refinement method	Full-matrix least-squares on F^2
Data / restraints / parameters	4920 / 6 / 370
Goodness-of-fit on F^2	1.030
Final R indices [I>2sigma(I)]	R1 = 0.0397, wR2 = 0.0947
R indices (all data)	R1 = 0.0428, wR2 = 0.0978
Extinction coefficient	n/a
Largest diff. peak and hole	0.209 and -0.308 $e.Å^{-3}$

Table S8. Crystal data and structure refinement for **10**.

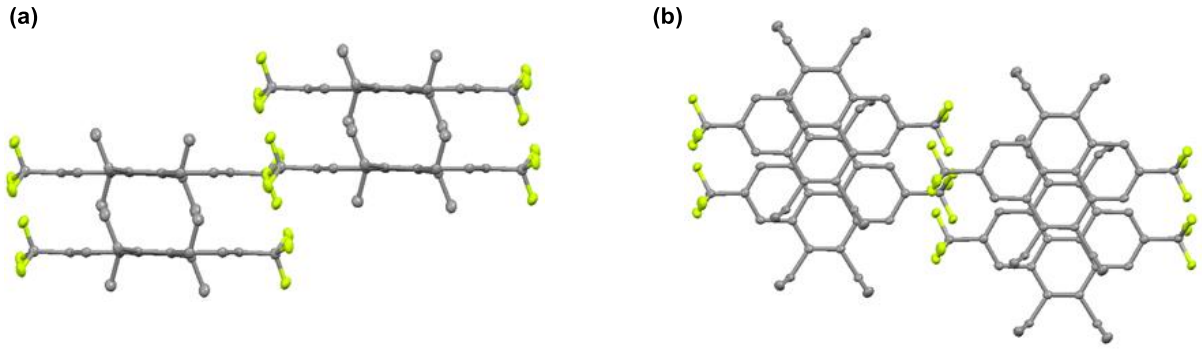

Figure S94. Solid state packing of **21** as determined by single-crystal X-ray diffraction: (a) side view; (b) top view.

Empirical formula	$C_{26}H_{24}F_6$	
Formula weight	450.45	
Temperature	100(2) K	
Wavelength	1.54178 Å	
Crystal system	Triclinic	
Space group	P -1	
Unit cell dimensions	a = 4.8048(2) Å	□□ = 116.788(2)°.
	b = 10.9498(5) Å	□□ = 98.857(3)°.
	c = 11.2373(6) Å	□ = 92.562(3)°.
Volume	517.09(4) $Å^3$	
Z	1	
Density (calculated)	1.447 Mg/m^3	
Absorption coefficient	1.033 mm^{-1}	
F(000)	234	
Crystal size	0.100 x 0.040 x 0.030 mm^3	
Theta range for data collection	4.494 to 68.268°.	
Index ranges	-5<=h<=4, -13<=k<=13, -13<=l<=13	
Reflections collected	11487	
Independent reflections	1855 [R(int) = 0.0361]	
Completeness to theta = 67.000°	98.1 %	
Absorption correction	Semi-empirical from equivalents	
Max. and min. transmission	0.6870 and 0.5549	
Refinement method	Full-matrix least-squares on F^2	
Data / restraints / parameters	1855 / 0 / 163	
Goodness-of-fit on F^2	1.047	
Final R indices [I>2sigma(I)]	R1 = 0.0317, wR2 = 0.0907	
R indices (all data)	R1 = 0.0355, wR2 = 0.0937	
Extinction coefficient	n/a	
Largest diff. peak and hole	0.232 and -0.201 $e.Å^{-3}$	

Table S9. Crystal data and structure refinement for **21**.

References for Supporting Information of Chapter 2

(1) Bong, D. T.-Y.; Chan, E. W. L.; Diercks, R.; Dosa, P. I.; Haley, M. M.; Matzger, A. J.; Miljanić, O. Š.; Vollhardt, K. P. C.; Bond, A. D.; Teat, S. J.; Stanger, A. *Org. Lett.* **2004**, *6* (13), 2249–2252.
(2) Levi, Z. U.; Tilley, T. D. *J. Am. Chem. Soc.* **2009**, *131* (8), 2796–2797.
(3) Körner, C.; Starkov, P.; Sheppard, T. D. *J. Am. Chem. Soc.* **2010**, *132* (17), 5968–5969.
(4) Gronowitz, S.; Holm, B.; Rappe, C.; Hänninen, O.; Vialle, J.; Anthonsen, T. *Acta Chem. Scand.* **1976**, *30b*, 423–429.
(5) Chanteau, S. H.; Tour, J. M. *J. Org. Chem.* **2003**, *68* (23), 8750–8766.
(6) Goldfinger, M. B.; Crawford, K. B.; Swager, T. M. *J. Am. Chem. Soc.* **1997**, *119* (20), 4578–4593.
(7) Hoye, T. R.; Eklov, B. M.; Voloshin, M. *Org. Lett.* **2004**, *6* (15), 2567–2570.
(8) Goldfinger, M. B.; Crawford, K. B.; Swager, T. M. *J. Am. Chem. Soc.* **1997**, *119* (20), 4578–4593.
(9) Chinchilla, R.; Nájera, C. *Chem. Rev.* **2007**, *107* (3), 874–922.
(10) Miyaura, Norio.; Suzuki, Akira. *Chem. Rev.* **1995**, *95* (7), 2457–2483.
(11) Miyake, Y.; Wu, M.; Rahman, M. J.; Kuwatani, Y.; Iyoda, M. *J. Org. Chem.* **2006**, *71* (16), 6110–6117.
(12) An, D.-L.; Zhang, Z.; Orita, A.; Mineyama, H.; Otera, J. *Synlett* **2007**, *2007* (12), 1909–1912.
(13) Benhamou, L.; Walker, D. W.; Bučar, D.-K.; Aliev, A. E.; Sheppard, T. D. *Org. Biomol. Chem.* **2016**, *14* (34), 8039–8043.
(14) Staab, H. A.; Mack, H.; Nissen, A. *Chem. Ber.* **1972**, *105* (7), 2310–2319.
(15) Bradsher, C. K.; Jackson, W. J. *J. Am. Chem. Soc.* **1954**, *76* (16), 4140–4143.
(16) Kanno, K.; Liu, Y.; Iesato, A.; Nakajima, K.; Takahashi, T. *Org. Lett.* **2005**, *7* (24), 5453–5456.
(17) Sheldrick, G. M. A *Acta Crystallogr. A* **2008**, *64* (1), 112–122.
(18) Sheldrick, G. M. *Acta Crystallogr. Sect. Found. Adv.* **2015**, *71* (1), 3–8.
(19) Palatinus, L.; Chapuis, G. *J. Appl. Crystallogr.* **2007**, *40* (4), 786–790.
(20) Sheldrick, G. M. *Acta Crystallogr. Sect. C Struct. Chem.* **2015**, *71* (1), 3–8.
(21) Macrae, C. F.; Edgington, P. R.; McCabe, P.; Pidcock, E.; Shields, G. P.; Taylor, R.; Towler, M.; Streek, J. van de. *J. Appl. Crystallogr.* **2006**, *39* (3), 453–457.

Chapter 3: Expanded Helicenes: General Synthetic Strategy and Remarkable Self-Assembly

This chapter was adapted with permission from: Kiel, G. R.; Patel, S. C.; Smith, P. W.; Levine, D. S.; Tilley, T. D., *J. Am. Chem. Soc.*, **2017**, 139, 18456–18459.

A helicene has been defined as "a polycyclic aromatic hydrocarbon (PAH) with a nonplanar, screw-shaped skeleton formed by ortho-fused benzene or other aromatic rings".[1] These compounds display remarkable properties[1d] such as large non-linear optical responses,[2] circularly polarized absorption and emission,[3] rich supramolecular chemistry,[4] and relatively high solubility. Thus, helicenes are now being investigated for applications in electronics and optoelectronics,[3b,3c,5] asymmetric catalysis (e.g. as ligands),[6] molecular recognition,[7] and as molecular machines and switches.[8] Due to their significant distortion from planarity and resulting three-dimensional structure, helicenes also offer the possibility of novel intermolecular interactions in the solid state (e.g. π-stacking in two or three dimensions).[9] Toward this end, helicenes play an important role in the growing field of crystal engineering with non-planar PAHs.[10]

Most reported helicenes possess all angularly-fused aromatic rings (**A**, Figure 1). Increasing the size of a helicene by alternation of linear and angular ring fusion ("expanded helicene", **B**) or lateral extension of its π-system ("laterally-extended helicene", **C**) might result in novel electronic, photophysical, and chirotopical properties. The possible increase in π-stacking could result in discovery of new or enhanced supramolecular or solid-state properties (e.g. higher charge-carrier mobilities). Their flexible structures should make them more soluble than analogous linear PAHs and their larger cavities are conducive to applications that rely on porosity (e.g., sensing or catalysis).

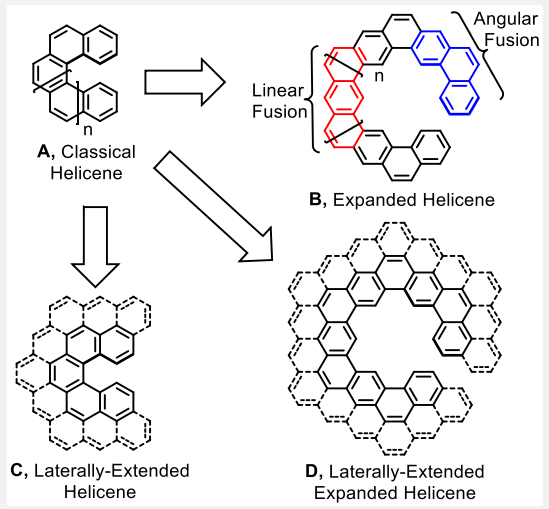

Figure 1. Simple Classification of Larger Helicenes.

A growing number of laterally-extended helicenes have been well-characterized,[11] but expanded helicenes are unexplored. The term "expanded heterohelicene" was used to describe a helicene-like compound with alternating angular and linear fusion of six-membered rings; however, this compound contains several saturated rings.[12] A few other helical PAHs with expanded cavities are known. For example, Vollhardt reported a series of heliphenes, which are composed of alternating six- and four-membered rings fused in an angular fashion.[13]

The central challenge associated with the investigation of helicenes is their difficult synthesis, which requires both the introduction of strain and regioselective fusion of many rings. Many methods have been developed,[1b] including photocyclization of stilbenes,[14] Diels-Alder cycloaddition,[15] and fully-intramolecular [2+2+2] cycloisomerization.[13,16] These methods have allowed exhaustive studies of classical helicenes, but they are difficult to apply to expanded helicenes, for which the central challenge is regioselective fusion of many rings.

As part of an effort to increase the utility of [2+2+n] cycloadditions in PAH synthesis, we recently developed a strategy for the synthesis of large PAHs *via* zirconocene coupling, involving the reductive cyclization of oligo(diynes) (**1**, Scheme 1a) to form zirconacyclopentadiene-annulated PAHs (**2**).[17] Two compelling features of this strategy are the near-quantitative nature of the zirconocene coupling reaction and the known synthetic versatility[18] of the resulting zirconacyclopentadiene functionality.

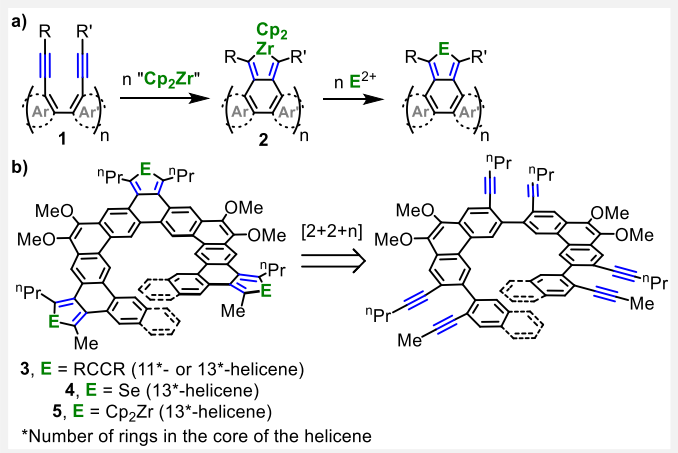

Scheme 1. (a) Previously Reported General Strategy; **(b)** Application of Strategy to Expanded Helicenes.

Here we report a general strategy for use of [2+2+n] cycloadditions in the synthesis of expanded helicenes (Scheme 1b). The effort was aided by identification of a *catalytic* and essentially *quantitative* [2+2+2] cycloaddition to access a series of benzannulated expanded helicenes (**3**). This partially-intermolecular[19] [2+2+2] reaction was enabled by a commercially-available Ir catalyst and is complementary to the stoichiometric zirconocene-coupling reaction used to access expanded helicenes **4** and **5**. One of the benzannulated expanded helicenes undergoes an unusual, diastereoselective dimerization *via* π-stacking, both in solution and in the solid state, while a quite different solid-state packing was observed for analogous **4**. Finally, the presence of diastereotopic Cp rings in **5** allowed the determination of its racemization barrier by dynamic ^{1}H NMR spectroscopy, suggesting that expanded helicenes are much more flexible than all-angularly-fused helicenes.

Execution of the synthetic strategy was enabled by the availability of **6** (Scheme 2) in large (>100 g) quantities.[20] This compound was reduced and methylated in one pot to give **7** using a scalable protocol for a similar compound,[21] and a subsequent Sonogashira reaction[22] gave diyne **8**. A selective mono-lithiation of **8** with ^{n}BuLi permitted a $CuCl_2$-mediated oxidative homocoupling to give tetrayne **9**. Finally, cross-coupling of **9** with metallated (alkynyl)benzene **10** and (alkynyl)naphthalene **11** gave tris(diynes) **12** and **13** in 52 and 64% yields, respectively.

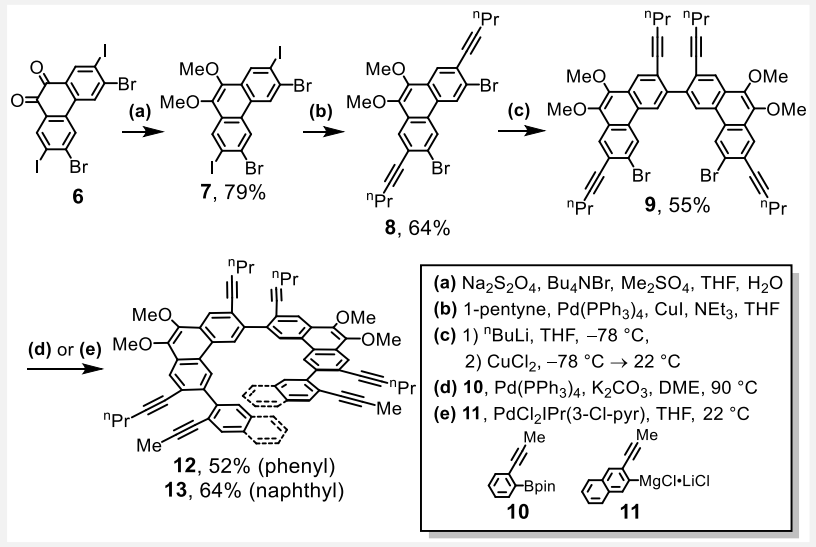

Scheme 2. Synthesis of Expanded Helicene Precursors.

An optimal [2+2+2] catalytic system was identified for the ring-fusion reaction (Scheme 3), based on modification of a previously-reported procedure[23] employing $[Ir(COD)Cl]_2$ and dppe. Treatment of tris(diyne)s **12** and **13** with six equiv (two equiv per diyne unit) of the corresponding monoyne in the presence of this catalyst produced the corresponding expanded 11-helicenes **3a-b** and expanded 13-helicene **3c** in good to excellent isolated yields. Helicenes **3a**–**3c** are very soluble in CH_2Cl_2 and THF (>100 mg/mL), which is notable given their size, and **3b** is similarly soluble in hexanes. The remarkable efficiency of this reaction is indicated by ^{1}H NMR spectroscopy, which revealed essentially

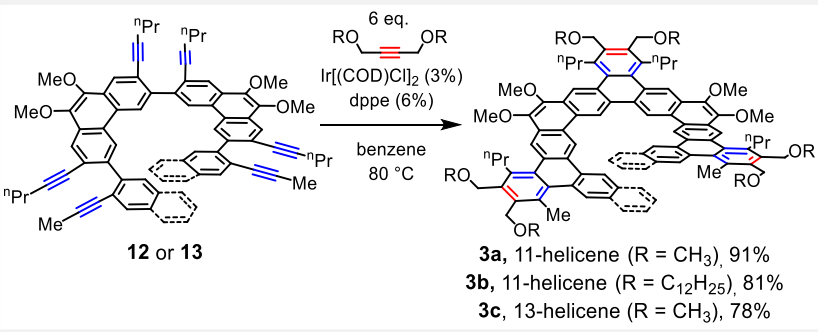

Scheme 3. Expanded Helicenes *via* a Three-fold, Partially-intramolecular, Ir-catalyzed [2+2+2] Cycloaddition.

quantitative formation of **3a–c**. This suggests its applicability to even larger expanded helicenes utilizing more than three couplings (including polymers).

A ^{1}H NMR analysis of a dilute (8.2 x 10^{-4} M) solution of **3c** in chloroform-*d* is consistent with a monomeric expanded 13-helicene; however, concentration of this solution results in the emergence of a new species with reduced symmetry and upfield-shifted aromatic resonances (Scheme 4). The structure of this new species was assigned *via* ^{1}H-^{1}H NOESY (see SI, Figure S1) as the homochiral, π-stacked dimer **3c-Dim**. The presence of a monomer-dimer equilibrium was confirmed by variable-concentration ^{1}H NMR spectroscopy (Figure S2). Variable-temperature ^{1}H NMR spectroscopy allowed measurement of thermodynamic parameters ($\Delta H° = -9.6 \pm 0.3$ kcal/mol and $\Delta S° = -26 \pm 1.0$ cal/mol·K) (Figures S3 and S4). The chemical shifts for **3c-Dim** do not vary with concentration, suggesting that there is no further aggregation (e.g. tetramers). This slow, unusual dimerization is likely driven by π-stacking between helicenes. Notably, PAH aggregation equilibria that are slow enough to be directly observed by ^{1}H NMR spectroscopy are extremely rare.[24]

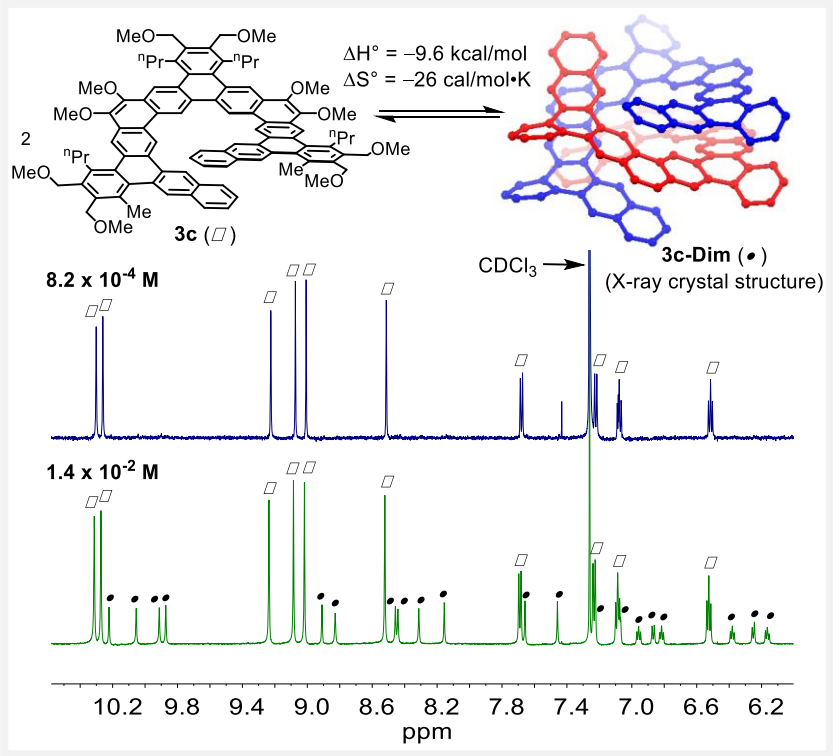

Scheme 4. Slow Equilibrium between Expanded 13-Helicene and its Homochiral, π-Stacked Dimer.

Single crystals of **3c** were grown by slow evaporation from chloroform-*d*, and X-ray crystallography revealed formation of the **3c-Dim** in the solid state (Scheme 4), with the helicenes in the dimer related by a pseudo-C_2 axis of symmetry. The distorted nature of the helicene in its dimeric form can be quantified by its pitch of 7.44 Å, which was calculated by fitting a helical curve to the thirteen centroids of the inner rings.[25] For comparison, the DFT-calculated structure of the monomer revealed a pitch of 3.30 Å (see SI). Due to the presence of the pseudo-C_2 axis in the dimer, half of the pitch of its monomeric component (3.72 Å) can be used as an estimate of the average π-stacking distance between

the two helicenes. The true average π-stacking distance is shorter since this is formally the distance between centroids, which are not aligned. The chiral dimers co-crystallize with their dimeric enantiomer in the centrosymmetric space group $P2_1/c$. There are no π-stacking interactions *between* dimers, which is consistent with the observed solution behavior (*vide supra*), and large voids in the crystal are filled by chloroform-*d* (2.5 equiv per helicene).

In contrast to expanded 13-helicene **3c**, no aggregation is apparent in chloroform-*d* solution for the analogous 11-helicene **3a**, as ^{1}H chemical shifts are invariant over concentrations between 4.2 x 10^{-2} and 8.4 x 10^{-5} M (Figure S5). However, when the more soluble analogue **3b** is dissolved in methylcyclohexane-d_{14} (at 22 °C), the ^{1}H NMR spectrum consists of a complex mixture of broadened and upfield-shifted resonances. Variable-temperature ^{1}H NMR spectroscopy (Figure S6) suggests this results from aggregation of some type.

While the dimerization of **3c** is interesting, extended π-stacking is often desirable (e.g. for applications that require efficient charge transport). Given that the presence of heteroatoms has a profound impact on self-assembly, selenophene-annulated expanded helicene **4** was targeted (Scheme 5). This compound was accessible in two steps from tris(diyne) **13**, *via* the intermediacy of zirconacyclopentadiene-annulated expanded helicene **5**. In contrast to the analogous **3c,** single crystal X-ray crystallography revealed long-range π-stacking for **4**. The helicenes stack as alternating *M* and *P* enantiomers, with a shortest intermolecular π-π distance of 3.6 Å. Helicene **4** exhibits a small pitch of 3.23 Å in the solid state, which is consistent with its DFT-calculated pitch of 3.29 Å. The small pitches for monomeric **3c** (calculated) and **4** (calculated and experimental) appear to be driven by a π-stacking interaction at their termini. These pitches are much smaller than those of topologically similar [7]helicene[26] and [7]heliphene,[13a] which are 3.82 and 4.29 Å, respectively.

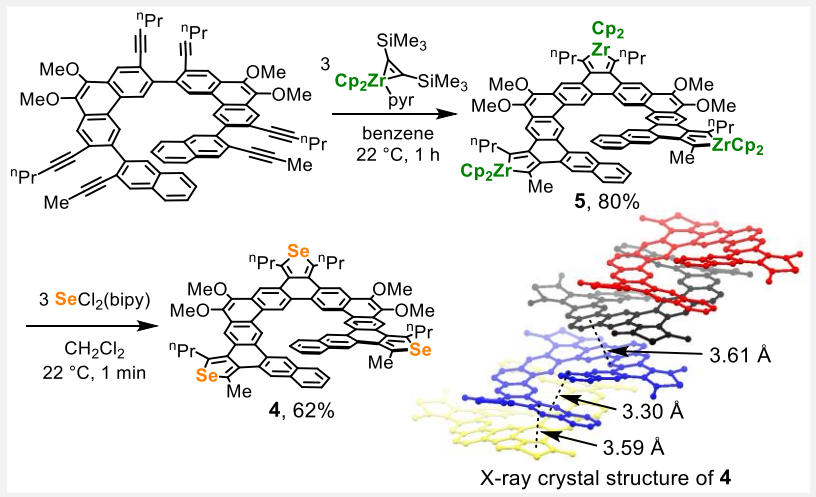

Scheme 5. Expanded Helicenes *via* Zirconocene Coupling.

The new expanded helicenes possess low racemization barriers, which is evident in their room temperature ^{1}H NMR spectra. There are sharp singlets for the diastereotopic methylene resonances in compounds **3a–c** and only two Cp-H singlets (in 2:1 ratio) for **5**. Due to its monomeric nature and diastereotopic Cp rings, **5** provides an opportunity to study the configurational lability of the expanded

13-helicene framework by dynamic ^{1}H NMR spectroscopy (Scheme 6). Upon cooling a toluene-d_8/tetrahydrofuran (3:1) solution of **5**, the more intense singlet decoalesces, giving a 1:1:1 singlet ratio. This allowed calculation of a racemization barrier ($\Delta G^{\ddagger}_{-62°C}$) of 10.7 kcal/mol. The barriers for [7]helicene[27] and [7]heliphene[13a] are 41.7 ($\Delta G^{\ddagger}_{27°C}$) and 12.6 kcal/mol ($\Delta G^{\ddagger}_{-27°C}$), respectively. The low barrier compared to [7]helicene might be attributed to the fact that the distortion required for racemization is spread over a larger number of bonds and angles (as for [7]heliphene).

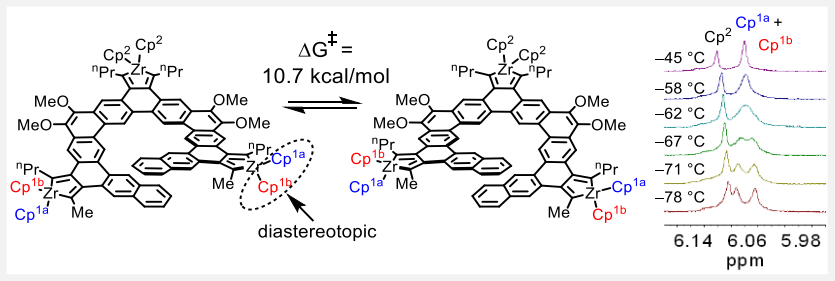

Scheme 6. Racemization Barrier for Expanded 13-Helicene **5**.

In conclusion, five highly functionalized expanded helicenes were synthesized using a general, divergent strategy, which allowed studies on supramolecular organization and configurational stability. This generality will allow a systematic investigation of this fascinating compound class. We are currently exploring ways to increase configurational stability and reliably control supramolecular organization. Most importantly, the synthetic strategy should be applicable to other PAH topologies and graphene nanostructures.

References for Main Text of Chapter 3

(1) (a) Shen, Y.; Chen, C.-F. *Chem. Rev.* **2012**, *112*, 1463. (b) Gingras, M. *Chem. Soc. Rev.* **2013***, 42*, 968. (c) Gingras, M.; Félix, G.; Peresutti, R. *Chem. Soc. Rev.* **2013**, *42*, 1007. (d) Gingras, M. *Chem. Soc. Rev.* **2013**, *42*, 1051. (e) Rickhaus, M.; Mayor, M.; Juríček, M. *Chem. Soc. Rev.* **2016**, *45*, 1542.

(2) Verbiest, T.; Elshocht, S. V.; Kauranen, M.; Hellemans, L.; Snauwaert, J.; Nuckolls, C.; Katz, T. J.; Persoons, A. *Science* **1998**, *282*, 913.

(3) (a) Field, J. E.; Muller, G.; Riehl, J. P.; Venkataraman, D. *J. Am. Chem. Soc.* **2003**, *125*, 11808. (b) Yang, Y.; Correa da Costa, R.; Fuchter, M. J.; Campbell, A. J. *Nat. Photonics* **2013**, *7*, 634. (c) Brandt, J. R.; Wang, X.; Yang, Y.; Campbell, A. J.; Fuchter, M. J. *J. Am. Chem. Soc.* **2016**, *138*, 9743.

(4) (a) Nuckolls, C.; Katz, T. J.; Castellanos, L. *J. Am. Chem. Soc.* **1996**, *118*, 3767. (b) Shcherbina, M. A.; Zeng, X.; Tadjiev, T.; Ungar, G.; Eichhorn, S. H.; Phillips, K. E. S.; Katz, T. J. *Angew. Chem. Int. Ed.* **2009**, *48*, 7837.

(5) (a) Brandt, J. R.; Salerno, F.; Fuchter, M. J. *Nat. Rev. Chem.* **2017**, *1*, 45. (b) Yang, Y.; Rice, B.; Shi, X.; Brandt, J. R.; Correa da Costa, R.; Hedley, G. J.; Smilgies, D.-M.; Frost, J. M.; Samuel, I. D. W.; Otero-de-la-Roza, A.; Johnson, E. R.; Jelfs, K. E.; Nelson, J.; Campbell, A. J.; Fuchter, M. J. *ACS Nano* **2017**, *11*, 8329. (c) Vacek, J.; Chocholoušová, J. V.; Stará, I. G.; Starý, I.; Dubi, Y. *Nanoscale* **2015**, *7*, 8793.

(6) Narcis, M. J.; Takenaka, N. *Eur. J. Org. Chem.* **2014**, 2014, 21.

(7) Chen, C.-F.; Shen, Y. In *Helicene Chemistry*; Springer, Berlin, Heidelberg, **2017**; pp 201–220.

(8) (a) Schweinfurth, D.; Zalibera, M.; Kathan, M.; Shen, C.; Mazzolini, M.; Trapp, N.; Crassous, J.; Gescheidt, G.; Diederich, F. *J. Am. Chem. Soc.* **2014**, *136*, 13045. (b) Shen, C.; Loas, G.; Srebro-Hooper, M.; Vanthuyne, N.; Toupet, L.; Cador, O.; Paul, F.; López Navarrete, J. T.; Ramírez, F. J.; Nieto-Ortega, B.; Casado, J.; Autschbach, J.; Vallet, M.; Crassous, J. *Angew. Chem. Int. Ed.* **2016**, *55*, 8062.

(9) (a) Ball, M.; Zhong, Y.; Wu, Y.; Schenck, C.; Ng, F.; Steigerwald, M.; Xiao, S.; Nuckolls, C. *Acc. Chem. Res.* **2015**, *48*, 267. (b) Fujikawa, T.; Segawa, Y.; Itami, K. *J. Am. Chem. Soc.* **2015**, *137*, 7763.

(10) Gsänger, M.; Oh, J. H.; Könemann, M.; Höffken, H. W.; Krause, A.-M.; Bao, Z.; Würthner, F. *Angew. Chem. Int. Ed.* **2010**, *49*, 740.

(11) We include contorted aromatics and related compounds containing multiple helicenes embedded in a larger PAH framework. Examples with a single helical axis: (a) Schlütter, F.; Nishiuchi, T.; Enkelmann, V.; Müllen, K. *Angew. Chem. Int. Ed.* **2014**, *53,* 1538. (b) Schuster, N. J.; Paley, D. W.; Jockusch, S.; Ng, F.; Steigerwald, M. L.; Nuckolls, C. *Angew. Chem. Int. Ed.* **2016**, 55, 13519. (c) Fujikawa, T.; Segawa, Y.; Itami, K. *J. Org. Chem.* **2017**, 82, 7745. Examples with multiple helical axes: (d) Ref 9. (e) Barnett, L.; Ho, D. M.; Baldridge, K. K.; Pascal Jr., R. A. *J. Am. Chem. Soc.* **1999**, *121*, 727. (f) Wang, X.-Y.; Wang, X.-C.; Narita, A.; Wagner, M.; Cao, X.-Y.; Feng, X.; Müllen, K. *J. Am. Chem. Soc.* **2016**, 138, 12783. (g) Fujikawa, T.; Segawa, Y.; Itami, K. *J. Am. Chem. Soc.* **2016**, *138*, 3587. (h) Pradhan, A.; Dechambenoit, P.; Bock, H.; Durola, F. *Chem. Eur. J.* **2016**, *22*, 18227. (i) Hu, Y.; Wang, X.-Y.; Peng, P.-X.; Wang, X.-C.; Cao, X.-Y.; Feng, X.; Müllen, K.; Narita, A. *Angew. Chem. Int. Ed.* **2017**, *56*, 3374. (j) Hosokawa, T.; Takahashi, Y.; Matsushima, T.; Watanabe, S.; Kikkawa, S.; Azumaya, I.; Tsurusaki, A.; Kamikawa, K. *J. Am. Chem. Soc.* **2017**, DOI: 10.1021/jacs.7b07113.

(12) Bell, T. W.; Jousselin, H. *J. Am. Chem. Soc.* **1991**, *113*, 6283.

(13) (a) Han, S.; Bond, A. D.; Disch, R. L.; Holmes, D.; Schulman, J. M.; Teat, S. J.; Vollhardt, K. P. C.; Whitener, G. D. *Angew. Chem. Int. Ed.* **2002**, *41*, 3223. (b) Han, S.; Anderson, D. R.; Bond, A. D.; Chu, H. V.; Disch, R. L.; Holmes, D.; Schulman, J. M.; Teat, S. J.; Vollhardt, K. P. C.; Whitener, G. D. *Angew. Chem. Int. Ed.* **2002**, *41*, 3227.
(14) (a) Flammang-Barbieux, M.; Nasielski, J.; Martin, R. H. *Tetrahedron Lett.* **1967**, *8*, 743. (b) Mallory, F. B.; Mallory, C. W. In Organic Reactions; John Wiley & Sons, Inc.: Hoboken, NJ, **1984**; Vol. 30, pp 1–456.
(15) Liu, L.; Katz, T. J. *Tetrahedron Lett.* **1990**, *31*, 3983.
(16) (a) Teplý, F.; Stará, I. G.; Starý, I.; Kollárovič, A.; Šaman, D.; Rulíšek, L.; Fiedler, P. *J. Am. Chem. Soc.* **2002**, *124*, 9175. (b) Šámal, M.; Chercheja, S.; Rybáček, J.; Vacek Chocholoušová, J.; Vacek, J.; Bednárová, L.; Šaman, D.; Stará, I. G.; Starý, I. *J. Am. Chem. Soc.* **2015**, *137*, 8469. (c) Tanaka, K. In *Transition-Metal-Mediated Aromatic Ring Construction*; Tanaka, K., Ed.; John Wiley & Sons, Inc.: Hoboken, NJ, **2013**; pp 281–298.
(17) Kiel, G. R.; Ziegler, M. S.; Tilley, T. D. *Angew. Chem. Int. Ed.* **2017**, *56*, 4839.
(18) (a) Nugent, W. A.; Thorn, D. L.; Harlow, R. L. *J. Am. Chem. Soc.* **1987**, *109*, 2788. (b) Yan, X.; Xi, C. *Acc. Chem. Res.* **2015**, *48*, 935. (c) Takahashi, T.; Xi, Z.; Yamazaki, A.; Liu, Y.; Nakajima, K.; Kotora, M. *J. Am. Chem. Soc.* **1998**, *120*, 1672. (d) Takahashi, T.; Hara, R.; Nishihara, Y.; Kotora, M. *J. Am. Chem. Soc.* **1996**, 118, 5154.
(19) While the fully-intramolecular [2+2+2] cycloaddition of triynes (i.e. "cycloisomerization") is heavily-developed for helicene synthesis (refs 13 and 16), there have been very few applications of the partially-intermolecular [2+2+2] of a diyne and monoyne. The latter is potentially more general, but it is also more difficult to control. For a notable example of a helicene-like compound produced in this way, see: Sawada, Y.; Furumi, S.; Takai, A.; Takeuchi, M.; Noguchi, K.; Tanaka, K. *J. Am. Chem. Soc.* **2012**, *134*, 4080.
(20) Shirai, Y.; Osgood, A. J.; Zhao, Y.; Yao, Y.; Saudan, L.; Yang, H.; Yu-Hung, C.; Alemany, L. B.; Sasaki, T.; Morin, J.-F.; Guerrero, J. M.; Kelly, K. F.; Tour, J. M. *J. Am. Chem. Soc.* **2006**, *128*, 4854.
(21) Paruch, K.; Katz, T. J.; Incarvito, C.; Lam, K.-C.; Rhatigan, B.; Rheingold, A. L. *J. Org. Chem.* **2000**, *65*, 7602.
(22) Chinchilla, R.; Nájera, C. *Chem. Rev.* **2007**, *107*, 874.
(23) Kezuka, S.; Tanaka, S.; Ohe, T.; Nakaya, Y.; Takeuchi, R. *J. Org. Chem.* **2006**, *71*, 543.
(24) (a) Wu, J.; Fechtenkötter, A.; Gauss, J.; Watson, M. D.; Kastler, M.; Fechtenkötter, C.; Wagner, M.; Müllen, K. *J. Am. Chem. Soc.* **2004**, *126*, 11311. (b) Shao, C.; Grüne, M.; Stolte, M.; Würthner, F. *Chem. Eur. J.* **2012**, *18*, 13665.
(25) All pitches were calculated as described in: Enkhbayar, P.; Damdinsuren, S.; Osaki, M.; Matsushima, N. *Comput. Biol. Chem.* **2008**, *32*, 307.
(26) Beurskens, P. T.; Beurskens, G.; van den Hark, T. E. M. *Cryst. Struct. Comm.* **1976**, *5*, 241.
(27) Martin, R. H., Marchant, M. J., *Tetrahedron*, **1974**, *30*, 347.

Supporting Information for Chapter 3

General Details

Unless otherwise stated, all manipulations of organometallic compounds were carried out in dry solvents under an atmosphere of nitrogen, using either standard Schlenk techniques or a glovebox. Dichloromethane (CH_2Cl_2) and tetrahydrofuran (THF) were dried using a JC Meyers Phoenix SDS solvent purification system. Benzene was dried using a Vacuum Atmosphere solvent purification system. Benzene-d_6 was freed from oxygen using three free-pump-thaw cycles and then dried for at least 24 h over 3 Å molecular sieves (5% by mass). All solvents were stored over 3 Å molecular sieves. $SeCl_2$(bipy),[1] Cp_2Zr(pyr)($Me_3SiC{\equiv}CSiMe_3$),[2] ^{i}PrMgCl·LiCl,[3] $PdCl_2$(IPr)(3-chloropyridine),[4] $[Ir(COD)Cl]_2$,[5] 1,4-dimethoxy-2-butyne,[6] 3,6-dibromo-2,7-diiodophenanthrene-9,10-dione (**6**),[7] 1-bromo-2-(propynyl)benzene,[8] and 2-Bromo-3-hydroxynaphthalene[9] were prepared by literature procedures or slight modifications thereof. ^{i}PrMgCl·LiCl and ^{n}BuLi were titrated by ^{1}H NMR spectroscopy immediately prior to use.[10] All other reagents and solvents were purchased from commercial suppliers and used as received. Melting points were determined on an SRS OptiMelt and are uncorrected. Mass spectrometry was performed by the QB3/Chemistry Mass Spectrometry Facility at the University of California, Berkeley. Elemental analyses were performed by the Microanalytical Laboratory in the College of Chemistry at the University of California, Berkeley. Column chromatography was carried out using Fischer Chemical 40–63μm, 230–400 mesh silica gel. Unless otherwise noted, NMR spectra were acquired at ambient temperature (~22 °C) using Bruker AV-600, AV-500, DRX-500, AV-400, and AV-300 spectrometers. Chemical shifts (δ) are given in ppm and referenced to residual solvent peaks for ^{1}H NMR spectra (δ = 7.26 ppm for chloroform-*d* and δ = 7.16 for benzene-d_6) and for $^{13}C\{^1H\}$ NMR spectra (δ = 77.16 ppm for chloroform-*d*).

Synthetic Procedures and Characterization of Compounds

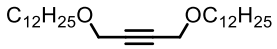

S1

1,4-bis(dodecyloxy)but-2-yne (S1). A 100 mL round-bottomed flask equipped with a magnetic stirbar was charged with 2-butyne-1,4-diol (3.00 g, 34.8 mmol), powdered KOH (7.80 g, 139 mmol), and dimethyl sulfoxide (30 mL). To the stirred solution was added 1-bromododecane (19.1 g, 76.6 mmol) over ~10 min (a rate that maintained the temperature below 45 °C). The flask was then placed on an oil bath at 50 °C and the reaction mixture was stirred for 4 h. The mixture was poured into ice-cold water (150 mL), then the waxy precipitate was collected by filtration and washed with water (50 mL). The solid was partitioned between hexanes (150 mL) and aqueous HCl (1 M, 100 mL), then the aqueous layer was extracted with hexanes (50 mL). The combined hexanes layers were dried with $MgSO_4$, filtered, and solvent was removed from the filtrate *via* rotary evaporation to give a white crystalline solid (14 g). The solid was dissolved in diethyl ether (50 mL), then the solution was diluted with methanol (50 mL) and cooled to –25 °C for ~12 h. The resulting needles were collected by filtration, washed with methanol (30 mL), and residual solvents were removed under a stream of air. The yield of colorless needles was 12.7 g (86%). ^{1}H NMR (chloroform-*d*, 400 MHz): δ 4.16 (s, 4H), 3.48 (t, *J* = 6.6 Hz, 4H), 1.57 (p, *J* = 6.8 Hz, 4H), 1.18 – 1.38 (m, 36H), 0.87 (t, *J* = 6.7 Hz, 6H); ^{13}C{^{1}H} NMR (chloroform-*d*, 101 MHz): δ = 82.42, 70.40, 58.41, 32.06, 29.81, 29.78, 29.76, 29.74, 29.68, 29.60, 29.50, 26.27, 22.83, 14.24; HRMS-EI (m/*z*): $[M]^+$ calcd. for $C_{28}H_{54}O_2$, 422.4124; found, 422.4123.

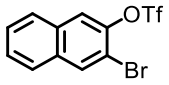

S2

3-bromonaphthalen-2-yl trifluoromethanesulfonate (S2). This compound was prepared by a modified literature procedure.[11] A 250 mL Schlenk flask was loaded with 2-bromo-3-hydroxynaphthalene (5.80 g, 26.0 mmol), dry pyridine (4.1 g, 52 mmol), and CH_2Cl_2 (50 mL) and the resulting solution was cooled to 0 °C with an ice/water bath. To the stirred solution was added Tf_2O (8.2 g, 29 mmol) dropwise over 10 min *via* syringe. The mixture was stirred for 2–3 min at this temperature, then it was allowed to warm to RT, stirred for a further 2 h, and quenched with aqueous HCl (1M, 100 mL). The layers were separated and the aqueous layer was extracted with CH_2Cl_2 (50 mL). The combined organic layers were dried over $MgSO_4$, filtered, and solvent was removed from the filtrate to give a red oil. The oil was purified by column chromatography (10–15% CH_2Cl_2 in hexanes) to afford **S2** (7.85 g, 84%) as a white solid. mp 42.7–43.4 °C (lit.[11] mp 47–48 °C). ^{1}H NMR data matches that in the literature.[11]

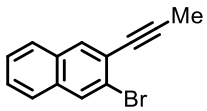

S3

2-bromo-3-(prop-1-ynyl)naphthalene (S3). A 150 mL flask with Teflon stopper and side arm was connected to a 225 mL gas addition apparatus and charged with **S2** (3.00 g, 8.45 mmol)**,** $Pd(PPh_3)_2Cl_2$ (0.18 g, 0.26 mmol), and CuI (0.099 g, 0.52 mmol). The apparatus was evacuated and refilled with N_2,

then the flask was charged with an N_2-sparged mixture of DMF (15 mL) and NH^iPr_2 (15 mL) *via* cannula transfer. The mixture was frozen with liquid N_2, the apparatus was evacuated, and propyne (0.37 g, 9.3 mmol, 225 mL at 1 atm) was added by condensation of the gas onto the frozen reaction mixture. The flask was sealed and the solution was warmed to 21 °C and stirred for 22 h. Cold (~0° C) aqueous HCl (3 M, 80 mL) was slowly added, then the mixture was extracted with hexanes (80 mL, then 40 mL). The combined extracts were dried with $MgSO_4$, filtered, and solvent was removed from the filtrate by rotary evaporation. The crude yellow oil was purified by column chromatography (100% hexanes) to afford **S3** (1.55 g, 75%) as a white solid. mp 55.9–57.0 °C. ^{1}H NMR (chloroform-*d*, 600 MHz): δ = 8.06 (s, 1H), 7.95 (s, 1H), 7.76 – 7.68 (m, 2H), 7.49 – 7.45 (m, 2H), 2.16 (s, 3H); ^{13}C{^{1}H} NMR (chloroform-*d*, 101 MHz): δ = 133.4, 133.0, 131.9, 130.9, 127.5, 127.3, 126.9, 126.8, 123.4, 122.2, 90.7, 78.8, 4.8; HRMS-EI (m/z): $[M]^+$ calcd. for $C_{13}H_9Br$, 243.9888; found, 243.9890.

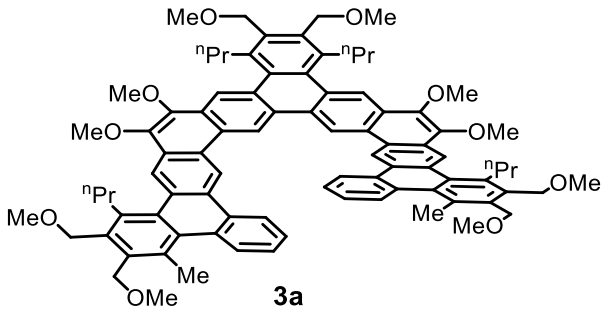

3a

Benzannulated Expanded 11-Helicene (3a). The following is a modification of the methodology reported by Takeuchi and coworkers.[12] To a solution of $[Ir(COD)Cl]_2$ (10 mg, 0.015 mmol) in benzene-d_6 (0.50 mL) was added (dropwise over ~1 min) a solution of dppe (12 mg, 0.030 mmol) in benzene-d_6 (0.50 mL). A 0.10 mL aliquot of this mixture, corresponding to 0.015 mmol $Ir(COD)Cl]_2$, was immediately added to a J-Young tube containing a solution of tris(diyne) **12** (48.4 mg, 0.0500 mmol), 1,4-dimethoxy-2-butyne (34 mg, 0.30 mmol), and 1,3,5-trimethoxybenzene (~6 mg; internal standard) in benzene-d_6 (1.0 mL). The tube was sealed with a Teflon stopper and the reaction mixture was heated at 80 °C for 2 h. The mixture was brought to RT and analyzed by ^{1}H NMR spectroscopy, which showed quantitative yield of **3a**. After 20–30 min, a yellow microcrystalline solid began to precipitate. After 1 h, hexanes (1.5 mL) was added, then the solid was collected by filtration, washed with hexanes (3 x 0.5 mL), and residual solvents were removed under vacuum to yield a yellow powder that was a mixture of **3a** and 5 mol% of cyclotrimerized dimethoxy-2-butyne. The solid was dissolved in CH_2Cl_2 (~2 mL), filtered into a 20 mL vial, and ethanol (4 mL) was added to the filtrate. The solution was concentrated to ~3 mL and the resulting precipitate was collected by filtration, washed with ethanol (1 mL), and dried *in vacuo*. The yield of pure **3a**, a pale-yellow powder, was 60 mg (91%). ^{1}H NMR (chloroform-*d*, 600 MHz, 4.2 x 10^{-2} M*): δ = 10.24 (s, 2H), 10.17 (s, 2H), 9.11 (s, 2H), 9.08 (s, 2H), 9.08 (d, *J* = 8 Hz, 2H), 8.30 (d, *J* = 7.9 Hz, 2H), 7.66 (t, *J* = 7.3 Hz, 2H), 7.62 (t, *J* = 7.3 Hz, 2H), 4.88 (s, 4H), 4.85 (s, 4H), 4.83 (s, 4H), 4.24 (s, 6H), 4.23 (s, 6H), 3.64 (s, 6H), 3.62 (s, 6H), 3.61 (s, 6H), 3.59 – 3.50 (m, 8H), 3.03 (s, 6H), 2.11 (sext, *J* = 7.3 Hz, 4H), 2.05 (sext, *J* = 7.3 Hz, 4H), 1.16 (t, *J* = 7.3 Hz, 6H), 1.09 (t, *J* = 7.3 Hz, 6H); ^{13}C{^{1}H} NMR (chloroform-*d*, 151 MHz): δ = 144.20, 144.19, 136.55, 136.11, 136.09, 136.08, 134.81, 134.55, 134.52, 133.69, 131.95, 131.76, 131.69, 131.21, 130.66, 130.08, 129.69, 129.63, 128.34, 127.96, 127.92, 127.50, 127.34, 126.34, 123.20, 122.78, 122.61, 117.84, 117.49, 69.37, 69.32, 69.20, 61.13, 61.06, 58.94, 58.92, 58.78, 35.29, 35.10, 26.05, 25.89, 20.71, 14.69, 14.68; HRMS-ESI (m/z): $[M]^+$ calcd. for $C_{88}H_{92}O_{10}$, 1308.6685; found, 1308.6713. *Chemical shifts are essentially invariant to concentration between 4.2 x 10^{-2} M and 8.4 x 10^{-5} M (see Figure S5).

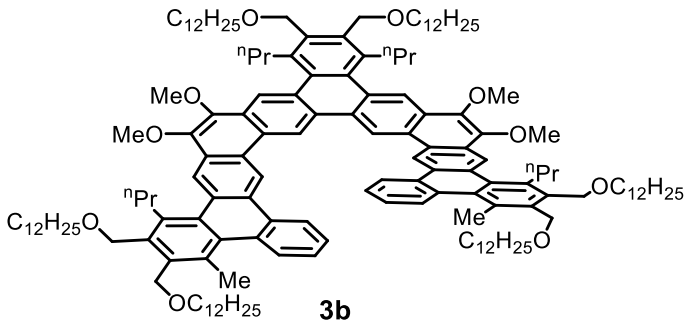

3b

Benzannulated Expanded 11-Helicene (3b). This compound was prepared according to the procedure for **3a**, with the following quantities (and noted differences): $[Ir(COD)Cl]_2$ (0.74 mg, 0.0011 mmol), dppe (0.88 mg, 0.0022 mmol), tris(diyne) **12** (34.0 mg, 0.0351 mmol), and monoyne **S1** (89 mg, 0.21 mmol). The reaction mixture was subjected (without workup) to column chromatography (1:1 hexanes:CH_2Cl_2) to give a viscous yellow oil that was a mixture of **3b** and monoyne **S1**.* The oil was dissolved in CH_2Cl_2 (1 mL) and to this solution was added ethanol (4 mL). The solution was concentrated to ~3 mL and sonicated, then the solvent was decanted from the yellow oil, which was subsequently washed with ethanol (1 mL). This procedure was repeated, then residual solvents were removed under high vacuum to afford pure **3b** (63 mg, 81%) as a glassy yellow solid. ^{1}H NMR (chloroform-*d,* 600 MHz): δ = 10.24 (s, 2H), 10.17 (s, 2H), 9.12 (s, 2H), 9.10 (s, 2H), 9.08 (d, *J* = 8.0 Hz, 2H), 8.31 (d, *J* = 7.8 Hz, 2H), 7.66 (t, *J* = 7.2 Hz, 2H), 7.62 (t, *J* = 7.4 Hz, 2H), 4.92 (s, 4H), 4.90 (s, 4H), 4.87 (s, 4H), 4.25 (s, 6H), 4.24 (s, 6H), 3.78 – 3.68 (m, 12H), 3.60 – 3.50 (m, 8H), 3.04 (s, 6H), 2.18 – 2.06 (m, 8H), 1.83 – 1.73 (m, 12H), 1.57 – 1.46 (m, 12H), 1.45 – 1.25 (m, 96H), 1.16 (t, *J* = 7.3 Hz, 6H), 1.11 (t, *J* = 7.2 Hz, 6H), 0.94 – 0.89 (m, 18H); ^{13}C{^{1}H} NMR (chloroform-*d,* 151 MHz): δ = 144.25, 144.23, 136.67, 136.45, 136.38, 136.20, 135.06, 134.53, 134.45, 133.68, 132.03, 131.79, 131.78, 131.29, 130.74, 130.10, 129.72, 129.63, 128.31, 127.93, 127.86, 127.50, 127.34, 126.27, 123.20, 122.82, 122.66, 117.80, 117.45, 71.64, 71.51, 71.50, 67.68, 67.63, 67.47, 61.13, 61.08, 35.40, 35.21, 32.09, 32.09, 32.09, 30.14, 30.14, 30.10, 29.89, 29.89, 29.89, 29.86, 29.86, 29.86, 29.83, 29.83, 29.83, 29.82, 29.82, 29.82, 29.74, 29.72, 29.71, 29.53, 29.52, 29.52, 26.74, 26.69, 26.60, 25.91, 25.76, 22.85, 22.85, 22.85, 20.77, 14.76, 14.75, 14.27, 14.27, 14.27; HRMS-ESI (m/z): $[M]^+$ calcd. for $C_{154}H_{224}O_{10}$, 2233.7014; found, 2233.7146.

*Compound **3b** eluted over a very broad range, but this eluent was effective at removing the major byproduct (cyclotrimerized **S1**). A similar result was obtained when toluene was employed as eluent. With a 20:1 hexanes:ethyl acetate eluent, the desired compound eluted over a narrow range, but both **S1** and cyclotrimerized **S1** co-eluted.

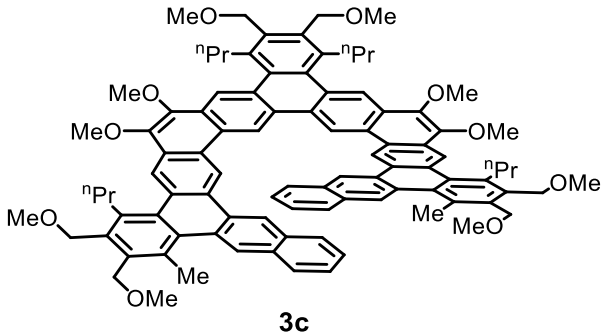

3c

Benzannulated Expanded 13-Helicene (3c). This compound was prepared according to a procedure analogous to that for **3a.** To a solution of $[Ir(COD)Cl]_2$ (2.8 mg, 0.0042) in benzene-d_6 (0.14 mL) was added, dropwise, a solution of dppe (3.3 mg, 0.0084 mmol) in benzene-d_6 (0.14 mL). This mixture was immediately added to a J-Young tube containing a solution of tris(diyne) **13** (150 mg, 0.141 mmol), 1,4-dimethoxy-2-butyne (97 mg, 0.85 mmol), and 1,3,5-trimethoxybenzene (~10 mg; internal standard) in benzene-d_6 (2.0 mL). The tube was sealed with a Teflon stopper and the reaction mixture was heated at 80 °C for 9 h. The mixture was brought to RT and allowed to stand for 2 h, over which time a solid precipitated. This solid was collected by filtration, washed with benzene (0.5 mL), and dried under vacuum to yield a yellow microcrystalline solid, which was **3c** with a small amount of cyclotrimerized 1,4-dimethoxy-2-butyne (~5 mol %). To remove this impurity, the yellow solid was dissolved in CH_2Cl_2 (~4 mL) and the solution was diluted with ethanol (4 mL). The resulting solution was concentrated to ~3 mL, producing a pale yellow microcrystalline precipitate that was collected by filtration, then washed with ethanol (2 mL) and methanol (2 mL). Residual solvents were removed under high vacuum to yield 155 mg (78%) of pure **3c** as a yellow powder. X-ray quality crystals (yellow needles) were grown by layering pentane onto a solution of **3c** in chloroform-*d* and the structure was elucidated by X-ray crystallography (see Scheme 4 in the main text and Figure S40 and Table S1 below).

Data for monomer **3c**: ^{1}H NMR (chloroform-*d*, 700 MHz): δ = 10.34 (s, 2H), 10.29 (s, 2H), 9.26 (s, 2H), 9.11 (s, 2H), 9.04 (s, 2H), 8.54 (s, 2H), 7.71 (d, *J* = 8.2 Hz, 2H), 7.25 (d, *J* = 8.3 Hz, 2H), 7.11 (t, *J* = 7.5 Hz, 2H), 6.54 (t, *J* = 7.5 Hz, 2H), 4.88 (s, 4H), 4.88 (s, 4H), 4.82 (s, 4H), 4.26 (s, 6H), 4.24 (s, 6H), 3.64 (s, 6H), 3.64 (s, 6H), 3.63 (s, 6H), 3.61 – 3.56 (m, 4H), 3.55 – 3.50 (m, 4H), 3.17 (s, 6H), 2.12 (sext, 4H, *J* = 7.7 Hz), 2.08 (sext, 4H, *J* = 7.7 Hz), 1.16 (t, *J* = 7.3 Hz, 6H), 1.12 (t, *J* = 7.3 Hz, 6H); ^{13}C{^{1}H} NMR (chloroform-*d*, 176 MHz): δ = 144.37, 144.29, 136.63, 136.53, 136.22, 136.12, 135.44, 134.58, 134.18, 132.16, 131.97, 131.86, 131.27, 131.23, 130.57, 130.29, 130.28, 129.91, 128.75, 128.52, 128.47, 127.65, 127.64, 127.53, 127.48, 127.40, 125.78, 125.45, 122.82, 122.56, 121.85, 118.37, 117.89, 69.42, 69.29, 69.19, 61.15, 61.09, 59.00, 58.95, 58.78, 35.29, 35.13, 26.03, 25.88, 20.77, 14.67, 14.66; HRMS-ESI(m/z): $[M+Na]^+$ calcd. for $C_{96}H_{96}O_{10}Na$, 1431.6896; found, 1431.6938;

Data for dimer **3c**-**Dim**: ^{1}H NMR (chloroform-*d*, 700 MHz): δ = 10.25 (s, 2H), 10.08 (s, 2H), 9.93 (s, 2H), 9.90 (s, 2H), 8.93 (s, 2H), 8.85 (s, 2H), 8.48 (s, 2H), 8.46 (s, 2H), 8.33 (s, 2H), 8.18 (s, 2H), 7.68 (s, 2H), 7.48 (s, 2H), 7.25 (d, *J* = 7.1 Hz, 2H), 7.10 (d, *J* = 7.1 Hz, 2H), 6.98 (t, *J* = 7.1 Hz, 2H), 6.89 (d, *J* = 7.9 Hz, 2H), 6.84 (t, *J* = 7.0 Hz, 2H), 6.40 (t, *J* = 7.1 Hz, 2H), 6.27 (d, *J* = 8.0 Hz, 2H), 6.19 (t, *J* = 7.1 Hz, 2H), 4.95 (d, *J* = 11 Hz, 2H), 4.72 (d, *J* = 11 Hz, 2H), 4.70 (d, *J* = 11 Hz, 2H), 4.69 (d, *J* = 11 Hz, 2H), 4.64 (d, *J* = 11 Hz, 2H), 4.64 (d, *J* = 11 Hz, 2H), 4.61 (d, *J* = 11 Hz, 2H), 4.58 (d, *J* = 11 Hz, 2H), 4.55 (d, *J* = 11 Hz, 2H), 4.54 (s, 6H), 4.54 (d, *J* = 11 Hz, 2H), 4.52 (d, *J* = 11 Hz, 2H), 4.49 (d, *J* = 11 Hz, 2H), 4.17 (s, 6H), 4.17 (s, 6H), 3.90 (s, 6H), 3.81 (s, 6H), 3.76 (s, 6H), 3.75 (s, 6H), 3.74 (s, 6H), 3.67 (s, 6H), 3.66 (s, 6H), 3.56 – 3.45 (m, 4H), 3.33 – 2.80 (m, 12H), 2.55 – 2.27 (m, 16H), 2.47 (s, 6H), 2.40 (s, 6H), 1.64 (t, 7.3 Hz, 6H), 1.41 (t, *J* = 7.5 Hz, 6H), 1.40 (t, *J* = 7.5 Hz, 6H); ^{13}C{^{1}H} NMR (chloroform-*d*, 176 MHz): δ = 143.64, 142.52, 142.49, 142.30, 136.97, 136.00, 135.96, 135.84, 135.74, 135.63, 134.62, 134.39, 134.25, 134.10, 134.06, 134.00, 133.56, 133.54, 133.17, 131.77, 131.71, 131.33, 131.17, 130.97, 130.64, 130.58, 130.37, 130.22, 130.03, 129.91, 129.63, 129.63, 129.44, 129.32, 129.04, 128.88, 128.48, 128.09, 127.64, 127.26, 127.17, 127.11, 126.90, 126.80, 126.78, 126.71, 126.63, 126.61, 126.40, 126.13, 125.89, 124.68, 124.56, 124.11, 123.86, 123.05, 122.64, 122.02, 121.37, 121.19, 120.89, 119.35, 119.13, 118.59, 117.98, 69.26, 69.11, 68.91, 68.85, 68.85, 68.78, 60.63, 60.11, 60.03, 60.03, 58.87, 58.87, 58.75, 58.72, 58.52, 58.43, 35.88, 35.71, 34.19, 34.19, 25.42, 25.42, 25.30, 25.30, 19.65, 19.38, 14.98, 14.98, 14.82, 14.30.

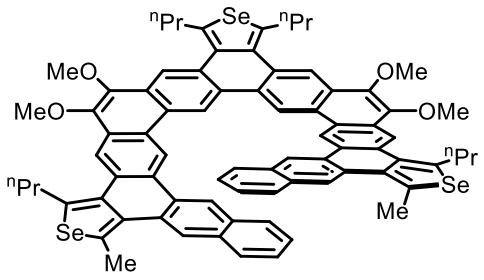

4

Selenophene-annulated expanded 13-helicene (4). To a vial containing $SeCl_2$(bipy) (16.8 mg, 0.0548 mmol) was added a solution of **5** (28.8 mg, 0.0166 mmol) in CH_2Cl_2 (5 mL). The mixture was stirred vigorously for 1 min, then filtered. The filtrate was concentrated to ~2mL and then cooled to –35 °C for 1 h. Compound **4** (13.5 mg, 62%), a yellow/orange crystalline solid, was collected by filtration. X-ray quality crystals (yellow/orange needles) precipitated from the reaction mixture during a smaller scale reaction in CD_2Cl_2, and the structure was elucidated by X-ray crystallography (see Scheme 5 in the main text and Figure S41 and Table S2 below). ^{1}H NMR (CS_2 with chloroform-*d* capillary, 600 MHz): δ = 10.37 (s, 2H), 10.31 (s, 2H), 9.30 (s, 2H), 9.20 (s, 2H), 9.16 (s, 2H), 8.65 (s, 2H), 7.77 (d, *J* = 8.1 Hz, 2H), 7.42 (d, *J* = 8.1 Hz, 2H), 7.24 (ddd, *J* = 8.1, 6.9, 1.1 Hz, 2H), 6.75 (ddd, *J* = 8.1, 6.8, 1.1 Hz, 2H), 4.55 (s, 6H), 4.54 (s, 6H), 3.88 (t, *J* = 8.0 Hz, 4H), 3.88 (t, *J* = 7.9 Hz, 4H), 3.50 (s*, 6H), 2.46 (sext, *J* = 7.4, 4H), 2.44 (sext, *J* = 7.4, 4H), 1.68 (t, *J* = 7.2 Hz, 6H), 1.67 (t, *J* = 7.3 Hz, 6H); ^{13}C{^{1}H} NMR (CS_2 with chloroform-*d* capillary, 151 MHz): δ = 145.04, 144.89, 144.57, 144.55, 137.04, 134.31, 133.60, 133.59, 132.80, 132.05, 131.63, 131.57, 130.72, 130.40, 130.37, 130.14, 129.32, 129.28, 127.93, 127.61, 127.54, 127.44, 126.29, 125.58, 125.52, 123.06, 120.21, 120.09, 118.56, 118.02, 61.07, 61.06, 37.62, 37.51, 26.42, 26.39, 21.93, 15.42, 15.40; HRMS-ESI (m/z): $[M]^+$ calcd. for $C_{78}H_{66}O_4Se_3$, 1306.2457; found, 1306.2491.

*This peak has satellites from coupling (*J* = 6.3 Hz) with Se^{77} (7.6% abundance).

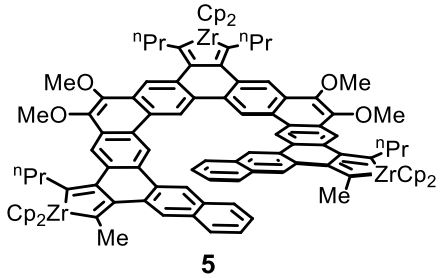

5

Zirconacyclopentadiene-annulated expanded 13-helicene (5). To a vial containing $Cp_2Zr(pyr)(Me_3SiC{\equiv}CSiMe_3)$ (0.146 g, 0.309 mmol) was added a solution of tris(diyne) **13** (0.100 g, 0.0937 mmol) in benzene (3 mL) to form an initially homogeneous mixture. After 1 h at RT, the precipitate was collected on a fritted funnel, washed with benzene (1 mL) and pentane (2 x 2 mL), and dried *in vacuo* to afford **5** (0.130 g, 80%) as an orange solid. ^{1}H NMR (chloroform-*d,* 500 MHz): δ = 9.40 (s, 2H), 9.39 (s, 2H), 8.47 (s, 2H), 8.26 (s, 2H), 8.22 (s, 2H), 7.74 (s, 2H), 7.66 (d, *J* = 8.1 Hz, 2H), 7.15 (d, *J* = 8.2 Hz, 2H), 7.12 (t, *J* = 7.5 Hz, 2H), 6.71 (t, *J* = 7.4 Hz, 2H), 6.30 (s, 10H), 6.29 (s, 20H), 4.22 (s, 6H), 4.20 (s, 6H), 3.23 – 3.10 (m, 8H), 2.61 (s, 6H), 1.49 – 1.34 (m, 8H), 1.01 (t, *J* = 7.2 Hz, 6H), 1.00 (t, *J* = 7.3 Hz, 6H); ^{13}C{^{1}H} NMR (chloroform-*d*, 101 MHz): δ = 200.26, 199.19, 192.94, 144.68, 144.64, 133.61, 133.49, 133.46, 133.12, 133.00, 132.81, 132.73, 131.58, 128.48, 128.24, 128.19, 128.05, 127.89, 127.74, 127.32, 125.77, 125.58, 122.99, 122.76, 122.70, 121.17, 120.96, 118.57, 118.55,

118.06, 109.52, 109.05, 61.64, 61.60, 44.43, 44.23, 27.40, 27.08, 26.77, 15.22, 15.19; Anal. Calcd for $C_{108}H_{96}O_4Zr_3$: C, 74.91; H, 5.59. Found: C, 74.57; H, 5.71.

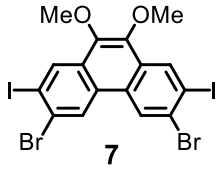

7

3,6-dibromo-2,7-diiodo-9,10-dimethoxyphenanthrene (7). This procedure was adapted from that published by Katz et al. for 9,10-dimethoxyphenanthrene.[13] To a 1000 mL round-bottomed flask equipped with a magnetic stirbar was added **6** (13.0 g, 21.0 mmol), $Na_2S_2O_4$ (11.0 g, 63.2 mmol), Bu_4NBr (2.08 g, 6.45 mmol), tetrahydrofuran (80 mL), and water (80 mL). The reaction mixture was stirred vigorously for 5 min, then dimethyl sulfate (13.8 g, 10.4 mL, 109 mmol) was added via syringe, followed by aqueous NaOH (13 M, 15 mL). The mixture was stirred for 40 min, then the precipitate was collected by filtration, washed with water (2 x 80 mL), MeOH (2 x 80 mL), and diethyl ether (2 x 40 mL), and dried under a stream of air to afford an off-white solid (12.0 g, mp 279–284 °C). This solid was purified by recrystallization from the minimal amount (~225 mL) of boiling toluene to afford **7** (10.7 g, 79%) as a flocculent, off-white solid. mp 285–288 °C. ^{1}H NMR (chloroform-*d*, 500 MHz): δ = 8.70 (s, 2H), 8.69 (s, 2H), 4.06 (s, 6H); ^{13}C{^{1}H} NMR (chloroform-*d*, 151 MHz): δ = 143.1, 134.4, 129.8, 128.1, 127.6, 126.3, 100.8, 61.2; HRMS-EI (m/z): $[M]^+$ calcd. for $C_{16}H_{10}Br_2I_2O_2$, 645.7137; found, 645.7130; Anal. Calcd for $C_{16}H_{10}Br_2I_2O_2$: C, 29.66; H, 1.56. Found: C, 29.82; H, 1.44.

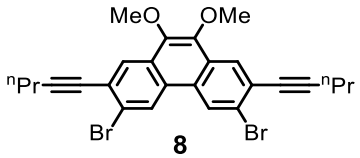

8

3,6-dibromo-2,7-bis(pent-1-ynyl)-9,10-dimethoxyphenanthrene (8). A 150 mL Schlenk flask with Teflon stopper was charged with **7** (3.62 g, 5.59 mmol), $Pd(PPh_3)_4$ (0.16 g, 0.14 mmol), and CuI (0.064 g, 0.34 mmol), then the flask was evacuated and refilled with N_2. To this flask was added an N_2-sparged mixture of tetrahydrofuran (36 mL) and triethylamine (18 mL), followed by 1-pentyne (0.97 g, 14 mmol). The flask was subjected to two freeze-pump-thaw cycles, backfilled with N_2, and sealed. The stirred reaction mixture was heated at 70 °C for 18 h, then brought to RT, diluted with CH_2Cl_2 (100 mL), washed with aqueous HCl (3 M, 80 mL), dried with $MgSO_4$, and filtered. Solvents were removed from the filtrate *via* rotary evaporation, then the crude product was dissolved in CH_2Cl_2 (50 mL) and this solution was diluted with hexanes (150 mL). The solution was eluted through a plug of silica gel (25 g) and the plug was flushed with 3:1 hexanes:CH_2Cl_2 (150 mL). Solvents were removed *via* rotary evaporation and further purification was carried out as follows (repeated 2x). The solid was dissolved in CH_2Cl_2 (30 mL), then methanol (60 mL) was added to produce an immediate precipitate that was collected by filtration and washed with methanol (30 mL). The yield of **8**, an off-white solid, was 1.89 g (64%). mp 199–200 °C. Note: the final product sometimes contained a small amount of CH_2Cl_2 and/or methanol, which is problematic for the next step. These solvents can be removed under high vacuum at 60–70 °C. ^{1}H NMR (chloroform-*d*, 600 MHz): δ = 8.64 (s, 2H), 8.24 (s, 2H), 4.05 (s, 6H), 2.52 (t, *J* = 6.9 Hz, 4H), 1.73 (sext, *J* = 7.2 Hz, 4H), 1.13 (t, *J* = 7.4 Hz, 6H); ^{13}C{^{1}H} NMR (chloroform-*d*, 101 MHz): δ = 143.6, 128.5, 127.4, 127.2, 126.5, 125.2, 123.4, 96.4, 79.9, 61.2, 22.2, 21.9, 13.8; HRMS-EI (m/z): $[M]^+$ calcd. for $C_{26}H_{24}Br_2O_2$, 526.0143; found, 526.0139.

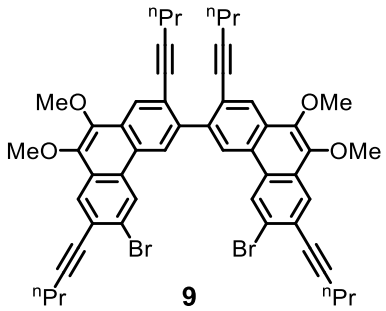

9

6,6'-dibromo-9,9',10,10'-tetramethoxy-2,2',7,7'-tetra(pent-1-ynyl)-3,3'-biphenanthrene (9). A 75 mL Schlenk flask was charged with diyne **8** (1.70 g, 3.22 mmol) and tetrahydrofuran (40 mL) and the solution was cooled to –78 °C with a dry ice / acetone bath. To this solution was added *n*-butyllithium (1.50 M in hexanes, 2.04 mL, 3.06 mmol) dropwise over 10–15 min and the resulting mixture was stirred for an additional 15 min at –78 °C. Anhydrous copper(II) chloride (0.693 g, 5.15 mmol) was then added in one portion, the cold bath was removed, and the reaction mixture was allowed to warm to 21 °C and stirred for 12 h at this temperature. The mixture was quenched with 10% aqueous NH_4OH (35 mL) and extracted with ethyl acetate (2 x 50 mL). The organic layer was washed with saturated aqueous NaCl (50 mL), dried with Na_2SO_4, filtered, and concentrated by rotary evaporation. Purification of the residue by column chromatography (25–40% CH_2Cl_2 in hexanes) afforded **9** as a viscous oil, which solidified upon addition of MeOH and sonication. Yield: 0.751 g (55%, off-white powder). mp 201–203 °C. ^{1}H NMR (chloroform-*d*, 500 MHz): δ 8.76 (s, 2H), 8.70 (s, 2H), 8.40 (s, 2H), 8.29 (s, 2H), 4.12 (s, 6H), 4.12 (s, 6H), 2.53 (t, *J* = 7.0 Hz, 4H), 2.19 (t, *J* = 6.9 Hz, 4H), 1.73 (sext, *J* = 7.2 Hz, 4H), 1.34 (sext, *J* = 7.2 Hz, 4H), 1.14 (t, *J* = 7.4 Hz, 6H), 0.70 (t, *J* = 7.4 Hz, 6H); ^{13}C{^{1}H} NMR (chloroform-*d*, 151 MHz): δ = 143.9, 143.6, 140.0, 128.83, 128.76, 128.3, 127.2, 126.6, 126.5, 125.9, 125.1, 124.5, 123.5, 123.1, 95.9, 95.2, 80.5, 80.1, 61.25, 61.16, 22.3, 22.1, 21.9, 21.7, 13.8, 13.4; HRMS-ESI (m/z): $[M]^+$ calcd. for $C_{52}H_{48}O_4Br_2$, 894.1914; found, 894.1908.

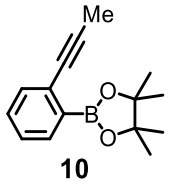

10

4,4,5,5-tetramethyl-2-(2-(prop-1-ynyl)phenyl)-1,3,2-dioxaborolane (10). A solution of 1-bromo-2-(propynyl)benzene (0.970 g, 4.97 mmol) in tetrahydrofuran (15 mL) was cooled to –78 °C and *n*-butyllithium (1.5 M in hexanes, 3.65 mL, 5.47 mmol) was added over 5 min. The resulting mixture was stirred for 1 h at –78 °C, then 2-isopropoxy-4,4,5,5-tetramethyl-1,3,2-dioxaborolane (1.57 mL, 1.39 g, 7.46 mmol) was added via syringe. The cold bath was removed and the reaction mixture was allowed to warm to 21 °C. After 1 day, water (15 mL) was added and the mixture was extracted with ethyl acetate (2 x 20 mL). The combined organic layers were washed with saturated aqueous NaCl (20 mL), dried with Na_2SO_4, and concentrated by rotary evaporation to yield **10** as a golden yellow oil (0.97g. 81%), which was used without purification. ^{1}H NMR (chloroform-*d*, 500 MHz): δ = 7.63 (dd, *J* = 7.6, 1.2 Hz, 1H), 7.39 (d, *J* = 7.6 Hz, 1H), 7.32 (td, *J* = 7.6, 1.5 Hz, 1H), 7.24 (td, *J* = 7.4, 1.2 Hz, 1H), 2.06 (s, 3H), 1.37 (s, 12H); ^{13}C{^{1}H} NMR* (chloroform-*d*, 151 MHz): δ = 134.6, 132.1, 130.3, 128.7, 126.8, 87.7, 83.9, 80.5, 25.0, 4.6; HRMS-EI (m/z): $[M]^+$ calcd. for $C_{15}H_{19}BO_2$, 242.1478; found, 242.1484. *One resonance was not observed (assumed to be for the carbon *ipso* to boron).

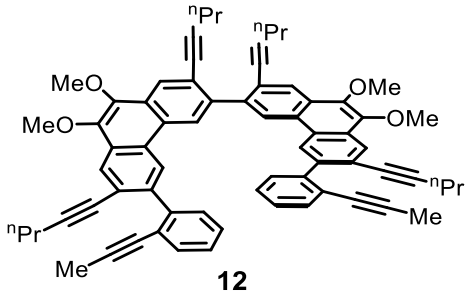

12

9,9',10,10'-tetramethoxy-2,2',7,7'-tetra(pent-1-ynyl)-6,6'-bis(2-(prop-1-ynyl)phenyl)-3,3'-biphenanthrene (12). A 30 mL flask with Teflon stopper was charged with $Pd(PPh_3)_4$ (20 mg, 0.017 mmol) and K_2CO_3 (169 mg, 1.22 mmol) and to this mixture was added a solution of tetrayne **9** (255 mg, 0.284 mmol) and boronic ester **10** (186 mg, 0.768 mmol) in dimethoxyethane (3.6 mL). Quickly thereafter, deionized water (0.9 mL) was added, then the solution was degassed by the freeze-pump-thaw method and backfilled with nitrogen. The flask was sealed and the stirred reaction mixture was heated for 8 h at 90 °C, then cooled to RT, diluted with ethyl acetate (20 mL), and washed with saturated aqueous NaCl (15 mL). The organic layer was dried with $MgSO_4$, filtered, and the filtrate was concentrated under reduced pressure. The residue was separated by column chromatography (33–50% CH_2Cl_2 in hexanes) to give the desired product contaminated with a red, hexanes-soluble oil. Most of this impurity was removed by trituration with hexanes (5 mL) and the resulting pale orange powder was recrystallized from CH_2Cl_2/hexanes as follows. The compound was dissolved in CH_2Cl_2 (~2 mL) and the solution was concentrated give a viscous oil. The oil was dissolved in hexanes (3 mL) and ~1 mL of solvents was allowed to slowly evaporate. The mother liquor was decanted from the resulting pale-yellow crystals, which were then washed with hexanes (2 x 1 mL) and dried under vacuum. The yield of tris(diyne) **12** was 144 mg (52%). ^{1}H NMR (benzene-d_6, 600 MHz): δ = 8.92 (s, 2H), 8.89 (s, 2H), 8.84 (s, 2H), 8.84 (s, 2H), 7.62 (dd, *J* = 7.7, 1.3 Hz, 2H), 7.52 (dd, *J* = 7.7, 1.4 Hz, 2H), 7.11 (td, *J* = 7.6, 1.4 Hz, 2H), 7.05 (td, *J* = 7.6, 1.4 Hz, 2H), 3.79 (s, 6H), 3.75 (s, 6H), 2.07 (t, *J* = 6.9 Hz, 4H), 1.98 (t, *J* = 6.9 Hz, 4H), 1.42 (s, 6H), 1.30 (sext, *J* = 7.2 Hz, 4H), 1.20 (sext, *J* = 7.2 Hz, 4H), 0.77 (t, *J* = 7.4 Hz, 6H), 0.63 (t, *J* = 7.4 Hz, 6H); ^{13}C{^{1}H} NMR (chloroform-*d*, 151 MHz): δ = 143.9, 143.8, 143.0, 140.7, 140.4, 132.4, 130.5, 128.5, 128.4, 127.3, 127.2, 127.2, 126.9, 126.02, 125.97, 124.7, 124.6, 123.8, 123.2, 122.7, 94.4, 94.2, 89.1, 80.7, 80.6, 79.2, 61.24, 61.19, 22.08, 22.05, 21.7, 21.6, 13.5, 13.3, 4.5; HRMS-ESI (m/z): $[M]^+$ calcd. for $C_{70}H_{62}O_4$, 966.4643; found, 966.4640.

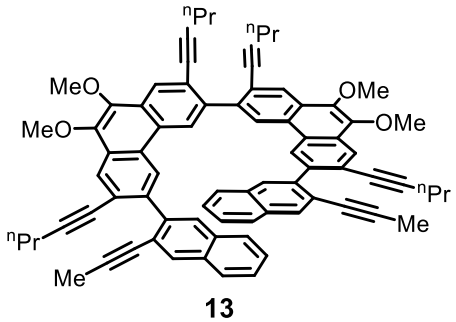

13

9,9',10,10'-tetramethoxy-2,2',7,7'-tetra(pent-1-ynyl)-6,6'-bis(3-(prop-1-ynyl)naphthalen-2-yl)-3,3'-biphenanthrene (13). A 30 mL flask equipped with Teflon stopper was charged with **S3** (370 mg, 1.51 mmol) and tetrahydrofuran (1.8 mL) and to this solution was added ^{i}PrMgCl·LiCl (1.1 M in tetrahydrofuran, 1.19 mL, 1.31 mmol) via syringe. The flask was sealed and the mixture was heated at

50 °C for 8 h. A 1 mL aliquot was analyzed by ^{1}H NMR spectroscopy[10] to ensure complete consumption of ^{i}PrMgCl·LiCl and the aliquot was recombined with the original solution. To this solution was added $PdCl_2$(IPr)(3-chloropyridine) (7.1 mg, 0.010 mmol), followed by tetrayne **9** (300 mg, 0.335 mmol). The resulting homogeneous mixture was allowed to stand at RT (~21 °C) for 18 h, then quenched with saturated aqueous NH_4Cl (5 mL), extracted with EtOAc (10 mL), washed with saturated aqueous NaCl (5 mL), dried with $MgSO_4$, filtered, and the filtrate was concentrated under reduced pressure. The residue was purified by column chromatography (33–50% CH_2Cl_2 in hexanes) to afford tris(diyne) **13** (230 mg, 64%) as a pale-yellow solid. ^{1}H NMR (benzene-d_6, 600 MHz): δ = 9.02 (s, 2H), 8.91 (s, 2H), 8.90 (s, 2H), 8.89 (s, 2H), 8.14 (s, 2H), 7.93 (s, 2H), 7.63 – 7.60 (m, 2H), 7.56 – 7.53 (m, 2H), 7.23 – 7.18 (m, 4H), 3.77 (s, 6H), 3.76 (s, 6H), 1.98 (t, J = 6.9 Hz, 4H), 1.96 (t, J = 6.8 Hz, 4H), 1.46 (s, 6H), 1.24 – 1.14 (m, 8H), 0.65 – 0.58 (m, 12H); ^{13}C{^{1}H} NMR (chloroform-*d*, 151 MHz): δ = 143.89, 143.79, 140.61, 140.29, 140.02, 132.47, 132.29, 131.89, 129.31, 128.53, 128.46, 127.91, 127.30, 127.27, 127.19, 126.45, 126.36, 126.05, 125.96, 124.88, 124.70, 123.13, 123.05, 122.18, 94.38, 94.22, 89.35, 80.68, 80.68, 79.50, 61.24, 61.18, 22.06, 22.05, 21.66, 21.65, 13.35, 13.32, 4.51; HRMS-ESI (m/z): $[M+H]^+$ calcd. for $C_{78}H_{67}O_4$, 1067.5034; found, 1067.5041.

Data Referenced in the Main Text

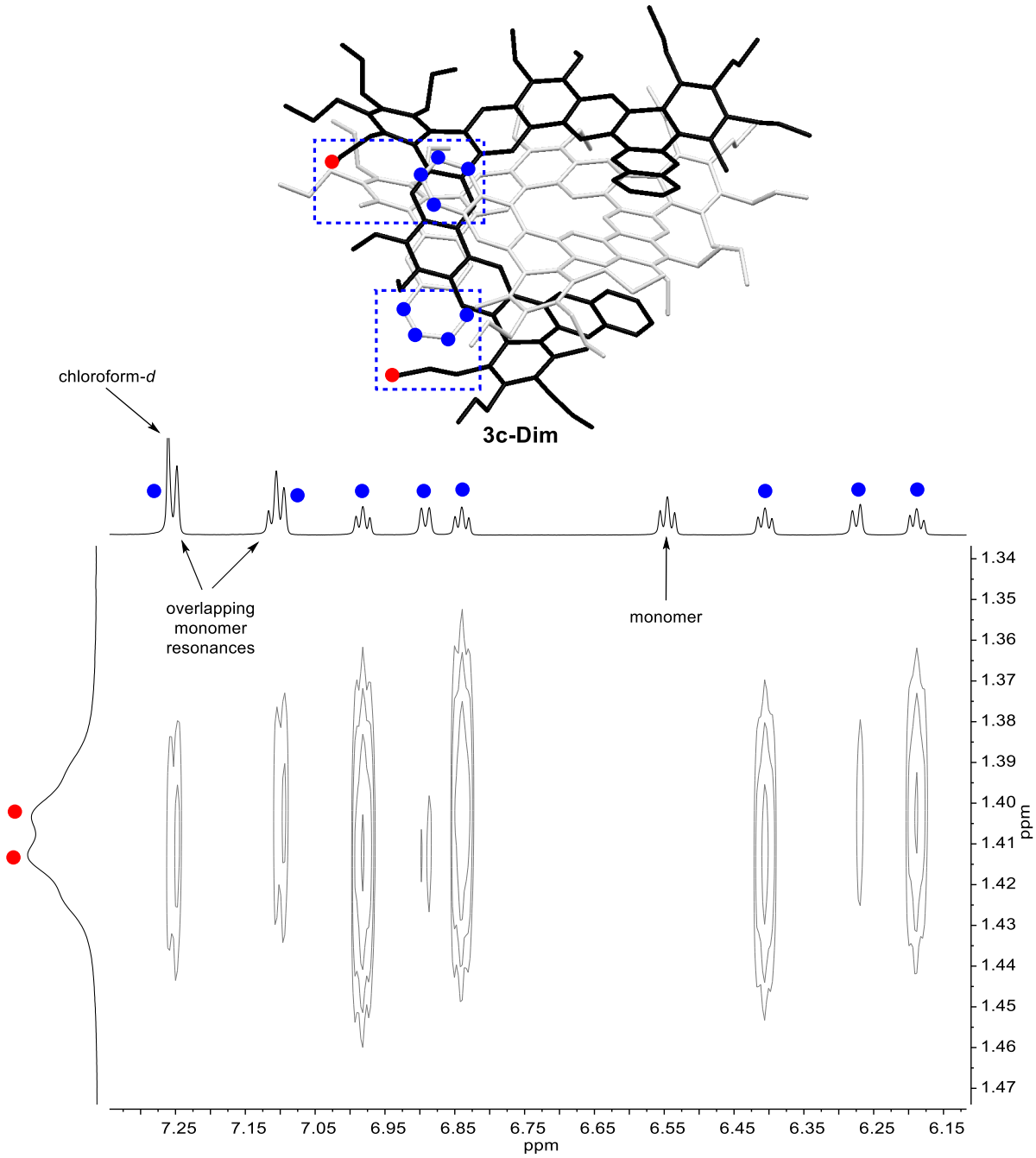

Figure S1. Partial ^{1}H-^{1}H NOESY spectrum (700 MHz, chloroform-*d*, [c] = 4.3 x 10^{-2} M, T = 298 K) of **3c**/**3c-Dim** equilibrium mixture, supporting the proposed dimeric structure of **3c-Dim**. The observed correlations are between C-H resonances on each terminal ring and a CH_3 (propyl) resonance on the other molecule in the dimer.

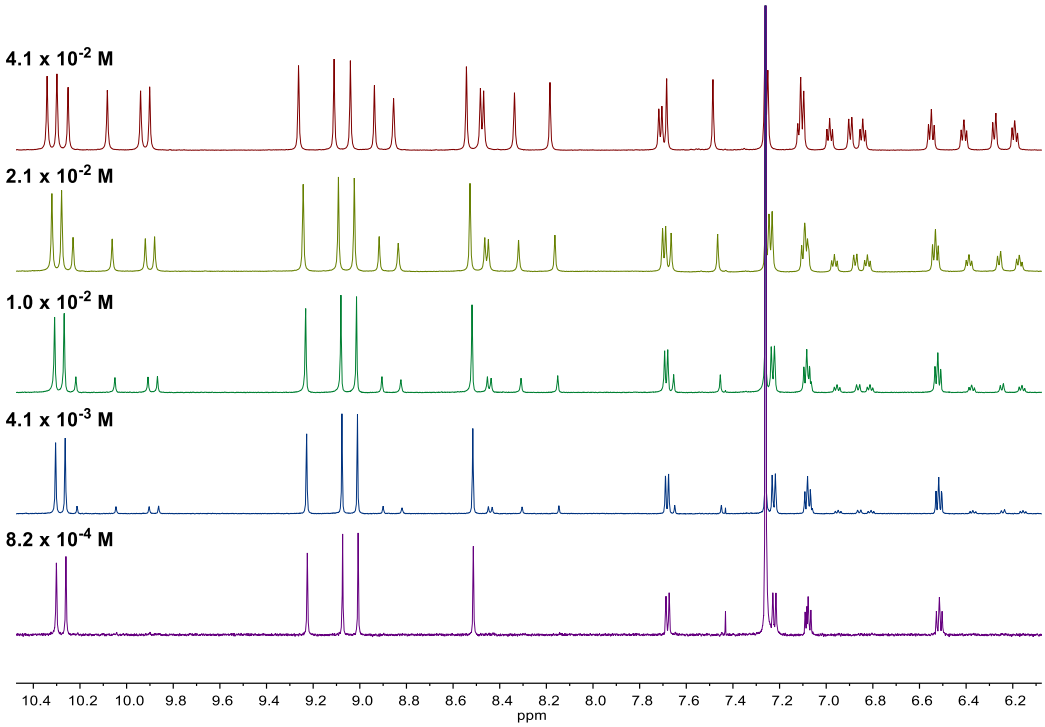

Figure S2. Variable concentration partial ^{1}H NMR spectra (600 MHz, chloroform-*d*) of **3c/3c-Dim** equilibrium mixture.

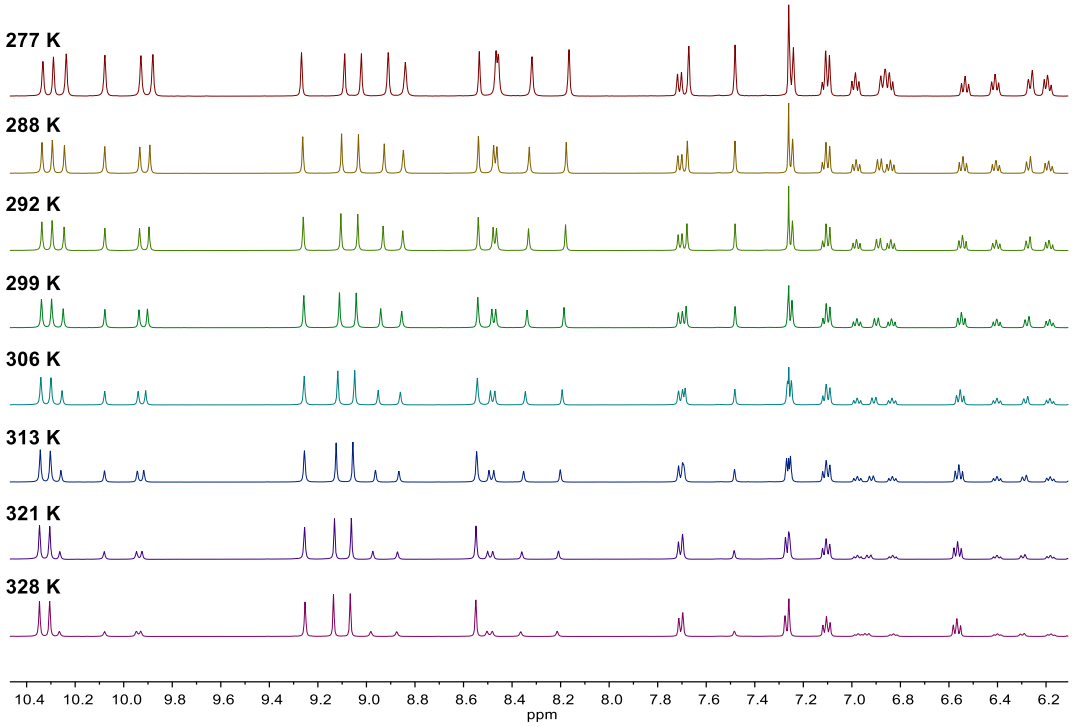

Figure S3. Variable temperature partial ^{1}H NMR spectra (600 MHz, chloroform-*d,* [c] = 4.3 x 10^{-2} M) of **3c/3c-Dim** equilibrium mixture.

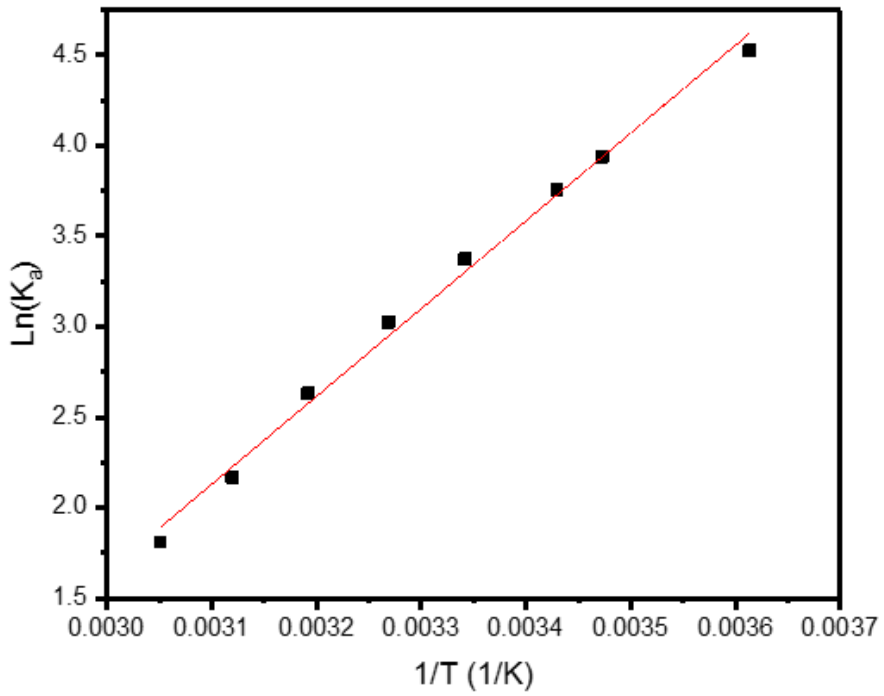

Figure S4. Van't Hoff plot for **3c/3c-Dim** equilibrium mixture.

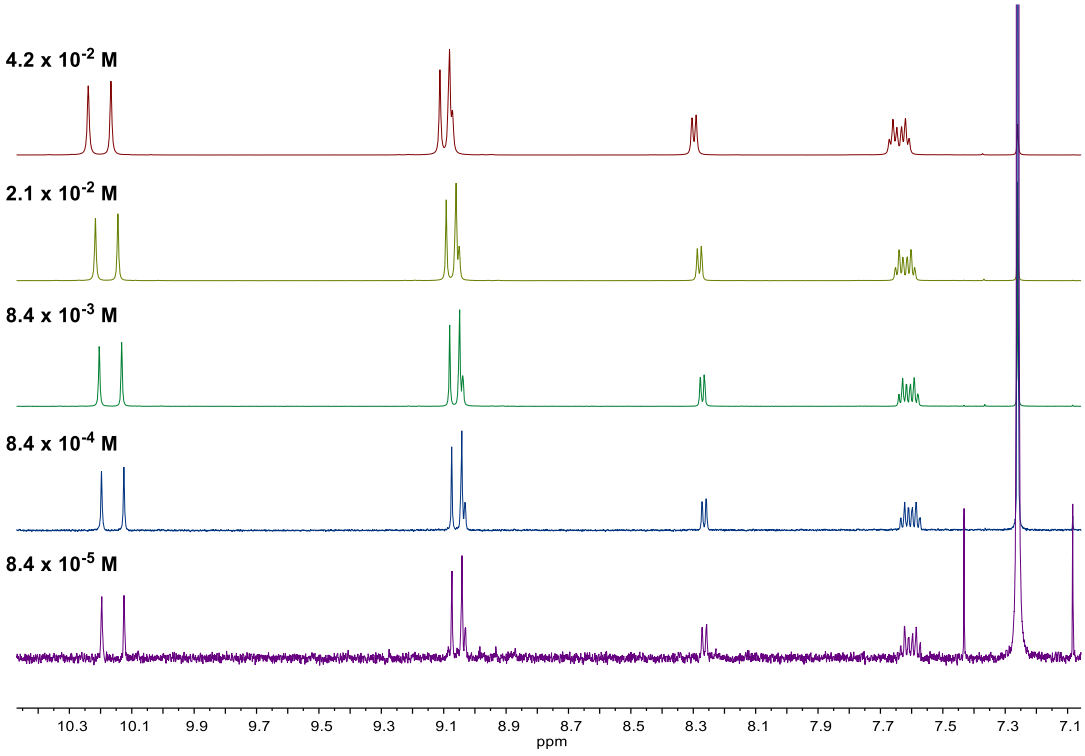

Figure S5. Variable concentration partial ^{1}H NMR spectra (600 MHz, chloroform-*d*) of **3a**.

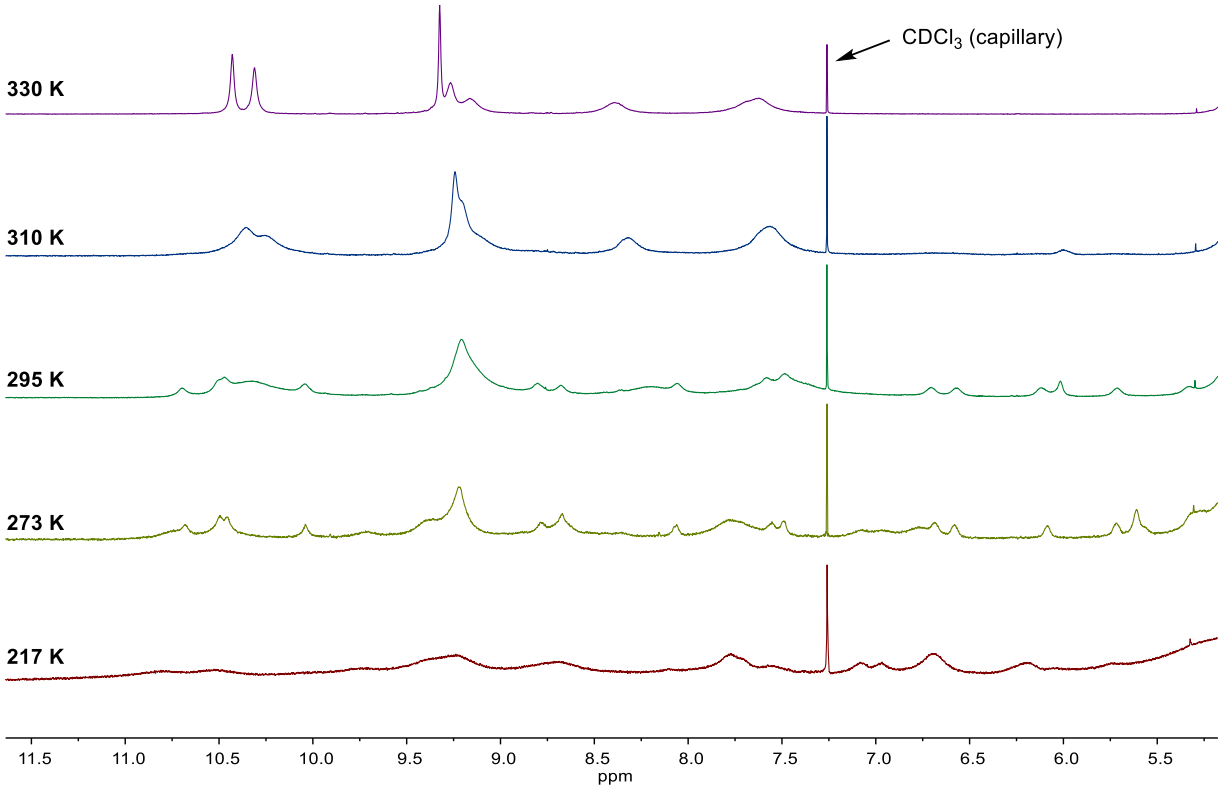

Figure S6. Variable temperature partial ^{1}H NMR spectra (500 MHz, methylcyclohexane-d_{14}, [c] = 3.8 x 10^{-2} M) of **3b**.

NMR Spectra

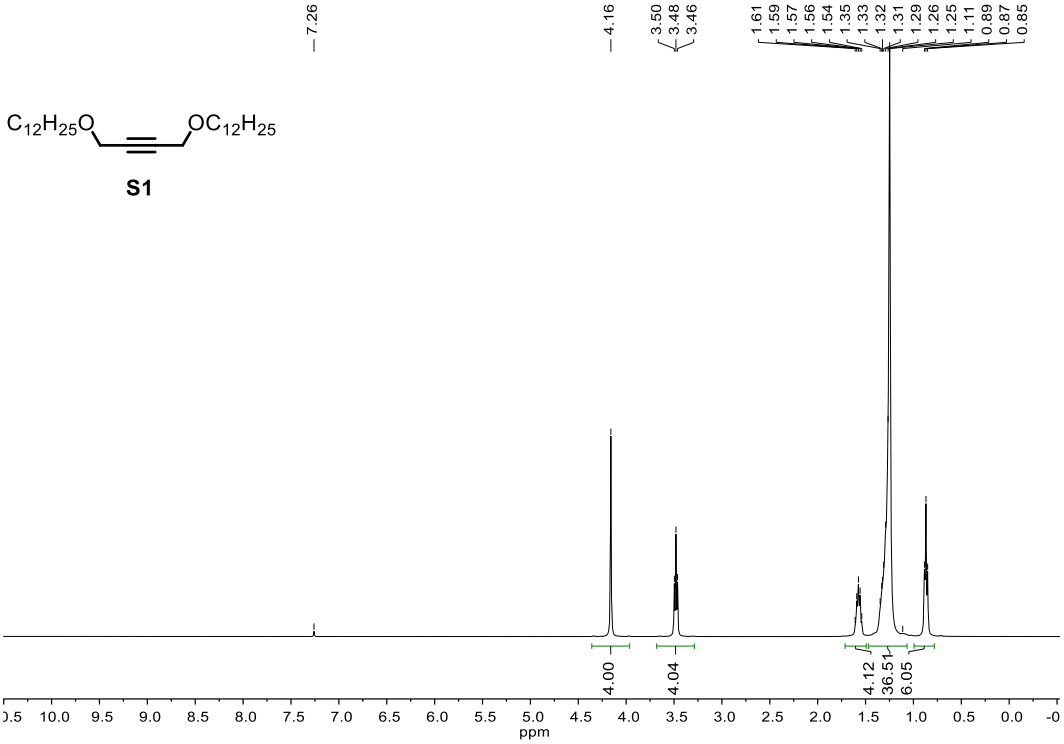

Figure S7. ^{1}H NMR Spectrum (400 MHz, chloroform-*d*) of **S1**.

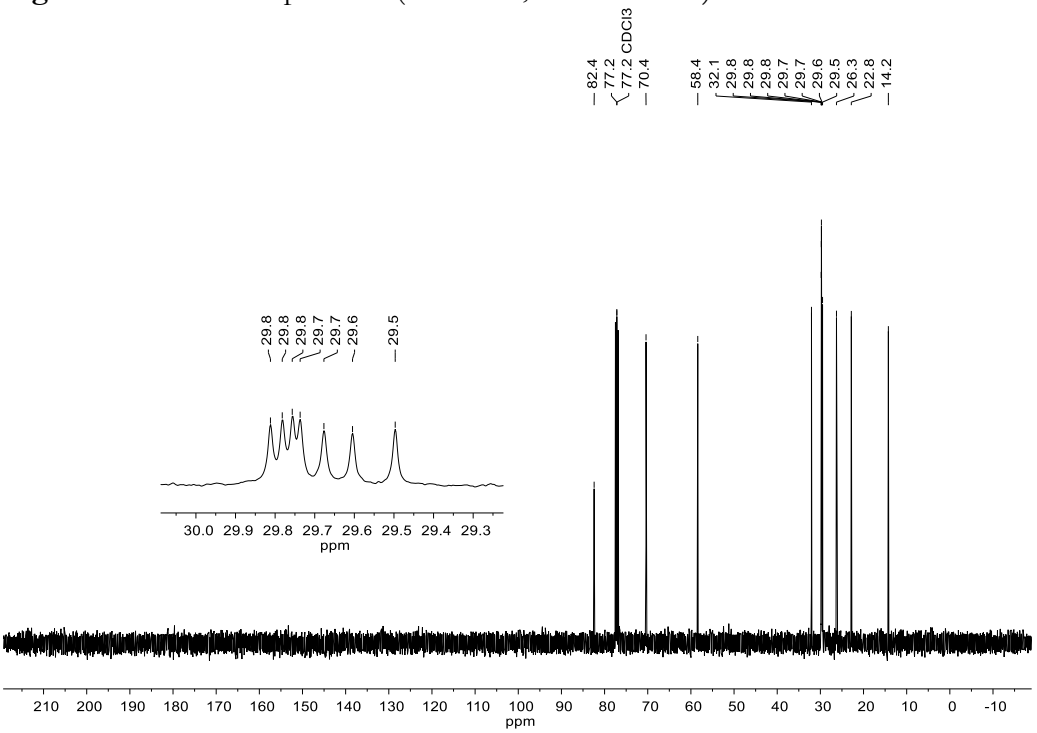

Figure S8. ^{13}C{^{1}H} NMR Spectrum (101 MHz, chloroform-*d*) of **S1**.

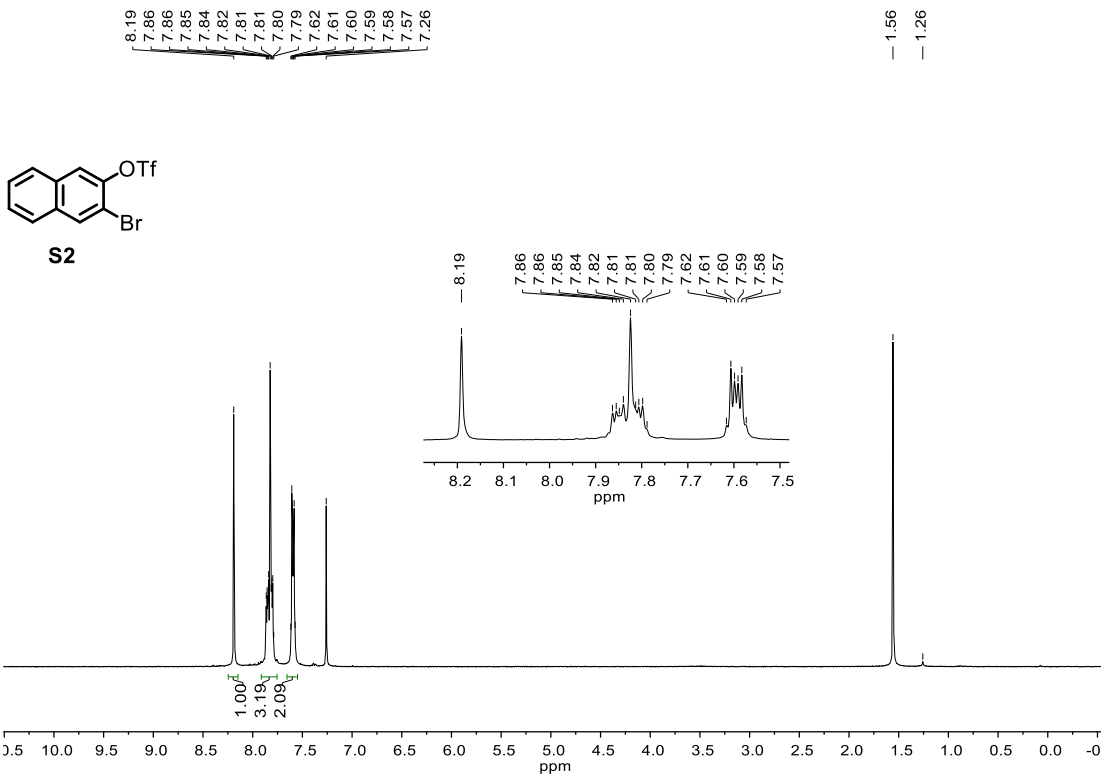

Figure S9. ^{1}H NMR Spectrum (400 MHz, chloroform-*d*) of **S2**.

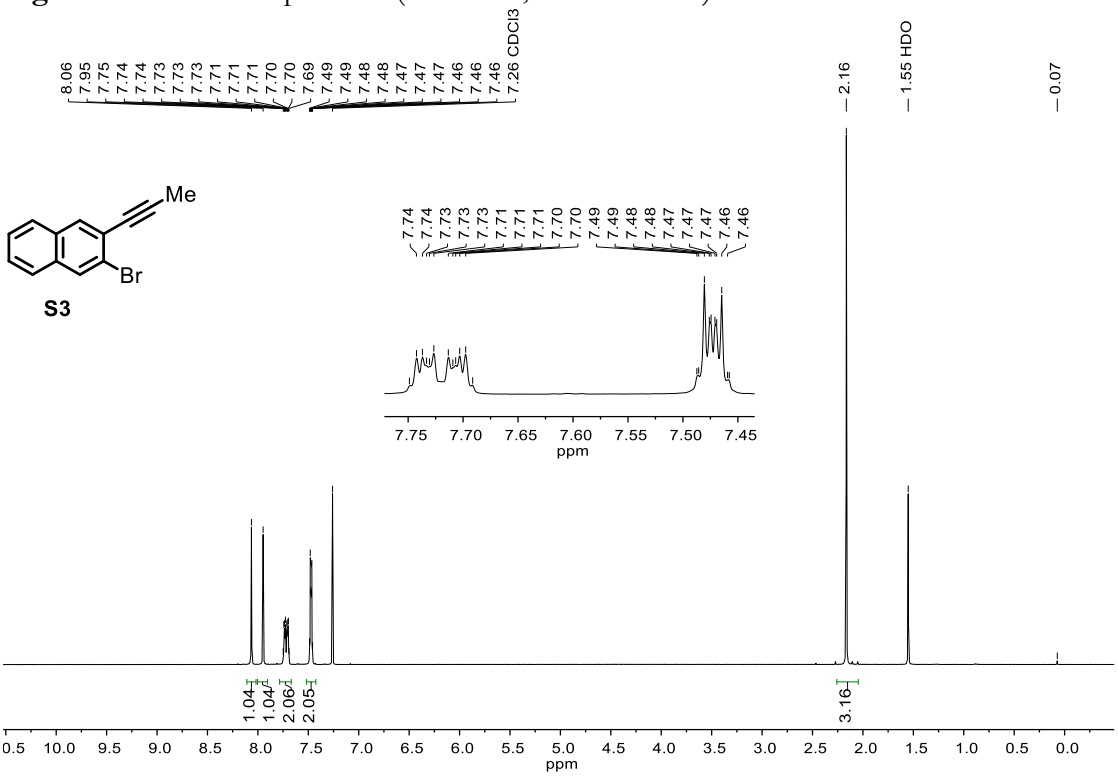

Figure S10. ^{1}H NMR Spectrum (600 MHz, chloroform-*d*) of **S3**.

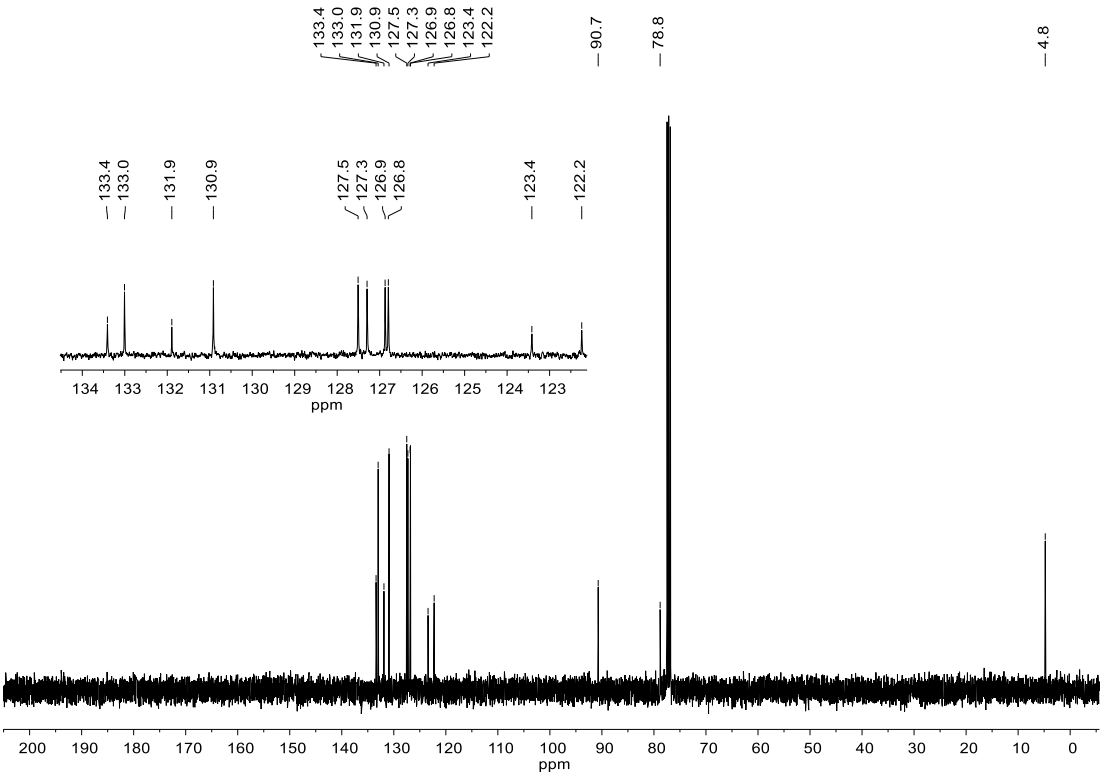

Figure S11. $^{13}C\{^{1}H\}$ NMR Spectrum (101 MHz, chloroform-*d*) of **S3**.

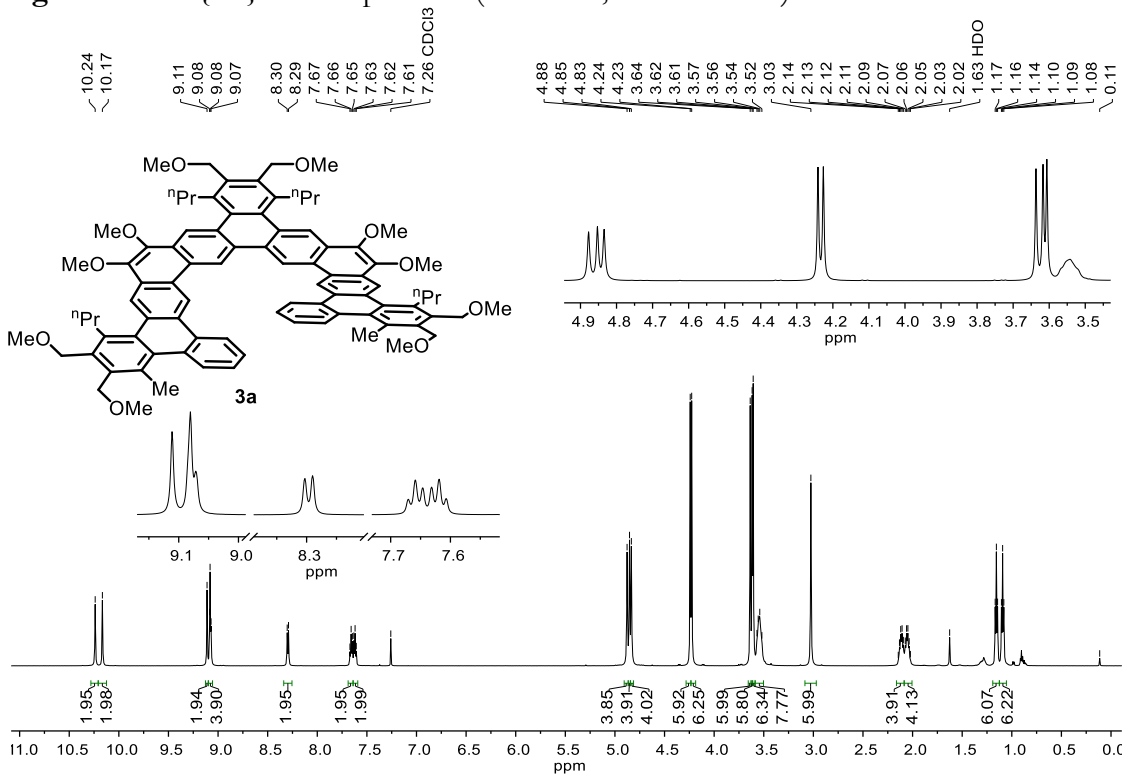

Figure S12. ^{1}H NMR Spectrum (600 MHz, chloroform-*d*) of **3a**.

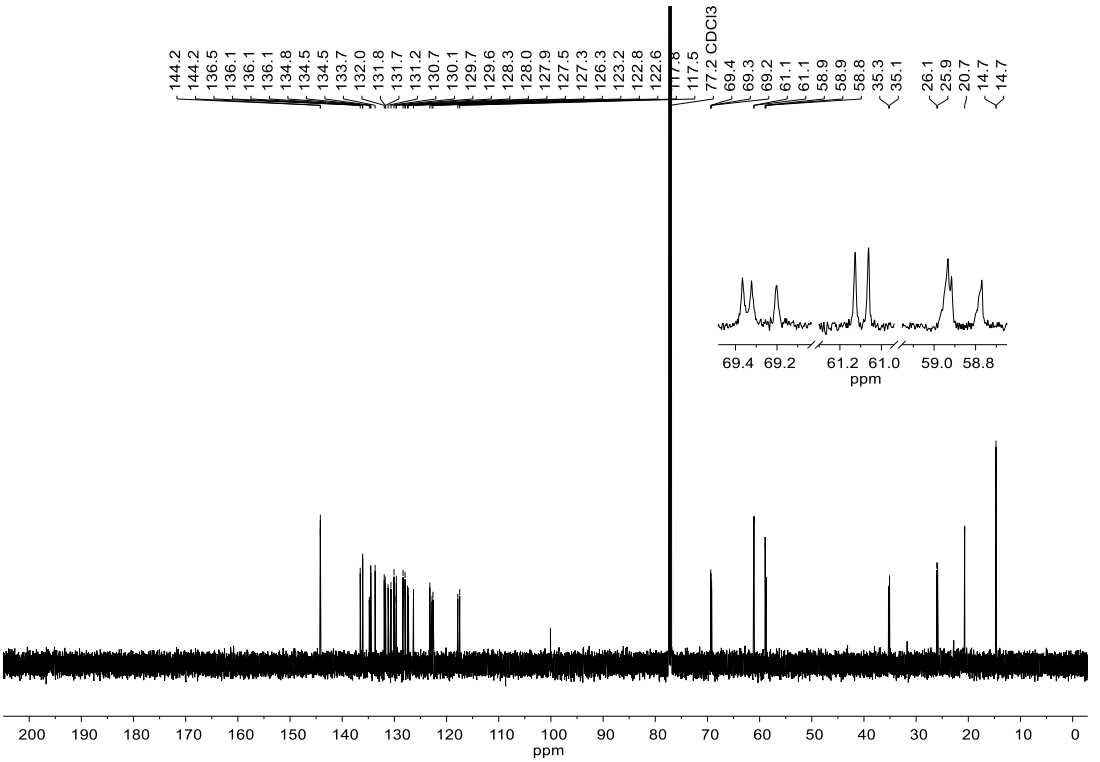

Figure S13. $^{13}C\{^{1}H\}$ NMR Spectrum (151 MHz, chloroform-*d*) of **3a**.

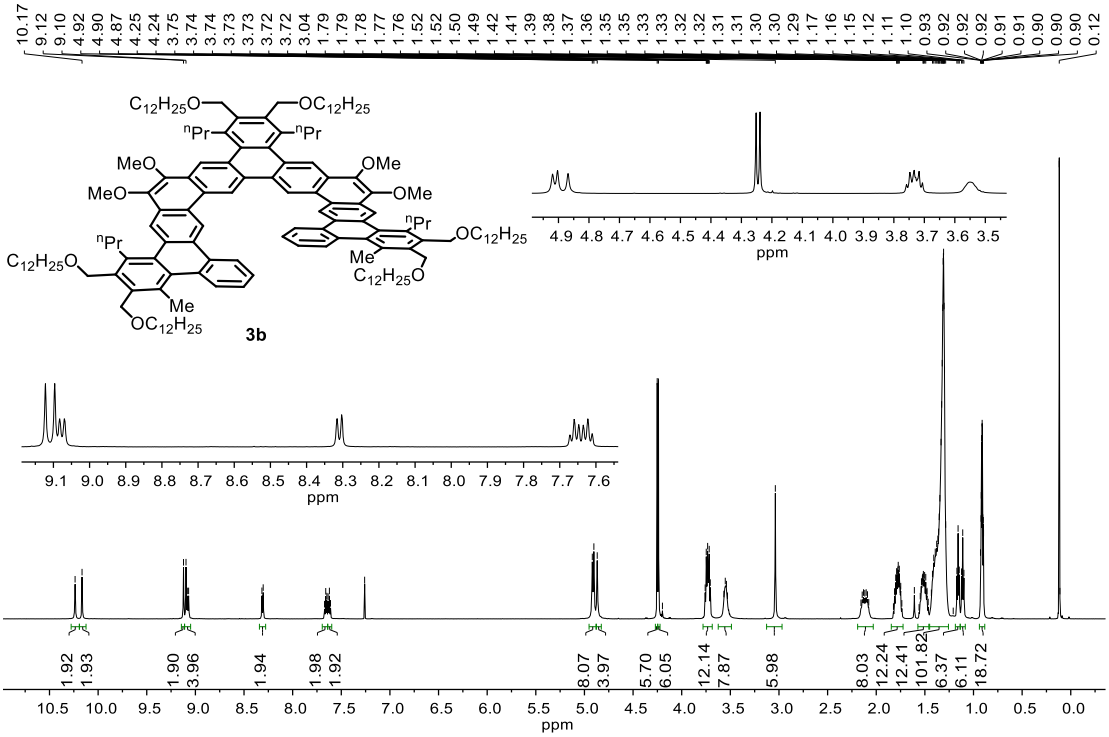

Figure S14. ^{1}H NMR Spectrum (600 MHz, chloroform-*d*) of **3b**.

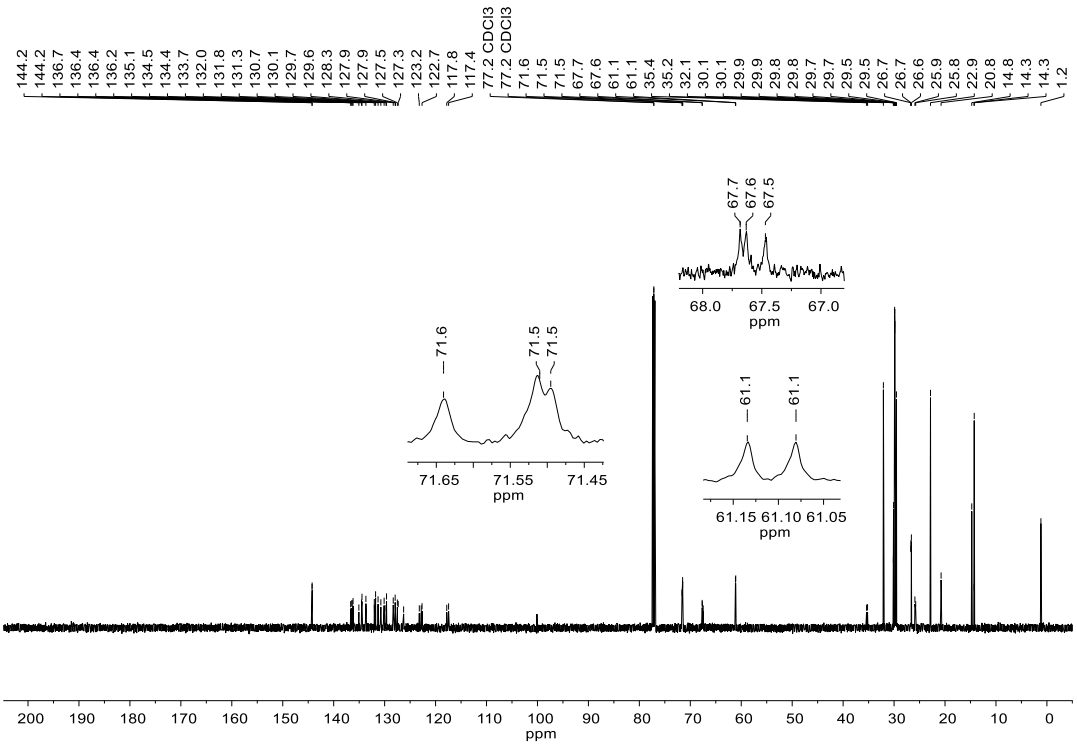

Figure S15. $^{13}C\{^{1}H\}$ NMR Spectrum (151 MHz, chloroform-*d*) of **3b**.

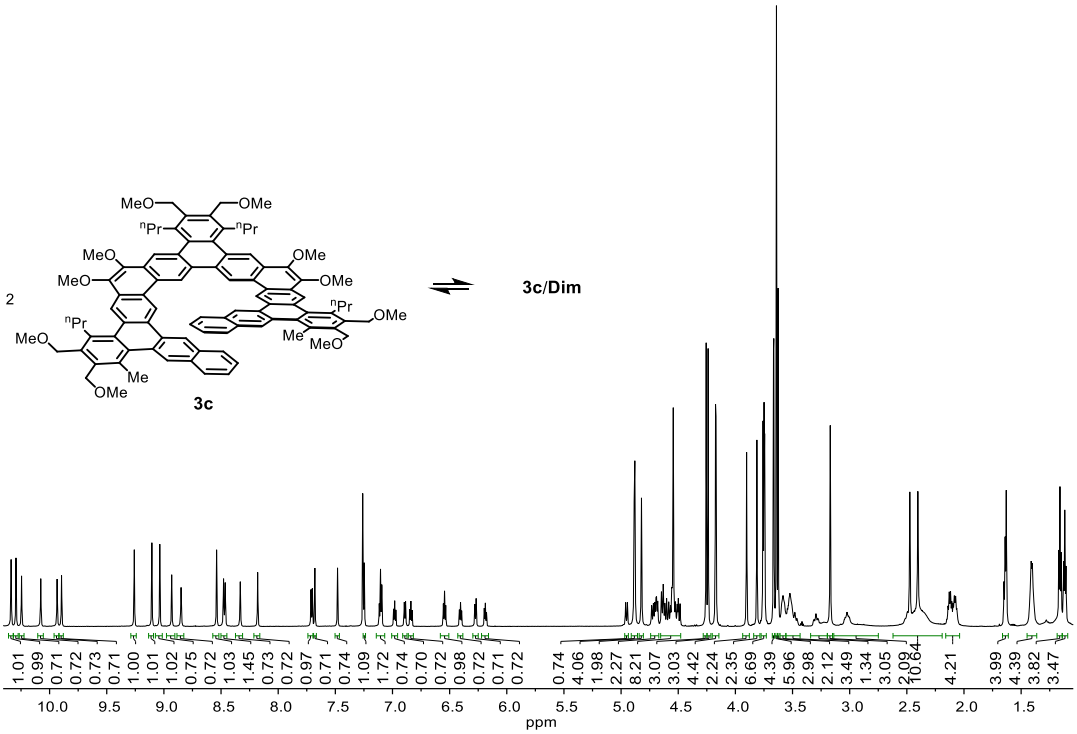

Figure S16. Full ^{1}H NMR Spectrum (700 MHz, chloroform-*d*, [c] = 4.3 x 10^{-2} M, T = 298 K) of the **3c**/**3c-Dim** equilibrium mixture. See Figures S17-S19 for a closer look at the various regions.

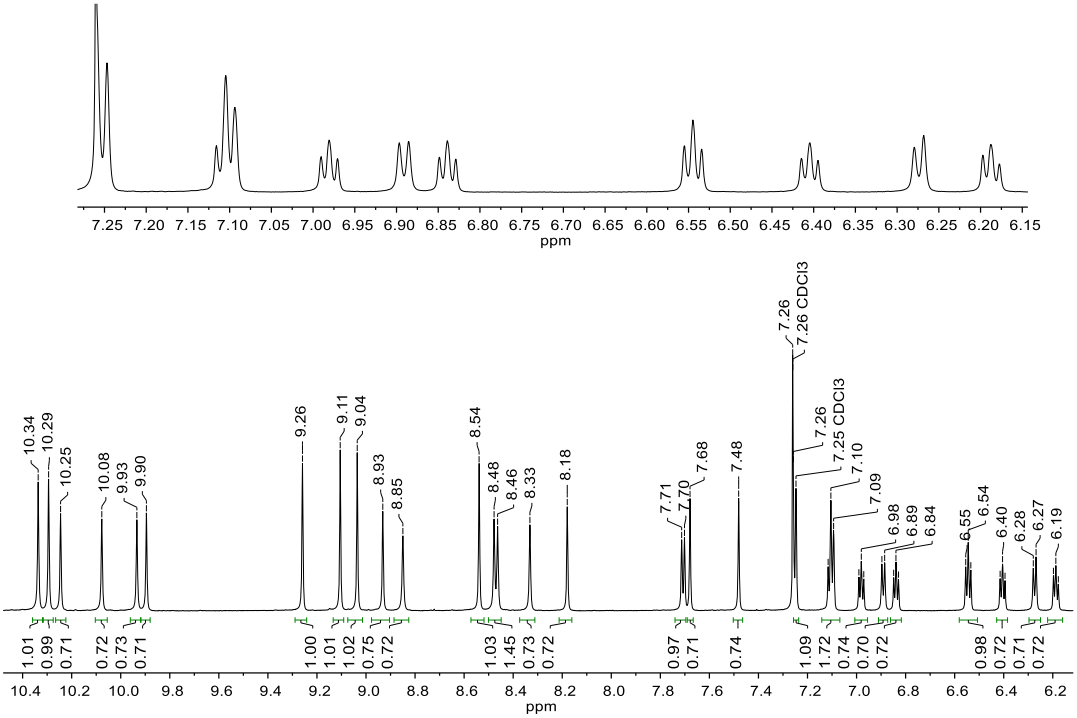

Figure S17. Aromatic region of the ^{1}H NMR Spectrum (700 MHz, chloroform-*d*, [c] = 4.3 x 10^{-2} M, T = 298 K) of the **3c**/**3c-Dim** equilibrium mixture. See Figure S16 for full spectrum.

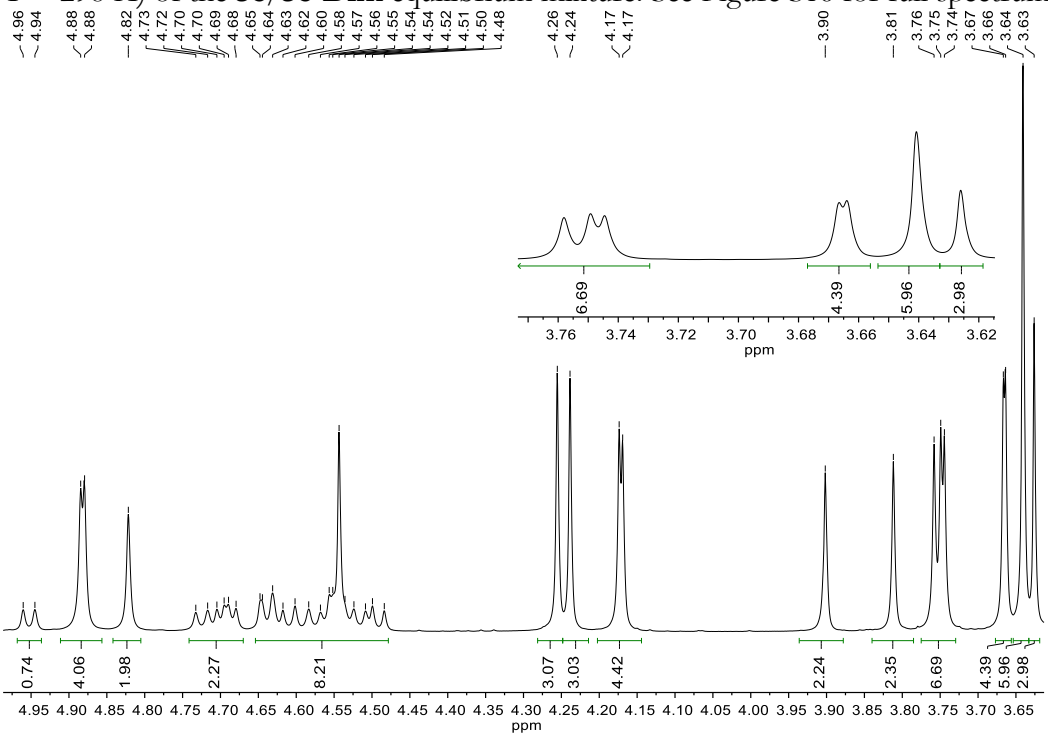

Figure S18. Alkoxy region of the ^{1}H NMR Spectrum (700 MHz, chloroform-*d*, [c] = 4.3 x 10^{-2} M, T = 298 K) of the **3c**/**3c-Dim** equilibrium mixture. See Figure S16 for full spectrum.

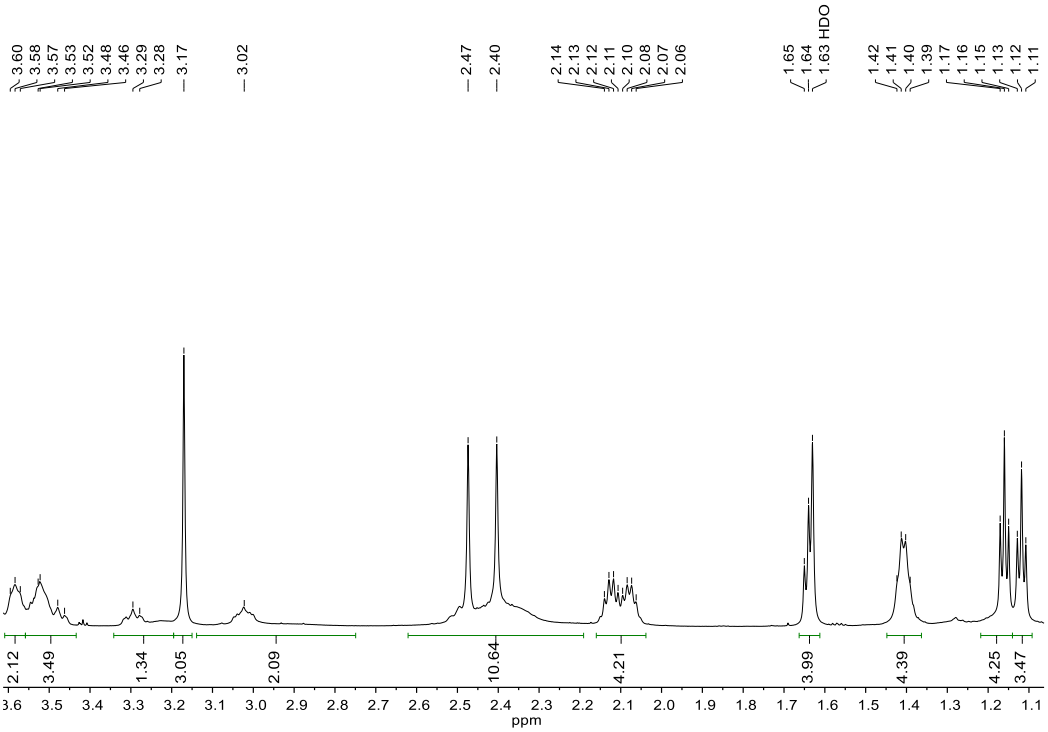

Figure S19. Alkyl region of the ^{1}H NMR Spectrum (700 MHz, chloroform-*d*, [c] = 4.3 x 10^{-2} M, T = 298 K) of the **3c**/**3c-Dim** equilibrium mixture. See Figure S16 for full spectrum.

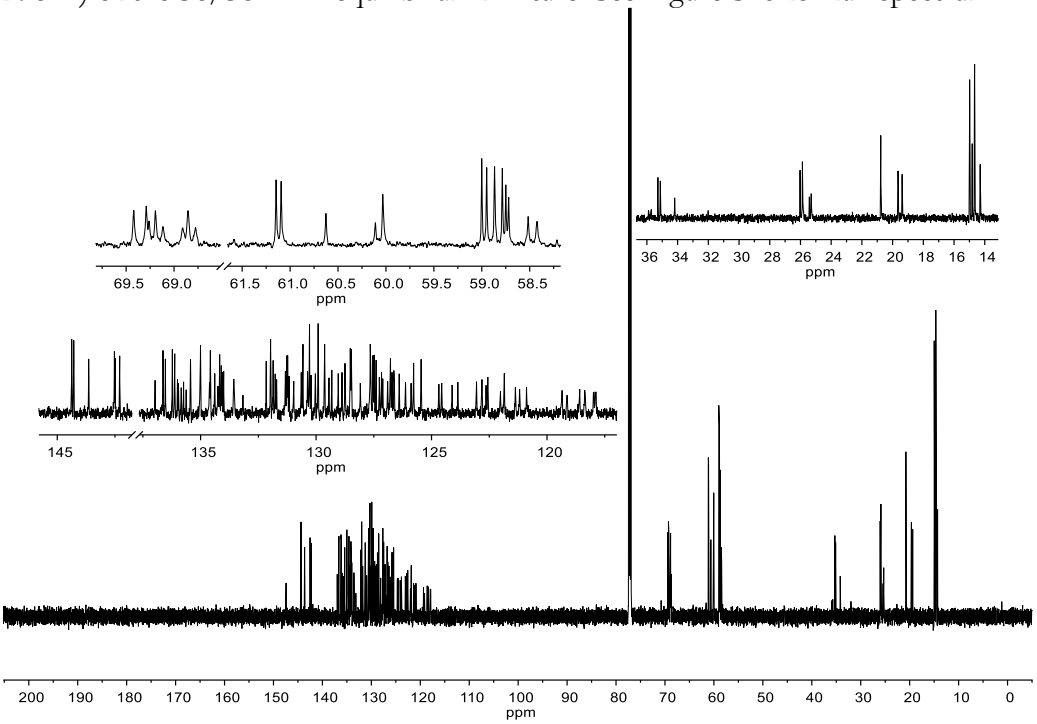

Figure S20. ^{13}C{^{1}H} NMR Spectrum (176 MHz, chloroform-*d*, [c] = 4.3 x 10^{-2} M, T = 298 K) of the **3c**/**3c-Dim** equilibrium mixture.

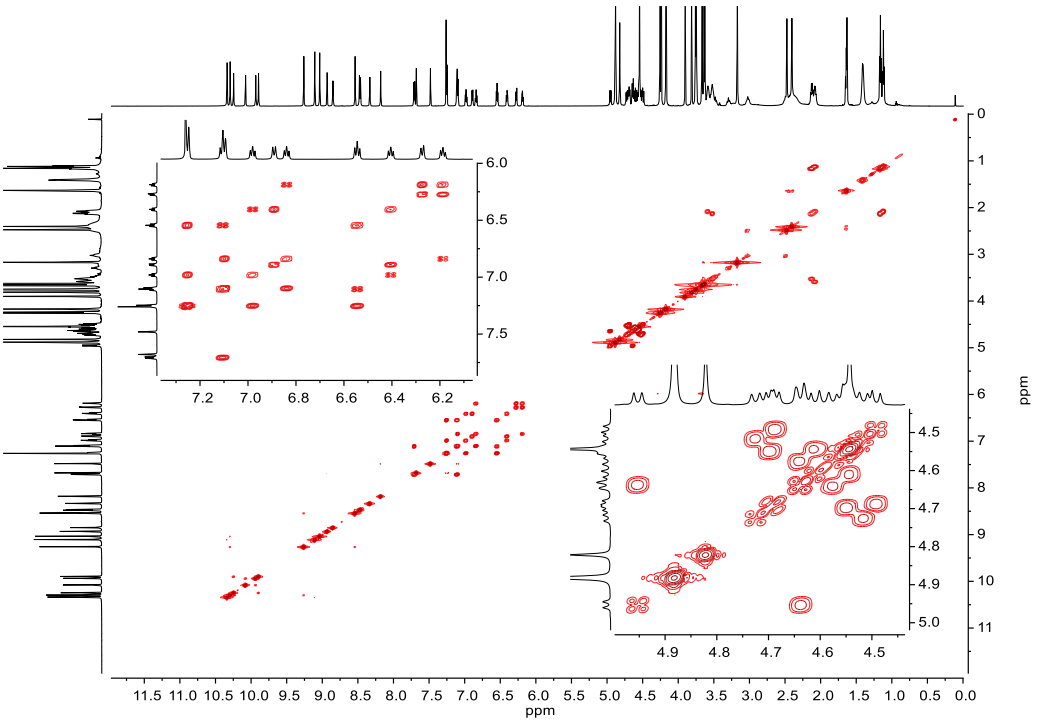

Figure S21. ^{1}H-^{1}H COSY spectrum (700 MHz, chloroform-*d*, [c] = 4.3 x 10^{-2} M, T = 298 K) of **3c**/**3c-Dim** equilibrium mixture.

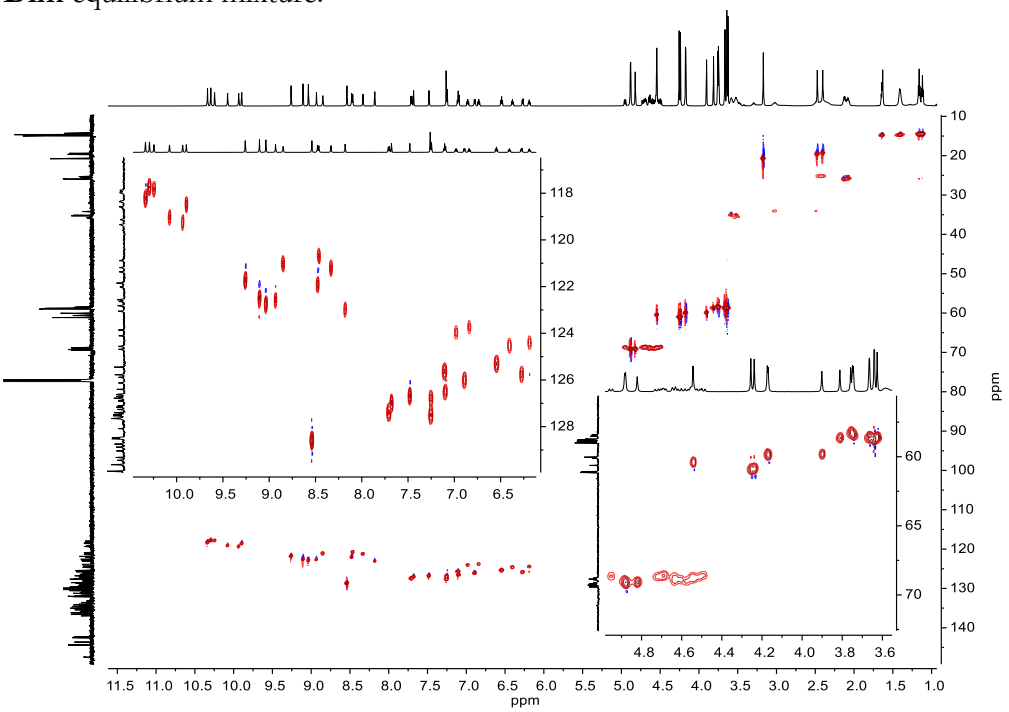

Figure S22. ^{1}H-^{13}C HSQC spectrum (700 MHz, chloroform-*d*, [c] = 4.3 x 10^{-2} M, T = 298 K) of **3c**/**3c-Dim** equilibrium mixture.

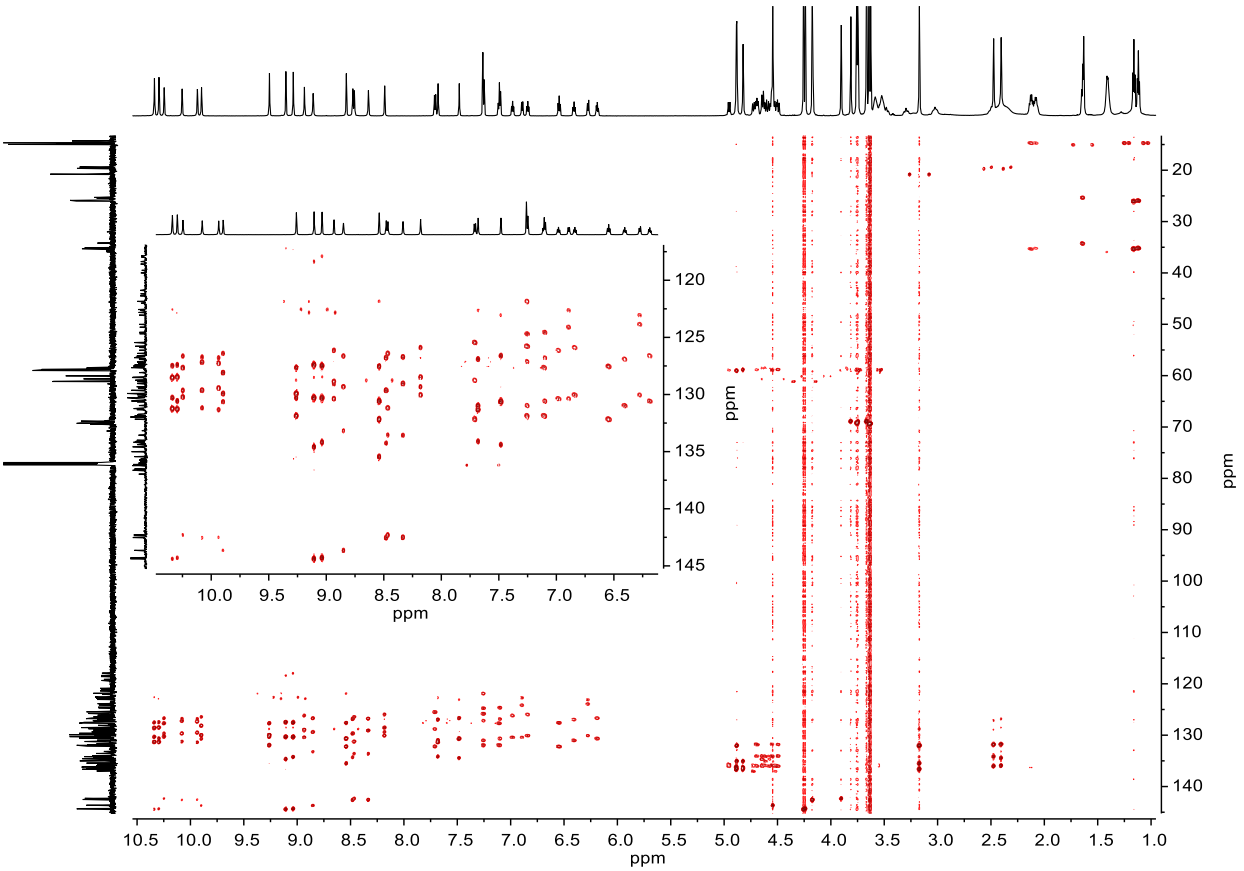

Figure S23. ^{1}H-^{13}C HMBC spectrum (700 MHz, chloroform-*d*, [c] = 4.3 x 10^{-2} M, T = 298 K) of **3c**/**3c-Dim** equilibrium mixture.

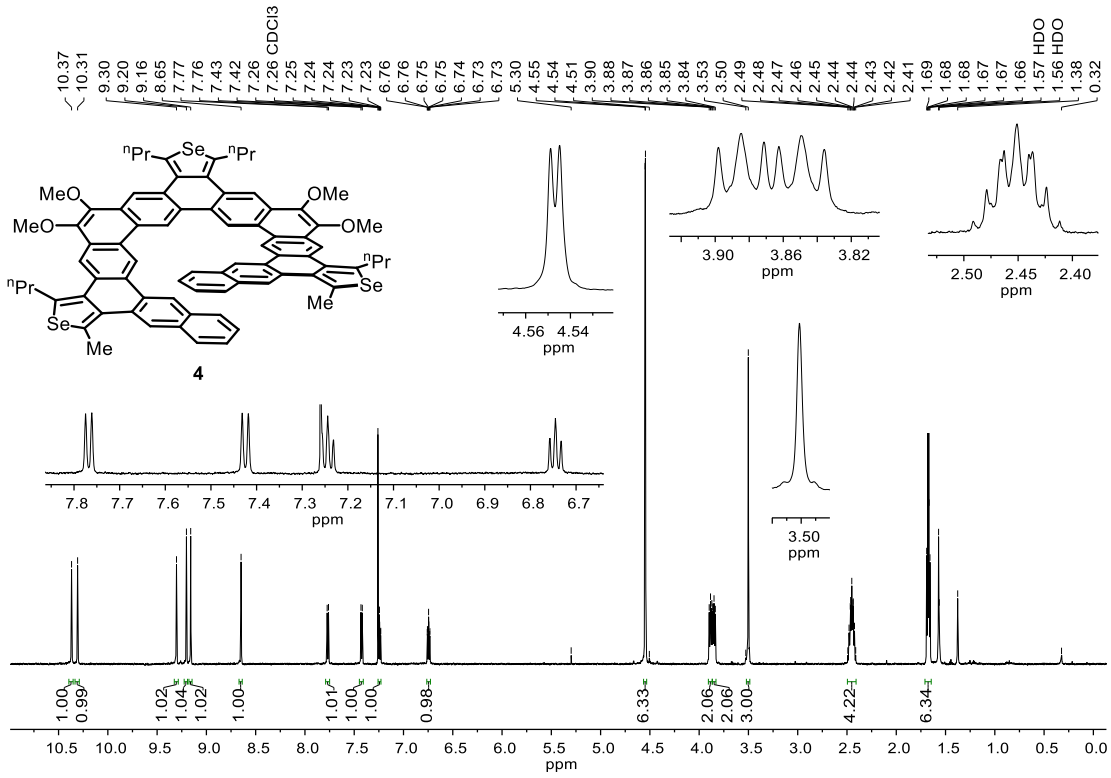

Figure S24. ^{1}H NMR Spectrum (600 MHz, CS_2 with chloroform-*d* capillary) of **4**.

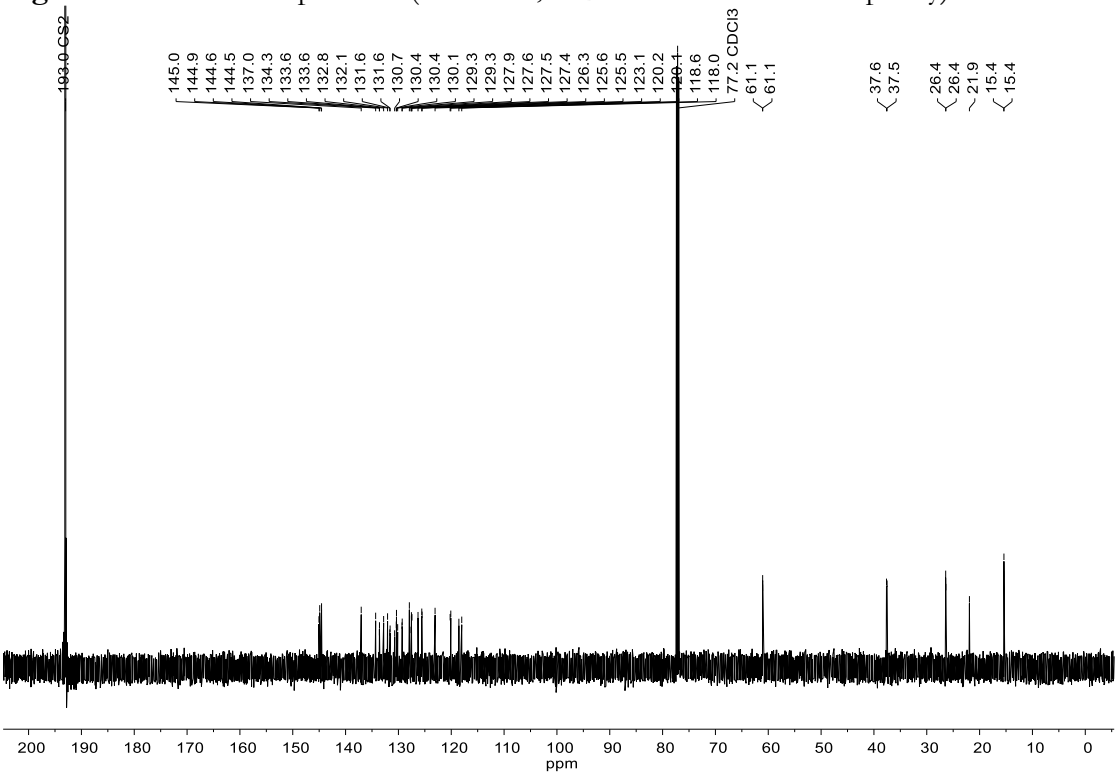

Figure S25. ^{13}C{^{1}H} NMR Spectrum (151 MHz, CS_2 with chloroform-*d* capillary) of **4**.

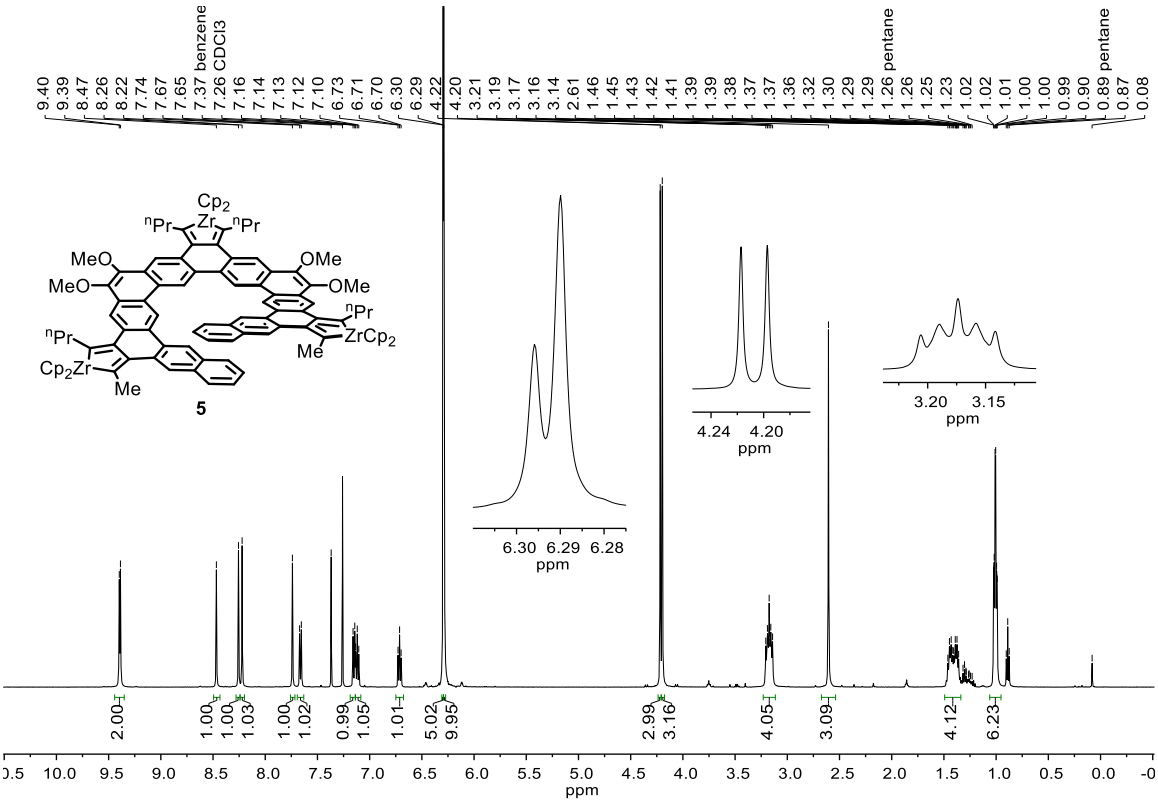

Figure S26. ^{1}H NMR Spectrum (500 MHz, chloroform-*d*) of **5**.

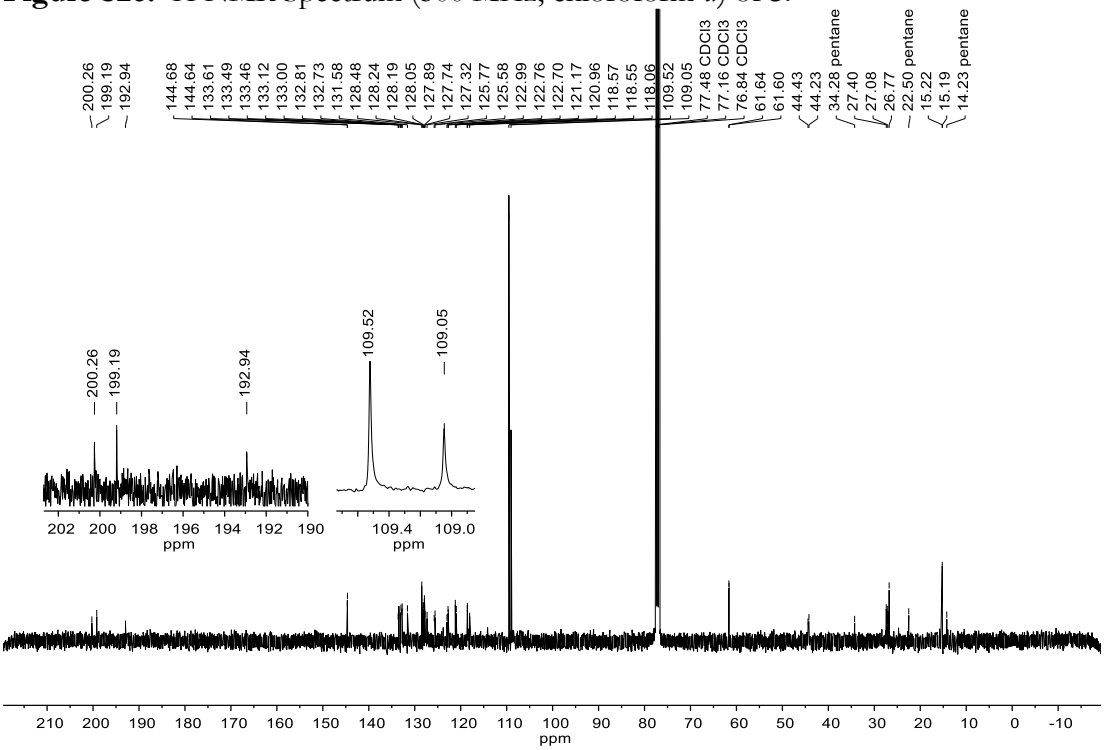

Figure S27. ^{13}C{^{1}H} NMR Spectrum (101 MHz, chloroform-*d*) of **5**.

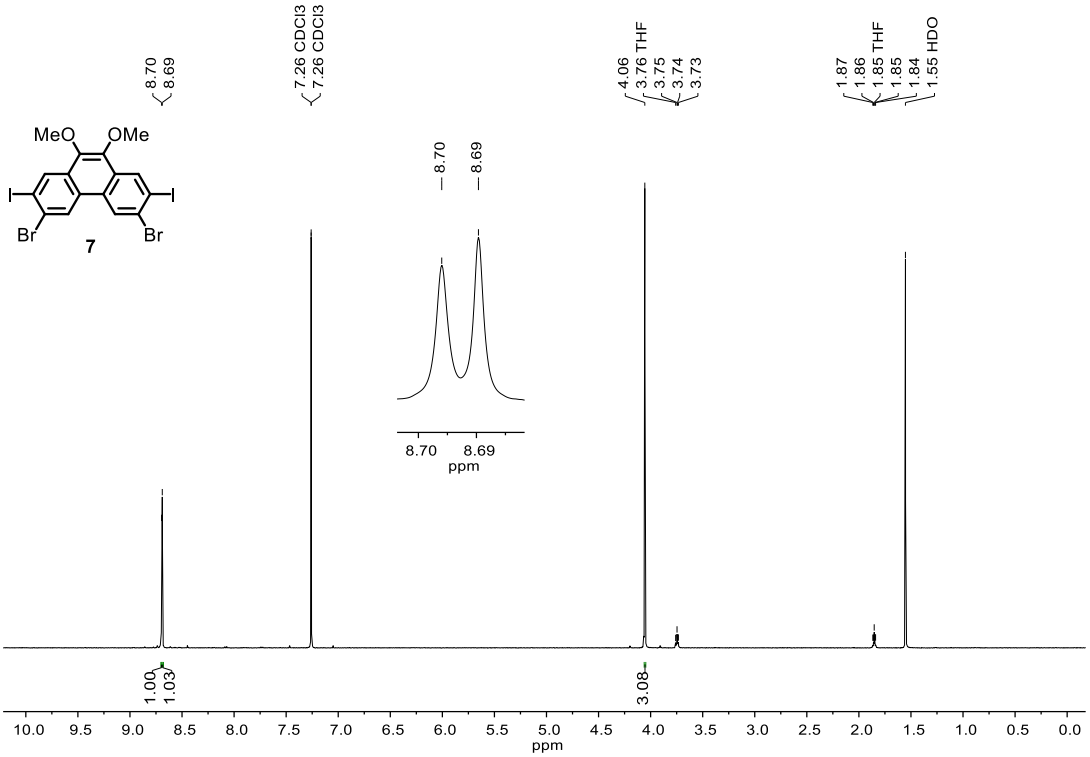

Figure S28. ^{1}H NMR Spectrum (500 MHz, chloroform-*d*) of **7**.

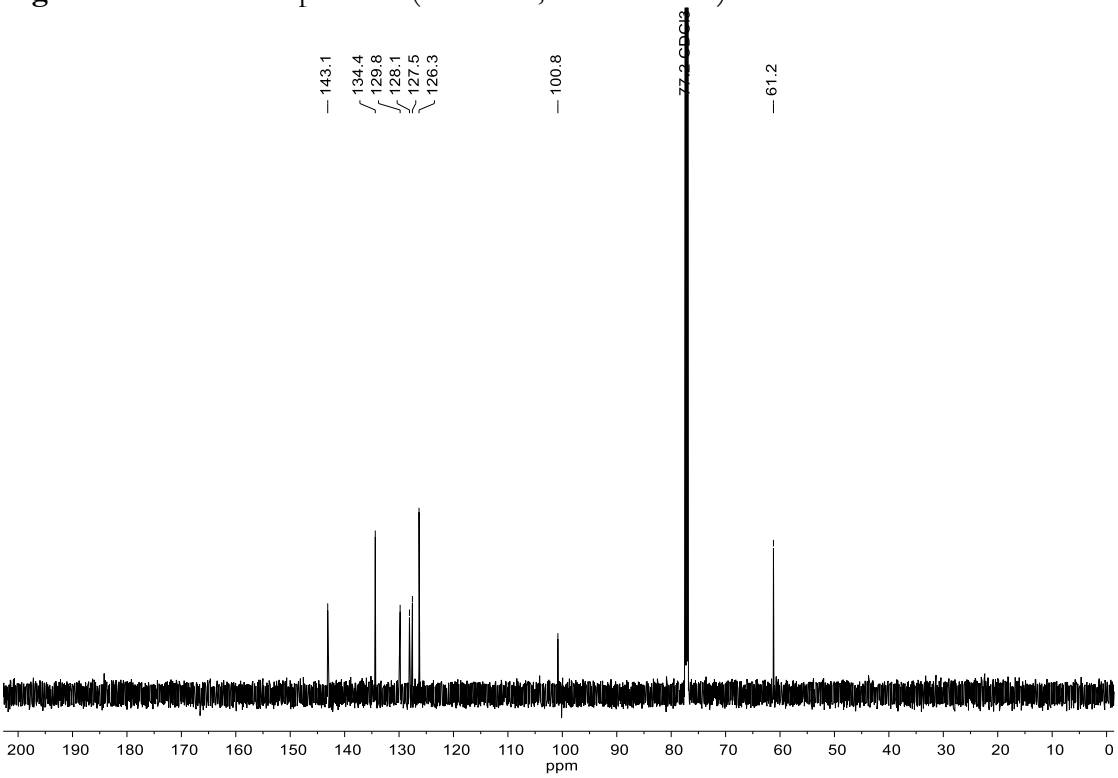

Figure S29. ^{13}C{^{1}H} NMR Spectrum (151 MHz, chloroform-*d*) of **7**.

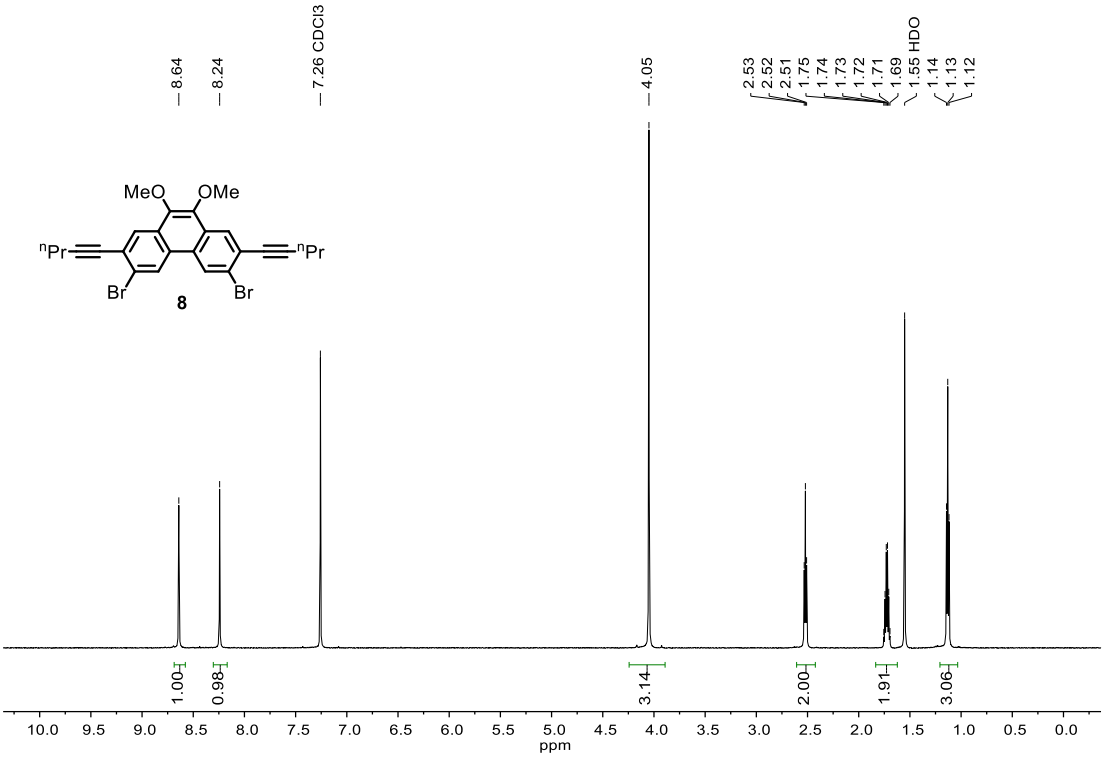

Figure S30. ^{1}H NMR Spectrum (600 MHz, chloroform-*d*) of **8**.

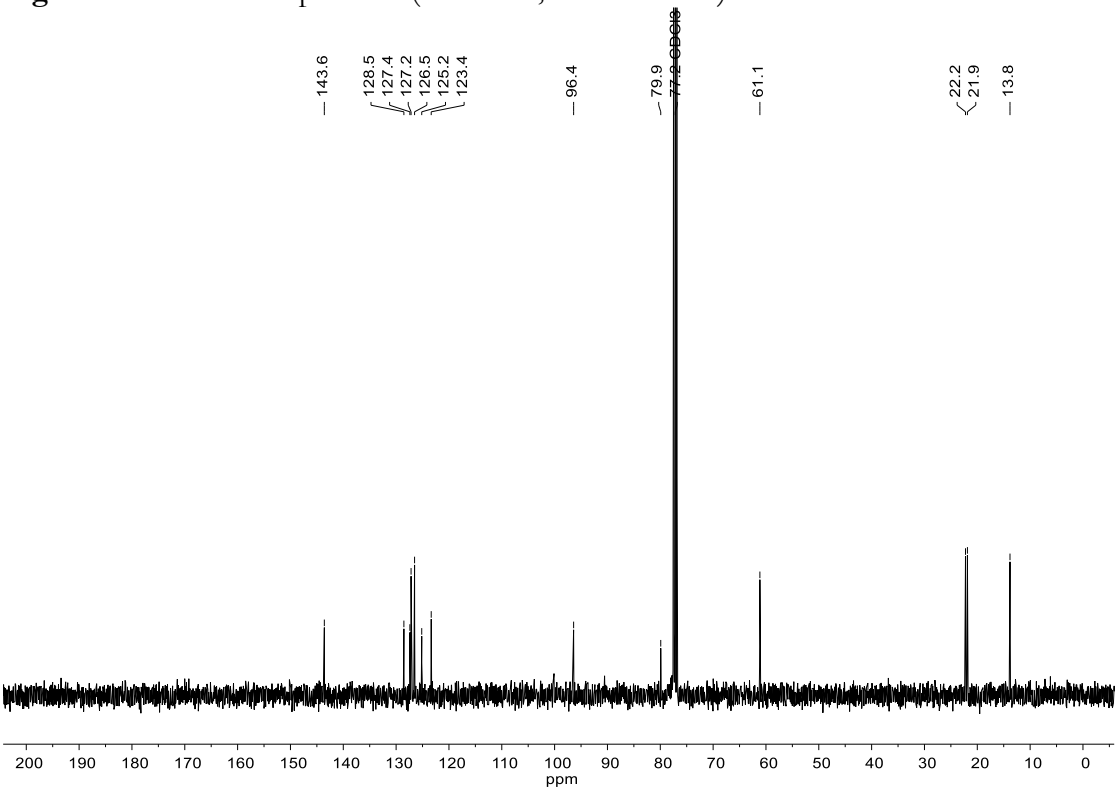

Figure S31. ^{13}C{^{1}H} NMR Spectrum (101 MHz, chloroform-*d*) of **8**.

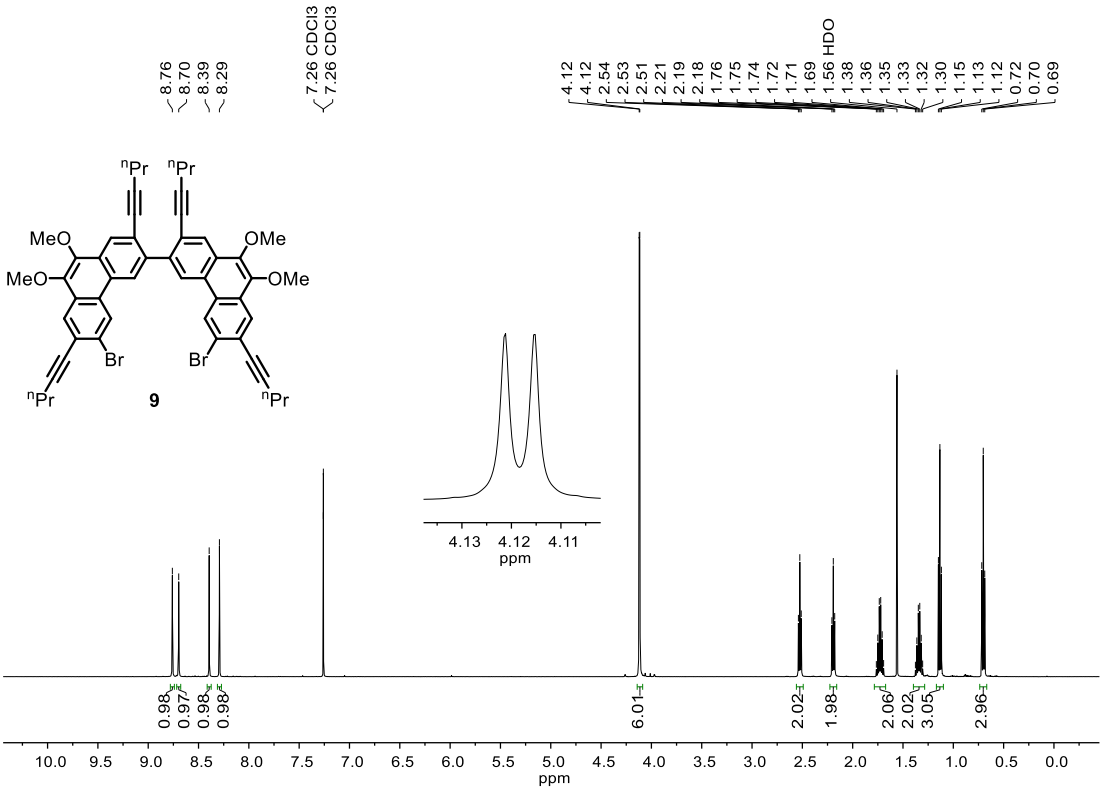

Figure S32. ^{1}H NMR Spectrum (500 MHz, chloroform-*d*) of **9**.

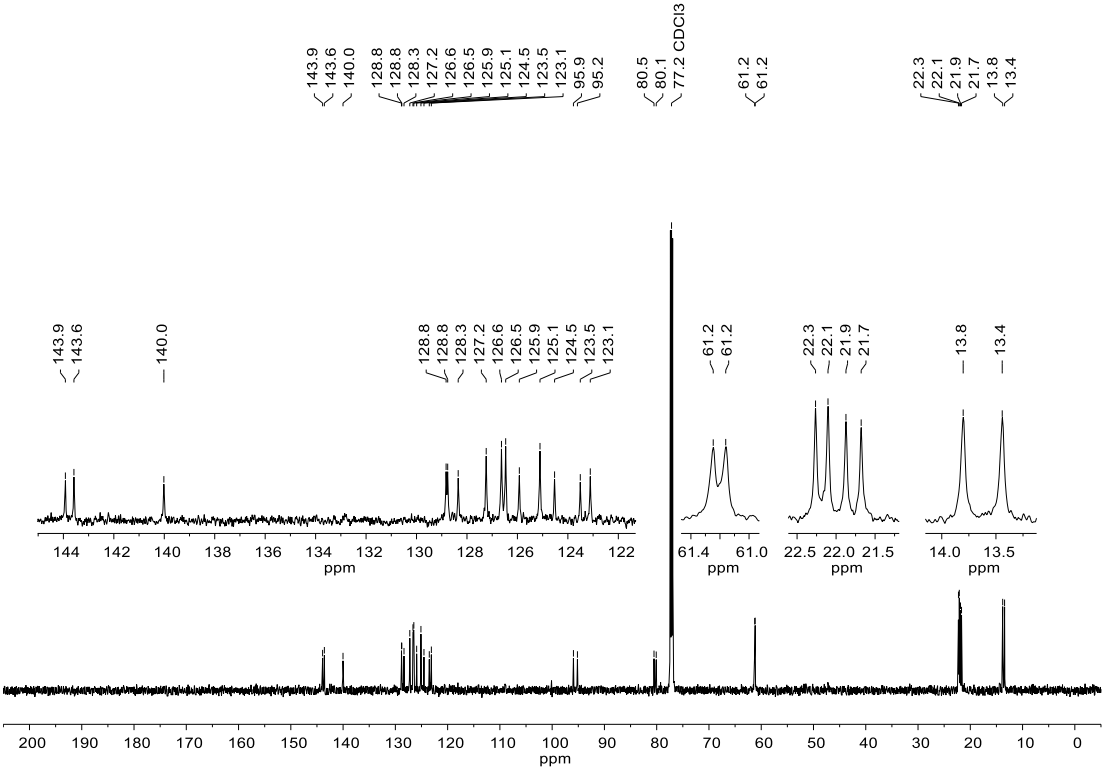

Figure S33. ^{13}C{^{1}H} NMR Spectrum (151 MHz, chloroform-*d*) of **9**.

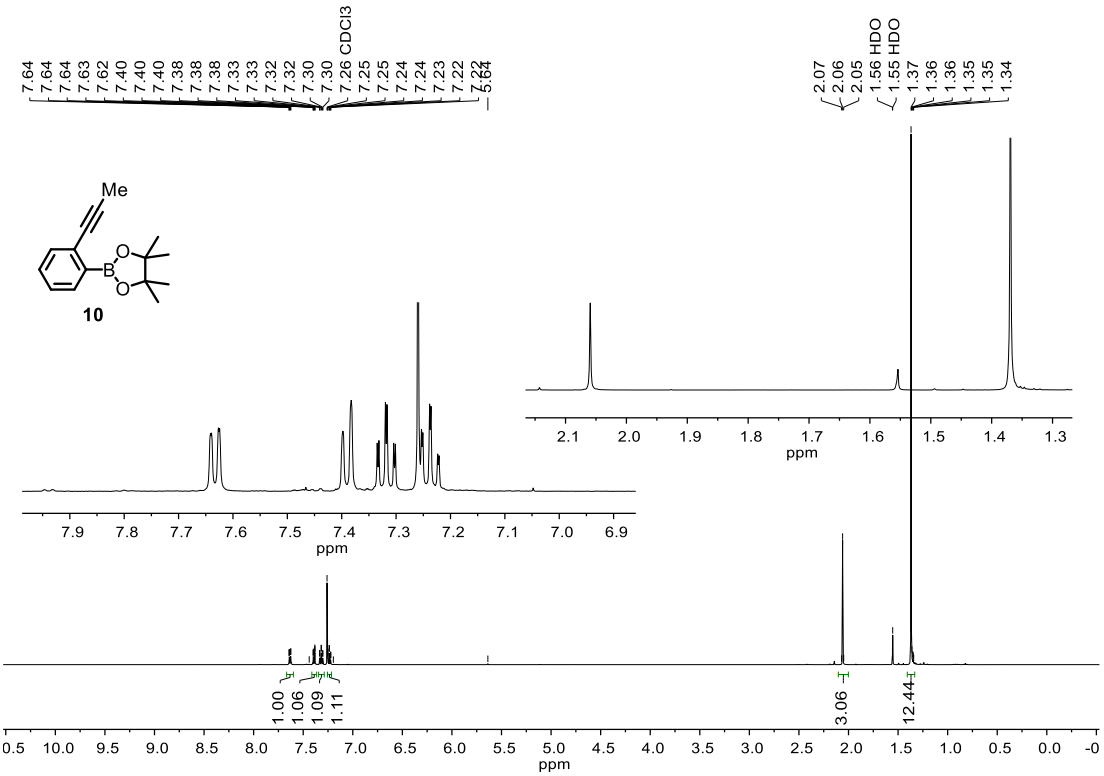

Figure S34. ^{1}H NMR Spectrum (500 MHz, chloroform-*d*) of **10**.

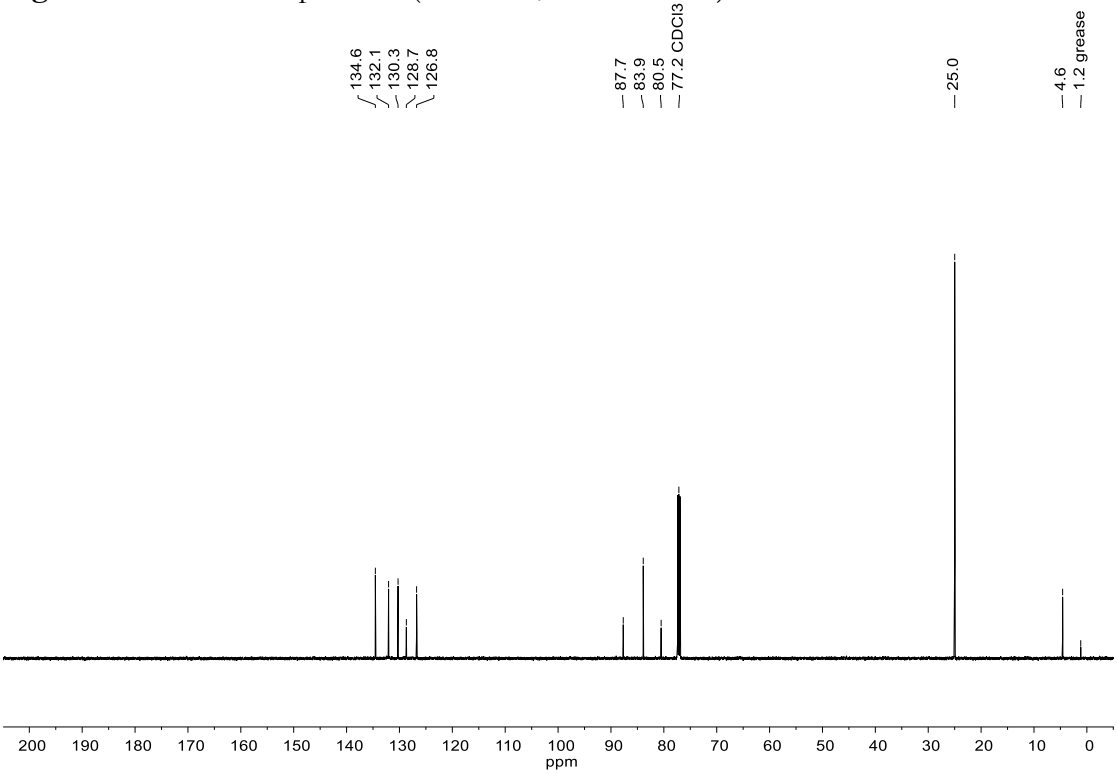

Figure S35. ^{13}C{^{1}H} NMR Spectrum (151 MHz, chloroform-*d*) of **10**.

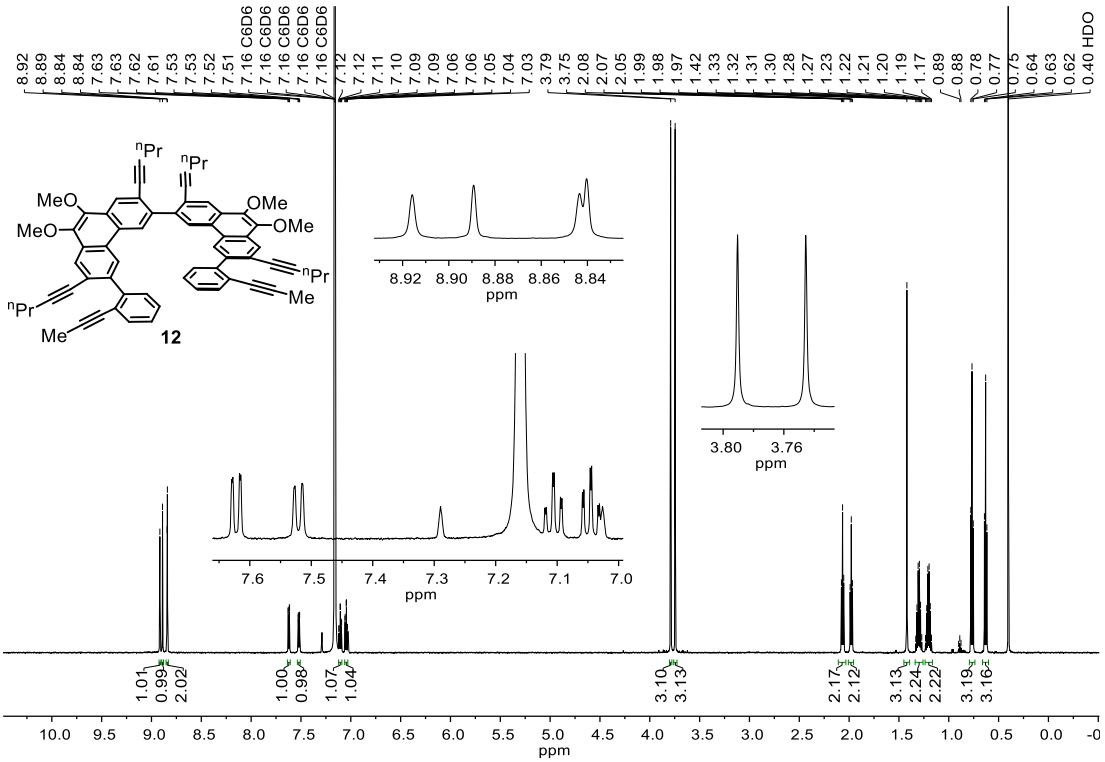

Figure S36. ^{1}H NMR Spectrum (600 MHz, benzene-d_6) of **12**.

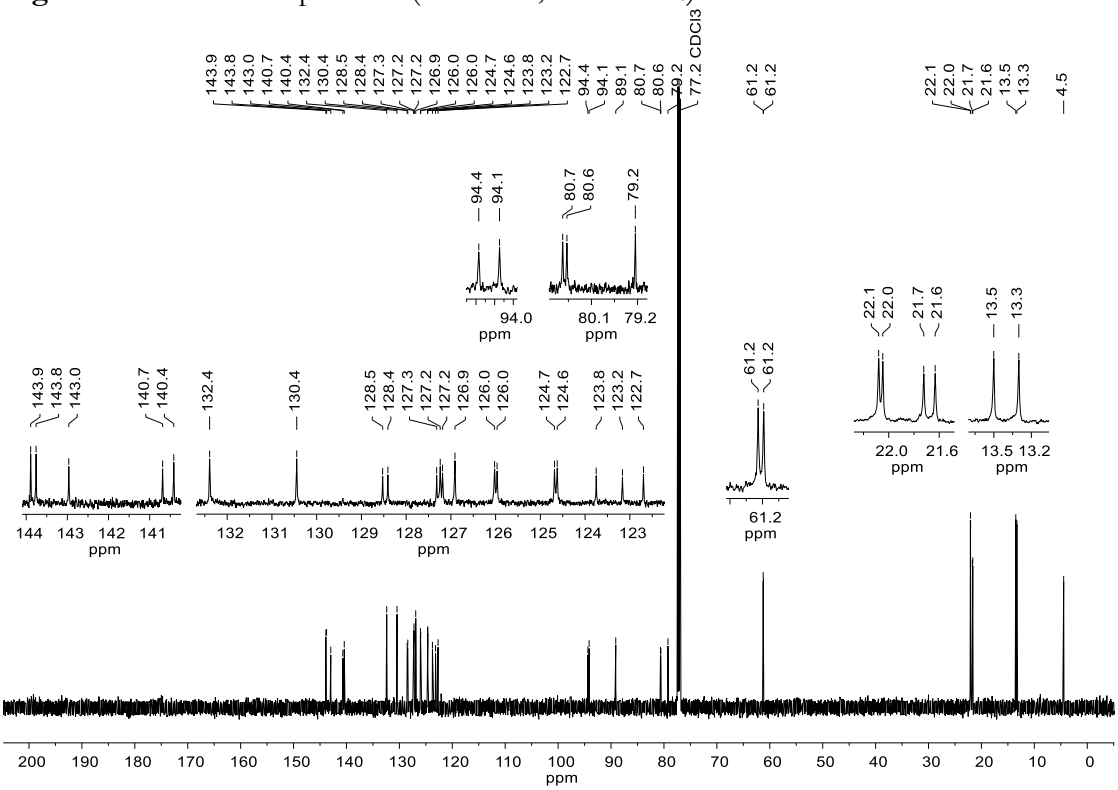

Figure S37. ^{13}C{^{1}H} NMR Spectrum (151 MHz, chloroform-*d*) of **12**.

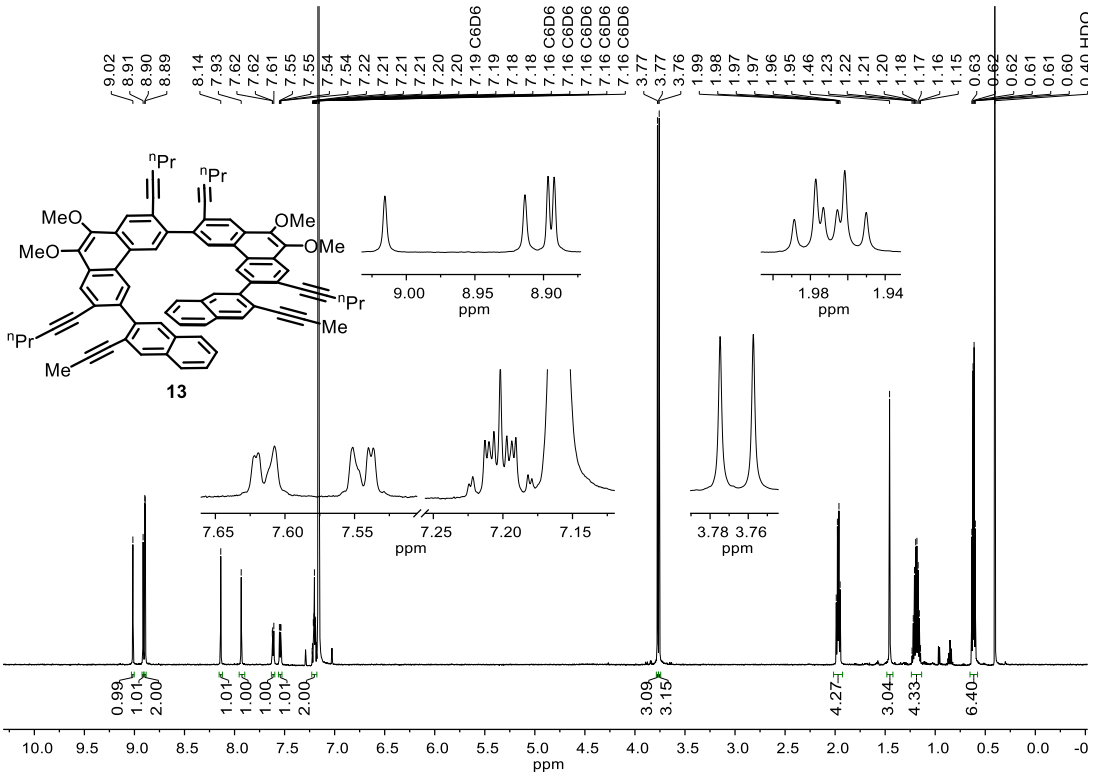

Figure S38. ^{1}H NMR Spectrum (600 MHz, benzene-d_6) of **13**.

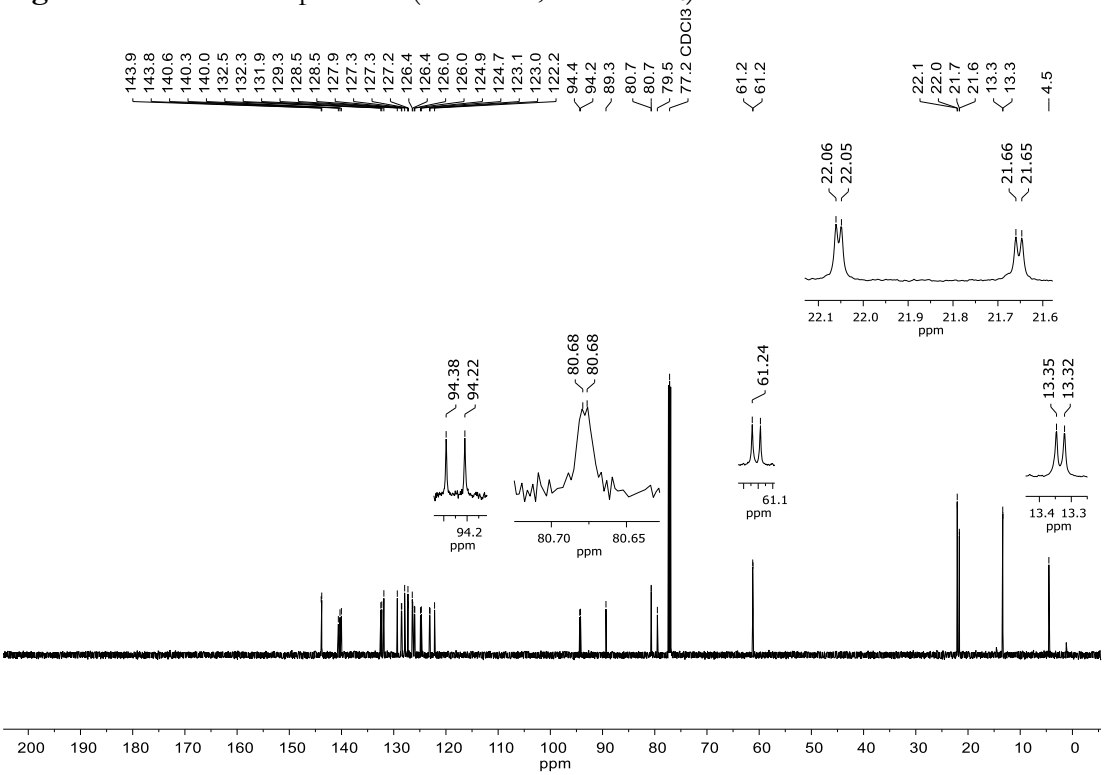

Figure S39. ^{13}C{^{1}H} NMR Spectrum (151 MHz, chloroform-*d*) of **13**.

X-Ray Crystallography

X-ray diffraction data were collected at beamline 11.3.1 of the Advanced Light Source at Lawrence Berkeley National Laboratory. Frames were collected on a PHOTON100 CMOS running shutterless using radiation with a wavelength of 0.7749 Å selected by a Si(111) monochromator and focused to 200 μm^2 with a toroidal mirror. Data collection, integration, scaling, and space group determination were performed with Bruker APEX3 (v. 2016.5-0) software. Structures were solved by SHELXT-2014 and refined with SHELXL-2014, with refinement of F^2 on all data by full-matrix least squares.[14–17] The 3D molecular structure figures were produced in Mercury 3.7.[18] See the synthetic procedures for compounds **3c** and **4** (above) for details on crystal growth. For compound **4**, due to residual electron density near the neighboring Se atom, C74 was restrained using ISOR.

Compound 3c

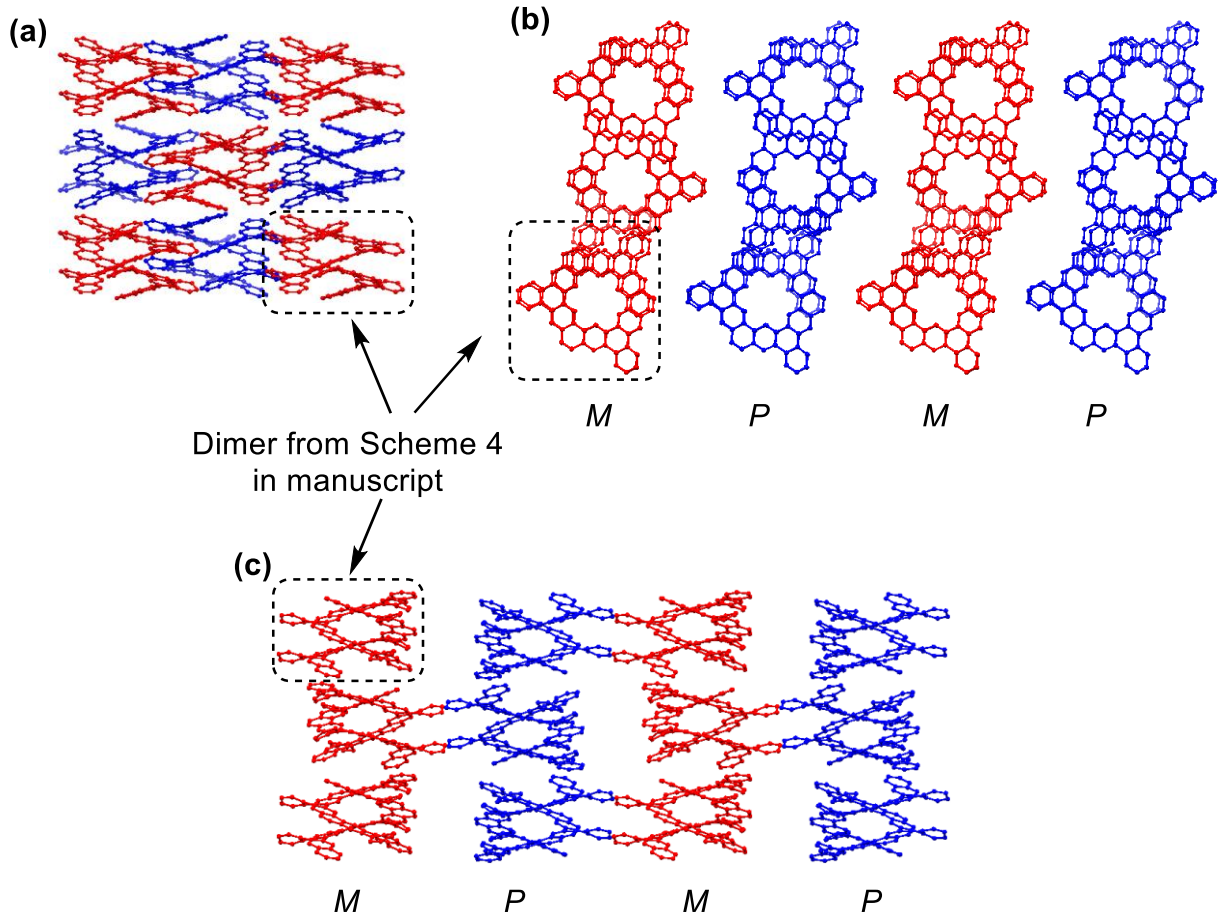

Figure S40. Solid-state packing of **3c** as determined by single-crystal X-ray diffraction. Red helicenes are left-handed (*M*) and blue helicenes are right-handed (*P*). Alkyl, methoxymethyl, and methoxy groups were omitted for clarity. Solvent molecules were also omitted. Views along the crystallographic (a) c axis, (b) b axis, and (c) a axis.

Empirical formula	$C_{195.55}H_{195.55}Cl_{10.66}O_{20}$
Formula weight	3243.59

Temperature	100.0 K
Crystal system	monoclinic
Space group	$P2_1/c$
Unit cell dimensions	a = 23.2934(8) Å
	b = 19.8397(8) Å
	c = 37.1735(13) Å
	α = 90°
	β = 100.129(2)°
	γ = 90°
Volume	16911.4(11) $Å^3$
Z	4
Density (calculated)	1.274 g/cm^3
μ	0.306 mm^{-1}
F(000)	6840.0
Radiation	Synchrotron (λ = 0.7749)
2Θ range for data collection	3.606 to 51.154°
Index ranges	$-25 \leq h \leq 25$, $-22 \leq k \leq 22$, $-41 \leq l \leq 41$
Reflections collected	118469
Independent reflections	24356 [R_{int} = 0.0692, R_{sigma} = 0.0514]
Data/restraints/parameters	24356/0/2126
Goodness-of-fit on F^2	1.126
Final R indexes [I>=2σ (I)]	R_1 = 0.0979, wR_2 = 0.2286
Final R indexes [all data]	R_1 = 0.1220, wR_2 = 0.2418
Largest diff. peak/hole	1.31/-0.78 e $Å^{-3}$

Table S1. Crystal data and structure refinement for helicene **3c**.

Compound 4

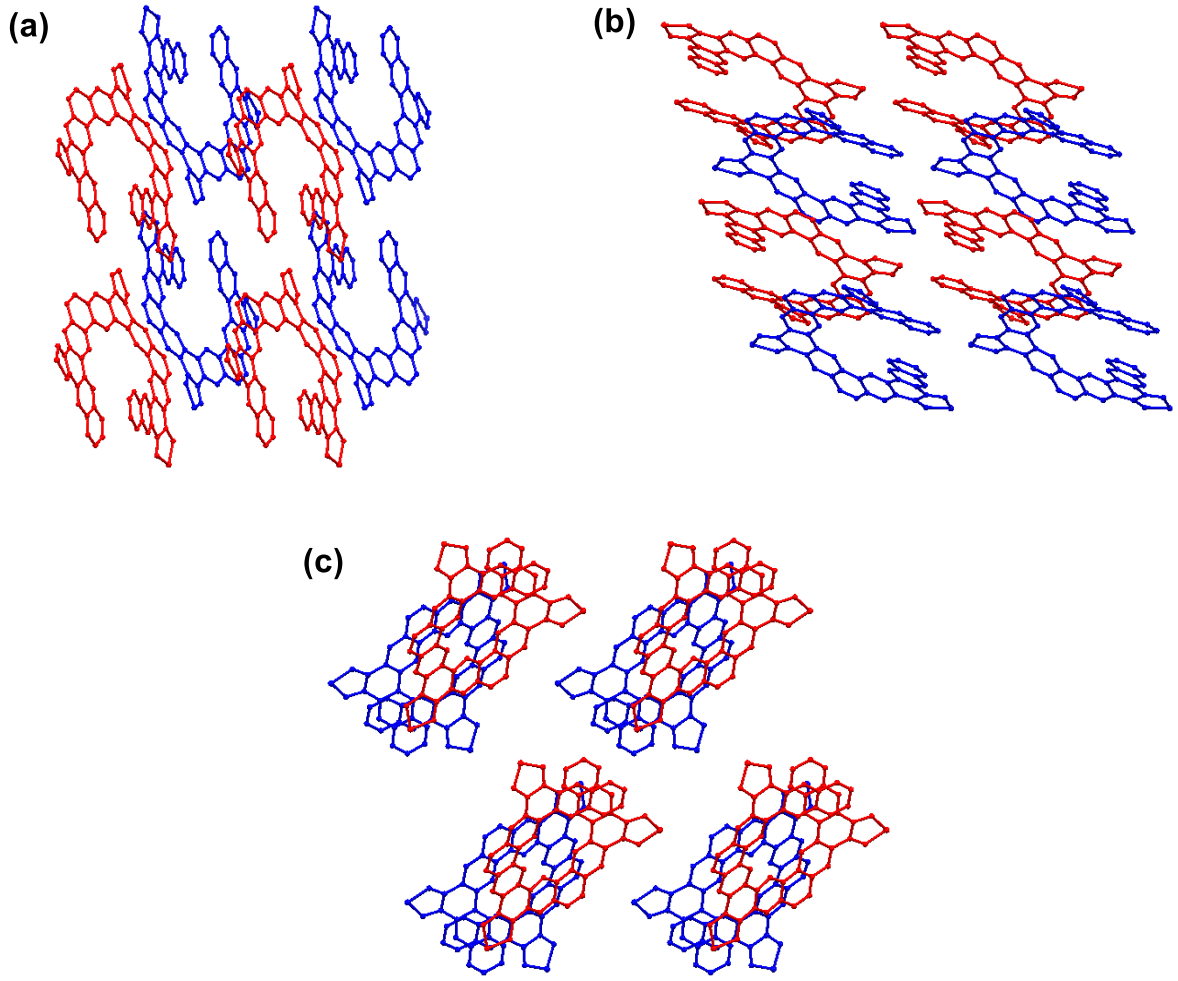

Figure S41. Solid-state packing of **4** as determined by single-crystal X-ray diffraction. Red helicenes are left-handed (*M*) and blue helicenes are right-handed (*P*). Alkyl and methoxy groups were omitted for clarity. Solvent molecules were also omitted. Views along the crystallographic (a) c axis, (b) b axis, and (c) a axis.

Empirical formula	$C_{80}H_{70}O_4Cl_4Se_3$
Formula weight	1474.04
Temperature	100(2) K
Crystal system	triclinic
Space group	P-1
Unit cell dimensions	a = 12.9527(7) Å
	b = 16.0679(8) Å
	c = 16.7417(9) Å
	α = 70.269(3)°

	$\beta = 77.377(3)°$
	$\gamma = 86.182(3)°$
Volume	3200.4(3) $Å^3$
Z	2
Density (calculated)	1.530 g/cm^3
μ	2.430 mm^{-1}
F(000)	1504.0
Crystal size	0.11 × 0.05 × 0.05 mm^3
Radiation	Synchrotron (λ = 0.7749)
2Θ range for data collection	4.426 to 56.586 °
Index ranges	$-15 \leq h \leq 15$, $-19 \leq k \leq 19$, $-20 \leq l \leq 20$
Reflections collected	29278
Independent reflections	12150 [R_{int} = 0.0678, R_{sigma} = 0.0898]
Data/restraints/parameters	12150/6/830
Goodness-of-fit on F^2	1.046
Final R indexes [I>=2σ (I)]	R_1 = 0.0832, wR_2 = 0.2348
Final R indexes [all data]	R_1 = 0.1165, wR_2 = 0.2566
Largest diff. peak/hole	3.25/-1.25 e $Å^{-3}$

Table S2. Crystal data and structure refinement for expanded helicene **4**.

DFT Calculations

Calculations were carried out using the QChem 4.4 software package[19] with the ωB97X-D functional[20] and the def2-svp basis set.[21] To save computational time, the compounds were truncated as follows. For compound **3c**, the four propyl groups were truncated to ethyl groups and the six peripheral (methoxy)methyl groups were removed. For compound **4**, the four propyl groups were truncated to ethyl groups.

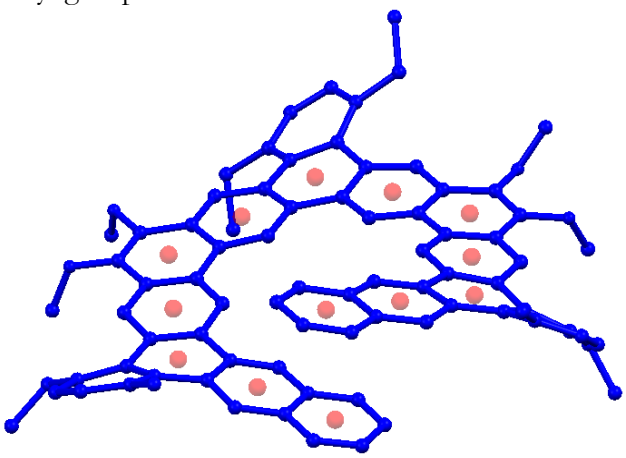

Figure S42. DFT-calculated structure of truncated **3c** (with centroids in red).

O	-2.264	1.121	6.922	C	-4.275	2.212	-4.401
O	0.396	0.477	7.296	C	4.448	2.045	5.907
O	6.890	-1.378	-1.767	C	-7.302	1.159	1.441
O	5.746	-1.107	-4.303	C	-7.606	2.006	3.692
C	-3.070	1.281	1.927	C	-8.115	1.427	2.538
C	-5.013	1.496	0.378	C	-7.967	0.530	0.237
C	-3.594	1.461	0.568	C	6.537	0.050	-4.493
C	0.729	0.271	4.911	C	7.441	-2.593	-2.236
C	-1.191	0.740	3.402	C	-2.492	2.472	7.250
C	4.498	-1.165	1.714	C	1.085	1.614	7.764
C	-1.754	0.890	2.131	H	-1.139	0.686	1.258
C	4.983	-1.106	-3.173	H	0.718	-1.228	-1.499
C	-0.827	-1.382	-7.604	H	-1.667	1.648	-0.369
C	1.342	-1.064	-2.373	H	0.571	-0.087	1.562
C	-5.915	1.431	1.555	H	-1.136	-1.206	-1.669
C	-2.015	0.978	4.522	H	-6.549	1.875	-1.082
C	1.559	-0.764	-4.765	H	3.605	-0.877	-5.462
C	0.943	-0.605	-6.100	H	-5.378	-1.335	-5.209
C	-1.448	0.888	5.857	H	1.546	-0.506	0.146
C	3.141	-0.791	1.549	H	-3.136	-1.138	-6.176
C	0.741	-0.976	-3.623	H	6.357	-1.389	0.617
C	0.189	0.331	3.607	H	-3.994	1.322	5.202

C	-0.131	0.568	6.044	H	-1.279	1.904	-2.790
C	-2.749	1.630	-0.515	H	-4.775	3.330	4.935
C	3.334	-1.011	-0.875	H	-5.597	2.155	5.953
C	-0.712	-1.135	-3.779	H	2.438	-0.165	6.093
C	2.724	-1.009	-2.192	H	2.950	1.192	-6.018
C	1.010	-0.051	2.552	H	3.812	0.213	-7.194
C	-3.515	-1.325	-4.087	H	-6.810	-1.596	-3.211
C	1.133	-0.243	-8.474	H	-3.337	-1.555	-0.658
C	3.547	-0.987	-3.338	H	-1.871	-2.741	-8.887
C	1.655	-0.050	-7.197	H	-2.948	-1.571	-8.121
C	-1.545	-1.241	-2.678	H	-2.303	-2.931	-7.175
C	-3.921	1.488	3.048	H	6.085	-3.341	1.658
C	-5.369	1.736	2.838	H	7.640	-2.529	1.728
C	-1.272	-1.190	-5.098	H	3.092	1.719	-9.047
C	-3.227	1.824	-1.826	H	2.019	2.603	-7.941
C	-5.485	1.744	-0.904	H	-2.199	2.226	-5.061
C	4.729	-1.186	-0.735	H	5.563	0.688	7.135
C	2.939	-0.332	3.998	H	3.875	0.289	7.052
C	2.946	-0.860	-4.599	H	-6.215	2.144	-3.491
C	-6.236	2.172	3.877	H	-5.785	-1.735	-0.934
C	-2.941	-1.376	-2.789	H	-7.638	3.582	6.038
C	5.110	-0.365	5.355	H	-6.930	4.700	4.849
C	-0.389	-1.081	-6.287	H	8.388	-4.014	3.588
C	-0.033	-0.971	-8.671	H	6.759	-4.717	3.706
C	4.382	-0.644	4.161	H	-4.671	2.356	-5.409
C	5.545	-1.240	-1.932	H	3.575	2.079	5.240
C	-4.932	-1.392	-4.213	H	5.315	2.414	5.339
C	2.591	-0.768	0.274	H	-7.277	-0.087	-0.351
C	-2.657	-1.219	-5.205	H	-8.406	1.278	-0.443
C	5.279	-1.275	0.554	H	-8.792	-0.113	0.576
C	-3.370	1.287	4.317	H	7.049	-0.067	-5.457
C	6.269	-1.998	3.324	H	7.284	0.164	-3.692
C	-2.358	1.962	-2.946	H	5.906	0.955	-4.529
C	-5.758	2.880	5.137	H	8.508	-2.580	-1.977
C	2.080	-0.076	5.074	H	7.327	-2.692	-3.327
C	2.898	0.815	-7.049	H	6.961	-3.456	-1.744
C	2.346	-0.395	2.710	H	-3.272	2.491	8.022
C	5.061	-1.286	3.077	H	-2.836	3.056	6.379
C	-4.633	1.887	-2.021	H	-1.584	2.950	7.652
C	6.887	-1.821	4.556	H	1.560	1.334	8.713
C	6.361	-0.954	5.506	H	0.400	2.458	7.946
C	-5.725	-1.537	-3.103	H	1.863	1.945	7.055

C	-3.786	-1.523	-1.654	H	1.660	0.153	-9.342
C	-2.056	-2.194	-7.952	H	-0.353	-1.202	-9.690
C	6.867	-3.007	2.354	H	7.820	-2.340	4.777
C	2.946	2.013	-7.998	H	6.935	-0.751	6.413
C	-2.871	2.142	-4.205	H	3.786	2.672	-7.730
C	4.717	0.634	6.435	H	-6.207	4.527	6.467
C	-5.134	2.094	-3.339	H	7.751	-4.982	2.253
C	-5.145	-1.613	-1.809	H	4.267	2.743	6.738
C	-6.691	3.979	5.645	H	-8.300	2.304	4.479
C	7.475	-4.242	3.019	H	-9.185	1.214	2.471

Final energy: -3384.53551730075

Table S3. Cartesian coordinates of calculated (truncated) **3c**.

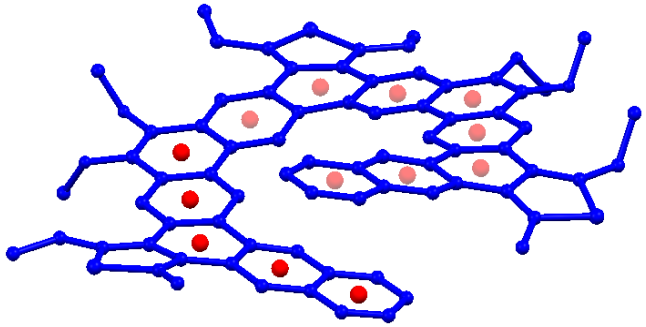

Figure S43. DFT-calculated structure of truncated **4** (with centroids in red).

Se	4.379	7.314	-1.879	C	0.057	-7.427	6.103
Se	1.479	-4.812	6.958	C	0.364	2.824	-5.799
Se	-5.719	-2.062	-6.194	C	-1.311	3.582	-1.873
O	-4.918	-5.402	-0.12	C	-3.149	-7.239	1.591
O	-3.467	-5.997	2.19	C	3.226	-2.904	8.635
O	4.747	1.157	5.358	C	-6.1	-5.362	0.655
O	5.435	3.239	3.638	C	-0.46	0.569	-5.473
C	-4.755	-0.53	-5.799	C	-7.251	-3.975	-3.291
C	3.046	5.017	-2.192	C	-4.533	0.463	-6.902
C	2.723	2.649	-0.576	C	6.774	2.787	3.696
C	3.175	0.304	3.748	C	4.356	2.128	6.31
C	3.636	3.653	-0.135	H	1.137	-0.501	1.178
C	0.051	-2.415	2.666	H	2.613	-1.321	7.319
C	2.133	2.697	-1.931	H	3.964	-2.278	6.715
C	-0.259	-3.574	3.431	H	-0.54	-1.167	1.04
C	1.59	-0.546	2.163	H	-1.666	-5.22	3.574
C	-3.617	-3.409	-0.461	H	-3.992	2.074	-5.272

C	3.843	4.85	-0.978	H	1.639	0.898	-0.029
C	2.567	0.399	2.477	H	0.039	-0.395	-3.624
C	2.27	3.881	-2.73	H	-3.048	4.335	-5.281
C	2.944	1.469	1.567	H	5.108	6.167	1.404
C	0.533	-3.845	4.648	H	6.293	5.229	0.5
C	1.172	-1.537	3.041	H	-1.685	6.07	-4.164
C	-2.082	2.565	-2.502	H	-1.787	1.12	-0.962
C	2.991	-2.352	7.231	H	-5.081	-3.841	-1.922
C	-2.949	0.271	-2.564	H	4.911	4.219	1.519
C	1.475	-2.84	5.145	H	5.946	8.286	0.34
C	1.824	-1.678	4.299	H	7.136	7.342	-0.595
C	-3.911	-4.592	0.317	H	-0.245	-6.546	4.165
C	-0.741	-2.089	1.575	H	-1.422	-6.046	5.377
C	-3.119	-1.049	-1.919	H	3.357	-0.785	5.548
C	-2.716	2.837	-3.742	H	-1.619	-0.676	-0.454
C	-1.804	-2.878	1.133	H	-5.202	-4.64	-3.621
C	-3.58	0.537	-3.824	H	-6.187	-4.579	-5.062
C	-1.344	-4.35	3.014	H	1.821	4.742	-4.65
C	-2.102	-4.043	1.871	H	1.397	0.676	-1.888
C	-2.589	-2.54	-0.042	H	-0.561	5.58	-1.983
C	3.901	2.421	1.976	H	-0.82	1.78	-7.244
C	-3.474	1.812	-4.355	H	2.556	7.969	-3.948
C	2.386	1.618	0.292	H	1.36	6.66	-3.922
C	-4.068	-1.991	-2.417	H	2.835	6.508	-4.908
C	0.135	0.503	-4.239	H	1.116	-7.693	5.959
C	-4.327	-0.548	-4.488	H	-0.101	-7.211	7.171
C	4.169	1.283	4.129	H	0.449	3.732	-6.402
C	-4.658	-1.77	-3.754	H	-0.818	3.364	-0.923
C	-2.562	4.126	-4.325	H	-3.751	-7.412	0.685
C	5.65	6.122	0.444	H	-3.372	-8.016	2.333
C	4.657	5.925	-0.674	H	-2.078	-7.286	1.329
C	-1.803	5.086	-3.704	H	2.288	-2.966	9.207
C	-2.242	1.282	-1.939	H	3.681	-3.907	8.608
C	-4.324	-3.12	-1.64	H	-6.824	-6.029	0.169
C	4.213	3.493	1.125	H	-6.517	-4.341	0.686
C	4.517	2.296	3.28	H	-5.915	-5.709	1.685
C	6.538	7.357	0.329	H	-1.036	-0.281	-5.847
C	0.437	-4.979	5.431	H	-7.098	-3.419	-2.354
C	-0.348	-6.249	5.221	H	-8.051	-3.464	-3.846
C	0.982	2.789	-4.518	H	-4.729	0.008	-7.884
C	2.811	-0.74	4.615	H	-3.492	0.821	-6.906
C	0.863	1.614	-3.73	H	-5.191	1.342	-6.816

C	-3.189	-4.895	1.438	H	7.096	2.383	2.721
C	-5.403	-2.683	-4.475	H	6.902	2.011	4.468
C	2.034	-3.139	6.373	H	7.395	3.656	3.947
C	-2.386	-1.371	-0.784	H	4.655	3.14	5.994
C	3.142	6.264	-2.771	H	4.861	1.874	7.251
C	-5.969	-4.035	-4.128	H	3.264	2.105	6.468
C	1.708	3.884	-3.997	H	7.233	7.405	1.179
C	1.466	1.604	-2.456	H	-0.55	-8.31	5.857
C	-1.17	4.812	-2.464	H	3.913	-2.25	9.19
C	-0.341	1.742	-6.262	H	-7.598	-4.987	-3.036
C	2.438	6.876	-3.948				

Final energy: -10356.4685141077

Table S4. Cartesian coordinates of calculated (truncated) **4**.

References for Supporting Information of Chapter 3

(1) Dutton, J. L.; Farrar, G. J.; Sgro, M. J.; Battista, T. L.; Ragogna, P. J. *Chem. – Eur. J.* **2009**, *15* (39), 10263.
(2) Nitschke, J. R.; Zürcher, S.; Tilley, T. D. *J. Am. Chem. Soc.* **2000**, *122* (42), 10345.
(3) Krasovskiy, A.; Knochel, P. *Angew. Chem. Int. Ed.* **2004**, *43* (25), 3333.
(4) O'Brien, C. J.; Kantchev, E. A. B.; Valente, C.; Hadei, N.; Chass, G. A.; Lough, A.; Hopkinson, A. C.; Organ, M. G. *Chem. – Eur. J.* **2006**, *12* (18), 4743.
(5) Herde, J. L.; Lambert, J. C.; Senoff, C. V.; Cushing, M. A. In *Inorganic Syntheses*; Parshall, G. W., Ed.; John Wiley & Sons, Inc., 1974; pp 18–20.
(6) Brandsma, L. *Best Synthetic Methods: Acetylenes, Allenes and Cumulenes*, 1st ed.; Elsevier Academic Press: Oxford, UK, 2003.
(7) Shirai, Y.; Osgood, A. J.; Zhao, Y.; Yao, Y.; Saudan, L.; Yang, H.; Yu-Hung, C.; Alemany, L. B.; Sasaki, T.; Morin, J.-F.; Guerrero, J. M.; Kelly, K. F.; Tour, J. M. *J. Am. Chem. Soc.* **2006**, *128* (14), 4854.
(8) Kiel, G. R.; Ziegler, M. S.; Tilley, T. D. *Angew. Chem. Int. Ed.* **2017**, *56* (17), 4839.
(9) Niimi, K.; Mori, H.; Miyazaki, E.; Osaka, I.; Kakizoe, H.; Takimiya, K.; Adachi, C. *Chem. Commun.* **2012**, *48* (47), 5892.
(10) Hoye, T. R.; Eklov, B. M.; Voloshin, M. *Org. Lett.* **2004**, *6* (15), 2567.
(11) Shao, J.; Zhao, X.; Wang, L.; Tang, Q.; Li, W.; Yu, H.; Tian, H.; Zhang, X.; Geng, Y.; Wang, F. *Tetrahedron Lett.* **2014**, *55* (41), 5663.
(12) Kezuka, S.; Tanaka, S.; Ohe, T.; Nakaya, Y.; Takeuchi, R. *J. Org. Chem.* **2006**, *71* (2), 543.
(13) Paruch, K.; Katz, T. J.; Incarvito, C.; Lam, K.-C.; Rhatigan, B.; Rheingold, A. L. *J. Org. Chem.* **2000**, *65* (22), 7602.
(14) Sheldrick, G. M. *Acta Crystallogr. A* **2008**, *64* (1), 112.
(15) Sheldrick, G. M. *Acta Crystallogr. Sect. Found. Adv.* **2015**, *71* (1), 3.
(16) Palatinus, L.; Chapuis, G. *J. Appl. Crystallogr.* **2007**, *40* (4), 786.
(17) Sheldrick, G. M. *Acta Crystallogr. Sect. C Struct. Chem.* **2015**, *71* (1), 3.
(18) Macrae, C. F.; Edgington, P. R.; McCabe, P.; Pidcock, E.; Shields, G. P.; Taylor, R.; Towler, M.; Streek, J. van de. *J. Appl. Crystallogr.* **2006**, *39* (3), 453.
(19) Shao, Y.; Gan, Z.; Epifanovsky, E.; Gilbert, A. T. B.; Wormit, M.; Kussmann, J.; Lange, A. W.; Behn, A.; Deng, J.; Feng, X.; Ghosh, D.; Goldey, M.; Horn, P. R.; Jacobson, L. D.; Kaliman, I.; Khaliullin, R. Z.; Kuś, T.; Landau, A.; Liu, J.; Proynov, E. I.; Rhee, Y. M.; Richard, R. M.; Rohrdanz, M. A.; Steele, R. P.; Sundstrom, E. J.; III, H. L. W.; Zimmerman, P. M.; Zuev, D.; Albrecht, B.; Alguire, E.; Austin, B.; Beran, G. J. O.; Bernard, Y. A.; Berquist, E.; Brandhorst, K.; Bravaya, K. B.; Brown, S. T.; Casanova, D.; Chang, C.-M.; Chen, Y.; Chien, S. H.; Closser, K. D.; Crittenden, D. L.; Diedenhofen, M.; Jr, R. A. D.; Do, H.; Dutoi, A. D.; Edgar, R. G.; Fatehi, S.; Fusti-Molnar, L.; Ghysels, A.; Golubeva-Zadorozhnaya, A.; Gomes, J.; Hanson-Heine, M. W. D.; Harbach, P. H. P.; Hauser, A. W.; Hohenstein, E. G.; Holden, Z. C.; Jagau, T.-C.; Ji, H.; Kaduk, B.; Khistyaev, K.; Kim, J.; Kim, J.; King, R. A.; Klunzinger, P.; Kosenkov, D.; Kowalczyk, T.; Krauter, C. M.; Lao, K. U.; Laurent, A. D.; Lawler, K. V.; Levchenko, S. V.; Lin, C. Y.; Liu, F.; Livshits, E.; Lochan, R. C.; Luenser, A.; Manohar, P.; Manzer, S. F.; Mao, S.-P.; Mardirossian, N.; Marenich, A. V.; Maurer, S. A.; Mayhall, N. J.; Neuscamman, E.; Oana, C. M.; Olivares-Amaya, R.; O'Neill, D. P.; Parkhill, J. A.; Perrine, T. M.; Peverati, R.; Prociuk, A.; Rehn, D. R.; Rosta, E.; Russ, N. J.; Sharada, S. M.; Sharma, S.; Small, D. W.; Sodt, A.; Stein, T.; Stück, D.; Su, Y.-C.; Thom, A. J. W.; Tsuchimochi, T.; Vanovschi, V.; Vogt, L.; Vydrov, O.;

Wang, T.; Watson, M. A.; Wenzel, J.; White, A.; Williams, C. F.; Yang, J.; Yeganeh, S.; Yost, S. R.; You, Z.-Q.; Zhang, I. Y.; Zhang, X.; Zhao, Y.; Brooks, B. R.; Chan, G. K. L.; Chipman, D. M.; Cramer, C. J.; III, W. A. G.; Gordon, M. S.; Hehre, W. J.; Klamt, A.; III, H. F. S.; Schmidt, M. W.; Sherrill, C. D.; Truhlar, D. G.; Warshel, A.; Xu, X.; Aspuru-Guzik, A.; Baer, R.; Bell, A. T.; Besley, N. A.; Chai, J.-D.; Dreuw, A.; Dunietz, B. D.; Furlani, T. R.; Gwaltney, S. R.; Hsu, C.-P.; Jung, Y.; Kong, J.; Lambrecht, D. S.; Liang, W.; Ochsenfeld, C.; Rassolov, V. A.; Slipchenko, L. V.; Subotnik, J. E.; Voorhis, T. V.; Herbert, J. M.; Krylov, A. I.; Gill, P. M. W.; Head-Gordon, M. *Mol. Phys.* **2015**, *113* (2), 184.

(20) Chai, J.-D.; Head-Gordon, M. *Phys. Chem. Chem. Phys.* **2008**, *10* (44), 6615.

(21) Schäfer, A.; Horn, H.; Ahlrichs, R. *J. Chem. Phys.* **1992**, *97* (4), 2571.

Chapter 4: A Site-Selective [2+2+2] Cycloaddition and its Orthogonality to Alkyne Metathesis: Rapid, General Synthesis of Macrocyclic Nanocarbons

A version of this chapter was submitted for publication on July 15, 2019: Kiel, G. R.; Tilley, T. D., *In Review*.

The recent surge of interest in molecular carbon nanoscience has been driven not only by the pursuit of atomic precision in larger nanostructures (e.g. graphene nanoribbons and carbon nanotubes),[1] but also by the extraordinary properties displayed by molecular nanocarbons themselves.[2] Macrocyclic nanocarbons represent a broad structural class of particular interest for their internal cavities and unique spatial arrangements of carbon-rich building blocks.[3–7] Such structures enable host-guest chemistry,[4g,5c,6a-d,7c,8] intramolecular through-space interactions,[7d] and electronic delocalization.[4c-d,5d] They also act as templates for growth of more complex functional materials *via* non-covalent[4e,6a-e,7e] and covalent[4f,6f] assembly. Among the many nanocarbon structures of this type, arylene ethynylene macrocycles (AEMs) stand out due to their remarkable shape-persistence, which reinforces their cavity and increases their tendency to assemble into more complex functional materials.[6,7b]

Polycyclic aromatic hydrocarbons (PAHs) are intriguing building blocks for more complex AEMs due to their structural diversity, rigidity, exceptional photophysical and electronic properties, and their ability to assemble into higher-order structures *via* π-stacking interactions.[9] PAHs comprise a vast chemical space that can be harnessed to significantly increase the number of conceivable AEM geometries and substitution patterns. However, despite their great promise, PAH-containing AEMs have remained a synthetic curiosity due to their difficult synthesis, which involves two challenging steps: 1) synthesis of an appropriately functionalized PAH precursor and 2) macrocyclization. Alkyne metathesis is useful for the latter since it provides thermodynamic products and thus high yields and scalability.[10] This is nicely demonstrated by the syntheses of AEMs from carbazole[10c] (Figure 1a) and phenanthrene,[9j] the smallest PAHs. Critically, these syntheses were only possible due to the availability of functionalized carbazole and phenanthrene precursors. Indeed, the bottleneck for more extensive investigations of these hybrid nanocarbons is the difficulty associated with synthesis of more complex PAH precursors.

The construction of PAHs is challenging as it requires regioselective fusion of many rings. Challenges are especially great when incorporation of a specific, reactive functionality such as an alkynyl group is desired. Thus, considerable effort has been devoted to PAH synthesis, especially with organometallic methods,[11] and metal-mediated [2+2+2] cycloadditions of alkynes have proven particularly valuable due to their efficacy in the formation of aromatic rings.[12,13] In the course of recent efforts in this area,[14] we discovered remarkably efficient cycloadditions involving biaryl-tethered diynes. The high selectivity associated with this reaction suggested that it might be site-selective,[15] which would enable its use in orthogonal reaction schemes. For example, a "diyne-selective" [2+2+2] cycloaddition that preserves peripheral alkynyl groups, as shown in the transformation of **1** to **2** in Figure 1b, would provide alkynylated PAHs in a single step from easily assembled, non-PAH precursors.

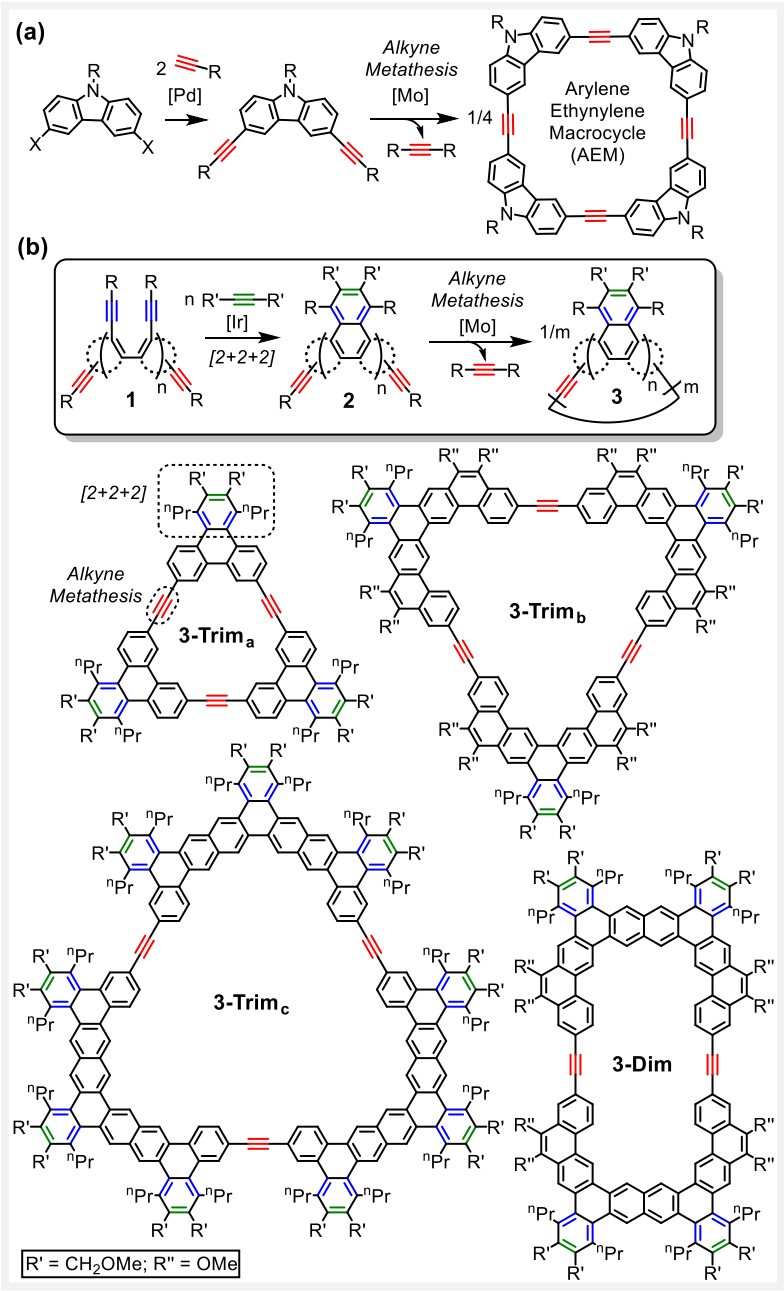

Figure 1. (a) Scalable, High-Yielding Synthesis of an AEM via Alkyne Metathesis **(b)** Orthogonal Application of Site-Selective [2+2+2] and Alkyne Metathesis Reactions for Synthesis of Large AEMs (This Work).

Here we demonstrate a general strategy for access to large, PAH-containing AEMs (**3,** Figure 1b) by the sequential, orthogonal application of [2+2+2] cycloaddition and alkyne metathesis reactions. Development of this strategy was enabled by the discovery that *substrates of general structure **1** undergo n-fold, "diyne-selective" [2+2+2] reactions to afford alkynylated PAHs **2** in a high-yielding, scalable fashion*. With the right substitution pattern, these PAHs are excellent substrates for macrocyclization *via* alkyne metathesis, as demonstrated by syntheses of AEMs **3-Dim**, **3-Trim$_a$**, **3-Trim$_b$**, and **3-Trim$_c$**, three of which are based on unknown PAH ring systems. The two-step strategy is scalable and provides

streamlined access to large AEMs from easily assembled precursors. The new AEMs possess a range of cavity sizes and shapes and retain the basic photophysical properties of their PAH precursors.

The sequential [2+2+2]/metathesis strategy was first investigated on the model triphenylene system shown in Scheme 1. Precursors **1a** and **1b** were synthesized by a Cu-mediated oxidative homocoupling of **4a** and **4b**, which was enabled by a highly selective desymmetrization of **4a** and **4b** *via* Li/Br exchange. The "Br-free" **1c** was subsequently synthesized by protodebromination of **1b** *via* Li/Br exchange followed by protic workup.

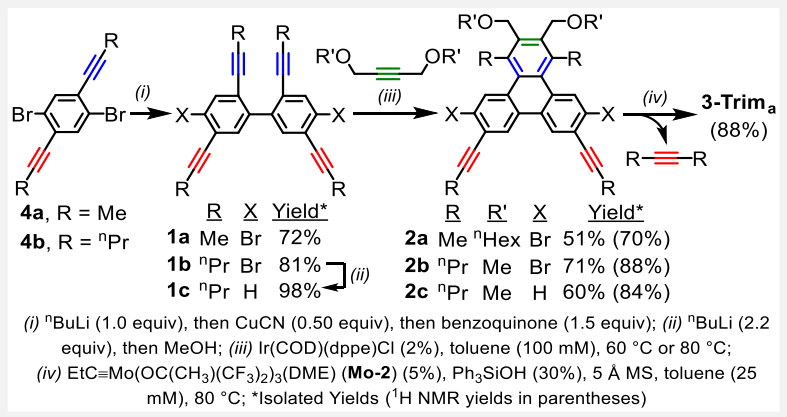

Scheme 1. Model System: Synthesis of Alkynylated Triphenylenes **2a–2c** and AEM **3-Trim$_a$**.

The [2+2+2] pre-catalyst Ir(COD)(dppe)Cl, which can either be isolated or generated *in situ* (see SI for details), proved to be highly effective for the synthesis of alkynylated triphenylenes **2a**–**2c**. Essentially no modification of the previously-developed conditions[14b,16] was required. These results reveal that bulkier pentynyl groups give higher yields than propynyl groups (70% and 88% for **2a** and **2b**, respectively, by ^{1}H NMR spectroscopy). In addition, the absence of the Br substituent in **2c** resulted in a slightly lower yield compared to **2b** (84% vs. 88%). The relatively low isolated yields (compared to those determined by ^{1}H NMR spectroscopy) result from unidentified side products that are difficult to separate. Importantly, this difficulty did not extend to the other examples given below. The remarkable preservation of the peripheral alkynyl groups in **2a**–**2c** was verified by ^{1}H NMR (one propargylic methylene triplet), ^{13}C NMR (two quaternary alkynyl resonances), and high-resolution mass spectrometry. Notably, the solubilizing groups on the PAH can be easily modified in the final step by use of a different monoyne reaction partner (e.g. 1,4-di(hexyloxy)butyne and 1,4-di(methoxy)butyne were used for **2a** and **2b**, respectively), which should prove invaluable for future applications.

For the macrocyclization step, the Fürstner-type catalyst[17] "EtC≡Mo(OSiPh$_3$)$_3$" (**Mo-1**) was employed. In analogy to the approach taken by Moore,[18] we found that **Mo-1** can be conveniently generated *in situ* by treatment of easily-prepared EtC≡Mo(OC(CH$_3$)(CF$_3$)$_2$)$_3$(DME) (**Mo-2**)[19] with 6 equiv of Ph$_3$SiOH (see SI for details on this ligand exchange). Triphenylene ethynylene macrocycle **3-Trim$_a$** was isolated in excellent yield (88%) after treatment of **2c** with a 5% loading of **Mo-1** in the presence of 5 Å molecular sieves[17] (16 h at 80 °C in toluene). The identity of **3-Trim$_a$** was unambiguously determined by ^{1}H and ^{13}C NMR (the former showed the absence of propargylic methylene resonances

and the latter showed only one quaternary alkynyl resonance) and MALDI-TOF. As is often the case for alkyne metathesis macrocyclizations,[10d] minimal purification was required (elution of the reaction mixture through a plug of silica gel followed by precipitation with MeOH), and high dilution was not necessary. The 5 Å MS were added to sequester 4-octyne and drive the reaction to completion. Notably, to our knowledge, this appears to be the first time that 5 Å MS have been used to sequester an alkyne larger than 2-butyne in a metathesis application. Attempts at the macrocyclization of Br-substituted **2a** and **2b** yielded complex mixtures that contained only small amounts of macrocycle, even at higher (20%) catalyst loading.

The Ir-catalyzed [2+2+2] reaction proved to be a general means to access alkynylated PAHs, as demonstrated by the isolation of **2d–2l** (Scheme 2). Precursors **1d–1l** were synthesized in a modular fashion *via* standard C-C bond-forming reactions (see SI). From the same benzene, naphthalene, and phenanthrene building blocks, a range of different shapes, sizes, and alkynyl group substitution patterns were obtained *via* onefold, twofold, or threefold cycloadditions. The nature of the building blocks does not play a large role in the yields for this series of compounds. This can be seen by the comparable yields for **2d** (89%), **2e** (80%), and **2f** (85%), which were derived from a onefold cycloaddition of a biphenyl (**1d**), binaphthalene (**1e**), and biphenanthrene (**1f**) precursor, respectively. Interestingly, the generally good-to-excellent yields do not appear to be correlated with the number of required cycloadditions. For example, a

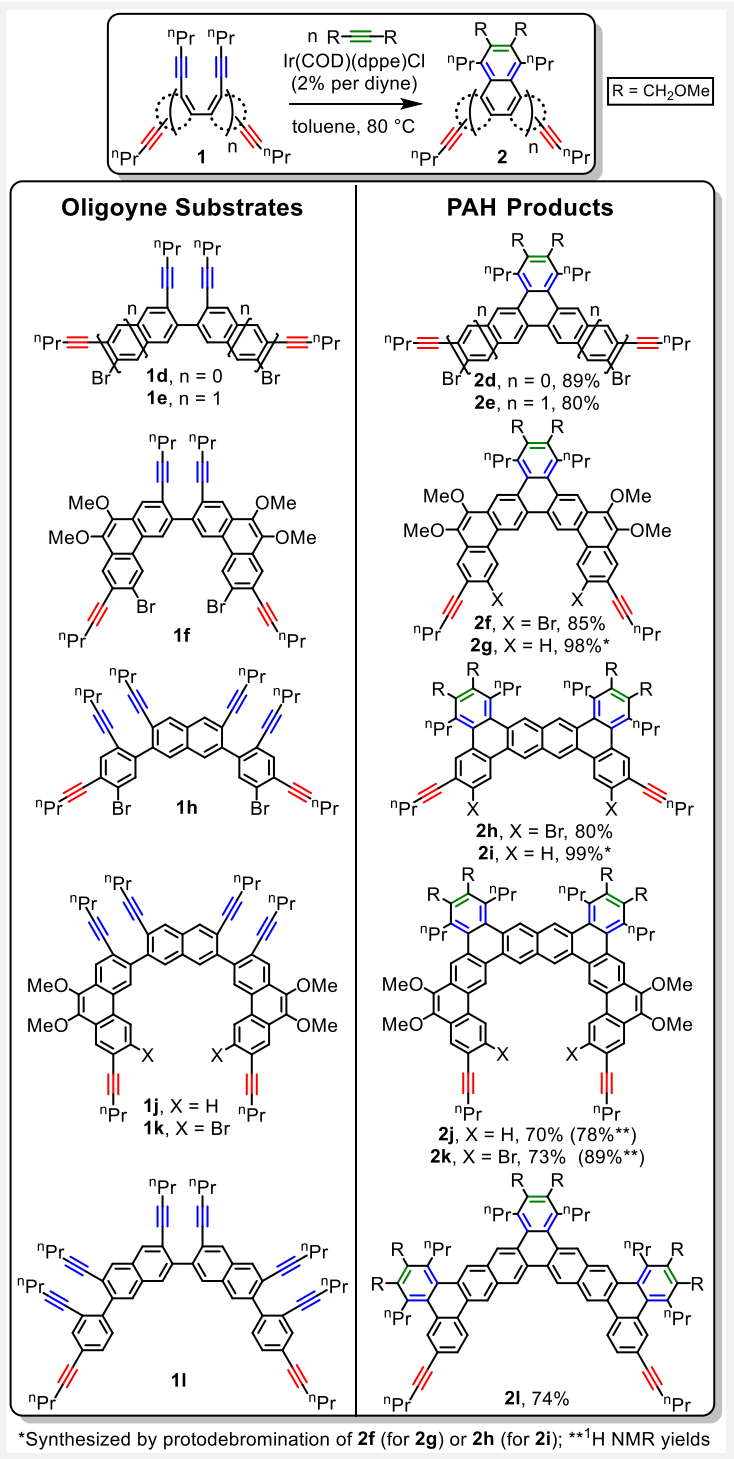

Scheme 2. Generalization of the "Diyne-Selective" [2+2+2] Reaction: Synthesis of Alkynylated PAHs **2d–l.**

twofold cycloaddition produced **2j** in 70% yield, whereas a threefold cycloaddition produced **2l** in 74% yield. As observed in the model system, the presence of Br substituents ortho to the alkynyl groups again resulted in a higher yield (78% for **2j** vs. 89% for **2k**, by ^{1}H NMR). Perhaps most importantly, since high dilution is not necessary (diyne concentration = 100 mM), the new strategy is highly scalable. For example, **2e**, **2f**, and **2h** were isolated on a 2.0, 3.4, and 1.3 gram scale, respectively.

The majority of **2d**–**2l** were designed with the subsequent macrocyclization in mind (see below), but this strategy is not limited to such applications (e.g. metathesis on **2d** or **2e** would give PAH-containing poly(arylene-ethnynylene)s[20] due to the linear disposition of the alkynyl groups). The substitution patterns of the new PAHs would be difficult or impossible to access using previous synthetic technology, even for the deceptively simple triphenylene systems **2a**–**d**. Represented among these examples are the first known tribenzo[a,h,o]pentaphene (**2f** and **2g**), tribenzo[a,h,o]phenanthro[2,3-q]hexaphene (**2j** and **2k**), and pentabenzo[a,c,j,q,s]heptaphene (**2l**) ring systems.

The angular disposition of the alkynyl groups in PAHs **2f**–**2l** makes them attractive for macrocyclization *via* alkyne metathesis. Since the presence of bulky Br substituents appears to inhibit macrocyclization with **Mo-1** as catalyst (see above), attention was focused on "Br-free" **2g**, **2i**, **2j**, and **2l**. Due to the larger sizes of these PAHs, the solvent was switched to *o*-dichlorobenzene (*o*-DCB) to limit the possibility of kinetic traps *via* precipitation of oligomeric or polymeric intermediates. Subjection of **2j**, **2g**, and **2l** to the slightly modified metathesis conditions (Scheme 3) afforded the elliptical macrocycle **3-Dim** and large, triangular macrocycles **3-Trim$_b$** and **3-Trim$_c$** in good to excellent isolated yields. While the yield of the largest of these macrocycles (**3-Trim$_c$**) did improve on dilution (from 43% at 25 mM to 74% at 9 mM), this is still quite concentrated for a macrocyclization reaction. Since no well-defined side products were observed in any case, purification was again streamlined. Unfortunately, subjection of **2i** to the conditions of Scheme 3 produced an intractable mixture composed primarily (~95% by mass) of insoluble material that could not be characterized. It is important to note that, except for the modest dilution in the case of **3-Trim$_c$**, we have not attempted to modify any parameter in these reactions.

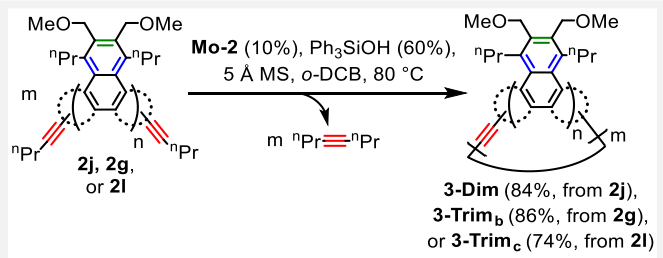

Scheme 3. Generalization of the Alkyne Metathesis Macrocyclization: Synthesis of AEMs **3-Dim, 3-Trim$_b$, and 3-Trim$_c$.**

In general, the new PAHs (**2**) and AEMs (**3**) are highly soluble in chlorinated solvents (>100 mg/mL) and insoluble in saturated hydrocarbons (e.g. hexanes) and more polar solvents (e.g. acetone and EtOH). The exception is **3-Dim**, which is only moderately soluble in chloroform (15–20 mg/mL). The ^{1}H NMR chemical shifts in chloroform-*d* of all except **3-Dim** and **3-Trim$_b$** are independent of concentration (see Figures S67–74), which suggests that the high solubility results from limited aggregation *via* π-stacking. This is likely a result of the alkyl groups in the bay positions, which induce

non-planarity. In contrast, despite this alkyl group substitution, the ^{1}H NMR spectra of **3-Dim** and **3-Trim$_b$** in chloroform-*d* solution exhibit significantly broadened aromatic resonances with chemical shifts that depend upon concentration, which suggests aggregation *via* π-stacking. Unfortunately, attempts to grow X-ray quality crystals of the aggregating AEMs were unsuccessful.

The UV/Vis absorption and emission spectra of AEMs (**3**) and their monomeric precursors (**2**) display the typical features of large, highly benzenoid PAH systems,[21] including high molar absorptivities (up to 5.0 x 10^5 $M^{-1}cm^{-1}$, for **3-Trim$_c$**), relatively large optical HOMO-LUMO gaps (between 2.8 to 3.3 eV), and fluorescence (see Table S1 and Figures S75–78). Despite the large increases in the sizes of the π-systems as a result of macrocyclization of **2** to form **3**, the expected red shifts in absorption maxima range from small (21 nm for **3-Dim**) to modest (54 nm for **3-Trim$_a$**). More strikingly, very small decreases in optical HOMO-LUMO gap (≤ 0.15 eV) and emission maxima (≤ 12 nm) are observed. Thus, to a large extent, the new PAH-containing AEMs retain the properties of their PAH precursors.

In conclusion, the orthogonal [2+2+2]/metathesis strategy was exploited to synthesize four structurally complex AEMs, but it is expected to be much more general due to the modularity of the precursor synthesis. Several opportunities are available for the introduction of structural and functional diversity, which might be systematically exploited to perturb self-assembly, photophysical, or electronic properties of a specific AEM, or to access entirely new AEMs. Alkynylated PAHs are also of interest in their own right due to the influence of the alkynyl group on properties (e.g. solid-state packing[22] and photophysics[23]). Perhaps most importantly, PAHs **2a**–**2l** are valuable synthons for a range of other interesting conjugated carbon nanostructures, which is the focus of ongoing work in our laboratory.

References for Main Text of Chapter 4

(1) (a) Müllen, K. In *Hierarchical Macromolecular Structures: 60 Years after the Staudinger Nobel Prize II*; Percec, V., Ed.; Advances in Polymer Science; Springer International Publishing, 2013; pp 61–92. (b) Segawa, Y.; Ito, H.; Itami, K. *Nat. Rev. Mater.* **2016**, *1* (1), 15002.

(2) (a) *Carbon-Rich Compounds: From Molecules to Materials*; Haley, M. M., Tykwinski, R. R., Eds.; Wiley-VCH Verlag GmbH & Co. KGaA: Weinheim, Germany, 2006. (b) Wu, J.; Pisula, W.; Müllen, K. *Chem. Rev.* **2007**, *107* (3), 718–747. (c) *Polycyclic Arenes and Heteroarenes: Synthesis, Properties, and Applications*; Miao, Q., Ed.; Wiley-VCH Verlag GmbH & Co. KGaA: Weinheim, Germany, 2015.

(3) General review: Iyoda, M.; Yamakawa, J.; Rahman, M. J. *Angew. Chem. Int. Ed.* **2011**, *50* (45), 10522–10553.

(4) Carbon Nanohoops: (a) Golder, M. R.; Jasti, R. *Acc. Chem. Res.* **2015**, *48* (3), 557–566. (b) Segawa, Y.; Yagi, A.; Matsui, K.; Itami, K. *Angew. Chem. Int. Ed.* **2016**, *55* (17), 5136–5158. (c) Kayahara, E.; Kouyama, T.; Kato, T.; Takaya, H.; Yasuda, N.; Yamago, S. *Angew. Chem. Int. Ed.* **2013**, *52* (51), 13722–13726. (d) Sprafke, J. K.; Kondratuk, D. V.; Wykes, M.; Thompson, A. L.; Hoffmann, M.; Drevinskas, R.; Chen, W.-H.; Yong, C. K.; Kärnbratt, J.; Bullock, J. E.; Malfois, M; Wasielewski, M. R.; Albinsson, B.; Herz, L. M.; Zigmantas, D.; Beljonne, D.; Anderson, H. L. *J. Am. Chem. Soc.* **2011**, *133* (43), 17262–17273. (e) Leonhardt, E. J.; Van Raden, J. M.; Miller, D.; Zakharov, L. N.; Alemán, B.; Jasti, R. *Nano Lett.* **2018**, *18* (12), 7991–7997. (f) Omachi, H.; Nakayama, T.; Takahashi, E.; Segawa, Y.; Itami, K. *Nat. Chem.* **2013**, *5* (7), 572–576. (g) Xu, Y.; Delius, M. von. *Angew. Chem. Int. Ed.* **2019**.

(5) Cycloarenes and related: (a) Miyoshi, H.; Nobusue, S.; Shimizu, A.; Tobe, Y. *Chem. Soc. Rev.* **2015**, *44*, 6560–6577. (b) Buttrick, J. C.; King, B. T. *Chem. Soc. Rev.* **2017**, *46*, 7–20. (c) Gregolińska, H.; Majewski, M.; Chmielewski, P. J.; Gregoliński, J.; Chien, A.; Zhou, J.; Wu, Y.-L.; Bae, Y. J.; Wasielewski, M. R.; Zimmerman, P. M.; Stępień, M. *J. Am. Chem. Soc.* **2018**, *140* (43), 14474–14480. (d) Liu, C.; Sandoval-Salinas, M. E.; Hong, Y.; Gopalakrishna, T. Y.; Phan, H.; Aratani, N.; Herng, T. S.; Ding, J.; Yamada, H.; Kim, D.; Casanova, D.; Wu, J. *Chem* **2018**, *4* (7), 1586–1595.

(6) Arylene ethynylene macrocycles: (a) Zhao, D.; Moore, J. S. *Chem. Commun.* **2003**, 807–818. (b) Höger, S. *Chem. – Eur. J.* **2004**, *10* (6), 1320–1329. (c) Sadowy, A. L.; Tykwinski, R. R. In *Modern Supramolecular Chemistry: Strategies for Macrocycle Synthesis*; Wiley-VCH Verlag GmbH & Co. KGaA: Weinheim, Germany, 2008; pp 185–231. (d) Smith, M. K.; Miljanić, O. Š. *Org. Biomol. Chem.* **2015**, *13* (29), 7841–7845. (e) Zang, L.; Che, Y.; Moore, J. S. *Acc. Chem. Res.* **2008**, *41* (12), 1596–1608. (f) Boese, R.; Matzger, A. J.; Vollhardt, K. P. C. *J. Am. Chem. Soc.* **1997**, *119* (8), 2052–2053.

(7) Other cyclophanes and cycloarylenes: (a) Ghasemabadi, P. G.; Yao, T.; Bodwell, G. J. *Chem. Soc. Rev.* **2015**, *44*, 6494–6518. (b) Iyoda, M.; Shimizu, H. *Chem. Soc. Rev.* **2015**, *44* (18), 6411–6424. (c) Lee, S.; Chen, C.-H.; Flood, A. H. *Nat. Chem.* **2013**, *5* (8), 704–710. (d) Schneebeli, S. T.; Frasconi, M.; Liu, Z.; Wu, Y.; Gardner, D. M.; Strutt, N. L.; Cheng, C.; Carmieli, R.; Wasielewski, M. R.; Stoddart, J. F. *Angew. Chem. Int. Ed.* **2013**, *52* (49), 13100–13104. (e) Liu, Z.; Liu, G.; Wu, Y.; Cao, D.; Sun, J.; Schneebeli, S. T.; Nassar, M. S.; Mirkin, C. A.; Stoddart, J. F. *J Am Chem Soc* **2014**, *136* (42), 16651–16660. (f) Ball, M.; Zhong, Y.; Fowler, B.; Zhang, B.; Li, P.; Etkin, G.; Paley, D. W.; Decatur, J.; Dalsania, A. K.; Li, H.; Li, H.; Xiao, S.; Ng, F.; Steigerwald, M. L.; Nuckolls, C. *J. Am. Chem. Soc.* **2016**, *138* (39), 12861–12867.

(8) Toyota, S.; Tsurumaki, E. *Chem. – Eur. J.* **2019**, *25* (28), 6878–6890.

(9) (a) Höger, S.; Cheng, X. H.; Ramminger, A.-D.; Enkelmann, V.; Rapp, A.; Mondeshki, M.; Schnell, I. *Angew. Chem. Int. Ed.* **2005**, *44* (18), 2801–2805. (b) Liu, W.-J.; Zhou, Y.; Zhou, Q.-F.; Ma, Y.; Pei, J. *Org. Lett.* **2008**, *10* (11), 2123–2126. (c) Chan, J. M. W.; Tischler, J. R.; Kooi, S. E.; Bulović, V.; Swager, T. M. *J. Am. Chem. Soc.* **2009**, *131* (15), 5659–5666. (d) Zhang, L.; Gopee, H.; Hughes, D. L.; Cammidge, A. N. *Chem. Commun.* **2010**, *46*, 4255–4257. (e) Chen, T.; Pan, G.-B.; Wettach, H.; Fritzsche, M.; Höger, S.; Wan, L.-J.; Yang, H.-B.; Northrop, B. H.; Stang, P. J. *J. Am. Chem. Soc.* **2010**, *132* (4), 1328–1333. (f) Finke, A. D.; Gross, D. E.; Han, A.; Moore, J. S. *J. Am. Chem. Soc.* **2011**, *133* (35), 14063–14070. (g) Venkataramana, G.; Dongare, P.; Dawe, L. N.; Thompson, D. W.; Zhao, Y.; Bodwell, G. J. *Org. Lett.* **2011**, *13* (9), 2240–2243. (h) Toyota, S. *Pure Appl. Chem.* **2012**, *84* (4), 917–929. (i) He, Z.; Xu, X.; Zheng, X.; Ming, T.; Miao, Q. *Chem. Sci.* **2013**, *4* (12), 4525–4531. (j) Yang, H.; Du, Y.; Wan, S.; Trahan, G. D.; Jin, Y.; Zhang, W. *Chem. Sci.* **2015**, *6* (7), 4049–4053. (k) Takaki, Y.; Ozawa, R.; Kajitani, T.; Fukushima, T.; Mitsui, M.; Kobayashi, K. *Chem. – Eur. J.* **2016**, *22* (47), 16760–16764.

(10) (a) Ge, P.-H.; Fu, W.; Herrmann, W. A.; Herdtweck, E.; Campana, C.; Adams, R. D.; Bunz, U. H. F. *Angew. Chem. Int. Ed.* **2000**, *39* (20), 3607–3610. (b) Miljanić, O. Š.; Vollhardt, K. P. C.; Whitener, G. D. *Synlett* **2003**, No. 1, 29–34. (c) Zhang, W.; Moore, J. S. *J. Am. Chem. Soc.* **2004**, *126* (40), 12796–12796. (d) Yu, C.; Jin, Y.; Zhang, W. In *Dynamic Covalent Chemistry*; John Wiley & Sons, Ltd, 2017; pp 121–163.

(11) Jin, T.; Zhao, J.; Asao, N.; Yamamoto, Y. *Chem. – Eur. J.* **2014**, *20* (13), 3554–3576.

(12) General [2+2+2] reviews: (a) Vollhardt, K. P. C. *Angew. Chem. Int. Ed. Engl.* **1984**, *23* (8), 539–556; (b) *Transition-Metal-Mediated Aromatic Ring Construction*; Tanaka, K., Ed.; John Wiley & Sons, Inc.: Hoboken, NJ, 2013; pp 1−320.

(13) Selected PAH applications: (a) Han, S.; Bond, A. D.; Disch, R. L.; Holmes, D.; Schulman, J. M.; Teat, S. J.; Vollhardt, K. P. C.; Whitener, G. D. *Angew. Chem. Int. Ed.* **2002**, *41* (17), 3223–3227. (b) Teplý, F.; Stará, I. G.; Starý, I.; Kollárovič, A.; Šaman, D.; Rulíšek, L.; Fiedler, P. *J. Am. Chem. Soc.* **2002**, *124* (31), 9175–9180. (c) Wu, Y.-T.; Hayama, T.; Baldridge, K. K.; Linden, A.; Siegel, J. S. *J. Am. Chem. Soc.* **2006**, *128* (21), 6870–6884. (d) Pérez, D.; Peña, D.; Guitián, E. *Eur. J. Org. Chem.* **2013**, *2013* (27), 5981–6013. (e) Takahashi, T.; Kitamura, M.; Shen, B.; Nakajima, K. *J. Am. Chem. Soc.* **2000**, *122* (51), 12876–12877. (f) Sawada, Y.; Furumi, S.; Takai, A.; Takeuchi, M.; Noguchi, K.; Tanaka, K. *J. Am. Chem. Soc.* **2012**, *134* (9), 4080–4083.

(14) (a) Kiel, G. R.; Ziegler, M. S.; Tilley, T. D. *Angew. Chem. Int. Ed.* **2017**, *56* (17), 4839–4844. (b) Kiel, G. R.; Patel, S. C.; Smith, P. W.; Levine, D. S.; Tilley, T. D. *J. Am. Chem. Soc.* **2017**, *139* (51), 18456–18459. (c) Kiel, G. R.; Samkian, A. E.; Nicolay, A.; Witzke, R. J.; Tilley, T. D. *J. Am. Chem. Soc.* **2018**, *140* (7), 2450–2454.

(15) Huang, Z.; Dong, G. *Acc. Chem. Res.* **2017**, *50* (3), 465–471.

(16) Kezuka, S.; Tanaka, S.; Ohe, T.; Nakaya, Y.; Takeuchi, R. *J. Org. Chem.* **2006**, *71* (2), 543–552.

(17) Heppekausen, J.; Stade, R.; Goddard, R.; Fürstner, A. *J. Am. Chem. Soc.* **2010**, *132* (32), 11045–11057.

(18) Lee, S.; Yang, A.; Moneypenny, T. P.; Moore, J. S. *J. Am. Chem. Soc.* **2016**, *138* (7), 2182–2185.

(19) Gdula, R. L.; Johnson, M. J. A. *J. Am. Chem. Soc.* **2006**, *128* (30), 9614–9615.

(20) *Poly(Arylene Ethynylene)s: From Synthesis to Application*; Weder, C., Ed.; Advances in Polymer Science; Springer-Verlag: Berlin Heidelberg, 2005.

(21) Rieger, R.; Müllen, K. *J. Phys. Org. Chem.* **2010**, *23* (4), 315–325.

(22) Anthony, J. E.; Brooks, J. S.; Eaton, D. L.; Parkin, S. R. *J. Am. Chem. Soc.* **2001**, *123* (38), 9482–9483.

(23) Hanhela, P. J.; Paul, D. B. *Aust. J. Chem.* **1984**, *37* (3), 553–559.

Supporting Information for Chapter 4

General Details

Unless otherwise stated, all manipulations of organometallic compounds were carried out in dry solvents under an atmosphere of nitrogen, using either standard Schlenk techniques or a glovebox. Pentane, toluene, tetrahydrofuran (THF), diethyl ether, and CH_2Cl_2 were dried using a JC Meyers Phoenix SDS solvent purification system. Benzene was dried using a Vacuum Atmosphere solvent purification system. 1,2-Dichlorobenzene was distilled from CaH_2 at atmospheric pressure. Benzene-d_6 was freed from oxygen using three free-pump-thaw cycles and then dried for at least 48 h over 3 Å molecular sieves (5% by mass). All reaction solvents were stored over 3 Å molecular sieves. $[Ir(COD)Cl]_2$ was either purchased from Strem chemical or prepared according to the literature.[1] 2,5-Dibromo-1,4-diiodobenzene (**S1**),[2] 2,4-dibromo-1,5-diiodobenzene (**S2**),[3] 3,6-dibromo-2,7-diiodo-9,10-dimethoxyphenanthrene (**S4**),[4] 3,6-dibromo-2,7-bis(pent-1-ynyl)-9,10-dimethoxyphenanthrene (**S7**),[4] EtC≡Mo(OC(CH_3)(CF_3)$_2$)$_3$(DME) (**Mo-2**),[5] $PdCl_2$(IPr)(3-chloropyridine),[6] ^{i}PrMgCl·LiCl,[7] Ir(COD)(dppe)Cl,[8] 1,4-bis(hexyloxy)but-2-yne,[9] 1,4-dimethoxy-2-butyne,[10] and 1,4-dibromo-2,5-di(prop-1-ynyl)benzene (**4a**)[11] were prepared by literature procedures or slight modifications thereof. Solutions of $ZnCl_2$ and CuCN·2LiCl in THF were prepared as follows. The precisely weighed masses of anhydrous salts were stirred in an approximate amount of THF until a homogeneous solution was obtained. For accurate determination of molarity, the solution was then quantitatively transferred to a graduated cylinder with the aid of additional THF. These solutions were stored over 3 Å molecular sieves (5% by mass) in a Teflon-stoppered flask. ^{n}BuLi and ^{i}PrMgCl·LiCl were titrated by ^{1}H NMR spectroscopy immediately prior to use.[12] 1,4-Benzoquinone was purified by sublimation. All other reagents and solvents were purchased from commercial suppliers and used as received. "Room temperature", "RT", or "ambient temperature" refers to ~22 °C. Reaction temperatures represent the oil bath temperature (with a fully submersed solution) unless otherwise stated. Mass spectrometry was performed by the QB3/Chemistry Mass Spectrometry Facility at UC Berkeley (for EI and ESI spectra) and the Mass Spectrometry Facility at UC Riverside (for MALDI spectra). For MALDI, α-cyano-4-hydroxycinnamic acid was used as the matrix. Unless otherwise noted, NMR spectra were acquired at ambient temperature (~22 °C) using Bruker AV-600, AV-500, DRX-500, AV-400, and AV-300 spectrometers. Chemical shifts (δ) are given in ppm and referenced to residual solvent peaks for ^{1}H NMR spectra (δ = 7.26 ppm for chloroform-*d* and δ = 7.16 for benzene-d_6) and for ^{13}C{^{1}H} NMR spectra (δ = 77.16 ppm for chloroform-*d* and δ = 128.06 for benzene-d_6). For ^{19}F NMR spectra, chemical shifts are referenced to a 1,3,5-tris(trifluoromethyl)benzene internal standard (δ = –63.17 ppm[13] in benzene-d_6) and are reported relative to $CFCl_3$ at 0.00 ppm. ^{1}H NMR yields were determined using 1,3,5-trimethoxybenzene as internal standard. For greatest accuracy, yields were typically measured by acquisition of ^{1}H NMR spectra both before and after the reaction of interest, then comparison of the amounts of starting material and desired product relative to the amount of added internal standard.

General Notes on Purification and Product Isolation

Chromatography: Column chromatography was carried out using Fischer Chemical 40–63μm, 230–400 mesh silica gel. Preparatory thin layer chromatography (prep TLC) was carried out using Analtech Silica Gel GF UNIPLATES (1000 μm, 20 x 20 cm). For prep TLC, in a typical procedure, 35–50 mg of material was loaded onto one side of the plate and the solvent front was allowed to elute halfway up (i.e. 70–100 mg was separated per plate). *Isolation of solids via rotary evaporation*: For most of the new

oligoyne precursors (**1**), PAHs (**2**), and AEMs (**3**), the concentration of their solutions in "good" solvents (e.g. CH_2Cl_2) typically furnished a glassy, yellow/orange residue. For isolation of these compounds in powder form, co-evaporation with a poor solvent (usually hexanes) was necessary. Typically, the solution (e.g. the combined fractions from column chromatography) was concentrated *via* rotary evaporation in a round-bottomed flask, then the residue was transferred to a 20 mL vial with the minimal amount of CH_2Cl_2. The CH_2Cl_2 solution was then co-evaporated with hexanes *via* rotary evaporation, and residual solvents were removed under high vacuum to give the desired powder. *Isolation of fine powders via filtration*: Several procedures below involve the precipitation of the desired product with an anti-solvent (e.g. MeOH). This often produced a very fine solid, which made filtration difficult. In these cases, filtration was greatly aided by celite, which was then extracted with CH_2Cl_2 for recovery of product. See above for important notes regarding rotary evaporation of CH_2Cl_2 solutions.

Comments About the $[Ir(COD)Cl]_2$ / dppe Catalyst System

The reaction of 1 equiv of $[Ir(COD)Cl]_2$ with 2 equiv of dppe (in toluene or benzene*) gives the [2+2+2] pre-catalyst Ir(COD)(dppe)Cl. If dppe is present in excess, an orange/red precipitate (likely $Ir(dppe)_2Cl$[14,15]) is observed. A reproducible way to use this catalyst system is with isolated Ir(COD)(dppe)Cl (see procedures for compounds **2a**–**2c** and **2j**–**2l** below), which can be easily prepared in one step in nearly quantitative yield.[8] Isolated Ir(COD)(dppe)Cl is especially useful for smaller scale reactions where it is harder to get the correct 2:1 ratio of dppe to $[Ir(COD)Cl]_2$. Alternatively, Ir(COD)(dppe)Cl can be pre-formed *in situ* by addition of a solution of dppe in toluene to a solution of $[Ir(COD)Cl]_2$ in toluene (in the absence of the alkyne-containing reactants). This is demonstrated for compounds **2d**, **2e**, and **2h** below. Finally, the most user-friendly procedure, which has been tested in only in one case (compound **2f**), is the addition of a solution of dppe in toluene to a solution of $[Ir(COD)Cl]_2$ *and* reactants in toluene.

*We did not notice any differences between toluene and benzene as solvents for the [2+2+2] reactions reported herein.

Important Note Regarding the Use of 5 Å Molecular sieves (MS) to Sequester 4-Octyne

We observed that the source of the molecular sieves is of critical importance for the alkyne metathesis reactions performed herein. All successful reactions used pre-powdered 5 Å MS that were purchased from Sigma Aldrich and activated under high vacuum at ~300 °C (until condensation of water ceased, then for another 24 h). The activated 5 Å MS were then stored in a solvent-free, nitrogen-filled glovebox until use. At the outset of our investigations, beaded 5 Å MS (3–5 mm, from Alfa Aesar) were activated as described above, then thoroughly ground with a mortar and pestle in a solvent-free, nitrogen-filled glovebox. *Use of these molecular sieves was not effective for the sequestration of 4-octyne.*

Generation of Hypothesized $EtC{\equiv}Mo(OSiPh_3)_3$ (Mo-1) from $EtC{\equiv}Mo(OC(CH_3)(CF_3)_2)_3(DME)$ (Mo-2) and Ph_3SiOH

The current best catalyst for many alkyne metathesis applications are complexes of the general form $R'C{\equiv}Mo(OSiAr_3)_3$ (R' = aryl or alkyl), which have been heavily developed Fürstner and coworkers.[16–19] There are several different isolable precursors, most notably the base-stabilized derivatives $R'C{\equiv}Mo(OSiAr_3)_3L$ (e.g., L = phen or Et_2O)[17] or bench stable $N{\equiv}Mo(OSiAr_3)_3L$ (L = phen or pyr)[16].

An alternative way to access these catalysts is by ligand exchange, as shown by Moore and coworkers *via in situ* treatment of EtC≡Mo(N^{t}BuAr)$_3$ with excess Ph_3SiOH.[20,21] In the course of the current study, it was discovered that **Mo-1** can be analogously generated from the easily-prepared **Mo-2**. Details of this ligand exchange are discussed in the following paragraph.

All alkyne metathesis reactions performed in this study use *in situ* generated **Mo-1**, which is typically formed by pre-mixing of **Mo-2** with 6 equiv of Ph_3SiOH. This ligand exchange reaction was initially investigated by ^1H and ^{19}F NMR spectroscopies, whereby a solution of **Mo-2** in benzene-d_6 was treated with 4, 6, and 9 equiv of Ph_3SiOH (Figures S1 and S2). With 6 and 9 equiv, the only observable species by ^{19}F NMR was free $(CH_3)(CF_3)_2COH$ (with 4 equiv, 95% of the theoretical amount of $(CH_3)(CF_3)_2COH$ was observed along with 5% of an unidentified species). Additionally, in all cases, the ^1H NMR spectra displayed identical, upfield-shifted propylidyne resonances (a methyl quartet at 1.5 ppm and a methylene triplet at –0.2 ppm). These data suggest that the ligand exchange goes to completion with > 4 equiv of Ph_3SiOH, producing metathesis active **Mo-1** that is likely in rapid equilibrium with various adducts of weakly bound[18] L-type ligands (e.g. Ph_3SiOH and DME).

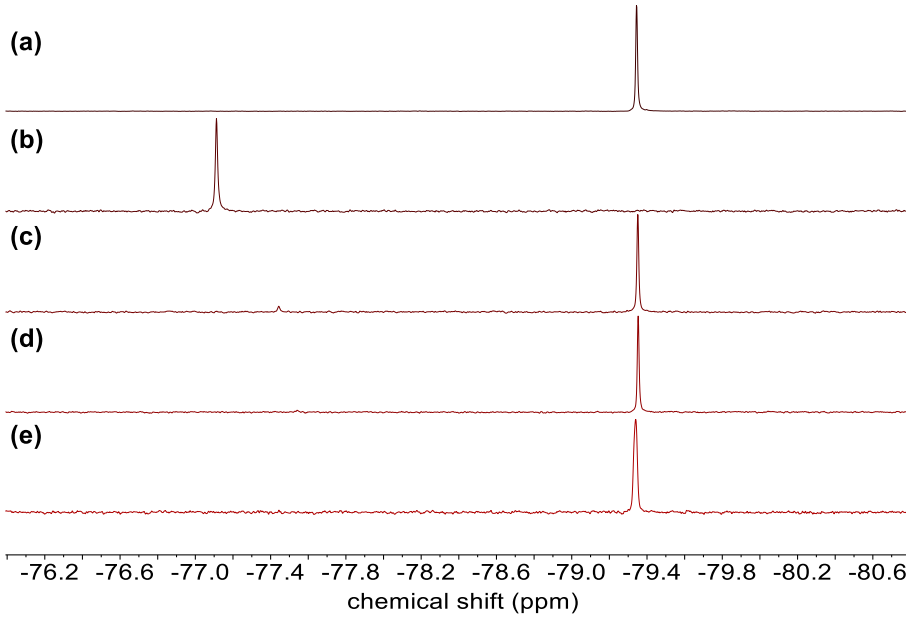

Figure S1. Partial ^{19}F NMR spectra (376 MHz, benzene-d_6) of **(a)** Authentic sample of $(CH_3)(CF_3)_2COH$; **(b) Mo-2**; **(c) Mo-2** + 4 equiv of Ph_3SiOH; **(d) Mo-2** + 6 equiv of Ph_3SiOH; **(e) Mo-2** + 9 equiv of Ph_3SiOH. These spectra suggest that free $(CH_3)(CF_3)_2COH$ is generated upon addition of > 4 equiv of Ph_3SiOH. Note that there is a small singlet (~5% by integration) at 77.4 ppm in spectrum (c), which suggests incomplete ligand exchange.

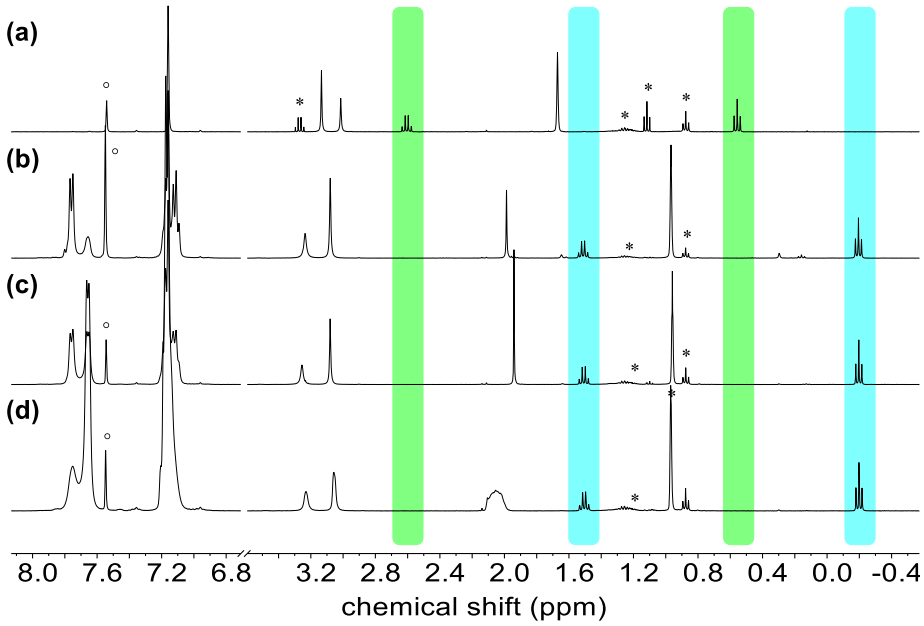

Figure S2. Partial ^{1}H NMR spectra (400 MHz, benzene-d_6) of **(a) Mo-2**; **(b) Mo-2** + 4 equiv of Ph_3SiOH; **(c) Mo-2** + 6 equiv of Ph_3SiOH; **(d) Mo-2** + 9 equiv of Ph_3SiOH. These spectra suggest that the same new species is formed in all cases, which is hypothesized to be **Mo-1**. Note that **Mo-1** is likely in rapid equilibrium with various adducts of weakly bound[18] L-type ligands (e.g. Ph_3SiOH and DME). The highlighted (green and blue) resonances are associated with the propylidyne group. Note that the hydroxyl resonances (between 1.8 and 2.3 ppm) are not comparable due to hydrogen bonding effects. *Glovebox solvents (pentane and diethyl ether); °1,3,5-tris(trifluoromethyl)benzene internal standard

Modular Synthesis of Oligo(Alkynyl)Arylene Precursors

The build-up of larger oligo(alkynyl)arylene substrates critically depends on the availability of unsymmetrical arylene building blocks for use as homo- and cross-coupling reaction partners. Lithium/bromine exchange, as depicted in Scheme S1, is highly effective for this purpose.[4,11,22] Generally, the dibrominated precursor is treated with 1 equiv of ^{n}BuLi to afford a mono-lithiated intermediate, which can then be either protodemetallated for isolation or transmetallated for direct use in a homo- or cross-coupling reaction (see below).

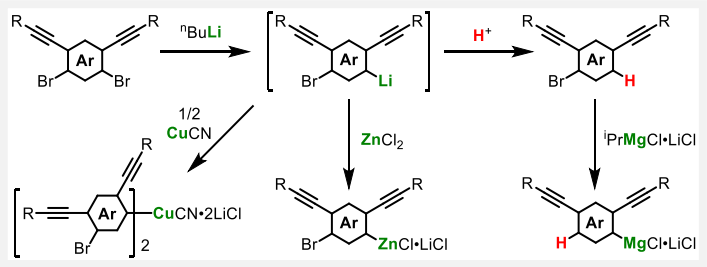

Scheme S1. General depiction of dibromoarene desymmetrization *via* lithium/bromine exchange.

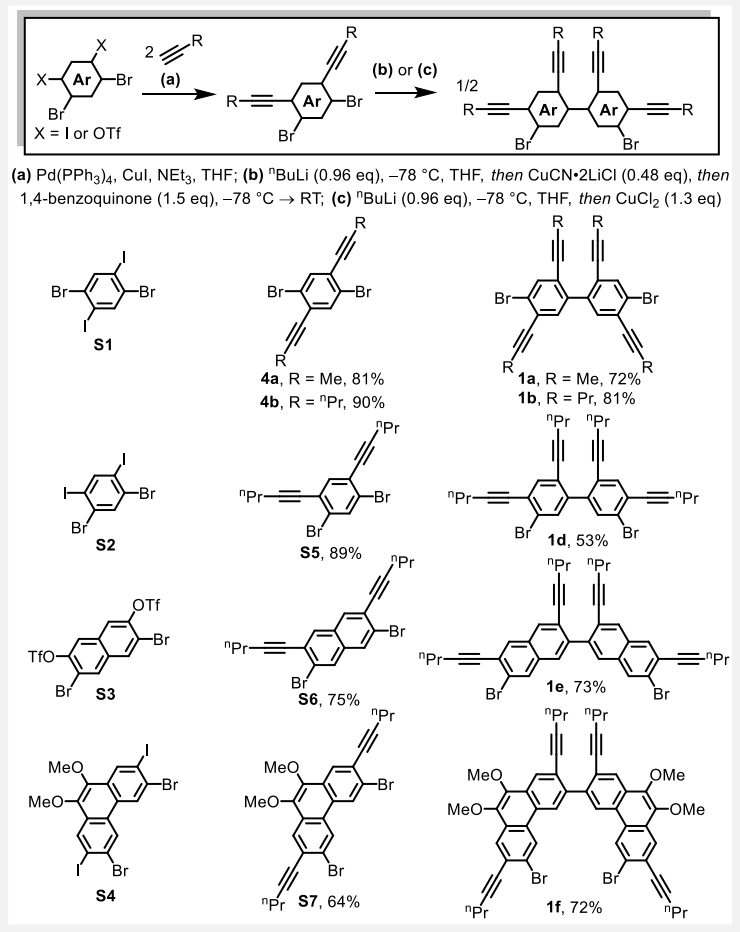

Scheme S2. Syntheses of substrates containing one diyne unit *via* Cu-mediated homocoupling.

The benzene, naphthalene, and phenanthrene building blocks **S1**–**S4** (Scheme S2) were synthesized in large quantities (30–100 grams per run) using previously-developed procedures (or slight modifications thereof).[2–4,23] These compounds were then be subjected to a highly selective Sonogashira protocol that takes advantage of the superior reactivity of iodides[3] (or triflates[23]) over bromides, affording dibromides **4a**–**b** and **S5**–**S7** in good yields. The selective desymmetrization of these dibromides *via* lithium/halogen exchange enabled a subsequent Cu-mediated, oxidative homocoupling reaction. The use of higher order cuprates (i.e. *via* transmetallation to CuCN before oxidation), as first developed by Lipshutz[24] and later improved by Iyoda,[25] consistently provided 70–80% yields for this this homocoupling reaction (i.e. **1a**, **1b**, **1e**, and **1f**). The use of $CuCl_2$ as oxidative coupling reagent,[26] while operationally more convenient, generally provides lower yields, as shown for compound **1d**.

The modularity of the precursor synthesis becomes evident when considering the synthesis of more complex substrates such as those shown in Scheme 3. Compounds **1h–1l** were isolated in moderate yields (51–65%) using standard Kumada or Negishi conditions. In addition to the modularity, there are a few other notable features of these cross-coupling reactions. First, they are directly analogous to those in our previous reports where both arene coupling partners possess an alkynyl group that is ortho to the coupling site.[4,11] Since only a few Pd catalysts have been screened, there is significant room for improvement in this transformation. Second, the Negishi coupling can be performed in an "iodide-selective" fashion, with the preservation of the less-reactive bromides, as shown for **1h** and **1k**. Third, the synthesis of **1l** demonstrates how coupling reactions can be used in sequence to build up more complex precursors (since cross coupling partner **1e** was synthesized *via* homocoupling). These features all point to the exciting possibility of iterative syntheses to build up arbitrarily complex substrates.

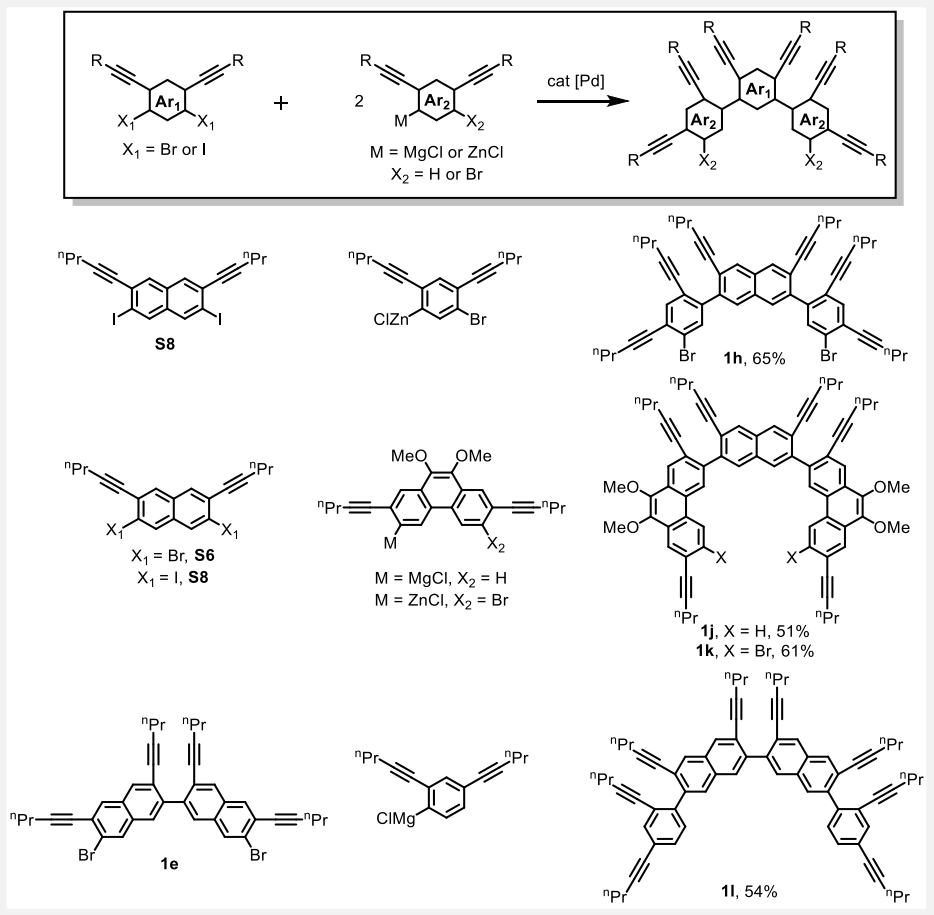

Scheme S3. Syntheses of substrates containing two or three diyne units *via* Kumada or Negishi cross-coupling.

Synthetic Procedures and Characterization Data

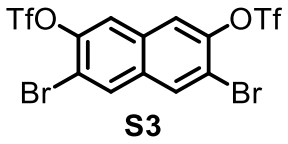

S3

3,6-Dibromo-2,7-bis(trifluoromethanesulfonyloxy)naphthalene (S3). This compound was prepared by a modified* literature procedure.[23] A 500 mL Schlenk flask was charged with **S11** (20.0 g, 62.9 mmol, 1.0 equiv), dry pyridine (20.0 g, 252 mmol, 4.0 equiv), and CH_2Cl_2 (170 mL), and the solution was cooled to 0 °C with an ice/water bath. To the stirred solution was added Tf_2O (41.0 g, 145 mmol, 2.3 equiv) dropwise over ~10 min. The cold bath was removed, then the mixture was stirred for 2 h and quenched with aqueous HCl (0.5 M, 200 mL). The layers were separated, and the aqueous layer was extracted with CH_2Cl_2 (30 mL). The combined organic layers were dried with $MgSO_4$, diluted** with hexanes (200 mL), filtered through a plug of silica gel (20-25 g), then the plug was flushed with 1:1 hexanes:CH_2Cl_2 (100 mL). The filtrate was concentrated to ~150 mL via rotary evaporation, then the crystalline precipitate was collected on a fritted funnel and washed with hexanes (2 x 30 mL). After removal of residual solvents from the solid *in vacuo*, the yield of **S3**, a pale-yellow (nearly colorless) crystalline solid, was 29.5 g (81%). ^{1}H NMR data matches that in the literature.[23]

*The major modifications were in the workup and purification steps

**In order to avoid precipitation of a solid, the mixture was filtered through the silica immediately after this dilution.

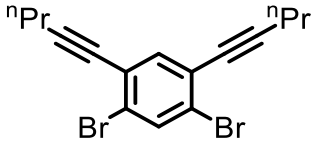

S5

1,5-dibromo-2,4-di(pent-1-ynyl)benzene (S5). This compound was prepared by a modified literature procedure.[22] A 250 mL Schlenk flask with Teflon stopper was charged with **S2** (10.0 g, 20.5 mmol, 1.0 equiv), $Pd(PPh_3)_4$ (0.36 g, 0.31 mmol, 0.015 equiv), and CuI (0.20 g, 1.03 mmol, 0.05 equiv), then the flask was evacuated and refilled with N_2. To this flask was added an N_2-sparged mixture of THF (28 mL) and triethylamine (14 mL), followed by 1-pentyne (3.07 g, 45.1 mmol, 2.2 equiv). The mixture was stirred at RT for 24 h, then diluted with hexanes (150 mL), washed with aqueous HCl (3 M, 100 mL), dried with $MgSO_4$, and filtered. Solvents were removed from the filtrate *via* rotary evaporation, then the crude product purified by column chromatography (100% hexanes) to afford **S5** (6.70 g, 89%) as yellow oil. ^{1}H NMR data matches that in the literature.[22]

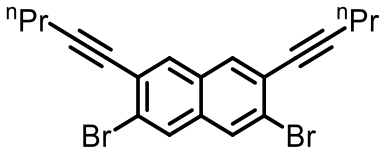

S6

2,7-dibromo-3,6-di(pent-1-yn-1-yl)naphthalene (S6). This procedure is a modified version of that reported by Takimiya and coworkers for a similar compound.[23] A 500 mL round-bottomed Schlenk flask was charged with **S3** (21.0 g, 36.1 mmol, 1.0 equiv)**,** $Pd(PPh_3)_4$ (1.25 g, 1.08 mmol, 0.03 equiv), and CuI (0.41 g, 2.17 mmol, 0.06 equiv), and the flask subjected to three vacuum/N_2 cycles. To this flask was added DMF (56 mL) and NH^iPr_2 (28 mL) (both of which had been thoroughly sparged with N_2), followed 1-pentyne (4.92 g, 72.2 mmol, 2.0 equiv*). The flask was sealed with a ground-glass stopper and stirred for 20 h at RT**. The mixture was diluted with hexanes (150 mL) and washed with water (200 mL). The aqueous layer was extracted with hexanes (2 x 100 mL), then the combined organic layers were washed with aqueous HCl (3 M, 100 mL), dried with $MgSO_4$, and filtered through a plug of silica gel (20 g). The plug was flushed with hexanes (150 mL), solvents were removed *via* rotary evaporation, and the crude solid was recrystallized from EtOH (150 mL; boiling, then –25 °C) to afford **S6** (11.3 g, 75%) as small colorless needles. ^{1}H NMR (500 MHz, Chloroform-*d*): δ = 7.92 (s, 2H), 7.80 (s, 2H), 2.48 (t, *J* = 6.9 Hz, 4H), 1.70 (h, *J* = 7.2 Hz, 4H), 1.11 (t, *J* = 7.4 Hz, 6H); ^{13}C{^{1}H} NMR (151 MHz, Chloroform-*d*): δ = 132.84, 132.05, 130.34, 129.74, 124.52, 123.98, 96.27, 79.52, 22.17, 21.81, 13.78; HRMS-EI (m/z): $[M]^+$ calcd. for $C_{20}H_{18}Br_2$, 415.9775; found, 415.9778.

*This reaction is very sensitive to stoichiometry.

**Toward the beginning of the reaction there was a (delayed) exotherm. It is thus prudent to monitor for this exotherm and equalize the pressure of the flask to avoid over-pressurization.

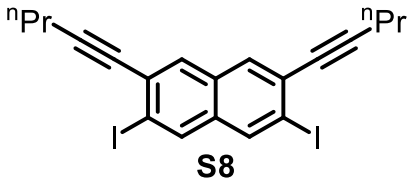

S8

2,7-diiodo-3,6-di(pent-1-yn-1-yl)naphthalene (S8). A solution of **S6** (2.09 g, 5.00 mmol, 1.0 equiv) in THF (25 mL) was cooled to –78 °C with a dry ice / acetone bath and to the stirred solution was added ^{t}BuLi (1.7 M in pentane, 11.8 mL, 20.0 mmol, 4.0 equiv) over 10–15 min. The resulting mixture was stirred for 1 h at –78 °C, then iodine (5.08 g, 20.0 mmol, 4.0 equiv) was added in one portion. After a further 10 min at –78 °C, the cold bath was removed, and the stirred mixture was allowed to warm to RT. After ~30 min at RT, the mixture was quenched with 3% aqueous sodium thiosulfate (120 mL) and extracted with CH_2Cl_2 (100 mL). The organic layer was washed with water (50 mL), dried with $MgSO_4$, filtered, and solvents were removed from the filtrate via rotary evaporation. The crude product was purified by elution through a plug of silica gel (15 g) with 9:1 hexanes:CH_2Cl_2 (150 mL), followed by recrystallization from hexanes (~20 mL total volume; boiling, then –25 °C), to afford **S8** (1.89 g, 77%) as beige needles. ^{1}H NMR (chloroform-*d,* 400 MHz): δ = 8.18 (s, 2H), 7.76 (s, 2H), 2.48 (t, *J* = 6.9 Hz, 4H), 1.71 (sext, *J* = 7.2 Hz, 4H), 1.12 (t, *J* = 7.3 Hz, 6H); ^{13}C{^{1}H} NMR (chloroform-*d*, 151 MHz): δ = 136.54, 133.38, 131.38, 130.85, 128.30, 99.37, 95.65, 82.99, 22.13, 21.81, 13.91; HRMS-EI (m/z): $[M]^+$ calcd. for $C_{20}H_{18}I_2$, 511.9498; found, 511.9495.

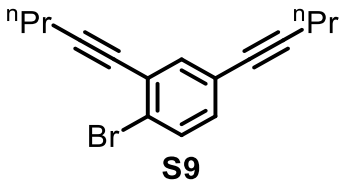

S9

1-bromo-2,4-di(pent-1-yn-1-yl)benzene (S9). A 250 mL Schlenk flask was charged with dibromide **S5** (2.51 g, 6.82 mmol, 1.00 equiv) and THF (34 mL), and the solution was cooled to –78 °C with a CO_2(s)/acetone bath. To the stirred solution was added *n*-butyllithium (1.64 M in hexanes, 4.28 mL, 7.02 mmol, 1.03 equiv) dropwise over 15-20 min, then the resulting mixture was stirred for a further 5 min at –78 °C. To this mixture was added N_2-sparged MeOH (0.83 mL, 21 mmol, 3.0 equiv) dropwise over 2-3 min, then the cold bath was removed. After 15 min (when most of the color had dissipated), the reaction mixture was quenched with saturated aqueous NH_4Cl (40 mL) and extracted with hexanes (40, then 20 mL). The organic layer was washed with saturated aqueous NaCl (50 mL), dried with $MgSO_4$, filtered, and concentrated by rotary evaporation. To remove residual THF, the residue was dissolved in hexanes and solvents were removed under vacuum to afford **S9** (1.92 g, 97%) as a light-yellow oil, which was directly employed for the next step. ^{1}H NMR (chloroform-*d,* 400 MHz): δ = 7.45 (d, *J* = 8.2 Hz, 1H), 7.45 (d, *J* = 2.1 Hz, 1H), 7.11 (dd, *J* = 8.3, 2.1 Hz, 1H), 2.43 (t, *J* = 7.0 Hz, 2H), 2.35 (t, *J* = 7.1 Hz, 2H), 1.66 (sext, *J* = 7.3 Hz, 2H), 1.61 (sext, *J* = 7.3 Hz, 2H), 1.08 (t, *J* = 7.4 Hz, 3H), 1.03 (t, *J* = 7.4 Hz, 3H); ^{13}C{^{1}H} NMR (chloroform-*d,* 101 MHz): = δ 136.25, 132.26, 131.60, 126.23, 124.54, 123.32, 95.88, 91.86, 79.36, 79.10, 22.18, 22.14, 21.66, 21.51, 13.68, 13.67; HRMS-EI (m/z): $[M]^+$ calcd. for $C_{16}H_{17}Br$, 288.0514; found, 288.0511.

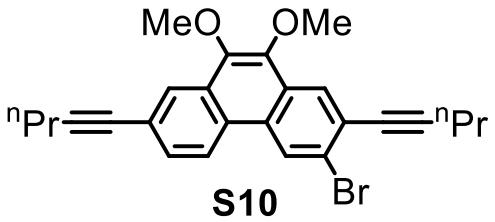

S10

3-bromo-9,10-dimethoxy-2,7-di(pent-1-yn-1-yl)phenanthrene (S10). A 250 mL Schlenk flask was charged with dibromide **S7** (6.00 g, 11.4 mmol, 1.0 equiv) and THF (115 mL) and the solution was cooled to –78 °C with a CO_2(s)/acetone bath. To this solution was added *n*-butyllithium (1.6 M in hexanes, 7.13 mL, 11.4 mmol, 1.0 equiv) dropwise over 15-20 min and the resulting mixture was stirred for a further 5 min at –78 °C. To this mixture was added N_2-sparged MeOH (4.5 mL, ~110 mmol, 10 equiv), then the cold bath was removed. As soon as the green color dissipated (~5 min), the reaction mixture was quenched with saturated aqueous NH_4Cl (40 mL) and extracted with ethyl acetate (90 mL, then 30 mL). The combined organic layers were washed with saturated aqueous NaCl (60 mL), dried with $MgSO_4$, filtered, and concentrated by rotary evaporation. The residue was dissolved in a 3:1 mixture of hexanes:CH_2Cl_2 (60 mL) and the solution was filtered through a plug of silica gel (15 g), which was then flushed with the same solvent mixture (240 mL). Removal of solvents from the filtrate *via* rotary evaporation, followed by high vacuum (at 80 °C for 1h), afforded a colorless oil (5.0 g; contained 3% starting **S7** and 9% doubly-debrominated **S7**, as determined by ^{1}H NMR spectroscopy) that was used without further purification. In a smaller-scale reaction, the pure compound was isolated *via* column chromatography (1:4 CH_2Cl_2:hexanes) in 72% yield. ^{1}H NMR (chloroform-*d*, 500 MHz): δ = 8.73 (s, 1H), 8.38 (d, *J* = 8.6 Hz, 1H), 8.26 (s, 1H), 8.23 (d, *J* = 1.7 Hz, 1H), 7.59 (dd, *J* = 8.6, 1.7 Hz, 1H), 4.06 (s, 3H), 4.06 (s, 3H), 2.52 (t, *J* = 7.0 Hz, 2H), 2.47 (t, *J* = 7.0 Hz, 2H), 1.73 (sext, *J* = 7.2 Hz, 2H), 1.69 (sext, *J* = 7.2 Hz, 2H), 1.13 (t, *J* = 7.4 Hz, 3H); 1.10 (t, *J* = 7.4 Hz, 3H); ^{13}C{^{1}H} NMR (chloroform-*d*, 101 MHz): δ = 143.99, 143.49, 129.63, 129.30, 128.54, 128.07, 127.15, 126.49, 126.36, 125.43, 124.45, 123.38, 123.04, 122.89, 95.89, 91.87, 81.07, 80.03, 61.16, 61.08, 22.37, 22.25, 21.85, 21.70, 13.81; 13.80; HRMS-EI (m/z): $[M]^+$ calcd. for $C_{26}H_{25}BrO_2$, 448.1038; found, 448.1045.

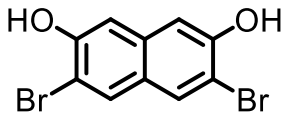

S11

3,6-dibromonaphthalene-2,7-diol (S11). This is a modified version of a literature procedure.[27] A 1000 mL round-bottom, 3-neck flask was equipped with a magnetic stirbar, dropping funnel, reflux condenser, and HBr trap (aqueous NaOH solution). The flask was charged with 2,7-dihydroxynaphthalene (12.7 g, 79.3 mmol, 1.0 equiv) and acetic acid (300 mL) and the dropping funnel with a solution of bromine (50.7 g, 317 mmol, 4.0 equiv) in acetic acid (100 mL). The third neck was sealed with a rubber septum (to permit addition of tin later in the reaction), then the bromine solution was added dropwise to the stirred solution over 10-15 min. To this mixture was added water (40 mL), then the mixture was heated to 130 °C (reflux) after which the first 10% of the mossy tin (2.0 g, 17 mmol, 0.2 equiv) was added. The remaining 90% of the tin (17.8 g, 150 mmol, 1.9 equiv) was added in three equal portions over ~30 min. The mixture was heated for a further 2 h, then the hot mixture was poured into ice cold water (800 mL) and the precipitate was collected on a fritted funnel packed with celite. The solid was extracted with ethyl acetate (200, then 100 mL), then the extract was washed with water (200 mL) and saturated aqueous NaCl (100 mL), dried with $MgSO_4$, filtered, concentrated via rotary evaporation. Residual solvents were removed *in vacuo* to afford **S11** (20.1 g, 80%) as an off-white solid that was pure enough for the next step. ^{1}H NMR data matches that in the literature.[28]

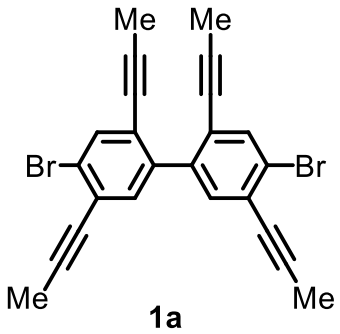

1a

4,4'-dibromo-2,2',5,5'-tetra(prop-1-yn-1-yl)-1,1'-biphenyl (1a). The following procedure is an adaptation* of methodology developed by Iyoda and coworkers.[25] A 250 mL Schlenk flask was charged with diyne **4a** (3.03 g, 9.71 mmol, 1.0 equiv) and THF (90 mL), and the solution was cooled to –78 °C. To the stirred solution was added *n*-butyllithium (1.64 M in hexanes, 5.68 mL, 9.32 mmol, 0.96 equiv) dropwise over ~15 min, and the resulting mixture was stirred for 5–10 min at –78 °C. Next, CuCN·2LiCl (0.47 M in THF, 9.91 mL, 4.66 mmol, 0.48 equiv**) was added dropwise over ~15 min, the mixture was stirred for a further 45 min at –78 °C, and 1,4-benzoquinone (1.58 g, 14.6 mmol, 1.5 equiv) was quickly added in one portion. The cold bath was removed, and the reaction mixture was allowed to warm to RT and stirred for a further 2 h. The mixture was quenched with saturated aqueous NH_4Cl (100 mL) and filtered through celite. The celite was rinsed with CH_2Cl_2 (150 mL), the layers of the filtrate were separated, and the aqueous layer was extracted with CH_2Cl_2 (50 mL). The combined organic layers were dried with $MgSO_4$, filtered, and the filtrate was concentrated to dryness *via* rotary evaporation. The residue was eluted through a short plug of silica gel (15 g) with CH_2Cl_2 (150 mL), the eluted solution was concentrated to ~25 mL via rotary evaporation, and MeOH (100 mL) was added. After ~1 h, the precipitate was collected by filtration, washed with MeOH (2 x 20mL),

and dried under vacuum to afford **1a** (1.62 g, 72%***) as a flocculent white solid. ^{1}H NMR (chloroform-*d,* 400 MHz): δ = 7.66 (s, 2H), 7.37 (s, 2H), 2.11 (s, 6H), 1.89 (s, 6H); ^{13}C{^{1}H} NMR (chloroform-*d,* 101 MHz): δ = 140.16, 135.72, 134.53, 124.77, 124.15, 123.99, 92.28, 92.20, 78.36, 77.39, 4.81, 4.65; HRMS-EI (m/z): $[M]^+$ calcd. for $C_{24}H_{16}Br_2$, 461.9619; found, 461.9617.

*The important changes include: 1) use of ^{n}BuLi instead of ^{t}BuLi; 2) use of THF-soluble CuCN·2LiCl rather than insoluble CuCN, which allows rapid formation of the cuprate at –78 °C.

**The relative stoichiometry of the Ar-Li intermediate and CuCN appears to be very important in achieving the optimal yield for this reaction.

***In the event that a smaller amount is recovered, more product should be isolable from the filtrate.

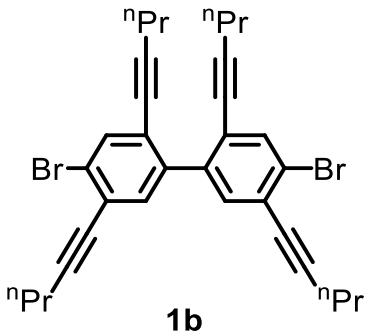

1b

4,4'-dibromo-2,2',5,5'-tetra(pent-1-yn-1-yl)-1,1'-biphenyl (1b). This compound was prepared by the same procedure as **1a**, with the following quantities and noted differences: dibromide **4b** (3.45 g, 9.37 mmol, 1.0 equiv), *n*-butyllithium (1.64 M in hexanes, 5.49 mL, 9.00 mmol, 0.96 equiv), CuCN·2LiCl (0.47 M in THF, 9.57 mL, 4.50 mmol, 0.48 equiv), 1,4-benzoquinone (1.52 g, 14.1 mmol, 1.5 equiv), and THF (90 mL). The crude product was purified by column chromatography (0–7% CH_2Cl_2 in hexanes) to give **1b** (2.19 g, 81%) as a waxy, white solid. ^{1}H NMR (chloroform-*d,* 500 MHz): δ = 7.66 (s, 2H), 7.42 (s, 2H), 2.44 (t, *J* = 7.0 Hz, 4H), 2.22 (t, *J* = 6.9 Hz, 4H), 1.65 (sext, *J* = 7.2 Hz, 4H), 1.45 (h, *J* = 7.2 Hz, 4H), 1.07 (t, *J* = 7.4 Hz, 6H), 0.85 (t, *J* = 7.4 Hz, 6H); ^{13}C{^{1}H} NMR (chloroform-*d,* 400 MHz): δ = 140.19, 135.52, 134.50, 124.77, 124.12, 124.01, 96.71, 96.65, 79.43, 78.57, 22.16, 21.92, 21.75, 21.60, 13.68, 13.44; HRMS-EI (m/z): $[M]^+$ calcd. for $C_{32}H_{31b}r_2$, 574.0871; found, 574.0865.

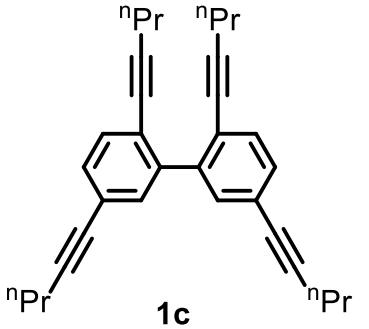

1c

2,2',5,5'-tetra(pent-1-yn-1-yl)-1,1'-biphenyl (1c). A 100 mL Schlenk flask was charged with dibromide **1b** (1.00 g, 1.73 mmol, 1.0 equiv) and THF (35 mL), and the solution was cooled to –78 °C with a CO_2(s)/acetone bath. To this stirred solution was added *n*-butyllithium (1.64 M in hexanes,

3.2 mL, 5.19 mmol, 3.0 equiv) dropwise over ~5 min, and the resulting mixture was stirred for a further 20 min at –78 °C. Anhydrous HCl (2.0 M in ether, 3.45 mL, 6.9 mmol, 4.0 equiv) was then added dropwise over 2-3 min, the cold bath was removed, and saturated aqueous NaCl (100 mL) was added. The mixture was extracted with hexanes (50 mL) and the organic layer was dried with $MgSO_4$, filtered, and concentrated by rotary evaporation. The residue was purified by elution through a plug of silica gel (10 g) with 10:1 hexanes/CH_2Cl_2 to afford **1c** (0.710 g, 98%) as a viscous, colorless oil. ^{1}H NMR (chloroform-*d,* 400 MHz): δ = 7.42 (d, *J* = 1.7 Hz, 2H), 7.37 (d, *J* = 8.0 Hz, 2H), 7.27 (dd, *J* = 8.0, 1.7 Hz, 2H), 2.38 (t, *J* = 7.0 Hz, 4H), 2.20 (t, *J* = 6.9 Hz, 4H), 1.61 (sext, *J* = 7.2 Hz, 4H), 1.42 (sext, *J* = 7.1 Hz, 4H), 1.03 (t, *J* = 7.4 Hz, 6H), 0.83 (t, *J* = 7.4 Hz, 6H); ^{13}C{^{1}H} NMR (chloroform-*d*, 101 MHz): δ = 142.47, 133.33, 131.96, 130.23, 122.78, 122.67, 95.02, 91.55, 80.69, 79.92, 22.33, 22.03, 21.66, 21.58, 13.67, 13.47; HRMS-EI (m/z): $[M]^+$ calcd. for $C_{32}H_{34}$, 418.2661; found, 418.2666.

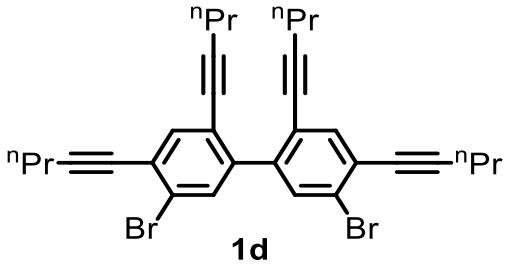

1d

2,2',4,4'-Tetra(pent-1-ynyl)-5,5'-dibromobiphenyl (1d). This procedure is a slightly modified version of a literature procedure for a similar compound.[11] A 100 mL Schlenk flask was charged with **S5** (3.50 g, 9.56 mmol, 1.0 equiv) and THF (48 mL), and the solution was cooled to –78 °C. To this solution was added *n*-butyllithium (1.6 M in hexanes, 5.7 mL, 9.1 mmol, 0.95 equiv) dropwise over 10–15 min and the resulting mixture was stirred for 10 min at –78 °C.* Copper(II) chloride (1.67 g, 12.4 mmol, 1.3 equiv) was then added in one portion, the cold bath was removed, and the reaction mixture was allowed to warm to 21 °C and stirred for 3 h at this temperature. The reaction mixture was quenched with 10% aqueous NH_4OH (50 mL) and extracted with ethyl acetate (50 mL). The organic layer was washed with saturated aqueous NaCl (50 mL) and dried with Na_2SO_4. Filtration and removal of solvents from the filtrate by rotary evaporation gave a crude brown oil. The oil was filtered through a plug of silica gel with excess hexanes, then the filtrate was concentrated to ~2 mL and diluted with EtOH (12 mL), which caused a large amount of crystalline solid to precipitate. The solid was collected by filtration, washed with EtOH (5 mL) and MeOH (5 mL), and dried under high vacuum. The yield of pure **1d** was 1.45 g (53%) as an off-white solid. ^{1}H NMR (chloroform-*d,* 500 MHz): δ = 7.63 (s, 2H), 7.53 (s, 2H), 2.46 (t, *J* = 7.0 Hz, 4H), 2.21 (t, *J* = 6.9 Hz, 4H), 1.68 (h, *J* = 7.2 Hz, 4H), 1.46 (h, *J* = 7.3 Hz, 4H), 1.09 (t, *J* = 7.4 Hz, 6H), 0.87 (t, *J* = 7.4 Hz, 6H); ^{13}C{^{1}H} NMR (chloroform-*d,* 75 MHz): δ 141.10, 136.79, 133.84, 125.53, 123.59, 122.55, 96.23, 95.61, 79.03, 78.37, 22.17, 21.99, 21.75, 21.58, 13.72, 13.53; HRMS-EI (m/z): $[M]^+$ calcd. for $C_{32}H_{31b}r_2$, 574.0871; found, 574.0868.

*Analysis of an aliquot (quenched with saturated aqueous NH_4Cl) by ^{1}H NMR spectroscopy revealed exclusive mono-metallation.

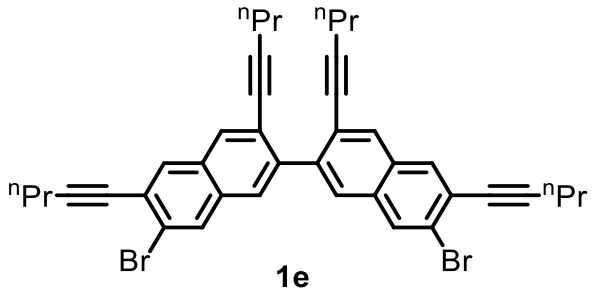

1e

7,7'-dibromo-3,3',6,6'-tetra(pent-1-yn-1-yl)-2,2'-binaphthalene (1e). This compound was prepared by the same procedure as **1a**, with the following quantities and noted differences: dibromide **S6** (4.60 g, 11.0 mmol, 1.0 equiv), *n*-butyllithium (1.64 M in hexanes, 6.6 mL, 10.8 mmol, 0.98 equiv), CuCN·2LiCl (0.47 M in THF, 11.5 mL, 5.39 mmol, 0.49 equiv), 1,4-benzoquinone (1.78 g, 16.5 mmol, 1.5 equiv), and THF (110 mL). The crude product was purified by column chromatography (0–10% CH_2Cl_2 in hexanes) to give **1e** (2.73 g, 73%) as a white solid. ^{1}H NMR (chloroform-*d*, 600 MHz): δ = 8.02 (s, 2H), 7.91 (s, 2H), 7.89 (s, 2H), 7.71 (s, 2H), 2.51 (t, *J* = 7.0 Hz, 4H), 2.13 (t, *J* = 6.8 Hz, 4H), 1.72 (sext, *J* = 7.2 Hz, 4H), 1.27 (sext, *J* = 7.2 Hz, 4H), 1.13 (t, *J* = 7.4 Hz, 6H), 0.67 (t, *J* = 7.4 Hz, 6H); ^{13}C{^{1}H} NMR (chloroform-*d*, 151 MHz): δ = 141.12, 132.04, 131.94, 130.96, 130.86, 130.80, 127.81, 124.05, 123.23, 123.03, 95.74, 94.94, 79.94, 79.80, 22.24, 21.92, 21.82, 21.55, 13.80, 13.30; HRMS-ESI (m/z): $[M]^+$ calcd. for $C_{40}H_{36}Br_2$, 674.1184; found, 674.1178.

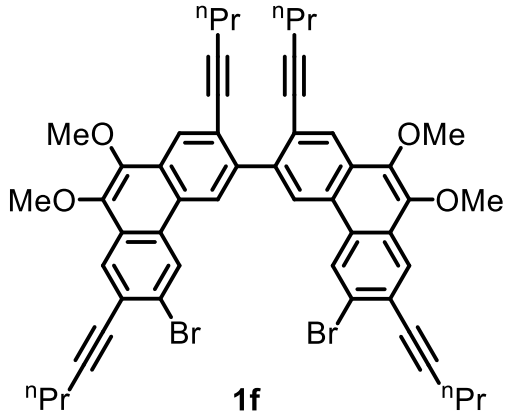

1f

6,6'-dibromo-9,9',10,10'-tetramethoxy-2,2',7,7'-tetra(pent-1-ynyl)-3,3'-biphenanthrene (1f). We previously synthesized **1f** *via* lithium/bromine exchange followed by oxidative coupling with $CuCl_2$.[4] This procedure gave diminished yield on a larger scale, so an alternative oxidative coupling method was sought. The following procedure is an adaptation* of methodology developed by Iyoda and coworkers.[25] A 500 mL Schlenk flask was charged with diyne **S7** (10.0 g, 18.9 mmol, 1.0 equiv) and THF (190 mL), and the solution was cooled to –78 °C. To the stirred solution was added *n*-butyllithium (1.64 M in hexanes, 11.0 mL, 18.1 mmol, 0.96 equiv) dropwise over 1 h, and the resulting mixture was stirred for 10 min at –78 °C. Next, CuCN·2LiCl (0.47 M in THF, 19.3 mL, 9.07 mmol, 0.48 equiv**) was added dropwise over ~30 min, the mixture was stirred for a further 30 min at –78 °C, then 1,4-benzoquinone (3.07 g, 28.4 mmol, 1.5 equiv) was added in one portion against light N_2 flow, immediately producing a deep purple color. The cold bath was removed and the reaction mixture was allowed to warm to RT and stirred for a further 2 h. The mixture was quenched with saturated aqueous NH_4Cl (200 mL), diluted with hexanes (200 mL), and filtered through celite. The aqueous

layer was extracted with hexanes (100 mL), then the combined organic layers were washed with saturated aqueous NaCl (100 mL), dried with $MgSO_4$, filtered, and the filtrate was concentrated *via* rotary evaporation. The residue was eluted through a short plug of silica gel with CH_2Cl_2 and solvents were removed *via* rotary evaporation. The crude was purified by column chromatography (33–40% CH_2Cl_2 in hexanes) to afford **1f** (6.10 g, 72%) as an off-white solid. ^{1}H NMR data matches the literature.[4]

*The important changes include: 1) use of ^{n}BuLi instead of ^{t}BuLi; 2) use of THF-soluble CuCN·2LiCl rather than insoluble CuCN, which allows rapid formation of the cuprate at –78 °C.

**The relative stoichiometry of the Ar-Li intermediate and CuCN appears to be important in achieving the optimal yield for this reaction.

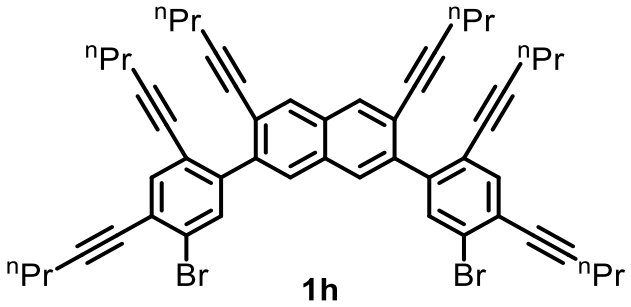

1h

2,7-bis(5-bromo-2,4-di(pent-1-yn-1-yl)phenyl)-3,6-di(pent-1-yn-1-yl)naphthalene (1h). A 250 mL Schlenk flask was charged with dibromide **S5** (3.24 g, 8.79 mmol, 3.0 equiv) and THF (38 mL), and the solution was cooled to –78 °C with a dry ice / acetone bath. To this solution was added *n*-butyllithium (1.62 M in hexanes, 5.06 mL, 8.20 mmol, 2.8 equiv) dropwise over ~10 min, and the resulting mixture was stirred for 5 min at –78 °C. Next, $ZnCl_2$ (0.84 M in THF, 11.9 mL, 9.96 mmol, 3.4 equiv) was added dropwise over ~2 min, the cold bath was removed, and the reaction mixture was allowed to warm to RT and stirred for 2 h (time after cold bath removal). To this solution was added diiodide **S8** (1.50 g, 2.93 mmol, 1.0 equiv) and $Pd(PPh_3)_4$ (0.34 g, 0.29 mmol, 0.10 equiv), then the flask was sealed with a ground glass stopper and the mixture was stirred at 35 °C for 12 h. The mixture was brought to RT, quenched with saturated aqueous NH_4Cl (50 mL), and extracted with EtOAc (2 x 50 mL). The combined extracts were washed with saturated aqueous NaCl (50 mL), dried with $MgSO_4$, filtered, and the filtrate was concentrated under reduced pressure. The residue was purified by column chromatography (mass of silica: 160 g; eluant: 0–10% CH_2Cl_2 in hexanes) to afford hexayne **1h** (1.59 g, 65%) as a sticky yellow/orange solid. ^{1}H NMR (chloroform-*d,* 600 MHz): δ = 7.92 (s, 2H), 7.75 (s, 2H), 7.67 (s, 2H), 7.57 (s, 2H), 2.47 (t, *J* = 6.9 Hz, 4H), 2.28 (t, *J* = 6.9 Hz, 4H), 2.10 (t, *J* = 6.9 Hz, 4H), 1.69 (sext, *J* = 7.2 Hz, 4H), 1.49 (sext, *J* = 7.2 Hz, 4H), 1.29 (sext, *J* = 7.2 Hz, 4H), 1.10 (t, *J* = 7.4 Hz, 6H), 0.89 (t, *J* = 7.4 Hz, 6H), 0.69 (t, *J* = 7.4 Hz, 6H); ^{13}C{^{1}H} NMR (chloroform-*d*, 151 MHz): δ = 143.10, 139.01, 136.61, 133.97, 131.68, 131.01, 130.68, 128.96, 125.12, 123.57, 123.18, 122.37, 95.88, 94.99, 94.80, 79.89, 79.14, 78.85, 22.20, 22.12, 21.90, 21.76, 21.66, 21.50, 13.71, 13.52, 13.32; HRMS-ESI (m/z): $[M+H]^+$ calcd. for $C_{52}H_{51}Br_2$, 833.2352; found, 833.2356.

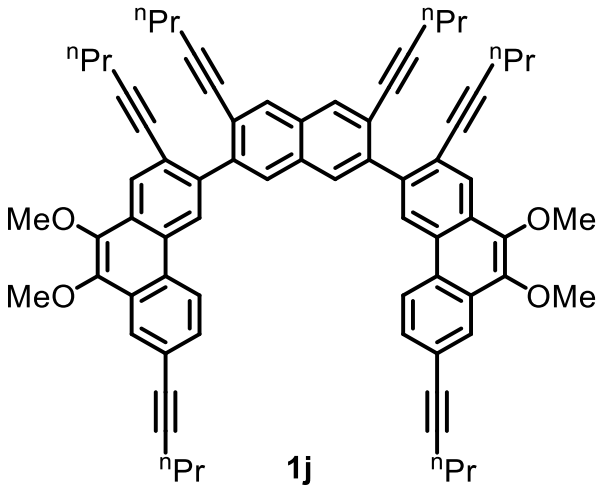

1j

3,3'-(3,6-di(pent-1-yn-1-yl)naphthalene-2,7-diyl)bis(9,10-dimethoxy-2,7-di(pent-1-yn-1-yl)phenanthrene) (1j). A 25 mL flask equipped with Teflon stopper was charged with monobromide **S10** (1.06 g, 2.36 mmol, 4.0 equiv) and ^{i}PrMgCl·LiCl (0.89 M in THF, 2.45 mL, 2.18 mmol, 3.7 equiv), then the mixture was diluted with THF (0.7 mL). The flask was sealed, and the stirred mixture was heated at 60 °C for 3 h. This mixture was transferred *via* syringe to another flask containing $PdCl_2$(IPr)(3-chloropyridine) (0.012 g, 0.018 mmol, 0.03 equiv) and dibromide **S6** (0.247 g, 0.590 mmol, 1.0 equiv), then THF (0.6 mL) was used for quantitative transfer. The resulting mixture was stirred at RT for 24 h, then quenched with saturated aqueous NH_4Cl (10 mL), extracted with CH_2Cl_2 (20 mL), dried with $MgSO_4$, filtered, and the filtrate was concentrated under reduced pressure. The residue was purified by column chromatography* (30–40% CH_2Cl_2 in hexanes) to afford hexayne **1j** (0.285 g, 51%) as a foamy, pale-orange solid. ^{1}H NMR (chloroform-*d,* 600 MHz): δ = 8.67 (s, 2H), 8.49 (d, *J* = 8.6 Hz, 2H), 8.37 (s, 2H), 8.28 (d, *J* = 1.7 Hz, 2H), 8.06 (s, 2H), 7.95 (s, 2H), 7.57 (dd, *J* = 8.6, 1.8 Hz, 2H), 4.12 (s, 6H), 4.12 (s, 6H), 2.47 (t, *J* = 7.0 Hz, 4H), 2.23 (t, *J* = 6.9 Hz, 4H), 2.16 (t, *J* = 6.9 Hz, 4H), 1.70 (sext, *J* = 7.3 Hz, 4H), 1.39 (sext, *J* = 7.2 Hz, 4H), 1.29 (sext, *J* = 7.1 Hz, 4H), 1.11 (t, *J* = 7.4 Hz, 6H), 0.78 (t, *J* = 7.3 Hz, 6H), 0.67 (t, *J* = 7.4 Hz, 6H); ^{13}C{^{1}H} NMR (chloroform-*d*, 151 MHz): δ = 143.93, 143.91, 140.98, 140.40, 131.57, 131.10, 131.03, 129.40, 129.25, 129.02, 128.36, 127.70, 127.07, 125.94, 125.47, 124.70, 123.20, 122.99, 122.88, 122.72, 94.35, 94.35, 91.40, 81.30, 80.68, 80.55, 61.19, 61.17, 22.41, 22.11, 22.02, 21.72, 21.71, 21.61, 13.78, 13.47, 13.32; MS-MALDI-TOF (m/z): $[M]^+$ calcd. for $C_{72}H_{68}O_4$, 996.51; found, 996.47.

*These reaction conditions produce some homocoupled **S10**, which is difficult to remove by column chromatography. Thus, a careful gradient is required.

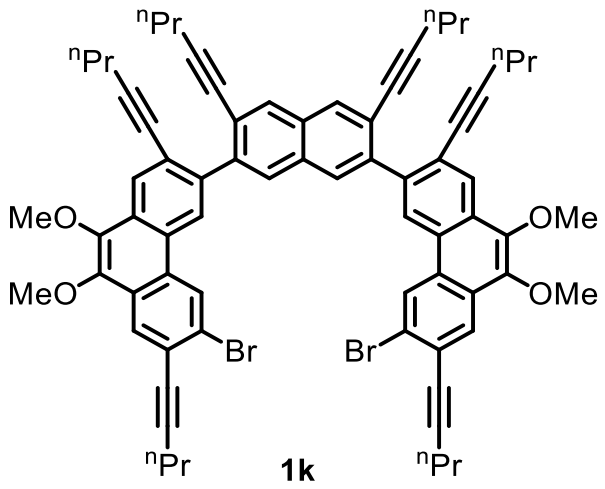

1k

6,6'-(3,6-di(pent-1-yn-1-yl)naphthalene-2,7-diyl)bis(3-bromo-9,10-dimethoxy-2,7-di(pent-1-yn-1-yl)phenanthrene) (1k). A 250 mL Schlenk flask was charged with dibromide **S7** (1.85 g, 3.51 mmol, 3.0 equiv) and THF (35 mL), and the solution was cooled to –78 °C with a dry ice / acetone bath. To this solution was added *n*-butyllithium (1.64 M in hexanes, 2.00 mL, 3.28 mmol, 2.8 equiv) dropwise over ~15 min, and the resulting mixture was stirred for 5 min at –78 °C. Next, $ZnCl_2$ (0.84 M in THF, 4.7 mL, 3.98 mmol, 3.4 equiv) was added dropwise over 3-4 min, the cold bath was removed, and the reaction mixture was allowed to warm to RT and stirred for 2 h (time after cold bath removal). To this solution was added (against light N_2 flow) diiodide **S8** (0.600 g, 1.17 mmol, 1.0 equiv) and $Pd(PPh_3)_4$ (0.135 g, 0.117 mmol, 0.10 equiv), then the flask was sealed with a ground glass stopper and the mixture was stirred at RT °C for 24 h. The mixture was poured into saturated aqueous NH_4Cl (50 mL) and extracted with CH_2Cl_2 (100 mL, then 50 mL). The combined extracts were dried with $MgSO_4$, filtered, and the filtrate was concentrated under reduced pressure. The residue was purified by column chromatography (mass of silica: 100 g; eluant: 25–40% CH_2Cl_2 in hexanes) to afford hexayne **1k** (0.825 g, 61%) as a foamy, orange/yellow solid. ^{1}H NMR (chloroform-*d,* 600 MHz): δ = 8.76 (s, 2H), 8.60 (s, 2H), 8.36 (s, 2H), 8.29 (s, 2H), 8.07 (s, 2H), 7.97 (s, 2H), 4.11 (s, 6H), 4.10 (s, 6H), 2.53 (t, *J* = 7.0 Hz, 4H), 2.24 (t, *J* = 6.9 Hz, 4H), 2.18 (t, *J* = 6.9 Hz, 4H), 1.73 (sext, *J* = 7.2 Hz, 4H), 1.40 (sext, *J* = 7.2 Hz, 4H), 1.33 (sext, *J* = 7.2 Hz, 4H), 1.14 (t, *J* = 7.4 Hz, 6H), 0.79 (t, *J* = 7.3 Hz, 6H), 0.70 (t, *J* = 7.4 Hz, 6H); ^{13}C{^{1}H} NMR (chloroform-*d,* 151 MHz): δ = 143.98, 143.50, 140.66, 140.65, 131.64, 131.15, 131.04, 129.27, 128.78, 128.75, 128.29, 127.21, 126.60, 126.01, 125.94, 124.69, 124.46, 123.85, 123.08, 122.82, 95.90, 94.85, 94.52, 80.52, 80.47, 80.08, 61.23, 61.13, 22.26, 22.08, 22.07, 21.86, 21.70, 21.63, 13.80, 13.51, 13.39; MS-MALDI-TOF (m/z): $[M]^+$ calcd. for $C_{72}H_{66}Br_2O_4$, 1152.33; found, 1152.26.

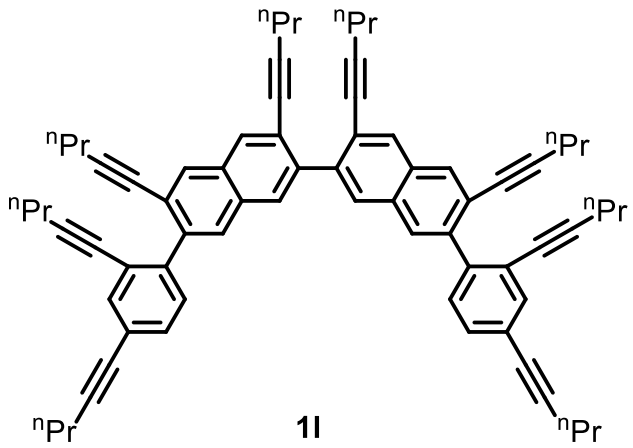

1l

7,7'-bis(2,4-di(pent-1-yn-1-yl)phenyl)-3,3',6,6'-tetra(pent-1-yn-1-yl)-2,2'-binaphthalene (1l). A 25 mL flask equipped with Teflon stopper was charged with monobromide **S9** (0.807 g, 2.79 mmol, 4.0 equiv) and ^{i}PrMgCl·LiCl (0.89 M in THF, 2.9 mL, 2.58 mmol, 3.7 equiv), then the mixture was diluted with THF (1.0 mL). The flask was sealed, and the stirred mixture was heated at 60 °C for 3 h. This mixture was transferred *via* syringe to another flask containing $PdCl_2$(IPr)(3-chloropyridine) (0.014 g, 0.021 mmol, 0.03 equiv) and dibromide **1e** (0.472 g, 0.697 mmol, 1.0 equiv), then THF (2 mL) was used for quantitative transfer. The resulting mixture was stirred at RT for 15 h, then quenched with saturated aqueous NH_4Cl (20 mL) and extracted with hexanes (20 mL). The organic layer was washed with saturated aqueous NaCl (20 mL), dried with $MgSO_4$, filtered, and the filtrate was concentrated under reduced pressure. The residue was purified by column chromatography (10–20% CH_2Cl_2 in hexanes) to afford octayne **1l** (0.375 g, 54%) as a foamy, pale yellow/orange solid. ^{1}H NMR (chloroform-*d,* 400 MHz): δ = 7.96 (s, 2H), 7.95 (s, 2H), 7.78 (s, 2H), 7.78 (s, 2H), 7.56 (d, *J* = 1.6 Hz, 2H), 7.37 (d, *J* = 7.9 Hz, 2H), 7.34 (dd, *J* = 8.0, 1.6 Hz, 2H), 2.41 (t, *J* = 7.0 Hz, 4H), 2.25 (t, *J* = 6.9 Hz, 4H), 2.16 (t, *J* = 7.0 Hz, 4H), 2.13 (t, *J* = 7.3 Hz, 4H), 1.65 (sext, *J* = 7.2 Hz, 4H), 1.46 (sext, *J* = 7.2 Hz, 4H), 1.32 (sext, *J* = 7.2, 4H), 1.31 (sext, *J* = 7.2, 4H), 1.07 (t, *J* = 7.4 Hz, 6H), 0.88 (t, *J* = 7.4 Hz, 6H), 0.71 (t, *J* = 7.4 Hz, 6H), 0.71 (t, *J* = 7.4 Hz, 6H); ^{13}C{^{1}H} NMR (chloroform-*d*, 101 MHz): δ = 142.23, 141.04, 140.38, 135.23, 131.48, 130.99, 130.93, 130.61, 130.26, 129.89, 128.87, 128.72, 124.07, 123.21, 122.98, 122.36, 94.18, 94.11, 93.79, 90.82, 80.43, 80.32, 80.27, 79.69, 22.35, 22.08, 22.02, 22.00, 21.67, 21.60, 21.58, 21.49, 13.69, 13.51, 13.36, 13.34; $[M+H]^+$ calcd. for $C_{72}H_{71}$, 935.5550; found, 935.5541.

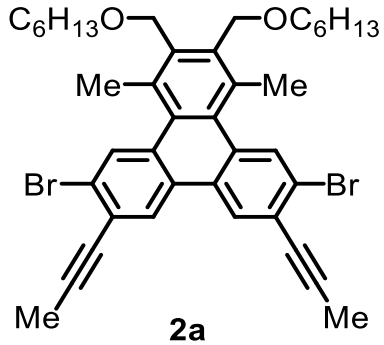

2a

6,11-dibromo-2,3-bis((hexyloxy)methyl)-1,4-dimethyl-7,10-di(prop-1-yn-1-yl)triphenylene (2a). A 100 mL Teflon-stoppered flask was charged with tetrayne **1a** (500 mg, 1.08 mmol, 1.0 equiv),

1,4-bis(hexyloxy)but-2-yne (550 mg, 2.16 mmol, 2.0 equiv), and toluene (9 mL). To this flask was added a solution of Ir(COD)(dppe)Cl (15.9 mg, 0.0216 mmol, 0.02 equiv) in toluene (2 mL). The flask was sealed, and the stirred mixture was heated at 60 °C for 2 h. In air, volatile materials were removed *via* rotary evaporation. The residue was purified by column chromatography (25–40% CH_2Cl_2 in hexanes) followed by recrystallization from boiling hexanes, affording PAH **2a** (396 mg, 51%) as a colorless, crystalline solid. Monitoring of a smaller-scale (0.2 x) reaction under identical conditions (in benzene-d_6) by ^{1}H NMR spectroscopy revealed that **2a** formed in 70% yield. ^{1}H NMR (chloroform-*d,* 600 MHz): δ = 8.43 (s, 2H), 8.33 (s, 2H), 4.74 (s, 4H), 3.62 (t, *J* = 6.6 Hz, 4H), 2.87 (s, 6H), 2.19 (s, 6H), 1.69 – 1.63 (m, 4H), 1.44 – 1.36 (m, 4H), 1.35 – 1.28 (m, 8H), 0.89 (t, *J* = 6.9 Hz, 6H); ^{13}C{^{1}H} NMR (chloroform-*d*, 101 MHz): δ = 136.28, 132.54, 132.18, 131.95, 131.49, 128.66, 128.26, 124.13, 122.91, 91.50, 78.80, 71.55, 67.42, 31.83, 29.93, 26.14, 22.80, 20.65, 14.23, 4.84; HRMS-ESI (m/z): $[M+Na]^+$ calcd. for $C_{40}H_{46}O_{1b}r_2Na$, 739.1757; found, 739.1763.

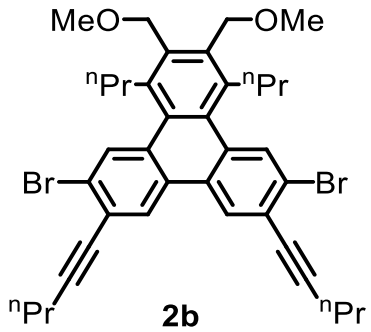

2b

6,11-dibromo-2,3-bis(methoxymethyl)-7,10-di(pent-1-yn-1-yl)-1,4-dipropyltriphenylene (2b). A 25 mL Teflon-stoppered flask was charged with tetrayne **1b** (300 mg, 0.521 mmol, 1.0 equiv), 1,4-dimethoxy-2-butyne (119 mg, 1.04 mmol, 2.0 equiv), and toluene (4.2 mL). To this flask was added a solution of Ir(COD)(dppe)Cl (7.6 mg, 0.0104 mmol, 0.02 equiv) in toluene (1.0 mL). The flask was sealed, and the stirred mixture was heated at 80 °C for 2 h. In air, volatile materials were removed *via* rotary evaporation, then the residue was subjected to column chromatography (40–50% CH_2Cl_2 in hexanes), affording PAH **2b** (254 mg, 71%) as a colorless solid. Monitoring of a smaller-scale (0.2 x) reaction under identical conditions (in benzene-d_6) by ^{1}H NMR spectroscopy revealed that **2b** formed in 88% yield. ^{1}H NMR (chloroform-*d,* 400 MHz): δ = 8.41 (s, 2H), 8.27 (s, 2H), 4.69 (s, 4H), 3.53 (s, 6H), 3.25 – 3.14 (m, 4H), 2.52 (t, *J* = 7.0 Hz, 4H), 1.80 – 1.68 (m, 8H), 1.14 (t, *J* = 7.4 Hz, 6H), 0.96 (t, *J* = 7.3 Hz, 6H); ^{13}C{^{1}H} NMR (chloroform-*d,* 101 MHz): δ = 136.51, 136.46, 132.52, 132.15, 131.55, 128.54, 128.03, 124.18, 123.23, 96.09, 79.73, 68.83, 58.96, 34.54, 25.66, 22.25, 21.83, 14.34, 13.81; HRMS-ESI (m/z): $[M+Na]^+$ calcd. for $C_{38}H_{42}O_{1b}r_2Na$, 711.1444; found, 711.1441.

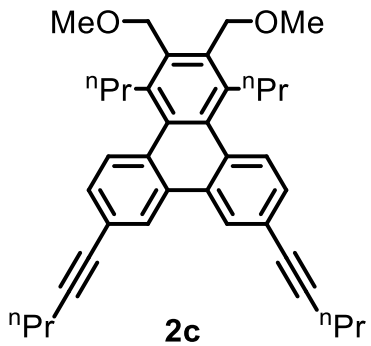

2c

2,3-bis(methoxymethyl)-7,10-di(pent-1-yn-1-yl)-1,4-dipropyltriphenylene (2c). A 25 mL Teflon-stoppered flask was charged with tetrayne **1c** (300 mg, 0.717 mmol, 1.0 equiv), 1,4-dimethoxy-2-butyne (163 mg, 1.43 mmol, 2.0 equiv), and toluene (5.2 mL). To this flask was added a solution of Ir(COD)(dppe)Cl (10.5 mg, 0.0143 mmol, 0.02 equiv) in toluene (2.0 mL). The flask was sealed, and the stirred mixture was heated at 80 °C for 2 h. In air, volatile materials were removed *via* rotary evaporation, then the residue was subjected to column chromatography (40–50% CH_2Cl_2 in hexanes), affording PAH **2c** (230 mg, 60%) as a sticky, colorless solid. Monitoring of a smaller-scale (0.2x) reaction under identical conditions (in benzene-d_6) by ^{1}H NMR spectroscopy revealed that **2c** formed in 84% yield. ^{1}H NMR (400 MHz, chloroform-*d*): δ = 8.45 (d, *J* = 1.7 Hz, 2H), 7.99 (d, *J* = 8.5 Hz, 2H), 7.47 (dd, *J* = 8.5, 1.7 Hz, 2H), 4.70 (s, 4H), 3.53 (s, 6H), 3.31 – 3.20 (m, 4H), 2.46 (t, *J* = 7.0 Hz, 4H), 1.73 – 1.60 (m, 4H), 1.70 (sext, *J* = 7.2 Hz, 4H), 1.10 (t, *J* = 7.3 Hz, 6H), 0.87 (t, *J* = 7.3 Hz, 6H); ^{13}C{^{1}H} NMR (101 MHz, chloroform-*d*): δ = 136.24, 135.45, 133.30, 130.53, 130.22, 129.09, 128.75, 126.66, 122.21, 91.18, 81.05, 69.02, 58.89, 34.72, 25.78, 22.42, 21.68, 14.50, 13.80; HRMS-ESI (m/z): $[M+Na]^+$ calcd. for $C_{38}H_{44}O_2Na$, 555.3234; found, 555.3239.

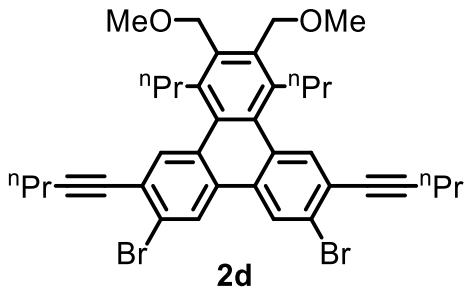

2d

7,10-dibromo-2,3-bis(methoxymethyl)-6,11-di(pent-1-yn-1-yl)-1,4-dipropyltriphenylene (2d). To a solution of $[Ir(COD)Cl]_2$ (3.5 mg, 0.0052 mmol, 0.01 equiv) in benzene (0.5 mL) was added (dropwise over ~1 min) a solution of dppe (4.2 mg, 0.010 mmol, 0.02 equiv) in benzene (0.5 mL). This mixture was immediately added to a flask containing a solution of tetrayne **1d** (300 mg, 0.521 mmol, 1.0 equiv) and 1,4-dimethoxy-2-butyne (89 mg, 0.782 mmol, 1.5 equiv) in benzene (4 mL). The flask was sealed with a Teflon stopper and the stirred reaction mixture was heated at 80 °C for 2 h. The mixture was allowed to cool to RT and directly subjected to column chromatography (1:1 CH_2Cl_2:hexanes, then 100% CH_2Cl_2) to afford triphenylene **2d** (322 mg, 89%) as a colorless solid. ^{1}H NMR (benzene-d_6, 500 MHz): δ = 8.31 (s, 2H), 8.27 (s, 2H), 4.71 (s, 4H), 3.26 (s, 6H), 3.22 – 3.15 (m, 4H), 2.25 (t, *J* = 6.9 Hz, 4H), 1.72 (sext, *J* = 7.5 Hz, 4H), 1.49 (sext, *J* = 7.2 Hz, 4H), 0.99 (t, *J* = 7.4 Hz, 6H), 0.86 (t, *J* = 7.3 Hz, 6H); ^{13}C{^{1}H} NMR (chloroform-*d*, 101 MHz): δ = 136.36, 136.23, 133.84, 132.36, 130.32, 129.86, 126.95, 124.20, 123.49, 95.91, 79.89, 68.90, 58.94, 34.54, 25.73, 22.22, 21.80, 14.27, 13.72; HRMS-ESI (m/z): $[M+Na]^+$ calcd. for $C_{38}H_{42}O_{1b}r_2Na$, 711.1444; found, 711.1444.

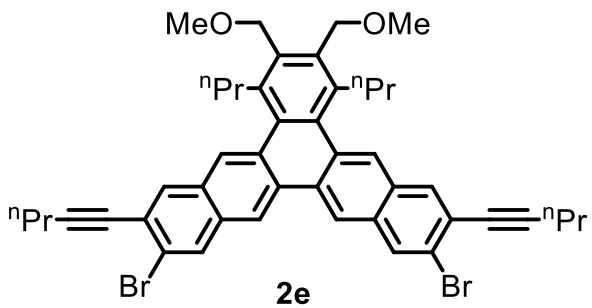

2e

2,13-dibromo-7,8-bis(methoxymethyl)-3,12-di(pent-1-yn-1-yl)-6,9-dipropylbenzo[h]pentaphene (2e). To a stirred solution of $[Ir(COD)Cl]_2$ (21.6 mg, 0.032 mmol, 0.01 equiv) in benzene (2 mL) was added (dropwise over ~1 min) a solution of dppe (25.6 mg, 0.064 mmol, 0.02 equiv) in benzene (2 mL). This mixture was immediately added to a flask containing a solution of tetrayne **1e** (2.17 g, 3.21 mmol, 1.0 equiv) and 1,4-dimethoxy-2-butyne (0.73 g, 6.42 mmol, 2.0 equiv) in benzene (28 mL). The flask was sealed with a Teflon stopper and the reaction mixture was heated at 80 °C for 2 h. The mixture was allowed to cool to RT, hexanes (65 mL) was added, then the solid was collected by filtration and washed with hexanes (2 x 10 mL). The light orange solid was then dissolved in boiling benzene (~25 mL) and hexanes (50 mL) was added to the hot, stirred solution to produce an immediate precipitate. The mixture was allowed to cool to RT, then the precipitate was collected *via* filtration, washed with hexanes (10 mL), and dried under high vacuum to afford pure **2e** (1.80 g) as a pale-yellow solid. The filtrate was concentrated via rotary evaporation and the residue was subjected to column chromatography (0–50% CH_2Cl_2 in hexanes) to provide a further 0.23 g of compound **2e**. Total yield: (2.03 g, 80%). ^{1}H NMR (chloroform-*d,* 500 MHz): δ = 8.72 (s, 2H), 8.28 (s, 2H), 8.28 (s, 2H), 8.00 (s, 2H), 4.72 (s, 4H), 3.57 (s, 6H), 3.39 – 3.31 (m, 4H), 2.53 (t, *J* = 7.0 Hz, 4H), 1.77 (sext, *J* = 7.2 Hz, 4H), 1.74 (sext, *J* = 7.2 Hz, 4H), 1.14 (t, *J* = 7.4 Hz, 6H), 0.94 (t, *J* = 7.3 Hz, 6H); ^{13}C{^{1}H} NMR (chloroform-*d*, 151 MHz): δ = 136.50, 136.48, 134.38, 132.90, 131.68, 131.26, 131.13, 130.70, 130.68, 127.68, 123.63, 122.80, 121.58, 95.80, 79.99, 69.02, 58.99, 34.62, 25.92, 22.27, 21.88, 14.68, 13.83; HRMS-ESI (m/z): $[M]^+$ calcd. for $C_{46}H_{46}Br_2O_2$, 788.1865; found, 788.1859.

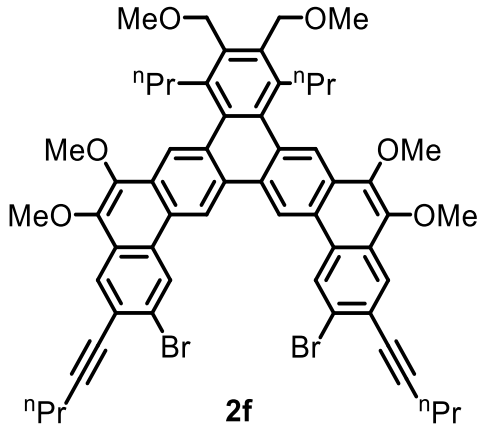

2f

2,17-dibromo-5,6,13,14-tetramethoxy-9,10-bis(methoxymethyl)-3,16-di(pent-1-yn-1-yl)-8,11-dipropyltribenzo[a,h,o]pentaphene (2f). A 150 mL Teflon-stoppered flask was charged with $[Ir(COD)Cl]_2$ (0.026 g, 0.039 mmol, 0.010 equiv), tetrayne **1f** (3.50 g, 3.90 mmol, 1.0 equiv), 1,4-dimethoxy-2-butyne (0.67 g, 5.9 mmol, 1.5 equiv), and toluene (37 mL). To the stirred, homogeneous solution was added (dropwise over ~1 min) a solution of dppe (0.031 g, 0.078 mmol, 0.020 equiv) in toluene (2 mL). The flask was sealed, and the stirred mixture was heated at 80 °C for 2 h. The mixture was allowed to cool to RT and diluted with hexanes (40 mL) under N_2. After 2-3 h, in air, the solid was collected on a fritted funnel and washed with hexanes (2 x 30 mL) to afford tribenzopentaphene **2f** (3.35 g, 85%) as a pale-yellow solid. ^{1}H NMR (chloroform-*d*, 600 MHz): δ = 9.64 (s, 2H), 9.17 (s, 2H), 8.93 (s, 2H), 8.34 (s, 2H), 4.80 (s, 4H), 4.13 (s, 6H), 4.13 (s, 6H), 3.59 (s, 6H), 3.46 – 3.38 (m, 4H), 2.57 (t, *J* = 7.0 Hz, 4H), 1.95 (sext, *J* = 7.3 Hz, 4H), 1.77 (sext, *J* = 7.2 Hz, 4H), 1.17 (t, *J* = 7.4 Hz, 6H), 1.01 (t, *J* = 7.3 Hz, 6H); ^{13}C{^{1}H} NMR (chloroform-*d*, 151 MHz): δ = 144.67, 143.05, 136.58, 136.36, 134.43, 131.58, 130.00, 128.91, 128.52, 128.34, 127.28, 126.71, 126.04, 124.69, 123.17, 122.81,

117.90, 95.99, 80.21, 69.13, 61.18, 61.06, 58.96, 34.97, 25.85, 22.28, 21.90, 14.63, 13.83; MS-MALDI-TOF (m/z): $[M]^+$ calcd. for $C_{58}H_{58}Br_2O_6$, 1008.26; found, 1008.21.

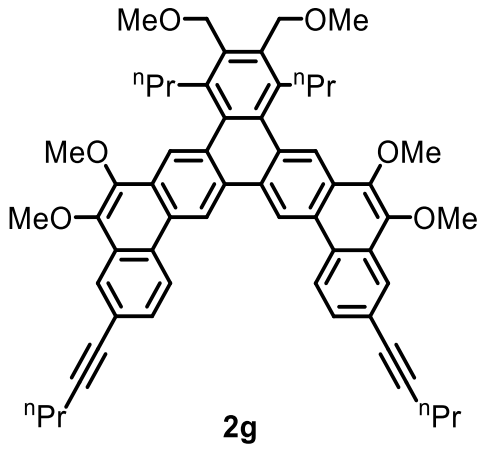

2g

5,6,13,14-tetramethoxy-9,10-bis(methoxymethyl)-3,16-di(pent-1-yn-1-yl)-8,11-dipropyltribenzo[a,h,o]pentaphene (2g). A 10 mL Schlenk tube was charged with dibromide **2f** (0.100 g, 0.0989 mmol, 1.0 equiv) and THF (2.0 mL), and the solution was cooled to –78 °C with a CO_2(s)/acetone bath. To this stirred solution was added *n*-butyllithium (1.6 M in hexanes, 0.14 mL, 0.22 mmol, 2.2 equiv) dropwise over ~5 min, and the resulting mixture was stirred for a further 20 min at –78 °C. Anhydrous HCl (2.0 M in ether, 0.15 mL, 0.30 mmol, 3.0 equiv) was then added dropwise over 2-3 min, the cold bath was removed, and saturated aqueous NH_4Cl (10 mL) was added. The mixture was extracted with CH_2Cl_2 (2 x 10 mL) and the combined organic layers were dried with $MgSO_4$, filtered, and concentrated by rotary evaporation to afford **2g** (0.083 g, 98%) as a yellow solid. ^{1}H NMR (chloroform-*d*, 500 MHz): δ = 9.77 (s, 2H), 8.95 (s, 2H), 8.94 (d, *J* = 8.4 Hz, 2H), 8.32 (d, *J* = 1.7 Hz, 2H), 7.77 (dd, *J* = 8.4, 1.7 Hz, 2H), 4.81 (s, 4H), 4.14 (s, 6H), 4.13 (s, 6H), 3.59 (s, 6H), 3.48 – 3.42 (m, 4H), 2.52 (t, *J* = 7.1 Hz, 4H), 1.95 (sext, *J* = 7.2 Hz, 4H), 1.74 (sext, *J* = 7.3 Hz, 4H), 1.14 (t, *J* = 7.4 Hz, 6H), 1.01 (t, *J* = 7.3 Hz, 6H); ^{13}C{^{1}H} NMR (chloroform-*d*, 101 MHz): δ = 144.59, 143.43, 136.49, 136.10, 134.44, 131.07, 129.93, 129.56, 129.04, 127.90, 127.77, 127.06, 125.58, 123.01, 122.85, 122.66, 117.68, 91.42, 81.40, 69.11, 61.09, 61.04, 58.87, 34.98, 25.82, 22.41, 21.73, 14.61, 13.79; MS-MALDI-TOF (m/z): $[M]^+$ calcd. for $C_{58}H_{60}O_6$, 852.44; found, 852.45.

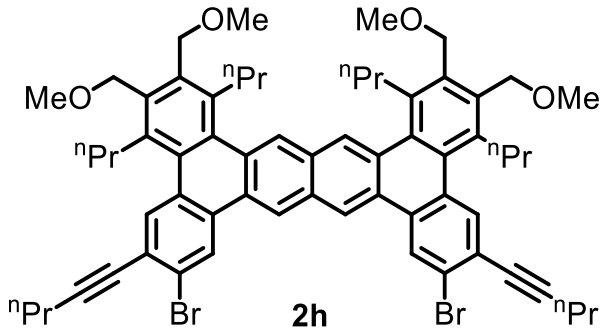

2h

7,12-dibromo-2,3,16,17-tetrakis(methoxymethyl)-6,13-di(pent-1-yn-1-yl)-1,4,15,18-tetrapropyltetrabenzo[a,c,j,l]tetracene (2h). To a stirred solution of $[Ir(COD)Cl]_2$ (0.031 g, 0.046 mmol, 0.03 equiv) in toluene (2 mL) was added (dropwise over ~1 min) a solution of dppe (0.037 g, 0.092 mmol, 0.06 equiv) in toluene (2 mL). This mixture was immediately added to a 150 mL flask

containing a solution of hexayne **1h** (1.28 g, 1.53 mmol, 1.0 equiv) and 1,4-dimethoxy-2-butyne (0.70 g, 6.1 mmol, 4.0 equiv) in toluene (26 mL). The flask was sealed with a Teflon stopper and the stirred reaction mixture was heated at 80 °C for 2 h. The mixture was allowed to cool to RT, then concentrated via rotary evaporation, and the residue was eluted through a plug of silica gel (40 g) with excess CH_2Cl_2 (until no more product was seen my TLC). The eluent was concentrated to ~10 mL, then MeOH (100 mL) was added. The resulting precipitate was collected on a fritted funnel, washed with MeOH (2 x 20 mL), and dried under high vacuum to afford **2h** (1.30 g, 80%) as a bright-yellow solid. ^{1}H NMR (chloroform-*d*, 500 MHz): δ = 8.96 (s, 2H), 8.76 (s, 2H), 8.56 (s, 2H), 8.08 (s, 2H), 4.74 (s, 4H), 4.72 (s, 4H), 3.57 (s, 6H), 3.56 (s, 6H), 3.42 – 3.34 (m, 4H), 3.29 – 3.20 (m, 4H), 2.51 (t, *J* = 6.9 Hz, 4H), 1.88 (sext, *J* = 7.4 Hz, 4H), 1.77 – 1.67 (m, 8H), 1.13 (t, *J* = 7.4 Hz, 6H), 1.00 (t, *J* = 7.3 Hz, 6H), 0.93 (t, *J* = 7.3 Hz, 6H); ^{13}C{^{1}H} NMR (chloroform-*d*, 151 MHz): δ = 136.46, 136.34, 136.30, 136.17, 134.36, 134.16, 133.00, 131.96, 130.83, 130.70, 130.53, 130.11, 129.23, 128.29, 127.60, 124.24, 123.67, 122.15, 95.67, 80.01, 69.03, 68.95, 58.97, 58.91, 34.80, 34.49, 25.91, 25.81, 22.26, 21.82, 14.80, 14.33, 13.72; MS-MALDI-TOF (m/z): $[M]^+$ calcd. for $C_{64}H_{70}Br_2O_4$, 1060.36; found, 1060.33.

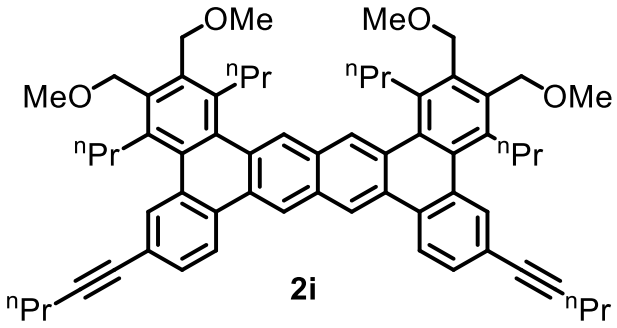

2i

2,3,16,17-tetrakis(methoxymethyl)-6,13-di(pent-1-yn-1-yl)-1,4,15,18-tetrapropyltetrabenzo[a,c,j,l]tetracene (2i). A 25 mL Schlenk tube was charged with dibromide **2h** (0.250 g, 0.235 mmol, 1.0 equiv) and THF (5 mL), and the solution was cooled to –78 °C with a CO_2(s)/acetone bath. To the stirred solution was added *n*-butyllithium (1.6 M in hexanes, 0.32 mL, 0.52 mmol, 2.2 equiv) dropwise over 7–10 min, and the resulting mixture was stirred for a further 5 min at –78 °C. Anhydrous HCl (2.0 M in ether, 0.35 mL, 0.71 mmol, 3.0 equiv) was then added dropwise over 2-3 min, the cold bath was removed, and saturated aqueous NH_4Cl (10 mL) was immediately added. The mixture was extracted with CH_2Cl_2 (2 x 10 mL) and the combined organic layers were dried with $MgSO_4$, filtered, and concentrated by rotary evaporation to afford **2i** (0.21 g, 99%) as a yellow solid, which was used without further purification. ^{1}H NMR (chloroform-*d,* 400 MHz, [c] = 48 mM): δ = 8.99 (s, 2H), 8.59 (s, 2H), 8.51 (d, *J* = 8.3 Hz, 2H), 8.08 (d, *J* = 1.6 Hz, 2H), 7.59 (dd, *J* = 8.3, 1.5 Hz, 2H), 4.77 (s, 4H), 4.75 (s, 4H), 3.58 (s, 6H), 3.57 (s, 6H), 3.46 – 3.36 (m, 4H), 3.36 – 3.27 (m, 4H), 2.46 (t, *J* = 7.0 Hz, 4H), 1.92 (sext, *J* = 7.6, 4H), 1.81 – 1.64 (m, 8H), 1.10 (t, *J* = 7.4 Hz, 9H), 1.03 (t, *J* = 7.3 Hz, 9H), 0.94 (t, *J* = 7.3 Hz, 9H); ^{13}C{^{1}H} NMR (chloroform-*d*, 101 MHz): δ = 136.39, 136.23, 135.97, 135.85, 134.51, 133.73, 132.75, 131.91, 130.60, 130.36, 130.35, 130.30, 130.27, 129.76, 128.19, 124.03, 122.47, 121.73, 91.01, 81.26, 69.08, 69.06, 58.92, 58.84, 34.86, 34.56, 25.93, 25.92, 22.41, 21.68, 14.83, 14.34, 13.70; HRMS-ESI (m/z): $[M]^+$ calcd. for $C_{64}H_{72}O_4$, 904.5431; found, 904.5422.

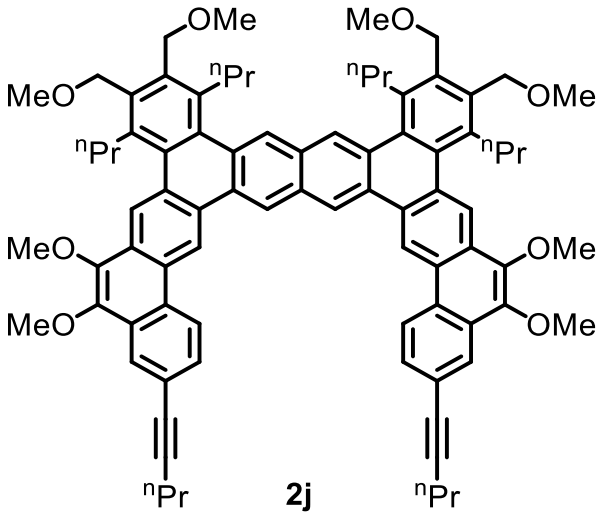

2j

5,6,19,20-tetramethoxy-9,10,15,16-tetrakis(methoxymethyl)-3,22-di(pent-1-yn-1-yl)-8,11,14,17-tetrapropyltribenzo[a,h,o]phenanthro[2,3-q]hexaphene (2j). *Procedure #1 (from hexayne **1j**):* A 25 mL Teflon-stoppered flask charged with hexayne **1j** (233 mg, 0.234 mmol, 1.0 equiv), 1,4-dimethoxy-2-butyne (107 mg, 0.936 mmol, 4.0 equiv), Ir(COD)(dppe)Cl (6.9 mg, 0.0094 mmol, 0.04 equiv), and toluene (4.7 mL). The flask was sealed, and the stirred mixture was heated at 80 °C for 2 h. In air, volatile materials were removed *via* rotary evaporation, then the residue was triturated with hexanes (10 mL) and solvents were removed again (to ensure complete removal of toluene). The resulting solid was dissolved in CH_2Cl_2 (~1 mL), then EtOH (30 mL) was added and the volume was reduced by to approximately 15 mL *via* rotary evaporation. The solid was collected on a fritted funnel, washed with MeOH (2 x 5 mL), and subjected to column chromatography (0–2% EtOAc in CH_2Cl_2), affording compound **2j** (201 mg, 70%) as a pale-yellow solid. Monitoring of a smaller-scale (0.1 x) reaction under identical conditions by ^{1}H NMR spectroscopy revealed that **2j** formed in 78% yield. *Procedure #2 (from dibromide **2k**):* A 50 mL Schlenk tube was charged with dibromide **2k** (0.440 g, 0.318 mmol, 1.0 equiv) and THF (7 mL), and the solution was cooled to –78 °C with a CO_2(s)/acetone bath. To the stirred solution was added *n*-butyllithium (1.64 M in hexanes, 0.43 mL, 0.70 mmol, 2.2 equiv) dropwise over ~5 min, and the resulting mixture was stirred for a further 20 min at –78 °C. Anhydrous HCl (2.0 M in ether, 0.48 mL, 0.95 mmol, 3.0 equiv) was then added dropwise over 2-3 min, the cold bath was removed, and saturated aqueous NH_4Cl (20 mL) was immediately added. The mixture was extracted with CH_2Cl_2 (2 x 15 mL) and the combined organic layers were dried with $MgSO_4$, filtered, and concentrated by rotary evaporation to afford **2j** (0.39 g, >99%) as a yellow solid, which was used without further purification. ^{1}H NMR (chloroform-*d,* 400 MHz): δ = 9.82 (s, 2H), 9.38 (s, 2H), 9.01 (d, *J* = 8.5 Hz, 2H), 8.90 (s, 2H), 8.59 (s, 2H), 8.34 (d, *J* = 1.8 Hz, 2H), 7.80 (dd, *J* = 8.5, 1.8 Hz, 1H), 4.81 (s, 4H), 4.79 (s, 4H), 4.15 (s, 6H), 4.14 (s, 6H), 3.61 (s, 6H), 3.60 (s, 6H), 3.53 – 3.39 (m, 8H), 2.53 (t, *J* = 7.0 Hz, 4H), 1.99 (sext, *J* = 7.6 Hz, 4H), 1.86 (sext, *J* = 7.7 Hz, 4H), 1.76 (sext, *J* = 7.2 Hz, 4H), 1.15 (t, *J* = 7.3 Hz, 6H), 1.05 (t, *J* = 7.2 Hz, 6H), 0.99 (t, *J* = 7.2 Hz, 6H); ^{13}C{^{1}H} NMR (chloroform-*d,* 151 MHz): δ = 144.54, 143.40, 136.50, 136.37, 135.98, 135.88, 134.97, 134.49, 131.19, 130.98, 130.73, 130.62, 130.57, 129.97, 129.44, 129.03, 128.41, 128.09, 127.76, 127.15, 125.41, 123.02, 122.78, 122.49, 121.98, 118.09, 91.41, 81.25, 69.03, 68.96, 61.02, 60.94, 58.71, 58.71, 34.80, 34.73, 25.89, 25.70, 22.28, 21.58, 14.58, 14.47, 13.63; MS-MALDI-TOF (m/z): $[M]^+$ calcd. for $C_{84}H_{88}O_8$, 1224.65; found, 1224.63.

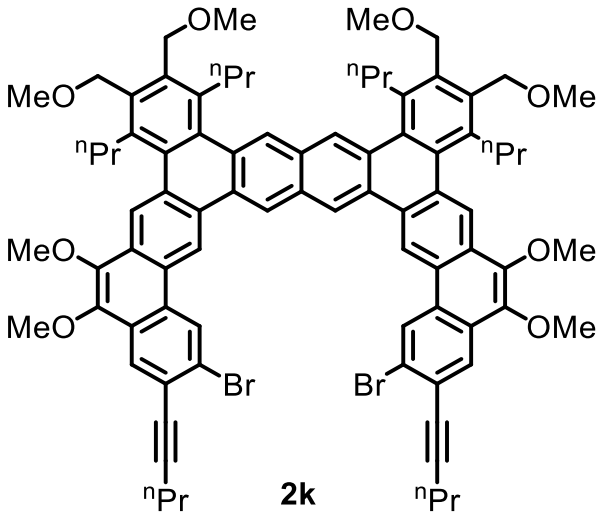

2k

2,23-dibromo-5,6,19,20-tetramethoxy-9,10,15,16-tetrakis(methoxymethyl)-3,22-di(pent-1-yn-1-yl)-8,11,14,17-tetrapropyltribenzo[a,h,o]phenanthro[2,3-q]hexaphene (2k). A 100 mL Teflon-stoppered flask charged with hexayne **1k** (550 mg, 0.476 mmol, 1.0 equiv), 1,4-dimethoxy-2-butyne (217 mg, 1.90 mmol, 4.0 equiv), Ir(COD)(dppe)Cl (17.5 mg, 0.0238 mmol, 0.05 equiv), and benzene (9.5 mL). The flask was sealed, and the stirred mixture was heated at 80 °C for 5 h. The mixture was allowed to cool to RT, then hexanes (10 mL) was added. After 3 h, the precipitate was collected by filtration and washed with a 1:1 mixture of benzene/hexanes (2 x 4 mL) and hexanes (10 mL) to afford pure **2k** (480 mg, 73%) as a yellow solid. Monitoring of a smaller-scale (0.1 x) reaction under identical conditions by ^{1}H NMR spectroscopy revealed that **2k** formed in 89% yield. It is also notable that the yield was essentially unchanged after 2 and 10 h of heating. ^{1}H NMR (chloroform-*d*, 600 MHz): δ = 9.74 (s, 2H), 9.48 (s, 2H), 9.27 (s, 2H), 8.88 (s, 2H), 8.59 (s, 2H), 8.34 (s, 2H), 4.81 (s, 4H), 4.79 (s, 4H), 4.13 (s, 6H), 4.13 (s, 6H), 3.61 (s, 6H), 3.60 (s, 6H), 3.51 – 3.46 (m, 4H), 3.46 – 3.40 (m, 4H), 2.58 (t, *J* = 7.0 Hz, 4H), 1.99 (sext, *J* = 7.2 Hz, 4H), 1.87 (sext, *J* = 6.8 Hz, 4H), 1.78 (sext, *J* = 7.1 Hz, 4H), 1.19 (t, *J* = 7.3 Hz, 6H), 1.05 (t, *J* = 7.2 Hz, 6H), 1.00 (t, *J* = 7.3 Hz, 6H); ^{13}C{^{1}H} NMR (chloroform-*d*, 151 MHz): δ = 144.75, 143.06, 136.64, 136.48, 136.38, 136.16, 135.19, 134.46, 131.83, 130.94, 130.90, 130.76, 130.70, 130.36, 129.00, 128.55, 128.52, 128.51, 127.22, 126.71, 126.17, 124.60, 123.23, 122.73, 122.34, 118.30, 95.93, 80.21, 69.16, 69.09, 61.16, 61.03, 58.93, 58.90, 34.98, 34.88, 26.02, 25.83, 22.28, 21.88, 14.79, 14.68, 13.83; MS-MALDI-TOF (m/z): $[M]^{+}$ calcd. for $C_{84}H_{86}Br_2O_8$, 1380.47; found, 1380.44.

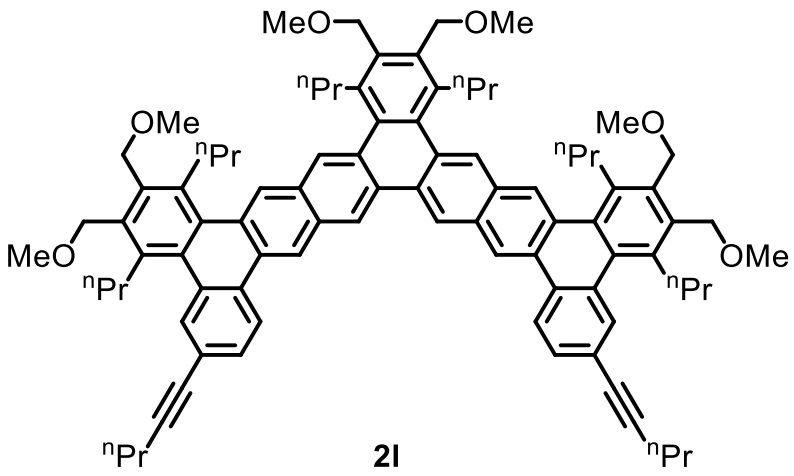

2l

Alkynylated PAH (2l). A 50 mL Teflon-stoppered flask was charged with octayne **1l** (313 mg, 0.335 mmol, 1.0 equiv), 1,4-dimethoxy-2-butyne (229 mg, 2.01 mmol, 6.0 equiv), and toluene (8 mL). To this flask was added a solution of Ir(COD)(dppe)Cl (14.8 mg, 0.0201 mmol, 0.06 equiv) in toluene (2.0 mL). The flask was sealed, and the stirred mixture was heated at 80 °C for 2 h. In air, volatile materials were removed *via* rotary evaporation, then the residue was subjected to column chromatography (0–2% EtOAc in CH_2Cl_2), affording PAH **2l** (305 mg, 74%) as a bright-yellow solid. ^{1}H NMR (chloroform-*d,* 400 MHz, [c] = 8.0 mM): δ = 9.20 (s, 2H), 9.05 (s, 2H), 8.58 (s, 2H), 8.55 (d, *J* = 8.4 Hz, 2H), 8.49 (s, 2H), 8.09 (d, *J* = 1.6 Hz, 2H), 7.62 (dd, *J* = 8.2, 1.5 Hz, 2H), 4.77 (s, 4H), 4.77 (s, 4H), 4.75 (s, 4H), 3.60 (s, 6H), 3.58 (s, 6H), 3.57 (s, 6H), 3.48 – 3.37 (m, 8H), 3.36 – 3.28 (m, 4H), 2.47 (t, *J* = 7.0 Hz, 4H), 1.97 – 1.82 (m, 8H), 1.81 – 1.64 (m, 8H), 1.11 (t, *J* = 7.3 Hz, 6H), 1.03 (t, *J* = 6.4 Hz, 6H), 1.00 (t, *J* = 6.4 Hz, 6H), 0.94 (t, *J* = 7.3 Hz, 6H); ^{13}C{^{1}H} NMR (chloroform-*d*, 101 MHz): δ = 136.44, 136.36, 136.22, 136.15, 135.93, 135.81, 135.22, 134.48, 133.70, 132.73, 131.87, 131.12, 130.97, 130.85, 130.59, 130.53, 130.35, 130.30, 129.77, 128.50, 128.16, 123.98, 122.44, 122.42, 121.77, 90.99, 81.26, 69.09, 69.06, 69.03, 58.92, 58.90, 58.83, 34.85, 34.83, 34.54, 25.97, 25.91, 25.89, 22.39, 21.66, 14.83, 14.81, 14.32, 13.69; MS-MALDI-TOF (m/z): $[M]^+$ calcd. for $C_{90}H_{100}O_6$, 1276.75; found, 1276.72.

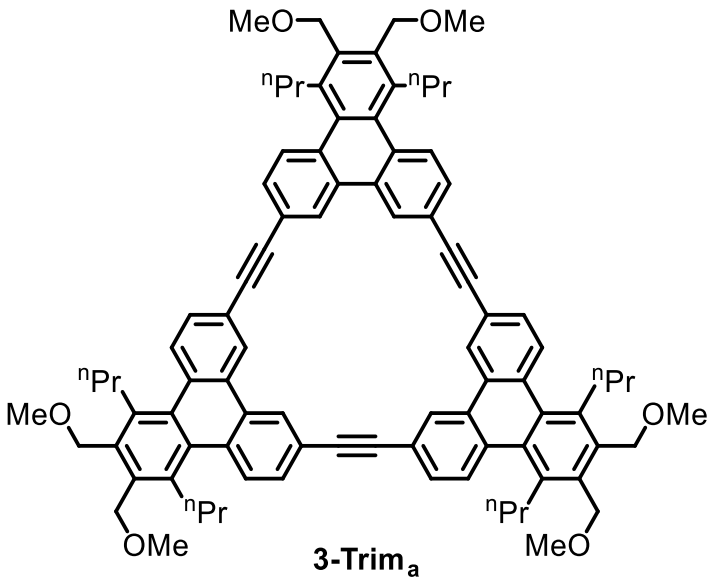

3-Trim$_a$

Small Trimeric Macrocycle (3-Trim$_a$). A 25 mL Teflon-stoppered flask equipped with magnetic stirbar was charged with PAH **2c** (117 mg, 0.220 mmol, 1.0 equiv), powdered 5 Å molecular sieves* (440 mg), and toluene (2 mL). To this flask was added a mixture of **Mo-2** (8.5 mg, 0.0110 mmol, 0.05 equiv), Ph_3SiOH (18.2 mg, 0.066 mmol, 0.30 equiv), and toluene (2.4 mL), which was prepared by addition of the latter to a mixture of the two solids. The flask was sealed, and the stirred mixture was heated at 80 °C for 16 h. The suspension, in addition to silica gel (1 g), was transferred to a round-bottomed flask, and volatile materials were removed *via* rotary evaporation. The powder was loaded onto a plug of silica gel (10 g), which was eluted with 10:1 CH_2Cl_2:EtOAc (100 mL, or until no further product was seen by TLC). The eluant was concentrated *via* rotary evaporation, the residue was dissolved in CH_2Cl_2 (1 mL), and MeOH (5 mL) was added.** The precipitate was collected by filtration and washed with MeOH (2 x 5 mL) to afford*** **3-Trim$_a$** (82 mg, 88%) as a beige solid. ^{1}H NMR (chloroform-*d,* 600 MHz): δ = 8.99 (d, *J* = 1.8 Hz, 6H), 8.13 (d, *J* = 8.4 Hz, 6H), 7.70 (dd, *J* = 8.4, 1.8 Hz, 6H), 4.75 (s, 12H), 3.56 (s, 18H), 3.38 – 3.26 (m, 12H), 1.74 (sext, *J* = 7.5 Hz, 12H), 0.95 (t, *J* = 7.3 Hz, 18H); ^{13}C{^{1}H} NMR (chloroform-*d*, 101 MHz): δ = 136.58, 135.87, 133.47, 131.20, 130.32, 129.03, 128.79, 127.48, 121.51, 90.90, 69.05, 58.93, 34.86, 25.90, 14.60; MS-MALDI-TOF (m/z): $[M]^+$ calcd. for $C_{90}H_{90}O_6$, 1266.67; found, 1266.63.

*See general section (above) for important details on the source of these molecular sieves.

**The purpose of this step is to remove Ph_3SiOH.

***See general section for details on optimal recovery of this solids.

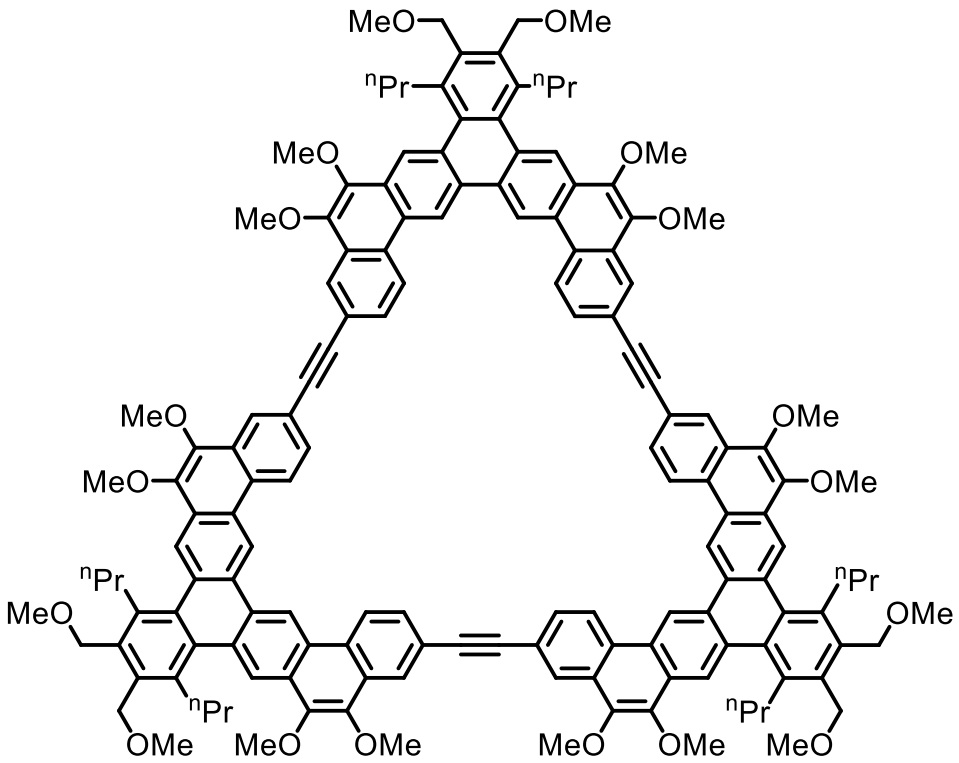

3-Trim$_b$

Medium-Sized Trimeric Macrocycle (3-Trim$_b$). A 50 mL Teflon-stoppered flask equipped with magnetic stirbar was charged with PAH **2g** (100 mg, 0.117 mmol, 1.0 equiv), powdered 5 Å molecular sieves (234 mg),* and 1,2-dichlorobenzene (2.0 mL). To this flask was added a mixture of **Mo-2** (9.0 mg, 0.0117 mmol, 0.10 equiv), Ph_3SiOH (19.4 mg, 0.0702 mmol, 0.60 equiv), and 1,2-dichlorobenzene (2.7 mL), which was prepared by addition of the latter to a mixture of the two solids. The flask was sealed, and the stirred mixture was heated at 80 °C for 16 h. After heating, the reaction mixture was cooled to RT, diluted with CH_2Cl_2 (40 mL), and directly loaded onto a silica gel column (20 g). The column was eluted with CH_2Cl_2 (~150 mL,** to ensure complete removal of 1,2-dichlorobenzene) and 10–20% EtOAc in CH_2Cl_2. The yield of **3-Trim$_b$**, a pale-yellow powder, was 75 mg (86%). ^{1}H NMR (chloroform-*d,* 400 MHz, [c] = 1.9 mM): δ = 9.78 (s, 6H), 9.06 (d, *J* = 8.4 Hz, 6H), 8.91 (s, 6H), 8.36 (s, 6H), 8.11 (dd, *J* = 8.3, 1.3 Hz, 6H), 4.83 (s, 12H), 4.14 (s, 18H), 4.12 (s, 18H), 3.64 (s, 18H), 3.51 – 3.30 (m, 12H), 2.10 – 1.96 (m, 12H), 1.09 (t, *J* = 7.2 Hz, 18H); ^{13}C{^{1}H} NMR (chloroform-*d,* 176 MHz): δ = 144.07, 143.10, 136.63, 136.11, 134.41, 130.71, 129.47, 129.40, 129.36, 128.01, 127.47, 126.76, 124.91, 122.94, 122.24, 121.88, 117.38, 91.40, 69.20, 60.83, 60.76, 58.87, 35.19, 25.85, 14.87; MS-MALDI-TOF (m/z): $[M]^+$ calcd. for $C_{150}H_{138}O_{18}$, 2226.99; found, 2226.98.

*See general section (above) for important details on the source of these molecular sieves.

**Note that all eluate was during the initial CH_2Cl_2 elution was colorless and was thus discarded. If the yellow band begins to elute, it likely contains desired product and thus should be collected.

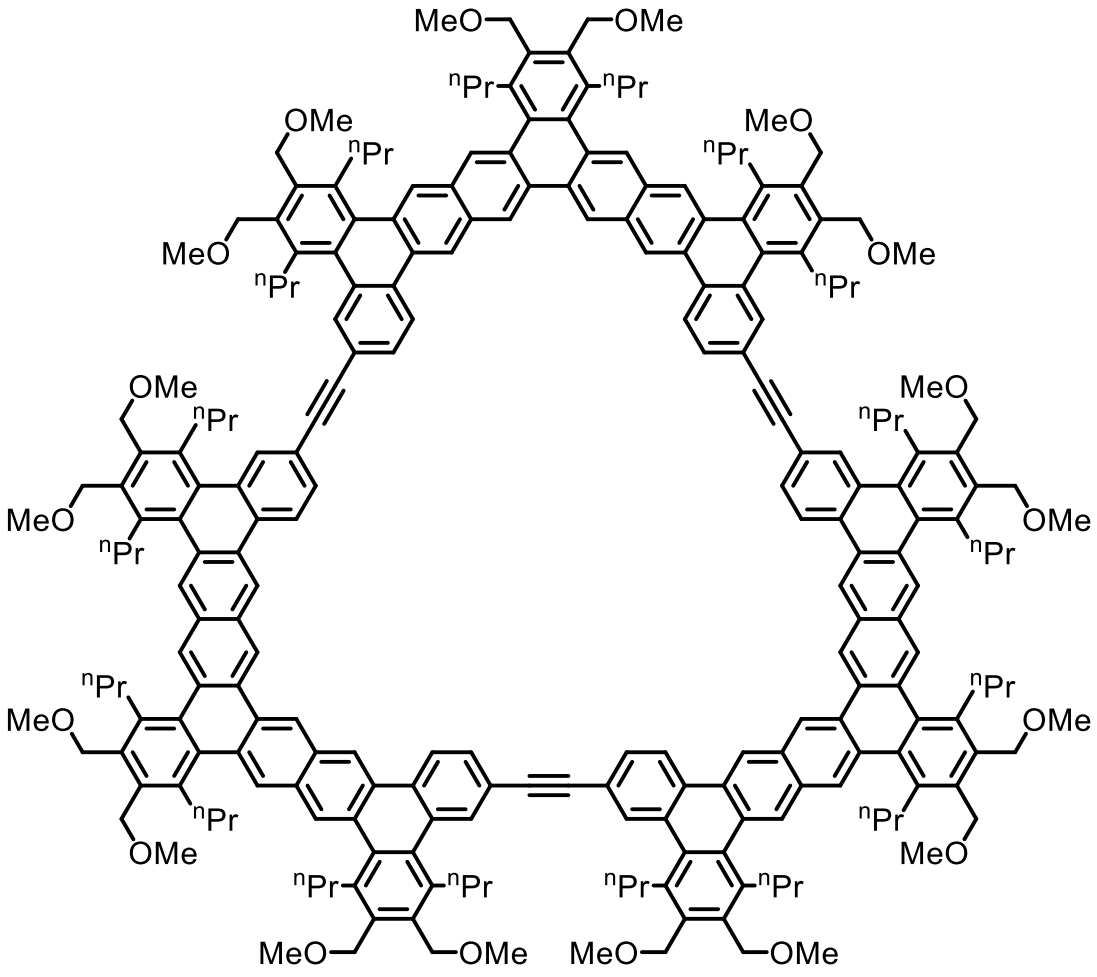

Large Trimeric Macrocycle (3-Trim$_c$). This compound was prepared by the same procedure as **3-Trim$_b$**, with the following quantities and noted differences: PAH **2l** (101 mg, 0.0790 mmol, 1.0 equiv), **Mo-2** (6.1 mg, 0.0079, 0.10 equiv), Ph_3SiOH (13.1 mg, 0.0474 mmol, 0.60 equiv), powdered 5 Å molecular sieves (158 mg), and 1,2-dichlorobenzene (9.0 mL). After heating, the reaction mixture was cooled to RT and directly loaded onto a silica gel column (20 g), which was eluted with CH_2Cl_2 (~200 mL,* to ensure complete removal of 1,2-dichlorobenzene) and 10–30% EtOAc in CH_2Cl_2. The yield of **3-Trim$_c$**, a bright-yellow powder, was 68 mg (74%). ^{1}H NMR (chloroform-*d,* 400 MHz): δ = 9.32 (s, 6H), 9.18 (s, 6H), 8.74 (d, *J* = 8.6 Hz, 6H), 8.64 (s, 6H), 8.55 (s, 6H), 8.29 (s, 6H), 7.94 (dd, *J* = 8.1, 1.0 Hz, 6H), 4.82 (s, 12H), 4.82 (s, 12H), 4.80 (s, 12H), 3.62 (s, 18H), 3.62 (s, 18H), 3.61 (s, 18H), 3.53 – 3.37 (m, 36H), 2.04 – 1.75 (m, 36H), 1.07 (t, *J* = 7.2 Hz, 18H), 1.04 (t, *J* = 7.2 Hz, 18H), 1.03 (t, *J* = 7.2 Hz, 18H); ^{13}C{^{1}H} NMR (chloroform-*d*, 101 MHz): δ = 136.63, 136.61, 136.44, 136.23, 136.12, 135.95, 135.14, 134.57, 133.55, 131.95, 131.69, 131.25, 130.99, 130.95, 130.88, 130.81, 130.53, 130.38, 130.13, 128.34, 128.08, 124.21, 122.48, 122.11, 121.74, 91.10, 69.17, 69.13, 69.11, 58.94, 58.91, 58.86, 34.95, 34.88, 34.74, 26.00, 25.95, 25.92, 14.84, 14.82, 14.50; MS-MALDI-TOF (m/z): $[M]^+$ calcd. for $C_{246}H_{258}O_{18}$, 3499.93; found, 3499.95.

*Note that all eluate was during the initial CH_2Cl_2 elution was colorless and was thus discarded. If the yellow band begins to elute, it likely contains desired product and thus should be collected.

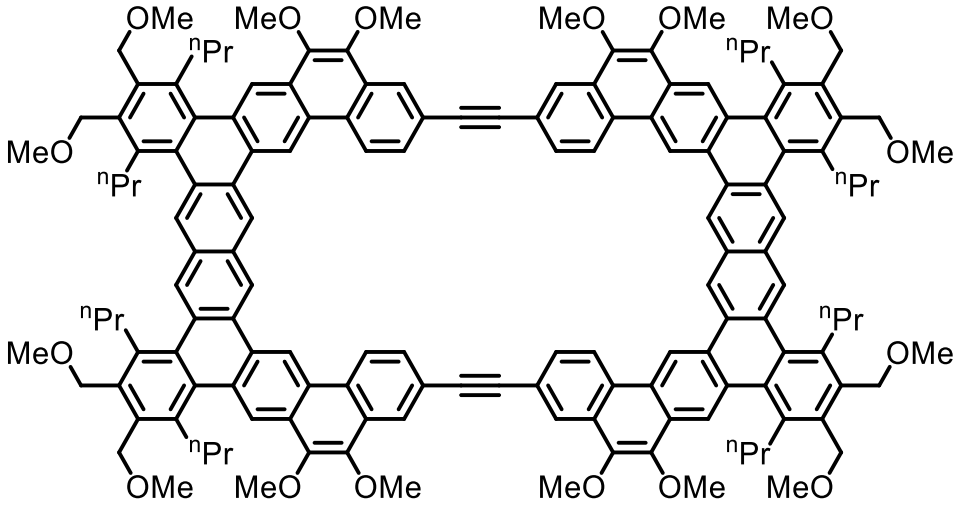

3-Dim

Dimeric Macrocycle (3-Dim). This compound was prepared by the same procedure as **3-Trim$_b$**, with the following quantities and noted differences: PAH **2j** (100 mg, 0.0816 mmol, 1.0 equiv), **Mo-2** (6.3 mg, 0.0082 mmol, 0.10 equiv), Ph_3SiOH (13.5 mg, 0.049 mmol, 0.60 equiv), powdered 5 Å molecular sieves* (160 mg), and 1,2-dichlorobenzene (3.3 mL). After heating, MeOH (20 mL) was added, the suspension was filtered, and the solids were washed with MeOH (2 x 5 mL). The solid was suspended in CH_2Cl_2 (50 mL), the mixture was stirred vigorously for 30 min and filtered through a plug of silica gel (5 g). The plug was flushed with 1:1 CH_2Cl_2:EtOAc (50 mL) and the filtrate was concentrated *via* rotary evaporation. The residue was suspended in benzene (3–4 mL), then the suspension was stirred vigorously for 1 h and filtered. The solid was washed with benzene (1 mL) and hexanes (3 mL) to afford* **3-Dim** (76 mg, 84%) as a yellow solid. ^{1}H NMR (chloroform-*d,* 500 MHz, [c] = 1.5 mM): δ = 9.94 (s, 4H), 9.51 (s, 4H), 9.23 (s, 4H), 8.92 (s, 4H), 8.61 (s, 4H), 8.53 (s, 4H), 8.24 (s, 4H), 4.84 (s, 8H), 4.81 (s, 8H), 4.17 (s, 12H), 4.16 (s, 12H), 3.64 (s, 12H), 3.63 (s, 12H), 3.57 – 3.36 (m, 16H), 2.09 – 1.97 (m, 8H), 1.97 – 1.85 (m, 8H), 1.09 (t, *J* = 7 Hz, 12H), 1.05 (t, *J* = 7 Hz, 12H); ^{13}C{^{1}H} NMR (chloroform-*d*, 151 MHz): δ = 144.83, 143.79, 136.97, 136.78, 136.54, 136.40, 135.24, 134.70, 131.60, 131.01, 130.93, 130.90, 130.82, 130.17, 130.08, 130.05, 128.61, 128.53, 128.41, 127.37, 125.13, 123.60, 122.68, 122.31, 122.13, 118.24, 91.86, 69.44, 69.38, 61.10, 61.05, 58.76, 58.76, 35.14, 35.07, 26.13, 25.88, 14.80, 14.72; MS-MALDI-TOF (m/z): $[M]^+$ calcd. for $C_{152}H_{148}O_{16}$, 2229.08; found, 2229.06.

*For optimal mass recovery, the solid was transferred to a 20 mL vial with the aid of CH_2Cl_2, which was then removed *via* rotary evaporation.

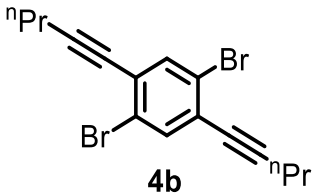

4b

1,4-dibromo-2,5-di(pent-1-yn-1-yl)benzene (4b). A 250 mL Schlenk flask with Teflon stopper was charged with **S1** (10.0 g, 20.5 mmol, 1.0 equiv), $Pd(PPh_3)_4$ (0.36 g, 0.31 mmol, 0.015 equiv), and CuI (0.20 g, 1.03 mmol, 0.05 equiv), then the flask was evacuated and refilled with N_2. To this flask was added an N_2-sparged mixture of THF (28 mL) and triethylamine (14 mL), followed by 1-pentyne (3.07 g, 45.1 mmol, 2.2 equiv). The mixture was stirred at RT for 16 h, then diluted with hexanes (150 mL), and filtered. The filter cake was rinsed with hexanes (50 mL) and solvents were removed from the filtrate *via* rotary evaporation.* The residue was purified by column chromatography (100% hexanes) to afford **4b** (6.77 g, 90%) as a white solid. ^{1}H NMR (chloroform-*d,* 400 MHz): δ = 7.59 (s, 2H), 2.44 (t, *J* = 7.0 Hz, 4H), 1.65 (q, *J* = 7.2 Hz, 4H), 1.07 (t, *J* = 7.4 Hz, 6H); ^{13}C{^{1}H} NMR (chloroform-*d,* 101 MHz): δ = 136.16, 126.59, 123.59, 98.12, 78.55, 22.04, 21.74, 13.69; HRMS-EI (m/z): $[M]^+$ calcd. for $C_{16}H_{16}Br_2$, 365.9619; found, 365.9613.

*To ensure complete removal of THF and triethylamine, which can adversely affect the separation in subsequent column chromatography, the residue obtained after the first concentration was dissolved in hexanes (30 mL) and solvents were removed again.

NMR Spectra

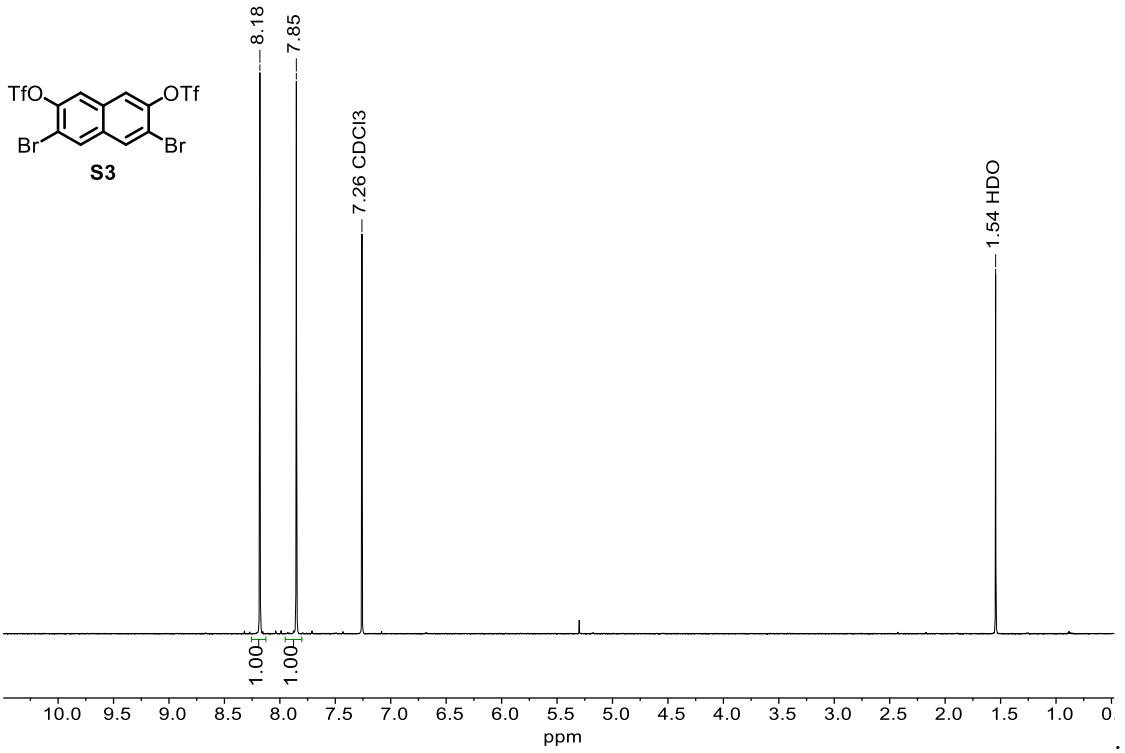

Figure S3. ^{1}H NMR Spectrum (500 MHz, chloroform-*d*) of **S3**.

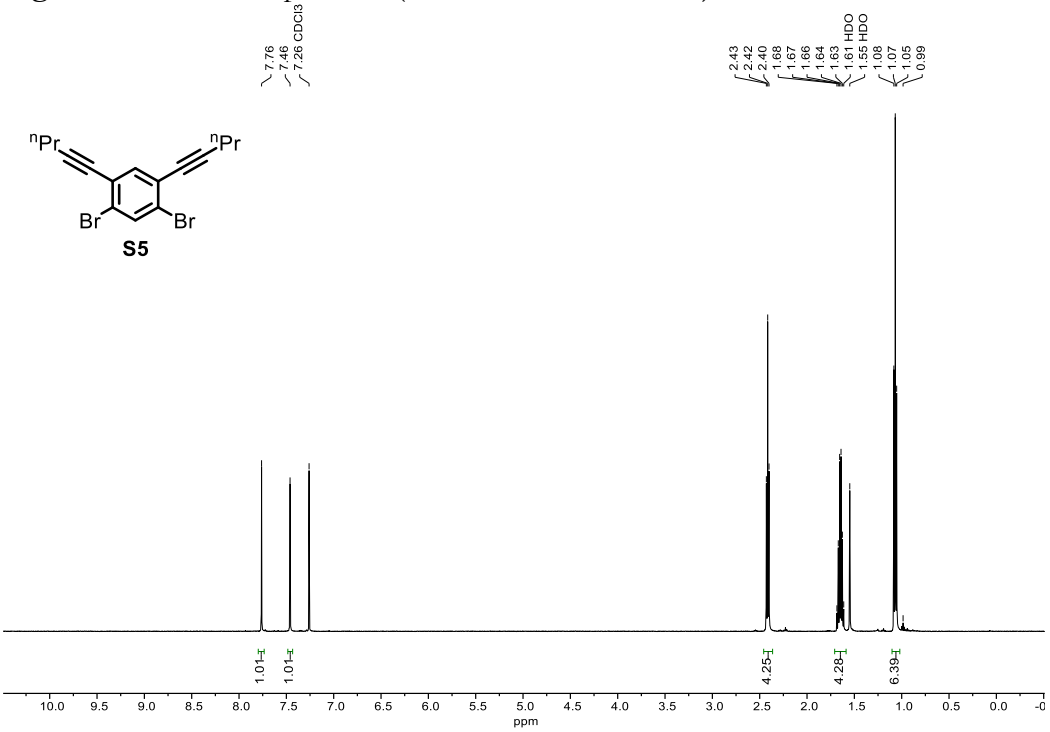

Figure S4. ^{1}H NMR Spectrum (500 MHz, chloroform-*d*) of **S5**.

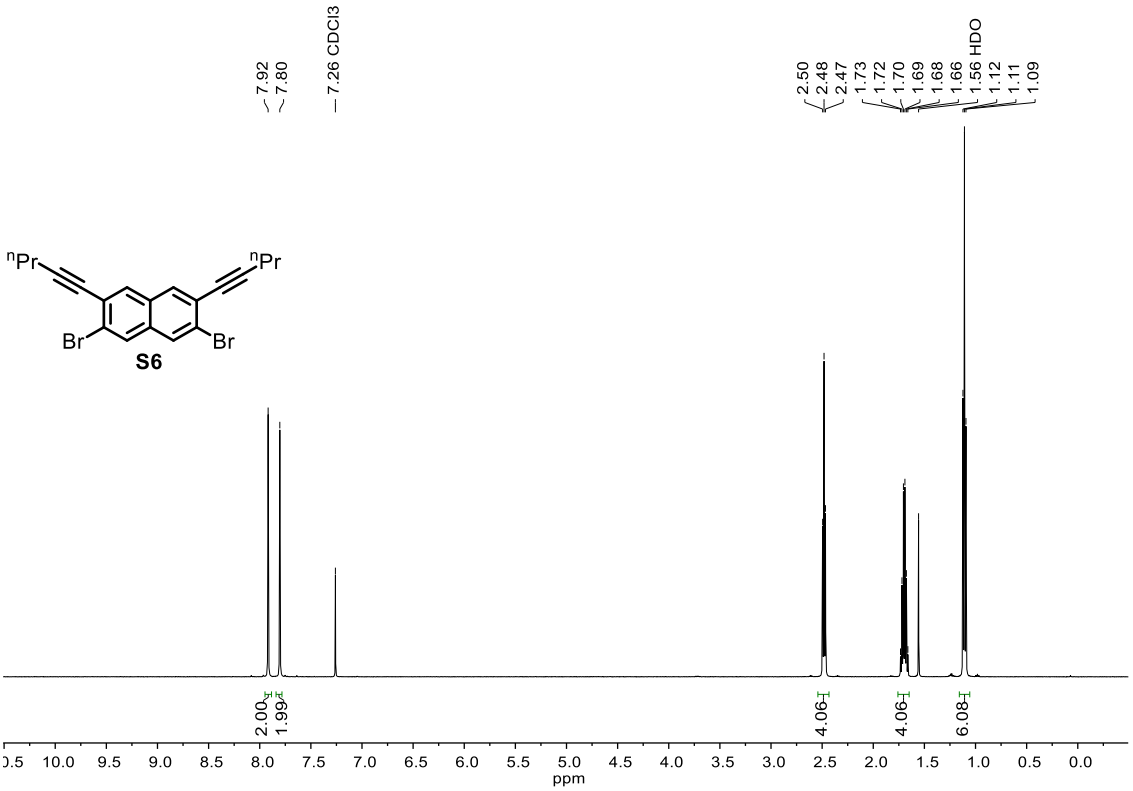

Figure S5. ^{1}H NMR Spectrum (500 MHz, chloroform-*d*) of **S6**.

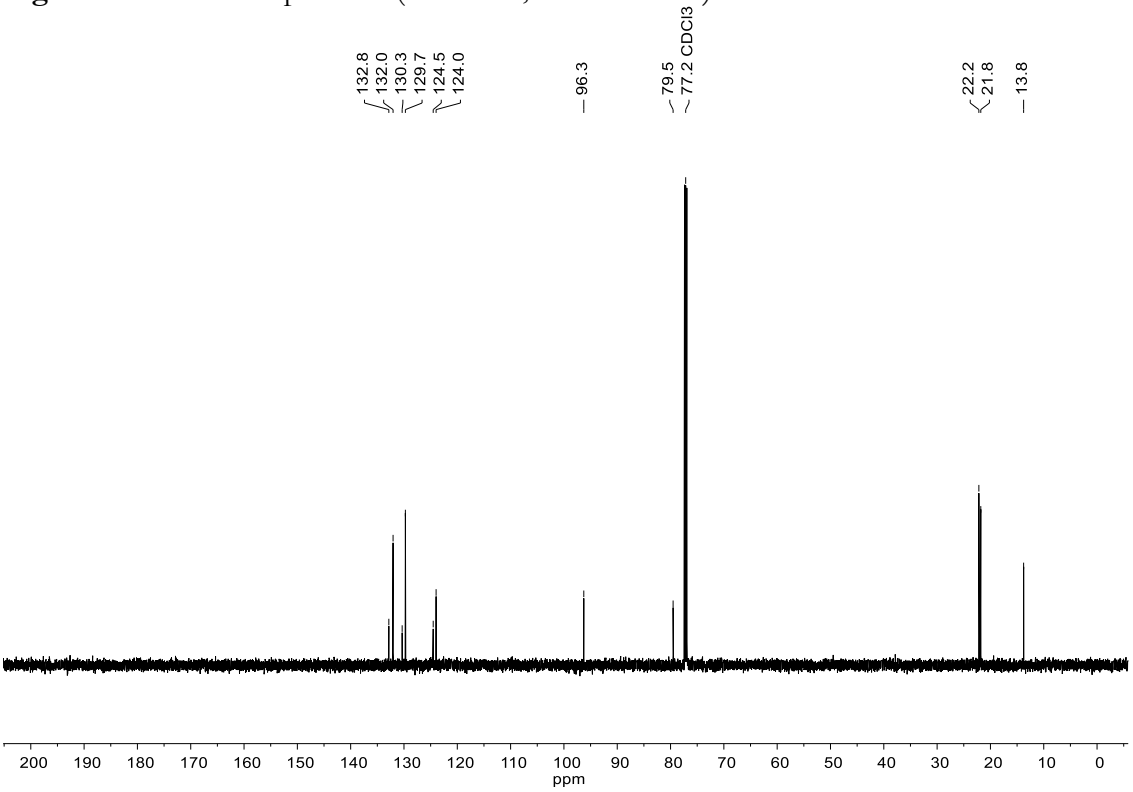

Figure S6. ^{13}C{^{1}H} NMR Spectrum (151 MHz, chloroform-*d*) of **S6**.

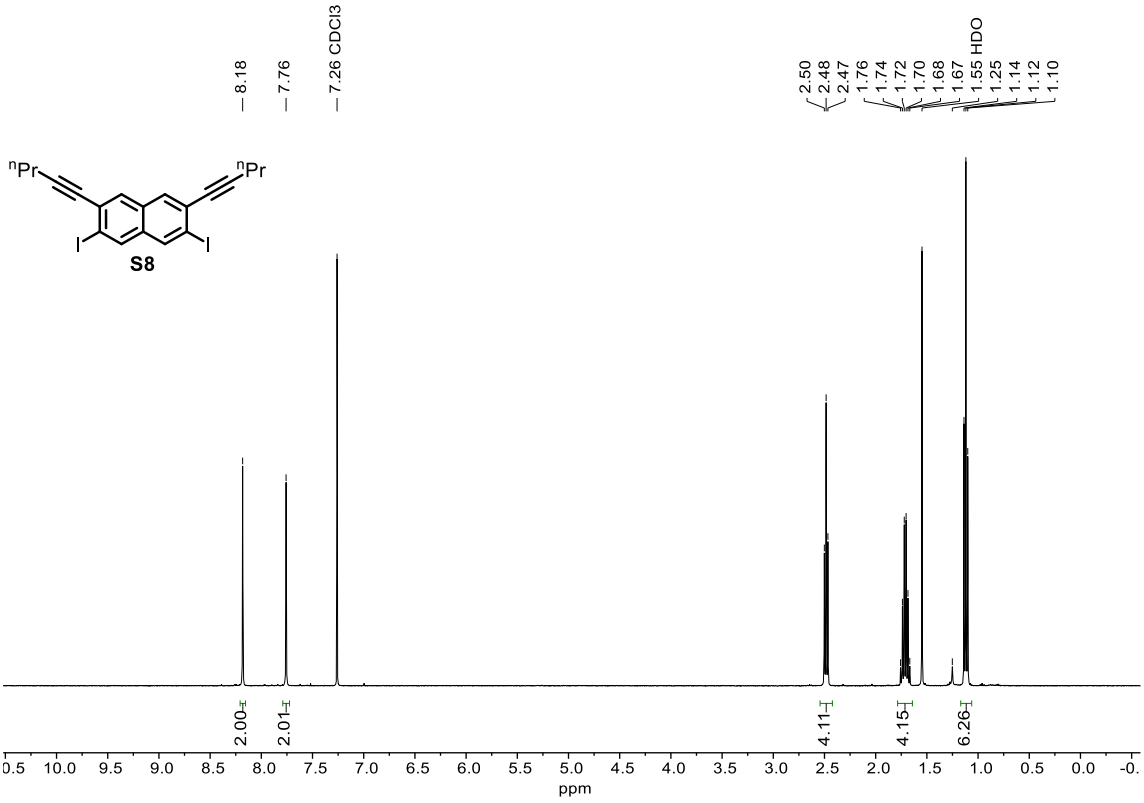

Figure S7. ^{1}H NMR Spectrum (400 MHz, chloroform-*d*) of **S8**.

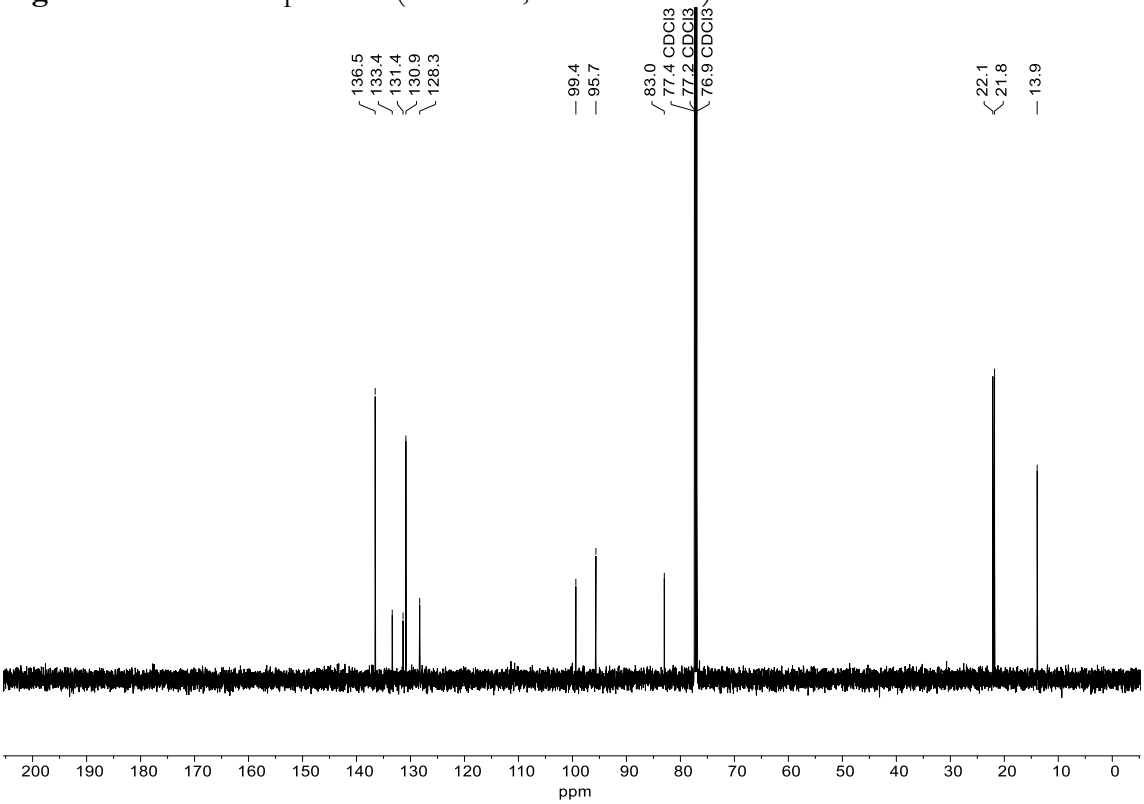

Figure S8. ^{13}C{^{1}H} NMR Spectrum (151 MHz, chloroform-*d*) of **S8**.

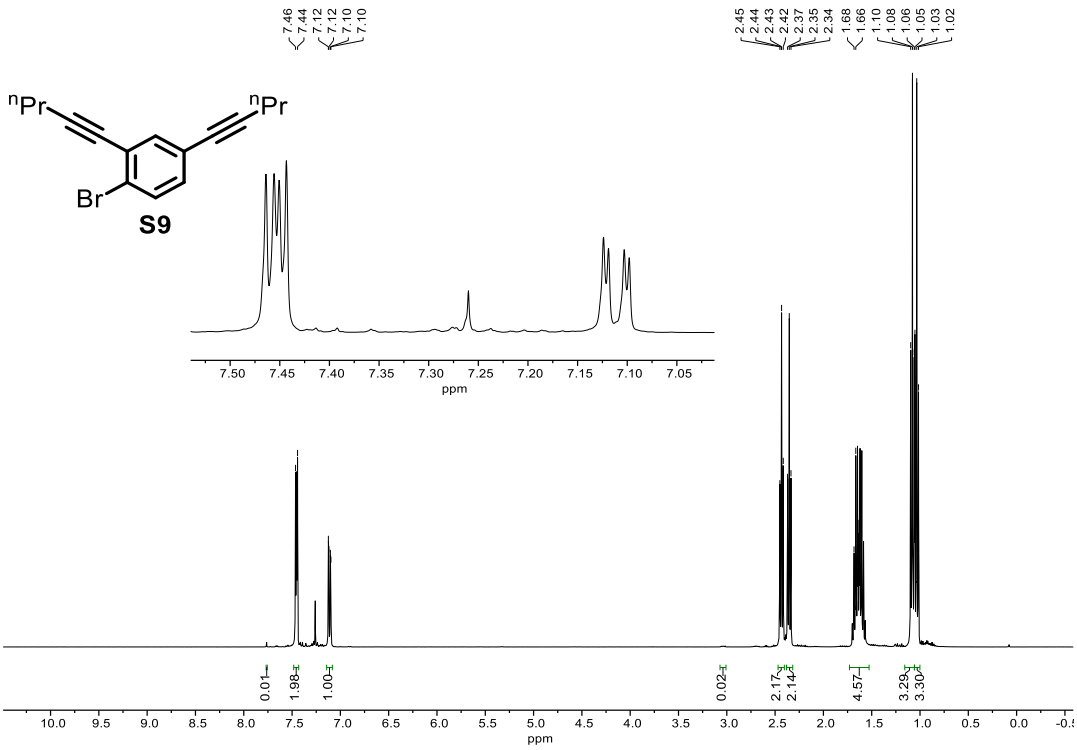

Figure S9. ^{1}H NMR Spectrum (400 MHz, chloroform-*d*) of **S9**.

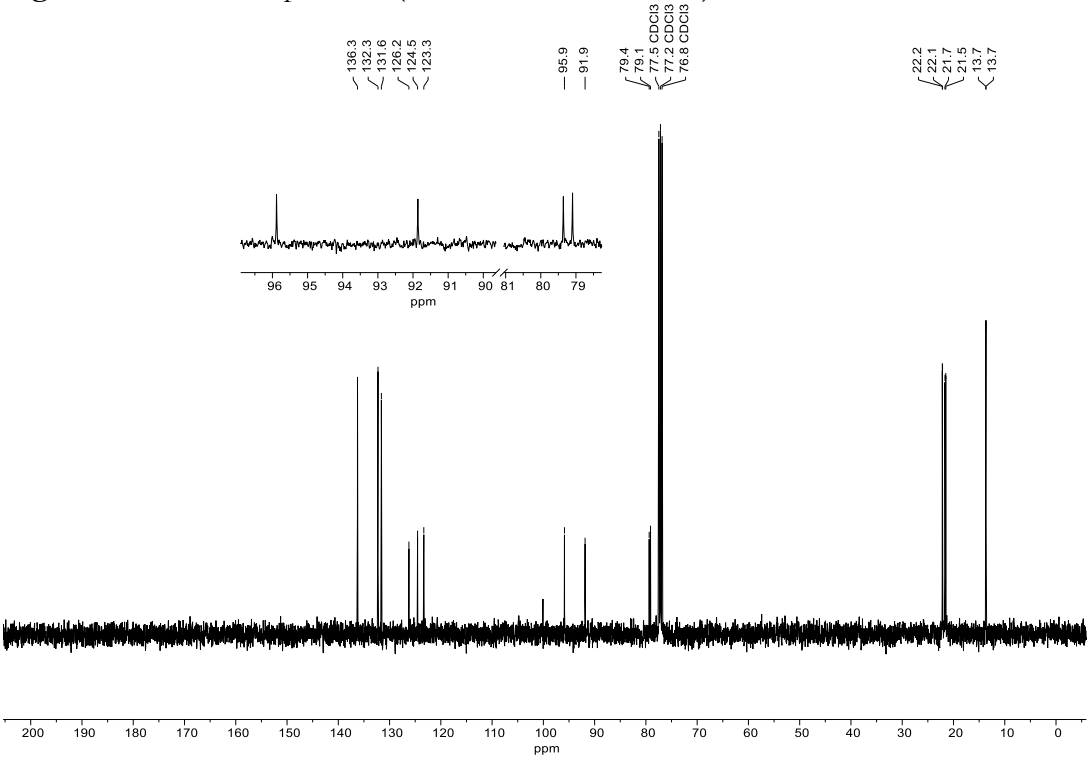

Figure S10. ^{13}C{^{1}H} NMR Spectrum (101 MHz, chloroform-*d*) of **S9**.

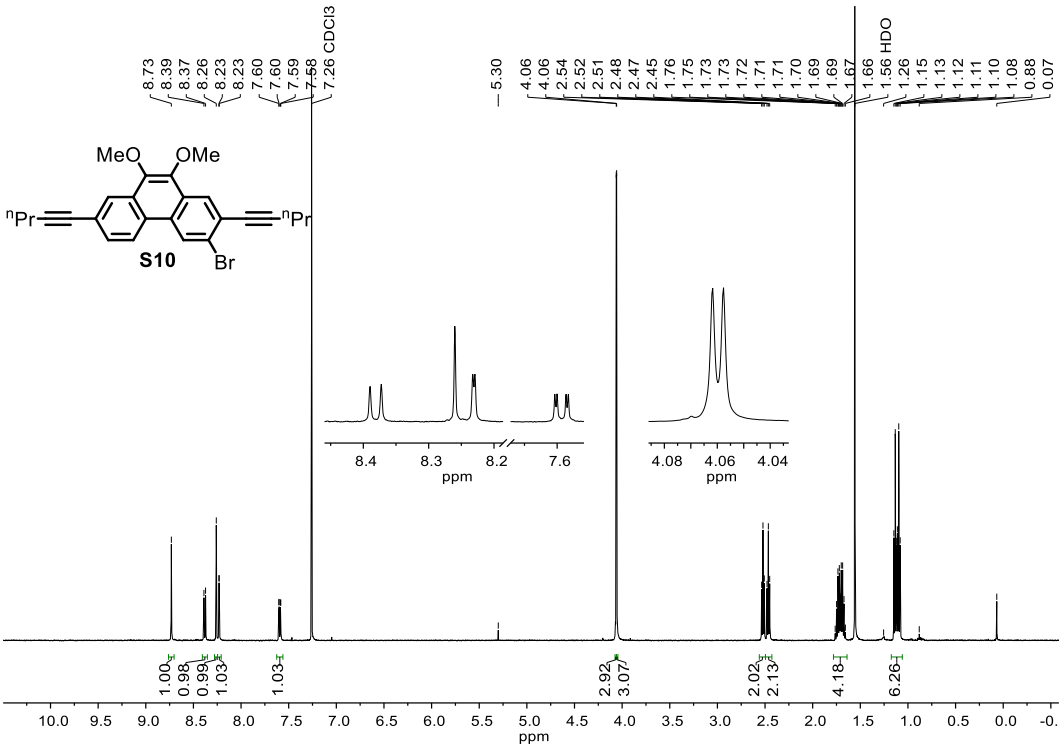

Figure S11. [1]H NMR Spectrum (500 MHz, chloroform-*d*) of purified **S10**.

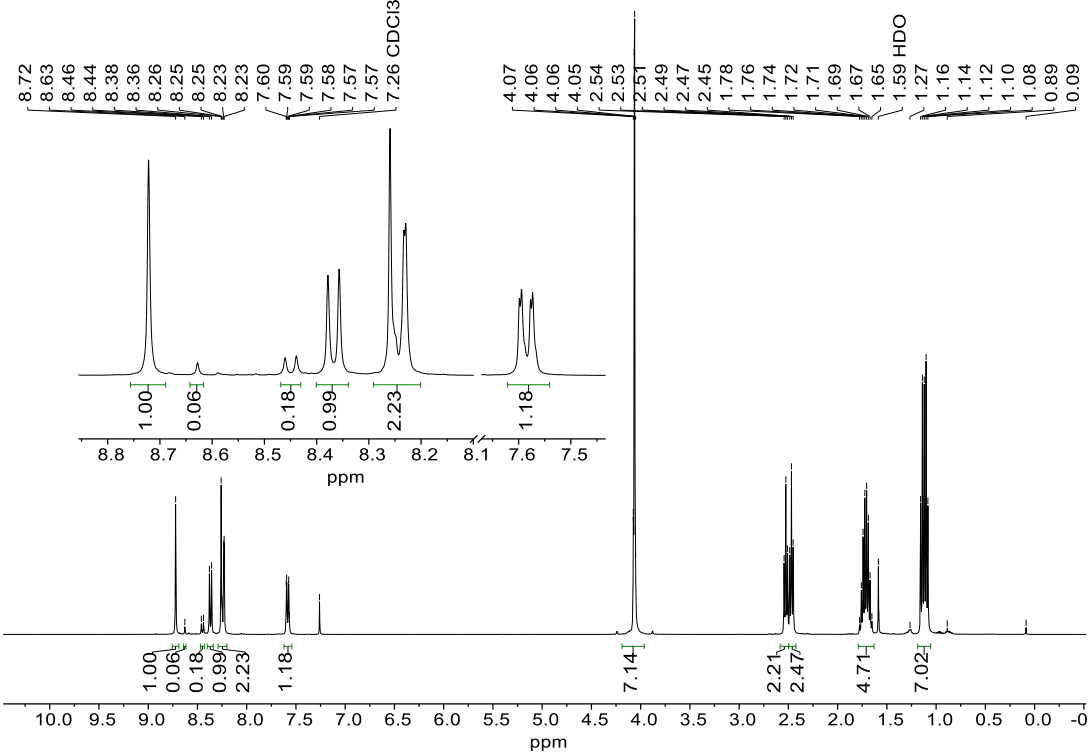

Figure S12. [1]H NMR Spectrum (101 MHz, chloroform-*d*) of the mixture of starting **S7**, **S10**, and doubly protodebrominated **S7** (molar ratio: 0.03 : 1.0 : 0.09). This mixture was used without purification in the subsequent cross-coupling reaction.

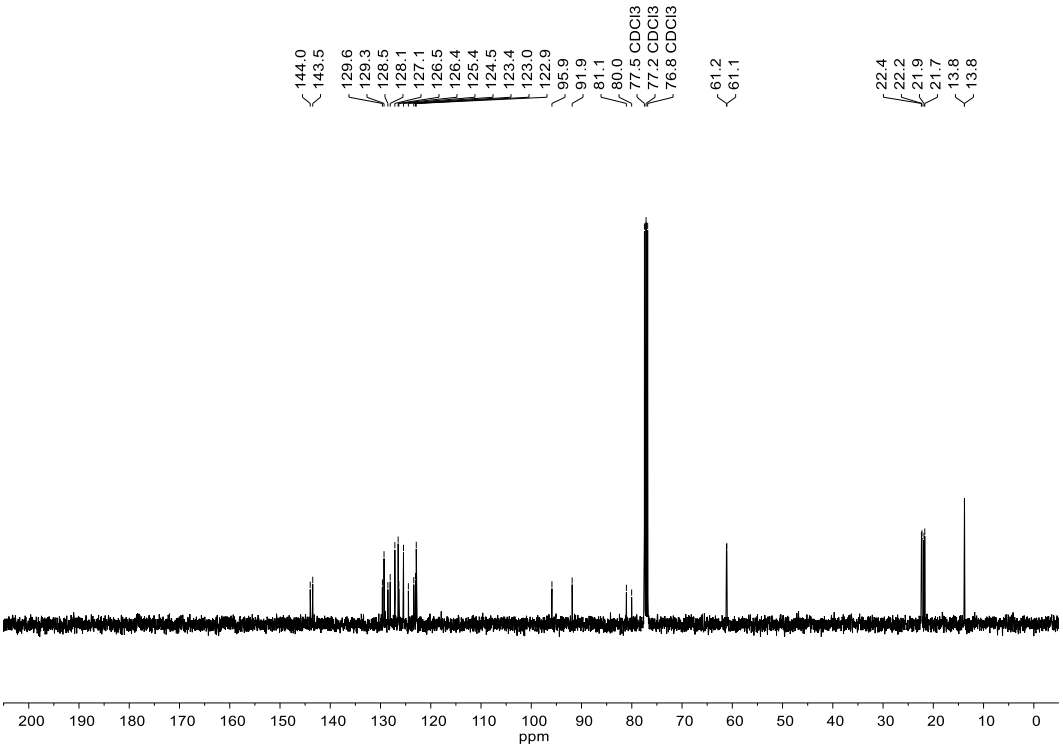

Figure S13. $^{13}C\{^{1}H\}$ NMR Spectrum (101 MHz, chloroform-*d*) of **S10**.

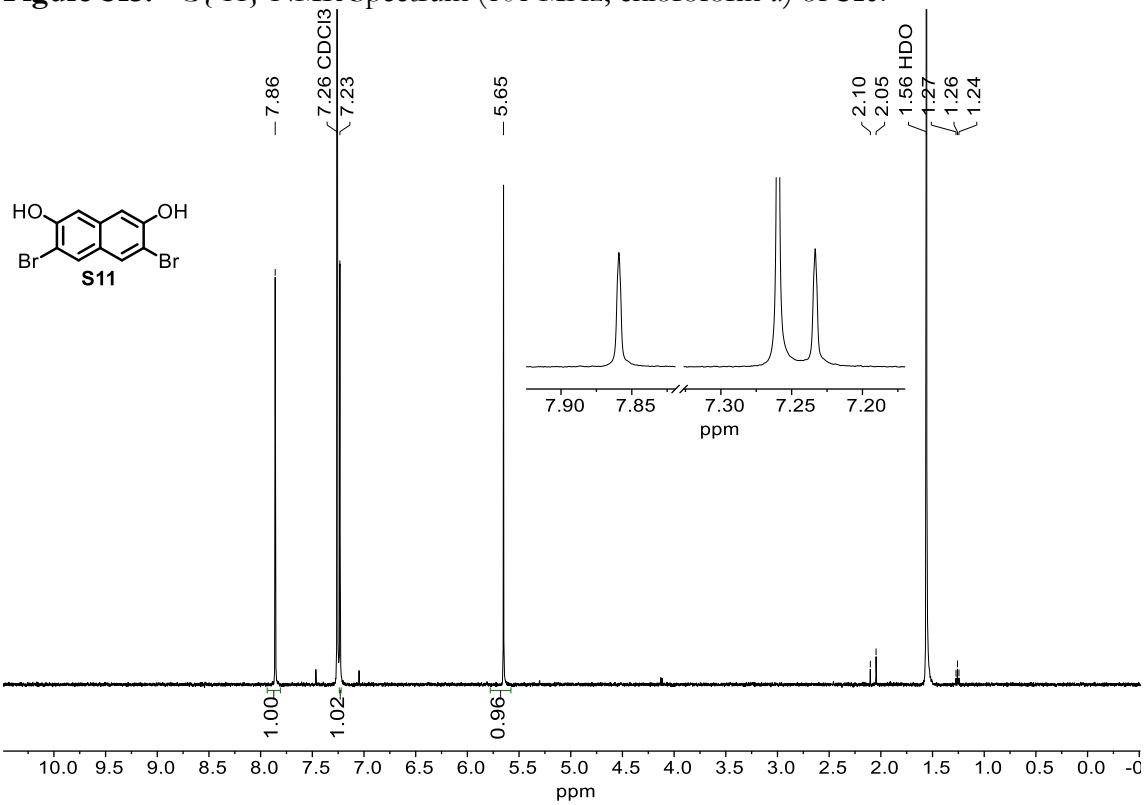

Figure S14. ^{1}H NMR Spectrum (500 MHz, chloroform-*d*) of **S11**.

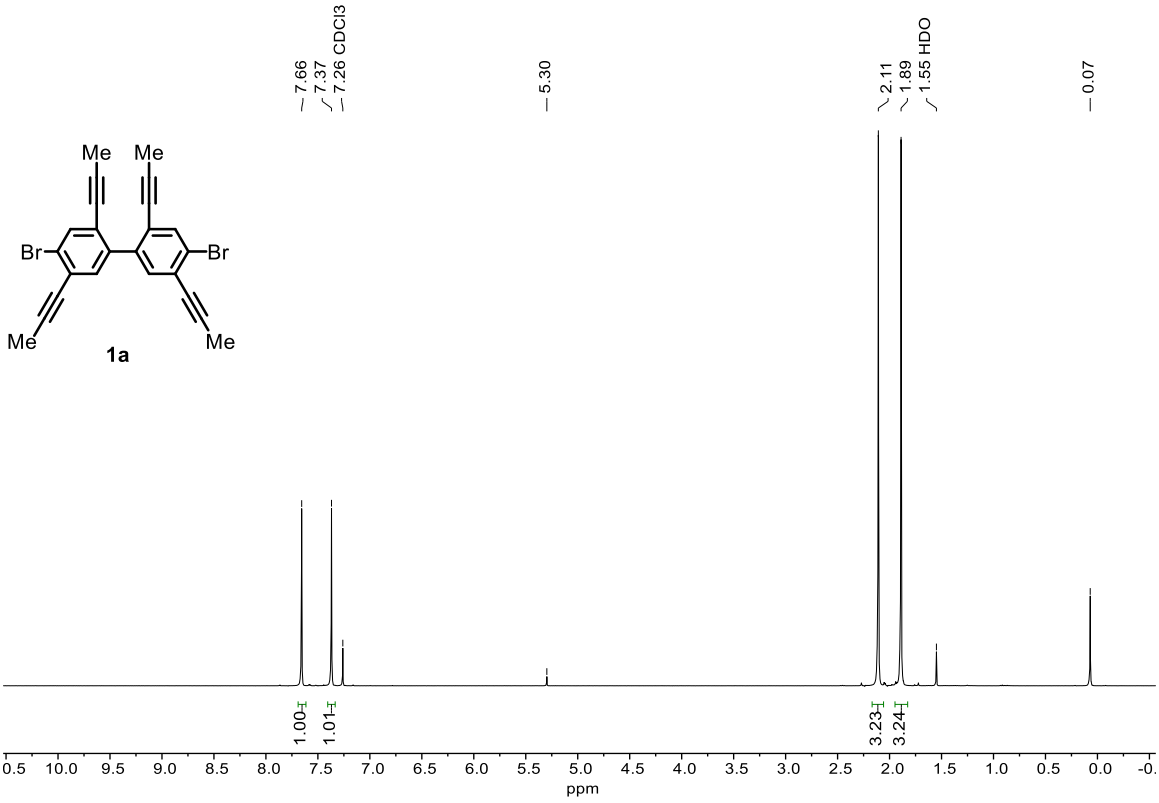

Figure S15. ^{1}H NMR Spectrum (400 MHz, chloroform-*d*) of **1a**.

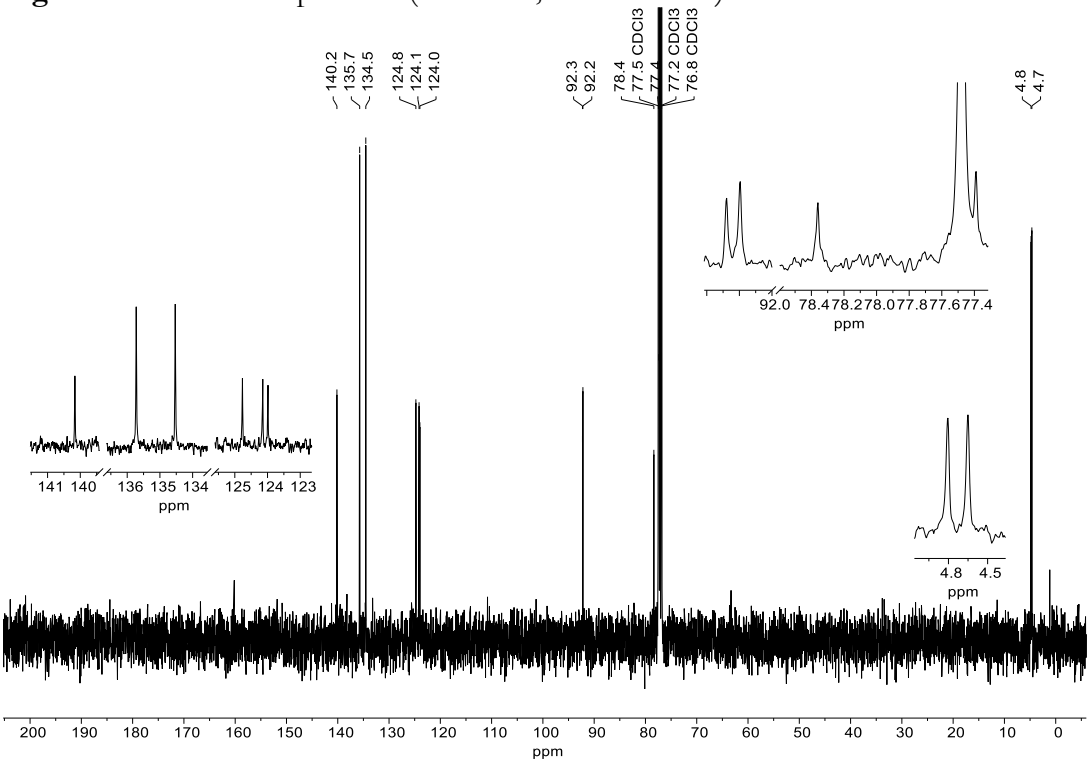

Figure S16. ^{13}C{^{1}H} NMR Spectrum (101 MHz, chloroform-*d*) of **1a**.

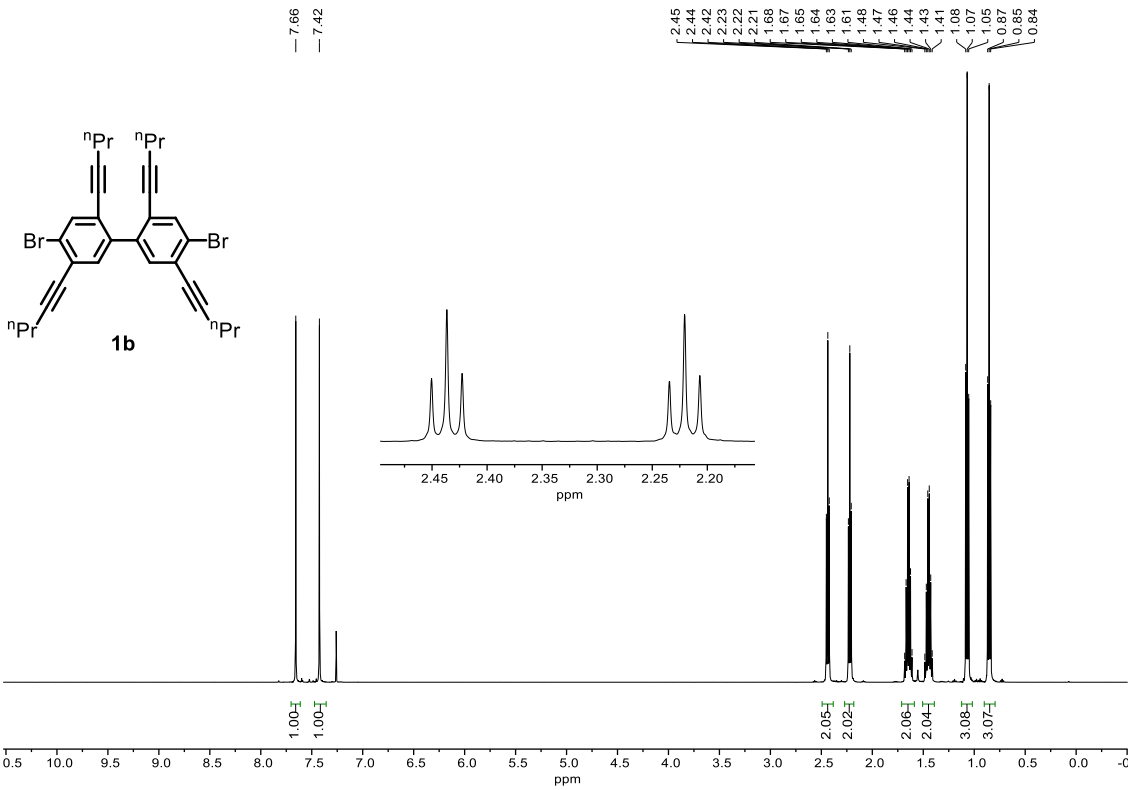

Figure S17. ^{1}H NMR Spectrum (500 MHz, chloroform-*d*) of **1b**.

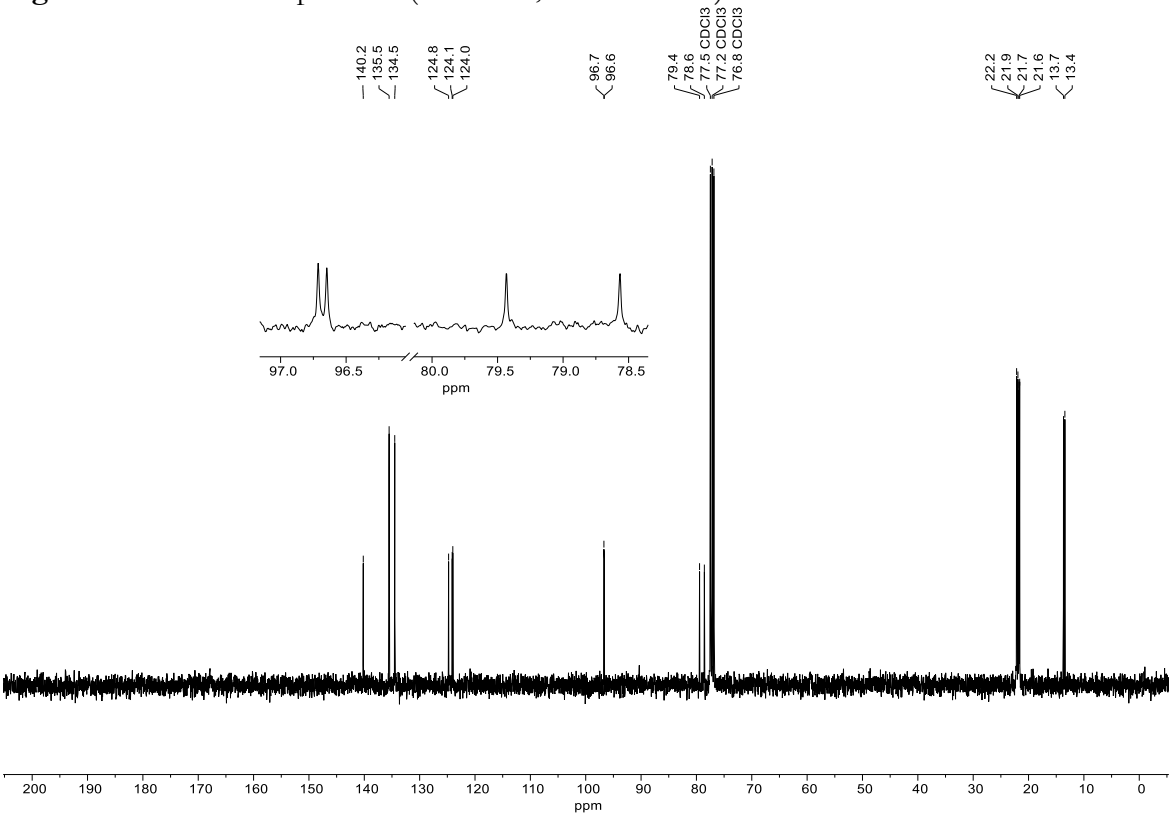

Figure S18. ^{13}C{^{1}H} NMR Spectrum (101 MHz, chloroform-*d*) of **1b**.

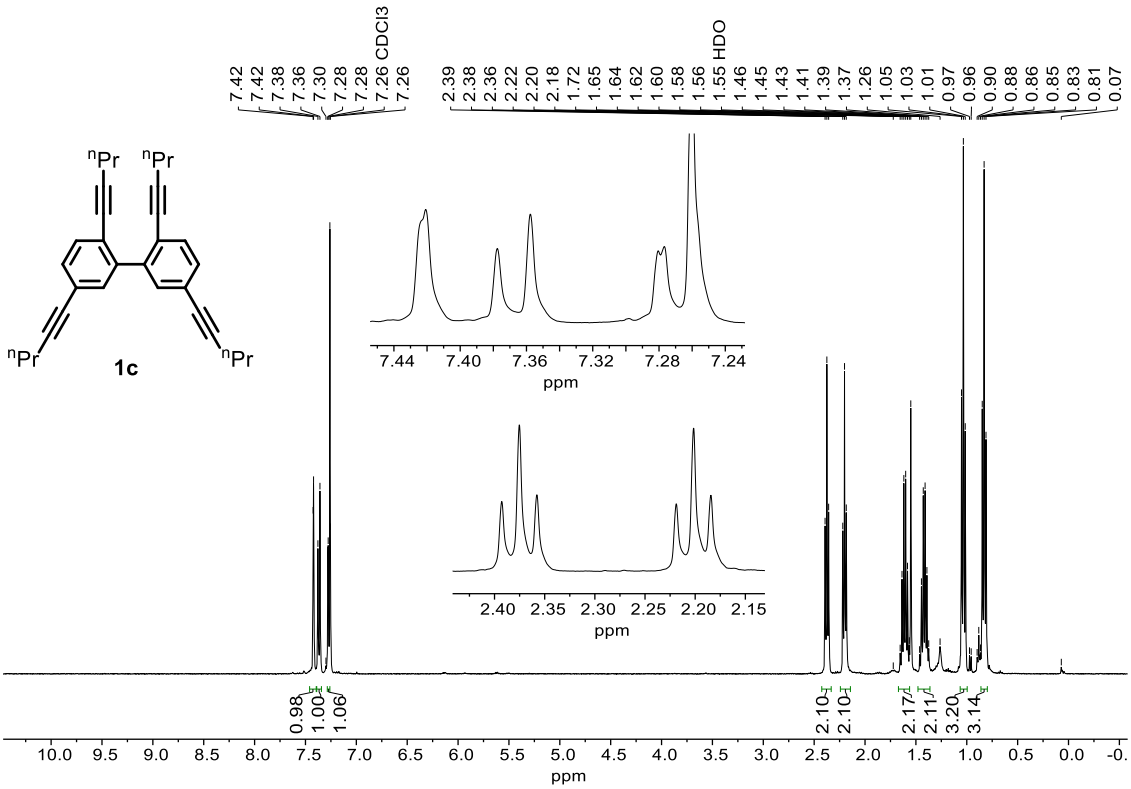

Figure S19. ^{1}H NMR Spectrum (400 MHz, chloroform-*d*) of **1c**.

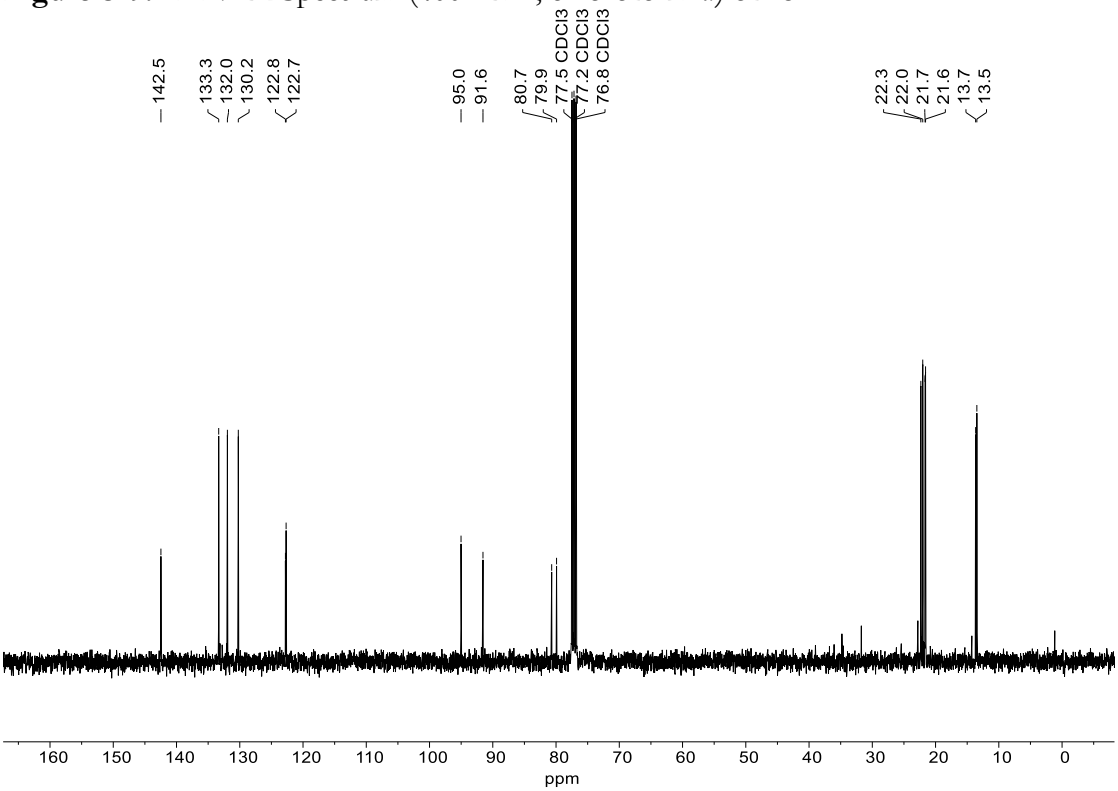

Figure S20. ^{13}C{^{1}H} NMR Spectrum (101 MHz, chloroform-*d*) of **1c**.

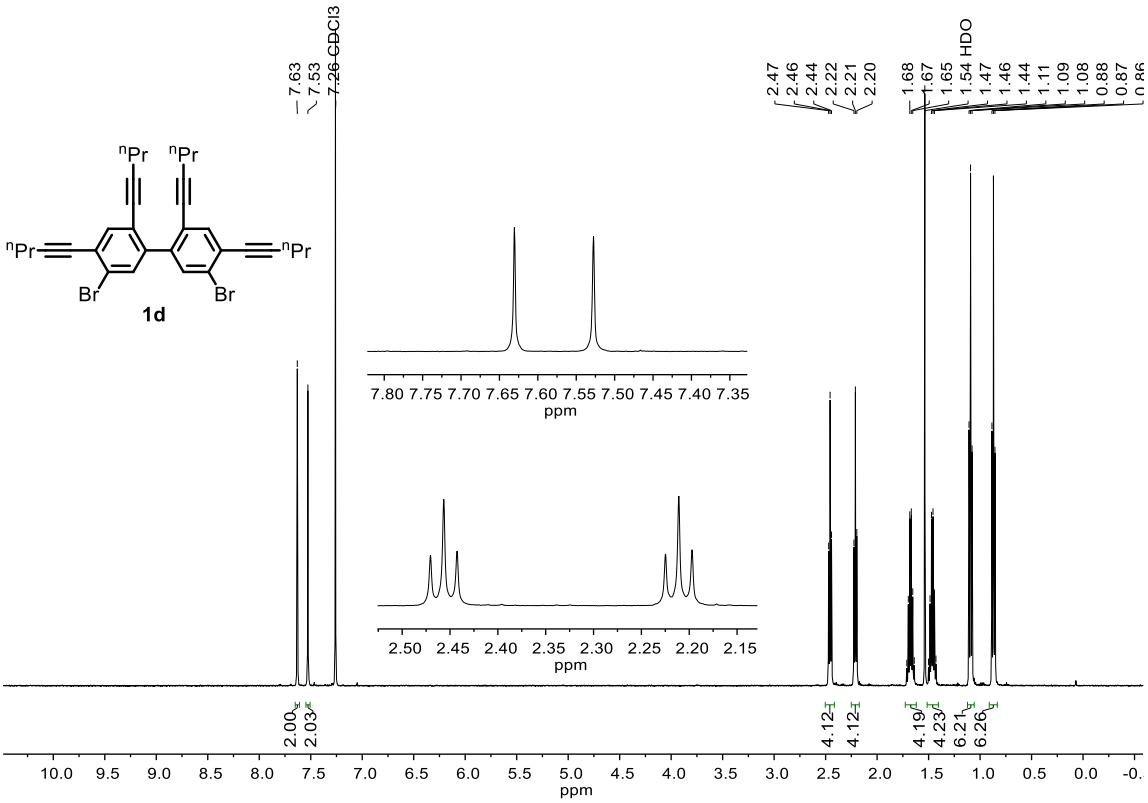

Figure S21. ^{1}H NMR Spectrum (500 MHz, chloroform-*d*) of **1d**.

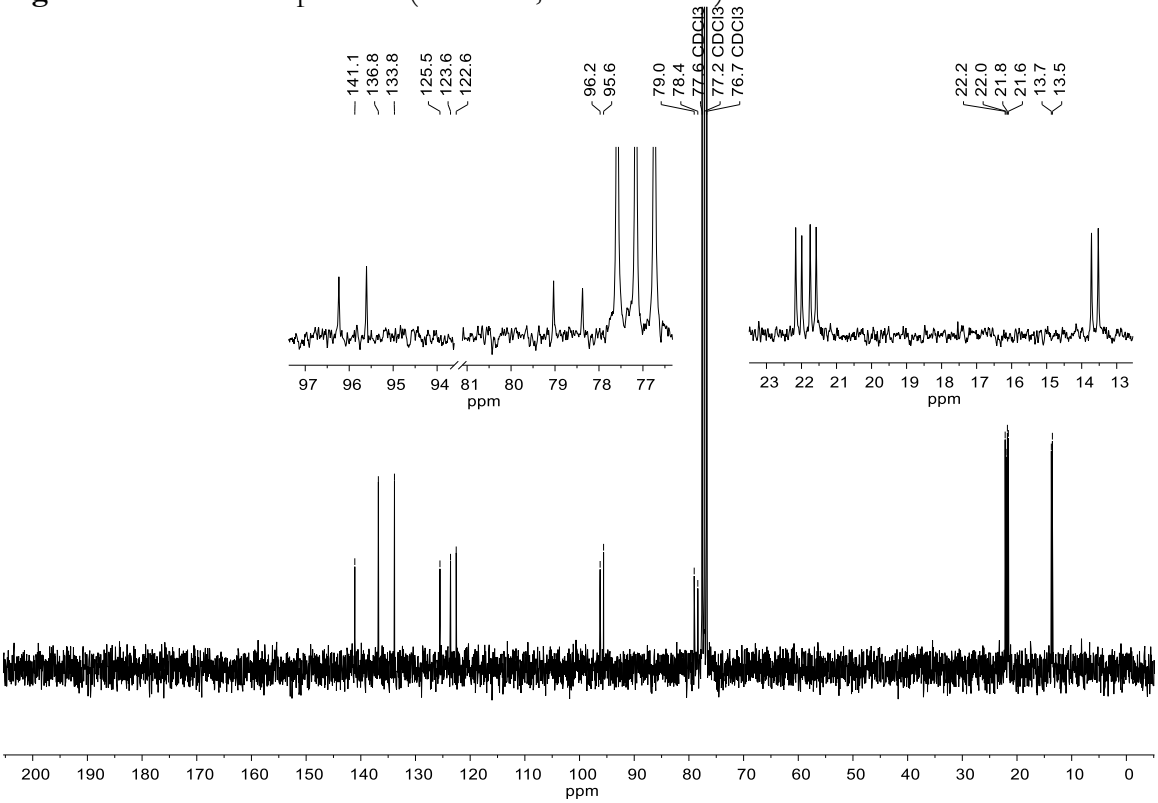

Figure S22. ^{13}C{^{1}H} NMR Spectrum (75 MHz, chloroform-*d*) of **1d**.

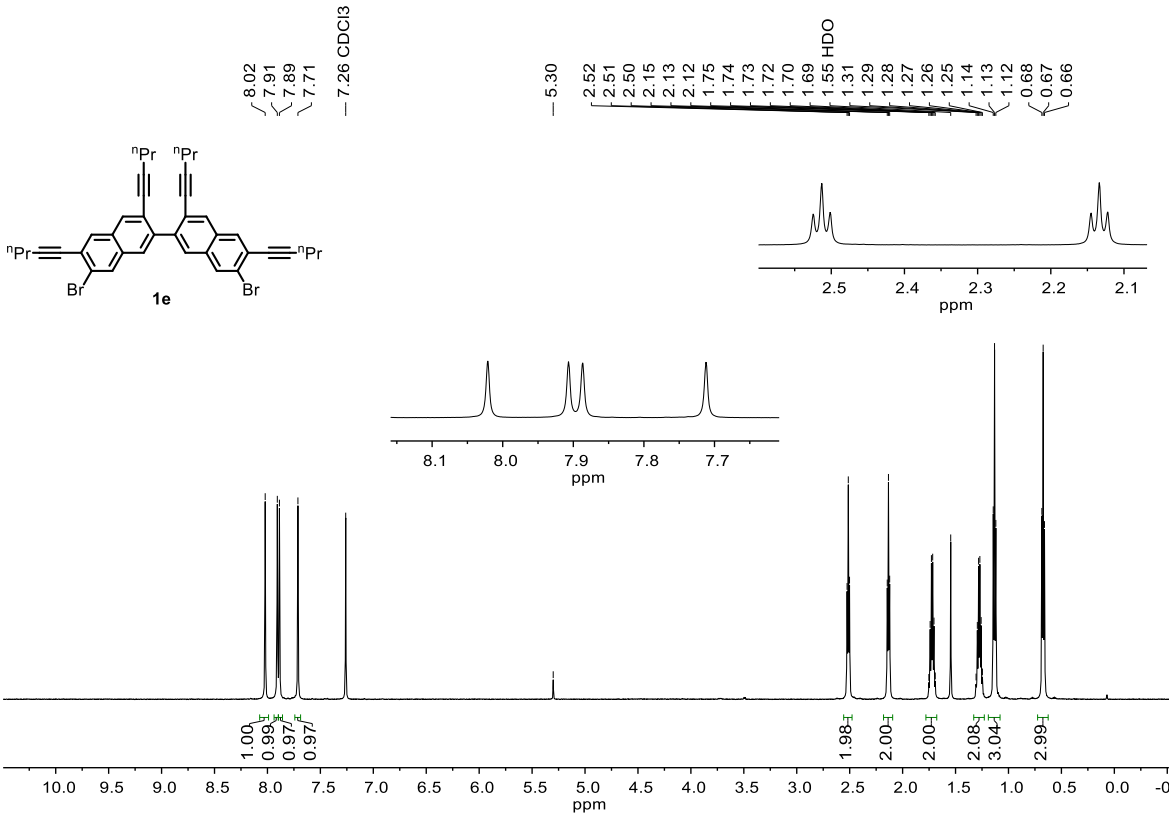

Figure S23. ^{1}H NMR Spectrum (600 MHz, chloroform-*d*) of **1e**.

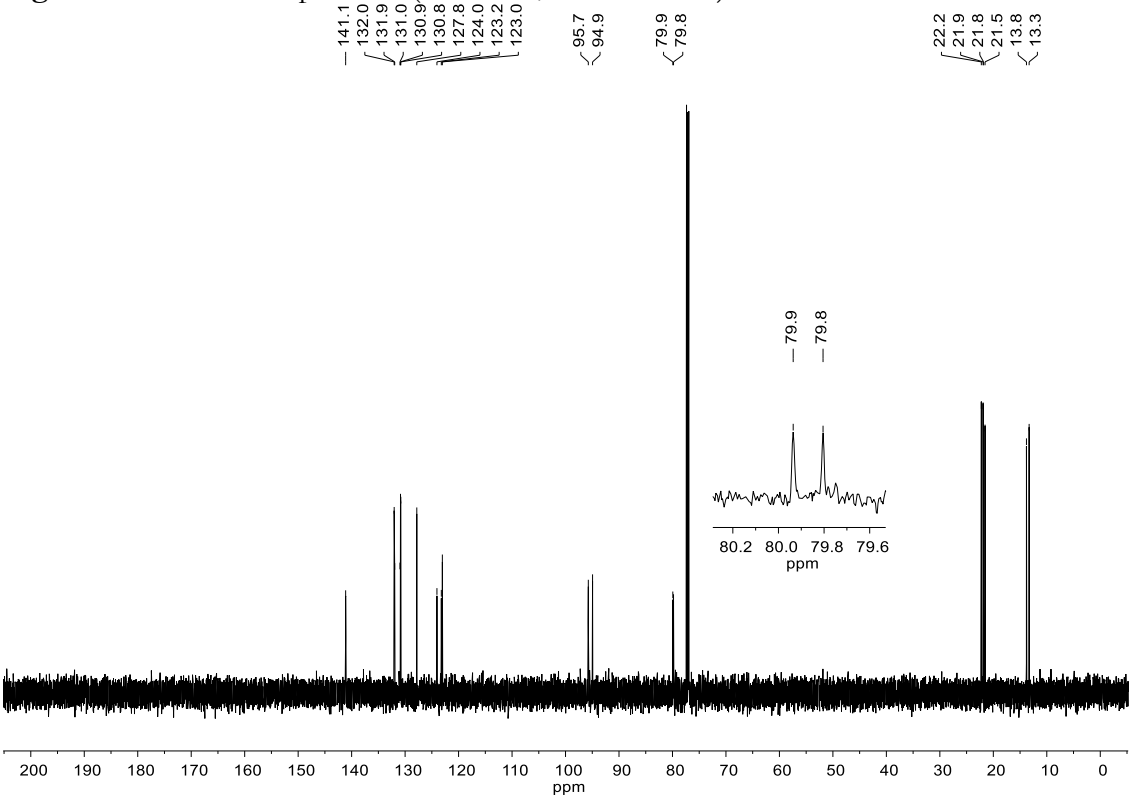

Figure S24. ^{13}C{^{1}H} NMR Spectrum (151 MHz, chloroform-*d*) of **1e**.

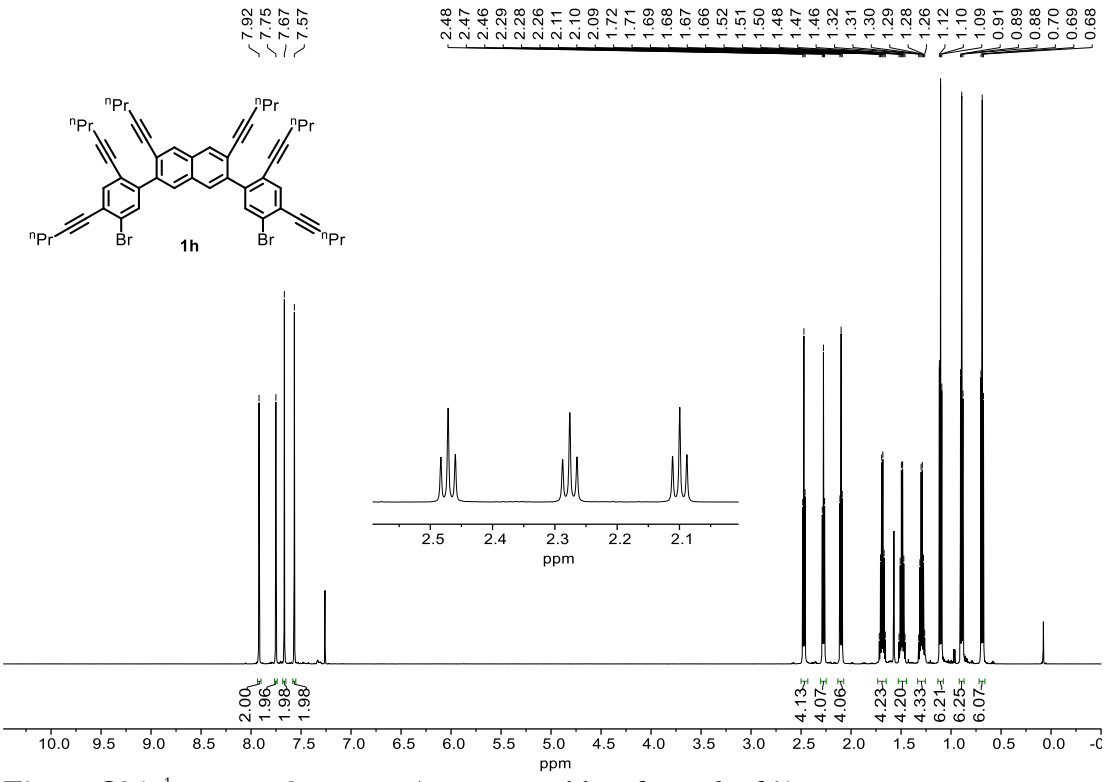

Figure S25. ^{1}H NMR Spectrum (600 MHz, chloroform-*d*) of **1h**.

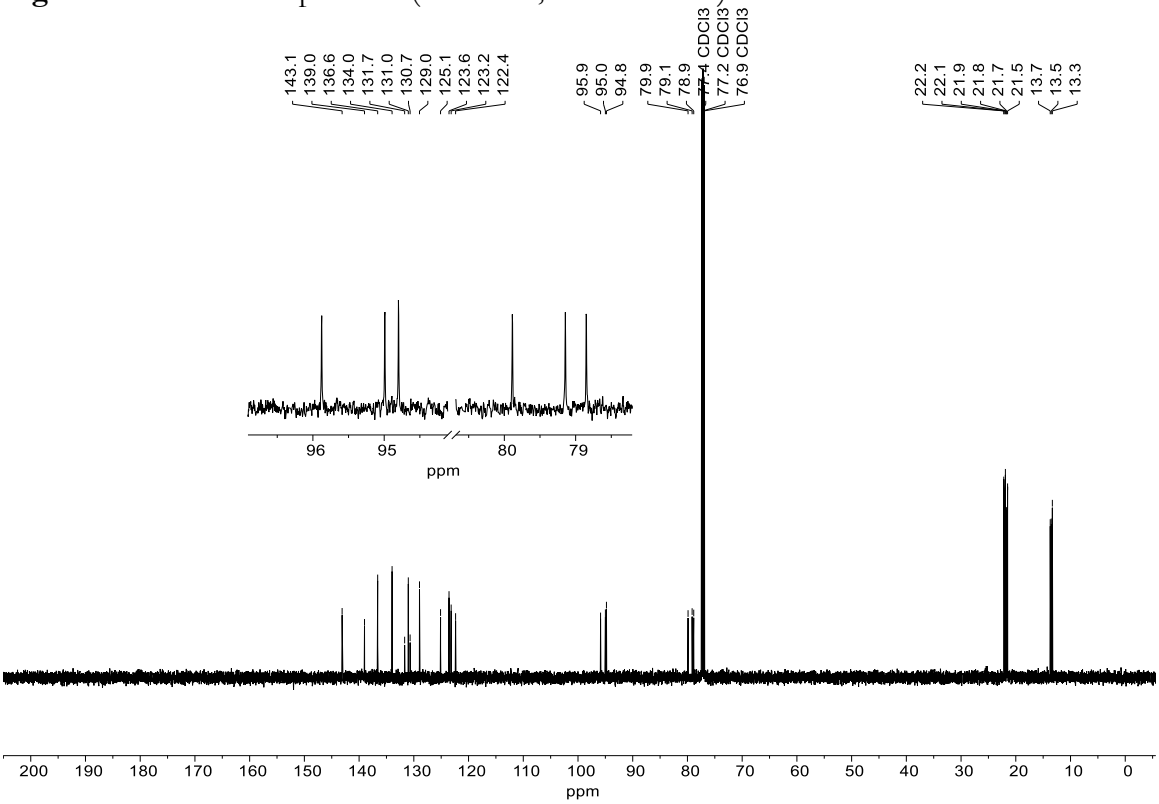

Figure S26. ^{13}C{^{1}H} NMR Spectrum (151 MHz, chloroform-*d*) of **1h**.

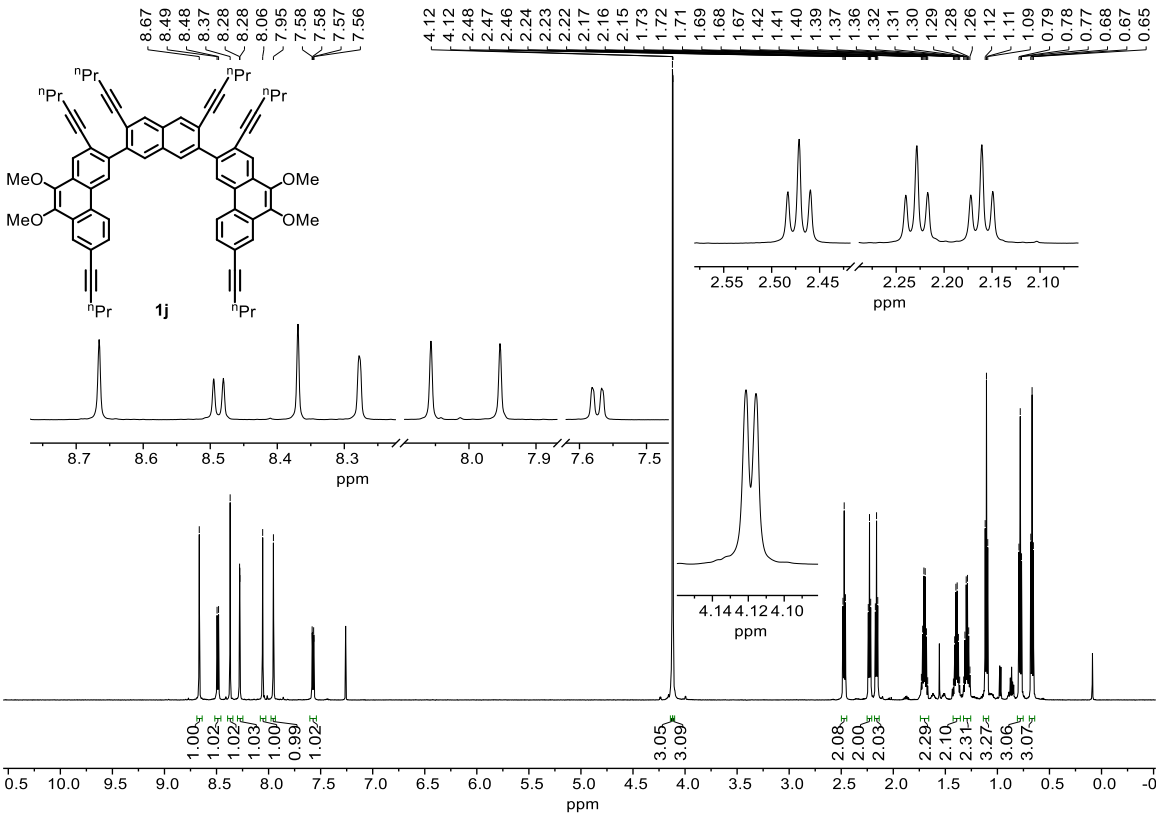

Figure S27. ^{1}H NMR Spectrum (600 MHz, chloroform-*d*) of **1j**.

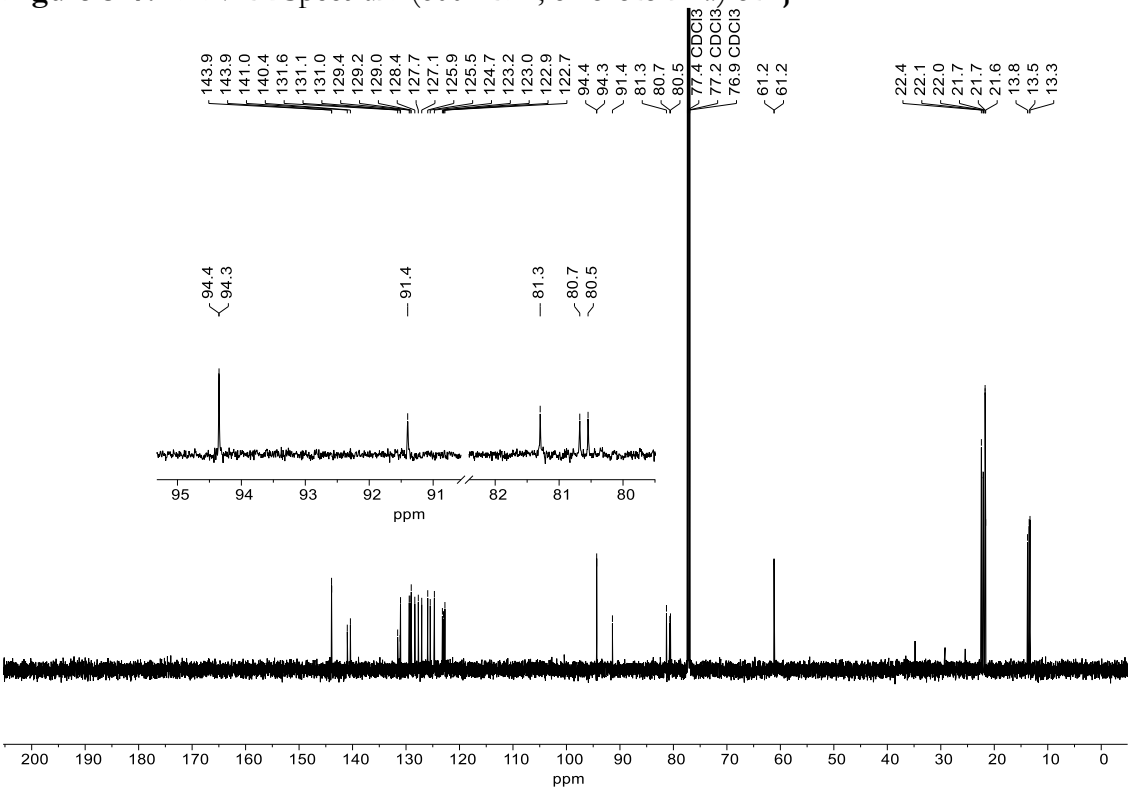

Figure S28. ^{13}C{^{1}H} NMR Spectrum (151 MHz, chloroform-*d*) of **1j**.

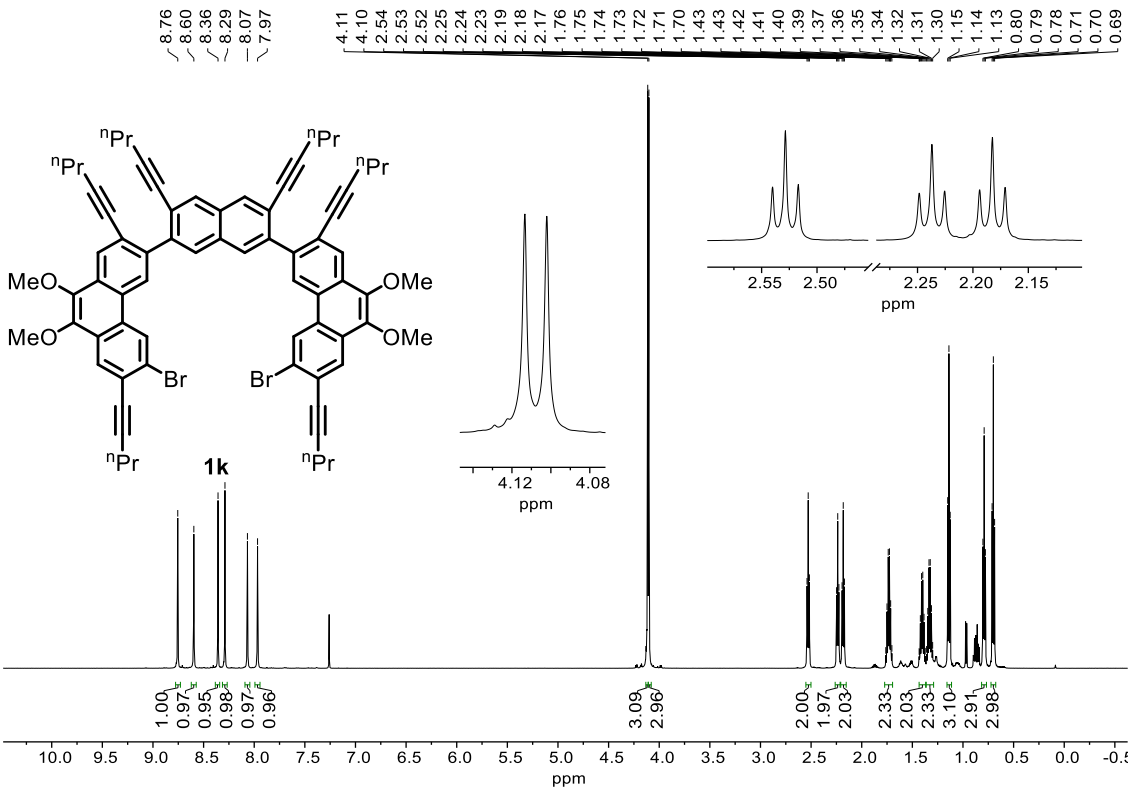

Figure S29. ^{1}H NMR Spectrum (600 MHz, chloroform-*d*) of **1k**.

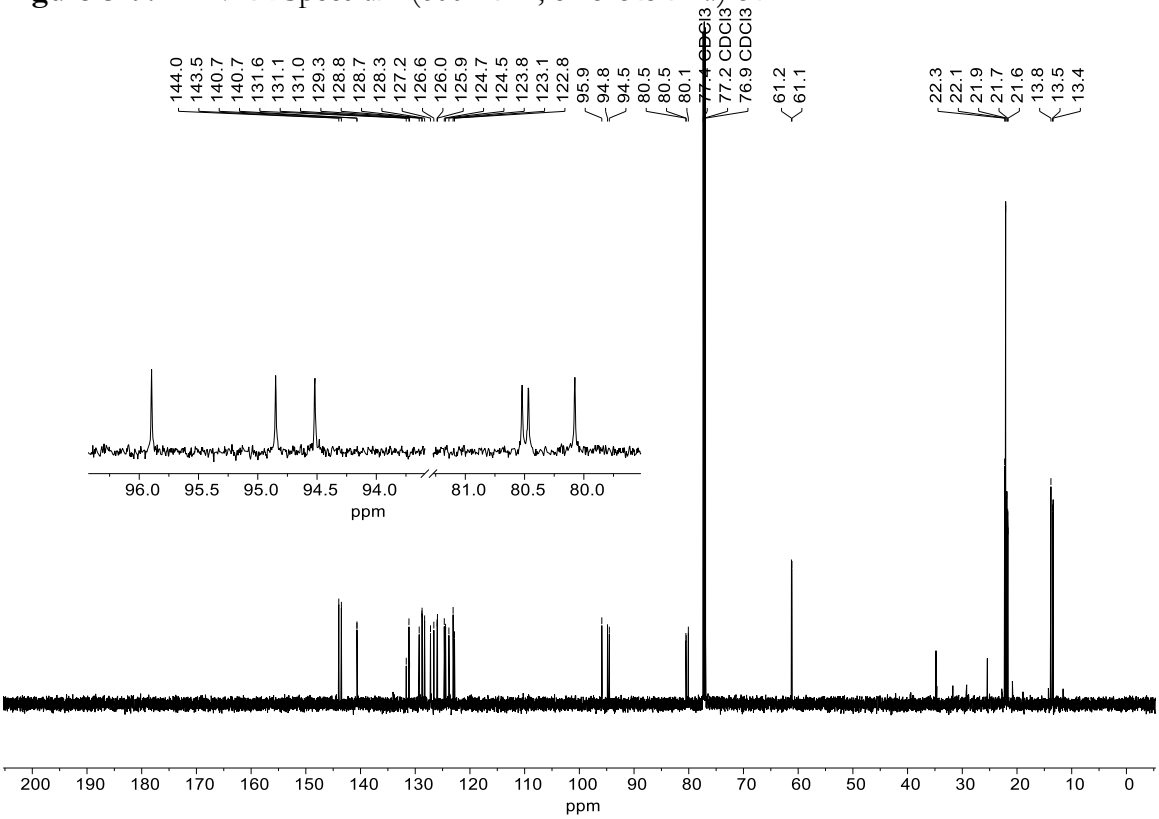

Figure S30. ^{13}C{^{1}H} NMR Spectrum (151 MHz, chloroform-*d*) of **1k**.

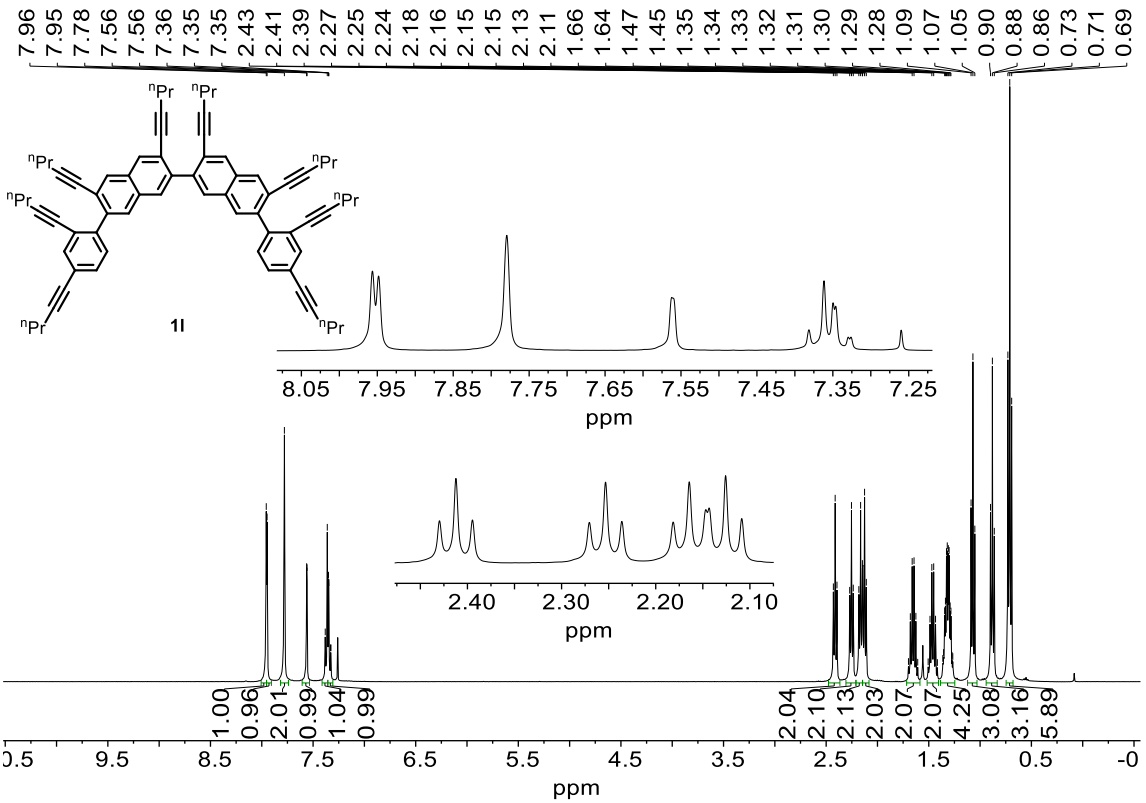

Figure S31. ^{1}H NMR Spectrum (101 MHz, chloroform-*d*) of **1l**.

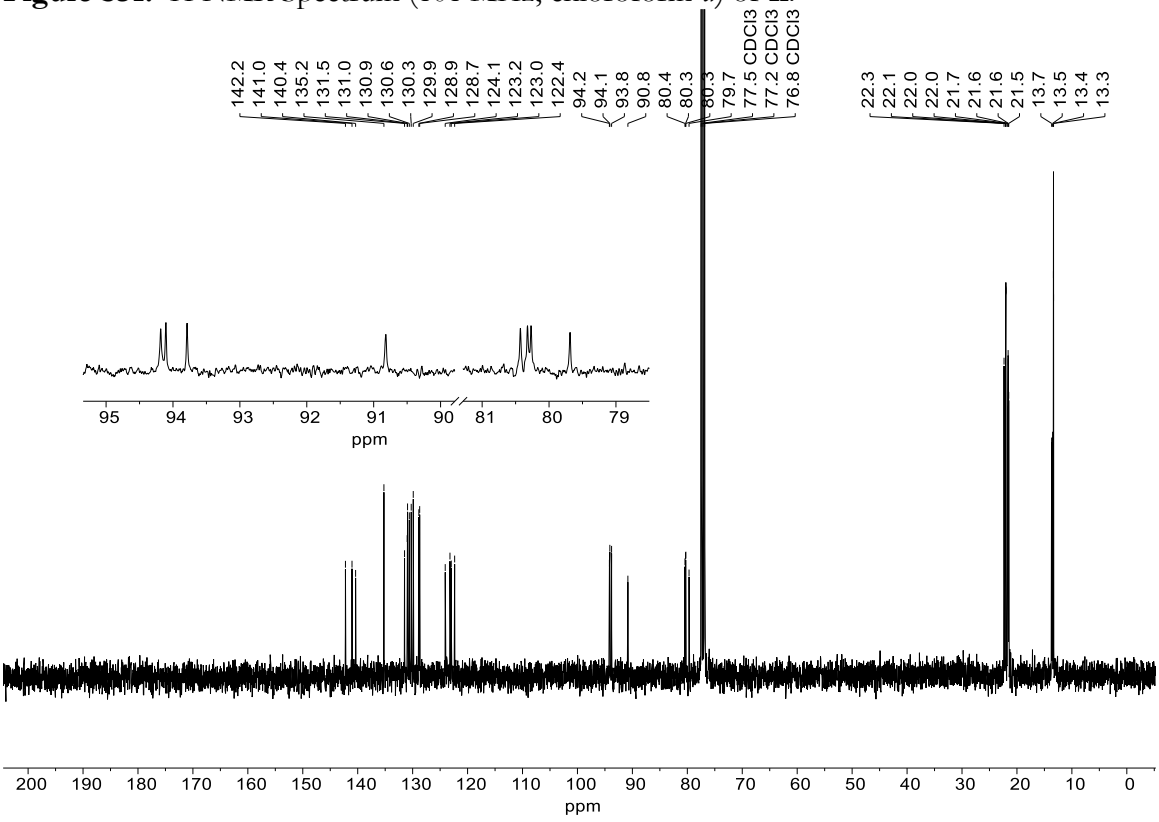

Figure S32. ^{13}C{^{1}H} NMR Spectrum (101 MHz, chloroform-*d*) of **1l**.

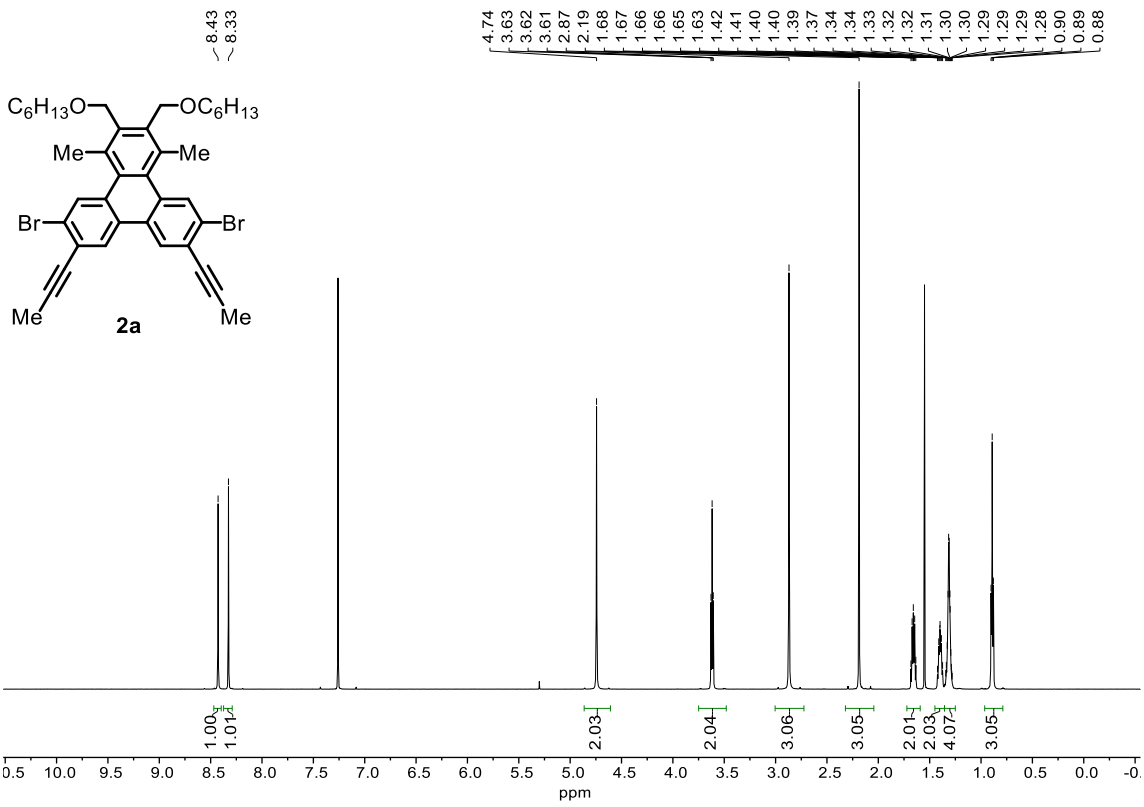

Figure S33. ^{1}H NMR Spectrum (600 MHz, chloroform-*d*) of **2a**.

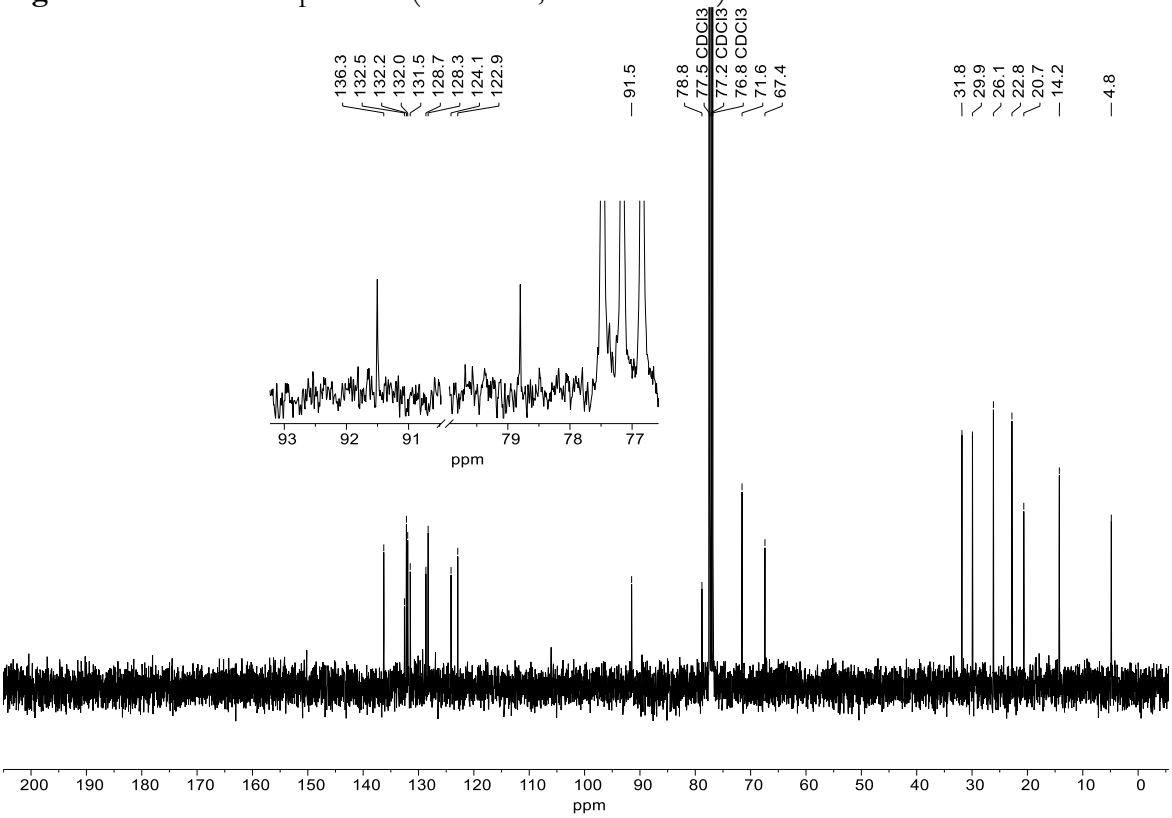

Figure S34. ^{13}C{^{1}H} NMR Spectrum (101 MHz, chloroform-*d*) of **2a**.

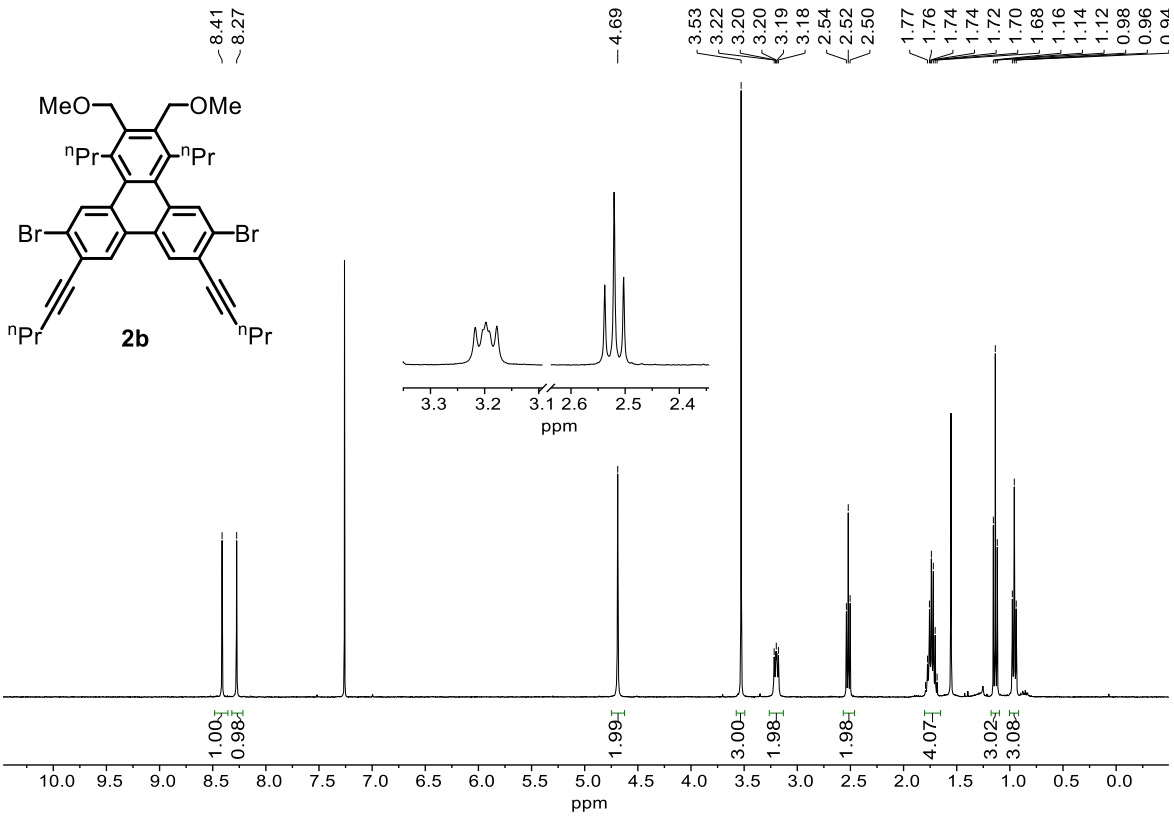

Figure S35. ^{1}H NMR Spectrum (400 MHz, chloroform-*d*) of **2b**.

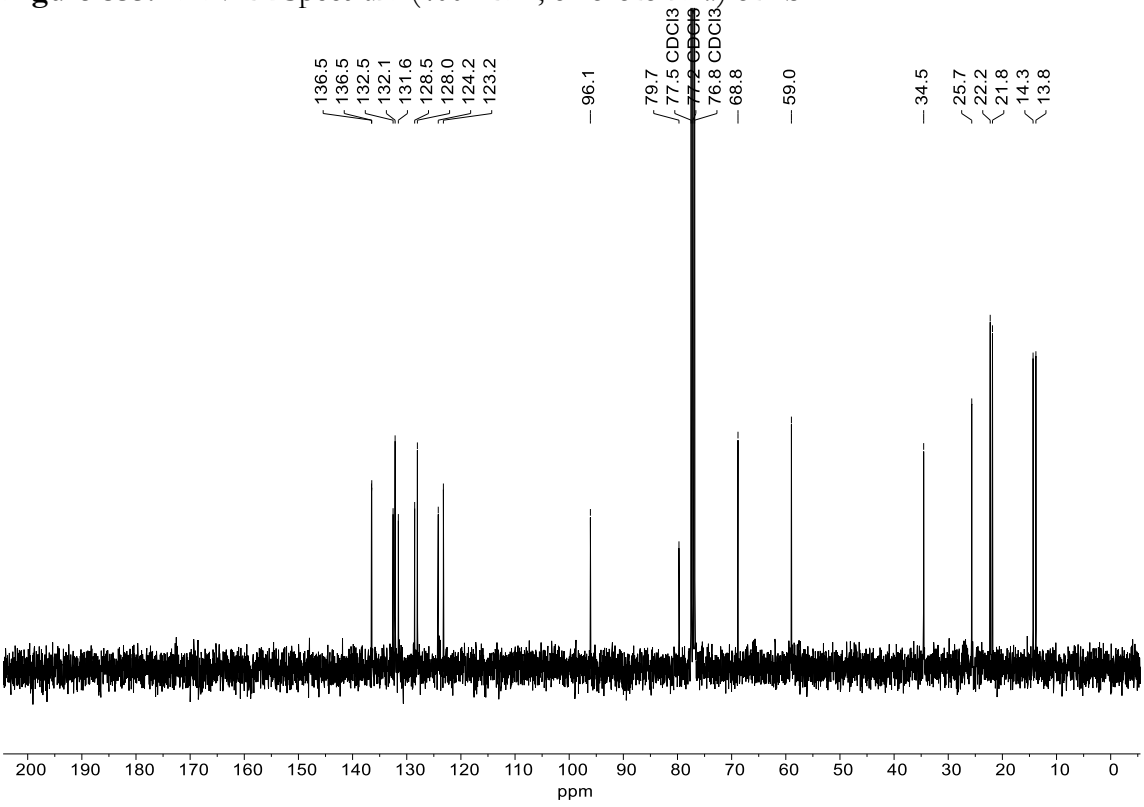

Figure S36. ^{13}C{^{1}H} NMR Spectrum (400 MHz, chloroform-*d*) of **2b**.

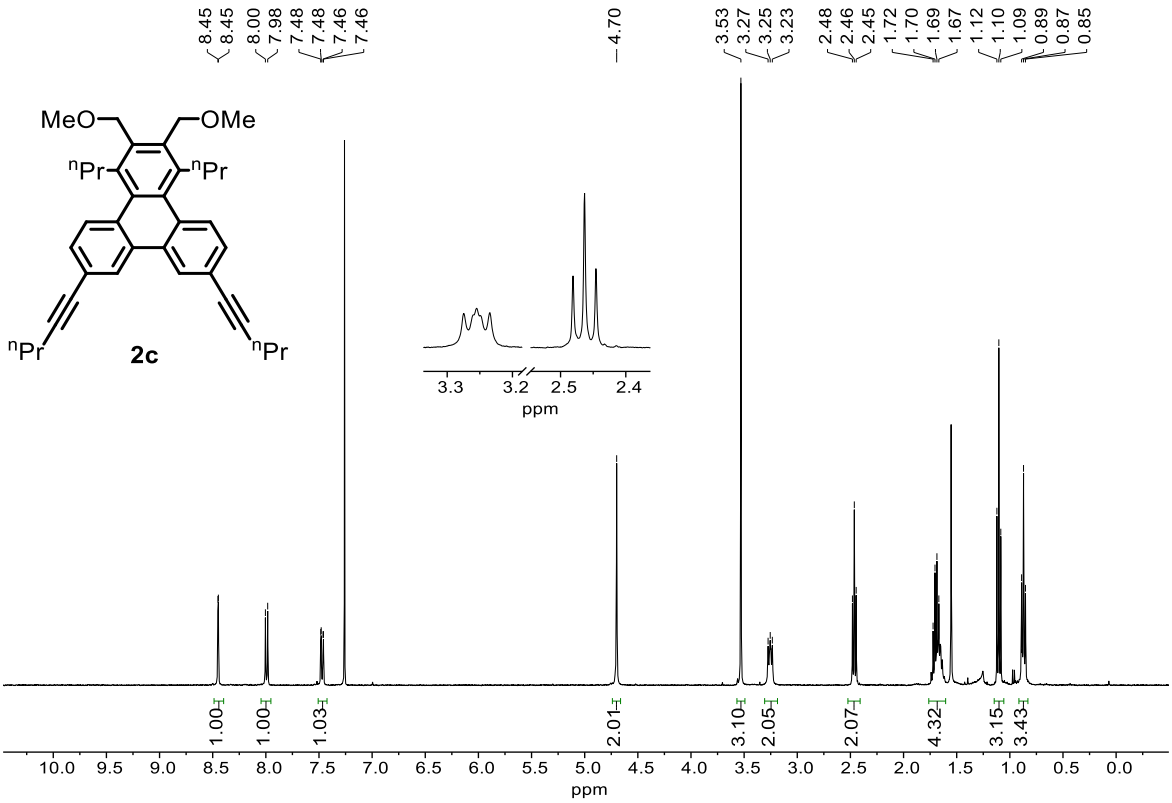

Figure S37. ^{1}H NMR Spectrum (400 MHz, chloroform-*d*) of **2c**.

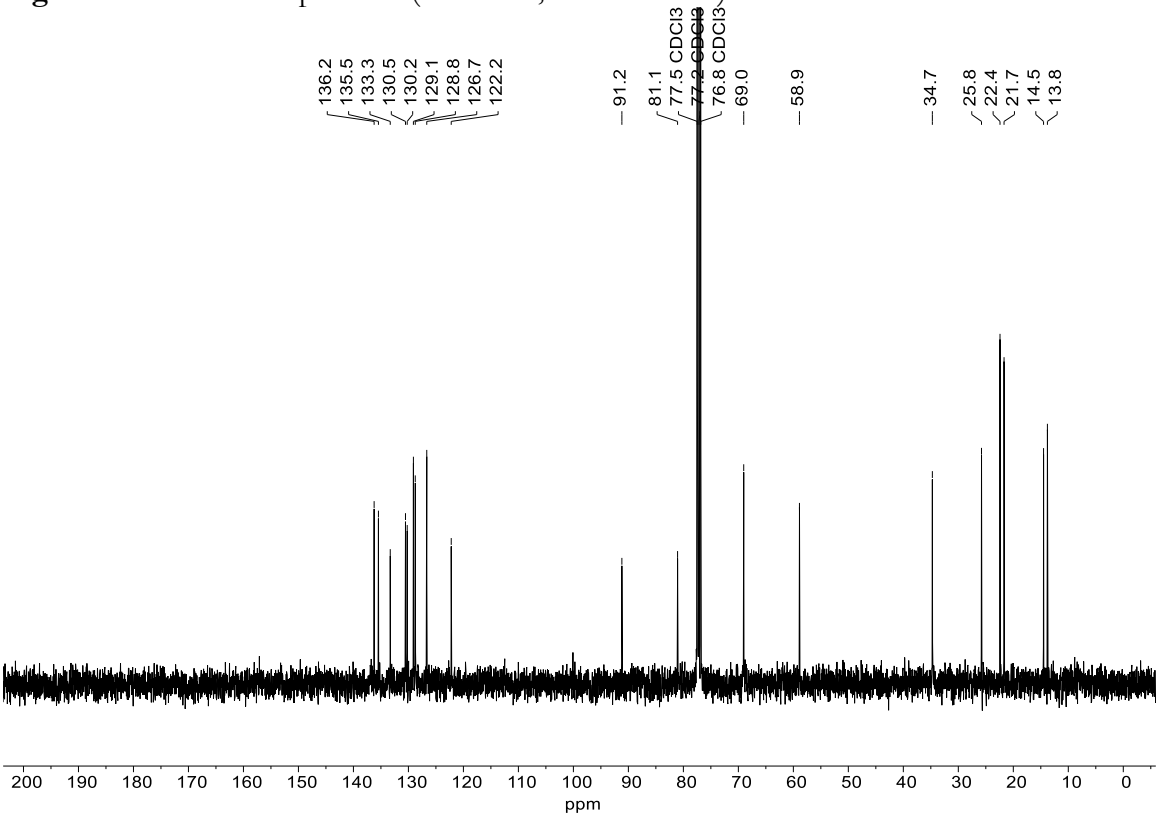

Figure S38. ^{13}C{^{1}H} NMR Spectrum (101 MHz, chloroform-*d*) of **2c**.

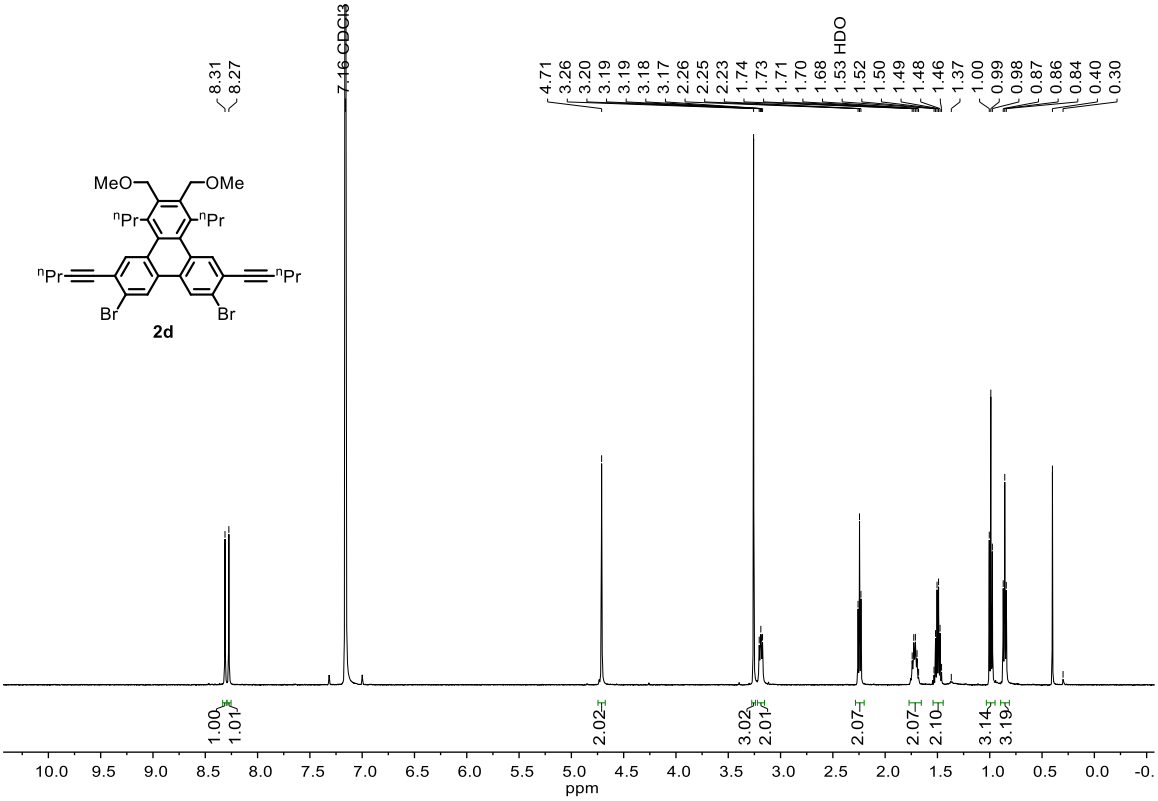

Figure S39. ^{1}H NMR Spectrum (500 MHz, benzene-d_6) of **2d**.

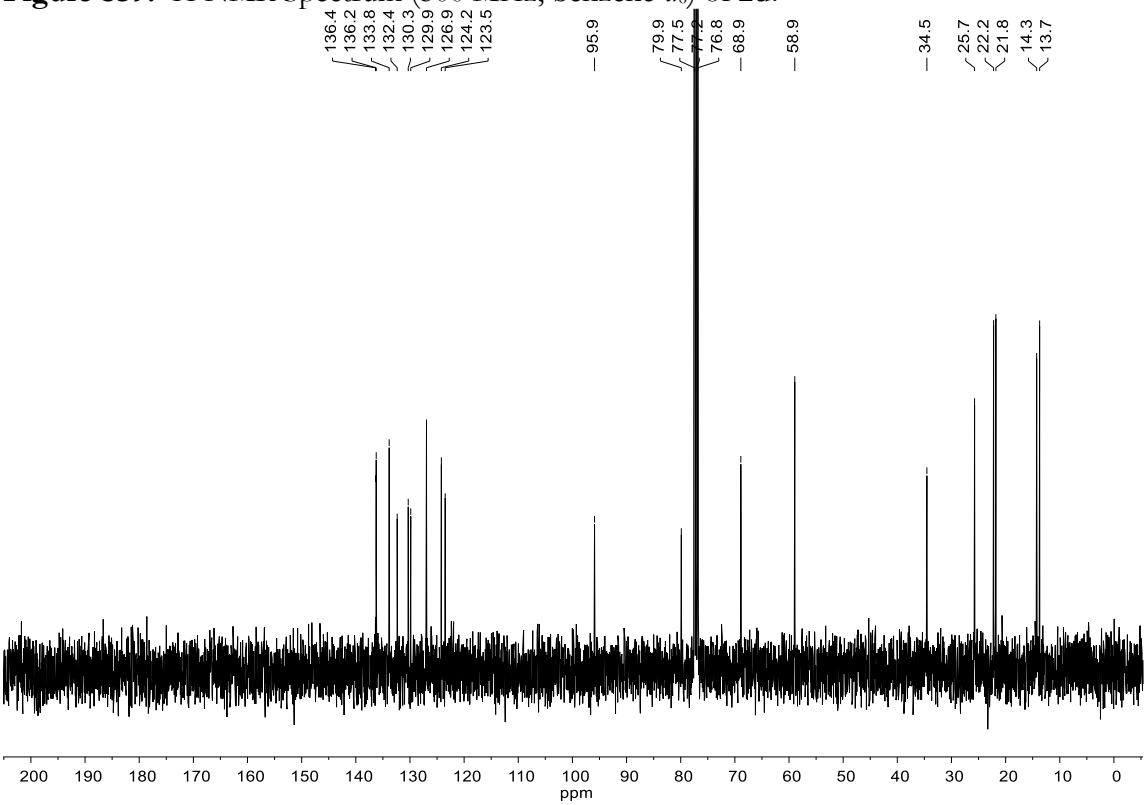

Figure S40. ^{13}C{^{1}H} NMR Spectrum (101 MHz, chloroform-d) of **2d**.

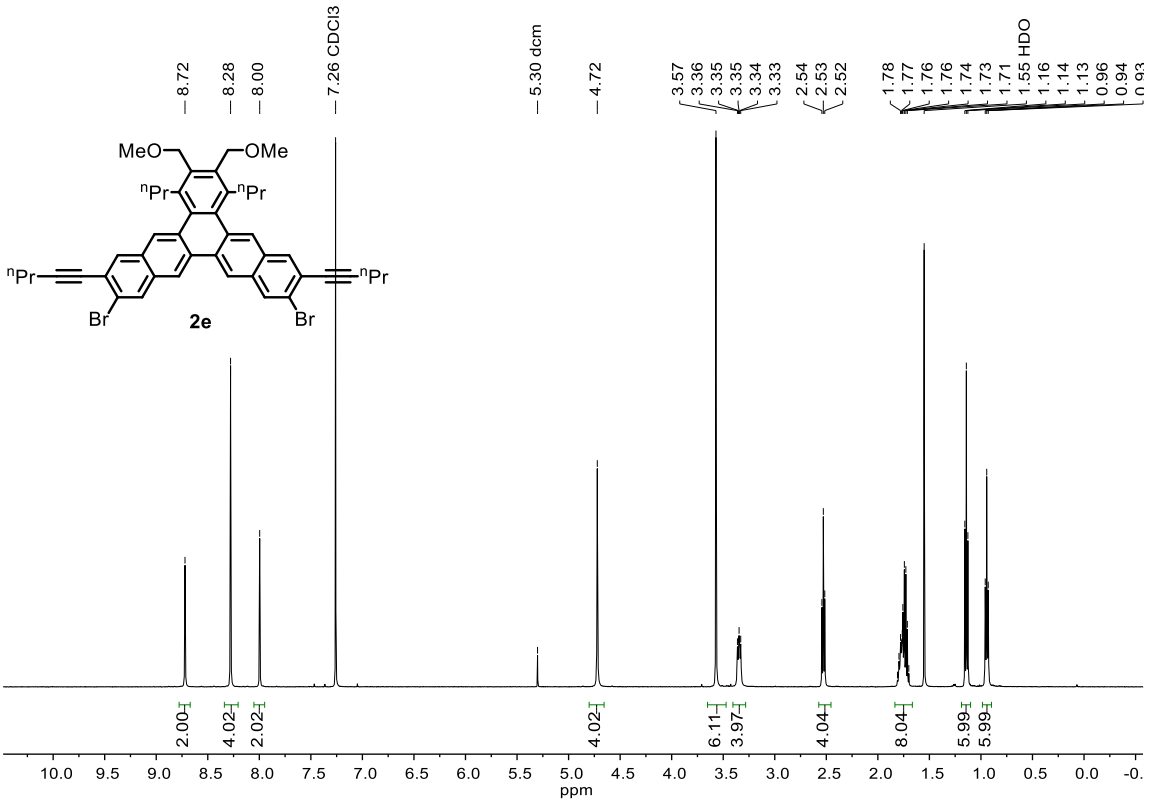

Figure S41. ^{1}H NMR Spectrum (500 MHz, chloroform-*d*) of **2e**.

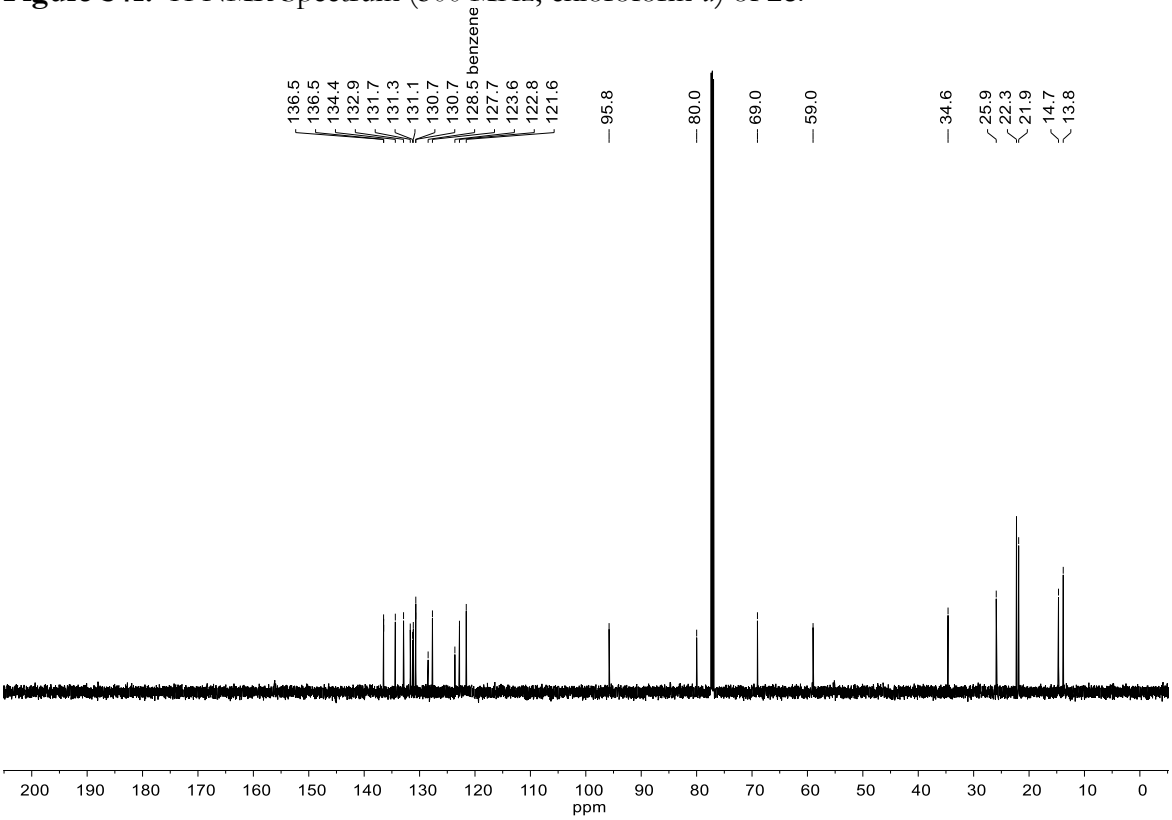

Figure S42. ^{13}C{^{1}H} NMR Spectrum (151 MHz, chloroform-*d*) of **2e**.

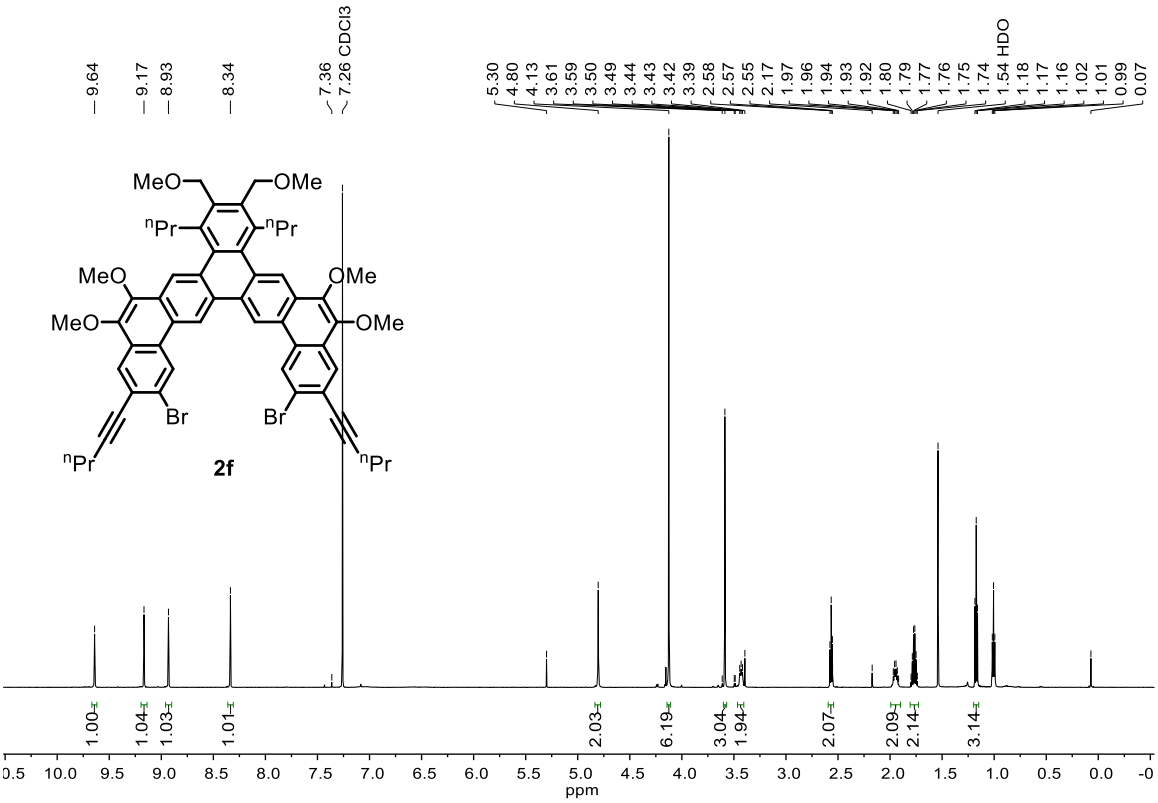

Figure S43. ^{1}H NMR Spectrum (600 MHz, chloroform-*d*) of **2f**.

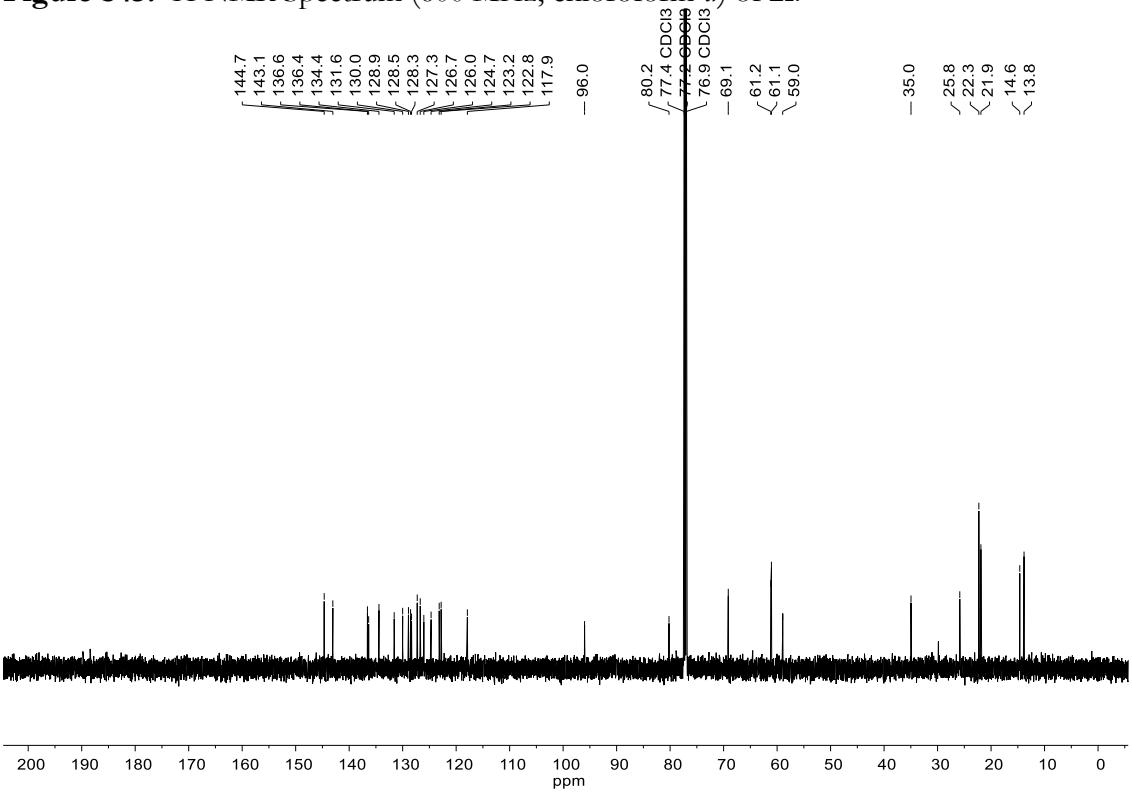

Figure S44. ^{13}C{^{1}H} NMR Spectrum (151 MHz, chloroform-*d*) of **2f**.

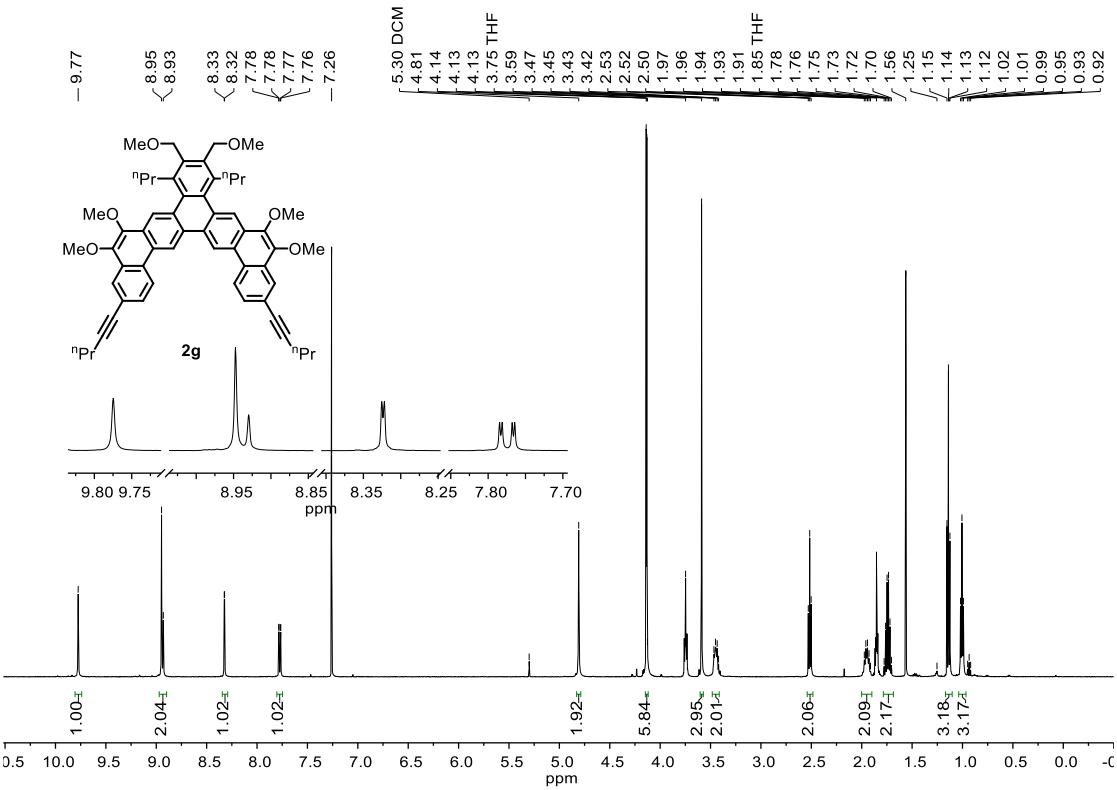

Figure S45. ^{1}H NMR Spectrum (500 MHz, chloroform-*d*) of **2g**.

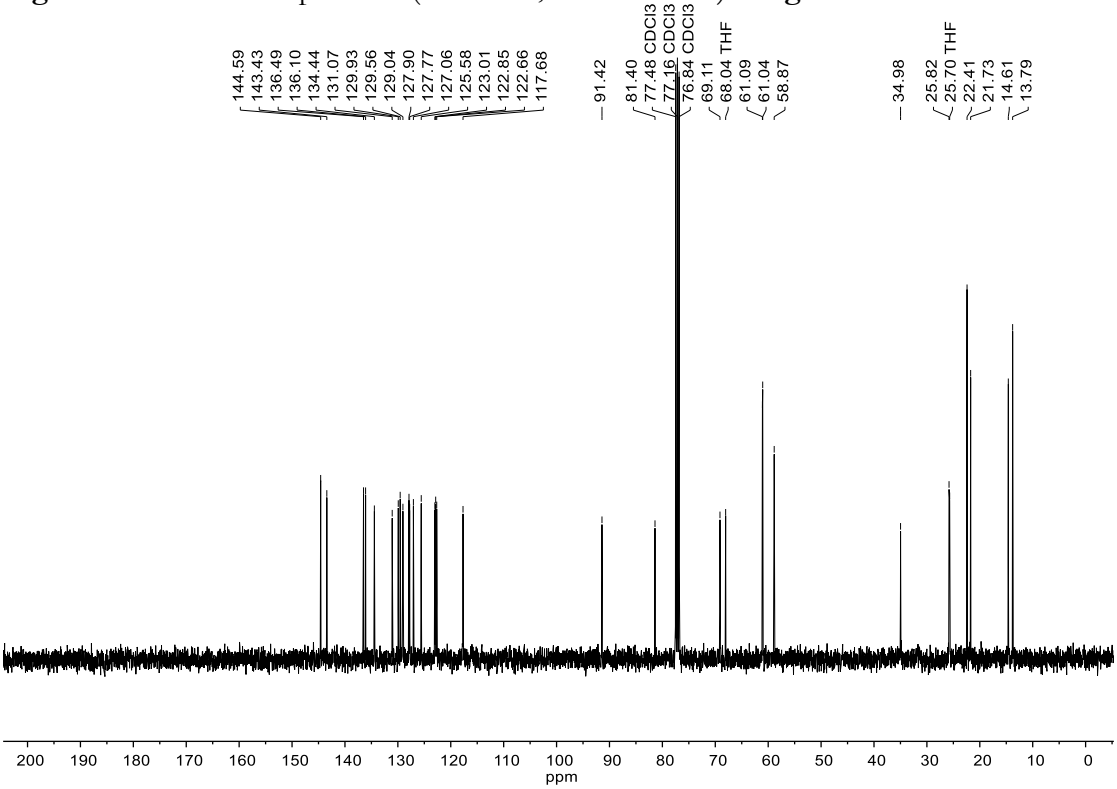

Figure S46. ^{13}C{^{1}H} NMR Spectrum (101 MHz, chloroform-*d*) of **2g**.

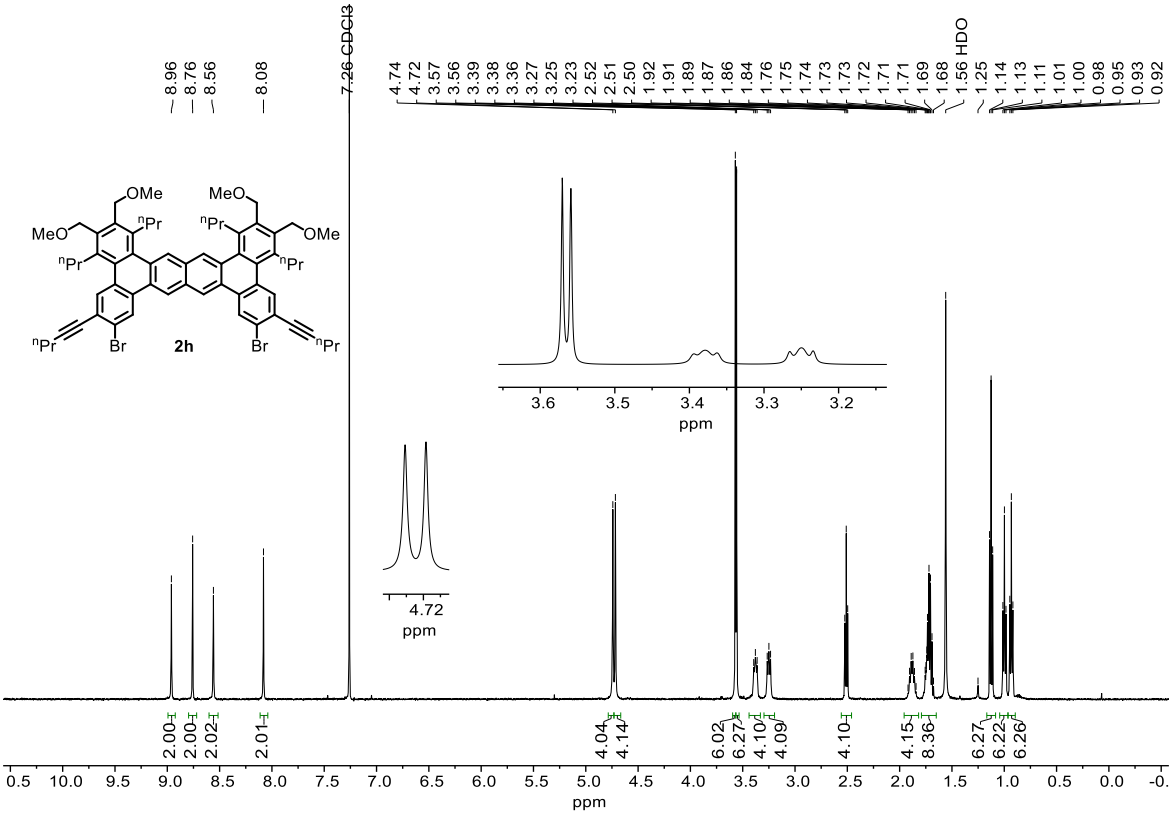

Figure S47. ^{1}H NMR Spectrum (500 MHz, chloroform-*d*) of **2h**.

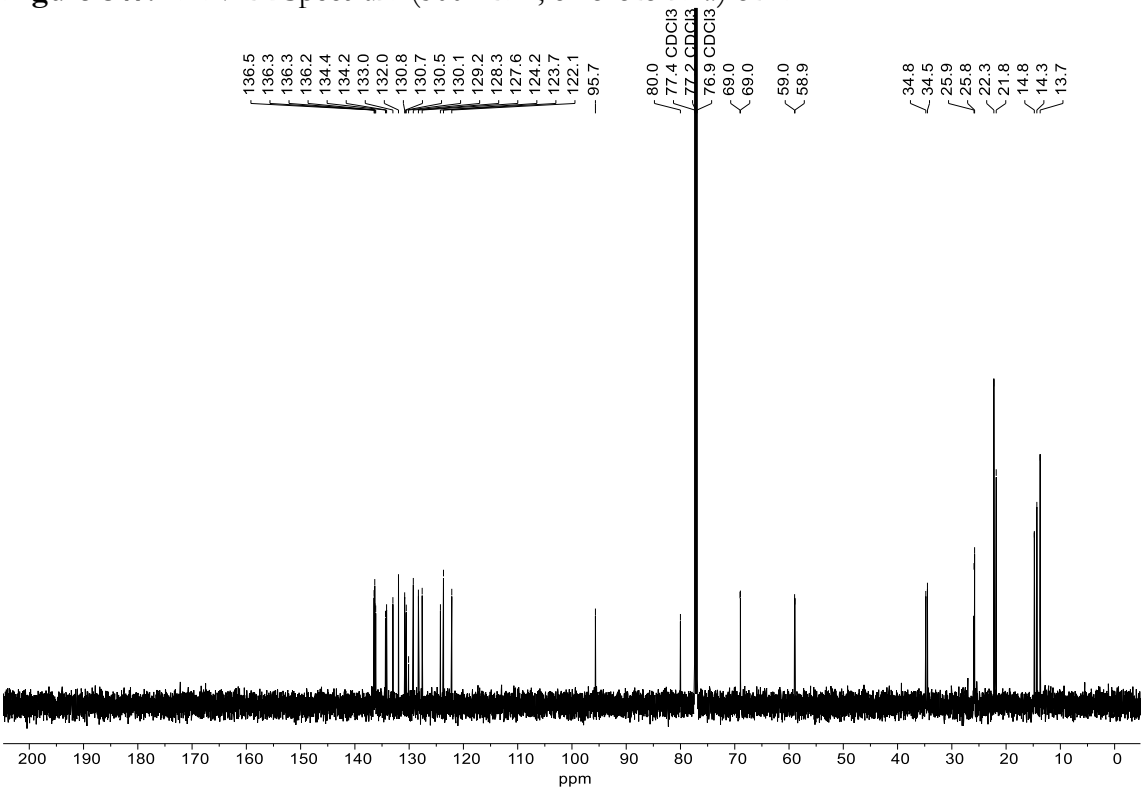

Figure S48. ^{13}C{^{1}H} NMR Spectrum (151 MHz, chloroform-*d*) of **2h**.

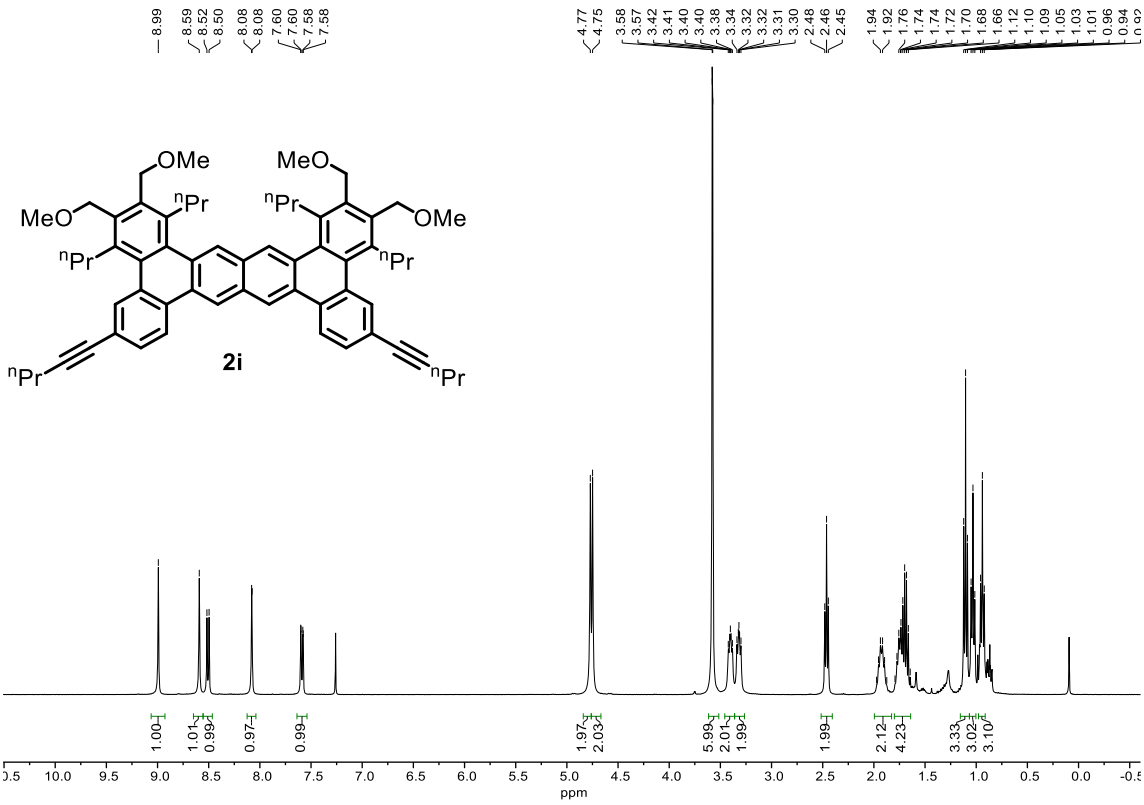

Figure S49. ^{1}H NMR Spectrum (400 MHz, chloroform-*d*) of **2i**.

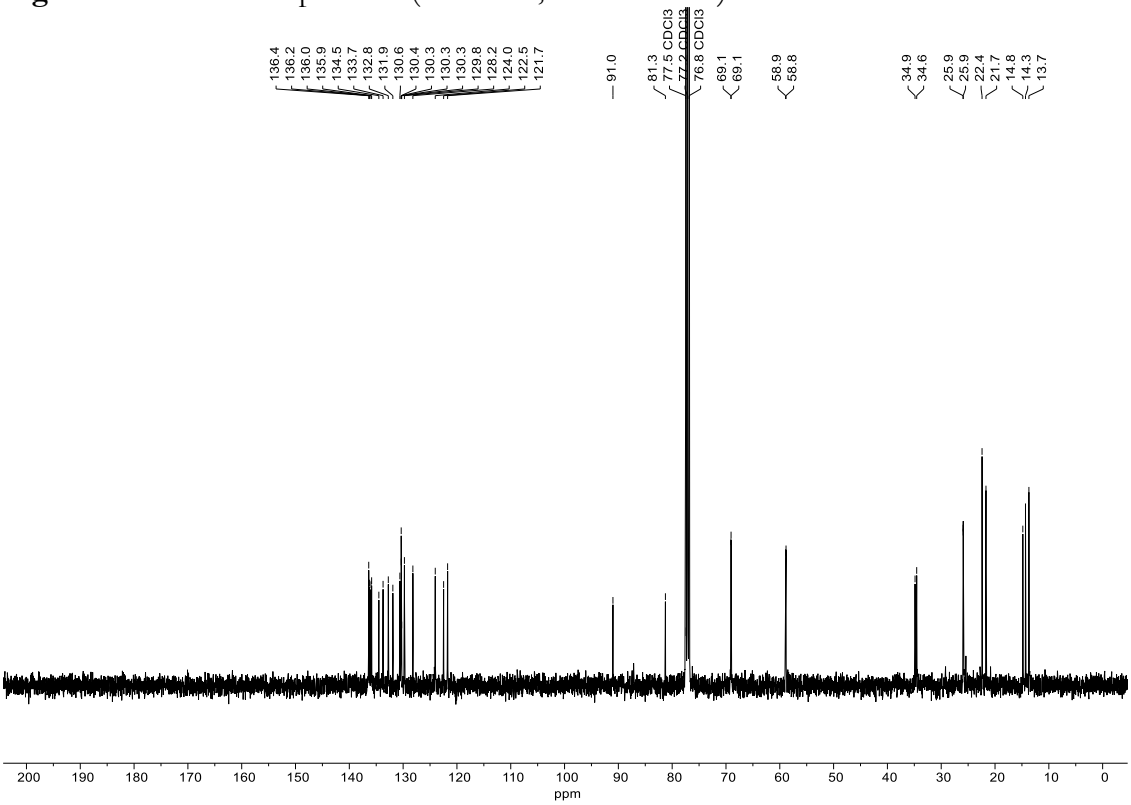

Figure S50. ^{13}C{^{1}H} NMR Spectrum (101 MHz, chloroform-*d*) of **2i**.

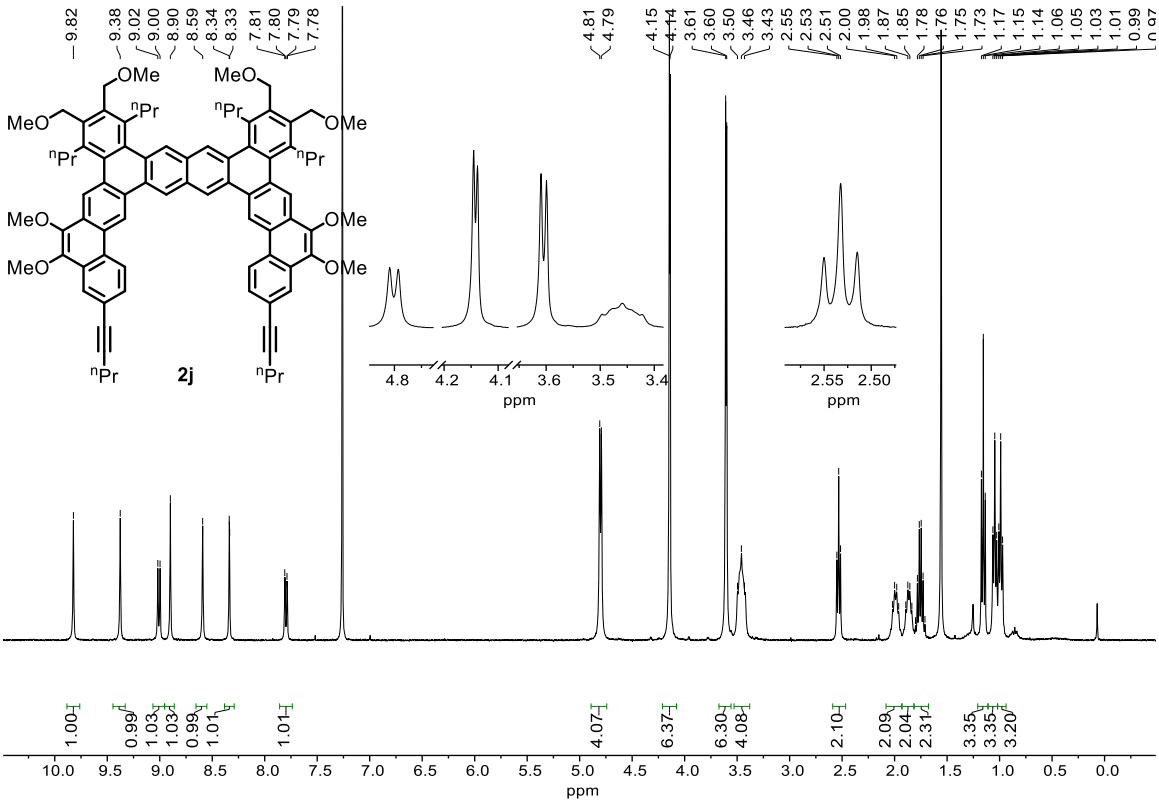

Figure S51. ^{1}H NMR Spectrum (400 MHz, chloroform-*d*) of **2j**.

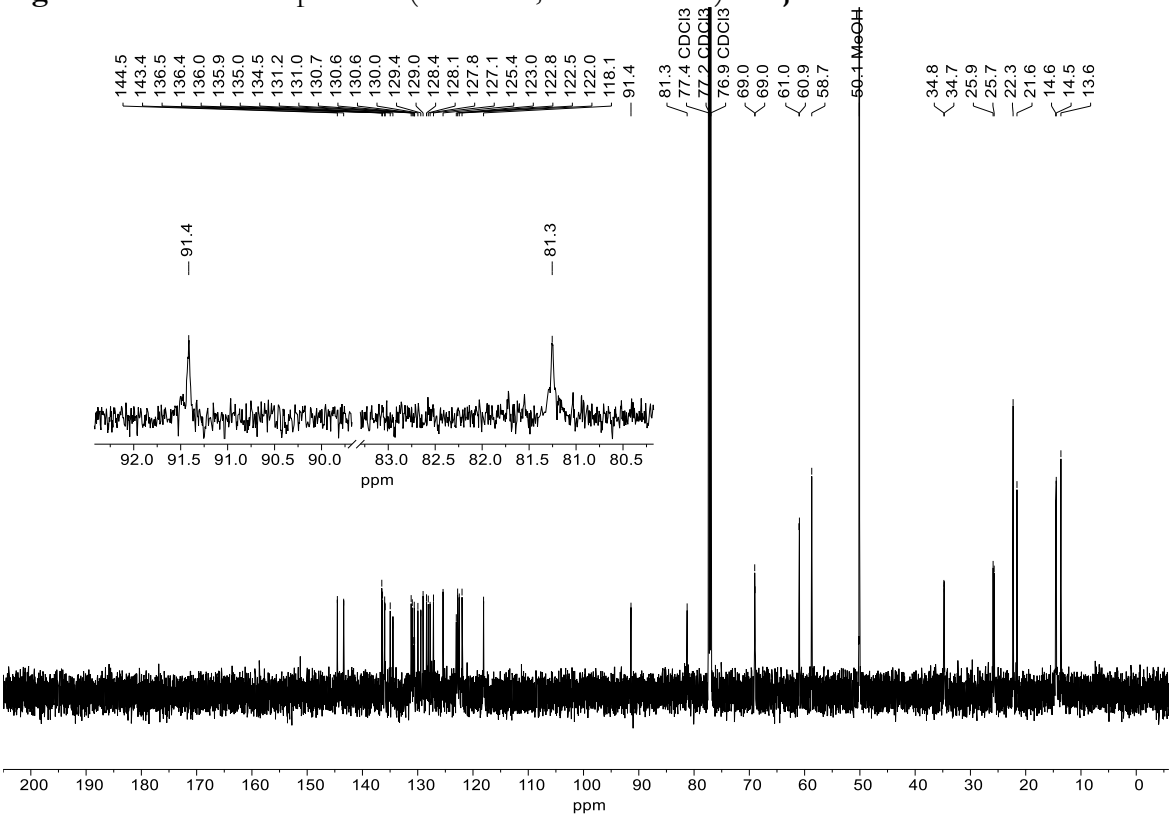

Figure S52. ^{13}C{^{1}H} NMR Spectrum (151 MHz, chloroform-*d*) of **2j**.

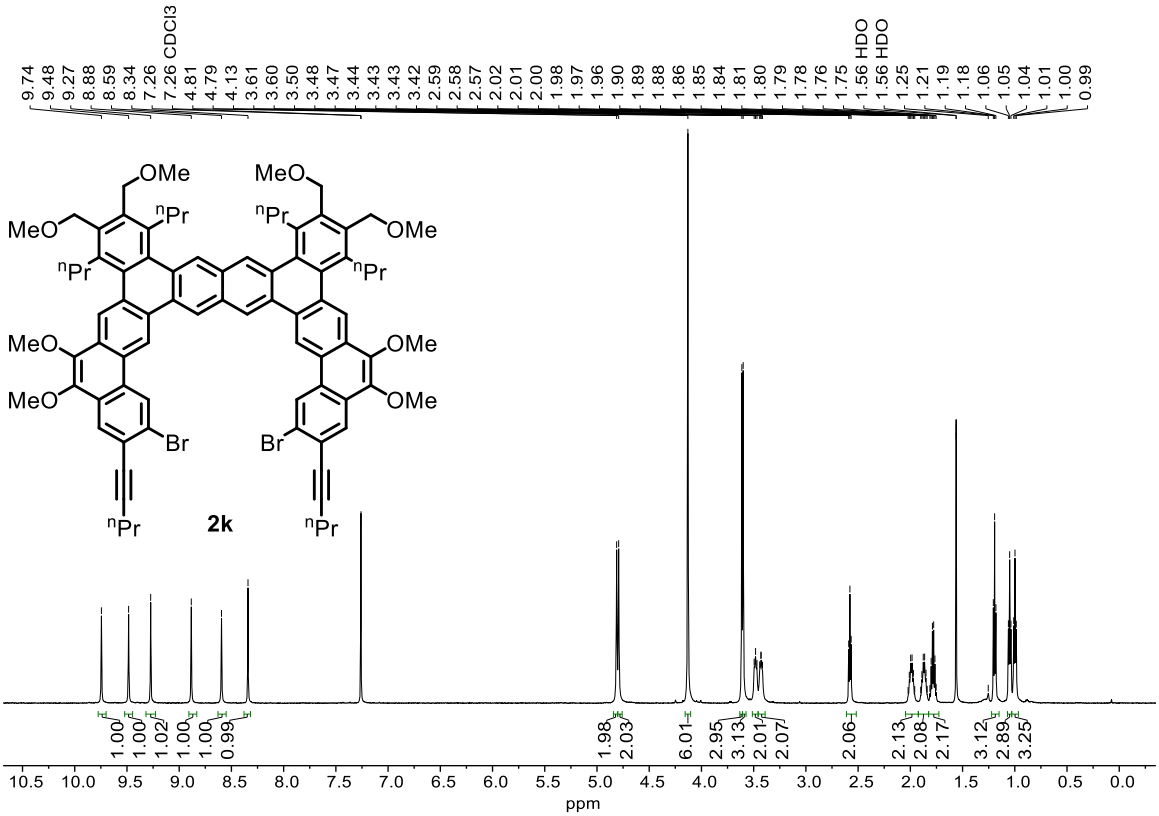

Figure S53. ^{1}H NMR Spectrum (600 MHz, chloroform-*d*) of **2k**.

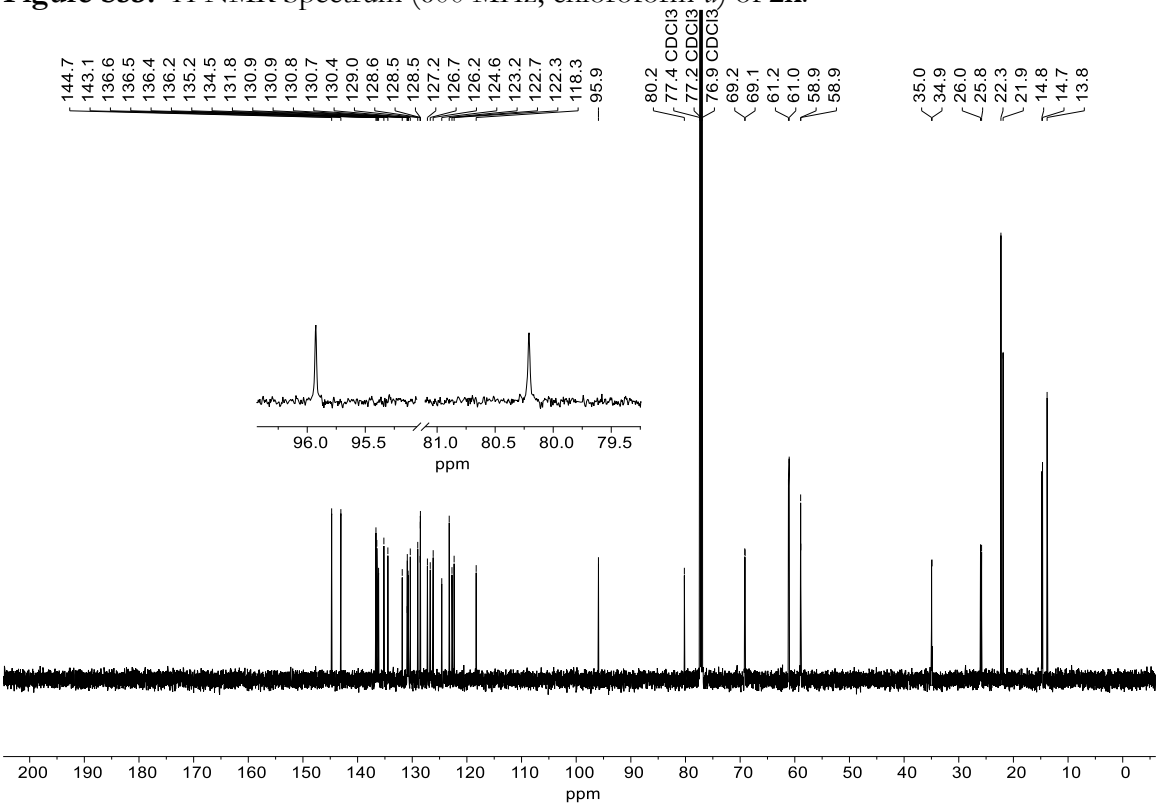

Figure S54. ^{13}C{^{1}H} NMR Spectrum (151 MHz, chloroform-*d*) of **2k**.

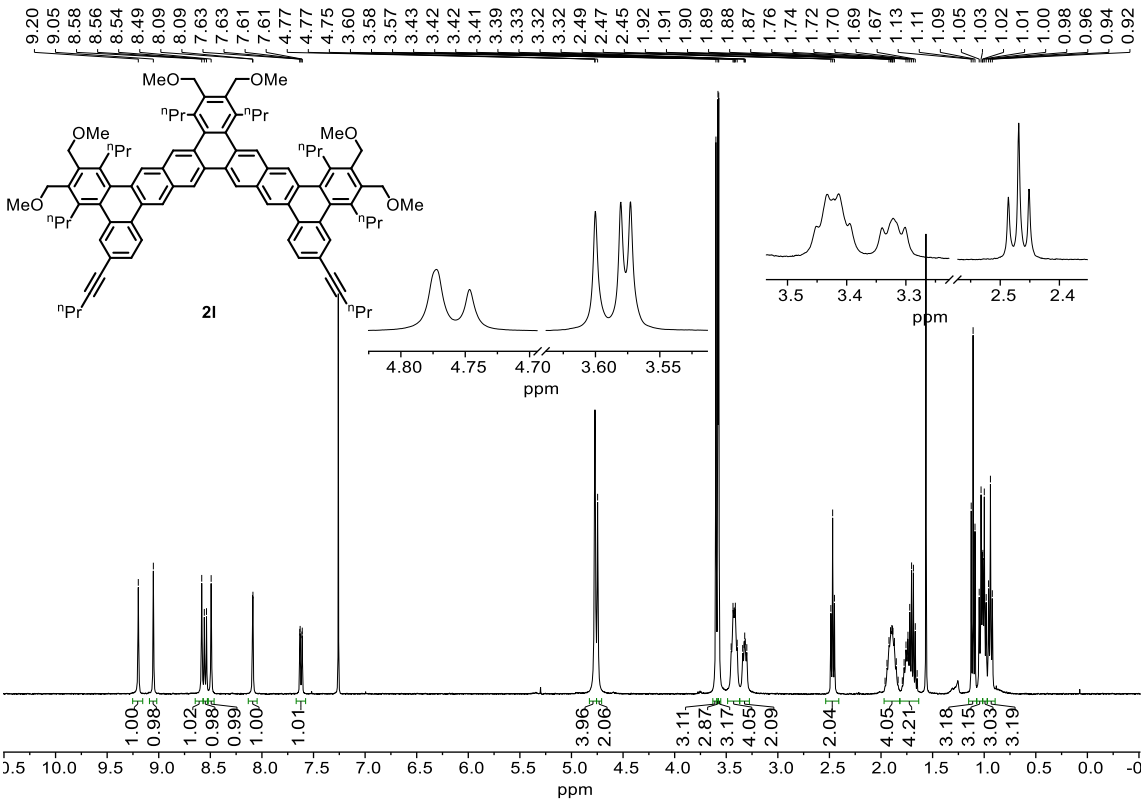

Figure S55. ^{1}H NMR Spectrum (400 MHz, chloroform-*d*) of **2l**.

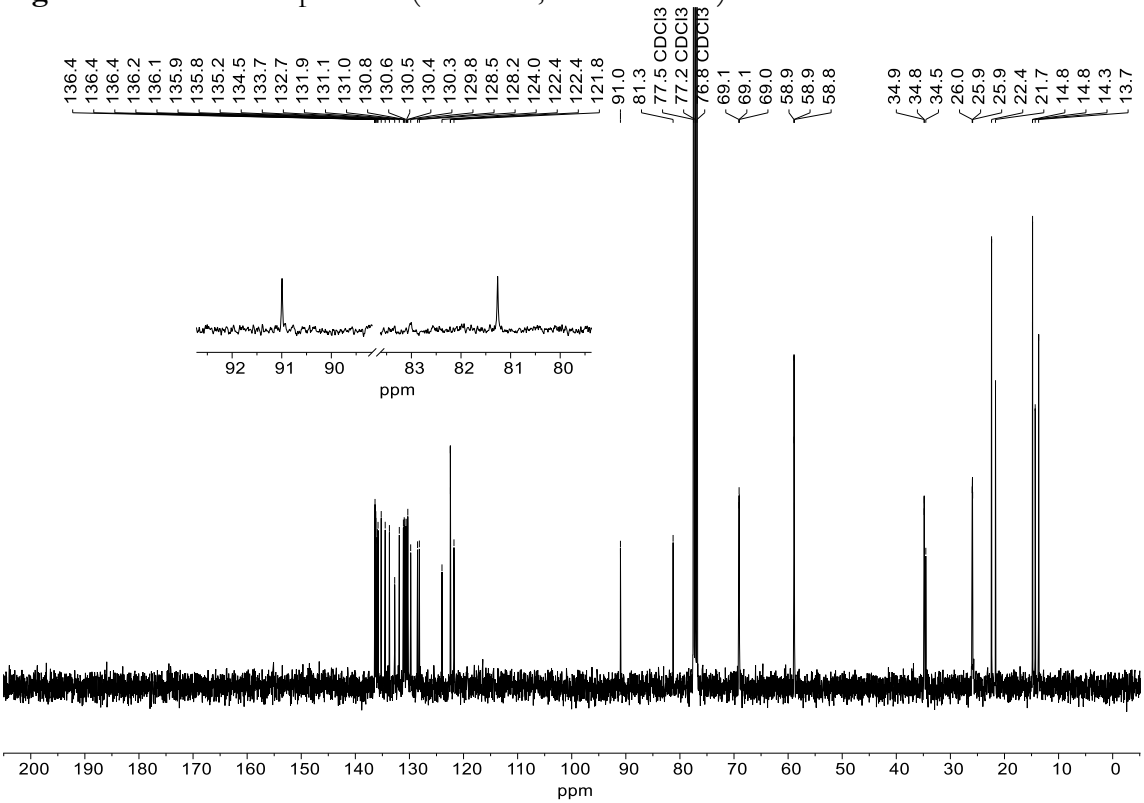

Figure S56. ^{13}C{^{1}H} NMR Spectrum (101 MHz, chloroform-*d*) of **2l**.

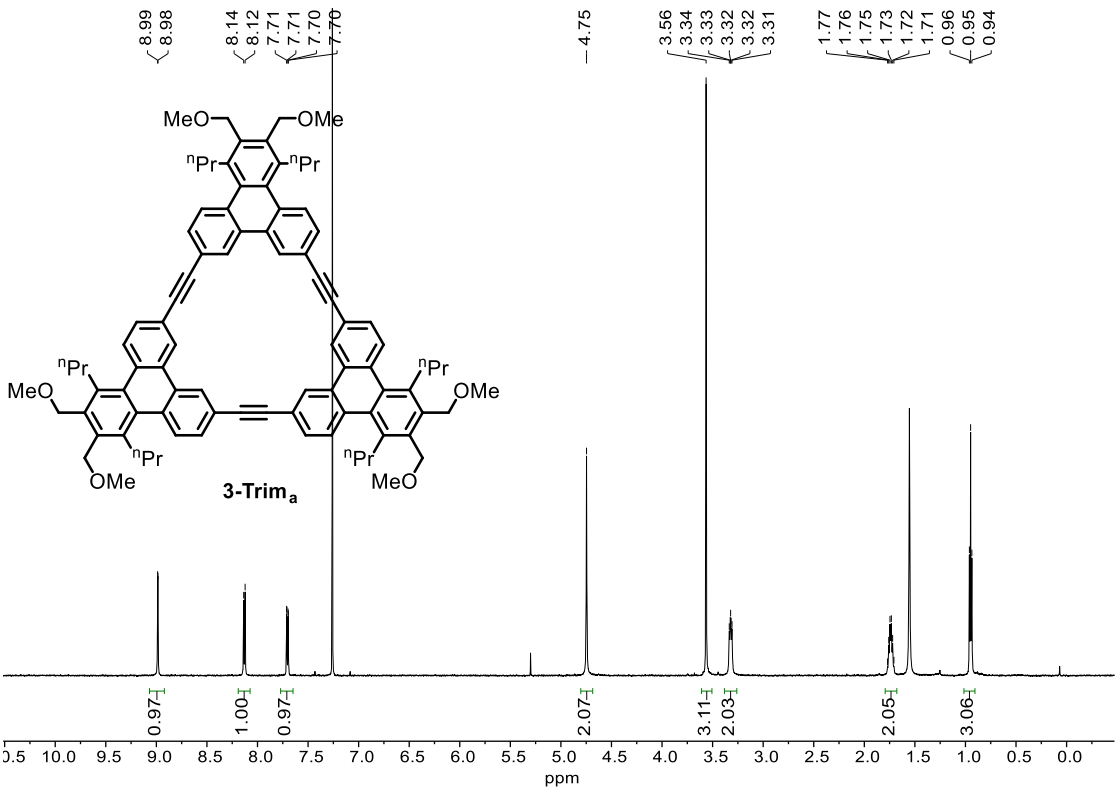

Figure S57. ^{1}H NMR Spectrum (600 MHz, chloroform-*d*) of **3-Trim$_a$**.

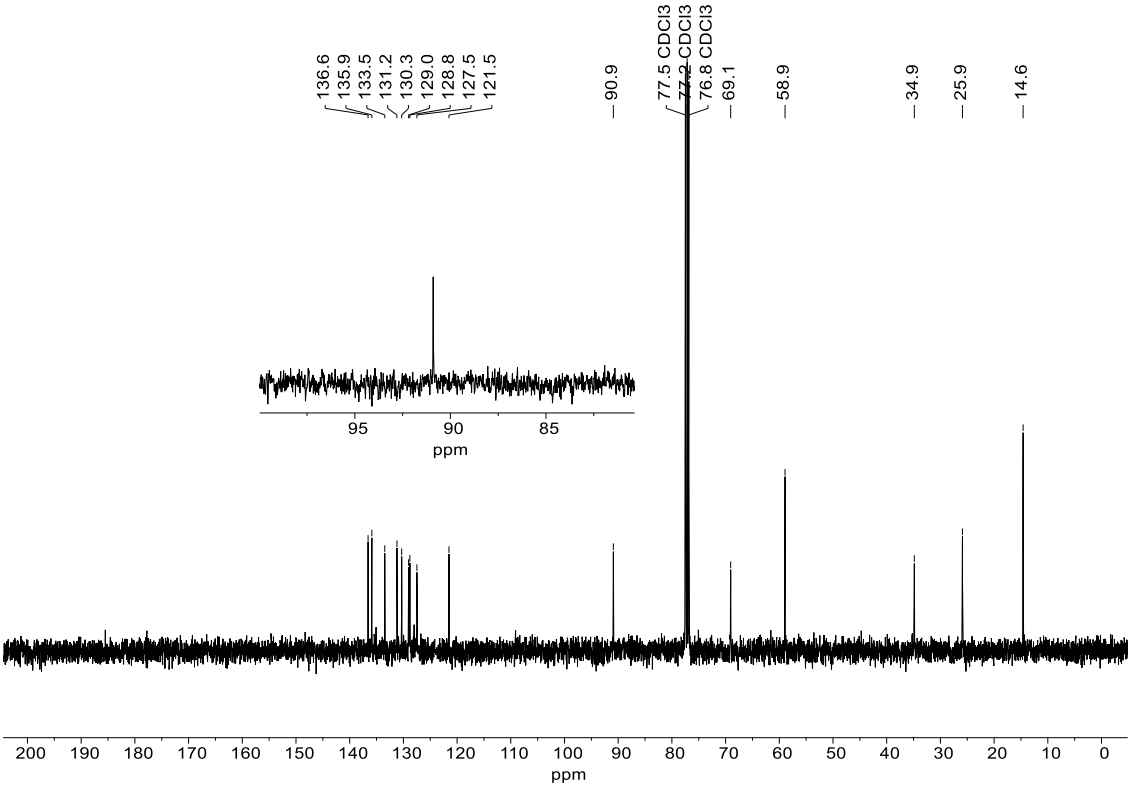

Figure S58. ^{13}C{^{1}H} NMR Spectrum (101 MHz, chloroform-*d*) of **3-Trim$_a$**.

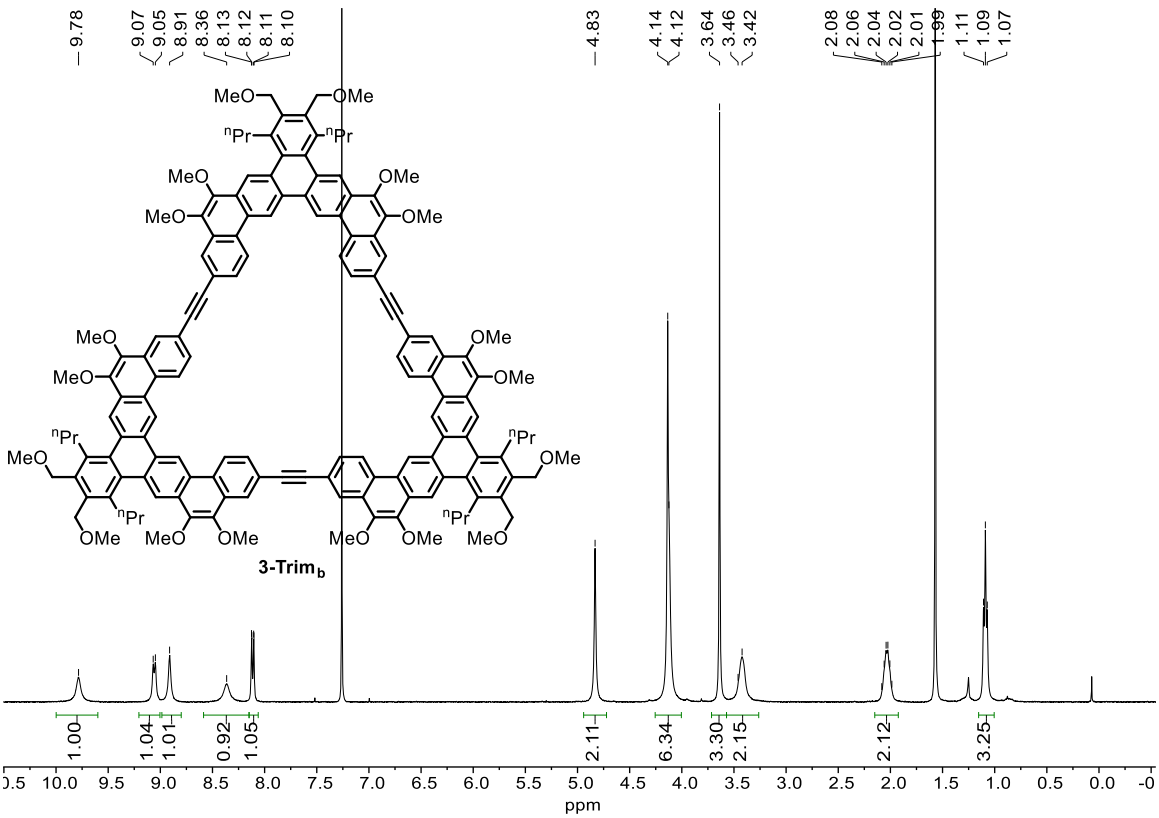

Figure S59. ^{1}H NMR Spectrum (400 MHz, chloroform-*d*, [c] = 1.9 mM) of **3-Trim$_b$**.

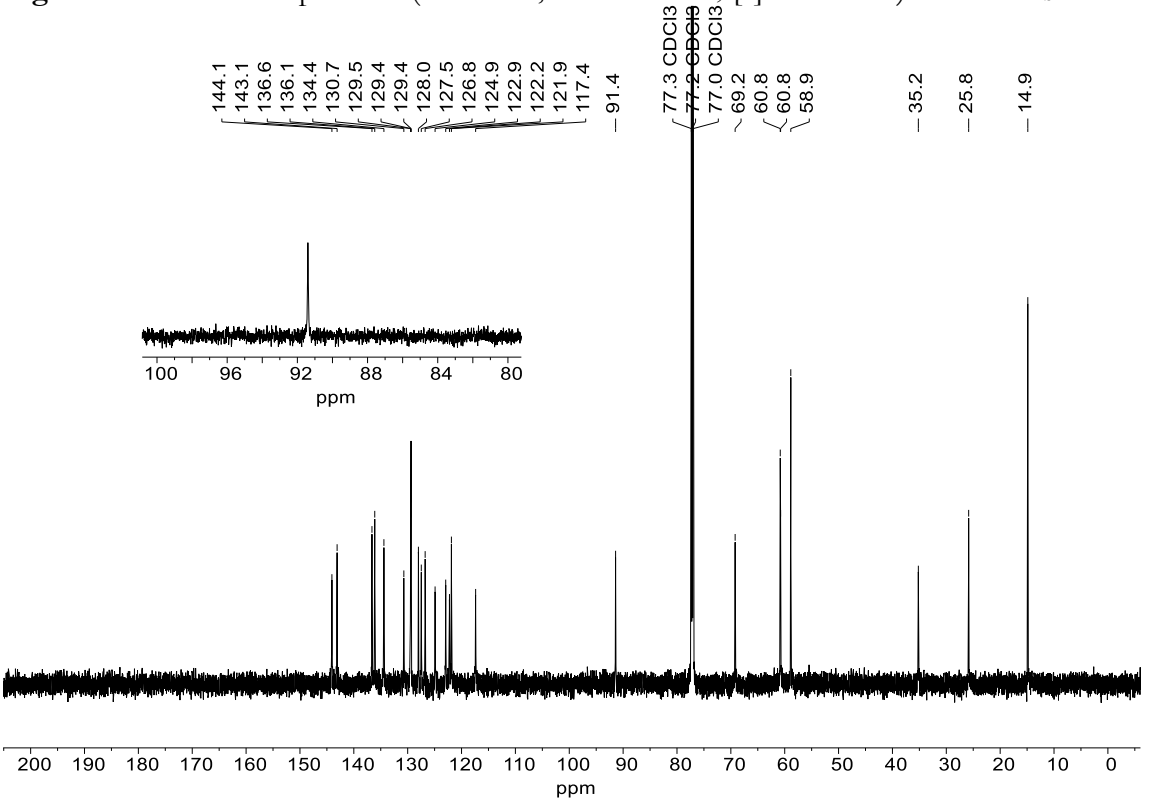

Figure S60. ^{13}C{^{1}H} NMR Spectrum (176 MHz, chloroform-*d*) of **3-Trim$_b$**.

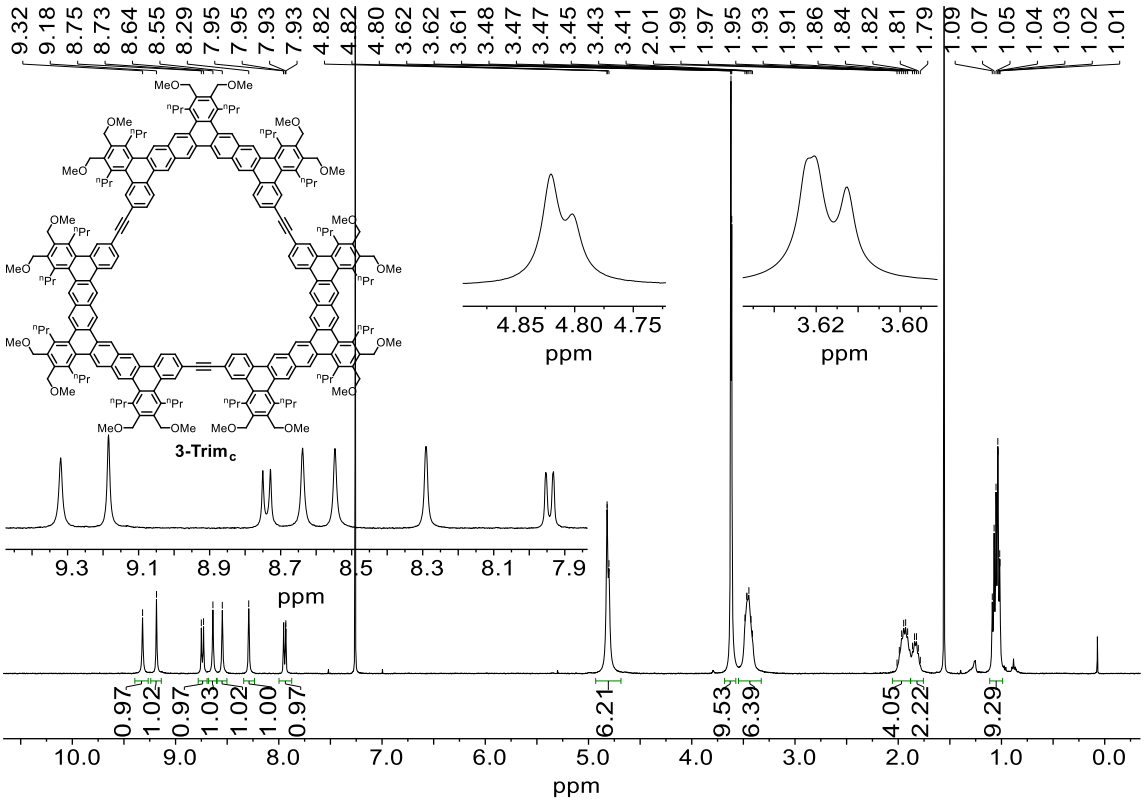

Figure S61. ^{1}H NMR Spectrum (400 MHz, chloroform-*d*) of **3-Trim$_c$**.

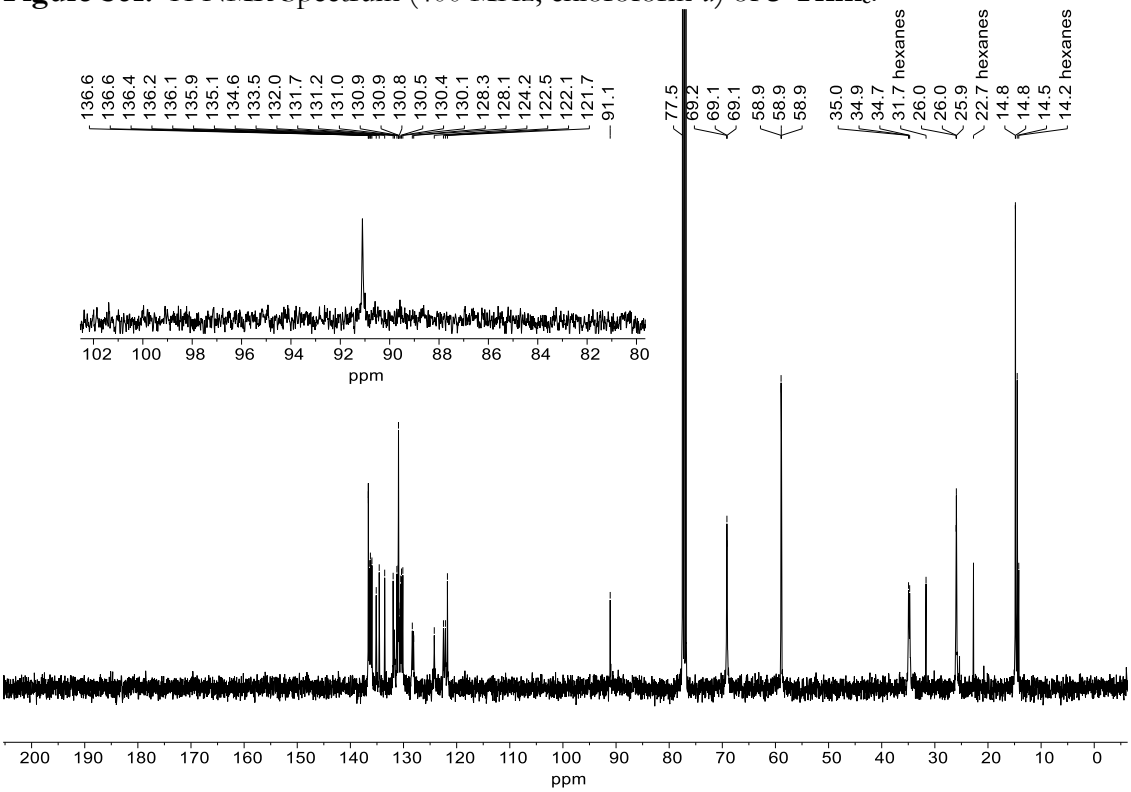

Figure S62. ^{13}C{^{1}H} NMR Spectrum (101 MHz, chloroform-*d*) of **3-Trim$_c$**.

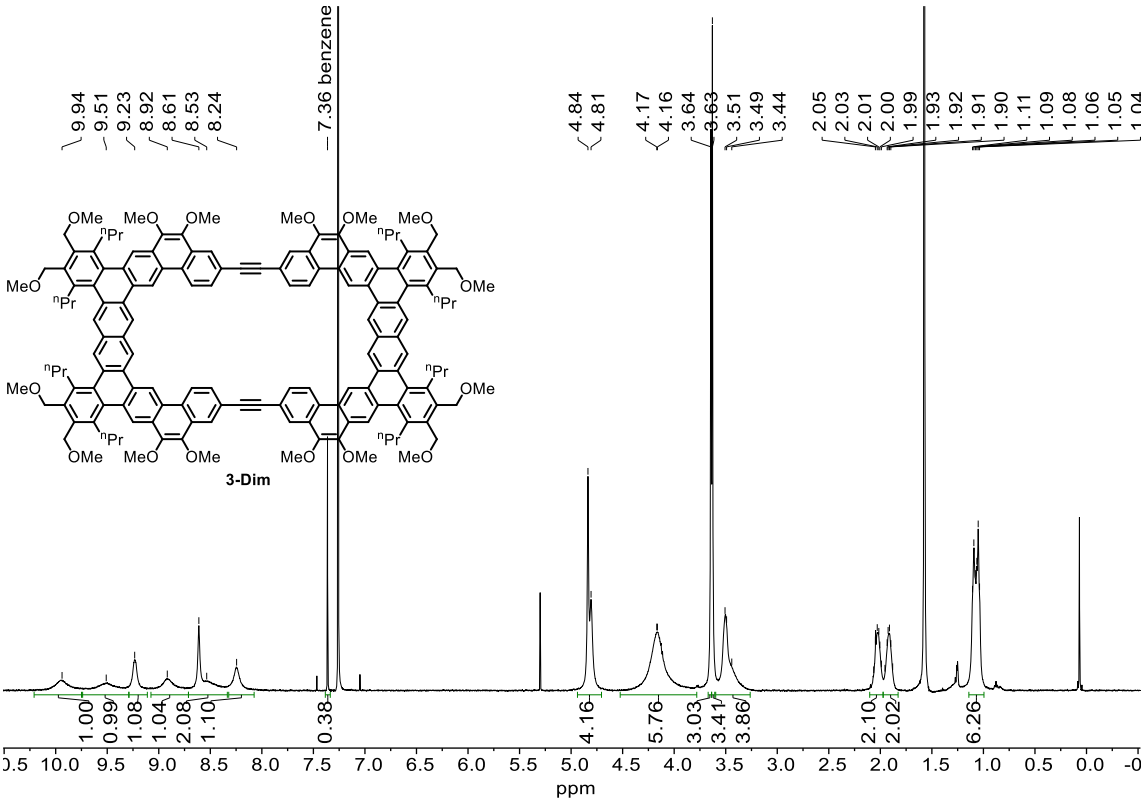

Figure S63. ^{1}H NMR Spectrum (500 MHz, chloroform-*d*, [c] = 1.5 mM) of **3-Dim**.

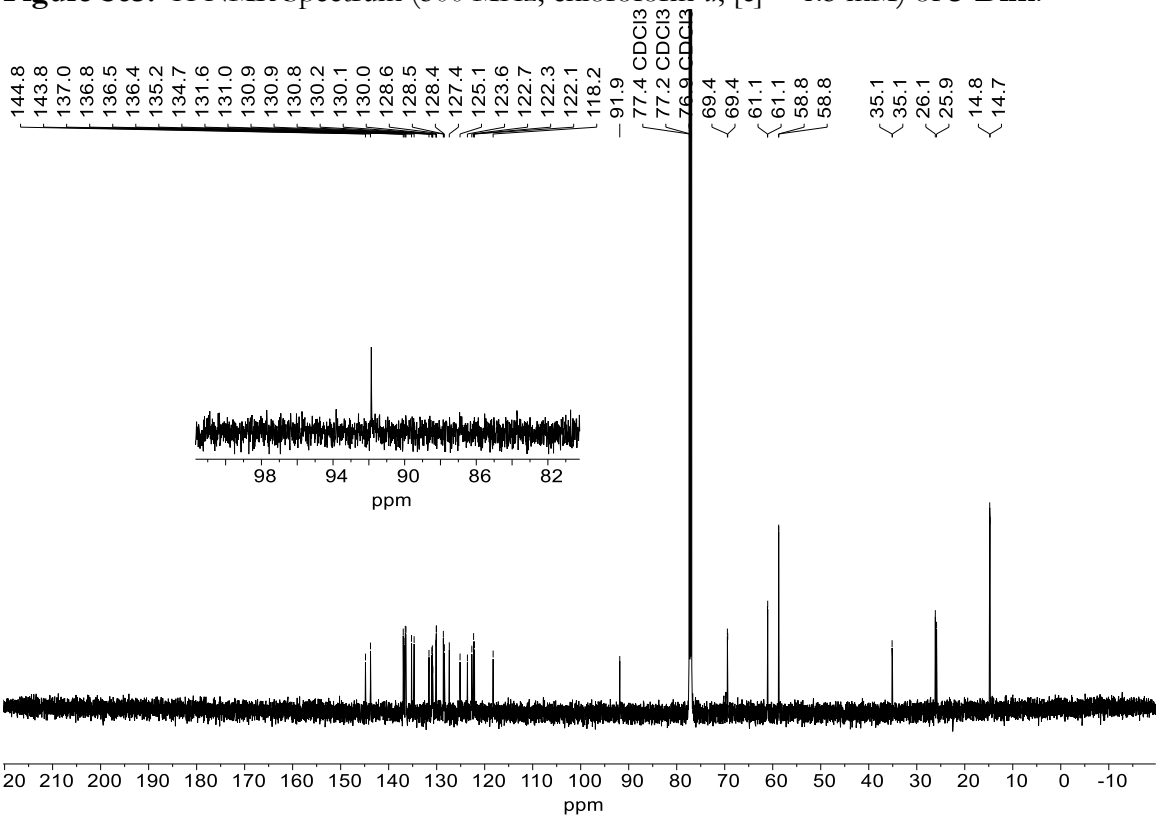

Figure S64. ^{13}C{^{1}H} NMR Spectrum (151 MHz, chloroform-*d*, 60 °C) of **3-Dim**.

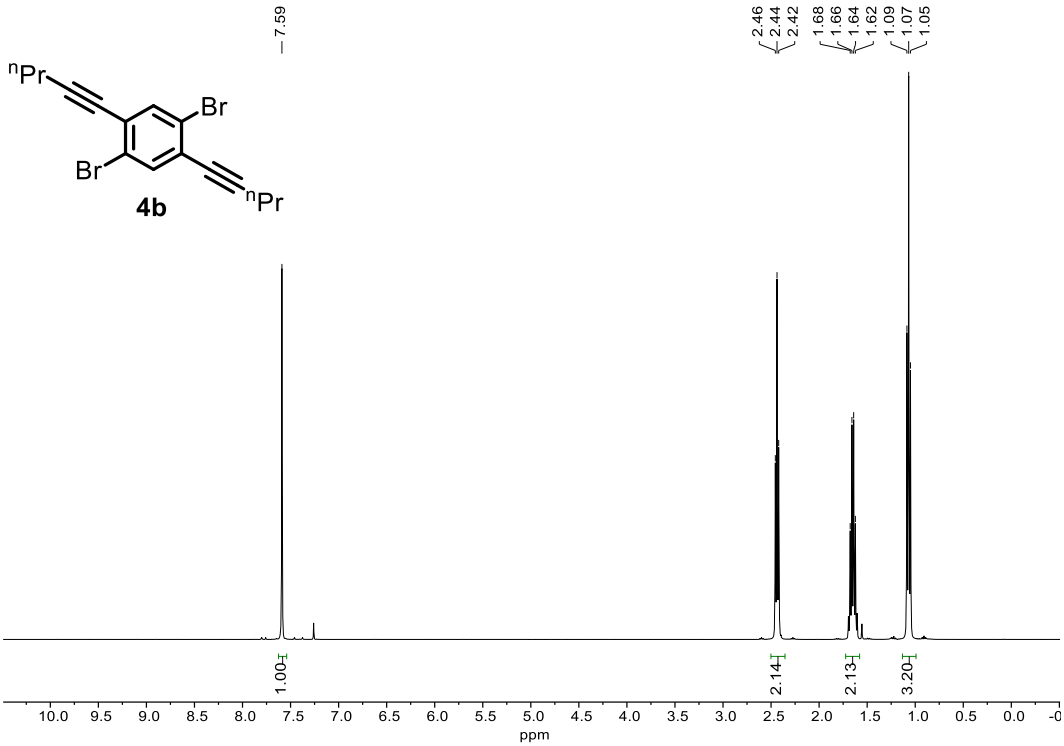

Figure S65. ^{1}H NMR Spectrum (400 MHz, chloroform-*d*) of **4b**.

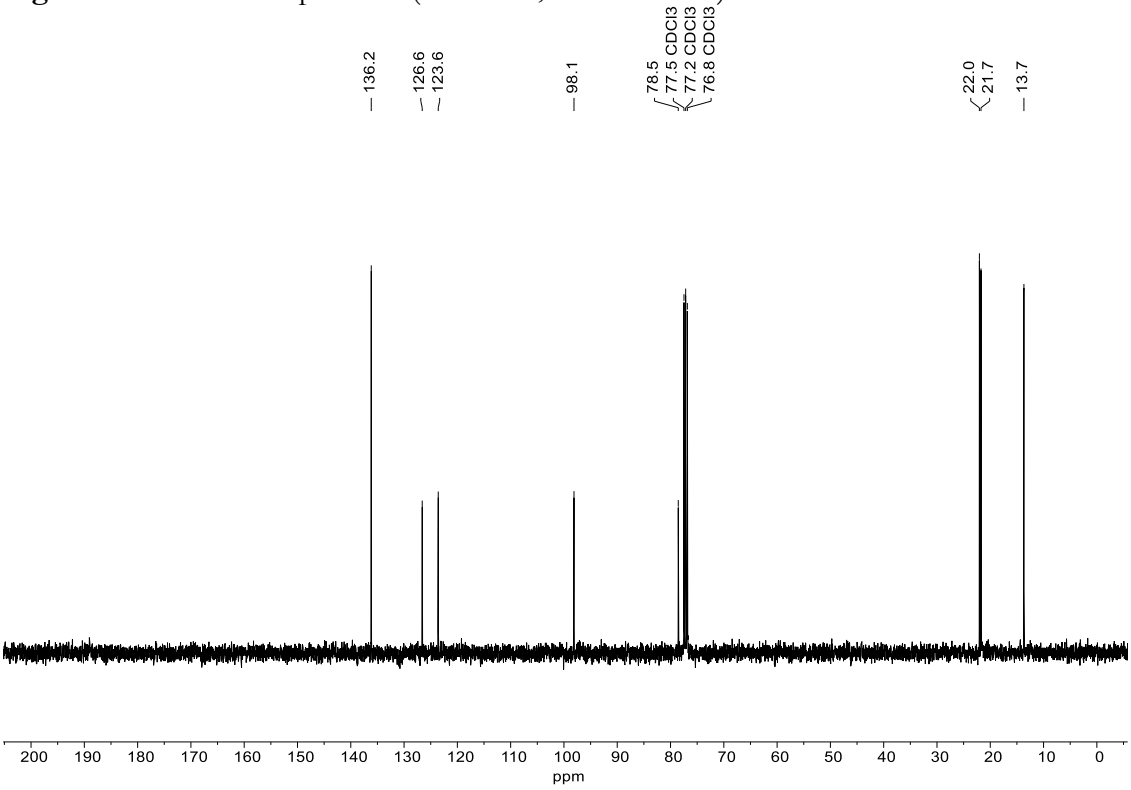

Figure S66. ^{13}C{^{1}H} NMR Spectrum (101 MHz, chloroform-*d*) of **4b**.

Variable Concentration ^{1}H NMR Spectra

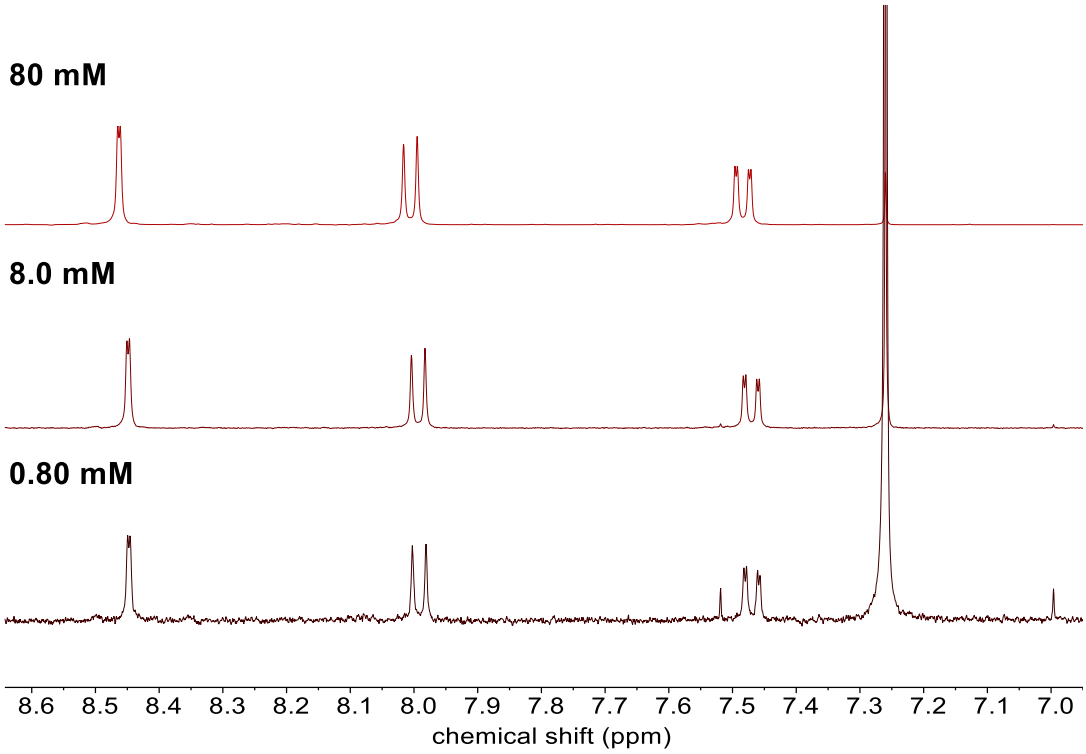

Figure S67. Variable concentration partial ^{1}H NMR spectra (400 MHz, chloroform-*d*) of **2c**.

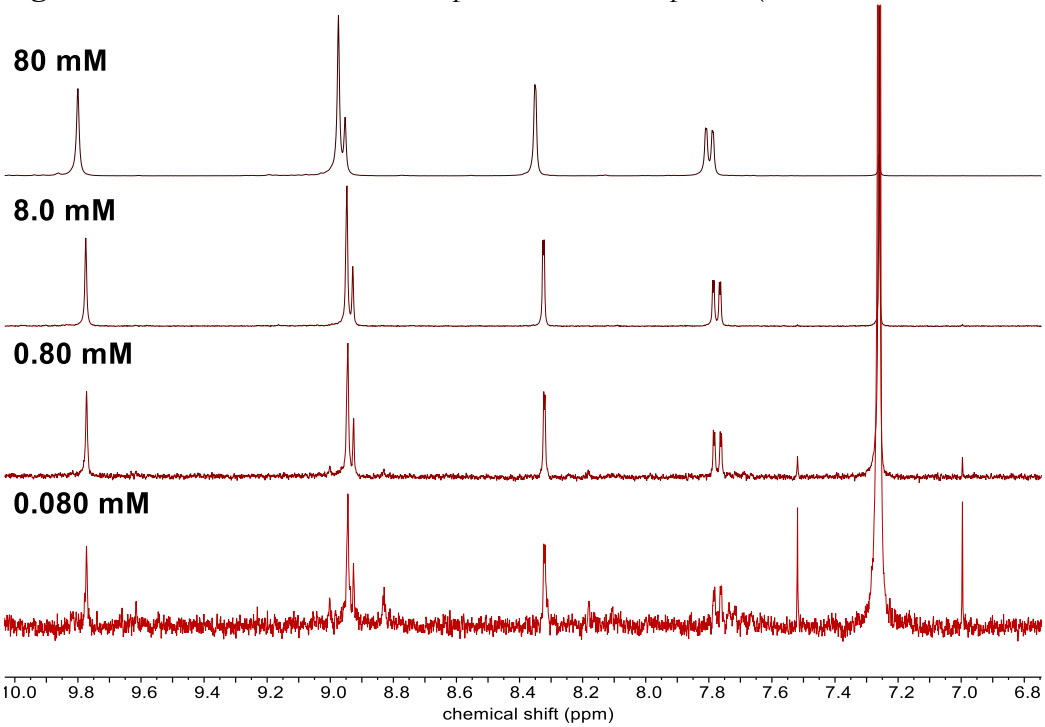

Figure S68. Variable concentration partial ^{1}H NMR spectra (400 MHz, chloroform-*d*) of **2g**.

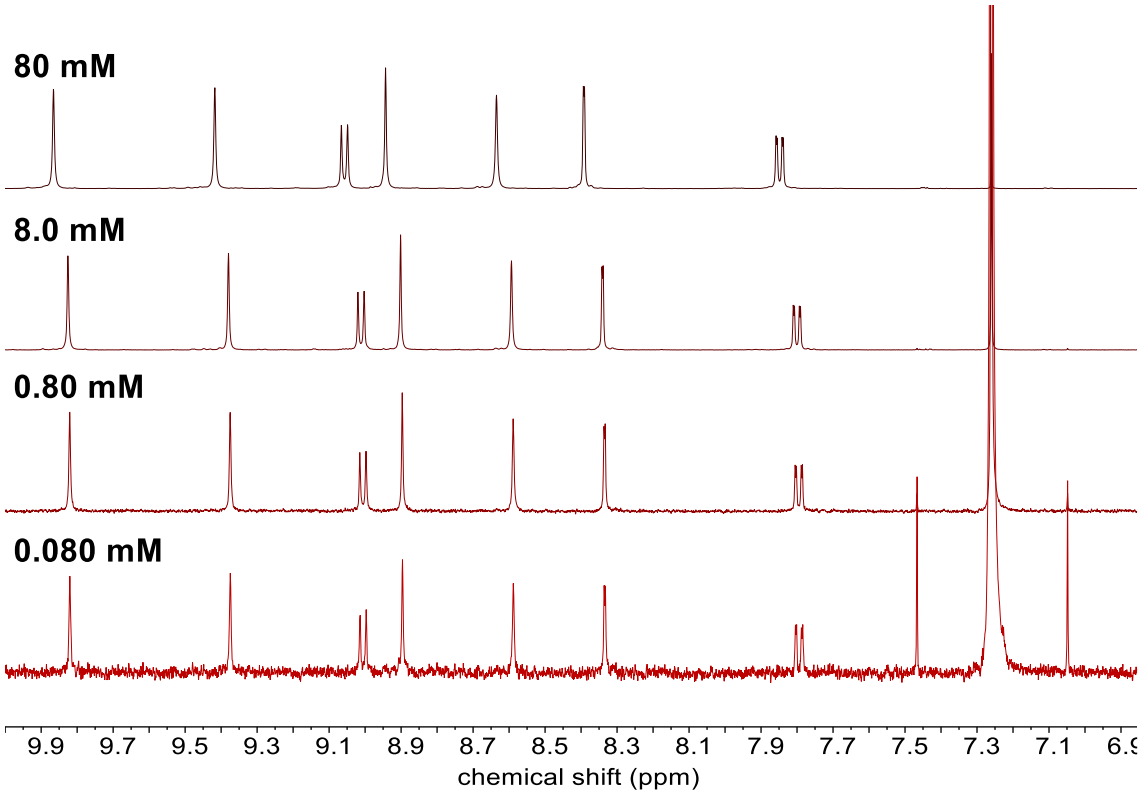

Figure S69. Variable concentration partial ^{1}H NMR spectra (500 MHz, chloroform-*d*) of **2j**.

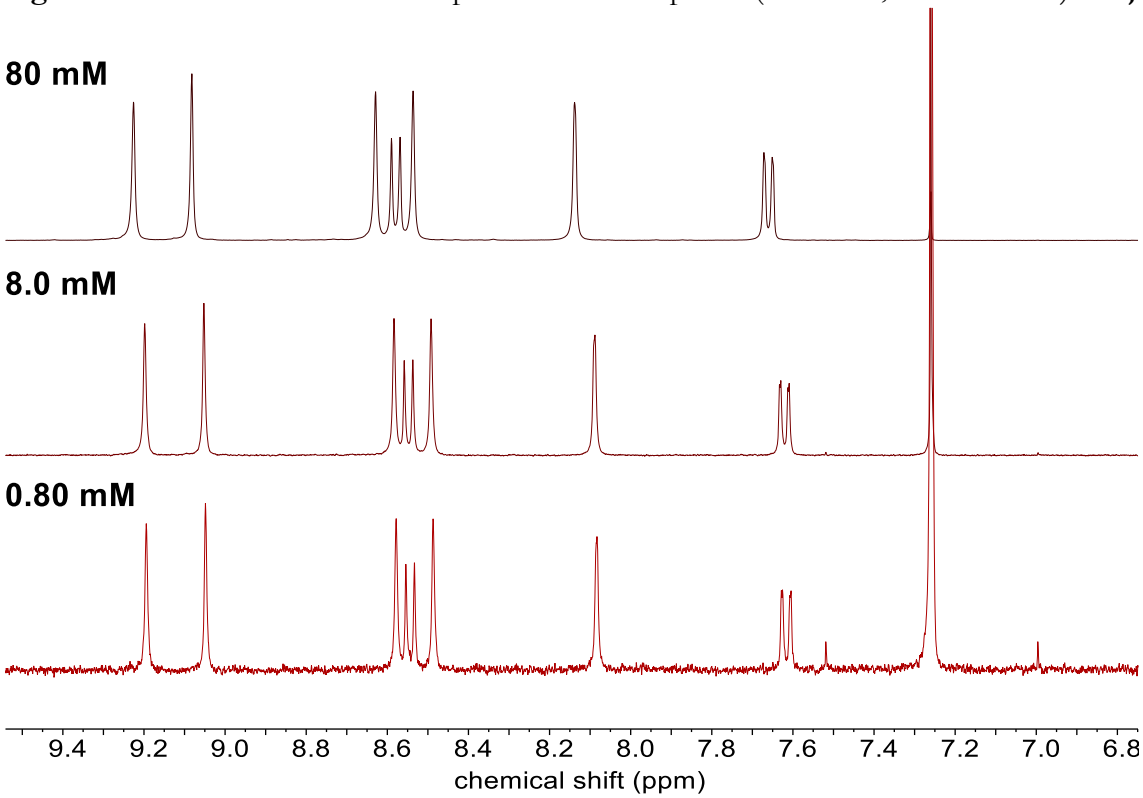

Figure S70. Variable concentration partial ^{1}H NMR spectra (400 MHz, chloroform-*d*) of **2l**.

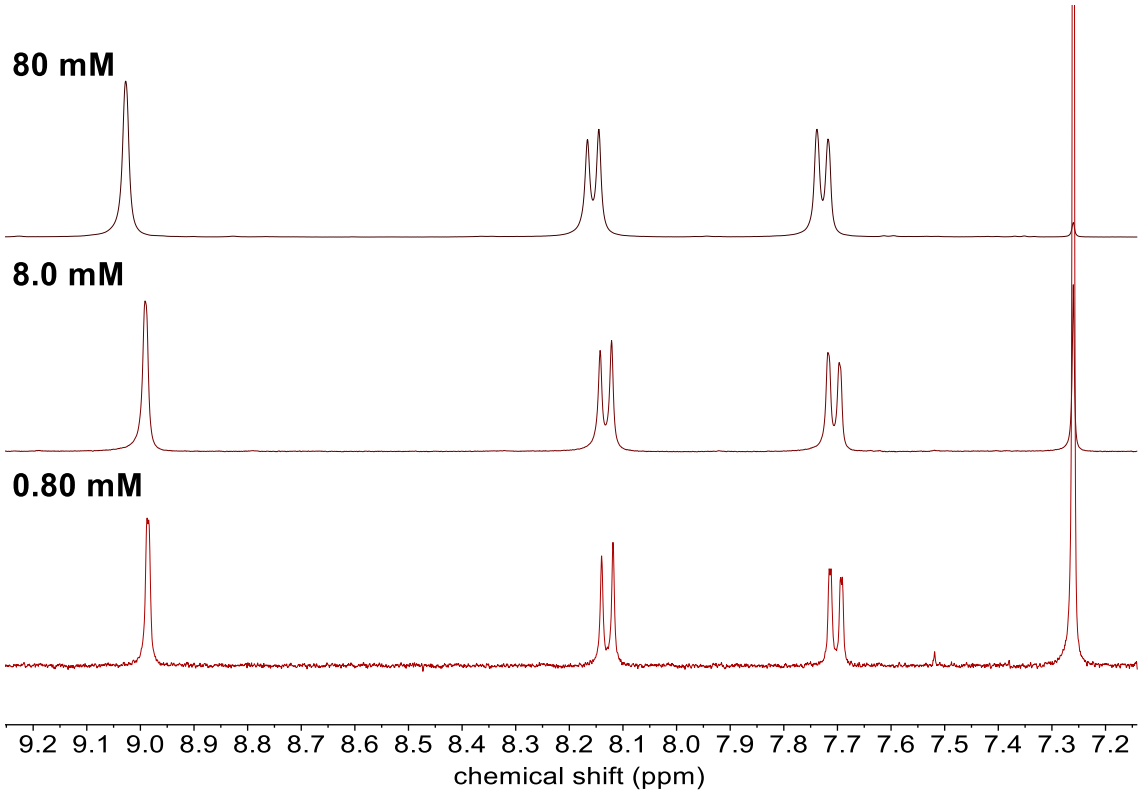

Figure S71. Variable concentration partial ^{1}H NMR spectra (400 MHz, chloroform-*d*) of **3-Trim$_a$**.

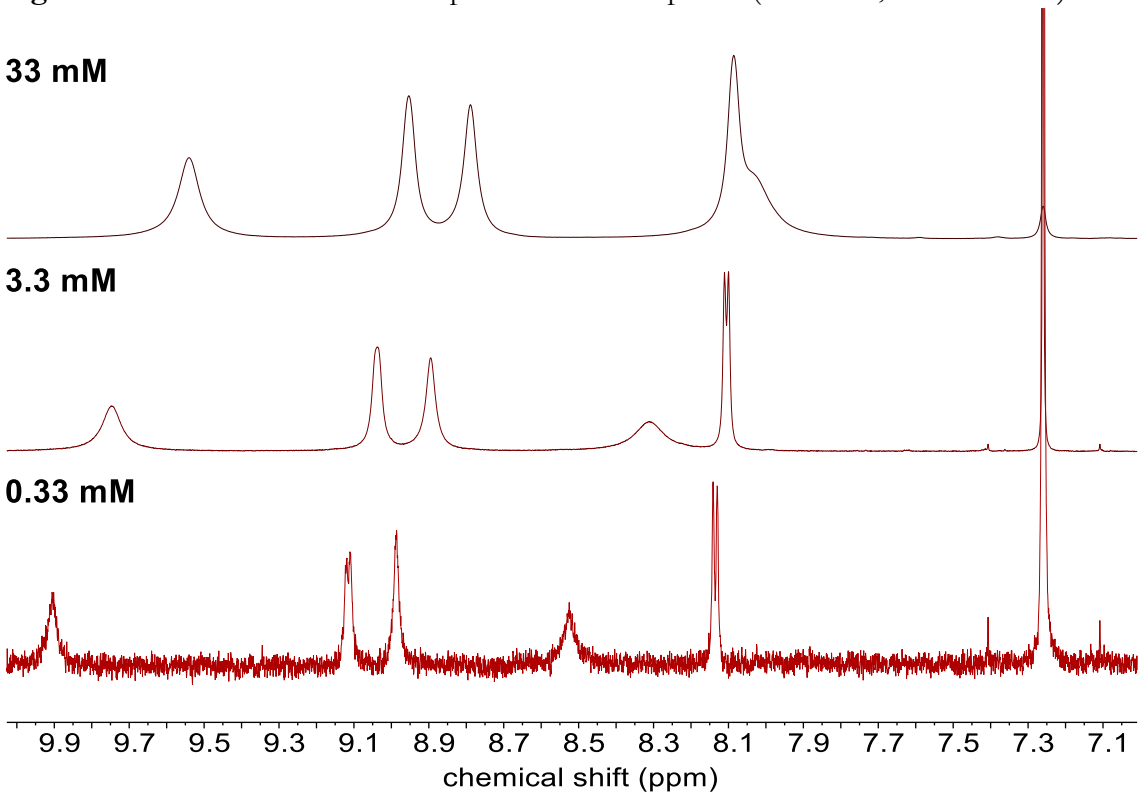

Figure S72. Variable concentration partial ^{1}H NMR spectra (700 MHz, chloroform-*d*) of **3-Trim$_b$**.

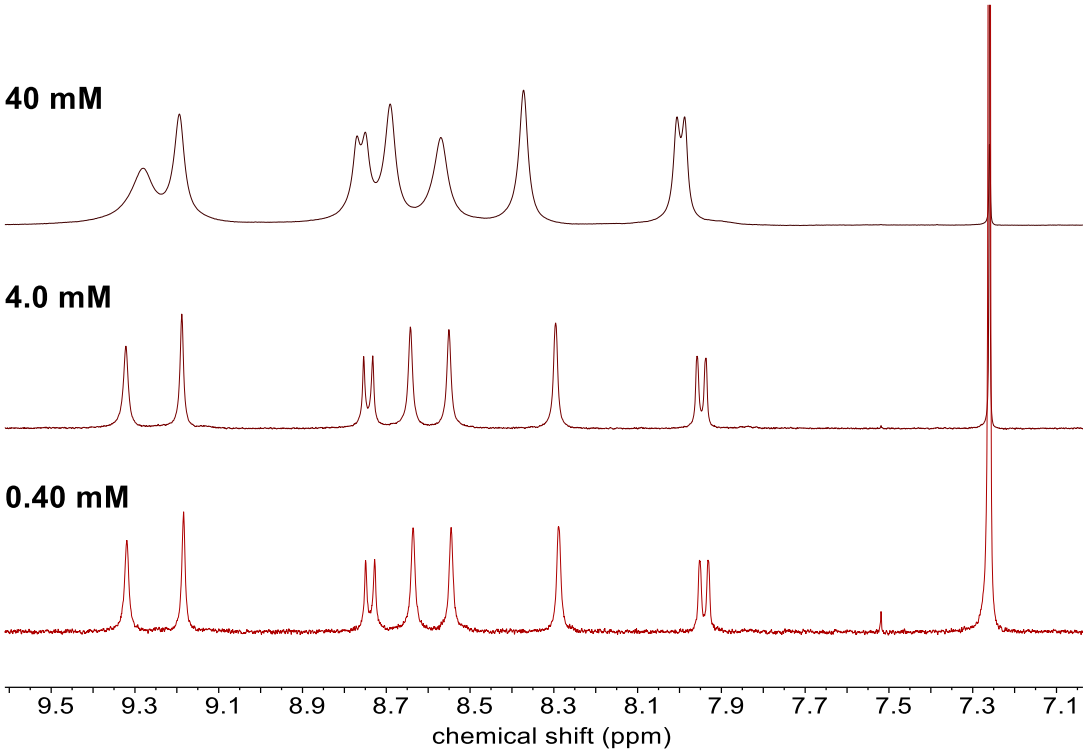

Figure S73. Variable concentration partial ^{1}H NMR spectra (400 MHz, chloroform-*d*) of **3-Trim$_c$**.

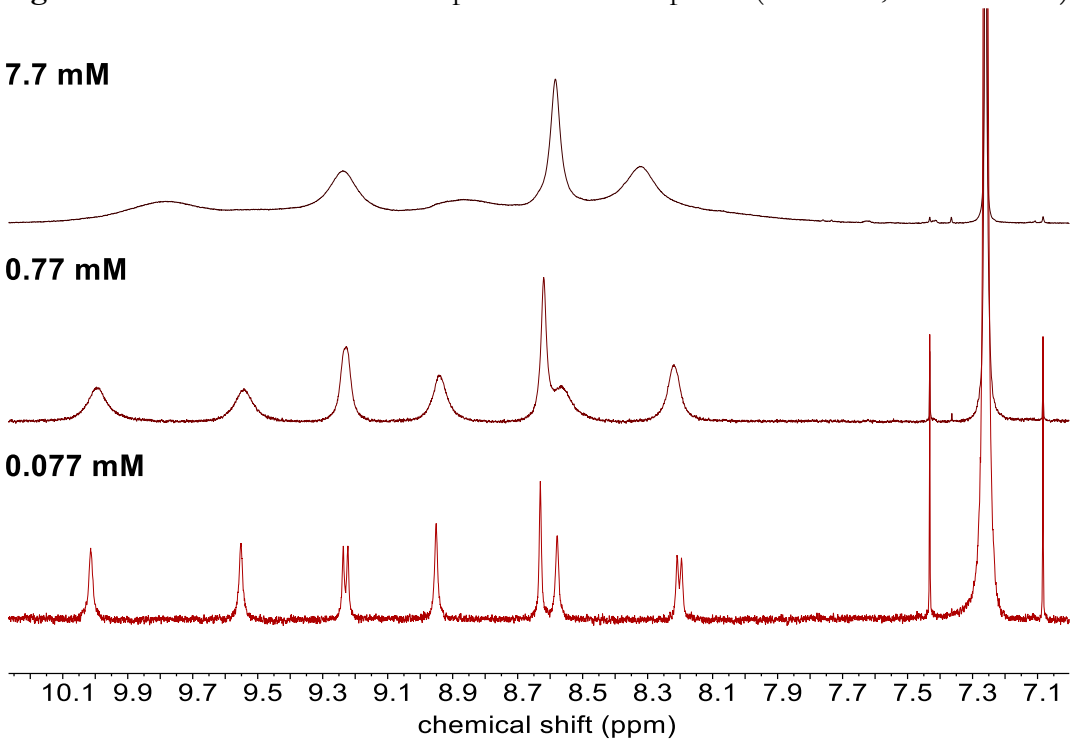

Figure S74. Variable concentration partial ^{1}H NMR spectra (600 MHz, chloroform-*d*) of **3-Dim**.

Photophysical Characterization

UV/Vis spectra were recorded on a Varian Cary 300 Bio UV-Visible spectrophotometer. Emission spectra were recorded on a Varian Cary Eclipse Spectrometer. All compounds were subjected to preparatory thin layer chromatography (CH_2Cl_2/hexanes or CH_2Cl_2/EtOAc solvent system) prior to analysis to ensure high purity. The UV/Vis spectra that are shown represent the average of two measurements on separate samples to ensure accuracy of extinction coefficients. For sample preparation, each analyte was weighed on an analytical balance and dissolved in the appropriate amount of CH_2Cl_2 using a volumetric flask. A single dilution experiment (10x) was performed for each compound. For all compounds, the UV/vis spectra (plotted by molar absorptivity) are unchanged by this dilution. Emission spectra for all compounds are independent of excitation wavelength.

Table S1. Summary of relevant photophysical properties

Compound	Absorption Onset, λ_{onset} (nm)[a,b]	Absorption Maximum, λ_{max} (nm)[a]	Emission Maximum, λ_{max} (nm)[a]	Photophysical E_g (eV)[a,c]
2c	375	297	414	3.31
3-Trim$_a$	393	351	426	3.16
2g	410	329	432	3.02
3-Trim$_b$	420	367	442	2.95
2l	438	339	465	2.83
3-Trim$_c$	442	384	468	2.81
2j	429	315, 344	452	2.89
3-Dim	431	365	453	2.88

(a) Solvent = CH_2Cl_2; (b) Defined as the point at which the absorption and emission spectra intersect;[29] (c) Estimated from the absorption onset (λ_{onset}): $E_g = 1240/\lambda_{onset}$.

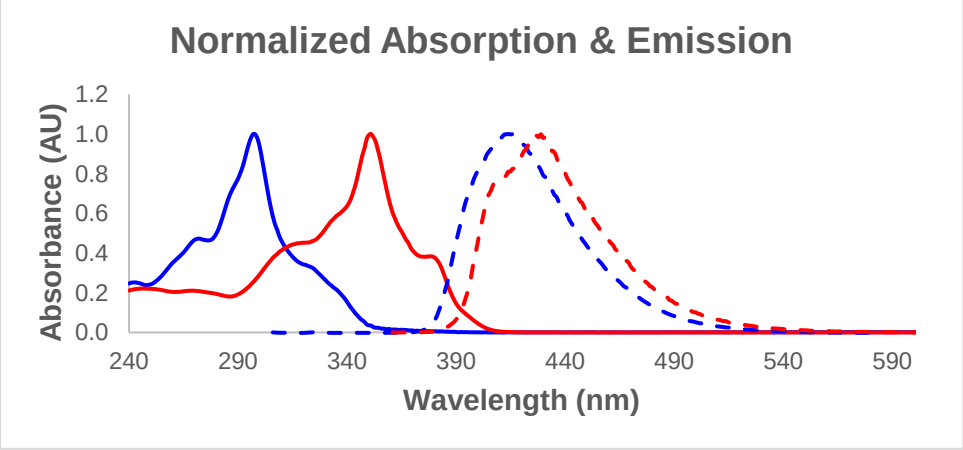

Figure S75. Normalized absorption (solid) and emission (dotted) spectra for AEM **3-Trim$_a$** (red) and its precursor PAH **2c** (blue) in CH_2Cl_2 solvent.

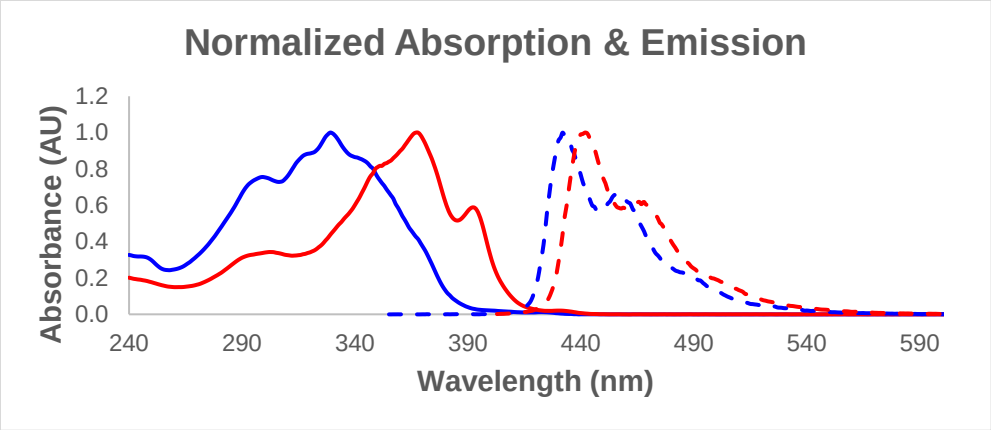

Figure S76. Normalized absorption (solid) and emission (dotted) spectra for AEM **3-Trim$_b$** (red) and its precursor PAH **2g** (blue) in CH_2Cl_2 solvent.

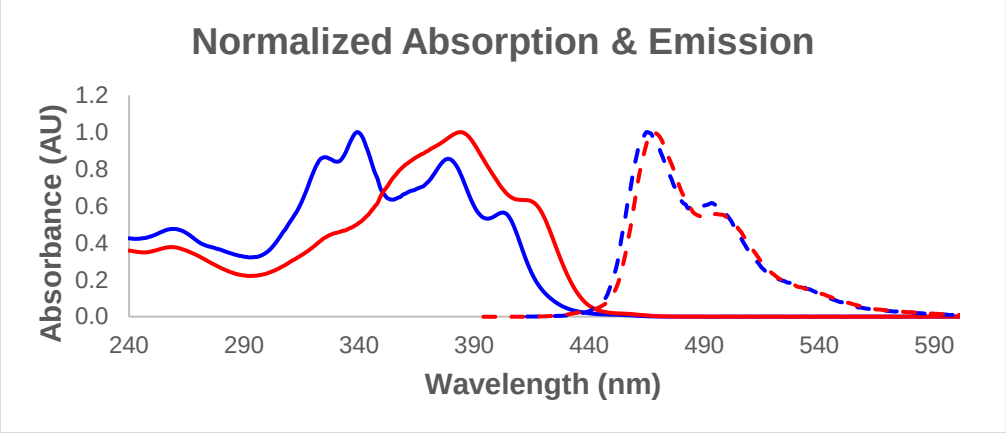

Figure S77. Normalized absorption (solid) and emission (dotted) spectra for AEM **3-Trim$_c$** (red) and its precursor PAH **2l** (blue) in CH_2Cl_2 solvent.

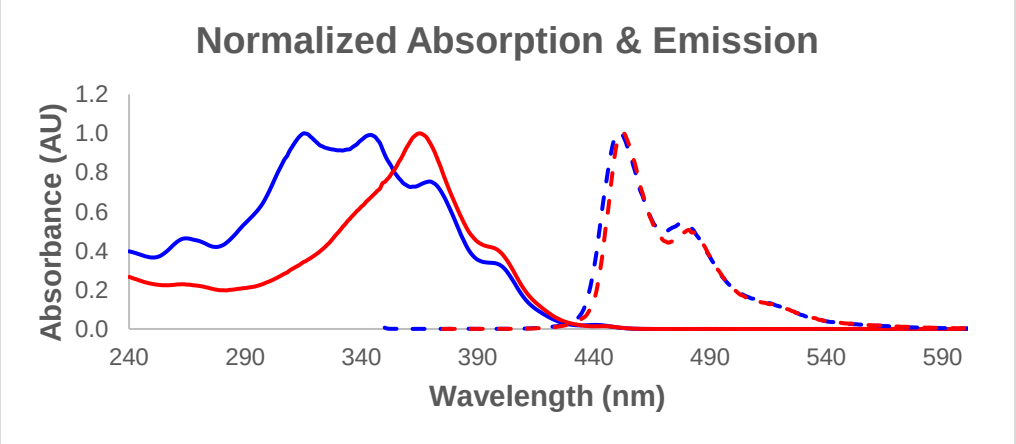

Figure S78. Normalized absorption (solid) and emission (dotted) spectra for AEM **3-Dim** (red) and its precursor PAH **2j** (blue) in CH_2Cl_2 solvent.

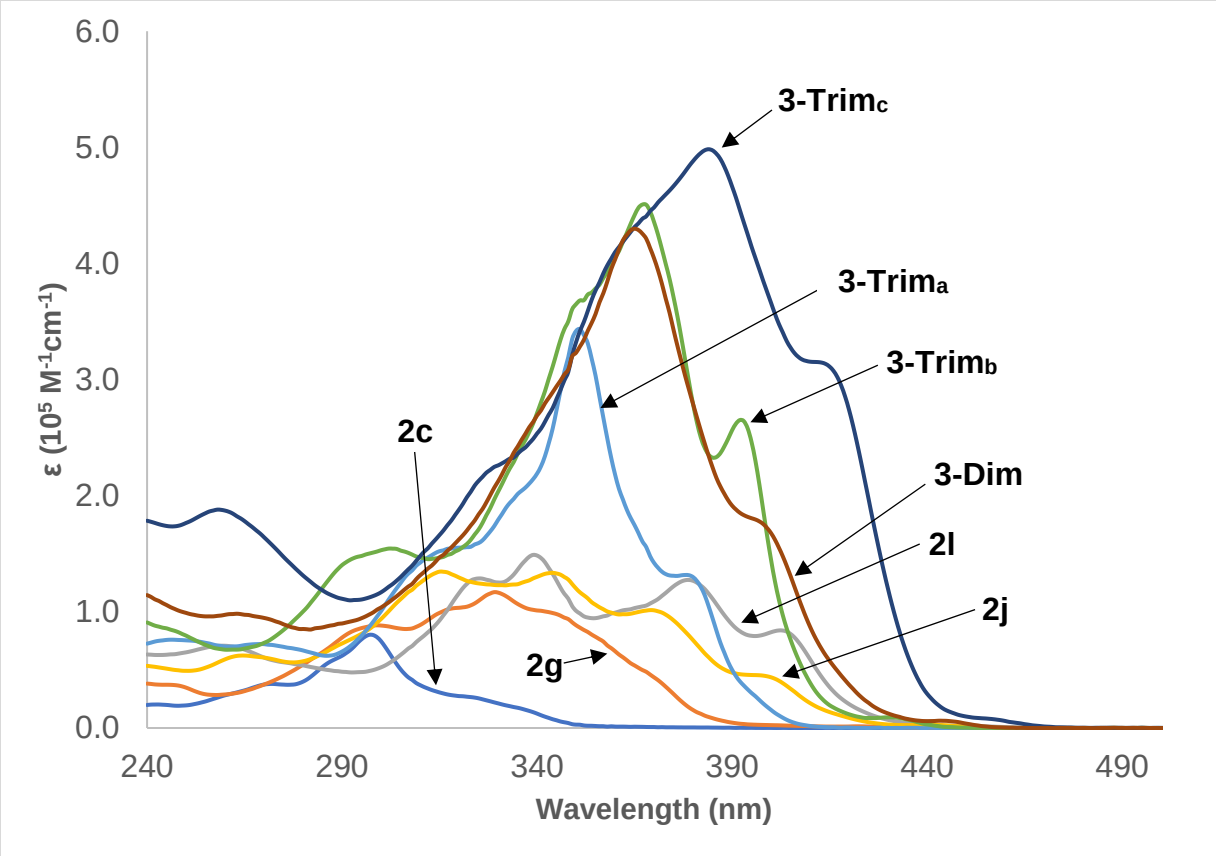

Figure S79. UV/Vis absorption spectra of PAHs **2c**, **2g**, **2l**, and **2j** and AEMs **3-Trim$_a$**, **3-Trim$_b$**, **3-Trim$_c$**, and **3-Dim** (ε = molar absorptivity).

References for Supporting Information of Chapter 4

(1) Herde, J. L.; Lambert, J. C.; Senoff, C. V.; Cushing, M. A. Cyclooctene and 1,5-Cyclooctadiene Complexes of Iridium(I). In *Inorganic Syntheses*; Parshall, G. W., Ed.; John Wiley & Sons, Inc., 1974; pp 18–20.
(2) Chanteau, S. H.; Tour, J. M. *J. Org. Chem.* **2003**, *68* (23), 8750–8766.
(3) Goldfinger, M. B.; Crawford, K. B.; Swager, T. M. *J. Am. Chem. Soc.* **1997**, *119* (20), 4578–4593.
(4) Kiel, G. R.; Patel, S. C.; Smith, P. W.; Levine, D. S.; Tilley, T. D. *J. Am. Chem. Soc.* **2017**, *139* (51), 18456–18459.
(5) von Kugelgen, S.; Bellone, D. E.; Cloke, R. R.; Perkins, W. S.; Fischer, F. R. *J. Am. Chem. Soc.* **2016**, *138* (19), 6234–6239.
(6) O'Brien, C. J.; Kantchev, E. A. B.; Valente, C.; Hadei, N.; Chass, G. A.; Lough, A.; Hopkinson, A. C.; Organ, M. G. *Chem. – Eur. J.* **2006**, *12* (18), 4743–4748.
(7) Krasovskiy, A.; Knochel, P. *Angew. Chem. Int. Ed.* **2004**, *43* (25), 3333–3336.
(8) Makino, T.; Yamamoto, Y.; Itoh, K. *Organometallics* **2004**, *23* (8), 1730–1737.
(9) Barbot, F.; Dauphin, B.; Miginiac, P. *Synthesis* **1985**, *1985* (8), 768–770.
(10) Brandsma, L. *Best Synthetic Methods: Acetylenes, Allenes and Cumulenes*, 1st ed.; Elsevier Academic Press: Oxford, UK, 2003.
(11) Kiel, G. R.; Ziegler, M. S.; Tilley, T. D. *Angew. Chem. Int. Ed.* **2017**, *56* (17), 4839–4844.
(12) Hoye, T. R.; Eklov, B. M.; Voloshin, M. *Org. Lett.* **2004**, *6* (15), 2567–2570.
(13) Ziegler, M. S.; Levine, D. S.; Lakshmi, K. V.; Tilley, T. D. *J. Am. Chem. Soc.* **2016**, *138* (20), 6484–6491.
(14) Vaska, L.; Catone, D. L. *J. Am. Chem. Soc.* **1966**, *88* (22), 5324–5325.
(15) Lilga, M. A.; Ibers, J. A. *Inorg. Chem.* **1984**, *23* (22), 3538–3543.
(16) Bindl, M.; Stade, R.; Heilmann, E. K.; Picot, A.; Goddard, R.; Fürstner, A. *J. Am. Chem. Soc.* **2009**, *131* (27), 9468–9470.
(17) Heppekausen, J.; Stade, R.; Goddard, R.; Fürstner, A. *J. Am. Chem. Soc.* **2010**, *132* (32), 11045–11057.
(18) Heppekausen, J.; Stade, R.; Kondoh, A.; Seidel, G.; Goddard, R.; Fürstner, A. *Chem. – Eur. J.* **2012**, *18* (33), 10281–10299.
(19) Fürstner, A. Alkyne Metathesis on the Rise. *Angew. Chem. Int. Ed.* **2013**, *52* (10), 2794–2819.
(20) Lee, S.; Yang, A.; Moneypenny, T. P.; Moore, J. S. *J. Am. Chem. Soc.* **2016**, *138* (7), 2182–2185.
(21) Lee, S.; Chénard, E.; Gray, D. L.; Moore, J. S. *J. Am. Chem. Soc.* **2016**, *138* (42), 13814–13817.
(22) Miljanić, O. Š.; Holmes, D.; Vollhardt, K. P. C. *Org. Lett.* **2005**, *7* (18), 4001–4004.
(23) Shinamura, S.; Osaka, I.; Miyazaki, E.; Nakao, A.; Yamagishi, M.; Takeya, J.; Takimiya, K. *J. Am. Chem. Soc.* **2011**, *133* (13), 5024–5035.
(24) Lipshutz, B. H.; Siegmann, K.; Garcia, E.; Kayser, F. *J. Am. Chem. Soc.* **1993**, *115* (20), 9276–9282.
(25) Miyake, Y.; Wu, M.; Rahman, M. J.; Kuwatani, Y.; Iyoda, M. *J. Org. Chem.* **2006**, *71* (16), 6110–6117.
(26) Kauffmann, T. *Angew. Chem. Int. Ed. Engl.* **1974**, *13* (5), 291–305.
(27) Cooke, R. G.; Johnson, B. L.; Owen, W. R. *Aust. J. Chem.* **1960**, *13* (2), 256–260.
(28) Yamashina, M.; Yuki, T.; Sei, Y.; Akita, M.; Yoshizawa, M. *Chem. – Eur. J.* **2015**, *21* (11), 4200–4204.
(29) Klan, P.; Wirz, J. *Photochemistry of Organic Compounds: From Concepts to Practice,* Pg. 194; John Wiley & Sons, Ltd., 2009.

Chapter 5: Expanded Helicenes as Synthons for Chiral Macrocyclic Nanocarbons

There is a rapidly growing appreciation that chirality endows conjugated nanocarbons and related polycyclic aromatic hydrocarbons (PAHs) with novel photophysical ("chiroptical"), electronic, and supramolecular properties.[1–5] Thus, chirality is an orthogonal design element for diverse applications in molecular nanotechnology (e.g. machines and switches) and organic electronics.[6] Chiral nanocarbons occupy a vast chemical space and tremendous effort has been devoted to their synthesis and evaluation.[7,8] Constraining a nanocarbon into a macrocyclic framework is a common way to introduce chirality into an otherwise achiral structure, and might provide a means to increase the configurational stability in those that are inherently chiral.[9–14] More importantly, new properties can result from a macrocyclic environment as a result of its impact on molecular topology[14] and spatial orientation of constituent units.[10–12,15]

As the prototypical chiral PAHs, helicenes (**A**, Figure 1a) are excellent building blocks for more complex chiral nanocarbons. For example, fusion of more than one helicene into a contiguous PAH framework gives rise to "multiple helicenes" (e.g. **B**),[16–23] which exhibit unique solid-state behavior (e.g. π-stacking in 3 dimensions[18]). Introduction of helicenes into "non-fused" oligomeric or polymeric structures has also yielded some remarkable results.[24–30] For example, Diedrich demonstrated that photophysical and chiroptical properties can be significantly enhanced in an oligomeric structure.[24] Yamaguchi has developed oligomeric helicene systems (e.g. **C**)[25,26] that exhibit a range of complex self-assembly phenomena. Notably, many of these self-assembling oligomers are cyclic. Helicene-containing macrocycles are also known to possess fascinating molecular topologies.[27–30] Three "figure-8" dimers have been constructed from 5-helicenes (e.g. **D**) and their heterocyclic analogues.[28,29] In addition, Isobe synthesized an analogous dimer of 4-helicene (**E**) that is a molecular manifestation of Penrose's illusory never-ending staircase.[30] Finally, Durola reported a trimer of 5-helicene (**F**) that displays Mobius aromaticity due to its rare "triply-twisted" Mobius topology.[27]

We recently introduced a new class of chiral nanocarbons, the "expanded helicenes" (**G**, Figure 1b), which have larger cavities and π-systems than **A** as a result of alternating angular and linear ring-fusion.[31] With the aid of a general, [2+2+*n*] cycloaddition strategy, these compounds were shown to exhibit remarkable self-assembly (e.g. a π-stacked double helix) and low enantiomerization barriers, both resulting from their highly flexible backbones. Such flexibility was more recently observed and studied computationally in an unsubstituted example by Matsuda and coworkers.[32] These authors also suggested that this class of molecules will possess exceptional chiroptical properties as a result of their larger diameters, but this has not yet been experimentally validated due to their low enantiomerization barriers.

This contribution describes a divergent synthetic route to two structurally and functionally distinct chiral macrocyclic nanocarbons (**1** and **2**, Figure 1b) from a single expanded helicene building block. The first, a geometrically constrained "arylene-bridged" expanded helicene (**1**), provides an effective platform to increase configurational stability, which is an important step toward elucidating the chiroptical properties of this broad class of nanocarbons. The second, a topologically distinct "figure-8" arylene ethynylene (**2**), retains the high flexibility and configurational lability of expanded helicenes and displays remarkable crystal packing (Figure 3). The critical step in the syntheses of **1** and **2** was development of a simple, gram-scale synthesis of the helicene precursor **3** (Scheme 1), which contains

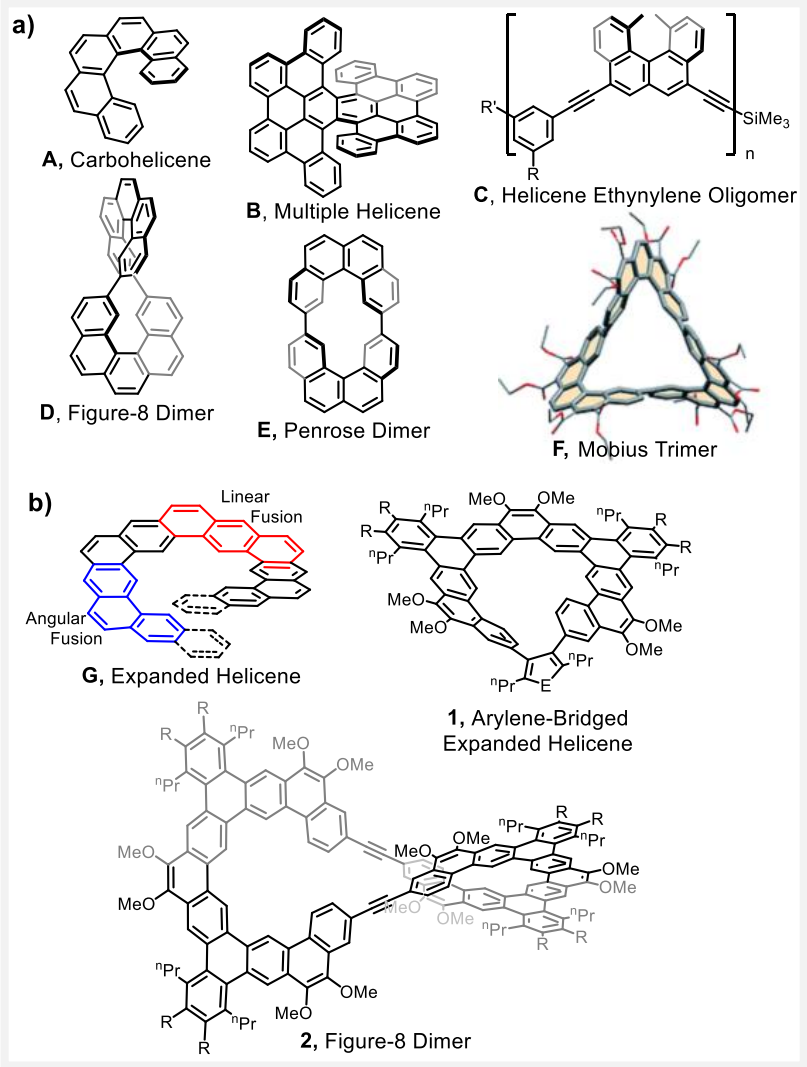

Figure 1. **(a)** Examples of Chiral Nanocarbons Derived from Carbohelicene Building Blocks; **(b)** New Chiral Macrocyclic Nanocarbons (**1** and **2**) Derived from an Expanded Helicene (***This Work***)

alkynyl groups at its termini. This was enabled by an application of the site-selective [2+2+2] reaction introduced in Chapter 4.[33] The preserved alkynyl groups at the termini of **3** undergo a formal [2+2+n] cycloaddition (two examples) and alkyne metathesis to give **1** and **2**, respectively (Scheme 2).

The synthesis of alkynylated expanded helicene **3** (Scheme 1) was accomplished in three steps from phenanthrene dibromide **4**. The previously-reported procedure[31] for **4** proved to be highly scalable, providing routine access to 35–40 grams of this compound (see SI). Treatment of **4** with 1.0 equiv of ^{n}BuLi resulted in a selective mono-lithiation *via* lithium-bromine exchange, giving **5** after a MeOH quench. The reaction of **5** with ^{i}PrMgCl·LiCl gave an *in situ*-generated Grignard reagent that was Kumada cross-coupled with **4** to give hexa(alkynyl)terphenanthrene **6** in 70% yield. Subjection of **6** to the previously-developed,[31,33,34] Ir-catalyzed [2+2+2] cycloaddition conditions afforded the desired helicene **3** in excellent yield (isolated: 80%; ^{1}H NMR: 88%). Notably, high dilution is not necessary for

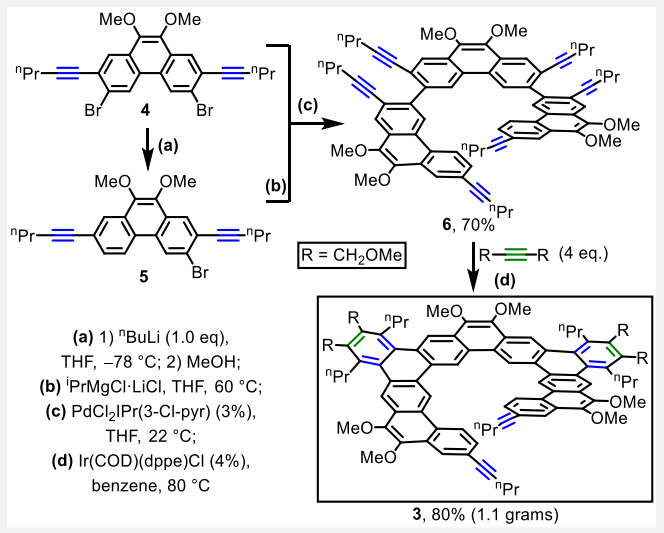

Scheme 1. Gram-Scale Synthesis of Alkynylated Expanded 11-Helicene **3**.

preservation of the reactive alkynyl groups (100 mM diyne concentration), which enabled the synthesis of **3** on a gram scale.

The spatial orientation of the alkynyl groups in **3** suggested the possibility of a formal [2+2+*n*] cycloaddition to form the conformationally-restricted, "bridged-helicene" structure **1** (Scheme 2).[35] Upon treatment of a solution of helicene **3** in benzene-d_6 with 1.2 equiv of $Cp_2Zr(pyr)(Me_3SiC{\equiv}CSiMe_3)$,[36,37] the intermediate zirconacyclopentadiene-bridged helicene **1-Zr** was observed in 86% yield by ^{1}H NMR spectroscopy. Zirconacyclopentadienes are typically isolable, but they are most conveniently generated *in situ* as synthetic intermediates. Treatment of *in situ* generated **1-Zr** with $SeCl_2(bipy)$[31] or DMAD[38] (the latter after transmetallation to Cu) afforded **1-Se** or **1-Benz** in 71 and 65% yields, respectively. It is important to note that, due to synthetic versatility of zirconacyclopentadiene intermediates,[39–42] many divergent functionalizations of this type should be possible.

Alkyne metathesis has proven effective for the scalable, high-yielding synthesis of carbon-rich macrocycles and cages, largely due to its reversibility.[43–46] The two alkynyl groups at the termini of helicene **3** are ideally poised to form the "figure-8" arylene ethynylene macrocycle **2** (Scheme 2). Compound **2** was isolated in excellent yield (95%) after treatment of **3** with a 10% loading of $EtC{\equiv}Mo(OC(CH_3)(CF_3)_2)_3(DME)$[47] (**Mo-1**) for 16 h at 80 °C, in the presence of powdered 5 Å molecular sieves (MS).[48] Purification required only a simple elution of the reaction mixture through silica gel. Notably, the metathesis reaction proceeded to ~95% conversion without removal of the 4-octyne byproduct (i.e. with no 5 Å MS), but this required more careful chromatography to remove unreacted **2** (see SI). The identity of **2** was unambiguously determined by ^{1}H and ^{13}C NMR spectroscopies (the former displayed an absence of propargylic methylene resonances and the latter only one quaternary alkynyl resonance), MALDI-TOF, and single crystal X-ray crystallography (Figure 2).

The new macrocycles can be accessed in a one-pot procedure from hexayne **6**, as demonstrated by the synthesis of **1-Benz** and **2** in 51 and 77% yields, respectively. These yields are comparable to those

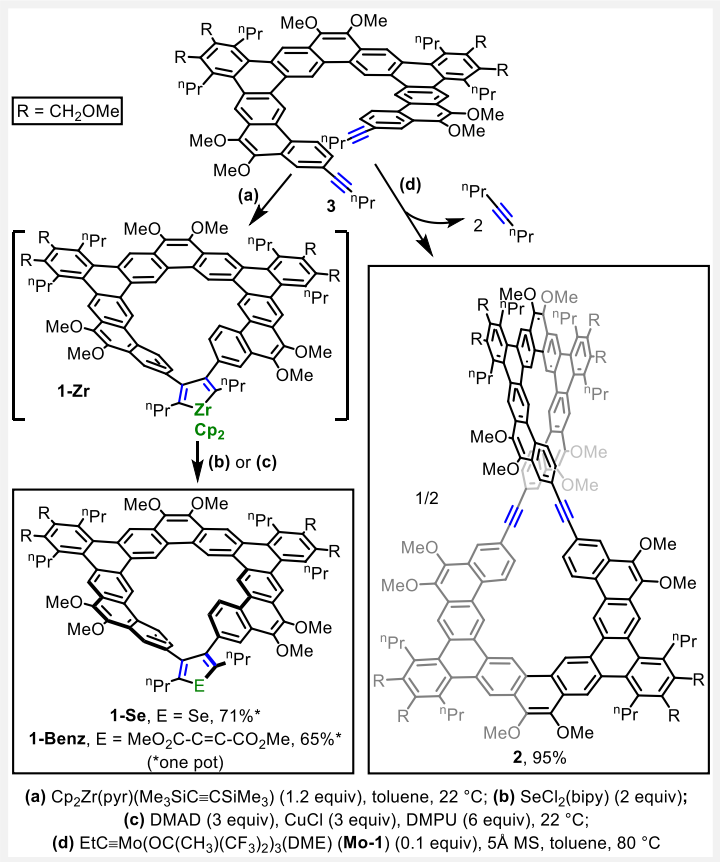

Scheme 2. Divergent Macrocyclization of Helicene **3** to Form Arylene-Bridged Helicenes **1** and "Figure-8" Dimer **2.**

from the two-step procedures outlined above. Remarkably, *the figure-8 macrocycle (**2**) was isolated on a 1.2 gram scale using this one-pot approach*.

All new compounds are highly soluble in common aromatic and chlorinated solvents and insoluble in more polar and non-polar solvents. The ^{1}H NMR chemical shifts of **1-Se**, **2**, and **3** in chloroform-*d* are independent of concentration (see Figures S12 and S14–15), suggesting that their high solubility results from limited aggregation *via* pi-stacking. In contrast, **1-Benz** appears to aggregate in chloroform-*d*, as evidenced by the moderate shielding of its aromatic resonances upon concentration (see Figure S13).

Single crystals of **2** were grown by slow evaporation of a CH_2Cl_2/hexanes solution, and the solid-state structure was elucidated by single crystal X-ray diffraction (Figure 2). Three notable molecular parameters are the distance between the centroids of the two triple bonds (3.55 Å), the pitch of each constituent helicene (3.54 Å), and the angle between the least-squares planes of the two constituent helicenes (30°). The latter two values are notably different from the gas-phase values of 3.60 Å, 3.30 Å, and 40°, respectively, which were calculated by density functional theory (DFT) at the B3LYP-D3/6-31G(d) level of theory. This variance suggests that crystal packing forces play a role in determining molecular structural parameters.

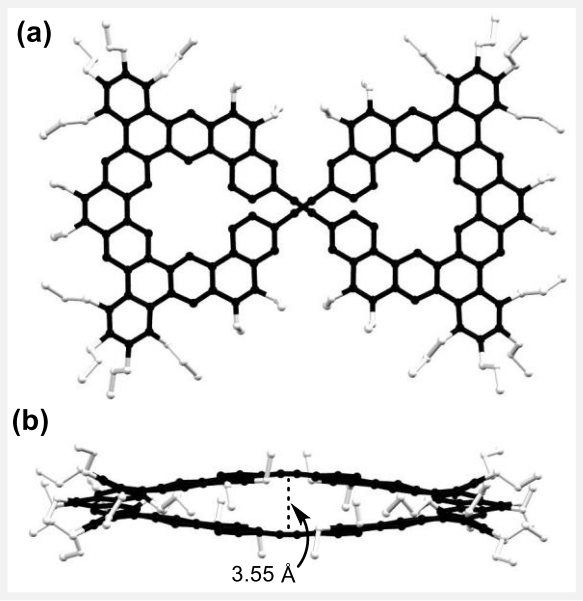

Figure 2. Molecular structure of **2** as determined by single crystal X-ray crystallography: (a) Top view; (b) Side view.

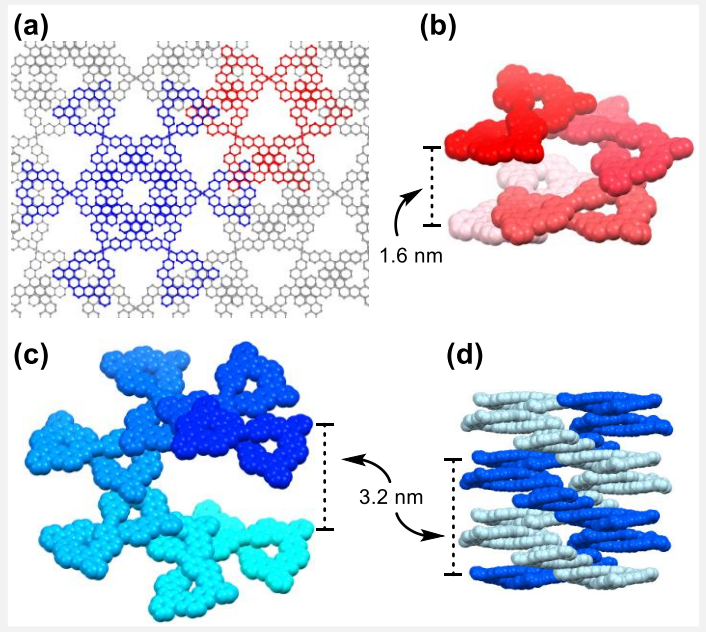

Figure 3. Solid-state packing of **2** as determined by single crystal X-ray diffraction (side chains and solvent molecules are omitted for clarity). **(a)** View along the crystallographic c-axis depicting the 3_1 (red) and 6_1 (blue) helical axes. Perspective view of a single turn of the **(b)** 3_1 and **(c)** 6_1 helices. **(d)** Double helix formed by two equivalent 6_1 helices.

Compound **2** crystallizes in the uncommon, non-centrosymmetric space group $P6_422$ (Figure 3). The remarkable solid-state packing features two parallel, interconnected helical axes (Figure 3a), containing three and six molecules of **2** per helical turn (Figure 3b and 3c, respectively). Here these are referred to as 3_1 and 6_1 helices, respectively, based on the symbol of the screw axis of symmetry that relates

their constituent molecules. The pitch of the former is 1.6 nm while that of the latter is 3.2 nm. In addition, the large pitch of the 6_1 helix serves to accommodate a symmetry-equivalent partner, forming a double helical structure (Figure 3d). Each molecule of **2** engages in π-stacking interactions with *eight* neighboring molecules, with a shortest π-stacking distance of 3.5 Å. The pores are occupied by solvent molecules, which are highly disordered and were removed with the SQUEEZE[49] program. Given the notable difference in the X-ray and DFT-calculated molecular structures (see above), we speculate that the flexibility of the helicene units is essential in enabling this remarkable crystal packing.

The basic photophysical properties of the helicene system are not significantly perturbed by either type of macrocyclization. Although the expected redshift in absorption maximum (λ_{max}) is observed upon dimerization of **3** to form **2**, it is small (from 322 to 334 nm; see Figure S16). The λ_{max} values for **1-Se**, **1-Benz**, and **3** are nearly identical (319–322 nm). The new compounds possess relatively large optical HOMO-LUMO gaps in the range of 2.9–3.0 eV, the magnitude of which is typical[50] for highly benzenoid PAHs. Likewise, the emission maxima (λ_{max}) are essentially unchanged (see Figure S17), each lying within 4 nm of the λ_{max} for **3** (448 nm).

The chirality of the new compounds results from their pseudo-C_2 (for **1-Benz**, **1-Se**, and **3**) and D_2 (for **2**) symmetries. The enantiomerization barriers ($\Delta G^{\ddagger}$) could be probed *via* variable temperature ^{1}H NMR spectroscopy due to the presence of diastereotopic methylene protons on the peripheral methoxymethyl groups. For the figure-8 dimer (**2**) and helicene (**3**) these measurements were complicated by aggregation and solvent viscosity at low temperatures. Nevertheless, ruling out accidental overlap, an upper bound of 13 kcal/mol was estimated for each compound (singlet decoelescence was not observed down to –25 °C in dichloromethane-d_2 or toluene-d_8). Thus, **2** retains the configurational lability of its precursor **3**. Due to their conformationally restricted structures, **1-Se** and **1-Benz** exhibit higher barriers of 17 and >20 kcal/mol, respectively (in toluene-d_8 and mesitylene-h_{12}). The lower bound for the latter was inferred by the absence of coalescence of methylene doublets up to 130 °C. Unfortunately, attempts to resolve **1-Benz** into its enantiomers *via* chiral HPLC have thus far proven unsuccessful. Resolution of **1-Se**, **2**, or **3** was not attempted using chiral HPLC due to their configurational lability. In principle, the spontaneous resolution of **2** in the solid state (see above) should enable a measurement of its chiroptical properties if the conglomerates could be manually separated; however, its low $\Delta G^{\ddagger}$ complicates the possibility of a solution measurement (the racemization half-life at –78 °C is expected to be only a few seconds).

In conclusion, the alkynylated expanded helicene **3**, which was produced in a high-yielding and scalable fashion, acts as a linchpin to two distinct chiral macrocyclic nanocarbons. The bridged helicene **1** provides a platform to increase expanded helicene configurational stability *via* a "covalent locking" strategy. The serendipitous resolution of the enantiomers of the "figure-8" macrocycle (**2**) in the solid-state hints at an alternative, non-covalent strategy to increase expanded helicene configurational stability. Here, it is the intricate, π-stacked network in the crystal structure that stabilizes the enantiomers of this otherwise highly flexible molecule. Importantly, the modularity of the synthetic tools presented here provide the means for a thorough exploration of these fascinating new nanocarbons.

References for Main Text of Chapter 5

(1) Rickhaus, M.; Mayor, M.; Juríček, M. *Chem. Soc. Rev.* **2016**, **45,** 1542–1556.
(2) Shen, Y.; Chen, C.-F. *Chem. Rev.* **2012**, *112* (3), 1463–1535.
(3) Gingras, M. *Chem. Soc. Rev.* **2013**, *42* (3), 1051–1095.
(4) Fernández-García, J. M.; Evans, P. J.; Filippone, S.; Herranz, M. Á.; Martín, N. *Acc. Chem. Res.* **2019**, 52 (6), 1565–1574.
(5) Tanaka, H.; Inoue, Y.; Mori, T. *ChemPhotoChem* **2018**, *2* (5), 386–402.
(6) Brandt, J. R.; Salerno, F.; Fuchter, M. J. *Nat. Rev. Chem.* **2017**, *1* (6), 45.
(7) Pascal, R. A. *Chem. Rev.* **2006**, *106* (12), 4809–4819.
(8) Rickhaus, M.; Mayor, M.; Juríček, M. *Chem. Soc. Rev.* **2017**, *46* (6), 1643–1660.
(9) Campbell, K.; Tykwinski, R. R. In *Carbon-Rich Compounds*; Haley, M. M., Tykwinski, R. R., Eds.; Wiley-VCH Verlag GmbH & Co. KGaA: Weinheim, Germany, 2006; pp 229–294.
(10) Ball, M.; Fowler, B.; Li, P.; Joyce, L. A.; Li, F.; Liu, T.; Paley, D.; Zhong, Y.; Li, H.; Xiao, S.; Ng, F.; Steigerwald, M. L.; Nuckolls, C. *J. Am. Chem. Soc.* **2015**, *137* (31), 9982–9987.
(11) Sato, S.; Yoshii, A.; Takahashi, S.; Furumi, S.; Takeuchi, M.; Isobe, H. *Proc. Natl. Acad. Sci.* **2017**, *114* (50), 13097–13101.
(12) Sun, Z.; Matsuno, T.; Isobe, H. *Bull. Chem. Soc. Jpn.* **2018**, *91* (6), 907–921.
(13) Weiland, K. J.; Brandl, T.; Atz, K.; Prescimone, A.; Häussinger, D.; Šolomek, T.; Mayor, M. *J. Am. Chem. Soc.* **2019**, *141* (5), 2104–2110.
(14) Senthilkumar, K.; Kondratowicz, M.; Lis, T.; Chmielewski, P. J.; Cybińska, J.; Zafra, J. L.; Casado, J.; Vives, T.; Crassous, J.; Favereau, L.; Stępień, M. *J. Am. Chem. Soc.* **2019**, 141 (18), 7421–7427.
(15) Schneebeli, S. T.; Frasconi, M.; Liu, Z.; Wu, Y.; Gardner, D. M.; Strutt, N. L.; Cheng, C.; Carmieli, R.; Wasielewski, M. R.; Stoddart, J. F. *Angew. Chem. Int. Ed.* **2013**, *52* (49), 13100–13104.
(16) Barnett, L.; Ho, D. M.; Baldridge, K. K.; Pascal, R. A. *J. Am. Chem. Soc.* **1999**, *121* (4), 727–733.
(17) Wang, X.-Y.; Wang, X.-C.; Narita, A.; Wagner, M.; Cao, X.-Y.; Feng, X.; Müllen, K. *J. Am. Chem. Soc.* **2016**.
(18) Fujikawa, T.; Segawa, Y.; Itami, K. *J. Am. Chem. Soc.* **2015**, *137* (24), 7763–7768.
(19) Pradhan, A.; Dechambenoit, P.; Bock, H.; Durola, F. *Chem. – Eur. J.* **2016**, *22* (50), 18227–18235.
(20) Hu, Y.; Wang, X.-Y.; Peng, P.-X.; Wang, X.-C.; Cao, X.-Y.; Feng, X.; Müllen, K.; Narita, A. *Angew. Chem. Int. Ed.* **2017**, *56* (12), 3374–3378.
(21) Hosokawa, T.; Takahashi, Y.; Matsushima, T.; Watanabe, S.; Kikkawa, S.; Azumaya, I.; Tsurusaki, A.; Kamikawa, K. *J. Am. Chem. Soc.* **2017**, 139 (51), 18512–18521.
(22) Ball, M.; Zhong, Y.; Wu, Y.; Schenck, C.; Ng, F.; Steigerwald, M.; Xiao, S.; Nuckolls, C. *Acc. Chem. Res.* **2015**, *48* (2), 267–276.
(23) Li, C.; Yang, Y.; Miao, Q. *Chem. – Asian J.* **2018**, *13* (8), 884–894.
(24) Schaack, C.; Arrico, L.; Sidler, E.; Górecki, M.; Di Bari, L.; Diederich, F. *Chem. – Eur. J.* **2019**, *25* (34), 8003–8007.
(25) Amemiya, R.; Mizutani, M.; Yamaguchi, M. *Angew. Chem. Int. Ed.* **2010**, *49* (11), 1995–1999.
(26) Saiki, Y.; Sugiura, H.; Nakamura, K.; Yamaguchi, M.; Hoshi, T.; Anzai, J. *J. Am. Chem. Soc.* **2003**, *125* (31), 9268–9269.
(27) Naulet, G.; Sturm, L.; Robert, A.; Dechambenoit, P.; Röhricht, F.; Herges, R.; Bock, H.; Durola, F. *Chem. Sci.* **2018**, *9* (48), 8930–8936.

(28) Robert, A.; Dechambenoit, P.; Hillard, E. A.; Bock, H.; Durola, F. *Chem. Commun.* **2017**, *53* (84), 11540–11543.
(29) Ushiyama, A.; Hiroto, S.; Yuasa, J.; Kawai, T.; Shinokubo, H. *Org. Chem. Front.* **2017**, *4* (5), 664–667.
(30) Nakanishi, W.; Matsuno, T.; Ichikawa, J.; Isobe, H. *Angew. Chem. Int. Ed.* **2011**, *50* (27), 6048–6051.
(31) Kiel, G. R.; Patel, S. C.; Smith, P. W.; Levine, D. S.; Tilley, T. D. *J. Am. Chem. Soc.* **2017**, *139* (51), 18456–18459.
(32) Nakakuki, Y.; Hirose, T.; Matsuda, K. *J. Am. Chem. Soc.* **2018**, *140* (45) 15461–15469.
(33) Kiel, G. R.; Tilley, T. D. *Submitted.*
(34) Kezuka, S.; Tanaka, S.; Ohe, T.; Nakaya, Y.; Takeuchi, R. *J. Org. Chem.* **2006**, *71* (2), 543–552.
(35) During the course of this work, Tanaka reported a remarkable synthesis of a [6]Cycloparaphenylene derivative using a similar, Rh-Catalyzed [2+2+2] macrocyclization strategy. See: Hayase, N.; Sugiyama, H.; Uekusa, H.; Shibata, Y.; Tanaka, K. *Org. Lett.* **2019**, *21* (11), 3895–3899.
(36) Rosenthal, U.; Ohff, A.; Baumann, W.; Tillack, A.; Görls, H.; Burlakov, V. V.; Shur, Vladimir. B. *Z. Für Anorg. Allg. Chem.* **1995**, *621* (1), 77–83.
(37) Nitschke, J. R.; Zürcher, S.; Tilley, T. D. *J. Am. Chem. Soc.* **2000**, *122* (42), 10345–10352.
(38) Takahashi, T.; Xi, Z.; Yamazaki, A.; Liu, Y.; Nakajima, K.; Kotora, M. *J. Am. Chem. Soc.* **1998**, *120* (8), 1672–1680.
(39) Fagan, P. J.; Nugent, W. A.; Calabrese, J. C. *J. Am. Chem. Soc.* **1994**, *116* (5), 1880–1889.
(40) Takahashi, T.; Hara, R.; Nishihara, Y.; Kotora, M. *J. Am. Chem. Soc.* **1996**, *118* (21), 5154–5155.
(41) Takahashi, T.; Li, Y.; Stepnicka, P.; Kitamura, M.; Liu, Y.; Nakajima, K.; Kotora, M. *J. Am. Chem. Soc.* **2002**, *124* (4), 576–582.
(42) Yan, X.; Xi, C. *Acc. Chem. Res.* **2015**, *48* (4), 935–946.
(43) Ge, P.-H.; Fu, W.; Herrmann, W. A.; Herdtweck, E.; Campana, C.; Adams, R. D.; Bunz, U. H. F. *Angew. Chem. Int. Ed.* **2000**, *39* (20), 3607–3610.
(44) Miljanić, O. Š.; Vollhardt, K. P. C.; Whitener, G. D. *Synlett* **2003**, No. 1, 29–34.
(45) Zhang, W.; Moore, J. S. *J. Am. Chem. Soc.* **2005**, *127* (33), 11863–11870.
(46) Yu, C.; Jin, Y.; Zhang, W. In *Dynamic Covalent Chemistry*; John Wiley & Sons, Ltd, 2017; pp 121–163.
(47) Gdula, R. L.; Johnson, M. J. A. *J. Am. Chem. Soc.* **2006**, *128* (30), 9614–9615.
(48) Heppekausen, J.; Stade, R.; Goddard, R.; Fürstner, A. *J. Am. Chem. Soc.* **2010**, *132* (32), 11045–11057.
(49) Spek, A. L. *Acta Crystallogr. Sect. C Struct. Chem.* **2015**, *71* (1), 9–18.
(50) Rieger, R.; Müllen, K. *J. Phys. Org. Chem.* **2010**, *23* (4), 315–325.

Supporting Information for Chapter 5

General Details

Unless otherwise stated, all manipulations of organometallic compounds were carried out in dry solvents under an atmosphere of nitrogen, using either standard Schlenk techniques or a glovebox. Toluene and tetrahydrofuran (THF) were dried using a JC Meyers Phoenix SDS solvent purification system. Benzene was dried using a Vacuum Atmosphere solvent purification system. Benzene-d_6 and DMPU were freed from oxygen using three free-pump-thaw cycles and then dried for at least 48 h over 3 Å molecular sieves (5% by mass). All reaction solvents were stored over 3 Å molecular sieves. $Cp_2Zr(pyr)(Me_3SiC{\equiv}CSiMe_3)$,[1] $SeCl_2(bipy)$[2], $[Ir(COD)Cl]_2$,[3] 1,4-dimethoxy-2-butyne,[4] $EtC{\equiv}Mo(OC(CH_3)(CF_3)_2)_3(DME)$,[5] Ir(COD)(dppe)Cl,[6] 3,6-dibromo-2,7-diiodo-9,10-dimethoxyphenanthrene,[7] 3-bromo-9,10-dimethoxy-2,7-di(pent-1-yn-1-yl)phenanthrene (**5**),[8] ^{i}PrMgCl·LiCl,[9] and $PdCl_2(IPr)(3\text{-chloropyridine})$[10] were prepared by literature procedures or slight modifications thereof. ^{i}PrMgCl·LiCl was titrated by ^{1}H NMR spectroscopy immediately prior to use.[11] All other reagents and solvents were purchased from commercial suppliers and used as received. "Room temperature", "RT", or "ambient temperature" refers to ~22 °C. Reaction temperatures represent the oil bath temperature (with a fully submersed solution) unless otherwise stated. MALDI-TOF mass spectrometry was performed at the Mass Spectrometry Facility at UC Riverside. α-Cyano-4-hydroxycinnamic acid was used as the matrix. Unless otherwise noted, NMR spectra were acquired at ambient temperature (~22 °C) using Bruker AV-600, AV-500, DRX-500, AV-400, and AV-300 spectrometers. Chemical shifts (δ) are given in ppm and referenced to residual solvent peaks for ^{1}H NMR spectra (δ = 7.26 ppm for chloroform-*d*, δ = 7.16 for benzene-d_6, δ = 5.32 for dichloromethane-d_2, and δ = 2.09 for toluene-d_8) and for $^{13}C\{^1H\}$ NMR spectra (δ = 77.16 ppm for chloroform-*d*). ^{1}H NMR yields were determined using 1,3,5-trimethoxybenzene as internal standard. For greatest accuracy, yields were typically measured by acquisition of ^{1}H NMR spectra both before and after the reaction of interest, then comparison of the amounts of starting material and desired product relative to the amount of added internal standard.

Comments About the $[Ir(COD)Cl]_2$ / dppe Catalyst System

As discussed in our previous report,[8] the reaction of 1 equiv of $[Ir(COD)Cl]_2$ with 2 equiv of dppe (in toluene or benzene) gives the [2+2+2] pre-catalyst Ir(COD)(dppe)Cl. If dppe is present in excess, an orange/red precipitate (likely $Ir(dppe)_2Cl$[12,13]) is observed. The most reproducible way to achieve the desired catalyst loading is with isolated Ir(COD)(dppe)Cl (prepared in a simple one-step procedure[6]). For some procedures below, Ir(COD)(dppe)Cl was pre-formed *in situ* by addition of a solution of dppe in toluene to a solution of $[Ir(COD)Cl]_2$ in toluene.

General Notes on Purification and Product Isolation

Chromatography

Column chromatography was carried out using Fischer Chemical 40–63μm, 230–400 mesh silica gel. Preparatory thin layer chromatography (prep TLC) was carried out using Analtech Silica Gel GF UNIPLATES (1000 μm, 20 x 20 cm). For prep TLC, in a typical procedure, 35–50 mg of material was loaded onto one side of the plate and the solvent front was allowed to elute halfway up (i.e. 70–100 mg was separated per plate).

Isolation of solids via rotary evaporation

For most of the new compounds, the concentration of their solutions in "good" solvents (e.g. CH_2Cl_2) typically furnished a glassy, yellow/orange residue. For isolation of these compounds in powder form, co-evaporation with a poor solvent (usually hexanes) was necessary. Typically, the solution (e.g. the extracted solution from prep TLC) was concentrated *via* rotary evaporation in a round-bottomed flask, then the residue was transferred to a 20 mL vial with the minimal amount of CH_2Cl_2. The CH_2Cl_2 solution was then co-evaporated with hexanes *via* rotary evaporation, and residual solvents were removed under high vacuum to give the desired powder.

Isolation of fine powders via filtration

Several procedures below involve the precipitation of the desired product with an anti-solvent (e.g. MeOH). This often produced a very fine solid, which made filtration difficult. In these cases, filtration was greatly aided by celite, which was then extracted with CH_2Cl_2 for recovery of product. See above for important notes regarding rotary evaporation of CH_2Cl_2 solutions.

Important Note Regarding the Use of 5 Å Molecular Sieves (MS) to Sequester 4-Octyne

We observed that the source of the molecular sieves is of critical importance for the alkyne metathesis reactions performed herein. All successful reactions used pre-powdered 5 Å MS that were purchased from Sigma Aldrich and activated under high vacuum at ~300 °C (until condensation of water ceased, then for another 24 h). The activated 5 Å MS were then stored in a solvent-free, nitrogen-filled glovebox until use. At the outset of our investigations, beaded 5 Å MS (3–5 mm, from Alfa Aesar) were activated as described above, then thoroughly ground with a mortar and pestle in a solvent-free, nitrogen-filled glovebox. *Use of these molecular sieves was not effective for the sequestration of 4-octyne.*

Synthetic Procedures and Characterization of Compounds

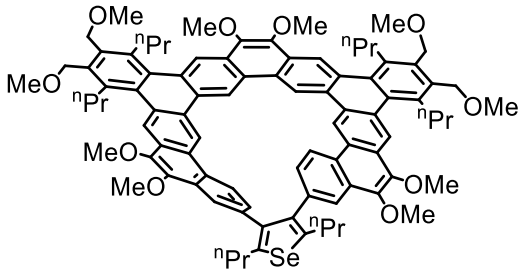

1-Se

Selenophene-bridged expanded helicene (1-Se). To a stirred solution of helicene **3** (100 mg, 0.0749 mmol, 1.0 equiv) in toluene (6 mL) was added, dropwise over 5–10 min, a solution of $Cp_2Zr(Me_3SiC{\equiv}CSiMe_3)pyr$ (42 mg, 0.090 mmol, 1.2 equiv) in toluene (1.0 mL).* The mixture was stirred for 5 min at RT, then $SeCl_2$(bipy) (46 mg, 0.15 mmol, 2.0 equiv) was added and the resulting suspension was stirred for a further 5 min. In air, the suspension was filtered through celite and the filter cake was rinsed with toluene (2 x 3 mL). Addition of MeOH (75 mL) to the filtrate resulted in the formation of a fine yellow/orange precipitate, which was collected via filtration** and washed with MeOH (2 x 5 mL). Subjection of the crude product to preparatory thin layer chromatography afforded **1-Se** (75 mg, 71%) as a pale-yellow solid. ^{1}H NMR (chloroform-*d,* 400 MHz, [c] = 6.2 mM): δ = 9.91 (s, 2H), 9.75 (s, 2H), 9.21 (s, 2H), 8.84 (s, 2H), 8.53 (d, *J* = 8.5 Hz, 2H), 8.34 (d, *J* = 1.8 Hz, 2H), 6.64 (dd, *J* = 8.4, 1.8 Hz, 2H), 4.88 (d, *J* = 10.3 Hz, 2H), 4.83 (d, *J* = 10.1 Hz, 2H), 4.81 (d, *J* = 10.7 Hz, 2H), 4.78 (d, *J* = 10.5 Hz, 2H), 4.21 (s, 6H), 4.21 (s, 6H), 4.17 (s, 6H), 3.61 (s, 6H), 3.60 (s, 6H), 3.67 – 3.40 (m, 8H), 3.41 – 3.33 (m, 2H), 3.26 – 3.16 (m, 2H), 2.29 – 1.79 (m, 12H), 1.25 (t, *J* = 7.2 Hz, 6H), 1.13 (t, *J* = 7.3 Hz, 6H), 1.02 (t, *J* = 7.2 Hz, 6H); ^{13}C{^{1}H} NMR (chloroform-*d*, 151 MHz): δ = 146.19, 144.64, 144.61, 144.16, 140.67, 137.31, 137.29, 136.52, 136.17, 136.12, 134.80, 133.41, 130.95, 130.60, 130.44, 130.14, 130.06, 129.31, 128.60, 127.83, 127.79, 127.60, 127.10, 125.00, 122.45, 121.78, 120.45, 119.79, 118.84, 69.29, 69.06, 61.26, 61.13, 61.02, 58.95, 58.85, 35.36, 35.04, 34.12, 27.21, 26.10, 25.17, 14.57, 14.55, 14.25; MS-MALDI-TOF (m/z): $[M]^+$ calcd. for $C_{90}H_{94}O_{10}Se$, 1414.60; found, 1414.58. *Order of addition and concentration play a critical role in the generation of the intermediate macrocyclic zirconacyclopentadiene **1-Zr** in high yield. Using this procedure, **1-Zr** was observed in 86% yield (by ^{1}H NMR spectroscopy). **The solid was very fine and filtration was greatly aided by celite. After filtration, the celite was extracted with CH_2Cl_2 for recovery of product.

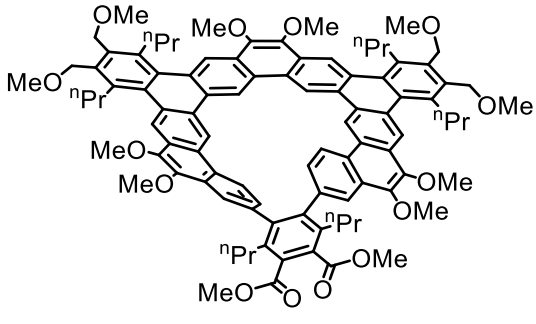

1-Benz

Phenylene-bridged expanded helicene (1-Benz).

*Procedure #1 (one-pot, from hexayne **6**)*

To a solution of $[Ir(COD)Cl]_2$ (1.2 mg, 0.0018 mmol, 0.02 equiv) in benzene (0.5 mL) was added (dropwise over ~1 min) a solution of dppe (1.4 mg, 0.0036 mmol, 0.04 equiv) in benzene (0.5 mL). This mixture was immediately added to a flask containing a solution of hexayne **6** (101 mg, 0.0909 mmol, 1.0 equiv), 1,4-dimethoxy-2-butyne (31 mg, 0.273 mmol, 3.0 equiv), and 1,3,5-trimethoxybenzene (14.6 mg, internal standard) in benzene (0.8 mL). The flask was sealed with a Teflon stopper and the reaction mixture was heated at 80 °C for 2 h. The mixture was allowed to cool to RT* and diluted with benzene (6 mL, to bring total concentration to 0.012 M relative to starting **6**). To the stirred mixture was added, dropwise over 5–10 min, a solution of $Cp_2Zr(Me_3SiC{\equiv}CSiMe_3)pyr$ (64 mg, 0.136 mmol, 1.5 equiv) in benzene (1.0 mL).** The mixture was stirred for 10 min at RT,*** then DMAD (39 mg, 0.27 mmol, 3.0 equiv), DMPU (70 mg, 0.55 mmol, 6.0 equiv), and copper(I) chloride (27 mg, 0.27 mmol, 3.0 equiv) were added in that order. The mixture was stirred for 1 h at RT and directly subjected (in air) to column chromatography (0–10% EtOAc in CH_2Cl_2) to give a light-yellow solid that was a mixture of **1-Benz** and DMAD. To remove DMAD, the solid was dissolved in CH_2Cl_2 (3-4 mL), filtered, then the filtrate was concentrated to ~2 mL. To this solution was added EtOH (6 mL), then the solution was concentrated to half of its volume to give a finely dispersed precipitate. The precipitate was collected by filtration**** and washed with MeOH (2 x 3 mL) to afford **1-Benz** (68 mg, 51%) as a light-yellow solid. *Analysis of an aliquot by ^{1}H NMR spectroscopy revealed formation of helicene **3** in 85% yield. **Order of addition and concentration play a critical role in the generation of the intermediate macrocyclic zirconacyclopentadiene **1-Zr** in high yield. ***Analysis of an aliquot by ^{1}H NMR spectroscopy revealed formation of **1-Zr** in 65% yield (*from hexayne **6***). ****The solid was very fine and filtration was greatly aided by celite. After filtration, the celite was extracted with CH_2Cl_2 for recovery of product.

*Procedure #2 (from isolated helicene **3**)*

This procedure was identical to *Procedure 1* above (starting with formation of **1-Zr**), except 1.2 equiv of $Cp_2Zr(Me_3SiC{\equiv}CSiMe_3)pyr$ was used. The isolated yield of **1-Benz** was 65% (from **3**).

Characterization

^{1}H NMR (chloroform-*d*, 500 MHz, [c] = 2.6 mM): δ = 9.83 (s, 2H), 9.67 (s, 2H), 9.23 (s, 2H), 8.84 (s, 2H), 8.42 (d, *J* = 8.5 Hz, 2H), 8.12 (d, *J* = 1.9 Hz, 2H), 6.56 (dd, *J* = 8.3, 1.8 Hz, 2H), 4.87 (d, *J* = 10.4 Hz, 2H), 4.82 (d, *J* = 10.2 Hz, 2H), 4.81 (d, *J* = 10.2 Hz, 2H), 4.77 (d, *J* = 10.4 Hz, 2H), 4.20 (s, 6H), 4.18 (s, 6H), 4.17 (s, 6H), 4.00 (s, 6H), 3.61 (s, 6H), 3.60 (s, 6H), 3.60 – 3.35 (m, 8H), 3.21 (ddd, *J* = 14.8, 10.3, 5.9 Hz, 2H), 2.86 (ddd, *J* = 14.4, 10.2, 5.0 Hz, 2H), 2.26 – 2.09 (m, 4H), 2.09 – 1.97 (m, 2H), 1.97 – 1.82 (m, 2H), 1.64 – 1.52 (m, 2H), 1.44 – 1.34 (m, 2H), 1.28 (t, *J* = 7.3 Hz, 6H), 1.05 (t, *J* = 7.2 Hz, 6H), 0.72 (t, *J* = 7.3 Hz, 6H); ^{13}C{^{1}H} NMR (chloroform-*d*, 101 MHz): δ = 169.87, 144.64, 144.48, 144.22, 143.78, 137.35, 137.18, 137.08, 136.65, 136.19, 134.69, 133.14, 132.64, 130.74, 130.65, 130.39, 130.23, 129.13, 129.02, 128.59, 127.85, 127.69, 127.56, 126.74, 126.21, 122.15, 121.91, 120.45, 120.37, 120.19, 118.58, 69.05, 68.95, 61.18, 61.03, 60.78, 58.96, 58.79, 52.71, 35.28, 35.02, 33.68, 25.94, 25.03, 25.01, 14.50, 14.49, 14.31; MS-MALDI-TOF (m/z): $[M]^+$ calcd. for $C_{96}H_{100}O_{14}$, 1476.71; found, 1476.66.

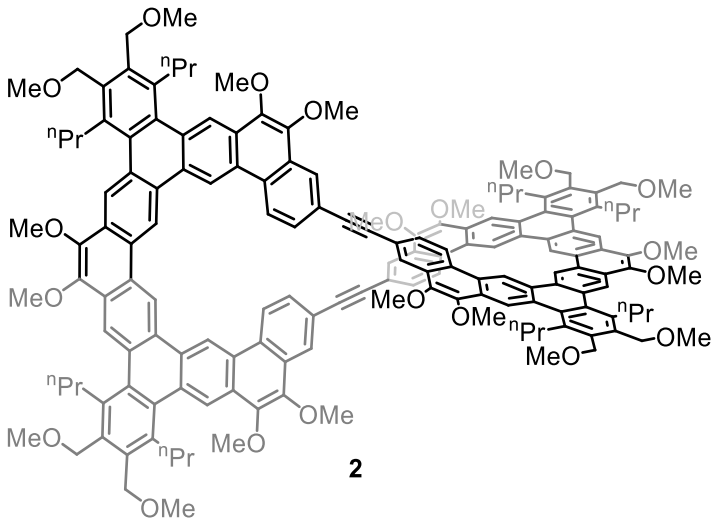

"Figure 8" Macrocycle (2).

*Procedure #1 (from helicene **3**, no 5 Å molecular sieves)*

A J-Young NMR tube was charged with **3** (50 mg, 0.0374 mmol, 1.0 equiv), 1,3,5-trimethoxybenzene (~5 mg, internal standard), EtC≡Mo(OC(CH_3)(CF_3)$_2$)$_3$(DME) (2.9 mg, 0.0037 mmol, 0.10 equiv), and benzene-d_6 (0.75 mL). The tube was sealed, and the mixture was heated at 80 °C for 16 h. Analyses of the mixture by ^{1}H NMR spectroscopy after 3 h and 16 h (see Figure S9d) both revealed 95% consumption of starting **3** and 93% yield of **2** (i.e. conversion halted after 3 h). The mixture was directly subjected to preparatory thin layer chromatography (4% EtOAc in CH_2Cl_2), which afforded **2** (41 mg, 89%) as a yellow solid.

*Procedure #2 (from helicene **3**, with 5 Å molecular sieves)*

A 10 mL Teflon-stoppered flask with magnetic stirbar was charged with **3** (100 mg, 0.0749 mmol, 1.0 equiv), EtC≡Mo(OC(CH_3)(CF_3)$_2$)$_3$(DME) (5.8 mg, 0.0075 mmol, 0.10 equiv), powdered 5 Å molecular sieves* (150 mg), and benzene-d_6 (3.0 mL). The flask was sealed, then the stirred mixture was heated at 80 °C for 16 h, cooled to RT, and an aliquot was filtered into an NMR tube. Analysis by ^{1}H NMR spectroscopy revealed complete consumption of **3** and the absence of byproduct 4-octyne (see Figure S9e). The mixture was quantitatively transferred to a 50 mL round-bottomed flask with the aid of toluene (2 x 2 mL), and silica gel (1 g) was added. Volatile materials were removed by rotary evaporation and resulting powder was layered onto a plug of silica gel (5 g) that had been equilibrated with 10% EtOAc in CH_2Cl_2. The plug was flushed with the same solvent mixture until the yellow color was very faint (~50 mL). Removal of solvents* from the eluent via rotary evaporation afforded **2** (87 mg, 95%) as a yellow solid. *See general section (above) for important details on the source of the molecular sieves and on solvent removal.

*Procedure #3 (one pot, gram-scale, from hexayne **6**)*

A 100 mL Teflon-stoppered flask was loaded with hexayne **6** (1.40 g, 1.26 mmol, 1.0 equiv), 1,4-dimethoxy-2-butyne (0.575 g, 5.04 mmol, 4.0 equiv), and toluene (15 mL), and to this flask was added a solution of Ir(COD)(dppe)Cl (0.037 g, 0.050 mmol, 0.04 equiv) in toluene (10 mL). The flask was sealed with a Teflon stopper and the stirred reaction mixture was heated at 80 °C for 2 h. The mixture

was allowed to cool to RT, then powdered 5 Å molecular sieves* (3.8 g) and a solution of EtC≡Mo(OC(CH_3)(CF_3)$_2$)$_3$(DME) (0.097 g, 0.126 mmol, 0.10 equiv) in toluene (10 mL) were added. The stirred mixture was heated at 80 °C for 16 h, then the mixture was cooled to RT and added to a 250 mL round-bottomed flask containing silica gel (35 g). Volatile materials were removed from the suspension by rotary evaporation and the resulting powder was layered onto a plug of silica gel (50 g) that had been equilibrated with 10% EtOAc in CH_2Cl_2. The plug was flushed with the same solvent mixture until the yellow color was very faint (~300 mL). The filtrate was concentrated to ~5 mL via rotary evaporation, then MeOH (50 mL) was added. The precipitate was collected by filtration**, affording **2** (1.19 g, 77%) as a yellow solid. *See general section (above) for important details on the source of the molecular sieves; **The precipitate was very fine, and filtration was greatly aided by celite. After filtration, the celite was extracted with CH_2Cl_2 for recovery of product.

Characterization:

^{1}H NMR (benzene-d_6, 500 MHz): δ = 10.38 (s, 4H), 10.20 (s, 4H), 9.46 (s, 4H), 9.46 (s, 4H), 9.16 (d, *J* = 8.6 Hz, 4H), 9.01 (d, *J* = 1.7 Hz, 4H), 8.27 (dd, *J* = 8.2, 1.8 Hz, 4H), 4.94 (s, 8H), 4.93 (s, 8H), 3.97 (s, 12H), 3.92 (s, 12H), 3.78 – 3.68 (m, 16H), 3.73 (s, 12H), 3.41 (s, 12H), 3.41 (s, 12H), 2.28 – 2.11 (m, 16H), 1.11 (t, *J* = 7.3 Hz, 12H), 1.07 (t, *J* = 7.3 Hz, 12H); ^{13}C{^{1}H} NMR (chloroform-*d*, 176 MHz): δ = 144.83, 144.42, 143.70, 136.76, 136.72, 136.21, 136.14, 134.58, 134.43, 131.29, 131.20, 130.11, 129.90, 129.87, 129.83, 128.57, 128.42, 128.22, 127.36, 127.17, 126.51, 122.77, 122.77, 122.41, 122.36, 117.94, 117.91, 90.26, 69.20, 69.19, 61.29, 61.16, 61.14, 58.97, 58.94, 35.12, 35.09, 25.92, 25.90, 14.71, 14.67; MS-MALDI-TOF (m/z): $[M]^+$ calcd. for $C_{164}H_{160}O_{20}$, 2449.15; found, 2449.17.

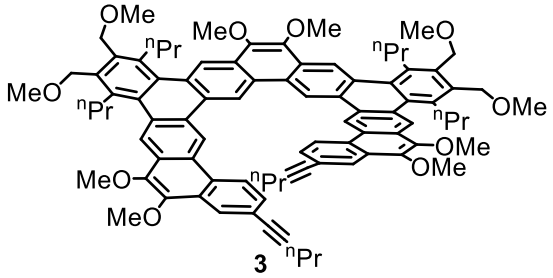

3

Di(alkynyl) Expanded Helicene (3). To a stirred solution of [Ir(COD)Cl]$_2$ (0.0133 g, 0.0199 mmol, 0.02 equiv) in benzene (0.5 mL) was added (dropwise over ~1 min) a solution of dppe (0.0158 g, 0.0397 mmol, 0.04 equiv) in benzene (0.5 mL). This mixture was immediately added to a flask containing a solution of hexayne **6** (1.10 g, 0.993 mmol, 1.0 equiv) and 1,4-dimethoxy-2-butyne (0.45 g, 4.0 mmol, 4.0 equiv) in benzene (19 mL). The flask was sealed with a Teflon stopper and the reaction mixture was heated at 80 °C for 2 h. The mixture was allowed to cool to RT and poured onto a fritted funnel packed with silica gel (20 g). The silica was eluted with 5% EtOAc in CH_2Cl_2 (~200 mL; until the yellow color in the eluent was faint) and the filtrate was concentrated via rotary evaporation. To fully remove solvents, the residue was suspended in hexanes (10 mL) and sonicated, then solvents were removed via rotary evaporation. The residue was again suspended in hexanes (40 mL) and stirred vigorously until a fine, light-yellow suspension was obtained (sonication is also effective). The suspension was filtered and the solid was washed with thoroughly with hexanes (2 x 10 mL). Residual solvents were removed under high vacuum to afford expanded helicene **3** (1.07 g, 80%) as a light-yellow solid. When this reaction was run on a smaller scale in benzene-d_6 solvent and monitored by ^{1}H NMR spectroscopy (1,3,5-trimethoxybenzene internal standard), **3** was observed in 88% yield. ^{1}H NMR (chloroform-*d,* 600 MHz): δ = 10.23 (s, 2H), 10.05 (s, 2H), 9.10 (d, *J* = 8.5 Hz, 2H), 9.05 (s,

2H), 9.03 (s, 2H), 8.38 (d, *J* = 1.7 Hz, 2H), 7.63 (dd, *J* = 8.5, 1.7 Hz, 2H), 4.85 (s, 4H), 4.85 (s, 4H), 4.22 (s, 6H), 4.20 (s, 6H), 4.19 (s, 6H), 3.62 (s, 6H), 3.62 (s, 6H), 3.57 – 3.49 (m, 8H), 2.50 (t, *J* = 7.1 Hz, 4H), 2.07 – 1.96 (m, 8H), 1.80 – 1.68 (m, 4H), 1.12 (t, *J* = 7.4 Hz, 6H), 1.07 (t, *J* = 7.3 Hz, 6H), 1.05 (t, *J* = 7.3 Hz, 6H); $^{13}C\{^{1}H\}$ NMR (chloroform-*d*, 151 MHz): δ = 144.67, 144.29, 143.62, 136.60, 136.57, 136.15, 136.08, 134.54, 134.52, 131.23, 131.18, 130.13, 130.01, 129.97, 129.67, 128.45, 127.97, 127.93, 127.40, 127.23, 125.65, 123.24, 122.81, 122.75, 122.34, 117.86, 117.84, 91.30, 81.30, 69.19, 69.20, 61.22, 61.16, 61.11, 58.95, 58.93, 35.10, 34.99, 25.89, 25.87, 22.50, 21.86, 14.68, 14.67, 13.89; MS-MALDI-TOF (m/z): $[M]^+$ calcd. for $C_{90}H_{94}O_{10}$, 1334.68; found, 1334.65.

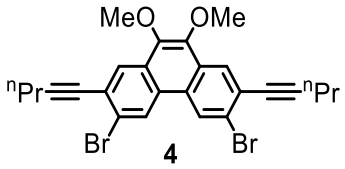

4

Large Scale Prep of 3,6-dibromo-2,7-bis(pent-1-ynyl)-9,10-dimethoxyphenanthrene (4). This is an adaptation of the previously reported procedure.[7] The only major difference is the scale, which required a modification of the reaction setup since the starting material, 3,6-dibromo-2,7-diiodo-9,10-dimethoxyphenanthrene, is a highly flocculent solid that is difficult to load into the narrow neck of a Teflon-stoppered flask. A 2000 mL Schlenk flask was charged with 3,6-dibromo-2,7-diiodo-9,10-dimethoxyphenanthrene (60.2 g, 92.9 mmol, 1.0 equiv), $Pd(PPh_3)_4$ (2.69 g, 2.32 mmol, 0.025 equiv), and CuI (1.06 g, 5.58 mmol, 0.06 equiv). The flask sealed with a rubber septum and subjected to three vacuum / N_2 cycles, then THF (580 mL) and triethylamine (290 mL) (both of which had been thoroughly sparged with N_2) were added via cannula transfer. To this mixture was added 1-pentyne (22.9 mL, 232 mmol, 2.5 equiv) via syringe, then (immediately after this addition) the septum was rapidly replaced with an efficient reflux condenser against N_2 flow. The mixture was heated at 70 °C under N_2 for 18 h, then brought to RT and poured into ice-cold aqueous HCl (3 M, 1300 mL). The mixture was extracted with CH_2Cl_2 (800 mL) and the extract was dried with $MgSO_4$ and filtered. Solvents were removed from the filtrate via rotary evaporation, then the crude product was dissolved in CH_2Cl_2 (300 mL) and this solution was diluted with hexanes (800 mL). The solution was eluted through a plug* of silica gel (200 g), and the plug was flushed with 3:1 hexanes:CH_2Cl_2 (~2000 mL, or until no more desired product was seen by TLC analysis). Solvents were removed via rotary evaporation and further purification was carried out as follows (repeated 2x). The solid was dissolved in CH_2Cl_2 (300 mL), then MeOH (600 mL) was added to produce an immediate precipitate that was collected by filtration and washed with MeOH (200 mL). The yield of **4**, after drying under high vacuum at 60–70 °C for 1 h, was 35 g (71%), as an off-white solid. ^{1}H NMR data matches that reported in the literature.[7] *The silica plug was set up like a standard silica column (i.e. it was thoroughly equilibrated before elution), but only a single fraction was collected.

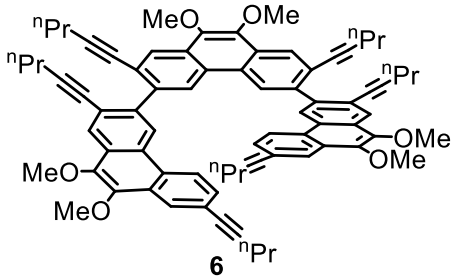

6

Hexa(pentynyl)terphenanthrene (6). A 50 mL flask equipped with Teflon stopper was charged with monobromide **5** (1.60 g, 3.56 mmol, 4.0 equiv) and THF (3.0 mL) and to this solution was added ^{i}PrMgCl·LiCl (0.81 M in THF, 4.06 mL, 3.29 mmol, 3.7 equiv) via syringe. The flask was sealed, and the mixture was heated at 60 °C for 3 h. A 1 mL aliquot was analyzed by ^{1}H NMR spectroscopy to ensure complete consumption of ^{i}PrMgCl·LiCl, then the aliquot was recombined with the original solution. To this solution was added $PdCl_2$(IPr)(3-chloropyridine) (0.018 g, 0.027 mmol, 0.03 equiv) in THF (2 mL), followed by dibromide **4** (0.470 g, 0.890 mmol, 1.0 equiv). The resulting homogeneous mixture was allowed to stand at RT (~21 °C) for 20 h, then quenched with saturated aqueous NH_4Cl (20 mL), extracted with EtOAc (30 mL), washed with saturated aqueous NaCl (20 mL), dried with $MgSO_4$, filtered, and the filtrate was concentrated under reduced pressure. The residue was purified by column chromatography (mass of silica: 120 g; eluant: 25–33% CH_2Cl_2 in hexanes) to afford hexayne **6** (0.69 g, 70%) as a pale-yellow solid. ^{1}H NMR (chloroform-*d,* 400 MHz): δ 8.74 (s, 2H), 8.69 (s, 2H), 8.44 (d, *J* = 8.7 Hz, 2H), 8.42 (s, 2H), 8.32 (s, 2H), 8.24 (d, *J* = 1.7 Hz, 2H), 7.53 (dd, *J* = 8.5, 1.8 Hz, 2H), 4.18 (s, 6H), 4.09 (s, 6H), 4.07 (s, 6H), 2.45 (t, *J* = 7.1 Hz, 4H), 2.17 (t, *J* = 6.9 Hz, 4H), 2.12 (t, *J* = 6.9 Hz, 4H), 1.68 (sext, *J* = 7.2 Hz, 4H), 1.30 (sext, *J* = 7.2 Hz, 4H), 1.25 (sext, *J* = 7.2 Hz, 4H), 1.08 (t, *J* = 7.3 Hz, 6H), 0.67 (t, *J* = 7.3 Hz, 6H), 0.59 (t, *J* = 7.3 Hz, 6H); ^{13}C{^{1}H} NMR (chloroform-*d*, 101 MHz): δ = 143.89, 143.89, 143.84, 140.44, 140.30, 129.36, 128.95, 128.54, 128.30, 127.68, 127.28, 127.04, 126.18, 126.13, 125.43, 125.07, 124.81, 123.06, 123.04, 122.99, 122.64, 94.45, 94.42, 91.34, 81.27, 80.73, 80.67, 61.27, 61.18, 61.14, 22.39, 22.04, 22.03, 21.70, 21.64, 21.64, 13.78, 13.35, 13.32; MS-MALDI-TOF (m/z): $[M]^+$ calcd. for $C_{78}H_{74}O_6$, 1106.55; found, 1106.51.

NMR spectra

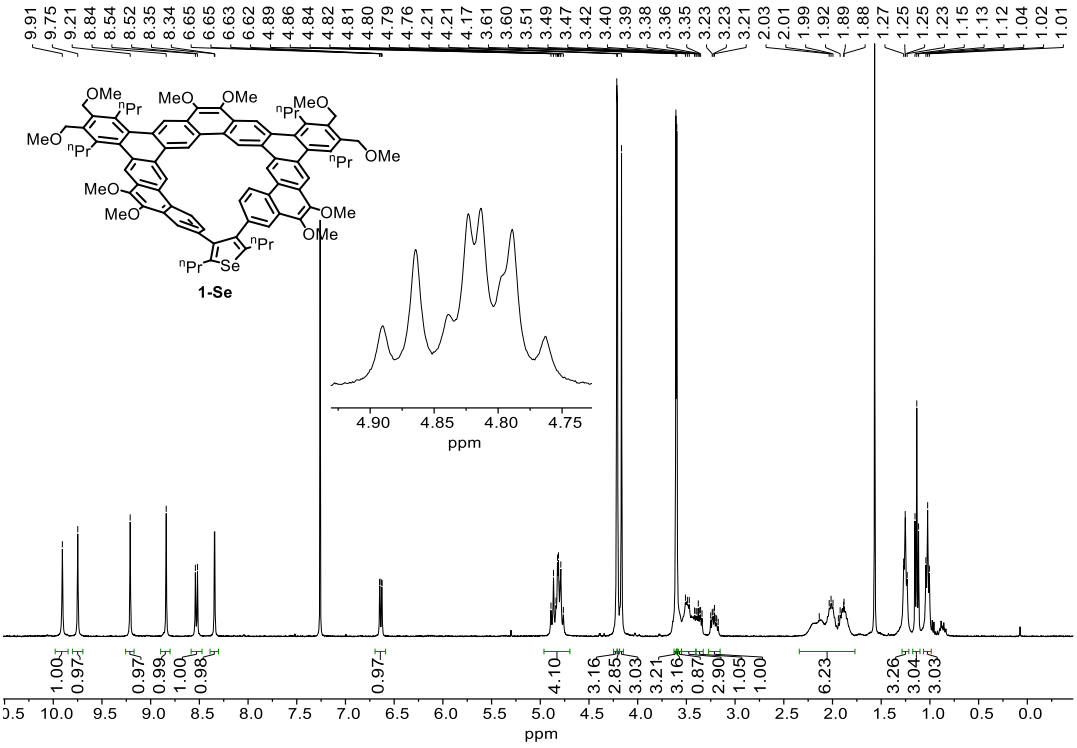

Figure S1. ^{1}H NMR Spectrum (400 MHz, chloroform-*d,* [c] = 6.2 mM) of **1-Se**

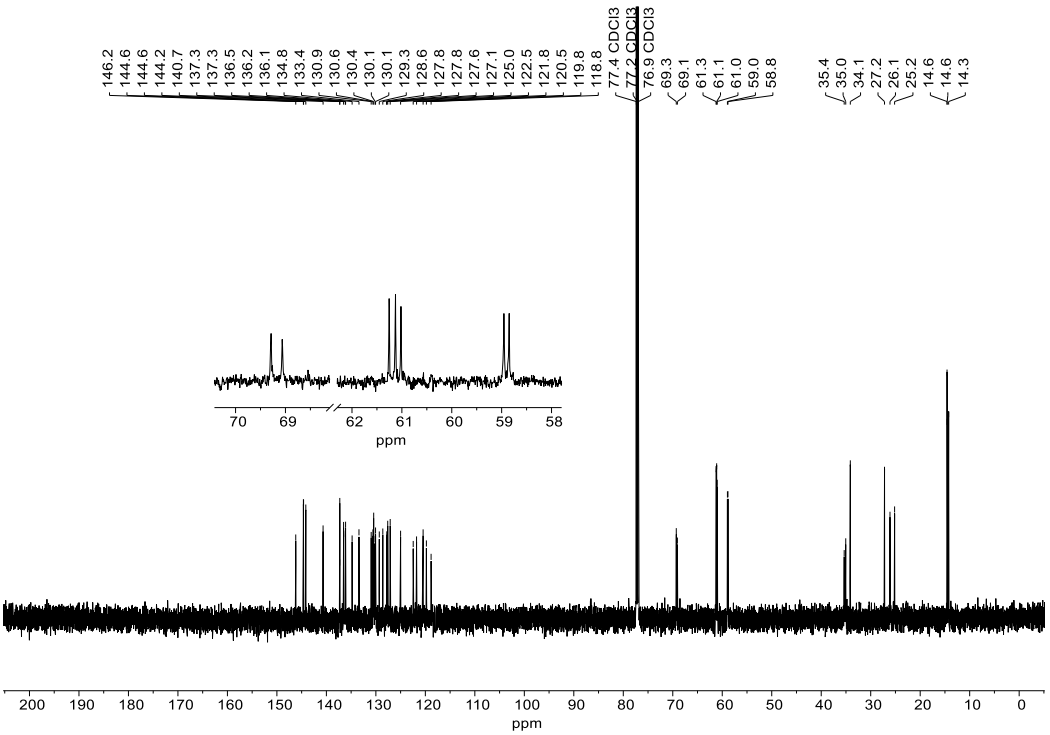

Figure S2. ^{13}C{^{1}H} NMR Spectrum (151 MHz, chloroform-*d*) of **1-Se**

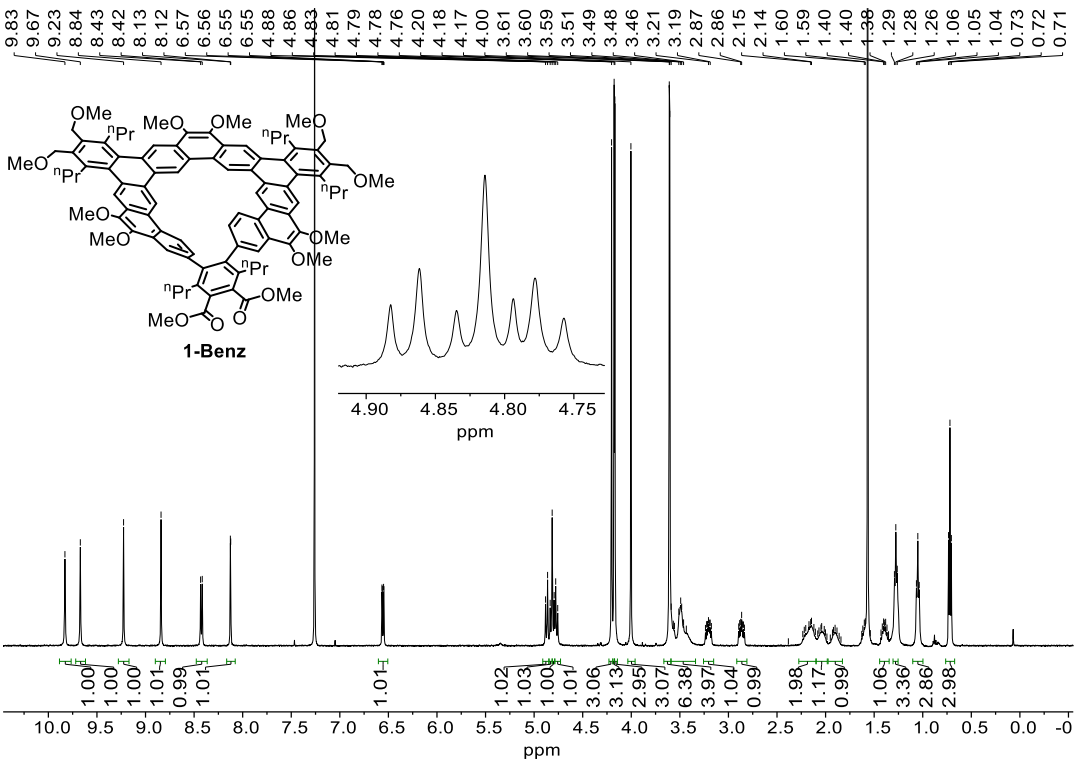

Figure S3. ^{1}H NMR Spectrum (500 MHz, chloroform-*d,* [c] = 2.6 mM) of **1-Benz**

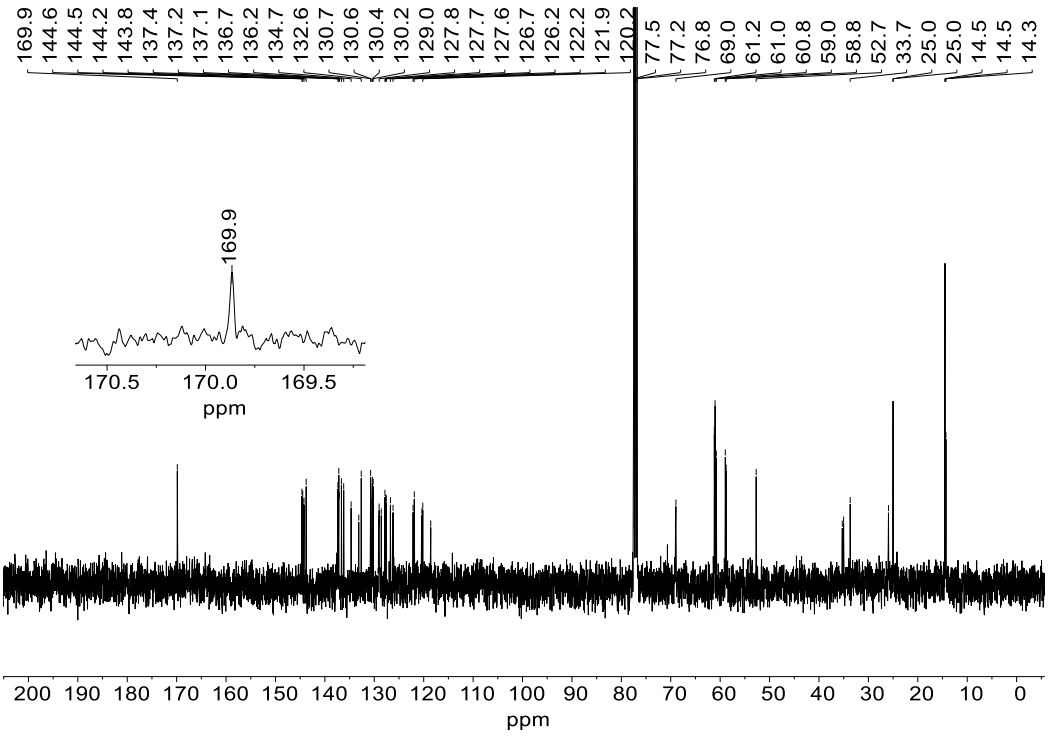

Figure S4. ^{13}C{^{1}H} NMR Spectrum (101 MHz, chloroform-*d*) of **1-Benz**

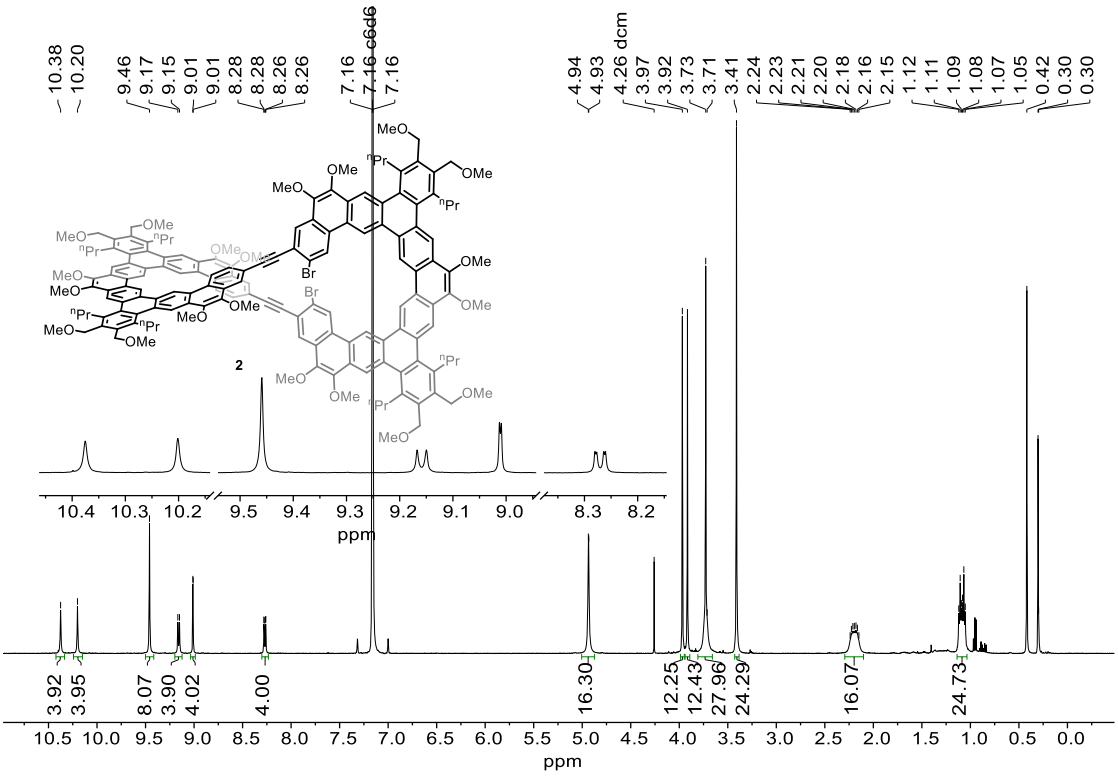

Figure S5. ^{1}H NMR Spectrum (500 MHz, benzene-d_6) of **2**

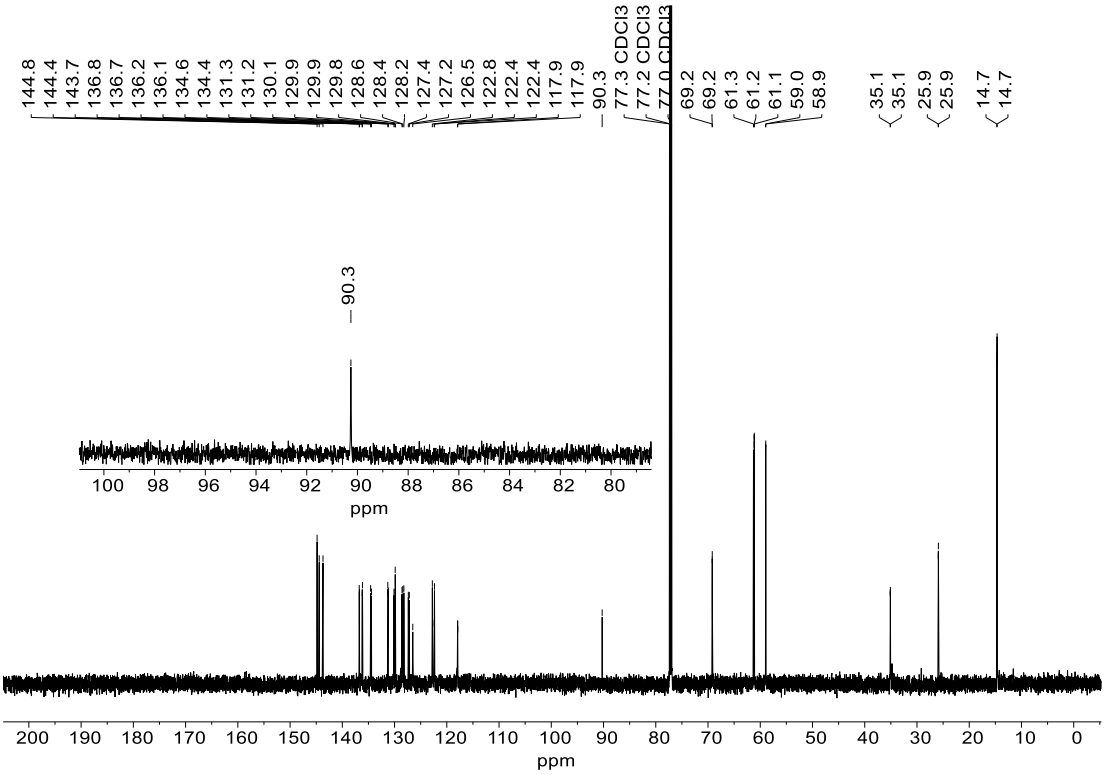

Figure S6. ^{13}C{^{1}H} NMR Spectrum (176 MHz, chloroform-*d*) of **2**

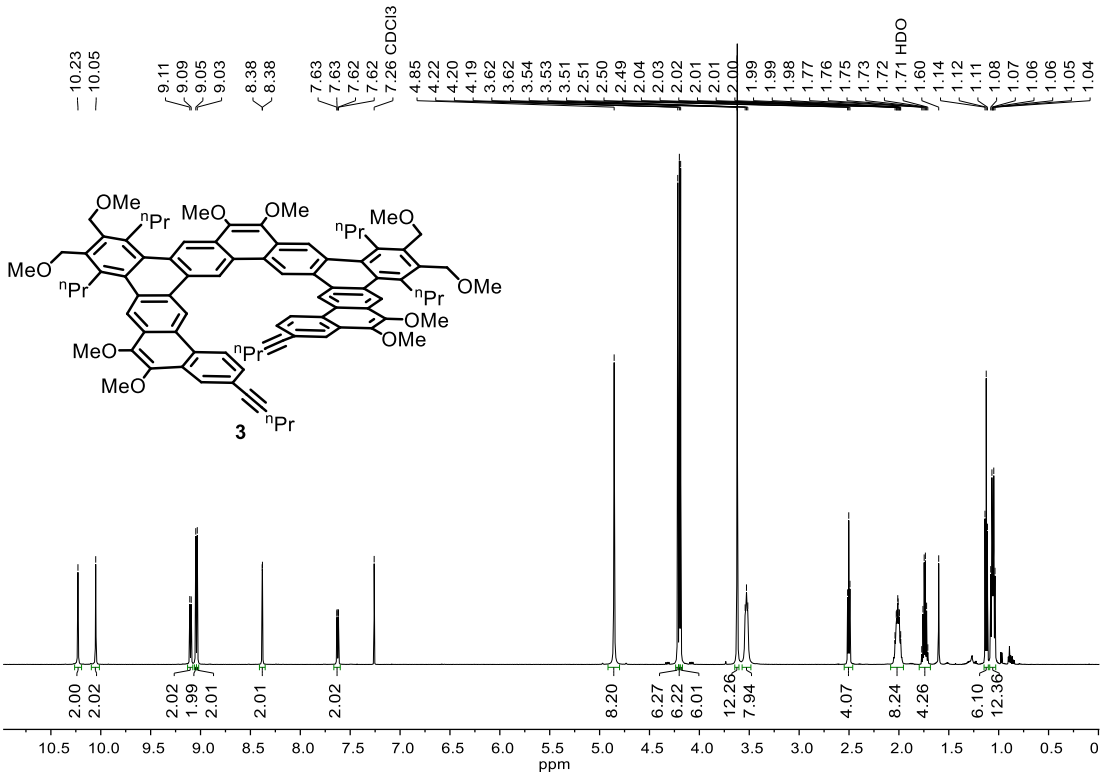

Figure S7. ^{1}H NMR Spectrum (600 MHz, chloroform-*d*) of **3**

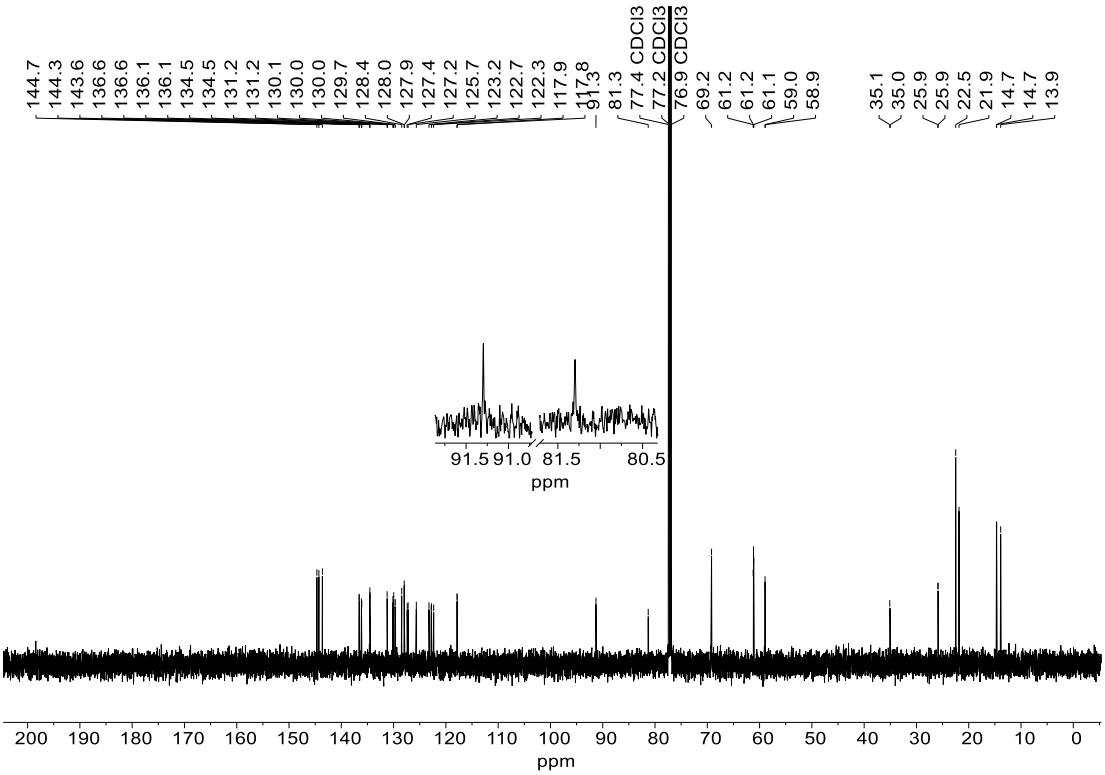

Figure S8. ^{13}C{^{1}H} NMR Spectrum (151 MHz, chloroform-*d*) of **3**

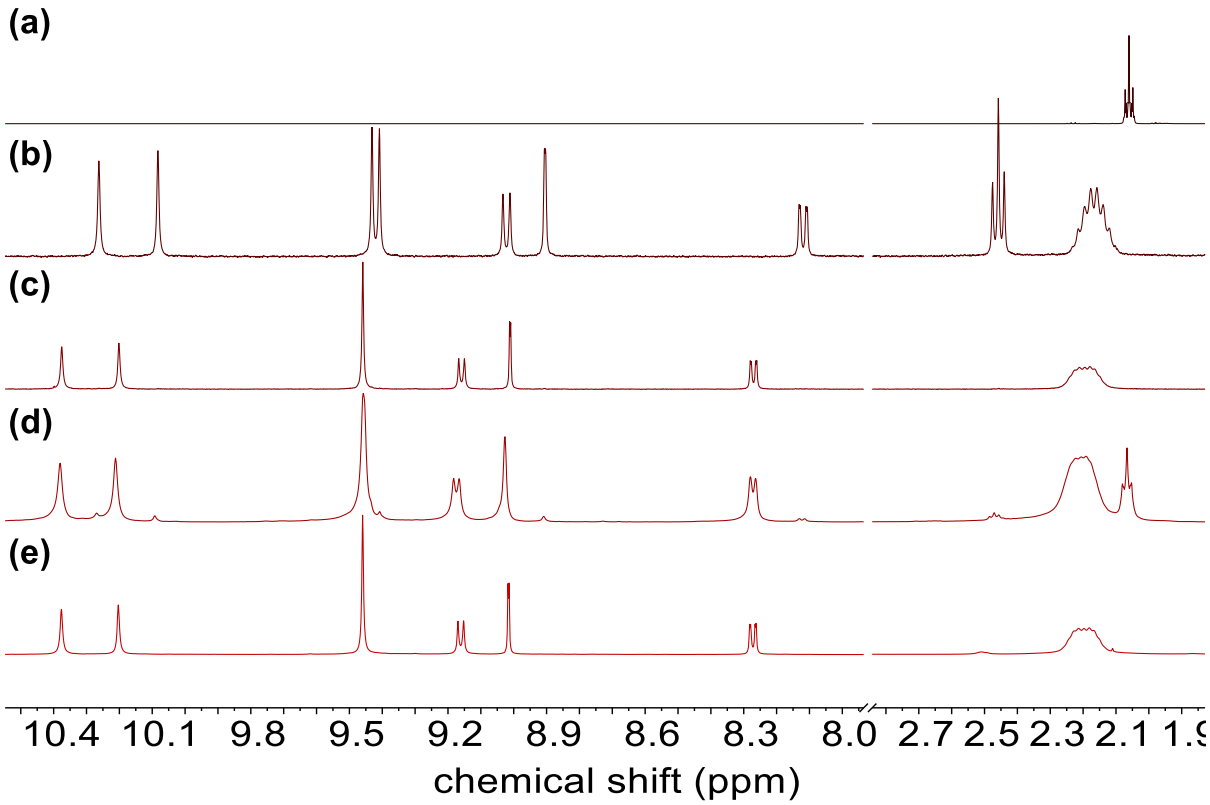

Figure S9. Partial ^{1}H NMR spectra (500 MHz, benzene-d_6) of **(a)** 4-octyne; **(b)** starting helicene **3**; **(c)** purified **2**; **(d)** reaction mixture after treatment of **3** with EtC≡Mo(OC(CH$_3$)(CF$_3$)$_2$)$_3$(DME) (10 mol%) for 16 h at 80 °C (no 5 Å molecular sieves); **(e)** reaction mixture after treatment of **3** with EtC≡Mo(OC(CH$_3$)(CF$_3$)$_2$)$_3$(DME) (10 mol%) for 16 h at 80 °C *in the presence of 5 Å molecular sieves*. Notably, all **3** and 4-octyne byproduct were consumed in this case.

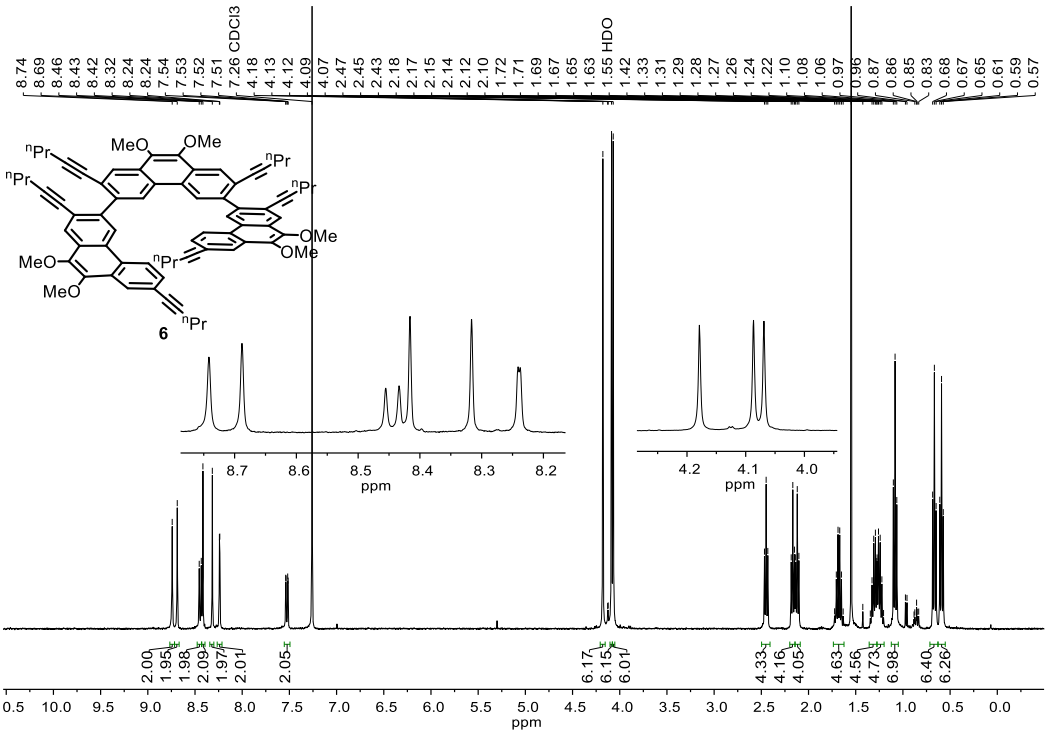

Figure S10. ^{1}H NMR Spectrum (400 MHz, chloroform-*d*) of **6**

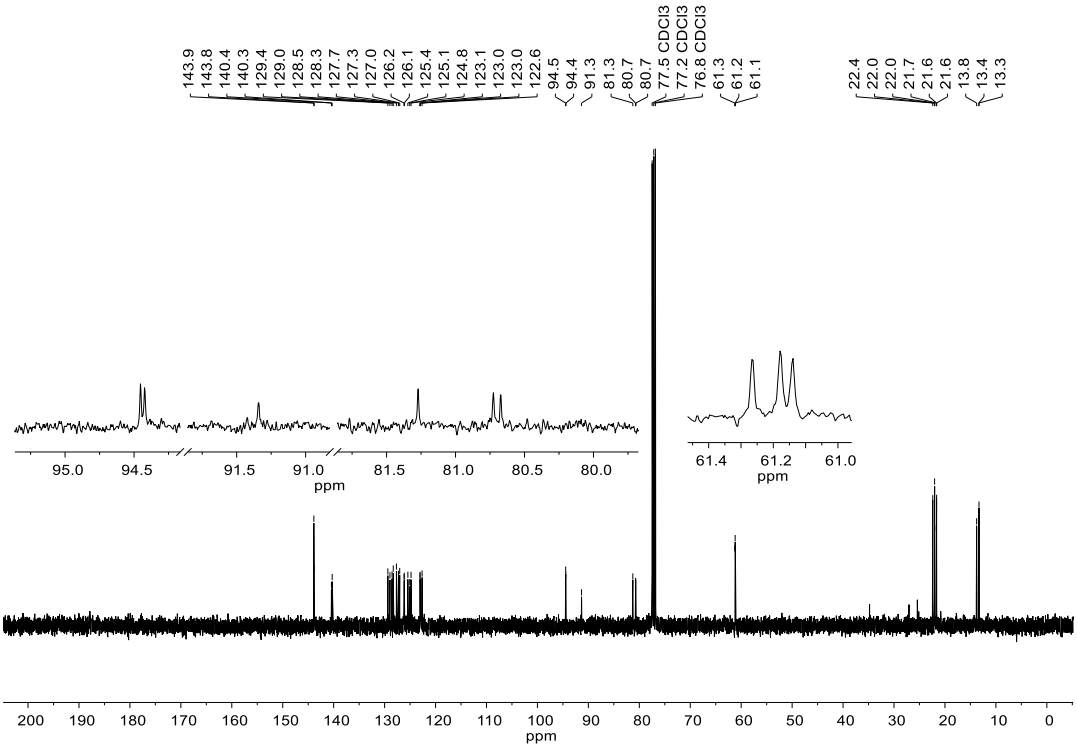

Figure S11. ^{13}C{^{1}H} NMR Spectrum (101 MHz, chloroform-*d*) of **6**

Variable Concentration ^{1}H NMR Spectra

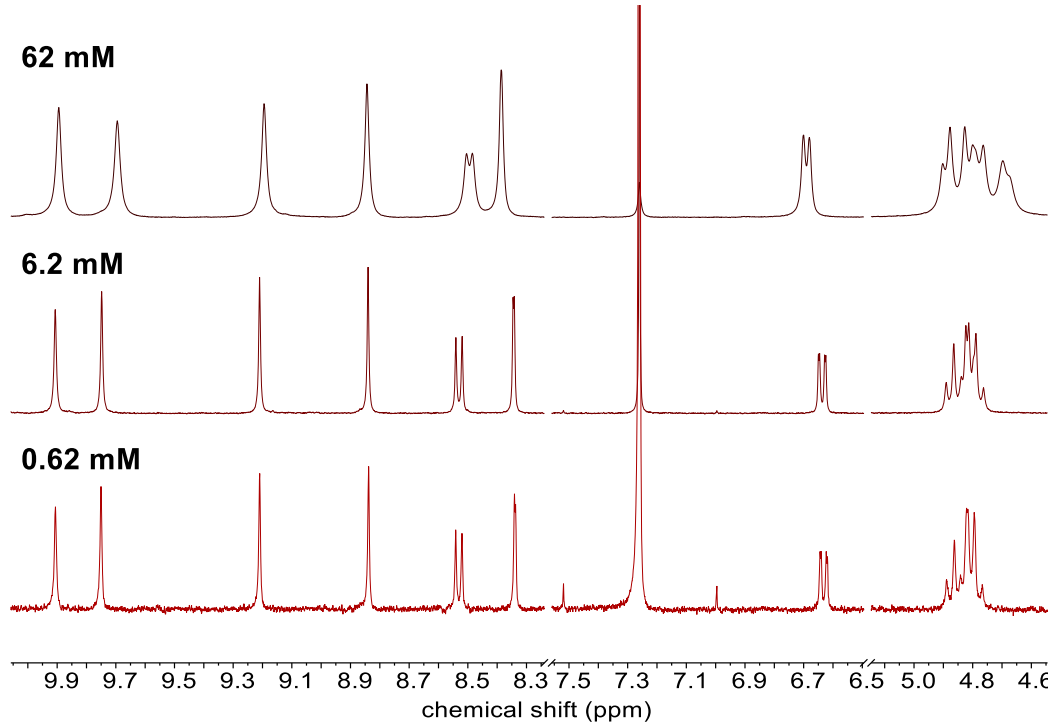

Figure S12. Variable concentration partial ^{1}H NMR spectra (400 MHz, chloroform-*d*) of **1-Se**.

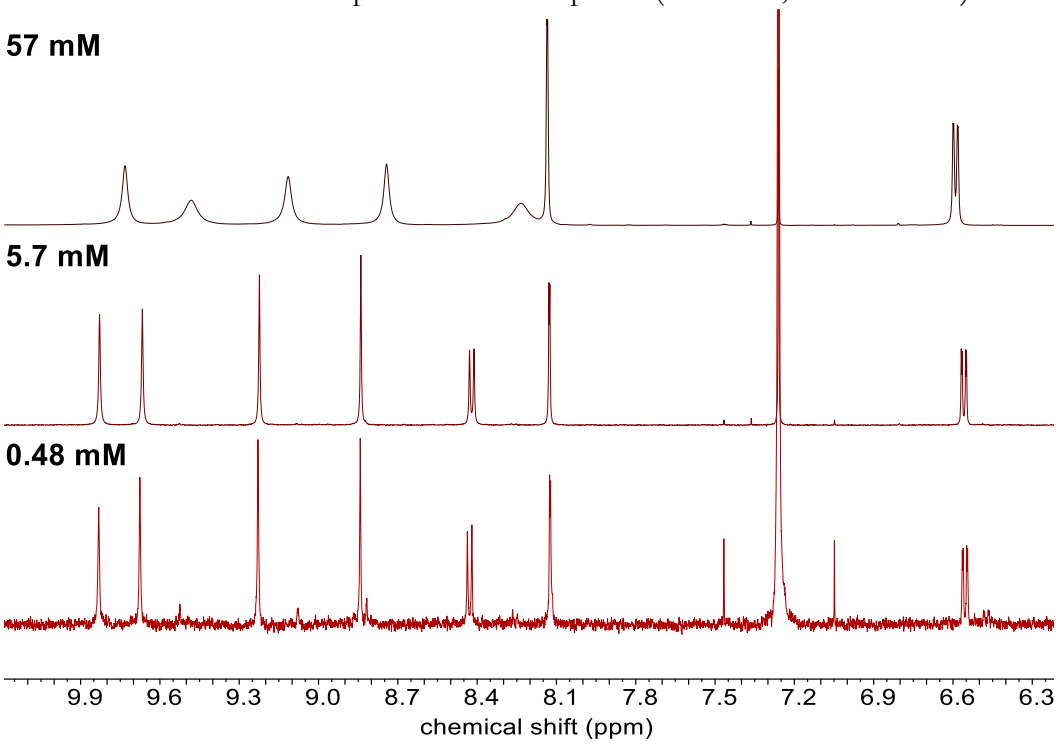

Figure S13. Variable concentration partial ^{1}H NMR spectra (500 MHz, chloroform-*d*) of **1-Benz**.

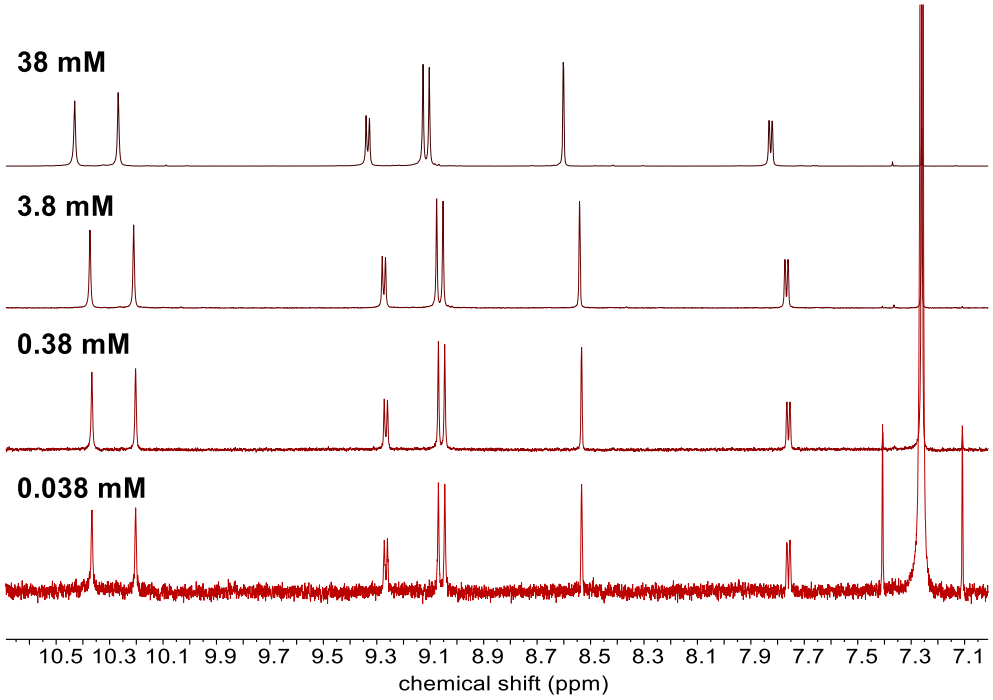

Figure S14. Variable concentration partial ^{1}H NMR spectra (700 MHz, chloroform-*d*) of **2**.

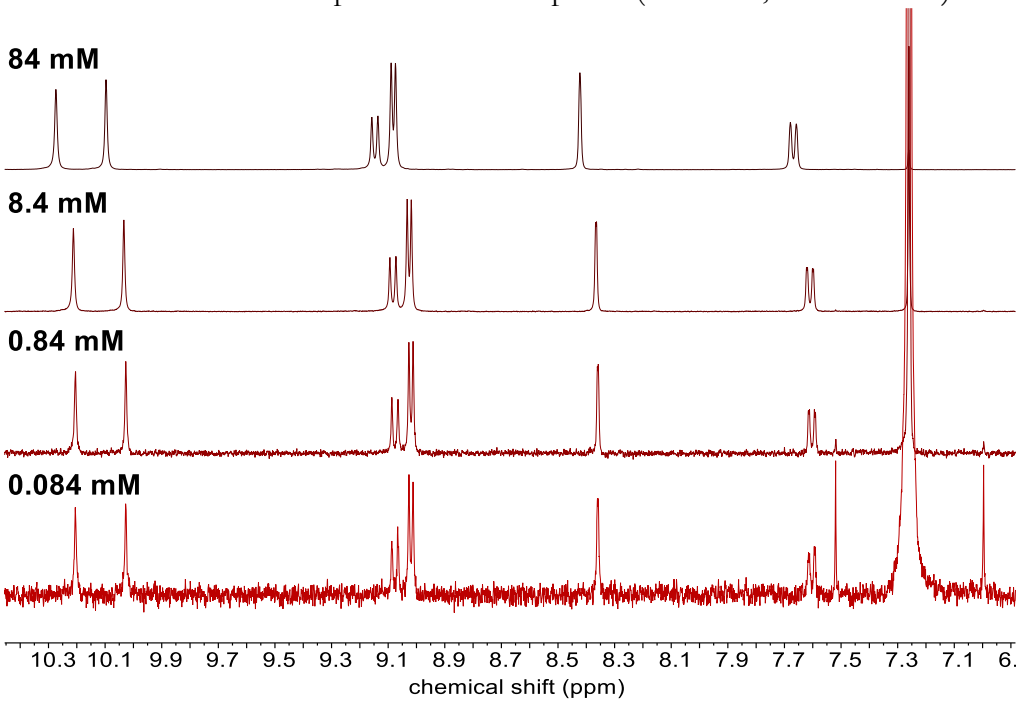

Figure S15. Variable concentration partial ^{1}H NMR spectra (400 MHz, chloroform-*d*) of **3**.

Photophysical Characterization

UV/Vis spectra were recorded on a Varian Cary 300 Bio UV-Visible spectrophotometer. Emission spectra were recorded on a Varian Cary Eclipse Spectrometer. All compounds were purified by preparatory thin layer chromatography (CH_2Cl_2/EtOAc solvent system) prior to analysis to ensure high purity. The UV/Vis spectra that are shown represent the average of two measurements on separate samples to ensure accuracy of extinction coefficients. For sample preparation, each analyte was weighed on an analytical balance and dissolved in the appropriate amount of CH_2Cl_2 using a volumetric flask. A single dilution experiment (10x) was performed for each compound and the UV/vis spectra (plotted by molar absorptivity) for all compounds were unchanged by this dilution. Emission spectra for all compounds were independent of excitation wavelength.

Compound	Absorption Onset, λ_{onset} (nm)[a,b]	Absorption Maximum, λ_{max} (nm)[a]	Emission Maximum, λ_{max} (nm)[a]	Photophysical HOMO-LUMO gap (eV)[a,c]
1-Benz	423	319	452	2.93
1-Se	424	322	451	2.92
2	424	334	449	2.92
3	420	322	448	2.95

Table S1. Summary of relevant photophysical properties. (a) Solvent = CH_2Cl_2; (b) Defined as the point at which the absorption and emission spectra intersect;[14] (c) Estimated from the absorption onset (λ_{onset}): $E_g = 1240/\lambda_{onset}$

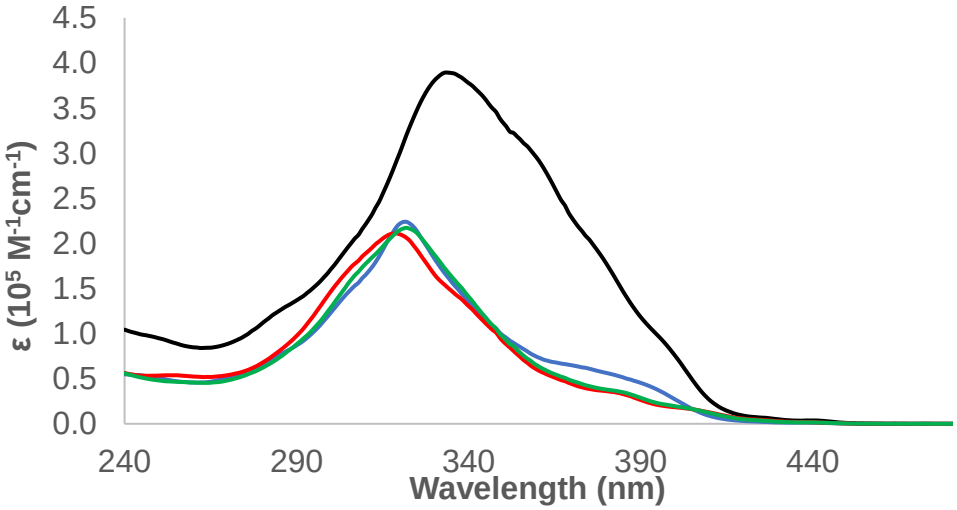

Figure S16. UV/Vis absorption spectra for helicene **3** (blue) and macrocyclic derivatives **1-Benz** (red), **1-Se** (green), and **2** (black) in CH_2Cl_2 solvent (ε = molar absorptivity).

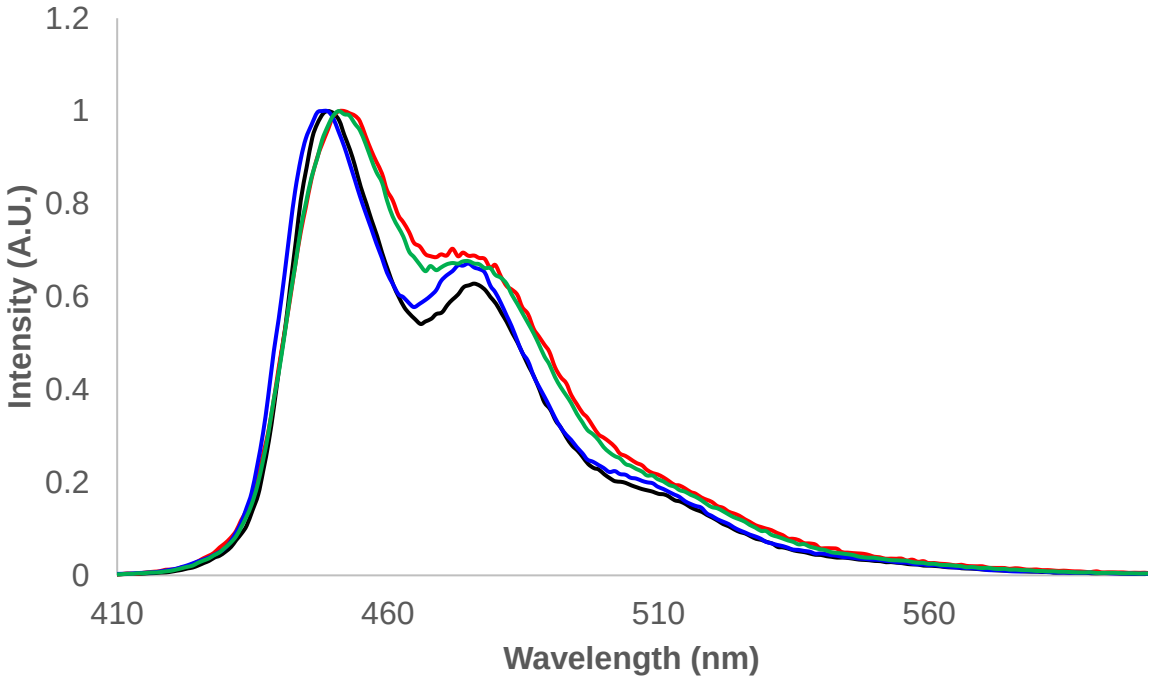

Figure S17. Normalized emission spectra for precursor helicene **3** (blue) and macrocyclic derivatives **1-Benz** (red), **1-Se** (green), and **2** (black) in CH_2Cl_2 solvent.

X-ray Crystallography

X-ray diffraction data were collected at beamline 12.2.1 of the Advanced Light Source at Lawrence Berkeley National Laboratory. Frames were collected on a PHOTON 100 CMOS detector using radiation with a wavelength of 0.7288 Å selected by a Si(111) monochromator and focused to 200 μm^2 with a toroidal mirror. Data collection, integration, scaling, and space group determination were performed with Bruker APEX3 (v. 2016.5-0) software. Structures were solved by SHELXT-2014 and refined with SHELXL-2014, with refinement of F^2 on all data by full-matrix least squares.[15–18] The 3D molecular structure figures were produced in Mercury 3.7.[19]

The single crystals that were used for this study were grown as follows. In a 6 mL vial, compound **2** (3 mg) was dissolved in CH_2Cl_2 (0.8 mL), then the solution was diluted with hexanes (0.8 mL). The vial was capped, and the lid was punctured with 2–3 pinholes. In a dark cabinet, the solvent was allowed evaporate to ~1/3 of the original volume over the course to 2–3 days, resulting in the formation of yellow, irregularly shaped crystals. Crystals of **2** were weakly diffracting, and substantially increased exposure times did not result in appreciably improved resolution. Extensive use of SIMU and ISOR restraints were required to maintain reasonable anisotropic displacement parameters for some of the atoms in the structural model. Because of the low resolution of the dataset, co-crystallized solvent molecules (presumably hexanes) in the unit cell could not be modeled atomistically and was instead treated with the SQUEEZE program.[20]

Empirical formula	$C_{160}H_{148}O_{20}$
Formula weight	2390.78
Temperature	100.15
Crystal system	Hexagonal
Space group	$P6_422$
Unit cell dimensions	a = 31.7473(18) Å
	b = 31.7473(18) Å
	c = 16.1631(10 Å
	α = 90°
	β = 90°
	γ = 120°
Volume	14108.1(18) $Å^3$
Z	3
Density (calculated)	0.844 g/cm^3
μ	0.058 mm^{-1}
F(000)	3804.0
Crystal size	0.15 × 0.15 × 0.15 mm^3
Radiation	Synchrotron (λ = 0.7288 Å)
2Θ range for data collection	1.518 to 45.412 °
Index ranges	-33 ≤ h ≤ 33, -33 ≤ k ≤ 33, -17 ≤ l ≤ 17

Reflections collected	128453
Independent reflections	5859 [R_{int} = 0.1259, R_{sigma} = 0.0408]
Data/restraints/parameters	5859/102/423
Goodness-of-fit on F^2	1.282
Final R indexes [I>=2σ (I)]	R_1 = 0.1084, wR_2 = 0.2776
Final R indexes [all data]	R_1 = 0.1296, wR_2 = 0.3056
Largest diff. peak/hole	0.57/-0.47 e $Å^{-3}$
Flack parameter	0(3)

Table S2. Crystal data and structure refinement for "Figure-8" Macrocycle **2**.

References for Supporting Information of Chapter 5

(1) Nitschke, J. R.; Zürcher, S.; Tilley, T. D. *J. Am. Chem. Soc.* **2000**, *122* (42), 10345–10352.
(2) Dutton, J. L.; Farrar, G. J.; Sgro, M. J.; Battista, T. L.; Ragogna, P. J. *Chem. – Eur. J.* **2009**, *15* (39), 10263–10271.
(3) Herde, J. L.; Lambert, J. C.; Senoff, C. V.; Cushing, M. A. Cyclooctene and 1,5-Cyclooctadiene Complexes of Iridium(I). In *Inorganic Syntheses*; Parshall, G. W., Ed.; John Wiley & Sons, Inc., **1974**; pp 18–20.
(4) Brandsma, L. *Best Synthetic Methods: Acetylenes, Allenes and Cumulenes*, 1st ed.; Elsevier Academic Press: Oxford, UK, **2003**.
(5) von Kugelgen, S.; Bellone, D. E.; Cloke, R. R.; Perkins, W. S.; Fischer, F. R. *J. Am. Chem. Soc.* **2016**, *138* (19), 6234–6239.
(6) Makino, T.; Yamamoto, Y.; Itoh, K. *Organometallics* **2004**, *23* (8), 1730–1737.
(7) Kiel, G. R.; Patel, S. C.; Smith, P. W.; Levine, D. S.; Tilley, T. D. *J. Am. Chem. Soc.* **2017**, *139* (51), 18456–18459.
(8) Kiel, G. R.; Tilley, T. D. A Site-Selective [2+2+2] Cycloaddition and Its Orthogonality to Alkyne Metathesis: Rapid, General Synthesis of Macrocyclic Nanocarbons. *Submitted.*
(9) Krasovskiy, A.; Knochel, P. *Angew. Chem. Int. Ed.* **2004**, *43* (25), 3333–3336.
(10) O'Brien, C. J.; Kantchev, E. A. B.; Valente, C.; Hadei, N.; Chass, G. A.; Lough, A.; Hopkinson, A. C.; Organ, M. G. *Chem. – Eur. J.* **2006**, *12* (18), 4743–4748.
(11) Hoye, T. R.; Eklov, B. M.; Voloshin, M. *Org. Lett.* **2004**, *6* (15), 2567–2570.
(12) Vaska, L.; Catone, D. L. *J. Am. Chem. Soc.* **1966**, *88* (22), 5324–5325.
(13) Lilga, M. A.; Ibers, J. A. *Inorg. Chem.* **1984**, *23* (22), 3538–3543.
(14) Klan, P.; Wirz, J. *Photochemistry of Organic Compounds: From Concepts to Practice, Pg. 194*; John Wiley & Sons, Ltd., **2009**.
(15) Sheldrick, G. M. *Acta Crystallogr. A* **2008**, *64* (1), 112–122.
(16) Sheldrick, G. M. *Acta Crystallogr. Sect. Found. Adv.* **2015**, *71* (1), 3–8.
(17) Palatinus, L.; Chapuis, G. *J. Appl. Crystallogr.* **2007**, *40* (4), 786–790.
(18) Sheldrick, G. M. *Acta Crystallogr. Sect. C Struct. Chem.* **2015**, *71* (1), 3–8.
(19) Macrae, C. F.; Edgington, P. R.; McCabe, P.; Pidcock, E.; Shields, G. P.; Taylor, R.; Towler, M.; Streek, J. van de. *J. Appl. Crystallogr.* **2006**, *39* (3), 453–457.
(20) Spek, A. L. *Acta Crystallogr. Sect. C Struct. Chem.* **2015**, *71* (1), 9–18.

Chapter 6: Titanocene-Mediated Dinitrile Coupling: A Divergent Route to Nitrogen-Containing Polycyclic Aromatic Hydrocarbons

This chapter was adapted with permission from: Kiel, G. R.; Samkian, A. E.; Nicolay, A.; Witzke, R. J.; Tilley, T. D., *J. Am. Chem. Soc.*, **2018**, 140, 2450–2454.

Heterocyclic rings have a profound impact on the electronic, photophysical, and supramolecular properties of polycyclic aromatic hydrocarbons (PAHs) and related carbon nanostructures.[1,2] In particular, nitrogen-containing PAHs have attracted tremendous interest in organic electronics, as they often are good electron-acceptors and have increased stability.[2] Such compounds are also models or building blocks for nitrogen-doped graphene, which is currently under intense investigation for its applications in electronics and catalysis.[3] The general, directed incorporation of nitrogen and other heteroatoms into PAHs is a significant challenge. Many synthetic methods have emerged, but few are *divergent,* which provide access to libraries of analogous compounds and facilitate the identification of structure-property relationships.[4] Indeed, the future success of PAHs as components in functional materials will critically depend on the availability of reliable synthetic methods that can be used to rationally tune properties in this way.

As part of an effort to expand the utility of [2+2+n] cycloadditions in PAH synthesis, we recently developed a general strategy for the synthesis of large PAHs, exemplified by the quantitative cyclization of oligo(diyne) compounds like **1** (Scheme 1a) with a zirconocene reagent or Ir catalyst.[5] The extension of this approach to include analogous precursors of general structure **2** (Scheme 1b), containing one or more tethered dinitrile units, would provide access to nitrogen-containing or other electron-deficient analogues. Notably, in contrast to diyne coupling,[6] there is little precedent for the

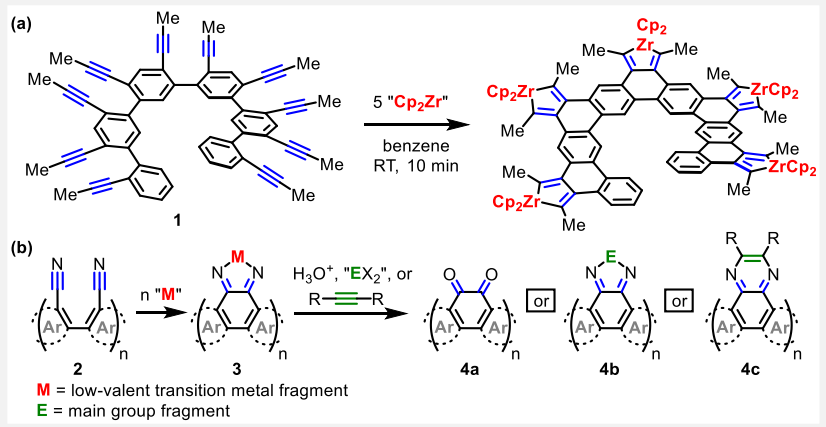

Scheme 1. (a) Previously reported oligo(diyne) coupling; **(b)** This report: extension of strategy to analogous oligo(dinitrile)s.

reductive coupling of two nitrile units to form a 2,5-di(aza)metallacyclopentadiene ring. Rosenthal and coworkers recently reported a breakthrough in this regard, demonstrating the competence of $Cp^*_2M(Me_3SiC{\equiv}CSiMe_3)$ (M = Ti or Zr) for the formation of several 2,5-di(aza)metallacyclopentadienes (the first unambiguous examples with any transition metal).[7]

This report describes a cheaper and more accessible coupling reagent, $Cp_2Ti(Me_3SiC{\equiv}CSiMe_3)$,[8] that efficiently cyclizes tethered dinitrile compounds of general structure **2**. Furthermore, treatment of the resulting π-extended di(aza)titanacycles **3** with aqueous acid, main-group dihalides, or acetylene dicarboxylates provides a divergent route to π-extended *o*-quinones (**4a**), diazoles (**4b**), or pyrazines (**4c**), respectively. These transformations represent the first development of metallacycle-transfer chemistry[6c-d] for di(aza)metallacyclopentadienes (to prepare **4b**) and the first examples of formal [2+2+2] reactions to form pyrazine rings. This chemistry was initially developed in the model system of Scheme 2, and then applied to *divergently* tune the HOMO-LUMO gap in two different PAH systems *via* installation of a range of substituents and heterocyclic rings.

The model system of Scheme 2 formed the basis of our investigations. Based on our favorable experience with biaryl-tethered diynes (e.g. **1**),[5] we hypothesized that the required *intra*molecular coupling of tethered dinitrile **5** might proceed with readily-accessible $Cp_2Ti(Me_3SiC{\equiv}CSiMe_3)$, despite the failure of this reagent in an analogous *inter*molecular coupling.[7a] Furthermore, it seemed that the relatively small Cp ligands would provide a reactive titanacycle better poised for further transformations. Indeed, treatment of **5** with 1.1 equiv of $Cp_2Ti(Me_3SiC{\equiv}CSiMe_3)$ gave the phenanthrene-annulated di(aza)titanacyclopentadiene **6** in 75% isolated yield. The structure of this compound was verified by X-ray crystallography (see SI, Figure S82) and its isolation allowed streamlined reactivity studies (*vide infra*).

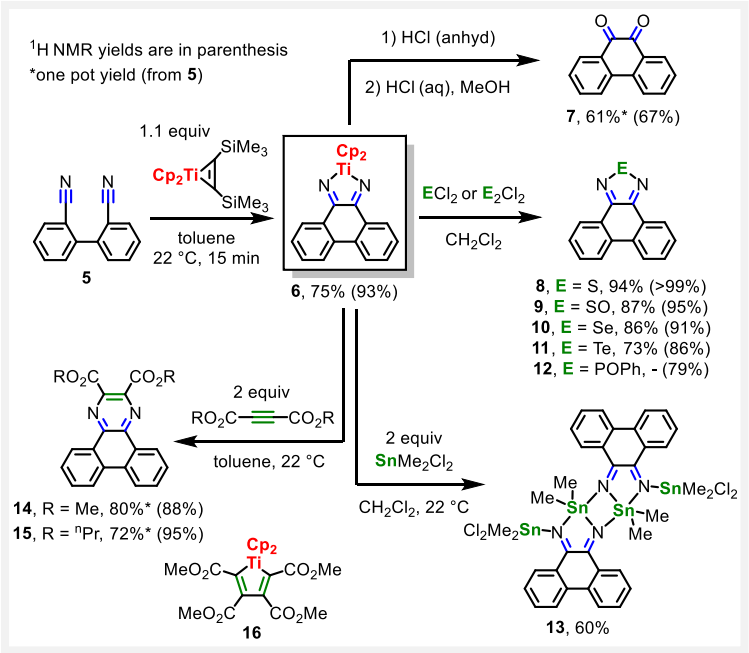

Scheme 2. Investigations of a model system.

The first transformation employed **6** *in situ* as a synthetic intermediate. A one-pot procedure involving coupling of **5**, protodemetallation of **6**, and hydrolysis of the resulting bis-imine gave 9,10-phenanthrenequinone **7** in 61% isolated yield. This represents a new way to access π-extended *o*-quinones, which are most commonly obtained by functionalization of one of the few commercially available *o*-quinones, or *via* oxidation of the parent PAH. These compounds are attractive for their electronic properties (most notably, their ability to reversibly accept electrons),[9] as ligands for transition metal complexes,[10] and as synthetic precursors.[2e,11]

In analogy to Fagan and Nugent's versatile and well-established zirconacyclopentadiene-transfer chemistry,[6c-d] the "Cp_2Ti" fragment in **6** can be exchanged for a range of heteroatoms. For example, this compound provided divergent access to chalcogenadiazoles **8–11**. Phenanthrene-annulated thiadiazole **8** and thiadiazole-oxide **9** were isolated in good yields by treatment of **6** with S_2Cl_2 and $SOCl_2$, respectively.[12] The reaction of **6** with SO_2Cl_2 failed to yield the corresponding thiadiazole-dioxide, resulting primarily in decyclization to re-form **5**. The heavier chalcogen analogues **10** and **11** were similarly synthesized by treatment of **6** with the isolable, base-stabilized chalcogen dihalides $SeCl_2$(bipy)[13] and $TeCl_2$(bipy),[13,14] respectively. Benzannulated chalcogenadiazole heterocycles are heavily-used as electron acceptors in conducting polymers and their unique self-assembly properties are well-documented.[15] These two features make them attractive for incorporation into PAHs; [15d-f, 16] however, this typically requires *o*-quinone or *o*-diamine functionality, which can be difficult to install.

The chemistry was extended to other main group diazole heterocycles, such as the π-extended phosphadiazole **12**,[17] which was produced in 79% yield (by ^{1}H NMR spectroscopy) upon treatment of titanacycle **6** with $POCl_2Ph$. Unfortunately, compound **12** could not be isolated due to the difficulty in separating the Cp_2TiCl_2 byproduct, which was complicated by the hydrolytic lability of the P–N bond in this compound. Treatment of a CH_2Cl_2 solution of **6** with 2 equiv of $SnMe_2Cl_2$ resulted in precipitation of dimeric **13**, as revealed by single crystal X-ray crystallography (Figure S83). It is well known that diazole heterocycles (e.g., **10** and **11**) associate non-covalently by formation of cyclic E–N–E–N linkages viewed as Lewis acid-base adducts,[15] but the short bonds in the central Sn–N–Sn–N ring of **13** suggest that this dimeric compound is associated through normal covalent bonding.

The formal [2+2+2] products **14** and **15** were produced in good yields by treatment of **6**, generated *in situ* from **5**, with excess di(alkyl)acetylene dicarboxylate. An interesting feature of this transformation is its occurrence in the absence of additives, as it formally requires the extrusion of thermally unstable "Cp_2Ti".[18] It is possible that the excess alkyne plays a role in this extrusion, as metallacyclopentadiene **16**[19] is observed (by ^{1}H NMR spectroscopy) as a byproduct in the synthesis of **14**. Furthermore, the yield drops to 63% when 1.1 equiv of acetylene is used. No reaction occurred with 3-hexyne and diphenylacetylene, even at elevated temperature, suggesting that an electron deficient alkyne is required. Surprisingly, this appears to be the first example of a [2+2+2] reaction to form a pyrazine ring, despite the extensive literature on [2+2+2] reactions involving nitriles.[20]

An appealing feature of the dinitrile precursors is the ease with which functionalized derivatives can be accessed. For example, the cyano group is a good activating group in nucleophilic aromatic substitution (S_NAr) reactions.[21] By subjection of commercially-available 2-bromo-4-fluorobenzonitrile to the simple three-step sequence of S_NAr, aryl-aryl coupling, and the [2+2+2] conditions described above, a range of 7,10-substituted dibenzo[f,h]quinoxalines **17–21** were produced (Scheme 3). The 57–70% yields for the [2+2+2] reactions are for the two-step, one-pot procedure. The S_NAr reactions are notable for their scalability and simplicity. For example, introduction of the amino substituent

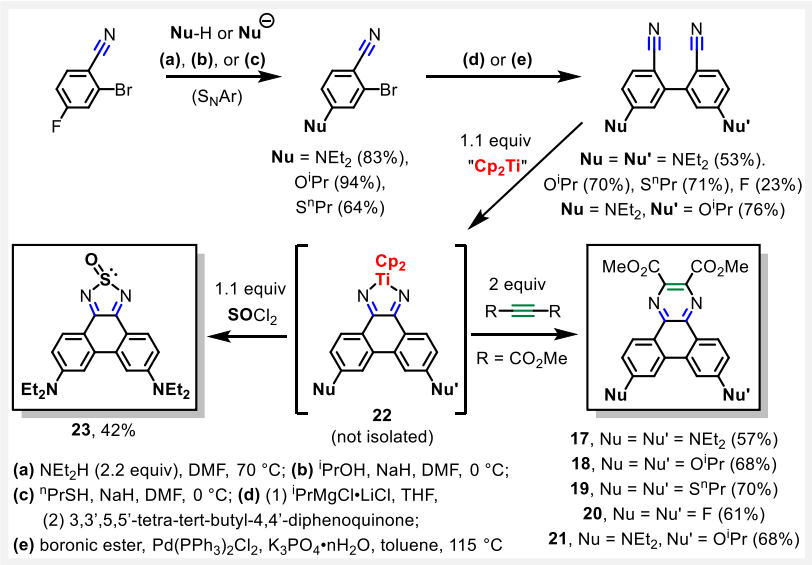

Scheme 3. Functionalized derivatives *via* an S_NAr / aryl-aryl coupling / [2+2+n] sequence

requires simple heating of a concentrated mixture of secondary amine (2.2 equiv) and 2-bromo-4-fluorobenzonitrile in DMF.

A critical feature of the new synthetic strategy is that the intermediate di(aza)titanacyclopentadienes (**22**) can be subjected to any of the reactions described in Scheme 2. This is shown in the synthesis of thiadiazole-oxide **23**, which was targeted for its expected small HOMO-LUMO gap due to its donor-acceptor (D-A) structure.

The advantages of this strategy are more apparent in the construction of larger PAHs, such as those resulting from multifold coupling reactions and containing two or more quinones, pyrazines, or diazoles. The focus here is on the series of large, angular PAHs **24–26** (Scheme 4), which were targeted in the context of our general interest in expanded helicenes.[5b] These compounds possess an alternation of donor and acceptor units, which might give rise to ambipolar charge transport and/or novel self-assembly. The bis(dinitrile) precursors **27–29** were obtained *via* Suzuki cross-coupling[22] of compound **30** with the appropriate boronic ester. The former was easily prepared on a gram scale using a Pd-catalyzed cyanation reaction[23] and the latter were produced *via* another exploitation of S_NAr chemistry (see SI).

The first targets were the pyrazine-annulated **24–26-pyr**, which differ only in the electron-donating ability of the "Nu" substituent, by employment of the [2+2+2] conditions described above. These compounds were isolated in 39–47% yields for the two-step, one-pot reaction, which are consistent with the yields expected based on the one-fold couplings described above. The side products were easily separated by column chromatography. Monitoring of the reactions by ^{1}H NMR spectroscopy revealed formation of the intermediate bis(di(aza)titanacyclopentadiene)s **24–26-Ti** in 58, 76, and 67% yields, respectively. The NEt_2-substituted bis(dinitrile) **28** was next subjected to the titanocene-coupling / chalcogen transfer reactions described above, which produced bis(chalcogenadiazoles) **25-S**, **25-SO**, and **25-Se** in 34, 47, and 52% yields, respectively. Compound **25-SO** is an inseparable mixture of two diastereomers, resulting from the chiral S=O centers. It is important to note that, in contrast to the model system (Scheme 2), these compounds were produced in a one-pot reaction from

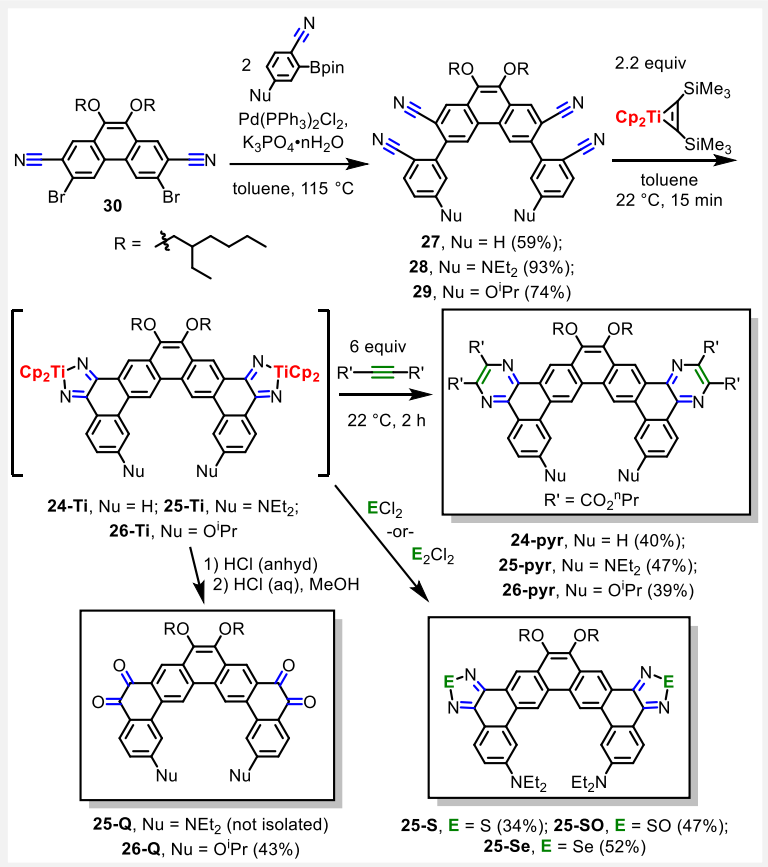

Scheme 4. Large, angular PAHs *via* twofold coupling.

bis(dinitrile) **28**. An attempt to produce the bis(*o*-quinone) **25-Q** using the conditions presented for **7** gave a complex mixture, probably due to the basicity of the NEt_2 group; however, synthesis of bis(*o*-quinone) **26-Q** using these conditions proceeded without difficulty.

A high level of control over HOMO and LUMO energy levels, and thus photophysical and electronic properties, can be achieved using the chemistry developed above. In the series of pyrazine-annulated PAHs **14** and **17**–**21**, a bathochromic shift in the absorption onset (λ_{onset}) value of 129 nm results on going from F-substituted **20** to NEt_2-substituted **17** (Figure 1a), with intermediate shifts for less-donating substituents. This results from an increase in the HOMO energy level, as supported by cyclic voltammetry (CV) and DFT calculations (see Figures S80 and S84 and Table S2). Emission λ_{max} values span a range of 158 nm in this series of compounds (Figure 1b). The LUMO energy level can be manipulated by modification of the heterocyclic ring,[16a] as shown for thiadiazole-oxide-annulated PAH **23**. Compared to pyrazine-annulated **17**, this compound exhibits a further bathochromic shift in absorption (λ_{onset}) of 84 nm and in emission (λ_{max}) of 91 nm. The total shifts in absorption and emission (from **20** to **23**) are 213 and 249 nm, respectively. Thus, a large decrease in the optical HOMO-LUMO gaps, from 3.20 eV for **20** to 2.06 eV for **23**, can be achieved from rational and independent perturbations of HOMO and LUMO energy levels in this PAH system.

The expected red-shift in absorption and emission is again seen on going from unsubstituted **24-pyr** to NEt_2-substituted **25-pyr** (Figures 2a and 2b); however, the effect of the substituent is attenuated

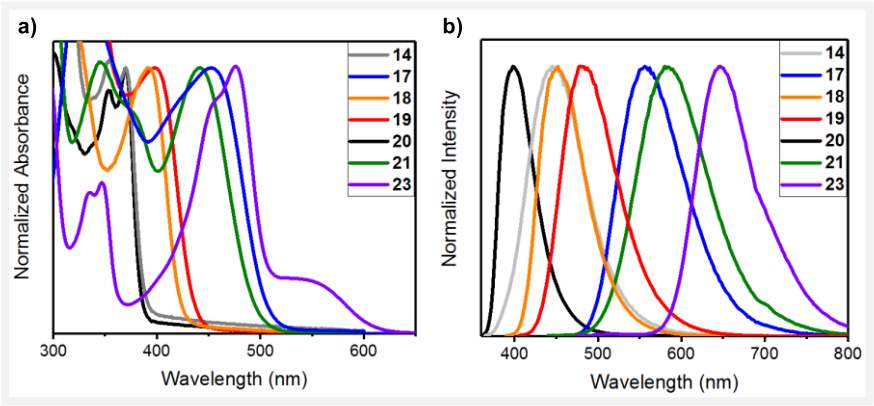

Figure 1. Normalized **(a)** absorption and **(b)** emission spectra (CH_2Cl_2) for PAHs **14**, **17–21**, and **23**.

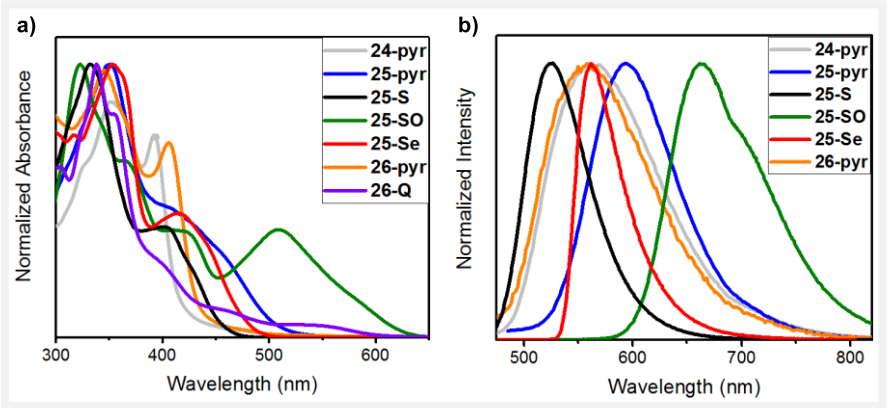

Figure 2. Normalized **(a)** absorption and **(b)** emission spectra (CH_2Cl_2) for **24–26**.

since the HOMO is partially distributed onto the central phenanthrene unit, which also contains electron-donating groups. Introduction of the thia- and selenadiazole rings in compounds **25-S** and **25-Se** results in blue-shifted absorption and emission maxima (λ_{max}) compared to compound **25-Pyr**; however, the absorption and emission (λ_{max}) of bis(thiadiazole-oxide) **25-SO** exhibit large red-shifts and a concomitant decrease in optical HOMO-LUMO gap of 0.35 eV (from 2.31 to 1.96 eV) compared to **25-pyr**. Bis(quinone) **26-Q** exhibits a weak, red-shifted absorption band and this compound is non-fluorescent.

Given the facility with which *o*-quinones accept electrons, the rare bis(*o*-quinone) **26-Q** was analyzed by CV in THF with 0.1 M $N^nBu_4PF_6$ as supporting electrolyte (Figure S81). This compound exhibits four reduction events (three reversible and one irreversible) with $E_{1/2}$ values of –1.16, –1.32, –1.91, and –3.01 V vs. Fc/Fc^+. No oxidation events could be observed within the solvent window.

In conclusion, a general, divergent synthetic strategy to rationally control the electronic and optical properties of nitrogen-substituted PAHs has been disclosed. The initial focus is on application of this strategy to PAHs and graphene nanostructures; however, this chemistry should find applications in other fields where *o*-quinone, diazole, or pyrazine functionalities are desirable. Metallacyclopentadiene intermediates have long been employed to access highly-substituted benzenes and metallole heterocycles (e.g., thiophenes, phospholes, and stannoles).[6] This strategy has now been extended to

seven di(aza)-analogues. Current efforts involve application of the method to synthesis of more complex electron-deficient PAHs (e.g. expanded helicenes), especially those containing multiple redox centers.

References for Main Text of Chapter 6

(1) (a) Jiang, W.; Li, Y.; Wang, Z. *Chem. Soc. Rev.* **2013**, *42*, 6113. (b) Stępień, M.; Gońka, E.; Żyła, M.; Sprutta, N. *Chem. Rev.* **2017**, *117*, 3479. (c) Anthony, J. E. *Chem. Rev.*, **2006**, *106*, 5028. (d) Vostrowsky, O.; Hirsch, A. *Chem. Rev.* **2006**, *106*, 5191. (e) *Polycyclic Arenes and Heteroarenes*; Miao, Q., Ed.; Wiley-VCH Verlag GmbH & Co. KGaA: Weinheim, Germany, **2015**. (f) Narita, A.; Wang, X.-Y.; Feng, X.; Müllen, K. *Chem. Soc. Rev.* **2015**, *44*, 6616.

(2) (a) Bunz, U. H. F.; Engelhart, J. U.; Lindner, B. D.; Schaffroth, M. *Angew. Chem. Int. Ed.* **2013**, *52*, 3810. (b) Bunz, U. H. F. *Acc. Chem. Res.* **2015**, *48*, 1676. (c) Miao, Q. *Adv. Mater.* **2014**, *26*, 5541. (d) Li, J.; Zhang, Q. *ACS Appl. Mater. Interfaces* **2015**, *7*, 28049. (e) Mateo-Alonso, A. *Chem. Soc. Rev.* **2014**, *43*, 6311.

(3) (a) Wang, H.; Maiyalagan, T.; Wang, X. *ACS Catal.* **2012**, *2*, 781. (b) Kong, X.-K.; Chen, C.-L.; Chen, Q.-W. *Chem. Soc. Rev.* **2014**, *43*, 2841.

(4) Many of the methods employed to date are summarized in refs 1 and 2. Notable examples of divergent approaches: (a) Jiang, W.; Qian, H.; Li, Y.; Wang, Z. *J. Org. Chem.* **2008**, *73*, 7369. (b) He, B.; Dai, J.; Zherebetskyy, D.; L. Chen, T.; A. Zhang, B.; J. Teat, S.; Zhang, Q.; Wang, L.; Liu, Y. *Chem. Sci.* **2015**, *6*, 3180.

(5) (a) Kiel, G. R.; Ziegler, M. S.; Tilley, T. D. *Angew. Chem. Int. Ed.* **2017**, *56*, 4839. (b) Kiel, G. R.; Patel, S. C.; Smith, P. W.; Levine, D. S.; Tilley, T. D. *J. Am. Chem. Soc.* **2017**, *139*, 18456**.**

(6) (a) Müller, E. *Synthesis* **1974**, *1974*, 761. (b) Vollhardt, K. P. C. *Acc. Chem. Res.* **1977**, *10*, 1. (c) Fagan, P. J.; Nugent, W. A. *J. Am. Chem. Soc.* **1988**, *110*, 2310. (d) Yan, X.; Xi, C. *Acc. Chem. Res.* **2015**, *48*, 935. (e) Agenet, N.; Buisine, O.; Slowinski, F.; Gandon, V.; Aubert, C.; Malacria, M. In *Organic Reactions*; Overman, L. E., Ed.; John Wiley & Sons: Hoboken, NJ, **2007**, Vol. 68, pp. 1–302. (f) *Transition-Metal-Mediated Aromatic Ring Construction*; Tanaka, K., Ed.; John Wiley & Sons, Inc.: Hoboken, NJ, **2013**.

(7) Initial report: (a) Becker, L.; Arndt, P.; Jiao, H.; Spannenberg, A.; Rosenthal, U. *Angew. Chem. Int. Ed.* **2013**, *52*, 11396. Follow-up reports: (b) Becker, L.; Arndt, P.; Spannenberg, A.; Jiao, H.; Rosenthal, U. *Angew. Chem. Int. Ed.* **2015**, *54*, 5523. (c) Becker, L.; Reiß, F.; Altenburger, K.; Spannenberg, A.; Arndt, P.; Jiao, H.; Rosenthal, U. *Chem. Eur. J.* **2016**, *22*, 10826.

(8) (a) Review: Rosenthal, U.; Burlakov, V. V.; Arndt, P.; Baumann, W.; Spannenberg, A. *Organometallics* **2003**, *22*, 884. (b) This reagent has also been used to construct hexaazatriphenylenes *via* an intermolecular, dehydrogenative C-C bond forming reaction: *J. Am. Chem. Soc.* **2005**, *127*, 14190.

(9) (a) Schweinfurth, D.; Zalibera, M.; Kathan, M.; Shen, C.; Mazzolini, M.; Trapp, N.; Crassous, J.; Gescheidt, G.; Diederich, F. *J. Am. Chem. Soc.* **2014**, *136*, 13045. (b) Urakawa, K.; Sumimoto, M.; Arisawa, M.; Matsuda, M.; Ishikawa, H. *Angew. Chem. Int. Ed.* **2016**, *128*, 7558.

(10) Pierpont, C. G.; Buchanan, R. M. *Coord. Chem. Rev.* **1981**, *38*, 45.

(11) Wasserfallen, D.; Kastler, M.; Pisula, W.; Hofer, W. A.; Fogel, Y.; Wang, Z.; Müllen, K. *J. Am. Chem. Soc.* **2006**, *128*, 1334.

(12) One thiadiazole-oxide has been synthesized by treatment of a di(aza)titanacyclopentadiene with $SOCl_2$, but the yield was low (ref 7c). To the best of our knowledge, this is the only previous example of metallacycle-transfer chemistry with a di(aza)metallacyclopentadiene.

(13) Dutton, J. L.; Farrar, G. J.; Sgro, M. J.; Battista, T. L.; Ragogna, P. J. *Chem. Eur. J.* **2009**, *15*, 10263.

(14) He, G.; Kang, L.; Torres Delgado, W.; Shynkaruk, O.; Ferguson, M. J.; McDonald, R.; Rivard, E. *J. Am. Chem. Soc.* **2013**, *135*, 5360.

(15) (a) Cozzolino, A. F.; Vargas-Baca, I.; Mansour, S.; Mahmoudkhani, A. H. *J. Am. Chem. Soc.* **2005**, *127*, 3184. (b) Ono, K.; Tanaka, S.; Yamashita, Y. *Angew. Chem. Int. Ed. Engl.* **1994**, *33*, 1977. (c) Langis-Barsetti, S.; Maris, T.; Wuest, J. D. *J. Org. Chem.* **2017**, *82*, 5034. (d) Neidlein, R.; Knecht, D.; Endres, H. *Z. f. Naturforsch.* **1987**, *42*, 84. (e) Appleton, A. L.; Miao, S.; Brombosz, S. M.; Berger, N. J.; Barlow, S.; Marder, S. R.; Lawrence, B. M.; Hardcastle, K. I.; Bunz, U. H. F. *Org. Lett.* **2009**, *11*, 5222. (f) Xia, D.; Wang, X.-Y.; Guo, X.; Baumgarten, M.; Li, M.; Müllen, K. *Cryst. Growth Des.* **2016**, *16*, 7124. (g) Wang, Y.; Michinobu, T. *J. Mater. Chem. C* **2016**, *4*, 6200.

(16) (a) Linder, T.; Badiola, E.; Baumgartner, T.; Sutherland, T. C. *Org. Lett.* **2010**, *12*, 4520. (b) Xie, Y.; Shuku, Y.; Matsushita, M. M.; Awaga, K. *Chem. Commun.* **2014**, *50*, 4178. (c) Xiao, J.; Xiao, X.; Zhao, Y.; Wu, B.; Liu, Z.; Zhang, X.; Wang, S.; Zhao, X.; Liu, L.; Jiang, L. *Nanoscale* **2013**, *5*, 5420.

(17) Linder, T.; Sutherland, T. C.; Baumgartner, T. *Chem. Eur. J.* **2010**, *16*, 7101.

(18) In contrast, the reaction between a zirconacyclopentadiene and a di(alkyl)acetylene dicarboxylate requires an initial transmetallation to Cu: Takahashi, T.; Xi, Z.; Yamazaki, A.; Liu, Y.; Nakajima, K.; Kotora, M. *J. Am. Chem. Soc.* **1998**, *120*, 1672.

(19) Demerseman, B.; H. Dixneuf, P. *J. Chem. Soc. Chem. Commun.* **1981**, 665.

(20) A closely related transformation is a 1,2,4-triazine synthesis *via* a [2+2+2] reaction between a dinitrile and a nitrile: Gesing, E. R. F.; Groth, U.; Vollhardt, K. P. C. *Synthesis*, **1984**, 351. For a review of [2+2+2] reactions involving nitriles, see: Varela, J. A.; Saá, C. *Chem. Rev.* **2003**, *103*, 3787.

(21) Bunnett, J. F.; Zahler, R. E. *Chem. Rev.* **1951**, *49*, 273.

(22) Urawa, Y.; Naka, H.; Miyazawa, M.; Souda, S.; Ogura, K. *J. Organomet. Chem.* **2002**, *653*, 269.

(23) Tschaen, D. M.; Desmond, R.; King, A. O.; Fortin, M. C.; Pipik, B.; King, S.; Verhoeven, T. R. *Synth. Commun.* **1994**, *2*

Supporting Information for Chapter 6

General Details

Unless otherwise stated, all manipulations of organometallic compounds were carried out in dry solvents under an atmosphere of nitrogen, using either standard Schlenk techniques or a glovebox. Pentane, toluene, tetrahydrofuran, and diethyl ether were dried using a JC Meyers Phoenix SDS solvent purification system. Benzene was dried using a Vacuum Atmosphere solvent purification system. $Cp_2Ti(Me_3SiC{\equiv}CSiMe_3)$,[1] $SeCl_2$(bipy),[2] $TeCl_2$(bipy),[2] 3,6-dibromo-2,7-diiodophenanthrene-9,10-dione,[3] dipropyl acetylenedicarboxylate,[4] ^{i}PrMgCl·LiCl,[5] and 3,3',5,5'-tetra-tert-butyl-4,4'-diphenoquinone[6] were prepared by literature procedures or slight modifications thereof. $K_3PO_4{\bullet}nH_2O$ and 2-bromo-4-fluorobenzonitrile were purchased from Fischer Scientific and Oakwood Chemical, respectively, and were used as received. Other reagents and solvents were purchased from various commercial suppliers and used as received. ^{i}PrMgCl·LiCl and ^{n}BuLi were titrated by ^{1}H NMR spectroscopy immediately prior to use.[7] "Room temperature" or "RT" refers to ~22 °C. Reaction temperatures represent the oil bath temperature unless otherwise stated. Melting points were determined on an SRS OptiMelt and are uncorrected. Mass spectrometry was performed by the QB3/Chemistry Mass Spectrometry Facility at the University of California, Berkeley. Elemental analyses were performed by the Microanalytical Laboratory in the College of Chemistry at the University of California, Berkeley. Column chromatography was carried out using Fischer Chemical 40–63μm, 230–400 mesh silica gel.

NMR spectra were acquired at ambient temperature (~22 °C) using Bruker AV-600, AV-500, DRX-500, AV-400, and AV-300 spectrometers. Chemical shifts (δ) are given in ppm and referenced to residual solvent peaks for ^{1}H NMR spectra (δ = 7.26 ppm for chloroform-*d*, δ = 7.16 for benzene-d_6, and δ = 5.32 for dichloromethane-d_2) and for $^{13}C\{^1H\}$ NMR spectra (δ = 77.16 ppm for chloroform-*d* and δ = 54.00 for dichloromethane-d_2). For ^{19}F NMR spectra, chemical shifts are referenced to a C_6F_6 internal standard (δ = –162.2 ppm) and are reported relative to $CFCl_3$ at 0 ppm. The chirality of the ethylhexyl group gives rise to diastereomers in compounds containing two or more of these substituents. For simplicity of analysis, especially with respect to NMR spectroscopy, this diastereomerism was ignored. In most cases, chemical shifts of the two diastereomers were indistinguishable (in ^{1}H and $^{13}C\{^1H\}$ NMR spectra). In cases where they could be distinguished (e.g., some alkyl carbons in $^{13}C\{^1H\}$ spectra), the average of the two chemical shifts is reported.

Comments About $Cp_2Ti(Me_3SiC{\equiv}CSiMe_3)$

This compound is typically stored at –35 °C in an N_2-filled glovebox. In the procedures below, the reagent's purity was typically 95–98%, as determined by ^{1}H NMR spectroscopy in benzene-d_6 (using hexamethylbenzene as internal standard). The masses reported below reflect the quantity of active species and the impurities do not noticeably affect results. This reagent can be routinely be synthesized[1] in decagram quantities.

Notes on Removal of Cp_2TiCl_2 Byproduct

Titanocene dichloride, which is generated as a stoichiometric byproduct in many of the reactions reported below, can be easily removed in several ways. We briefly discuss three of those ways here, all of which are used below. The compound decomposes under basic conditions and we found quenching a reaction mixture with 10% aqueous NH_4OH to be the most effective. Since a lot of solid is generated,

the biphasic mixture is typically filtered after quenching. For reactions that are run in CH_2Cl_2, the PAH product can be precipitated with MeOH, leaving Cp_2TiCl_2 in solution. Use of diethyl ether or hexanes results in co-precipitation of Cp_2TiCl_2. Finally, Cp_2TiCl_2 can be removed by a short silica column, as it has an R_f of zero with many eluents.

Synthetic Procedures and Characterization of Compounds

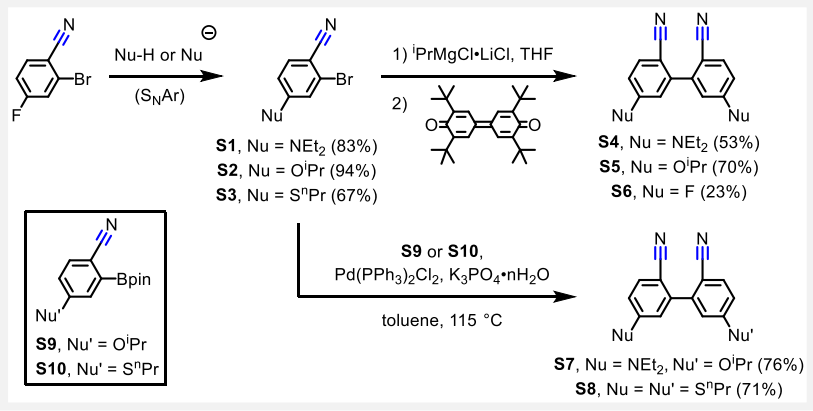

Scheme S1. Two-step synthesis of substituted dinitriles *via* S_NAr / aryl-aryl coupling

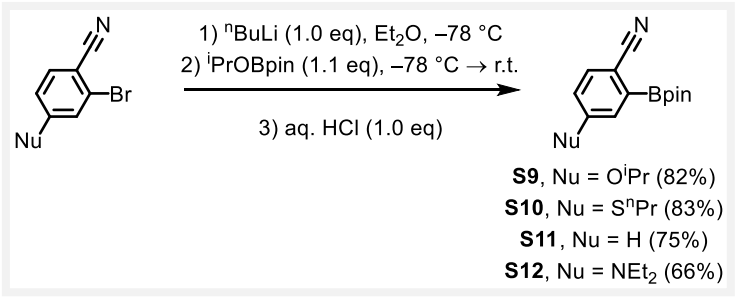

Scheme S2. Synthesis of boronic esters *via* lithium/bromine exchange

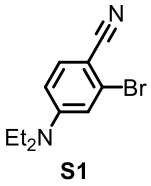

2-bromo-4-(diethylamino)benzonitrile (S1). A Schlenk flask equipped with Teflon stopper and a magnetic stirbar was loaded with 2-bromo-4-fluorobenzonitrile (5.00 g, 25.0 mmol), diethylamine (4.00 g, 55.0 mmol), and DMF (25 mL), the flask was sealed, and the stirred reaction mixture was heated at 70 °C for 12 h. The mixture was cooled to RT and diluted with diethyl ether (100 mL), washed with water (100 mL) and saturated aqueous NaCl (100 mL), dried with Na_2SO_4, filtered, and the filtrate was concentrated *via* rotary evaporation. The crude solid was dissolved in CH_2Cl_2 (10 mL) and filtered through a plug of silica gel (6 g). The plug was flushed with fresh CH_2Cl_2 (40 mL), then the filtrate was concentrated to ~5 mL. Hexanes (50 mL) was added, which caused a large amount of crystalline solid to gradually separate. This solid was collected on a fritted funnel, washed with hexanes, and dried in a stream of air to afford **S1** (5.25 g, 83%) as pale orange needles. ^{1}H NMR (chloroform-*d*, 400 MHz): δ = 7.36 (d, *J* = 9.0 Hz, 1H), 6.79 (d, *J* = 2.6 Hz, 1H), 6.53 (dd, *J* = 9.0, 2.6 Hz, 1H), 3.37 (q, *J* = 7.1 Hz, 4H), 1.18 (t, *J* = 7.1 Hz, 6H); ^{13}C{^{1}H} NMR (chloroform-*d*, 101 MHz): δ = 151.1,

135.0, 126.7, 119.2, 114.6, 110.0, 99.8, 44.7, 12.4; HRMS-ESI (m/z): $[M+H]^+$ calcd. for $C_{11}H_{14}N_2Br$, 253.0335; found, 253.0343.

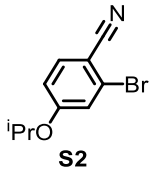

S2

2-bromo-4-isopropoxybenzonitrile (S2). A 100 mL Schlenk tube was charged with NaH (0.502 g, 20.9 mmol) and DMF (16 mL) and to this mixture was added isopropyl alcohol (1.16 g, 19.3 mmol) dropwise over ~10 min *via* syringe.* This mixture was stirred for 1 h. In a separate 150 mL Schlenk tube, a solution of 2-bromo-4-fluorobenzonitrile (3.22 g, 16.1 mmol) in DMF (16 mL) was cooled to 0 °C with an ice/water bath. The alkoxide solution was drawn into a syringe and added dropwise to the stirred 2-bromo-4-fluorobenzonitrile/DMF solution over 5-10 min. The reaction mixture was stirred for an additional 1 h at 0 °C, then it was diluted with ethyl acetate (60 mL) and quenched by addition of water (60 mL; added dropwise until bubbling subsided, then all at once). The layers were separated, then the aqueous layer was extracted with ethyl acetate (30 mL). The combined organic layers were washed with saturated aqueous NaCl (40 mL), dried with $MgSO_4$, filtered, and volatile materials were removed from the filtrate *via* rotary evaporation to give an oil. Addition of hexanes (10 mL) to the oil induced the formation of a crystalline solid. Removal of the hexanes *via* decantation, then high vacuum, gave pure **S2** as a beige crystalline solid (3.65 g, 94%). ^{1}H NMR (chloroform-*d*, 400 MHz): δ = 7.54 (d, *J* = 8.7 Hz, 1H), 7.14 (d, *J* = 2.4 Hz, 1H), 6.86 (dd, *J* = 8.7, 2.4 Hz, 1H), 4.59 (hept, *J* = 6.1 Hz, 1H), 1.36 (d, *J* = 6.1 Hz, 6H); ^{13}C{^{1}H} NMR (chloroform-*d*, 101 MHz): δ = 161.8, 135.4, 126.5, 120.1, 117.8, 115.1, 107.0, 71.3, 21.8; HRMS-EI (m/z): $[M]^+$ calcd. for $C_{10}H_{10}NOBr$, 238.9946; found, 238.9942.

*The reaction of NaH with the alcohol causes a large amount of bubbles (H_2) to form. Use of a large flask is beneficial in this regard.

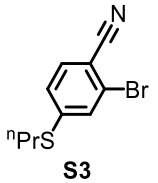

S3

2-bromo-4-(propylthio)benzonitrile (S3). A 150 mL Schlenk tube was charged with NaH (0.660 g, 27.5 mmol) and DMF (50 mL) and the mixture was cooled to 0 °C with an ice/water bath. To the vigorously stirred mixture was added 2-bromo-4-fluorobenzonitrile (5.00 g, 25.0 mmol) in one portion, followed by propane-1-thiol (1.96 g, 25.8 mmol) dropwise over 30 min. The mixture was stirred at 0 °C for an additional 30 min, then quenched by careful addition of saturated aqueous NH_4Cl (40 mL). The mixture was extracted with ethyl acetate (40, then 30 mL), then the combined organic layers were washed with water (2 x 30 mL) and saturated aqueous NaCl (40 mL), dried over $MgSO_4$, filtered, and the filtrate was concentrated via rotary evaporation. The crude product was recrystallized from boiling hexanes (25-30 mL) to furnish **S3** (4.26 g, 67%) as a white solid. ^{1}H NMR (chloroform-*d*, 400 MHz): δ = 7.48 (d, *J* = 8.3 Hz, 1H), 7.47 (d, *J* = 1.8 Hz, 1H), 7.21 (dd, *J* = 8.3, 1.8 Hz, 1H), 2.95 (t, *J* = 7.3 Hz, 2H), 1.73 (h, *J* = 7.3 Hz, 2H), 1.06 (t, *J* = 7.4 Hz, 3H); ^{13}C{^{1}H} NMR (chloroform-

d, 75 MHz): δ = 147.4, 133.9, 129.8, 125.6, 125.2, 117.5, 111.1, 33.9, 21.9, 13.6; HRMS-EI (m/z): $[M]^+$ calcd. for $C_{10}H_{10}NSBr$, 254.9717; found, 254.9720.

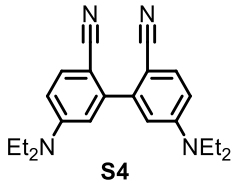

S4

5,5'-bis(dialkylamino)-[1,1'-biphenyl]-2,2'-dicarbonitrile (S4). This oxidative homocoupling was adapted from a report by Knochel and coworkers.[6] A 10 mL Schlenk tube was charged with **S1** (0.180 g, 0.711 mmol) and tetrahydrofuran (1.0 mL). To the stirred solution was added ^{i}PrMgCl·LiCl (0.81 M in THF, 0.97 mL, 0.79 mmol) dropwise over ~2 min at RT. The reaction mixture was stirred for 2 h at RT, then 3,3',5,5'-tetra-tert-butyl-4,4'-diphenoquinone (0.160 g, 0.391 mmol) was added in one portion. The mixture was stirred for a further 3 h, then quenched with saturated aqueous NH_4Cl (3 mL) and extracted with ethyl acetate (2 x 3 mL). The combined organic layers were washed with saturated aqueous NaCl (5 mL), dried with $MgSO_4$, filtered, and concentrated by rotary evaporation. Purification of the residue by column chromatography (100% CH_2Cl_2), followed by trituration with hexanes (2 mL), afforded **S4** as a white powder (0.065 g, 53%). ^{1}H NMR (chloroform-*d*, 400 MHz): δ = 7.55 (d, *J* = 8.8 Hz, 2H), 6.72 (d, *J* = 2.6 Hz, 2H), 6.65 (dd, *J* = 8.8, 2.7 Hz, 2H), 3.42 (q, *J* = 7.1 Hz, 8H), 1.22 (t, *J* = 7.1 Hz, 12H); ^{13}C{^{1}H} NMR (chloroform-*d*, 101 MHz): δ = 150.0, 144.1, 135.1, 120.2, 112.7, 110.7, 96.2, 44.8, 12.6; HRMS-ESI (m/z): $[M+H]^+$ calcd. for $C_{22}H_{27}N_4$, 347.2230; found, 347.2236.

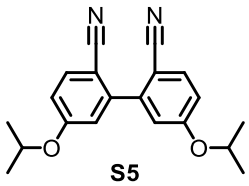

S5

5,5'-diisopropoxy-[1,1'-biphenyl]-2,2'-dicarbonitrile (S5). This oxidative homocoupling was adopted from a report by Knochel and coworkers.[6] A 100 mL Schlenk tube was charged with **S2** (0.738 g, 3.07 mmol) and tetrahydrofuran (7 mL), then the solution was cooled to 0 °C with an ice/water bath. To the stirred solution was added ^{i}PrMgCl·LiCl (0.81 M in THF, 4.0 mL, 3.2 mmol) dropwise over 4–5 min. The resulting mixture was stirred for 90 min at 0 °C, then 3,3',5,5'-tetra-tert-butyl-4,4'-diphenoquinone (0.691 g, 1.69 mmol) was added in one portion. The mixture was stirred for 2 h at 0 °C, then the cold bath was removed and the reaction mixture was allowed to warm to RT and stirred for 45 min at this temperature. The reaction mixture was quenched with saturated aqueous NH_4Cl (10 mL) and extracted with ethyl acetate (20 mL). The organic layer was washed with saturated aqueous NaCl (15 mL), dried with $MgSO_4$, filtered, and concentrated by rotary evaporation. Purification of the residue by column chromatography (15% ethyl acetate in hexanes), followed by trituration with hexanes (4 mL), afforded **S5** as a white powder (0.343 g, 70%). ^{1}H NMR (chloroform-*d*, 400 MHz): δ = 7.70 (d, *J* = 8.5 Hz, 2H), 7.02 – 6.97 (m, 4H), 4.66 (hept, *J* = 6.1 Hz, 2H), 1.40 (d, *J* = 6.1 Hz, 12H); ^{13}C{^{1}H} NMR (chloroform-*d*, 151 MHz): δ = 161.2, 143.7, 135.4, 118.3, 117.2, 116.6, 103.2, 71.0, 22.0; HRMS-ESI (m/z): $[M]^+$ calcd. for $C_{20}H_{20}N_2O_2$, 320.1523; found, 320.1525.

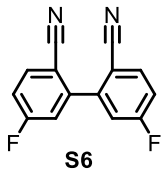

S6

5,5'-difluoro-[1,1'-biphenyl]-2,2'-dicarbonitrile (S6). A 150 mL Schlenk tube was charged with 2-bromo-4-fluorobenzonitrile (2.00 g, 10.0 mmol) and diethyl ether (50 mL) and the solution was cooled to –78 °C with a dry ice / acetone bath. To the resulting heterogeneous mixture was added ^{n}BuLi (1.67 M in hexanes, 5.9 mL, 9.8 mmol) dropwise over 10 min, then the resulting mixture was stirred for a further 10 min at –78 °C. Copper(II) chloride (2.08 g, 15.5 mmol) was then added in one portion, the cold bath was removed, and the reaction mixture was allowed to warm to RT and stirred for 2 h at this temperature. The reaction mixture was quenched with 10% aqueous NH_4OH (50 mL) and extracted with ethyl acetate (2 x 50 mL). The combined organic layers were washed with saturated aqueous NaCl (50 mL) and dried with $MgSO_4$. Filtration and removal of solvents from the filtrate by rotary evaporation gave a crude solid, which was purified by recrystallization from boiling methanol to afford **S6** (0.275 g, 23%*) as an off-white crystalline solid. ^{1}H NMR (chloroform-*d*, 400 MHz): δ = 7.86 (dd, *J* = 8.6, 5.3 Hz, 2H), 7.34 – 7.26 (m, 4H); ^{13}C{^{1}H} NMR (chloroform-*d*, 75 MHz): δ = 164.7 (d, *J* = 259 Hz), 143.3 (d, *J* = 10 Hz), 136.2 (d, *J* = 9.8 Hz), 118.4 (d, *J* = 23.6 Hz), 117.6 (d, *J* = 22.3 Hz), 116.6, 108.8 (d, *J* = 3.6 Hz); ^{19}F NMR (chloroform-*d*, 376 MHz): δ = -101.4 (td, *J* = 8.0, 5.4 Hz); HRMS-EI (m/z): $[M]^+$ calcd. for $C_{14}H_6F_2N_2$, 240.0499; found, 240.0500.

*This low yield is likely due to the use of diethyl ether in place of THF (the latter appears to be the solvent of choice for the $CuCl_2$-mediated coupling reaction). The use of ether was necessary to avoid competing deprotonation of 2-bromo-4-fluorobenzonitrile in the 3-position.[8] The conditions[6] that were employed for compounds **S4** and **S5** are likely to give better results.

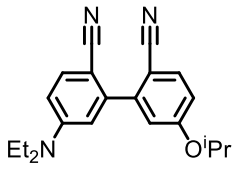

S7

5-(diethylamino)-5'-isopropoxy-[1,1'-biphenyl]-2,2'-dicarbonitrile (S7). This procedure is a modified version of that reported by Souda and coworkers.[9] Some important general comments are provided below. A 30 mL flask equipped with Teflon stopper was charged with bromide **S1** (0.203 g, 0.802 mmol, 1.0 equiv), boronic ester **S9** (0.299 g, 1.04 mmol, 1.3 equiv), $Pd(PPh_3)_2Cl_2$ (0.017 g, 0.024 mmol, 0.03 equiv), K_3PO_4•nH_2O* (0.240 g, 1.04 mmol, 1.3 equiv), and toluene (4 mL). The solution was degassed by the freeze-pump-thaw method, then the flask was backfilled with N_2 and sealed. The stirred reaction mixture was heated for 12 h** at 120 °C, then cooled to RT, diluted with CH_2Cl_2 (10 mL), filtered through celite, and the filtrate was concentrated to under reduced pressure. The crude solid was subjected to column chromatography*** with CH_2Cl_2, followed by recrystallization from CH_2Cl_2/hexanes, to give **S7** (0.203 g, 76%) as colorless crystals. ^{1}H NMR (chloroform-*d*, 600 MHz): δ = 7.68 (d, *J* = 8.7 Hz, 1H), 7.57 – 7.54 (m, 1H), 7.03 (d, *J* = 2.5 Hz, 1H), 6.96 (dd, *J* = 8.7, 2.5 Hz, 1H), 6.70 – 6.65 (m, 2H), 4.65 (hept, *J* = 6.1 Hz, 1H), 3.42 (q, *J* = 7.1 Hz, 4H), 1.39 (d, *J* = 6.1 Hz, 6H), 1.23 (t, *J* = 7.1 Hz, 6H); ^{13}C{^{1}H} NMR (chloroform-*d*, 75 MHz): δ = 161.1, 150.1, 144.9, 143.0,

135.3, 135.1, 119.9, 118.7, 117.1, 116.5, 112.6, 111.1, 103.2, 96.1, 70.9, 44.8, 22.0, 12.6; HRMS-ESI (m/z): $[M+H]^+$ calcd. for $C_{21}H_{24}ON_3$, 334.1914; found, 334.1917.

General comments about this Suzuki cross-coupling reaction (also applies to the preparation of compounds **S8**, **27**, **28**, and **29**):

*K_3PO_4•nH_2O was assumed to be the monohydrate, but the actual water content is unknown.

**Completion of this reaction appears to be indicated by the formation of metallic Pd (the reaction mixture turns grey or black). The reproducibility of the reaction time is affected by the source of K_3PO_4•nH_2O. For example, reactions with a new bottle of K_3PO_4•nH_2O appeared to proceed more rapidly than with the same batch that was a few months old (stored in a tightly sealed bottle in air). As previously reported,[9] the use of anhydrous K_3PO_4 with the addition of 1–2 equiv of water was found to be unreliable (due to formation of large K_3PO_4 / H_2O aggregates). Fortunately, if the reaction fails to go to completion in a reasonable time, the crude product can be re-treated with the original amounts of $Pd(PPh_3)_2Cl_2$ and K_3PO_4•nH_2O under the same conditions (since the boronic ester is stable under the reaction conditions).

***These boronic esters tend to streak down the column, which can result in a contaminated product. This contaminant was easily removed *via* recrystallization (compounds **S7** and **S8**) or trituration (compound **27**). Alternatively, we found that $B(OH)_3$-impregnated silica gel[10] prevented the streaking (compound **29**). The streaking was not a problem when we separated compound **28**.

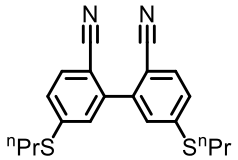

S8

5,5'-bis(propylthio)-[1,1'-biphenyl]-2,2'-dicarbonitrile (S8). This compound was prepared by the same procedure as **S7**, with the following quantities: bromide **S3** (0.250 g, 0.981 mmol, 1.0 equiv), boronic ester **S10** (0.385 g, 1.27 mmol, 1.3 equiv), $Pd(PPh_3)_2Cl_2$ (0.020 g, 0.029 mmol, 0.03 equiv), K_3PO_4•nH_2O (0.293 g, 1.27 mmol, 1.3 equiv), and toluene (5 mL). Compound **S8** was isolated as a colorless crystalline solid (0.246 g, 71%). ^{1}H NMR (chloroform-*d,* 400 MHz): δ = 7.65 (d, *J* = 8.2 Hz, 2H), 7.36 (dd, *J* = 8.2, 1.9 Hz, 2H), 7.33 (d, *J* = 1.9 Hz, 2H), 3.00 (t, *J* = 7.3 Hz, 4H), 1.76 (sext, *J* = 7.3 Hz, 4H), 1.07 (t, *J* = 7.4 Hz, 6H); ^{13}C{^{1}H} NMR (chloroform-*d,* 101 MHz): δ = 146.2, 141.7, 133.6, 127.7, 126.9, 117.9, 107.9, 34.1, 22.2, 13.7; HRMS-EI (m/z): $[M]^+$ calcd. for $C_{20}H_{20}N_2S_2$, 352.1068; found, 352.1063.

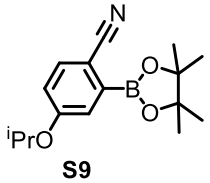

S9

4-isopropoxy-2-(4,4,5,5-tetramethyl-1,3,2-dioxaborolan-2-yl)benzonitrile (S9). A solution of **S2** (1.00 g, 4.16 mmol, 1.0 equiv) in diethyl ether (20 mL) was cooled to –78 °C with a dry ice / acetone bath. To the stirred, heterogeneous mixture was added ^{n}BuLi (1.67 M in hexanes, 2.5 mL, 4.2 mmol, 1.0 equiv) dropwise over 10 min. The mixture was stirred for a further 10 min at –78 °C, then 2-

isopropoxy-4,4,5,5-tetramethyl-1,3,2-dioxaborolane (0.85 g, 4.6 mmol, 1.1 equiv) was added quickly *via* syringe. After 10 min, the cold bath was removed and the reaction mixture was allowed to warm to RT and stirred for a further 1 h. The LiO^{i}Pr salt of the desired product was extracted with water (20, 10, then 10 mL), then the combined aqueous extracts were acidified by dropwise addition of aqueous HCl (12 M, 0.35 mL, 1.0 equiv) over ~1 min to the stirred aqueous solution. The resulting cloudy mixture was extracted with EtOAc (30, 20, then 20 mL) and the combined extracts were washed with saturated aqueous NaCl (30 mL), dried with $MgSO_4$, filtered, the filtrate was concentrated by rotary evaporation. Residual volatile materials were removed *in vacuo* to give pure **S9** (0.97 g, 82%) as a viscous, pale yellow oil. ^{1}H NMR (chloroform-*d*, 400 MHz): δ = 7.59 (d, *J* = 8.6 Hz, 1H), 7.32 (d, *J* = 2.7 Hz, 1H), 6.95 (dd, *J* = 8.6, 2.7 Hz, 1H), 4.65 (hept, *J* = 6.1 Hz, 1H), 1.36 (s, 12H), 1.33 (d, *J* = 6.1 Hz, 6H); ^{13}C{^{1}H} NMR* (chloroform-*d*, 101 MHz): δ = 160.4, 135.5, 122.7, 119.6, 118.0, 108.3, 84.9, 70.3, 24.9, 22.0; HRMS-EI (m/z): [M]$^+$ calcd. for $C_{16}H_{22}NO_3B$, 286.1729; found, 286.1723. *One resonance was not observed (assumed to be for the carbon *ipso* to boron)

General comment about this borylation reaction (also applies to the preparation of compounds **S10**, **S11**, and **S12**):

For some boronic esters, the desired compound was contaminated with a small amount of its acid and oligomeric derivatives, resulting from hydrolysis of the ester (likely during the acidification step). This hydrolysis reaction can easily be reversed by treatment of the mixture with pinacol in CH_2Cl_2 at RT. See the procedure for **S12** for an example.

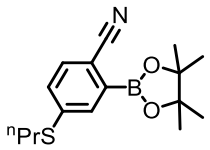

S10

4-(propylthio)-2-(4,4,5,5-tetramethyl-1,3,2-dioxaborolan-2-yl)benzonitrile (S10). The procedure of **S9** was employed with bromide **S3** instead of **S2**. Compound **S10** was isolated as a colorless crystalline solid (1.95 g, 83%). ^{1}H NMR (chloroform-*d,* 400 MHz): δ = 7.69 (d, *J* = 2.0 Hz, 1H), 7.55 (d, *J* = 8.2 Hz, 1H), 7.33 (dd, *J* = 8.2, 2.1 Hz, 1H), 2.96 (t, *J* = 7.2 Hz, 2H), 1.72 (sext, *J* = 7.5 Hz, 2H), 1.37 (s, 12H), 1.04 (t, *J* = 7.4 Hz, 3H); ^{13}C{^{1}H} NMR* (chloroform-*d,* 101 MHz): δ = 143.9, 133.8, 133.6, 128.6, 119.2, 112.9, 85.0, 33.9, 24.9, 22.1, 13.6; HRMS-EI (m/z): [M]$^+$ calcd. for $C_{16}H_{22}NO_2SB$, 303.1464; found, 303.1467. *One resonance was not observed (assumed to be for the carbon *ipso* to boron)

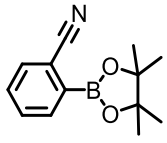

S11

2-(4,4,5,5-tetramethyl-1,3,2-dioxaborolan-2-yl)benzonitrile (S11). The procedure of **S9** was employed with 2-bromobenzonitrile instead of **S2**. Compound **S11** was isolated as a colorless crystalline solid (4.72 g, 75%). ^{1}H NMR (chloroform-*d*, 400 MHz): δ = 7.89 (d, *J* = 7.5, 1H), 7.70 (dd, *J* = 7.7, 1.5 Hz, 1H), 7.57 (td, *J* = 7.5, 1.5 Hz, 1H), 7.52 (td, *J* = 7.6, 1.6 Hz, 1H), 1.39 (s, 12H); ^{13}C{^{1}H}

NMR (chloroform-*d*, 75 MHz): δ = 162.4, 135.9, 133.5, 131.7, 131.2, 119.1, 117.3, 84.9, 24.9; HRMS-EI (m/z): $[M]^+$ calcd. for $C_{13}H_{16}NO_2B$, 229.1274; found, 229.1268.

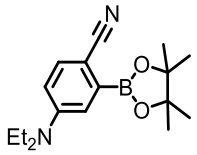

S12

4-(diethylamino)-2-(4,4,5,5-tetramethyl-1,3,2-dioxaborolan-2-yl)benzonitrile (S12). The procedure of **S9** was employed with the following quantities: bromide **S1** (1.00 g, 3.95 mmol, 1.0 equiv), ^{n}BuLi (1.67 M in hexanes, 2.4 mL, 4.0 mmol, 1.0 equiv), 2-isopropoxy-4,4,5,5-tetramethyl-1,3,2-dioxaborolane (0.81 g, 4.4 mmol, 1.1 equiv), and aqueous HCl (12 M, 0.33 mL, 1.0 equiv). The crude product contained a small amount of acid and oligomeric impurities, which were removed as follows. The crude product was dissolved in CH_2Cl_2 (1.5 mL) and pinacol (0.093 g, 0.2 equiv based on starting **S1**) was added. The mixture was stirred for 10 min, then hexanes (10 mL) was added. The mixture was concentrated to 2-3 mL, diluted with hexanes (8 mL), then filtered, affording pure **S12** (0.78 g, 66%) as a white solid. ^{1}H NMR (chloroform-*d,* 300 MHz): δ = 7.48 (d, *J* = 8.8 Hz, 1H), 7.03 (d, *J* = 2.9 Hz, 1H), 6.66 (dd, *J* = 8.8, 2.9 Hz, 1H), 3.41 (q, *J* = 7.1 Hz, 4H), 1.37 (s, 12H), 1.18 (t, *J* = 7.1 Hz, 6H); ^{13}C{^{1}H} NMR* (chloroform-*d*, 101 MHz): δ = 149.3, 135.2, 121.1, 117.8, 112.8, 101.4, 84.5, 44.3, 24.9, 12.5; HRMS-ESI (m/z): $[M+H]^+$ calcd. for $C_{17}H_{26}O_2N_2B$, 301.2082; found, 301.2086. *One resonance was not observed (assumed to be for the carbon *ipso* to boron).

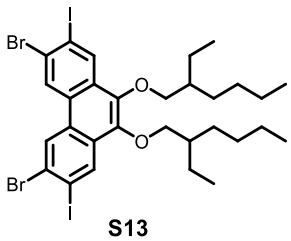

S13

3,6-dibromo-9,10-bis((2-ethylhexyl)oxy)-2,7-diiodophenanthrene (S13). To a 250 mL round-bottomed flask equipped with a magnetic stirbar was added 3,6-dibromo-2,7-diiodophenanthrene-9,10-dione (5.00 g, 8.10 mmol), $Na_2S_2O_4$ (4.23 g, 24.3 mmol), Bu_4NBr (0.79 g, 2.5 mmol), tetrahydrofuran (30 mL), and water (30 mL). The mixture was stirred vigorously for 5 min, diluted with water (30 mL), then the pale-yellow precipitate was collected by filtration and washed with water (2 x 30 mL). The damp solid* was transferred back to the same flask, which was then placed under high vacuum until the mass remained constant. To this flask was rapidly added K_2CO_3 (4.48 g, 32.4 mmol), 2-ethylhexylbromide (4.69 g, 24.3 mmol), and KI (0.14 g, 0.85 mmol). The flask was sealed with a rubber septum and purged with N_2 for 15 min, then dry, deoxygenated DMF (25 mL) was added *via* syringe. The reaction mixture was stirred for 18 h at 125 °C, then the mixture was brought to RT, and water (100 mL) was added. The resulting suspension was stirred for 15 min and the solid was collected by filtration and washed with water (2 x 30 mL) and methanol (2 x 30 mL). The solid was dissolved in CH_2Cl_2 (100 mL), then the solution was diluted with hexanes (100 mL) and filtered through a plug of silica gel (~15 g). The plug was flushed with 1:1 hexanes:CH_2Cl_2 (80 mL) and the filtrate was concentrated to ~90 mL to give a white precipitate. The precipitate was collected by filtration, dried under a stream of air, and used without further purification. Yield: 3.75 g (55%). This procedure was also performed on a 10 g scale (isolated product) with the same yield. ^{1}H NMR

(chloroform-*d,* 400 MHz): δ = 8.71 (s, 2H), 8.69 (s, 2H), 4.08 – 3.99 (m, 4H), 1.82 (h, *J* = 6.2 Hz, 2H), 1.68 – 1.45 (m, 8H), 1.43 – 1.33 (m, 8H), 1.00 (t, *J* = 7.5 Hz, 6H), 0.94 (t, *J* = 6.9 Hz, 6H); $^{13}C\{^{1}H\}$ NMR (chloroform-*d,* 101 MHz): δ = 142.7, 134.6, 130.2, 128.0, 127.2, 126.2, 100.6, 76.7, 40.7, 30.7, 29.3, 23.9, 23.3, 14.3, 11.3; HRMS-EI (m/z): $[M]^+$ calcd. for $C_{30}H_{38}Br_2I_2O_2$, 841.9328; found, 841.9320.

*Exposure to air was minimized (< 15 min), as decomposition can result on prolonged exposure (decomposition is indicated by darkening of the color). The decomposition rate appeared to increase as the compound dried. Decomposition also resulted when the solid was washed with organic solvents (EtOH, MeOH, and diethyl ether).

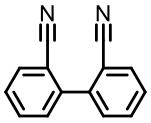

5

[1,1'-biphenyl]-2,2'-dicarbonitrile (5). A 500 mL Schlenk flask was charged with 2-bromobenzonitrile (5.00 g, 27.5 mmol) and tetrahydrofuran (140 mL) and the solution was cooled to –78 °C with a dry ice / acetone bath. To this solution was added ^{n}BuLi (1.60 M in hexanes, 17.2 mL, 27.5 mmol) dropwise over 10 min and the resulting mixture was stirred for a further 5 min at –78 °C. Copper(II) chloride (5.20 g, 38.7 mmol) was then added in one portion, the cold bath was removed, and the reaction mixture was allowed to warm to RT and stirred for 2 h at this temperature. The reaction mixture was quenched with 10% aqueous NH_4OH (140 mL) and extracted with ethyl acetate (2 x 100 mL). The combined organic layers were washed with saturated aqueous NaCl (2 x 50 mL) and dried with Na_2SO_4. Filtration and removal of solvents from the filtrate by rotary evaporation gave a crude solid. Purification by recrystallization from boiling methanol afforded **5** (1.60 g, 57%) as colorless crystals. ^{1}H NMR data matches the literature.[11]

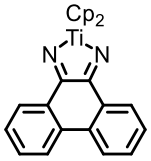

6

Model di(aza)titanacyclopentadiene (6). To a stirred suspension of dinitrile **5** (0.990 g, 4.85 mmol, 1.0 equiv) in toluene (50 mL) was added a solution of $Cp_2Ti(Me_3SiC{\equiv}CSiMe_3)$ (1.86 g, 5.34 mmol, 1.1 equiv) in toluene (5 mL) over ~3 min. The mixture was stirred for 15 min, then pentane (70 mL) was added. After 30 min, the precipitate was collected by filtration, washed pentane (2 x 15 mL), and dried under vacuum to give titanacycle **6** as a purple powder (1.48 g, 75%*). X-ray quality crystals were grown by layering of pentane onto a solution of **6** in toluene and the structure was elucidated by single crystal X-ray crystallography (see Figure S82). When this reaction was run on a smaller scale in benzene-d_6 solvent and monitored by ^{1}H NMR spectroscopy (hexamethylbenzene internal standard), titanacycle **6** was observed in 93% yield. ^{1}H NMR (chloroform-*d*, 400 MHz): δ = 7.98 (d, *J* = 8.0 Hz, 2H), 7.63 (d, *J* = 7.5 Hz, 2H), 7.40 (t, *J* = 7.6 Hz, 2H), 7.28 (t, *J* = 7.4 Hz, 2H), 6.33 (s, 10H); $^{13}C\{^{1}H\}$ NMR (chloroform-*d*, 101 MHz): δ = 154.9, 133.4, 132.6, 129.6, 127.8, 126.7, 123.4, 115.4; Anal. Calcd for $C_{24}H_{18}N_2Ti$: C, 75.4; H, 4.8; N, 7.3. Found: C, 74.6; H, 4.4; N, 7.3. *This yield accounts for the fact that the product was 94% pure (by mass), as determined by quantitative ^{1}H NMR spectroscopy with hexamethylbenzene as internal standard.

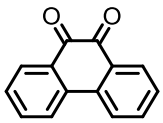

7

Phenanthrene-9,10-dione (7). To a stirred suspension of **5** (47.7 mg, 0.234 mmol, 1.0 equiv) in toluene (2.3 mL) was added a solution of $Cp_2Ti(Me_3SiC{\equiv}CSiMe_3)$ (90 mg, 0.26 mmol, 1.1 equiv) in toluene (0.6 mL) dropwise over ~1 min. The reaction mixture was stirred for 15 min, then HCl (2.0 M in diethyl ether, 0.70 mL, 1.4 mmol) was added dropwise over ~1 min. The mixture was stirred for 5 min, then volatile materials were removed *via* rotary evaporation. The residue was dissolved in MeOH (3 mL) and aqueous HCl (3.0 M, 0.3 mL) was added. The mixture was stirred for 15 h, then diluted with CH_2Cl_2 (10 mL), washed with water (10 mL), dried with $MgSO_4$, filtered, and solvents were removed from the filtrate *via* rotary evaporation. The residue was analyzed by ^{1}H NMR spectroscopy (hexamethylbenzene internal standard), which revealed the formation of **7** in 67% yield. The residue was purified by column chromatography (100% CH_2Cl_2) to afford **7** (30 mg, 61%) as a golden yellow solid. ^{1}H NMR (chloroform-*d,* 500 MHz): δ = 8.19 (dd, *J* = 7.8, 1.5 Hz, 2H), 8.02 (d, *J* = 8.0 Hz, 2H), 7.72 (td, *J* = 7.7, 1.5 Hz, 2H), 7.47 (td, *J* = 7.6, 1.0 Hz, 2H); ^{13}C{^{1}H} NMR (chloroform-*d,* 101 MHz): δ = 180.4, 136.2, 135.9, 131.1, 130.6, 129.7, 124.1. ^{1}H and ^{13}C{^{1}H} NMR data match that of an authentic sample from Sigma Aldrich.

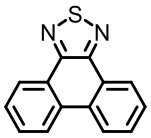

8

Phenanthro[9,10-c][1,2,5]thiadiazole (8).[12] Titanacycle **6** (70.9 mg, 0.186 mmol, 1.0 equiv) was dissolved in CH_2Cl_2 (2 mL) and the resulting solution was cooled to –78 °C with a dry ice / acetone bath. To the stirred solution was added S_2Cl_2 (0.018 mL, 30 mg, 0.22 mmol, 1.2 equiv) *via* syringe over ~10 seconds. The cold bath was immediately removed, and the reaction mixture was allowed to warm to RT and stirred for a further 1 h at this temperature. In air, the mixture was diluted to 10 mL with CH_2Cl_2 and hexamethylbenzene was added as internal standard. An aliquot was taken for ^{1}H NMR analysis, which revealed formation of **8** in quantitative yield. The solution was directly subjected to column chromatography (CH_2Cl_2) to afford **8** (41 mg, 94%) as an off-white solid. ^{1}H NMR (chloroform-*d*, 600 MHz): δ 8.75 (dd, *J* = 7.8, 1.5 Hz, 2H), 8.55 (d, *J* = 8.0 Hz, 2H), 7.76 (ddd, *J* = 8.3, 7.1, 1.5 Hz, 2H), 7.70 (td, *J* = 7.5, 1.1 Hz, 2H); ^{13}C{^{1}H} NMR (chloroform-*d*, 151 MHz): δ = 153.5, 131.7, 129.8, 128.3, 126.4, 126.2, 123.6. ^{1}H and ^{13}C{^{1}H} NMR data matches the literature.[12]

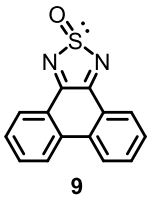

9

Phenanthro[9,10-c][1,2,5]thiadiazole 2-oxide (9).[12] Titanacycle **6** (105 mg, 0.275 mmol, 1.0 equiv) was dissolved in CH_2Cl_2 (3 mL) and the resulting solution was cooled to –78 °C with a dry ice / acetone bath. To the stirred solution was added $SOCl_2$ (0.025 mL, 41 mg, 0.34 mmol, 1.2 equiv) over

~30 seconds. The cold bath was removed, and the reaction mixture was allowed to warm to RT and stirred for a further 1 h at this temperature. In air, the mixture was diluted to 20 mL with CH_2Cl_2 and hexamethylbenzene (12.7 mg, 0.0783 mmol) was added as internal standard. A small aliquot was taken for ^{1}H NMR analysis, which revealed formation of **9** in 95% yield. The solution was washed with 10% aqueous NH_4OH (20 mL), the mixture was filtered, and the layers were separated. The organic layer was dried over $MgSO_4$ and filtered, then the filtrate was concentrated by rotary evaporation. The residue was subjected to column chromatography (100% CH_2Cl_2) to afford **9** (60 mg, 87%) as a bright yellow solid. ^{1}H NMR* (chloroform-*d*, 500 MHz): δ = 8.52 (dd, *J* = 7.9, 1.5 Hz, 2H), 8.21 (d, *J* = 8.1 Hz, 2H), 7.80 (ddd, *J* = 8.2, 7.3, 1.5 Hz, 2H), 7.57 (td, *J* = 7.6, 1.1 Hz, 2H); ^{13}C{^{1}H} NMR (chloroform-*d*, 101 MHz): δ = 161.4, 135.6, 130.4, 129.8, 125.0, 124.5. *These values are slightly different than the literature,[12] which appears to be a concentration effect.

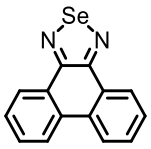

10

Phenanthro[9,10-*c*][1,2,5]selenadiazole (10).[13] A 10 mL Schlenk flask was loaded with titanacycle **6** (66.1 mg, 0.173 mmol, 1.0 equiv) and $SeCl_2$(bipy) (58 mg, 0.19 mmol, 1.1 equiv), then CH_2Cl_2 (2 mL) was added. The heterogeneous mixture was stirred vigorously for 5 min at RT, then (in air) filtered through a fritted funnel. The flask and filter cake were washed with CH_2Cl_2 (10 mL) and the filtrate was analyzed by ^{1}H NMR spectroscopy, which indicated formation of **10** in 91% yield. The filtrate was concentrated to ~1 mL, then MeOH (5 mL) was added and the precipitate was collected by filtration. The crude solid was purified by elution through a plug of silica gel with CH_2Cl_2 to afford **10** (42 mg, 86%) as a pale-yellow solid. ^{1}H NMR (chloroform-*d*, 500 MHz): δ = 8.75 (dd, *J* = 7.9, 1.4 Hz, 2H), 8.45 (dd, *J* = 8.2, 1.1 Hz, 2H), 7.74 (ddd, *J* = 8.3, 7.1, 1.5 Hz, 2H), 7.66 (td, *J* = 7.6, 1.2 Hz, 2H); ^{13}C{^{1}H} NMR (chloroform-*d*, 151 MHz): δ = 158.5, 132.0, 130.1, 128.6, 128.4, 127.1, 123.5. ^{1}H NMR data is consistent with the literature.[13]

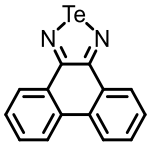

11

Phenanthro[9,10-c][1,2,5]telluradiazole (11).[14] A 10 mL Schlenk flask was loaded with titanacycle **6** (61.5 mg, 0.161 mmol, 1.0 equiv) and $TeCl_2$(bipy) (54.0 mg, 0.153 mmol, 0.95 equiv), then CH_2Cl_2 (2 mL) was added. The heterogeneous mixture was stirred vigorously for 10 min at RT, then (in air) the light brown solid was collected on a fritted funnel and washed with CH_2Cl_2 (0.5 mL) and diethyl ether (1 mL). ^{1}H NMR analysis suggested formation of the desired product in 86% yield. The solid was dissolved in DMSO (5 mL), then the solution was stirred for 10 min and filtered through celite. The filtrate was added dropwise to ice-cold water (10 mL), then the precipitate was collected by filtration and washed with water (1 mL), methanol (2 x 1 mL), and diethyl ether (1 mL). This afforded **11** (37 mg, 73%) as a greenish-yellow solid. ^{1}H NMR (dimethyl sulfoxide-d_6, 400 MHz): δ = 8.58 (d, *J* = 7.5 Hz, 2H), 8.56 (d, *J* = 7.5 Hz, 2H), 7.72 (t, *J* = 7.5 Hz, 2H), 7.66 (t, *J* = 7.4 Hz, 2H); ^{13}C{^{1}H}

NMR (dimethyl sulfoxide-d_6, 151 MHz,): δ = 162.2, 133.1, 131.0, 129.4, 128.0, 126.8, 123.5. ^{1}H and ^{13}C{^{1}H} NMR data matches the literature.[14]

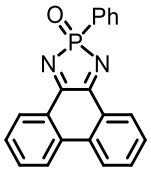

12

Generation of 2-phenylphenanthro[9,10-d][1,3,2]diazaphosphole 2-oxide (12).[15] To a stirred solution of titanacycle **6** (47.4 mg, 0.124 mmol, 1.0 equiv) in CD_2Cl_2 (1.5 mL) was added a solution of $POPhCl_2$ (26.5 mg, 0.136 mmol, 1.1 equiv) in CD_2Cl_2 (0.3 mL) dropwise over ~30 seconds. The mixture was allowed to stand for 24 h at RT, then analyzed by ^{1}H NMR (hexamethylbenzene internal standard), which revealed formation of **12** in 79% yield. Attempts to isolate pure compound were unsuccessful, primarily due to the difficulty in separating the Cp_2TiCl_2 byproduct (which in this case was complicated by the hydrolytic lability of the P–N bond in **12**).

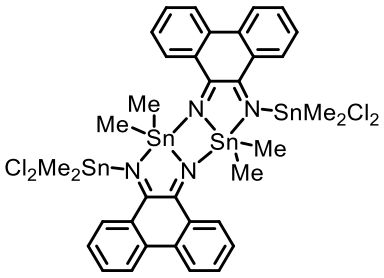

13

Di(aza)stannole dimer (13). To a solution of titanacycle **6** (82.3 mg, 0.215 mmol, 1.0 equiv) in CH_2Cl_2 (2.4 mL) was added $SnCl_2Me_2$ (95 mg, 0.43 mmol, 2.0 equiv). The mixture was allowed to stand for 24 h at RT, then the supernatant was decanted from the precipitated crystals. The crystals were washed with toluene (2 x 1 mL) and pentane (2 x 1 mL) and dried *in vacuo* to afford 82 mg (60%) of orange needles, which was identified as dimeric **13**. X-ray quality crystals were grown by performing this reaction on a smaller scale and forgoing the washing and drying steps and the structure was elucidated by single crystal X-ray crystallography (see Figure S83). ^{1}H NMR* (tetrahydrofuran, 600 MHz): δ 8.43 (d, J = 7.9 Hz, 2H), 8.24 (d, J = 8.0 Hz, 2H), 7.60 (t, J = 7.6 Hz, 2H), 7.46 (t, J = 7.5 Hz, 2H), 0.65 (s, 6H); Anal. Calcd for $C_{37}H_{42}Cl_6N_4Sn_4$: C, 36.1; H, 3.4; N, 4.6. Found: C, 36.4; H, 3.5; N, 4.5.

*Note that the ^{1}H NMR spectrum displays higher symmetry than that seen in the solid-state. The cause of this is currently unclear, but it could result from a rapid fluxional process or monomer-dimer equilibrium.

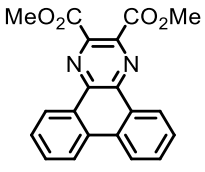

14

Dimethyl dibenzo[f,h]quinoxaline-2,3-dicarboxylate (14). To a stirred mixture of dinitrile **5** (60.1 mg, 0.294 mmol), hexamethylbenzene (21.1 mg, 0.130 mmol, internal standard), and toluene (3 mL) was added a solution of $Cp_2Ti(Me_3SiC{\equiv}CSiMe_3)$ (113 mg, 0.323 mmol) in toluene (1 mL) dropwise over ~1 min at RT. The mixture was stirred for 15 min, then a solution of dimethyl acetylenedicarboxylate (84 mg, 0.59 mmol) in toluene (0.5 mL) was added and the mixture was stirred for a further 1 h. In air, the mixture was diluted with CH_2Cl_2 (5 mL) to ensure homogeneity, then an aliquot was drawn, and solvents were removed *via* rotary evaporation. Analysis of the residue by ^{1}H NMR spectroscopy revealed formation of the desired product in 88% yield. The aliquot was recombined with the original mixture, solvents were removed by rotary evaporation, and the residue was subjected to column chromatography* (100% CH_2Cl_2) to afford **14** (82 mg, 80%) as a colorless solid. ^{1}H NMR (chloroform-*d*, 400 MHz): δ = 9.26 (dd, *J* = 8.1, 1.6 Hz, 2H), 8.63 (dd, *J* = 8.2, 1.1 Hz, 2H), 7.86 (ddd, *J* = 8.3, 7.1, 1.5 Hz, 2H), 7.77 (ddd, *J* = 8.2, 7.0, 1.1 Hz, 2H), 4.12 (s, 6H); ^{13}C{^{1}H} NMR (chloroform-*d*, 101 MHz): δ = 165.8, 142.7, 141.4, 132.5, 131.1, 128.7, 128.2, 126.6, 123.0, 53.5; HRMS-ESI (m/z): $[M+H]^+$ calcd. for $C_{20}H_{15}O_4N_2$, 347.1026; found, 347.1027.

*A dark-brown band partially elutes down the column and then halts, presumably due to decomposing "Cp_2Ti" species. We found that a 5 min "waiting period" after loading the compound onto the column limits the length of this dark-brown band. This is general for all the [2+2+2] reactions in this manuscript.

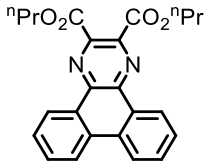

15

Dipropyl dibenzo[f,h]quinoxaline-2,3-dicarboxylate (15). This compound was prepared by the same procedure as **14** (with dipropyl acetylenedicarboxylate used in place of dimethyl acetylene dicarboxylate) and was isolated as a pale-yellow, nearly colorless solid (56 mg, 72%). The yield by ^{1}H NMR yield was 95%. ^{1}H NMR (chloroform-*d,* 400 MHz): δ = 9.27 (dd, *J* = 8.1, 1.4 Hz, 2H), 8.63 (d, *J* = 8.1, 2H), 7.86 (ddd, *J* = 8.3, 7.1, 1.5 Hz, 2H), 7.77 (ddd, *J* = 8.1, 7.0, 1.2 Hz, 2H), 4.48 (t, *J* = 6.7 Hz, 4H), 1.90 (h, *J* = 7.2 Hz, 4H), 1.10 (t, *J* = 7.4 Hz, 6H); ^{13}C{^{1}H} NMR (chloroform-*d,* 151 MHz): δ = 165.5, 143.0, 141.0, 132.2, 130. 8, 128.7, 128.0, 126.4, 122.8, 68.2, 22.1, 10.6; HRMS-ESI (m/z): $[M+H]^+$ calcd. for $C_{24}H_{23}O_4N_2$, 403.1652; found, 403.1661.

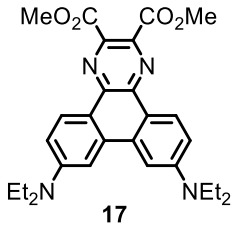

17

Dimethyl 7,10-bis(diethylamino)dibenzo[f,h]quinoxaline-2,3-dicarboxylate (17). This compound was prepared by the same procedure as **14** and was further purified by recrystallization from CH_2Cl_2/hexanes. The compound was isolated as bright orange crystals (40 mg, 57%). The yield by ^{1}H NMR spectroscopy was 69%. ^{1}H NMR (chloroform-*d,* 400 MHz): δ = 8.96 (d, *J* = 9.0 Hz, 2H), 7.49 (d, *J* = 2.5 Hz, 2H), 7.07 (dd, *J* = 9.2, 2.4 Hz, 2H), 4.07 (s, 6H), 3.56 (q, *J* = 7.1 Hz, 8H), 1.30 (t,

J = 7.0 Hz, 12H); $^{13}C\{^{1}H\}$ NMR (chloroform-*d*, 101 MHz): δ = 166.7, 149.5, 141.0, 140.1, 134.2, 128.4, 118.3, 113.5, 102.5, 53.1, 45.0, 12.7; HRMS-ESI (m/z): $[M+H]^+$ calcd. for $C_{28}H_{33}O_4N_4$, 489.2496; found, 489.2507.

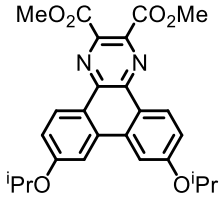

18

Dimethyl 7,10-diisopropoxydibenzo[f,h]quinoxaline-2,3-dicarboxylate (18). This compound was prepared by the same procedure as **14** and was isolated as a yellow solid (47 mg, 68%). ^{1}H NMR (chloroform-*d*, 400 MHz): δ = 9.14 (d, *J* = 9.0 Hz, 2H), 7.88 (d, *J* = 2.4 Hz, 2H), 7.31 (dd, *J* = 9.0, 2.4 Hz, 2H), 4.87 (hept, *J* = 6.1 Hz, 2H), 4.10 (s, 6H), 1.48 (d, *J* = 6.0 Hz, 12H); $^{13}C\{^{1}H\}$ NMR (chloroform-*d*, 151 MHz): δ = 166.1, 160.4, 141.7, 140.8, 134.1, 128.7, 122.7, 117.4, 108.4, 70.5, 53.4, 22.2; HRMS-ESI (m/z): $[M+H]^+$ calcd. for $C_{26}H_{27}O_6N_2$, 463.1864; found, 463.1876.

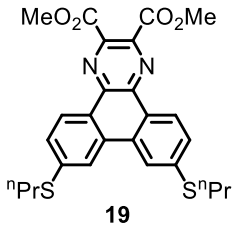

19

Dimethyl 7,10-bis(propylthio)dibenzo[f,h]quinoxaline-2,3-dicarboxylate (19). This compound was prepared by the same procedure as **14** and was isolated as a yellow solid (47 mg, 70%). ^{1}H NMR (chloroform-*d*, 300 MHz): δ = 8.90 (d, *J* = 8.5 Hz, 2H), 8.15 (d, *J* = 1.9 Hz, 2H), 7.52 (dd, *J* = 8.6, 1.7 Hz, 2H), 3.10 (t, *J* = 7.3 Hz, 4H), 1.81 (h, *J* = 7.3 Hz, 4H), 1.12 (t, *J* = 7.3 Hz, 6H); $^{13}C\{^{1}H\}$ NMR (chloroform-*d*, 75 MHz): δ = 165.9, 142.3, 142.1, 140.7, 131.9, 127.3, 126.8, 126.2, 120.6, 53.5, 34.8, 22.5, 13.8; HRMS-ESI (m/z): $[M+H]^+$ calcd. for $C_{26}H_{27}N_2O_4S_2$, 495.1407; found, 495.1430.

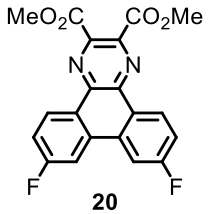

20

Dimethyl 7,10-difluorodibenzo[f,h]quinoxaline-2,3-dicarboxylate (20). This compound was prepared by the same procedure as **14** and was isolated as a colorless solid (51 mg, 61%). ^{1}H NMR (chloroform-*d,* 400 MHz): δ = 9.10 (dd, *J* = 9.0, 6.0 Hz, 2H), 7.96 (dd, *J* = 10.3, 2.4 Hz, 2H), 7.44 (ddd, *J* = 9.9, 7.8, 2.4 Hz, 2H), 4.12 (s, 6H); $^{13}C\{^{1}H\}$ NMR (chloroform-*d*, 101 MHz): δ = 165.5, 164.6 (d, *J* = 252 Hz), 142.7, 140.1, 133.6 (dd, *J* = 9.0, 2.9 Hz), 129.4 (d, *J* = 9.3 Hz), 125.5 (d, *J* = 1.8 Hz), 117.3 (d, *J* = 23 Hz), 109.1 (d, *J* = 23 Hz), 53.6; HRMS-ESI (m/z): $[M+H]^+$ calcd. for $C_{20}H_{13}O_4N_2F_2$, 383.0838; found, 383.0850.

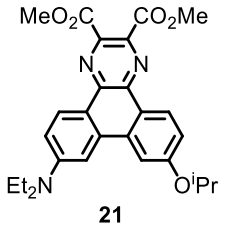

21

Dimethyl 7-(diethylamino)-10-isopropoxydibenzo[f,h]quinoxaline-2,3-dicarboxylate (21). This compound was prepared by the same procedure as **14** and was isolated as a bright orange solid (51 mg, 68%). ^{1}H NMR (chloroform-*d*, 400MHz): δ = 9.13 (d, *J* = 9.0 Hz, 1H), 8.99 (d, *J* = 9.1 Hz, 1H), 7.87 (d, *J* = 2.4 Hz, 1H), 7.52 (d, *J* = 2.6 Hz, 1H), 7.30 (dd, *J* = 9.0, 2.4 Hz, 1H), 7.11 (dd, *J* = 9.3, 2.4 Hz, 1H), 4.84 (hept, *J* = 6.1 Hz, 1H), 4.08 (s, 3H), 4.08 (s, 3H), 3.60 (q, *J* = 7.1 Hz, 4H), 1.48 (d, *J* = 6.0 Hz, 6H), 1.32 (t, *J* = 7.1 Hz, 6H); ^{13}C{^{1}H} NMR (chloroform-*d*, 151 MHz): δ = 166.7, 166.2, 160.1, 149.8, 142.5, 141.7, 140.1, 139.2, 134.4, 134.0, 128.6, 128.4, 122.9, 118.0, 116.2, 113.9, 108.9, 102.6, 70.5, 53.2, 53.2, 44.8, 22.2, 12.8; HRMS-ESI (m/z): $[M+H]^+$ calcd. for $C_{27}H_{30}O_5N_3$, 476.2180; found, 476.2188.

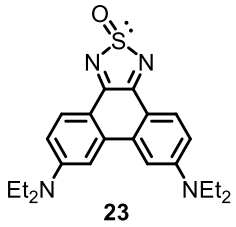

23

6,9-bis(diethylamino)phenanthro[9,10-c][1,2,5]thiadiazole 2-oxide (23). To a stirred mixture of dinitrile **S4** (62.5 mg, 0.180 mmol, 1.0 equiv) and toluene (1.8 mL) was added a solution of $Cp_2Ti(Me_3SiC{\equiv}CSiMe_3)$ (69 mg, 0.20 mmol, 1.1 equiv) in toluene (0.4 mL) dropwise over ~1 min. The reaction mixture was stirred for 15 min, then cooled to –78 °C with a dry ice / acetone bath and $SOCl_2$ (0.016 mL, 26 mg, 0.22 mmol, 1.2 equiv) was added *via* syringe. The mixture was allowed to warm to room temperature, stirred for a further 10 min, quenched with 10% aqueous NH_4OH (5 mL), diluted with CH_2Cl_2 (10 mL), and filtered through celite. The layers were separated, and the organic layer was dried with Na_2SO_4, filtered, and solvents were removed from the filtrate *via* rotary evaporation. The residue was purified by column chromatography (0–10% EtOAc in CH_2Cl_2) followed by recrystallization from CH_2Cl_2/hexanes to afford **23** (30 mg, 42%) as black* needles. ^{1}H NMR (dichloromethane-d_2, 400 MHz): δ = 8.14 (d, *J* = 8.9 Hz, 2H), 7.17 (d, *J* = 2.5 Hz, 2H), 6.74 (dd, *J* = 9.0, 2.5 Hz, 2H), 3.55 (q, *J* = 7.2 Hz, 8H), 1.29 (t, *J* = 7.1 Hz, 12H); ^{13}C{^{1}H} NMR (dichloromethane-d_2, 101 MHz): δ = 161.9, 152.9, 137.7, 132.4, 113.0, 112.9, 105.6, 45.7, 12.9; HRMS-ESI (m/z): $[M+H]^+$ calcd. for $C_{22}H_{27}ON_4S$, 395.1900; found, 395.1908. *The needles appear black by eye, but are dark red under a microscope.

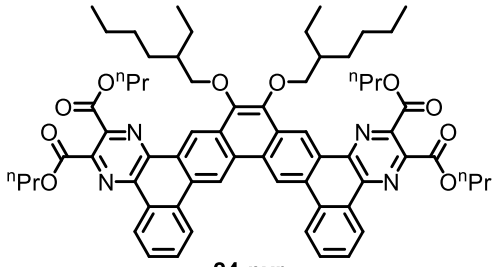

24-pyr

Bis(pyrazine)-annulated PAH (24-pyr). To a stirred solution of bis(dinitrile) **27** (48.5 mg, 0.0706 mmol, 1.0 equiv) in toluene (1.4 mL) was added a solution of $Cp_2Ti(Me_3SiC{\equiv}CSiMe_3)$ (54 mg, 0.155 mmol, 2.2 equiv) in toluene (0.5 mL) dropwise over ~1 min. The mixture was stirred for 15 min, then a solution of dipropyl acetylenedicarboxylate (84 mg, 0.42 mmol, 6.0 equiv) in toluene (0.3 mL) was added in one portion. The mixture was stirred for a further 2 h, then it was loaded directly onto a silica gel column* (25 g) and allowed to stand (in air) for ~5 min. The column was eluted with CH_2Cl_2 to afford (after evaporation of solvents by rotary evaporation) compound **24-pyr** (31 mg, 40%) as a yellow-orange solid. The reaction was also run in benzene-d_6 and monitored by ^{1}H NMR spectroscopy, which revealed the formation of the bis(di(aza)titanacyclopentadiene) intermediate **24-Ti** in 58% yield. ^{1}H NMR (chloroform-*d*, 400 MHz): δ = 10.13 (s, 2H), 10.10 (s, 2H), 9.27 (dd, *J* = 8.1, 1.4 Hz, 2H), 9.03 (d, *J* = 8.1 Hz, 2H), 8.02 (td, *J* = 7.6, 1.5 Hz, 2H), 7.83 (t, *J* = 7.5 Hz, 2H), 4.51 (t, *J* = 6.9 Hz, 4H), 4.47 (t, *J* = 6.8 Hz, 4H), 4.41 – 4.32 (m, 2H), 4.31 – 4.23 (m, 2H), 2.11 – 2.01 (m, 2H), 2.00 – 1.86 (m, 10H), 1.85 – 1.58 (m, 6H), 1.50 – 1.32 (m, 8H), 1.12 (t, *J* = 7.3 Hz, 6H), 1.11 (t, *J* = 7.3 Hz, 6H), 1.09 (t, *J* = 7.5 Hz, 6H), 0.90 (t, *J* = 7.2, 6H); ^{13}C{^{1}H} NMR (chloroform-*d*, 101 MHz): δ = 165.79, 165.02, 144.14, 144.12, 144.04, 144.01, 141.53, 132.35, 130.90, 130.21, 130.06, 129.39, 128.87, 128.27, 128.00, 126.45, 123.12, 121.04, 117.52, 76.66, 68.14, 68.08, 40.87, 30.76, 29.60, 24.10, 23.28, 22.18, 22.06, 14.32, 11.27, 10.63, 10.55; HRMS-ESI (m/z): $[M+H]^+$ calcd. for $C_{66}H_{75}O_{10}N_4$, 1083.5478; found, 1083.5544.

*There are two things to note about this chromatography purification: 1) a dark-brown band partially elutes down the column and then halts, presumably due to decomposing "Cp_2Ti" species. We found that a 5 min "waiting period" after loading the compound onto the column limits the length of this dark-brown band. This is general for all the [2+2+2] reactions in this manuscript; 2) the desired compound eluted over a very large range. Alternative eluents were not explored since this gave a product of good purity with collection of a single fraction.

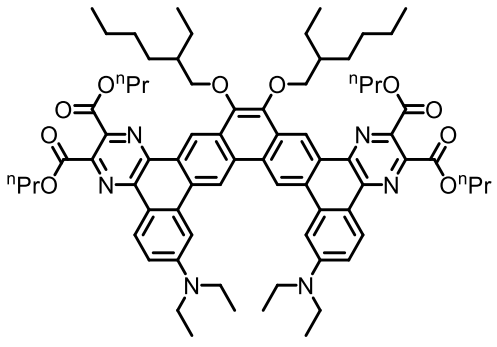

25-pyr

Bis(pyrazine)-annulated PAH (25-pyr). This compound was prepared by the same procedure as **24-pyr** and was isolated as a bright orange solid (28 mg, 47%). The bis(di(aza)titanacyclopentadiene) intermediate **25-Ti** was observed by ^{1}H NMR spectroscopy in 76% yield. ^{1}H NMR (chloroform-*d*; 400 MHz): δ = 10.16 (s, 2H), 9.91 (s, 2H), 9.09 (d, *J* = 9.1 Hz, 2H), 7.99 (d, *J* = 2.5 Hz, 2H), 7.21 (dd, *J* = 9.2, 2.4 Hz, 2H), 4.48 (t, *J* = 6.9 Hz, 8H), 4.41 – 4.22 (m, 4H), 3.73 (q, *J* = 7.0 Hz, 8H), 2.11 – 2.01 (m, 2H), 1.99 – 1.85 (m, 10H), 1.83 – 1.56 (m, 6H), 1.49 – 1.30 (m, 8H), 1.42 (t, *J* = 7.1, 12H), 1.11 (t, *J* = 7.4, 6H), 1.10 (t, *J* = 7.4, 6H), 1.08 (t, *J* = 7.3, 6H), 0.88 (t, *J* = 7.2, 6H); ^{13}C{^{1}H} NMR (chloroform-*d*, 151 MHz): δ = 166.15, 165.73, 149.98, 143.99, 143.96, 143.95, 142.89, 140.38, 140.13, 134.71, 130.34, 130.16, 129.72, 129.00, 128.68, 121.22, 118.38, 117.33, 114.23, 103.32, 76.81, 68.02, 67.86, 44.91, 40.88, 30.81, 29.52, 24.19, 23.25, 22.23, 22.09, 14.27, 13.09, 11.28, 10.60, 10.60; HRMS-ESI (m/z): $[M+H]^+$ calcd. for $C_{74}H_{93}O_{10}N_6$, 1225.6948; found, 1225.6996.

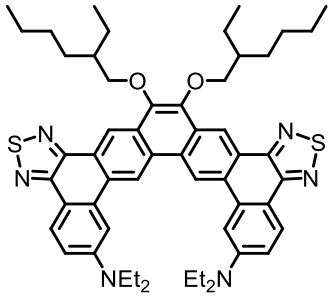

25-S

Bis(thiadiazole)-annulated PAH (25-S). To a stirred solution of bis(dinitrile) **28** (54.7 mg, 0.0660 mmol, 1.0 equiv) in toluene (1.3 mL) was added a solution of $Cp_2Ti(Me_3SiC{\equiv}CSiMe_3)$ (50.5 mg, 0.145 mmol, 2.2 equiv) in toluene (0.4 mL) dropwise over ~1 min. The mixture was stirred for 15 min, then volatile materials were removed *in vacuo*. The residue was dissolved in CH_2Cl_2 (1.5 mL), the solution was cooled to –78 °C with a dry ice / acetone bath, and S_2Cl_2 (0.015 mL, 25 mg, 0.19 mmol, 2.8 equiv) was added to the stirred solution *via* syringe. The mixture was allowed to warm to RT, stirred for a further 4 h, quenched with 10% aqueous NH_4OH (5 mL), diluted with CH_2Cl_2 (10 mL), and filtered through celite. The filtrate was added to a separatory funnel and layers were separated. The organic layer was washed with water (5 mL), dried with Na_2SO_4, filtered, and solvents were removed from the filtrate *via* rotary evaporation. The residue was purified by column chromatography (1:2 hexanes:CH_2Cl_2, then 100% CH_2Cl_2) followed by recrystallization from toluene (~1 mL) at –25 °C to afford **25-S** (20 mg, 34%) as golden yellow crystals. ^{1}H NMR (dichloromethane-d_2, 400 MHz): δ = 9.86 (s, 2H), 9.61 (s, 2H), 8.55 (d, *J* = 8.8 Hz, 2H), 8.00 (d, *J* = 2.5 Hz, 2H), 7.18 (dd, *J* = 8.9, 2.5 Hz, 2H), 4.30 (d, *J* = 5.9 Hz, 4H), 3.71 (q, *J* = 7.1 Hz, 8H), 2.08 – 1.98 (m, 2H), 1.90 – 1.58 (m, 8H), 1.51 – 1.42 (m, 8H), 1.38 (t, *J* = 7.0 Hz, 12H), 1.09 (t, *J* = 7.5 Hz, 6H), 0.94 (t, *J* = 6.9 Hz, 6H); ^{13}C{^{1}H} NMR (chloroform-*d*, 151 MHz): δ = 154.42, 152.64, 149.15, 143.85, 133.56, 130.12, 129.33, 129.30, 127.85, 126.08, 120.58, 117.42, 116.62, 114.29, 104.61, 76.77, 44.90, 40.97, 30.85, 29.46, 24.06, 23.36, 14.35, 13.04, 11.45; HRMS-ESI (m/z): $[M+H]^+$ calcd. for $C_{54}H_{65}N_6O_2S_2$, 893.4605; found, 893.4603.

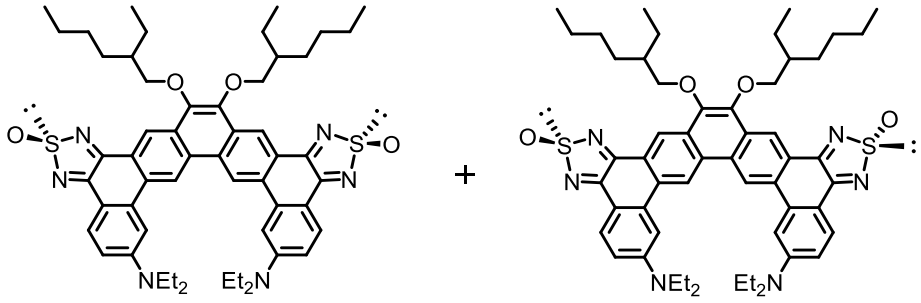

25-SO

Bis(thiadiazole-oxide)-annulated PAH (25-SO). To a stirred solution of bis(dinitrile) **28** (63.0 mg, 0.0760 mmol, 1.0 equiv) in toluene (1.5 mL) was added a solution of $Cp_2Ti(Me_3SiC{\equiv}CSiMe_3)$ (58.2 mg, 0.167 mmol, 2.2 equiv) in toluene (0.5 mL) dropwise over ~1 min. The mixture was stirred for 15 min, then the solution was cooled to –78 °C with a dry ice / acetone bath, and $SOCl_2$ (0.013 mL, 22 mg, 0.18 mmol, 2.4 equiv) was added to the stirred solution *via* syringe. The mixture was allowed to warm to RT, stirred for a further 30 min, quenched with 10% aqueous NH_4OH (5 mL), diluted with CH_2Cl_2 (10 mL), and filtered through celite. The filtrate was added to a separatory funnel and layers were separated. The organic layer was washed with water (5 mL), dried with Na_2SO_4, filtered, and solvents were removed from the filtrate. The residue was purified by column chromatography (0–10% EtOAc in CH_2Cl_2) to afford **25-SO** (35 mg, 47%) as a purple solid that was a mixture of two diastereomers. HRMS-ESI (m/z): $[M+Na]^+$ calcd. for $C_{54}H_{64}N_6O_4S_2Na$ 947.4323; found, 947.4328. *Diastereomer 1*: ^{1}H NMR (chloroform-*d*, 500 MHz): δ = 9.36 (s, 2H), 9.23 (s, 2H), 8.05 (d, *J* = 9 Hz, 2H), 7.69 (d, *J* = 2 Hz, 2H), 6.75 (dd, *J* = 9, 2 Hz, 2H), 4.16 – 4.06 (m, 4H), 3.86 – 3.66 (m, 8H), 1.93 – 1.83 (m, 2H), 1.72 – 1.48 (m, 8H), 1.44 (t, *J* = 7.2 Hz, 12H), 1.41 – 1.34 (m, 8H), 1.00 (t, *J* = 7.4 Hz, 6H), 0.95 – 0.89 (m, 6H); ^{13}C{^{1}H} NMR (chloroform-*d*, 176 MHz): δ = 162.8, 160.9, 153.4, 144.3, 137.6, 132.6, 132.5, 131.6, 131.1, 124.9, 124.7, 121.5, 112.8, 112.0, 107.4, 76.8, 45.1, 40.7, 30.5, 29.3, 23.7, 23.3, 14.3, 13.5, 11.3. *Diastereomer 2*: ^{1}H NMR (chloroform-*d*, 500 MHz): δ = 9.34 (s, 2H), 9.18 (s, 2H), 7.99 (d, *J* = 9 Hz, 2H), 7.68 (d, *J* = 2 Hz, 2H), 6.73 (dd, *J* = 9, 2 Hz, 2H), 4.22 – 4.17 (m, 2H), 4.06 – 3.99 (m, 2H), 3.86 – 3.66 (m, 8H), 1.93 – 1.83 (m, 2H), 1.72 – 1.48 (m, 8H), 1.44 (t, *J* = 7.2 Hz, 12H), 1.41 – 1.34 (m, 8H), 1.00 (t, *J* = 7.4 Hz, 6H), 0.95 – 0.89 (m, 6H); ^{13}C{^{1}H} NMR (chloroform-*d*, 176 MHz): δ = 162.8, 160.9, 153.4, 144.3, 137.6, 132.6, 132.5, 131.4, 131.1, 124.9, 124.7, 121.4, 112.8, 111.7, 107.4, 76.8, 45.1, 40.7, 30.5, 29.3, 23.7, 23.3, 14.3, 13.5, 11.3.

Note: Compound **25-SO** exhibits peculiar behavior in solution. After NMR characterization of solution of **25-SO** in chloroform-*d* (~20 mg/mL), a large amount of crystalline solid precipitated out of solution. A representative sample of this precipitate was re-dissolved in chloroform-*d* (despite its greatly diminished solubility) and ^{1}H NMR spectroscopy revealed that it was significantly enriched in one of the diastereomers. The diastereomeric ratio converged to 1:1 over the next 6 h (monitored by ^{1}H NMR; see Figure S65). Another ^{1}H NMR spectrum was acquired after 7 days and the ratio was still 1:1.

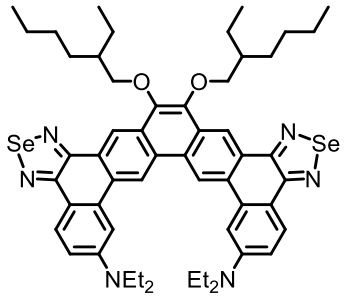

25-Se

Bis(selenadiazole)-annulated PAH (25-Se). To a stirred solution of bis(dinitrile) **28** (53.1 mg, 0.0640 mmol, 1.0 equiv) in toluene (1.3 mL) was added a solution of $Cp_2Ti(Me_3SiC{\equiv}CSiMe_3)$ (49.1 mg, 0.141 mmol, 2.2 equiv) in toluene (0.4 mL) dropwise over ~1 min. The mixture was stirred for 15 min, then $SeCl_2$(bipy) (59 mg, 0.19 mmol, 3.0 equiv) was added. The mixture was stirred for a further 5 min and filtered. Methanol (5 mL) was added to the filtrate, then the precipitated solid was collected by filtration and purified by column chromatography (100% CH_2Cl_2) to afford **25-Se** (33 mg, 52%) as a bright yellow solid. ^{1}H NMR (dichloromethane-d_2, 400 MHz): δ = 9.73 (s, 2H), 9.61 (s, 2H), 8.56 (d, *J* = 8.9 Hz, 2H), 7.88 (d, *J* = 2.5 Hz, 2H), 7.11 (dd, *J* = 8.9, 2.4 Hz, 2H), 4.33 – 4.24 (m, 4H), 3.69 (q, *J* = 7.1 Hz, 8H), 2.02 (hept, *J* = 6.0 Hz, 2H), 1.90 – 1.57 (m, 8H), 1.52 – 1.41 (m, 8H), 1.38 (t, *J* = 7.1 Hz, 12H), 1.08 (t, *J* = 7.4 Hz, 6H), 0.94 (t, *J* = 7.0 Hz, 6H); ^{13}C{^{1}H} NMR (dichloromethane-d_2, 151 MHz): δ = 159.5, 158.3, 149.9, 144.3, 134.1, 130.6, 130.1, 129.8, 129.0, 128.7, 121.9, 119.1, 117.9, 114.6, 104.7, 77.16, 45.23, 41.44, 31.26, 29.87, 24.51, 23.79, 14.57, 13.26, 11.67; HRMS-ESI (m/z): $[M+H]^+$ calcd. for $C_{54}H_{65}N_6O_2Se_2$, 989.3494; found, 989.3486.

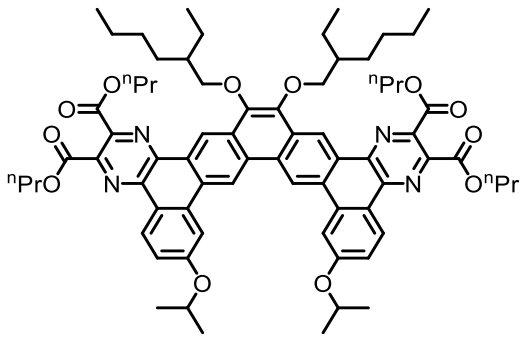

26-pyr

Bis(pyrazine)-annulated PAH (26-pyr). This compound was prepared by the same procedure as **24-pyr** and was further purified by recrystallization from CH_2Cl_2/hexanes. The compound was isolated as a yellow/orange microcrystalline solid (17 mg, 39%). The bis(di(aza)titanacyclopentadiene) intermediate **26-Ti** was observed by ^{1}H NMR spectroscopy in 67% yield. ^{1}H NMR (chloroform-*d,* 400 MHz): δ = 10.13 (s, 2H), 10.05 (s, 2H), 9.21 (d, *J* = 8.9 Hz, 2H), 8.42 (d, *J* = 2.3 Hz, 2H), 7.40 (dd, *J* = 9.0, 2.3 Hz, 2H), 5.04 (hept, *J* = 6.0 Hz, 2H), 4.49 (t, *J* = 7.0 Hz, 4H), 4.47 (t, *J* = 6.9 Hz, 4H), 4.41 – 4.31 (m, 2H), 4.32 – 4.23 (m, 2H), 2.11 – 2.01 (m, 2H), 1.99 – 1.85 (m, 10H), 1.83 – 1.58 (m, 6H), 1.63 (d, *J* = 6.0 Hz, 12H), 1.48 – 1.32 (m, 8H), 1.11 (t, *J* = 7.4 Hz, 6H), 1.10 (t, *J* = 7.4 Hz, 6H), 1.09 (t, *J* = 7.5 Hz, 6H), 0.89 (t, *J* = 7.1, 6H); ^{13}C{^{1}H} NMR (chloroform-*d,* 101 MHz): δ = 165.83, 165.35, 160.67, 144.22, 144.18, 142.62, 142.14, 140.79, 134.63, 130.40, 129.92, 129.23, 128.71, 128.49, 122.51, 121.07, 117.75, 116.78, 109.14, 76.70, 70.57, 68.06, 68.02, 40.85, 30.77, 29.56, 24.11, 23.27,

22.48, 22.17, 22.05, 14.30, 11.23, 10.61, 10.55; HRMS-ESI (m/z): $[M+H]^+$ calcd. for $C_{72}H_{87}O_{12}N_4$, 1199.6315; found, 1199.6373.

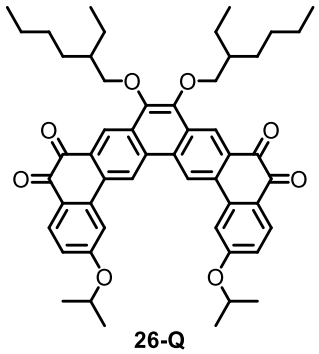

26-Q

Bis(*o*-quinone) (26-Q). To a stirred solution of bis(dinitrile) **29** (50.8 mg, 0.0633 mmol, 1.0 equiv) in toluene (1.3 mL) was added a solution of $Cp_2Ti(Me_3SiC{\equiv}CSiMe_3)$ (48.4 mg, 0.139 mmol, 2.2 equiv) in toluene (0.5 mL) dropwise over ~1 min. The reaction mixture was stirred for 15 min, then HCl (2.0 M in diethyl ether, 0.48 mL, 0.95 mmol, 15 equiv) was added dropwise over ~1 min. The mixture was stirred for 2 h, then volatile materials were removed *via* rotary evaporation. The residue was transferred to a 20 mL vial as a MeOH (2 mL) suspension, then aqueous HCl (3.0 M, 0.3 mL) was added, the vial was sealed, and the stirred mixture was heated at 70 °C for 24 h. The suspended solid was collected by filtration, washed with MeOH (2 x 2 mL), and purified by column chromatography (3% EtOAc in CH_2Cl_2) to afford **26-Q** (22 mg, 43%) as a red solid. ^{1}H NMR (chloroform-*d*, 500 MHz): δ = 9.21 (s, 2H), 9.11 (s, 2H), 8.29 (d, *J* = 8.7 Hz, 2H), 7.78 (d, *J* = 2.3 Hz, 2H), 7.02 (dd, *J* = 8.8, 2.3 Hz, 2H), 4.91 (hept, *J* = 6.3 Hz, 2H), 4.16 (d, *J* = 6.0 Hz, 4H), 1.93 (hept, *J* = 6.1 Hz, 2H), 1.76 – 1.58 (m, 8H), 1.55 (d, *J* = 6.1 Hz, 12H), 1.44 – 1.36 (m, 8H), 1.02 (t, *J* = 7.5 Hz, 6H), 0.97 – 0.91 (m, 6H); ^{13}C{^{1}H} NMR (chloroform-*d*, 151 MHz): δ = 180.9, 178.7, 164.7, 145.2, 138.5, 134.1, 132.2, 132.1, 131.5, 130.8, 126.9, 125.3, 119.0, 115.3, 111.6, 71.2, 40.8, 30.7, 29.9, 29.4, 24.0, 23.3, 22.2, 14.3, 11.3; HRMS-ESI (m/z): $[M+H]^+$ calcd. for $C_{52}H_{59}O_8$, 811.4204; found, 811.4202.

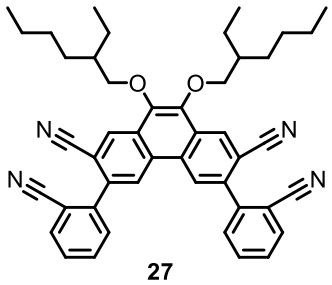

27

3,6-bis(2-cyanophenyl)-9,10-bis((2-ethylhexyl)oxy)phenanthrene-2,7-dicarbonitrile (27). This compound was prepared by the same procedure as **S7** with the following quantities: bromide **30** (0.200 g, 0.311 mmol, 1.0 equiv), boronic ester **S11** (0.185 g, 0.809 mmol, 2.6 equiv), $Pd(PPh_3)_2Cl_2$ (0.013 g, 0.019 mmol, 0.06 equiv), $K_3PO_4{\bullet}nH_2O$ (0.186 g, 0.809 mmol, 2.6 equiv), and toluene (3 mL). The crude mixture was purified by column chromatography (100% CH_2Cl_2) followed by trituration with boiling hexanes to afford bis(dinitrile) **27** as a pale-yellow solid (0.128 g, 59%). ^{1}H NMR (chloroform-*d*, 500 MHz): δ = 8.79 (s, 2H), 8.73 (s, 2H), 7.87 (dd, *J* = 7.9, 1.3 Hz, 2H), 7.78 (td, *J* = 7.7, 1.4 Hz, 2H), 7.70 (dd, *J* = 7.7, 1.2 Hz, 2H), 7.62 (td, *J* = 7.7, 1.3 Hz, 2H), 4.22 – 4.14 (m, 4H), 1.94 (hept, *J* = 5.6 Hz, 2H), 1.76 – 1.65 (m, 2H), 1.65 – 1.52 (m, 6H), 1.46 – 1.35 (m, 8H), 1.04 (t, *J* = 7.5 Hz, 6H),

1.00 – 0.90 (m, 6H); $^{13}C\{^{1}H\}$ NMR (chloroform-*d*, 151 MHz): δ = 144.1, 141.6, 137.4, 133.8, 133.2, 131.1, 131.1, 129.8, 129.6, 129.5, 125.9, 117.9, 117.7, 112.9, 112.3, 77.5, 40.8, 30.6, 29.3, 24.0, 23.3, 14.7, 11.3; HRMS-EI (m/z): $[M]^+$ calcd. for $C_{46}H_{46}O_2N_4$, 686.3621; found, 686.3605.

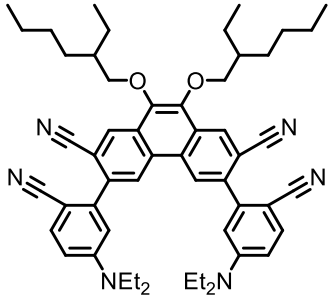

28

3,6-bis(2-cyano-5-(diethylamino)phenyl)-9,10-bis((2-ethylhexyl)oxy)phenanthrene-2,7-dicarbonitrile (28). This compound was prepared by the same procedure as **S7** with the following quantities: bromide **30** (0.395 g, 0.615 mmol, 1.0 equiv), boronic ester **S12** (0.48 g, 1.60 mmol, 2.6 equiv), $Pd(PPh_3)_2Cl_2$ (0.026 g, 0.037 mmol, 0.06 equiv), K_3PO_4•nH_2O (0.37 g, 1.60 mmol, 2.6 equiv), and toluene (6 mL). The crude mixture was purified by column chromatography (100% CH_2Cl_2) to afford bis(dinitrile) **28** as a yellow solid (0.475 g, 93%). ^{1}H NMR (chloroform-*d,* 400 MHz): δ = 8.77 (s, 2H), 8.74 (s, 2H), 7.59 (d, *J* = 8.9 Hz, 2H), 6.76 (d, *J* = 2.6 Hz, 2H), 6.72 (dd, *J* = 8.9, 2.6 Hz, 2H), 4.23 – 4.08 (m, 4H), 3.46 (q, *J* = 7.1 Hz, 8H), 1.93 (hept, *J* = 6.2 Hz, 2H), 1.78 – 1.48 (m, 8H), 1.48 – 1.35 (m, 8H), 1.25 (t, *J* = 7.1 Hz, 12H), 1.04 (t, *J* = 7.4 Hz, 6H), 1.00 – 0.91 (m, 6H); $^{13}C\{^{1}H\}$ NMR (chloroform-*d,* 151 MHz): δ = 150.2, 143.8, 142.9, 138.6, 135.1, 130.6, 129.7, 129.6, 126.0, 120.1, 118.2, 113.2, 112.0, 111.2, 96.5, 77.3, 44.8, 40.8, 30.6, 29.3, 24.0, 23.3, 14.3, 12.6, 11.3; HRMS-ESI (m/z): $[M+H]^+$ calcd. for $C_{54}H_{65}O_2N_6$, 829.5164; found, 829.5201.

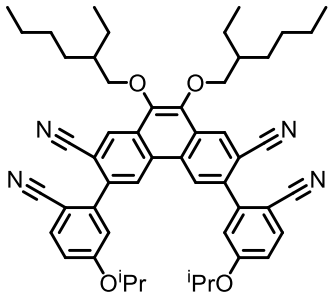

29

3,6-bis(2-cyano-5-isopropoxyphenyl)-9,10-bis((2-ethylhexyl)oxy)phenanthrene-2,7-dicarbonitrile (29). This compound was prepared by the same procedure as **S7** with the following quantities: bromide **30** (0.390 g, 0.607 mmol, 1.0 equiv), boronic ester **S9** (0.454 g, 1.58 mmol, 2.6 equiv), $Pd(PPh_3)_2Cl_2$ (0.025 g, 0.036 mmol, 0.06 equiv), K_3PO_4•nH_2O (0.364 g, 1.58 mmol, 2.6 equiv), and toluene (6 mL). The crude mixture was purified by column chromatography on $B(OH)_3$-impregnated[10] silica gel (100% CH_2Cl_2) to afford bis(dinitrile) **29** as a sticky yellow solid (0.360 g, 74%). ^{1}H NMR (chloroform-*d*, 400 MHz): δ = 8.77 (s, 2H), 8.73 (s, 2H), 7.75 (d, *J* = 8.7 Hz, 2H), 7.11 (d, *J* = 2.4 Hz, 2H), 7.04 (dd, *J* = 8.7, 2.5 Hz, 2H), 4.69 (hept, *J* = 6.1 Hz, 2H), 4.23 – 4.13 (m, 4H), 1.93 (h, *J* = 6.2 Hz, 2H), 1.77 – 1.49 (m, 8H), 1.48 – 1.33 (m, 20H), 1.04 (t, *J* = 7.5 Hz, 6H), 1.00 – 0.92 (m, 6H); $^{13}C\{^{1}H\}$ NMR (chloroform-*d*, 101 MHz): δ = 161.4, 144.0, 143.5, 137.4, 135.4, 130.9, 129.7,

129.6, 125.8, 118.5, 117.8, 117.8, 116.7, 112.1, 103.6, 77.4, 71.1, 40.7, 30.6, 29.2, 23.9, 23.3, 22.0, 14.3, 11.3; HRMS-ESI (m/z): $[M+Na]^+$ calcd. for $C_{52}H_{58}O_4N_4Na$, 825.4350; found, 825.4384.

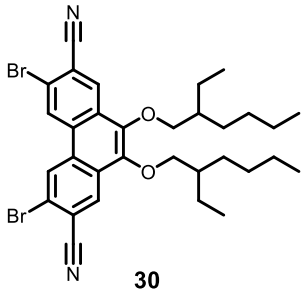

30

3,6-dibromo-9,10-bis((2-ethylhexyl)oxy)phenanthrene-2,7-dicarbonitrile (30). A 50 mL Schlenk flask equipped with Teflon stopper and a magnetic stirbar was loaded with **S13** (2.50 g, 2.96 mmol, 1.0 equiv), $Zn(CN)_2$ (0.347 g, 2.96 mmol, 1.0 equiv), and $Pd(PPh_3)_4$ (0.068 g, 0.059 mmol, 0.02 equiv), and the atmosphere of the flask was exchanged for N_2 with three vacuum/N_2 cycles. Dry, degassed DMF (14 mL) was added *via* syringe, the flask was sealed, and the stirred reaction mixture was heated at 120 °C for 12 h. The mixture was cooled to room temperature, 10% aqueous NH_4OH (30 mL) was added, and the suspension was stirred for 5 min. The solid was collected on a fritted funnel and washed with water (2 x 30 mL) and MeOH (2 x 20 mL). The crude solid was purified by column chromatography (33–50% CH_2Cl_2 in hexanes) to afford **30** (1.45 g, 76%) as a bright yellow solid. ^1H NMR (chloroform-*d*, 500 MHz): δ = 8.78 (s, 2H), 8.57 (s, 2H), 4.13 – 4.05 (m, 4H), 1.87 (hept, *J* = 6.2 Hz, 2H), 1.69 – 1.45 (m, 8H), 1.42 – 1.32 (m, 8H), 0.99 (t, *J* = 7.5 Hz, 6H), 0.95 – 0.91 (m, 6H); $^{13}C\{^1H\}$ NMR (chloroform-*d*, 101 MHz): δ = 143.5, 130.2, 130.0, 129.8, 127.9, 121.0, 117.2, 115.8, 77.3, 40.7, 30.5, 29.2, 23.9, 23.2, 14.2, 11.2; HRMS-EI (m/z): $[M]^+$ calcd. for $C_{32}H_{38}N_2O_2Br_2$, 640.1300; found, 640.1291.

NMR Spectra

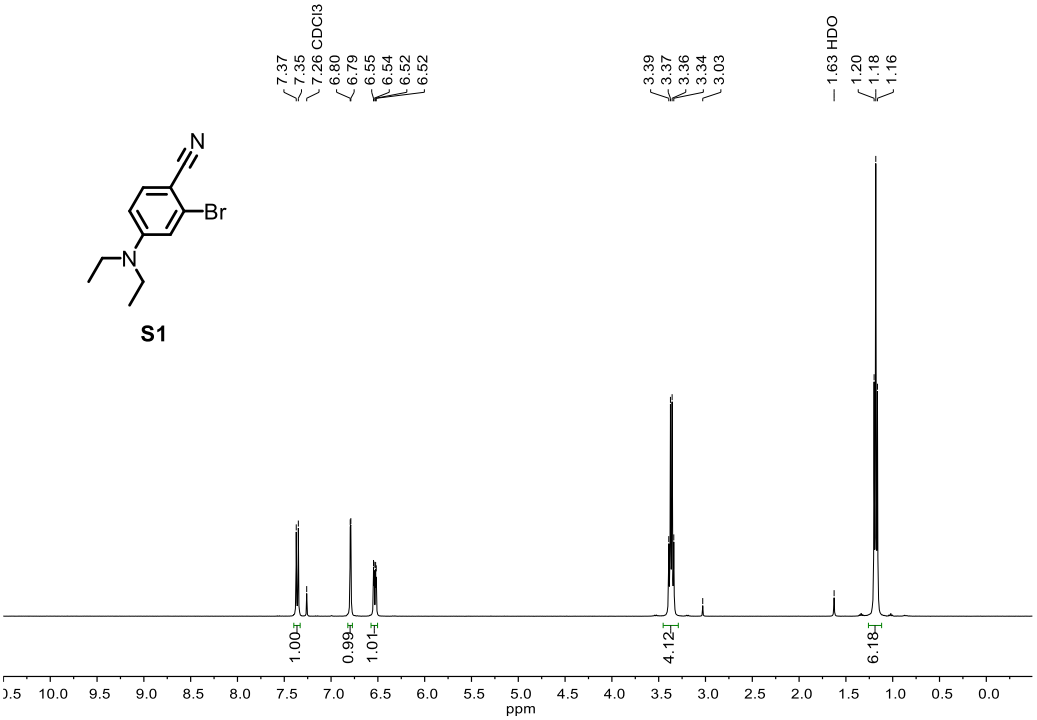

Figure S1. ^{1}H NMR Spectrum (400 MHz, Chloroform-*d*) of **S1**.

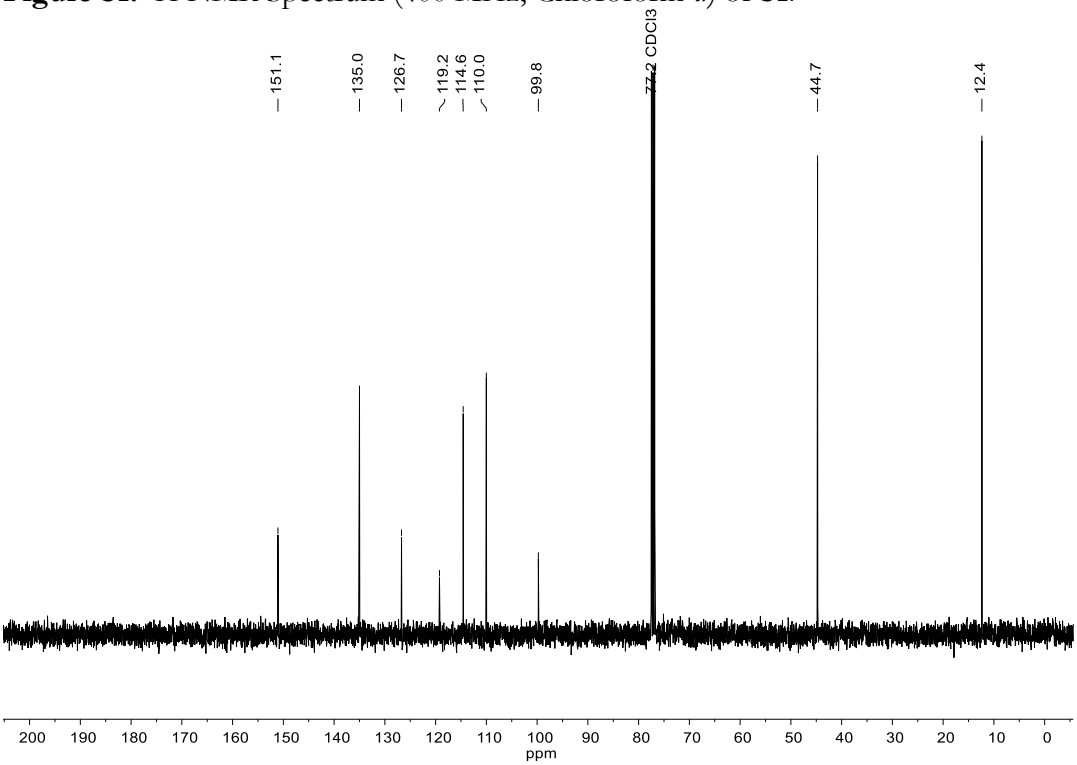

Figure S2. ^{13}C{^{1}H} NMR Spectrum (101 MHz, Chloroform-*d*) of **S1**.

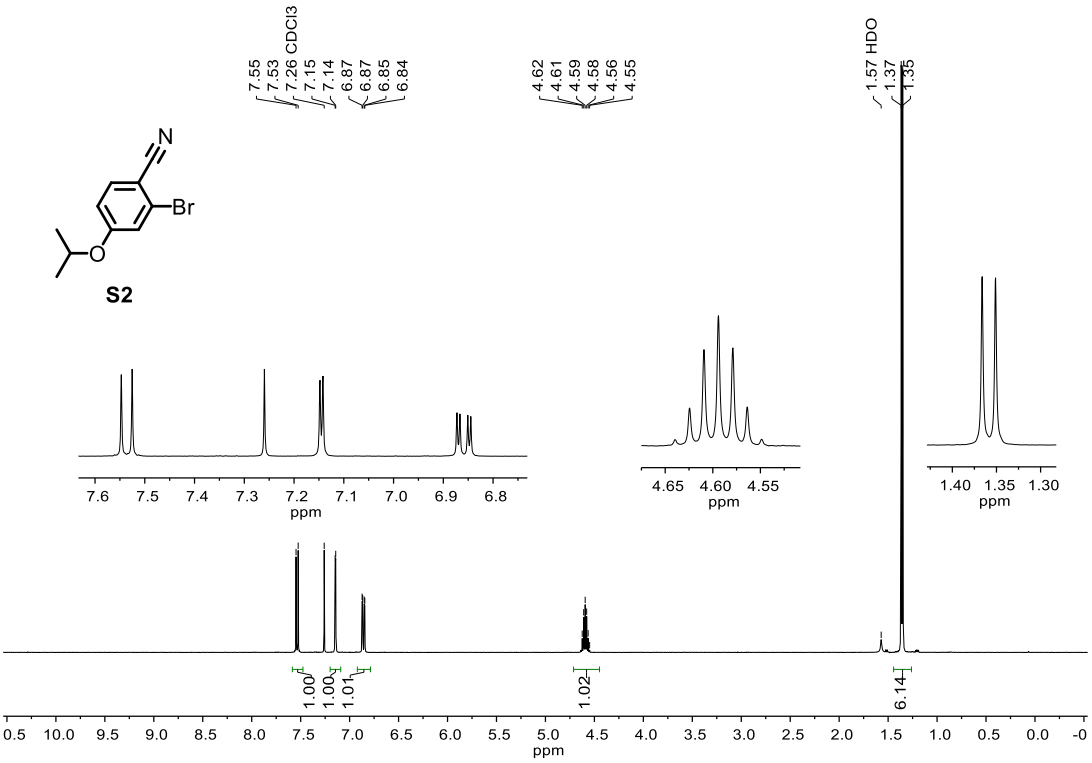

Figure S3. ^{1}H NMR Spectrum (400 MHz, Chloroform-*d*) of **S2**.

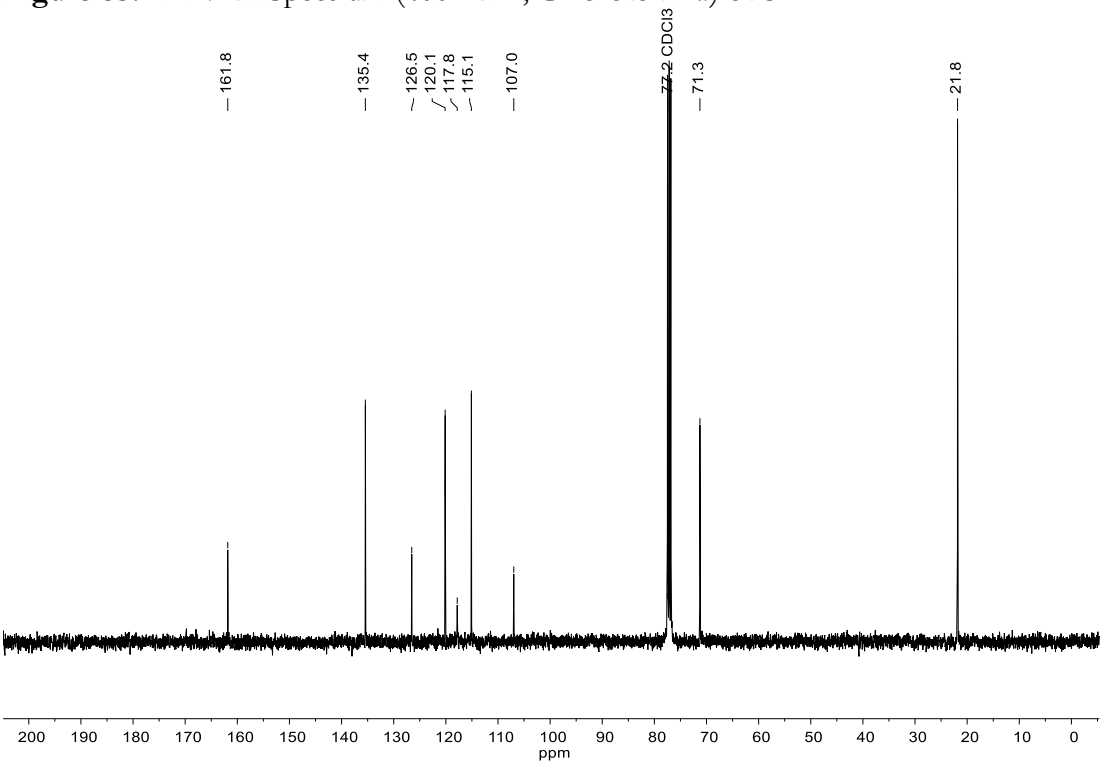

Figure S4. ^{13}C{^{1}H} NMR Spectrum (101 MHz, Chloroform-*d*) of **S2**.

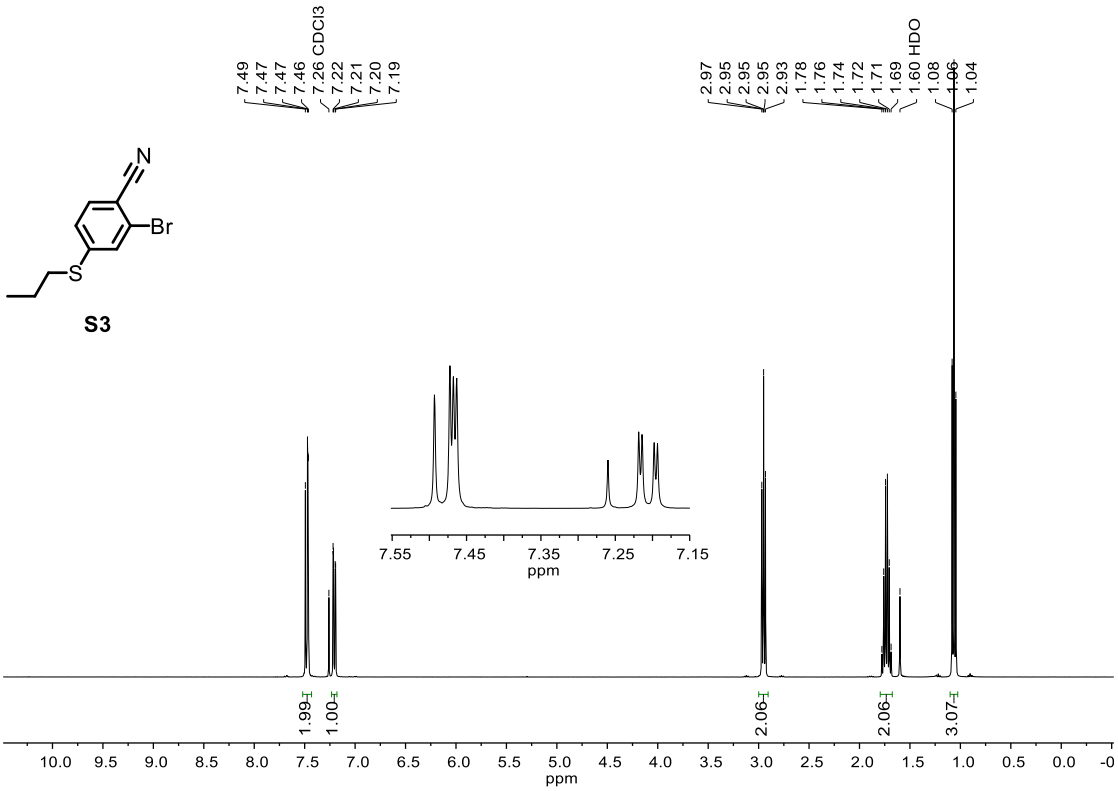

Figure S5. ^{1}H NMR Spectrum (400 MHz, Chloroform-*d*) of **S3**.

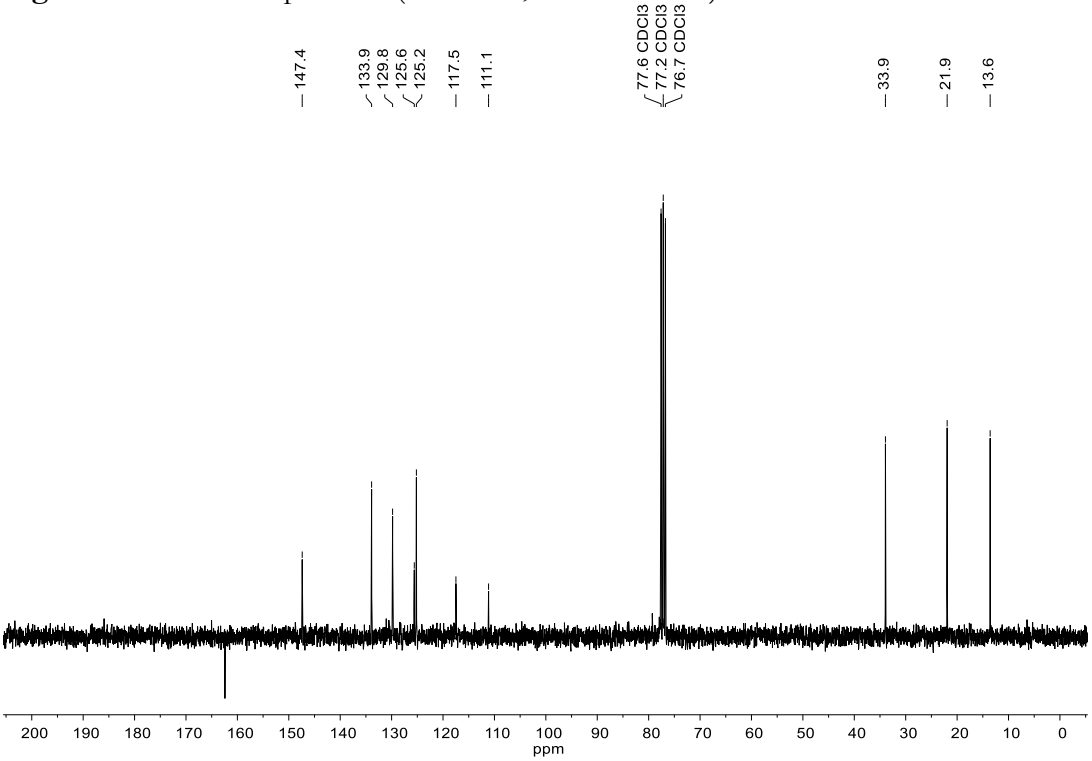

Figure S6. ^{13}C{^{1}H} NMR Spectrum (75 MHz, Chloroform-*d*) of **S3**.

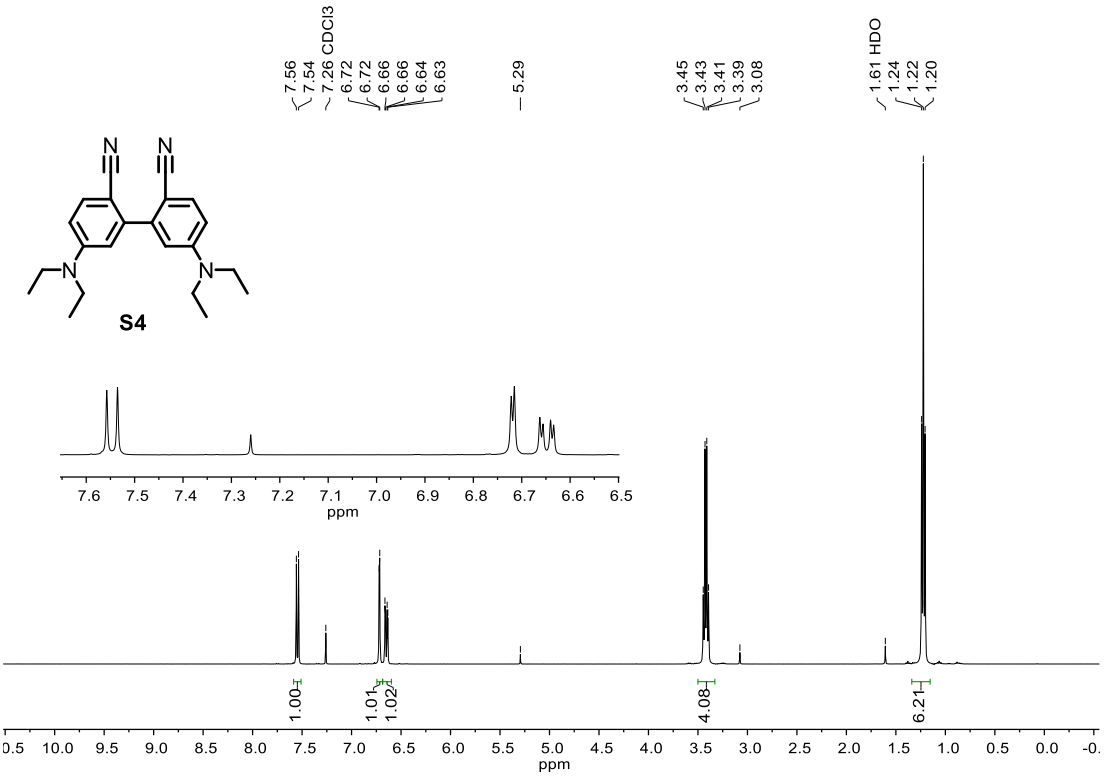

Figure S7. ^{1}H NMR Spectrum (400 MHz, Chloroform-*d*) of **S4**.

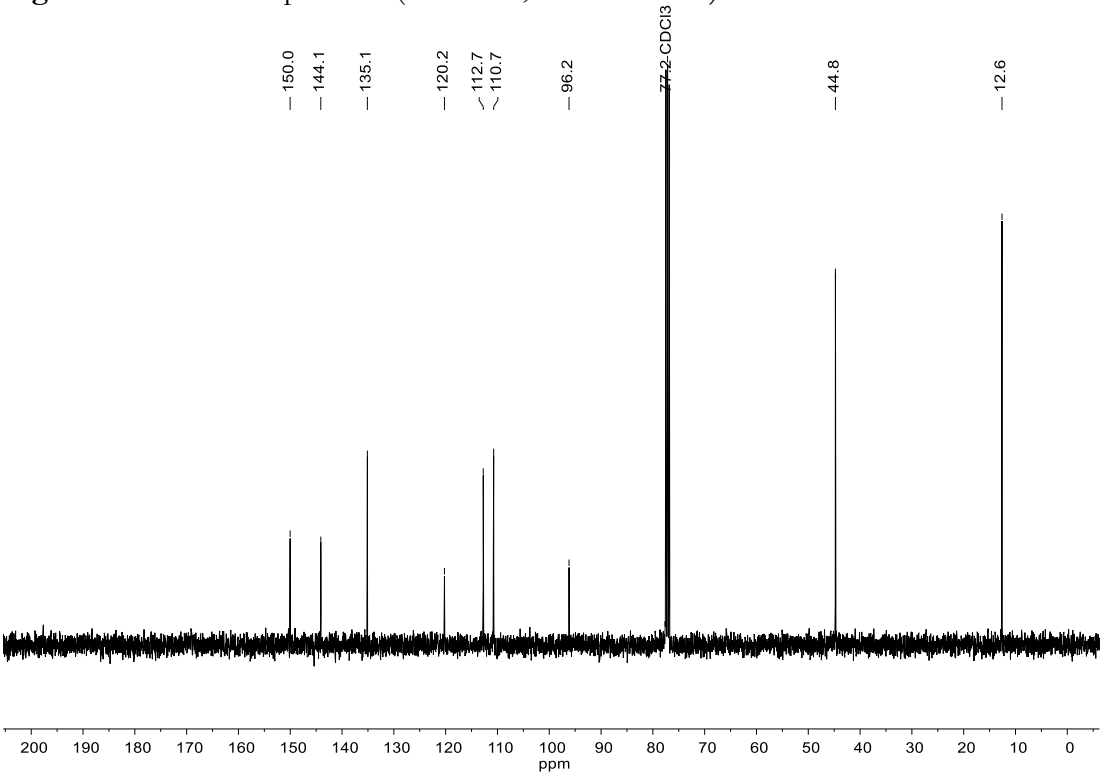

Figure S8. ^{13}C{^{1}H} NMR Spectrum (101 MHz, Chloroform-*d*) of **S4**.

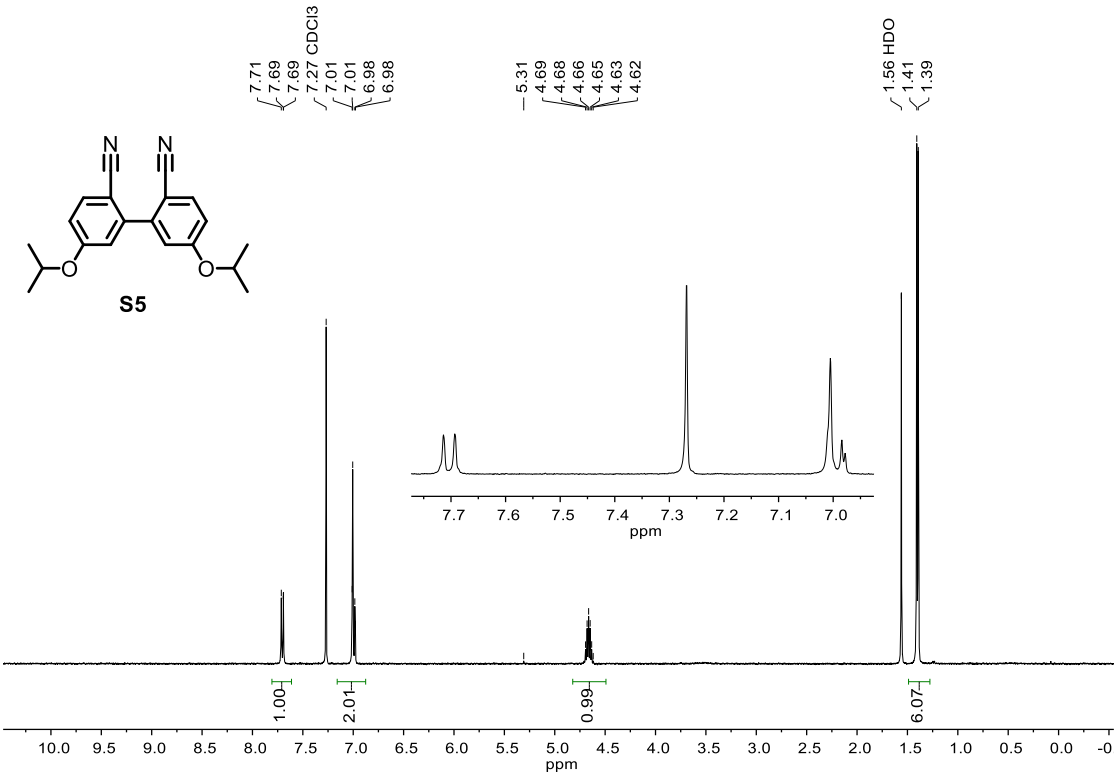

Figure S9. ^{1}H NMR Spectrum (400 MHz, Chloroform-*d*) of **S5**.

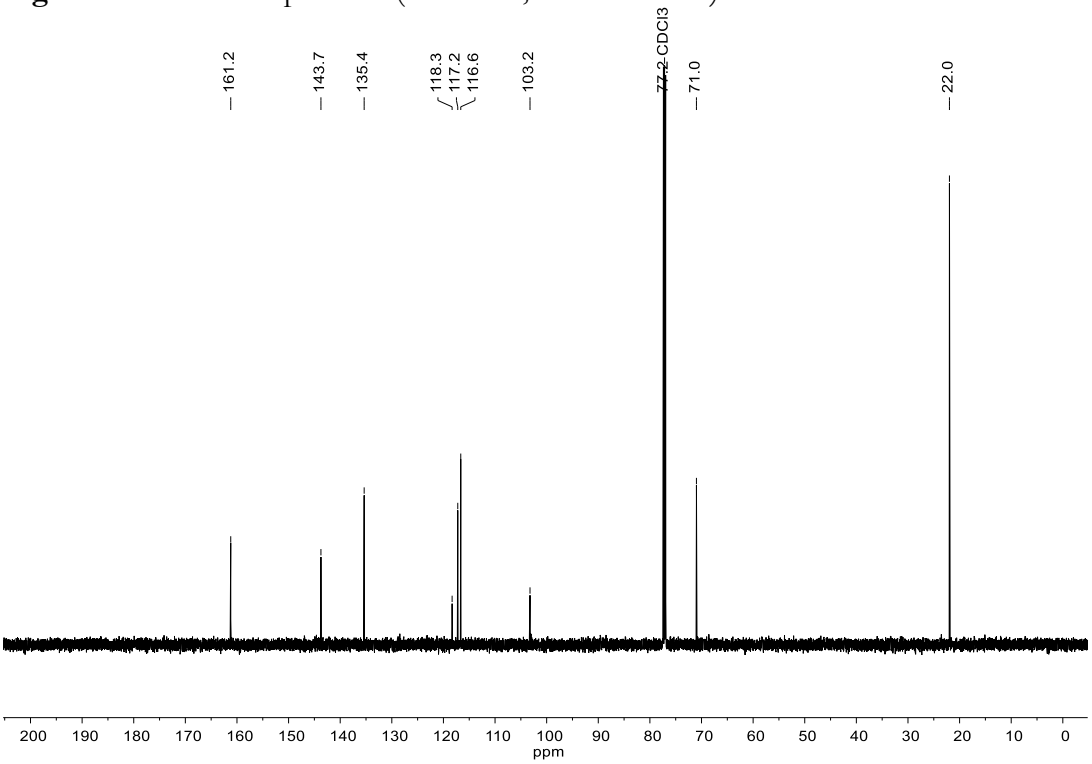

Figure S10. ^{13}C{^{1}H} NMR Spectrum (151 MHz, Chloroform-*d*) of **S5**.

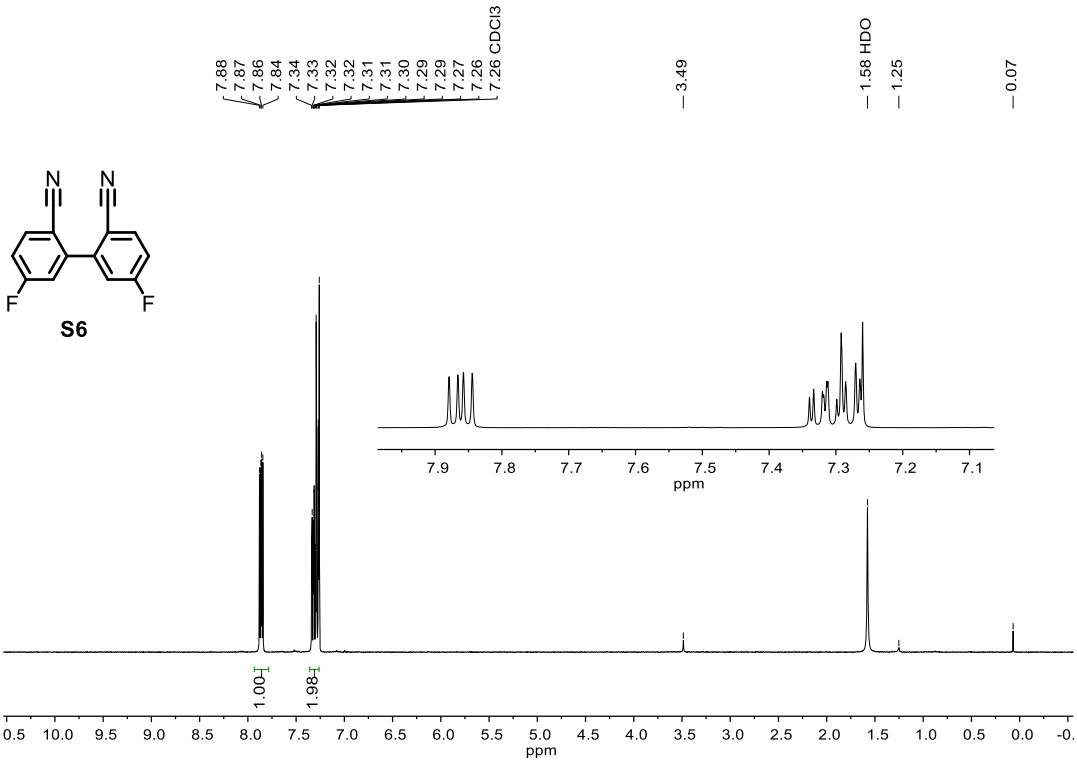

Figure S11. ^{1}H NMR Spectrum (400 MHz, Chloroform-*d*) of **S6**.

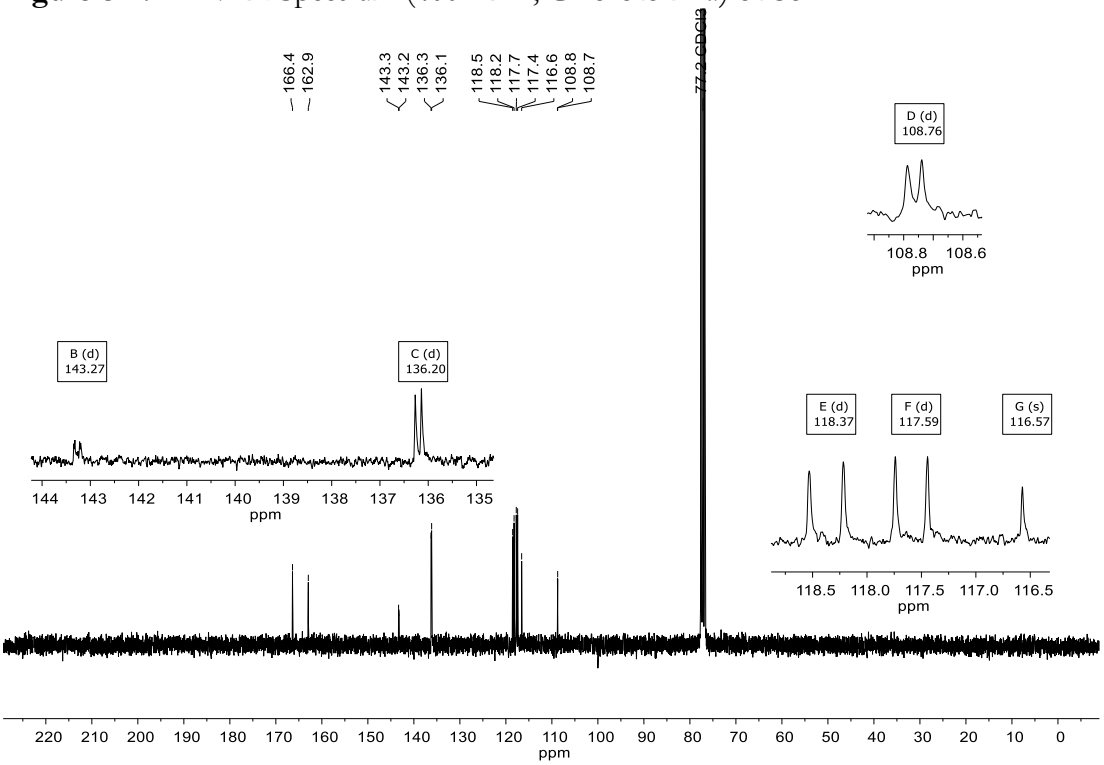

Figure S12. ^{13}C{^{1}H} NMR Spectrum (75 MHz, Chloroform-*d*) of **S6**.

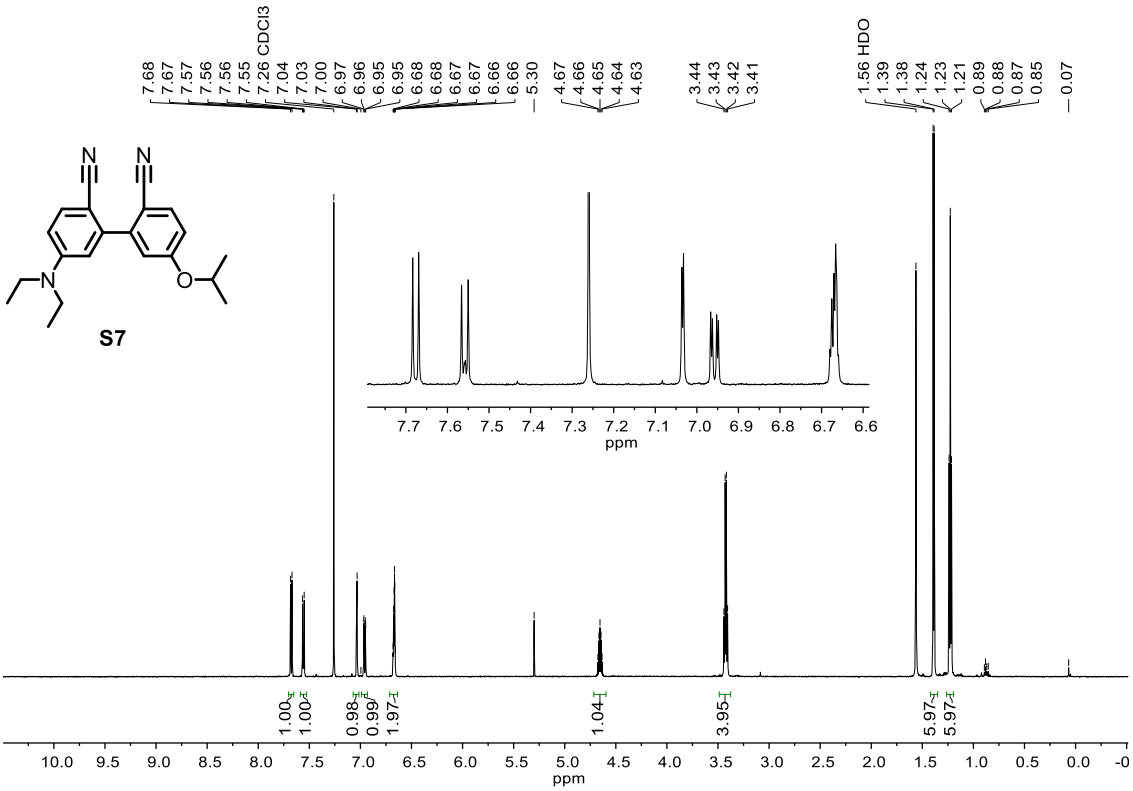

Figure S13. ^{1}H NMR Spectrum (600 MHz, Chloroform-*d*) of **S7**.

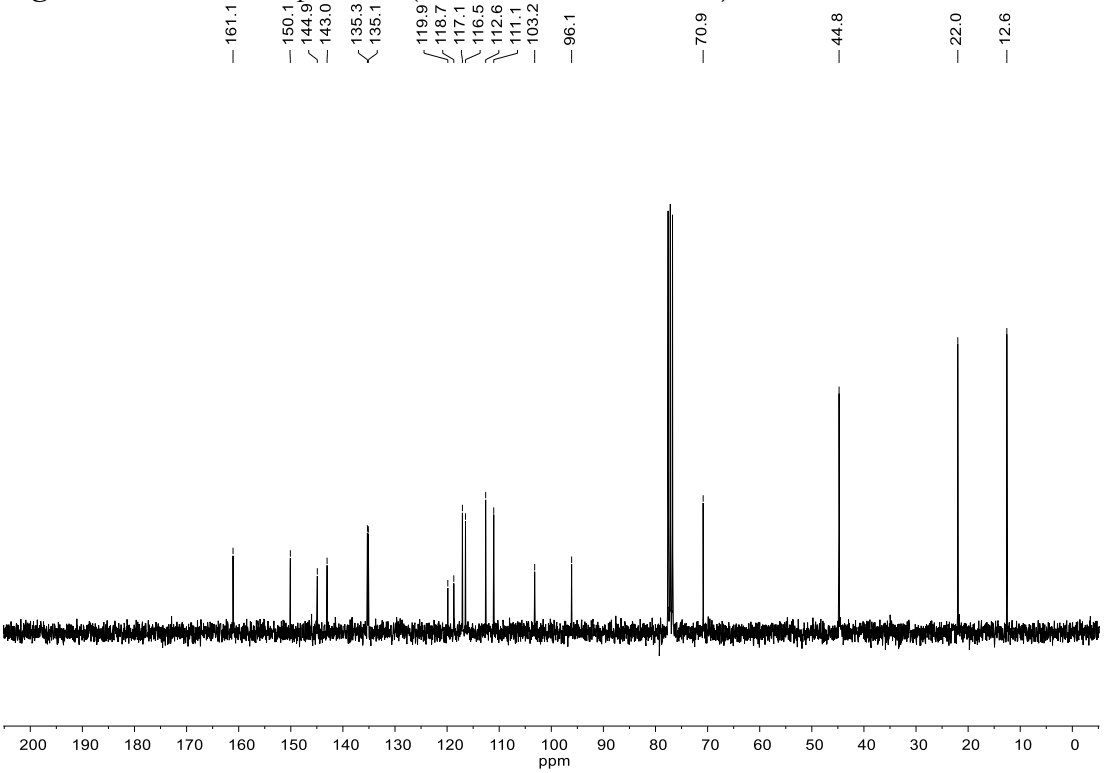

Figure S14. ^{13}C{^{1}H} NMR Spectrum (75 MHz, Chloroform-*d*) of **S7**.

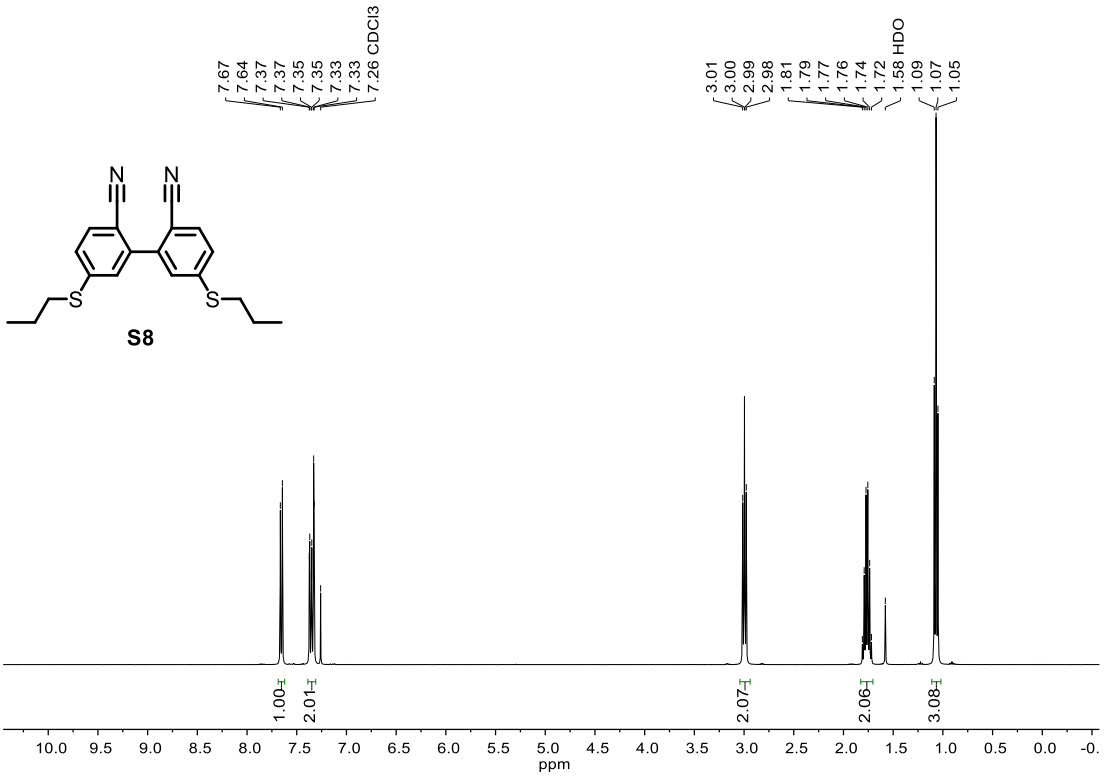

Figure S15. ^{1}H NMR Spectrum (400 MHz, Chloroform-*d*) of **S8**.

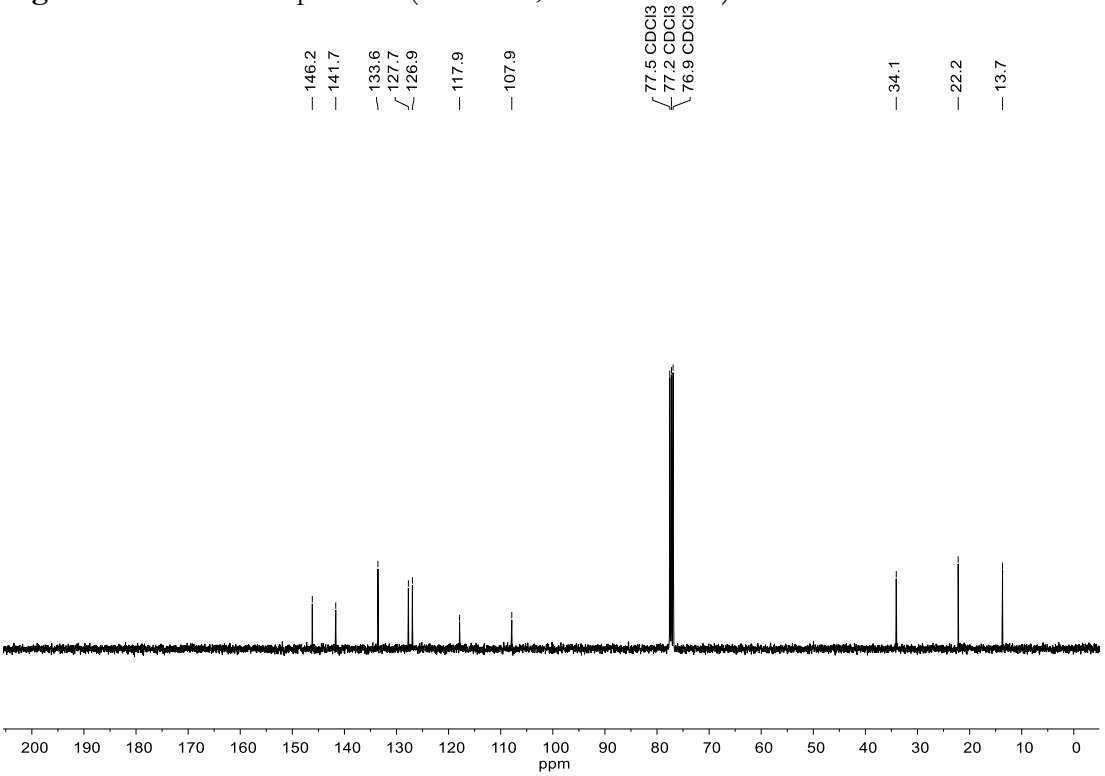

Figure S16. ^{13}C{^{1}H} NMR Spectrum (101 MHz, Chloroform-*d*) of **S8**.

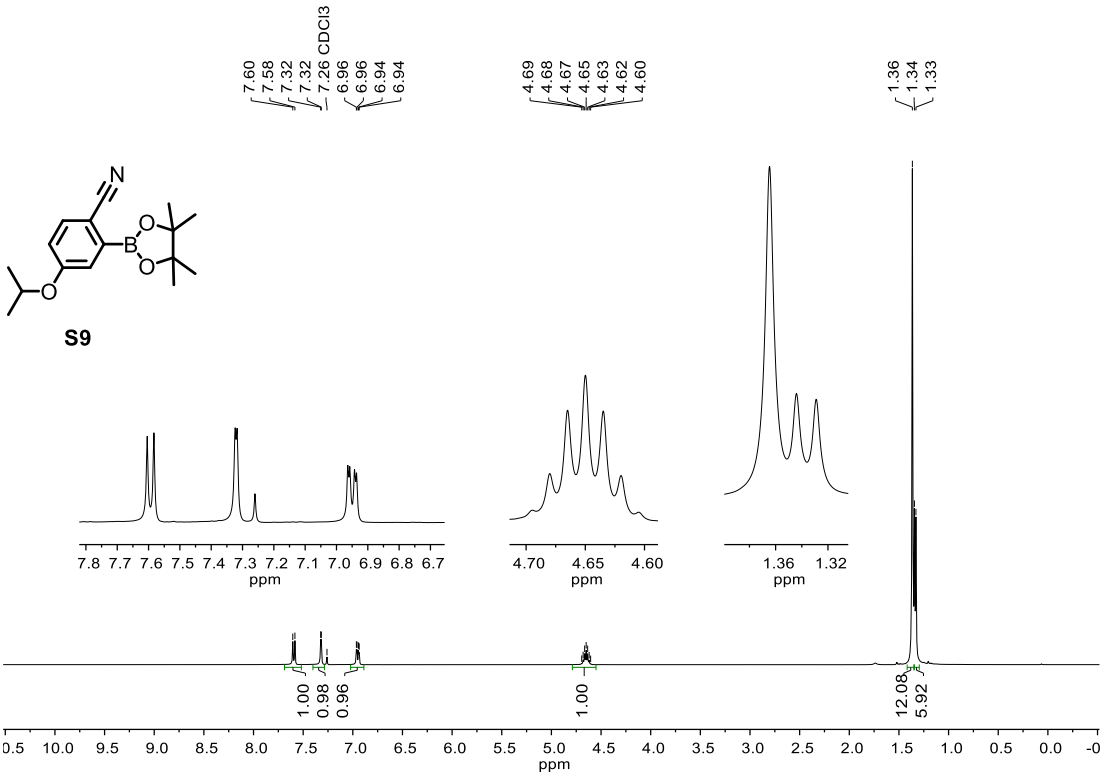

Figure S17. ^{1}H NMR Spectrum (400 MHz, Chloroform-*d*) of **S9**.

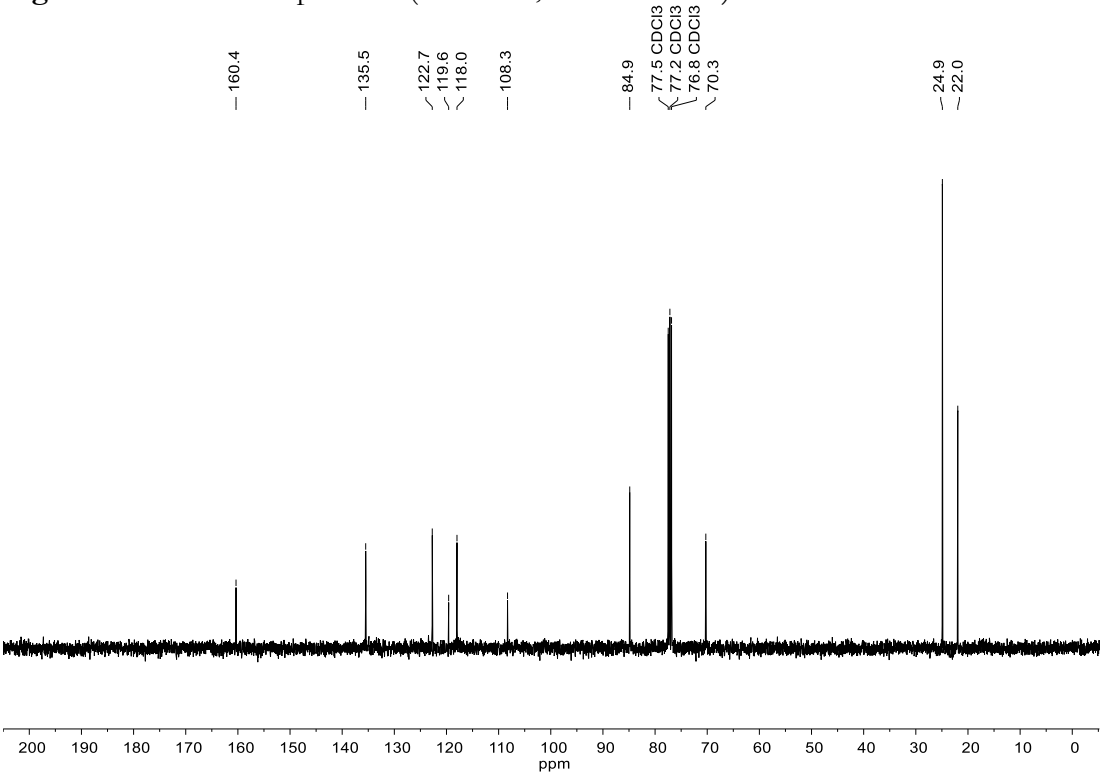

Figure S18. ^{13}C{^{1}H} NMR Spectrum (101 MHz, Chloroform-*d*) of **S9**.

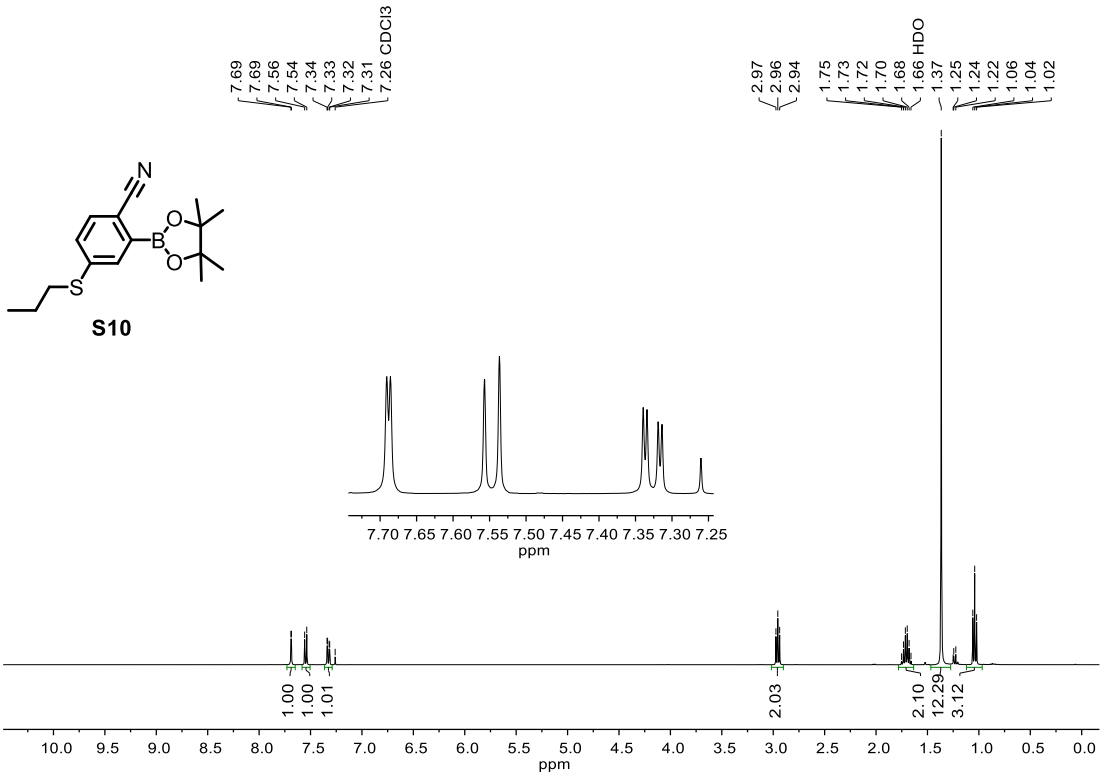

Figure S19. ^{1}H NMR Spectrum (400 MHz, Chloroform-*d*) of **S10**.

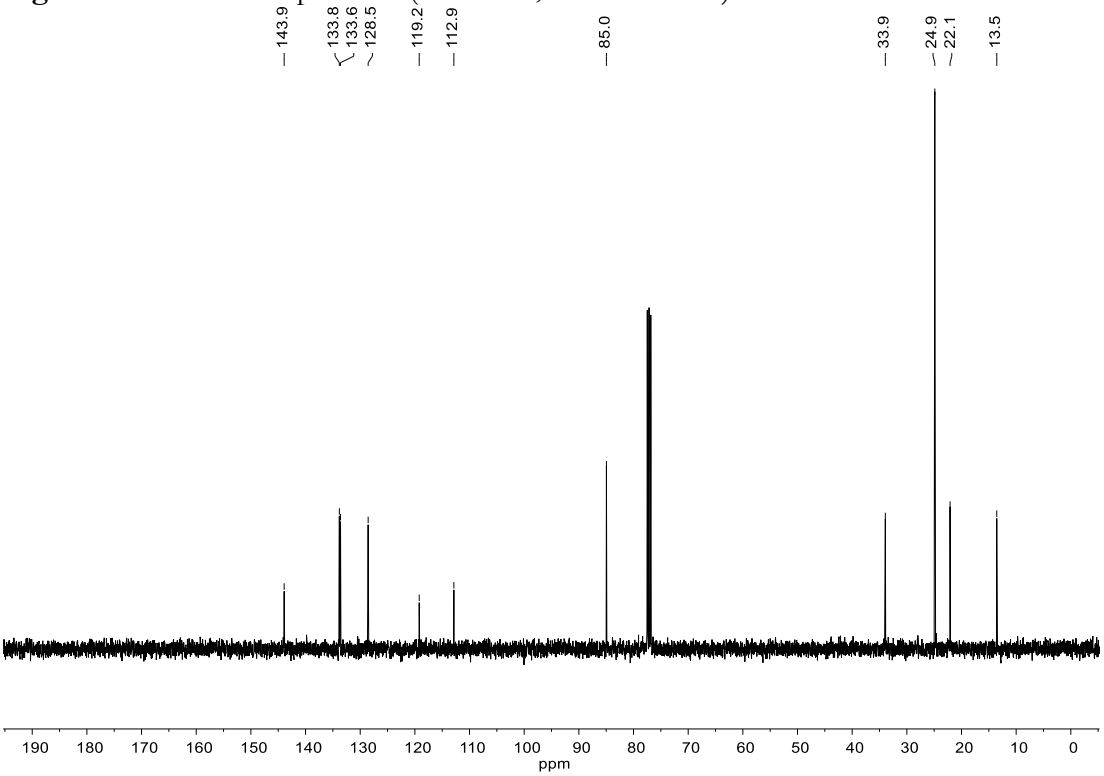

Figure S20. ^{13}C{^{1}H} NMR Spectrum (101 MHz, Chloroform-*d*) of **S10**.

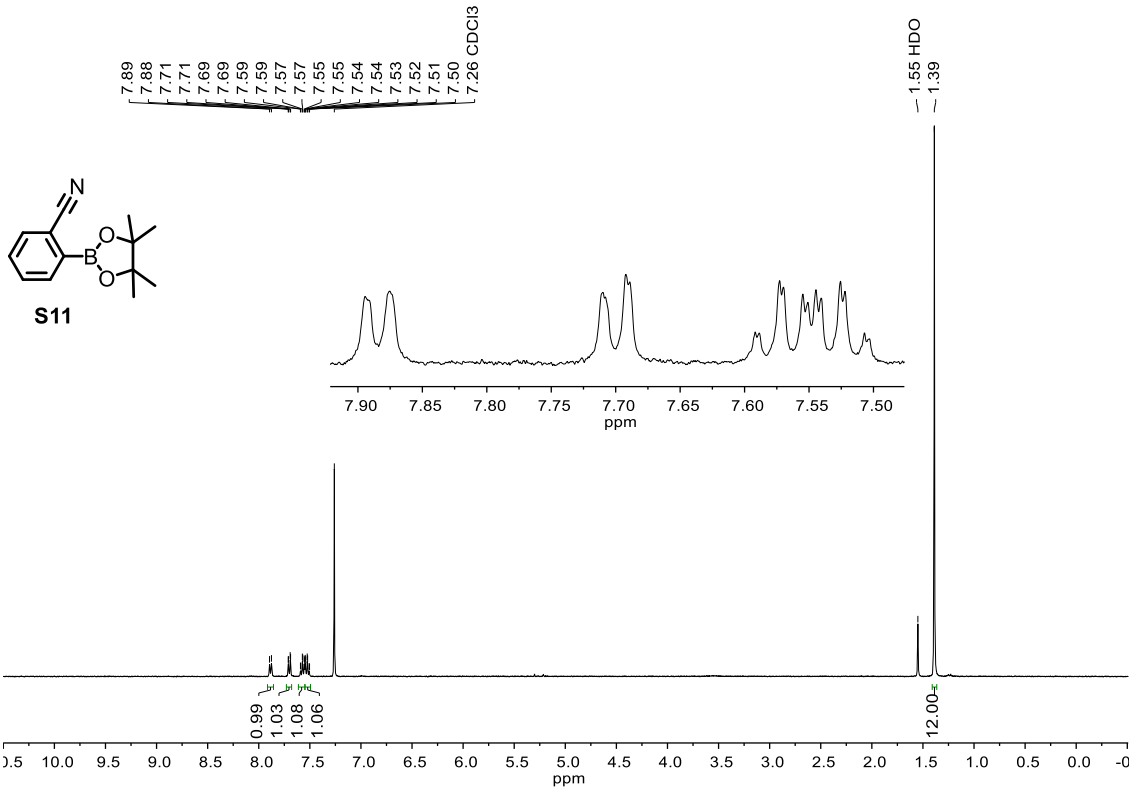

Figure S21. ^{1}H NMR Spectrum (400 MHz, Chloroform-*d*) of **S11**.

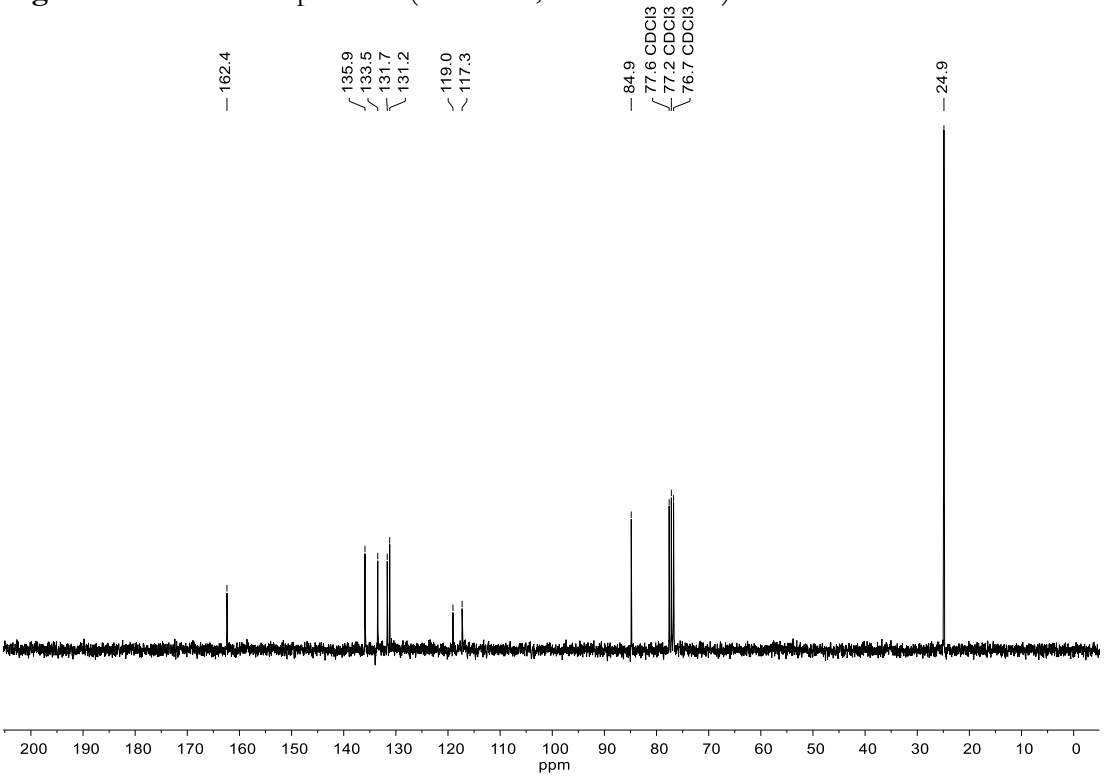

Figure S22. ^{13}C{^{1}H} NMR Spectrum (75 MHz, Chloroform-*d*) of **S11**.

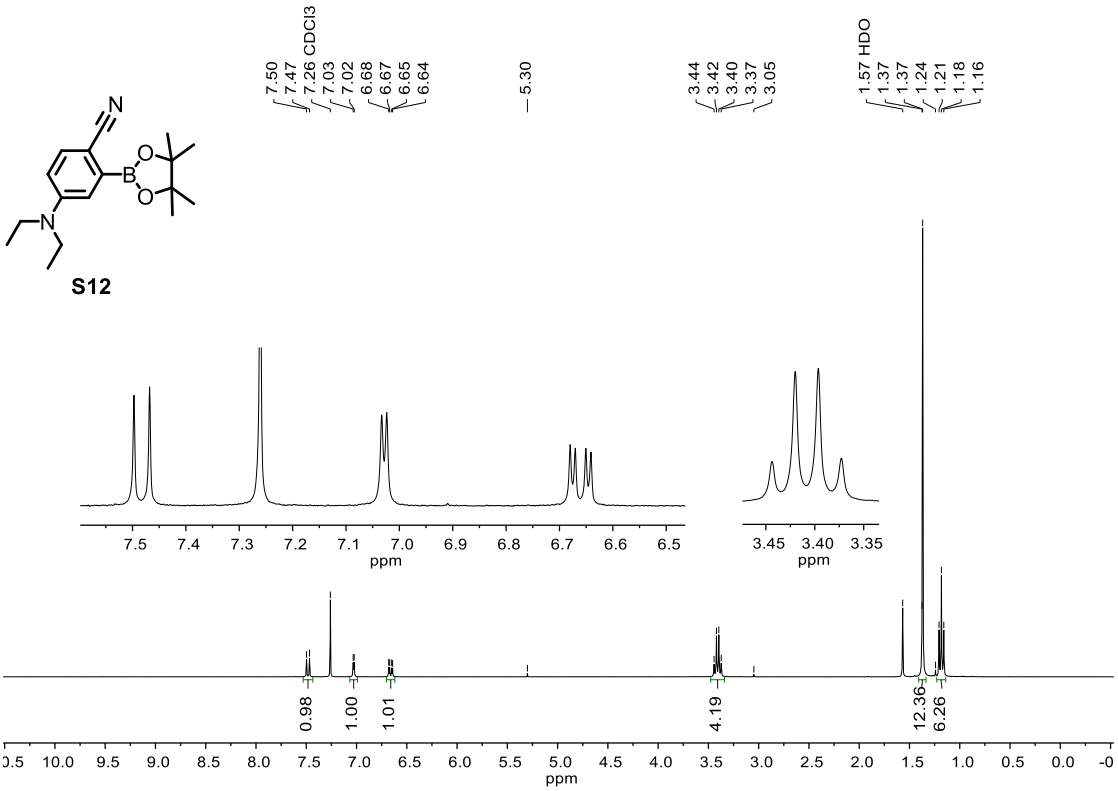

Figure S23. ^{1}H NMR Spectrum (300 MHz, Chloroform-*d*) of **S12**.

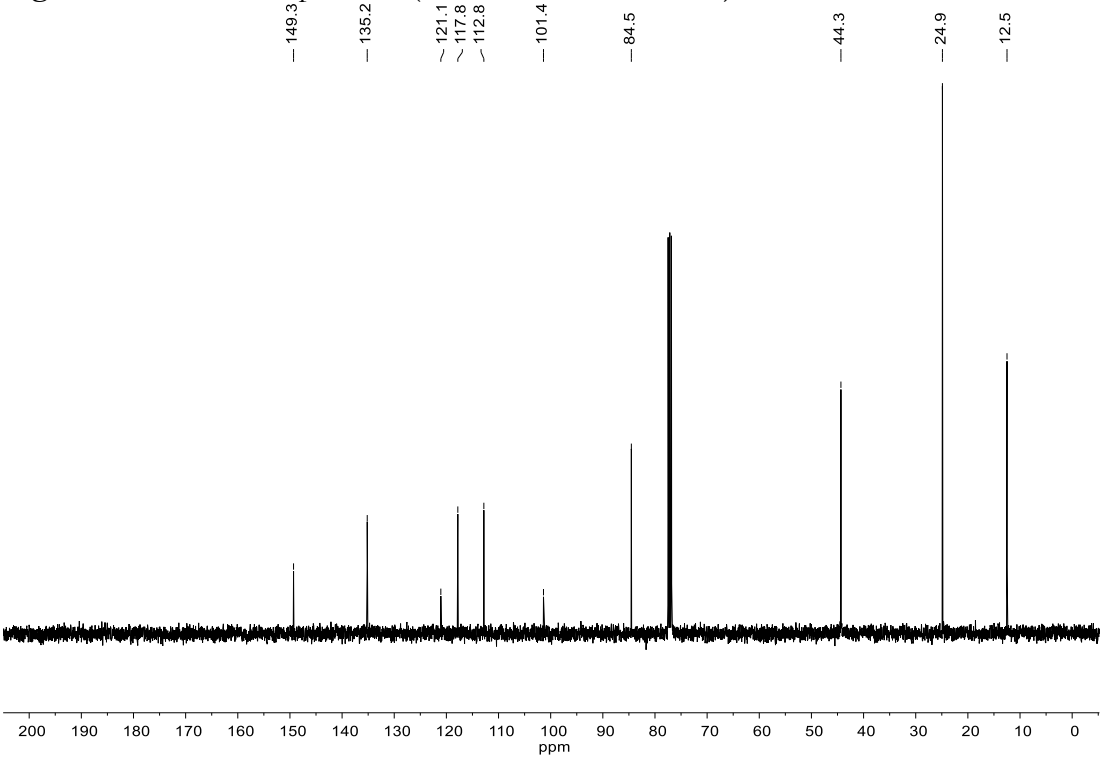

Figure S24. ^{13}C{^{1}H} NMR Spectrum (101 MHz, Chloroform-*d*) of **S12**.

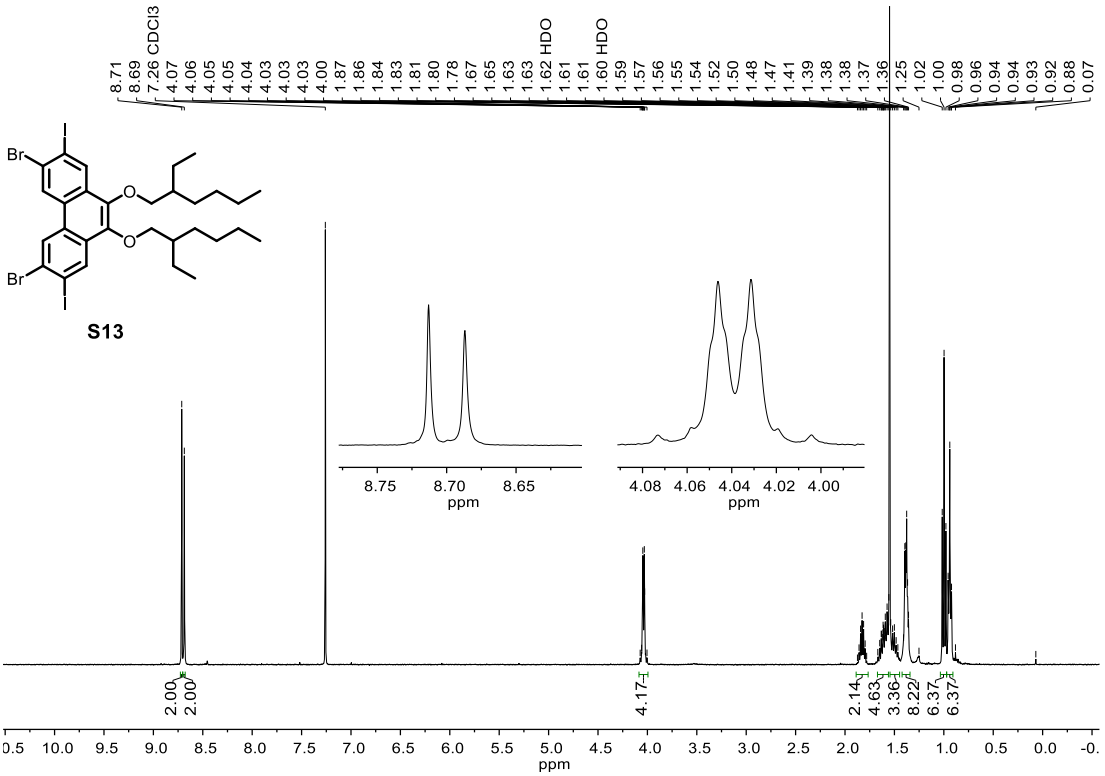

Figure S25. ^{1}H NMR Spectrum (400 MHz, Chloroform-*d*) of **S13**.

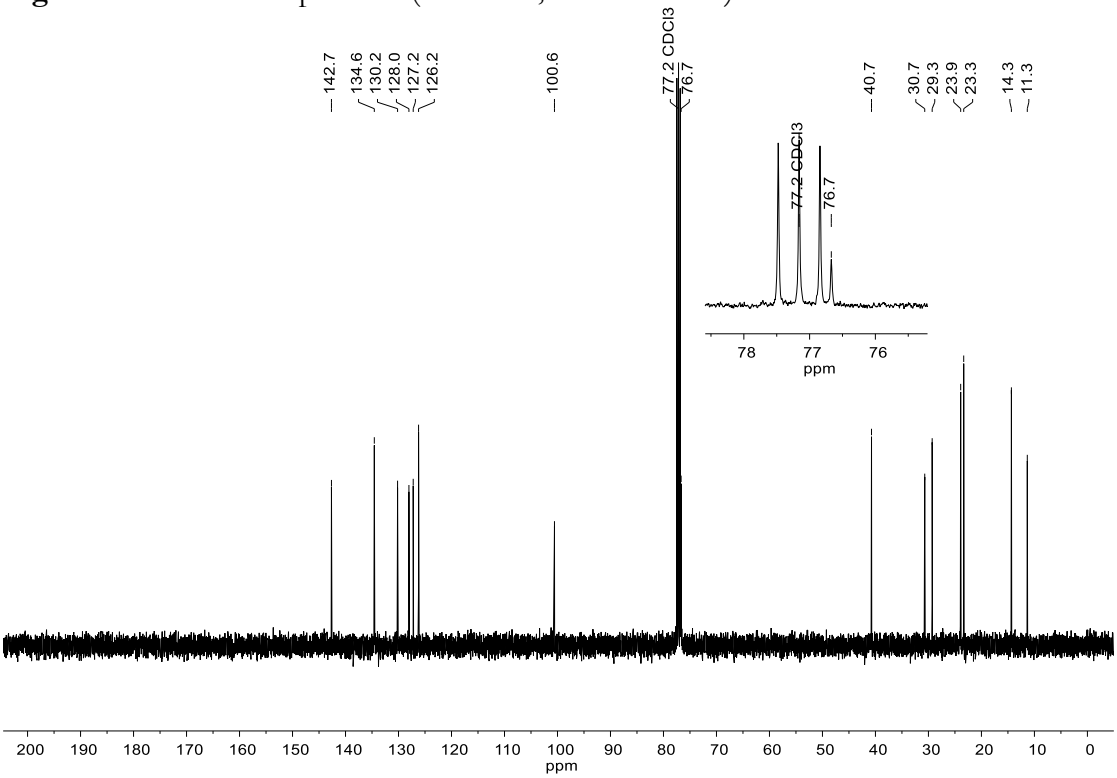

Figure S26. ^{13}C{^{1}H} NMR Spectrum (101 MHz, Chloroform-*d*) of **S13**.

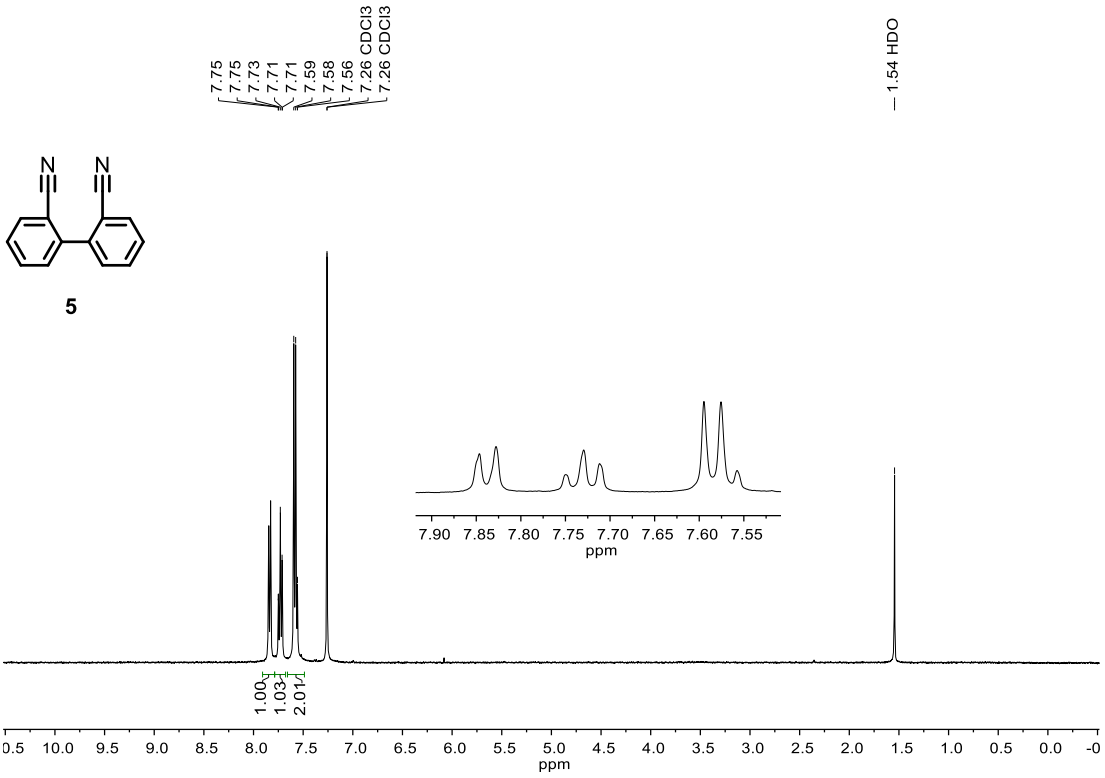

Figure S27. ^{1}H NMR Spectrum (400 MHz, Chloroform-*d*) of **5**.

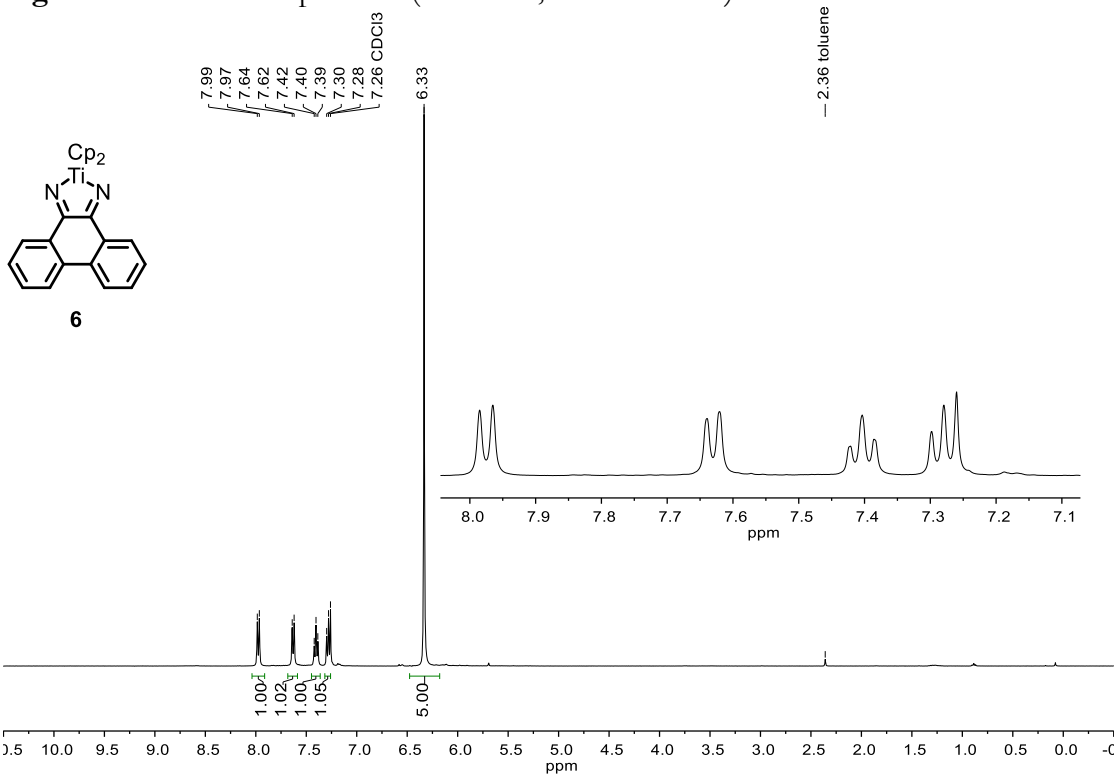

Figure S28. ^{1}H NMR Spectrum (400 MHz, Chloroform-*d*) of **6**.

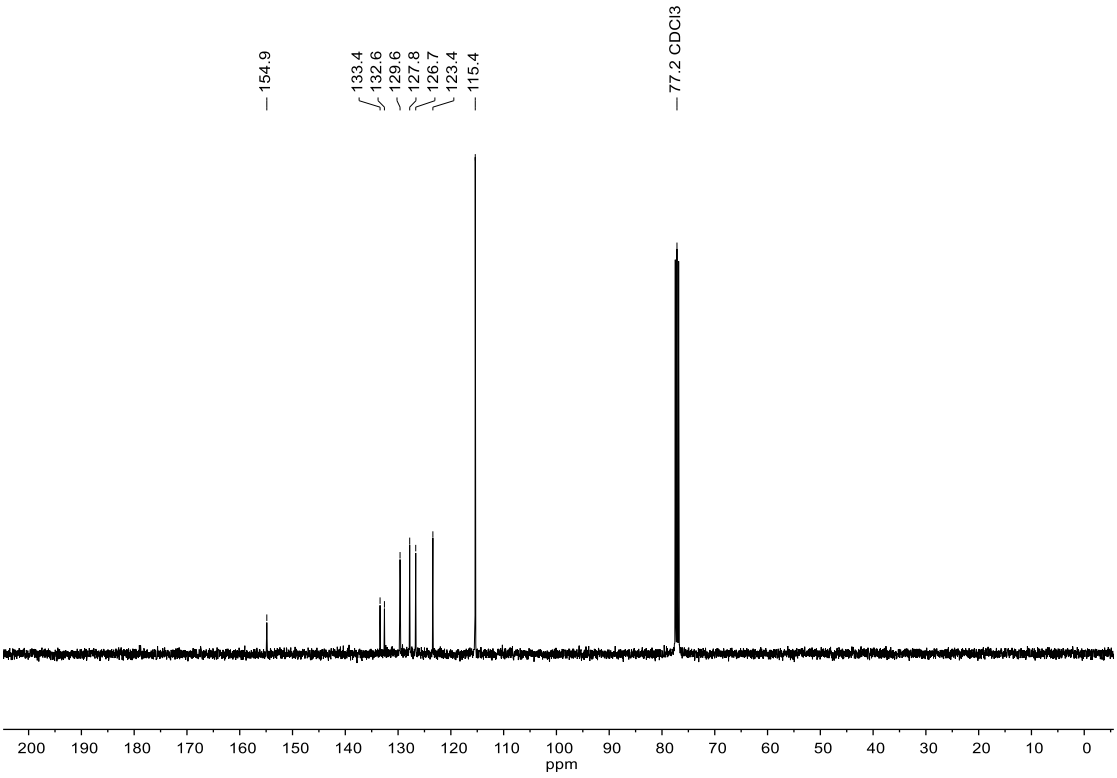

Figure S29. $^{13}C\{^{1}H\}$ NMR Spectrum (101 MHz, Chloroform-*d*) of **6**.

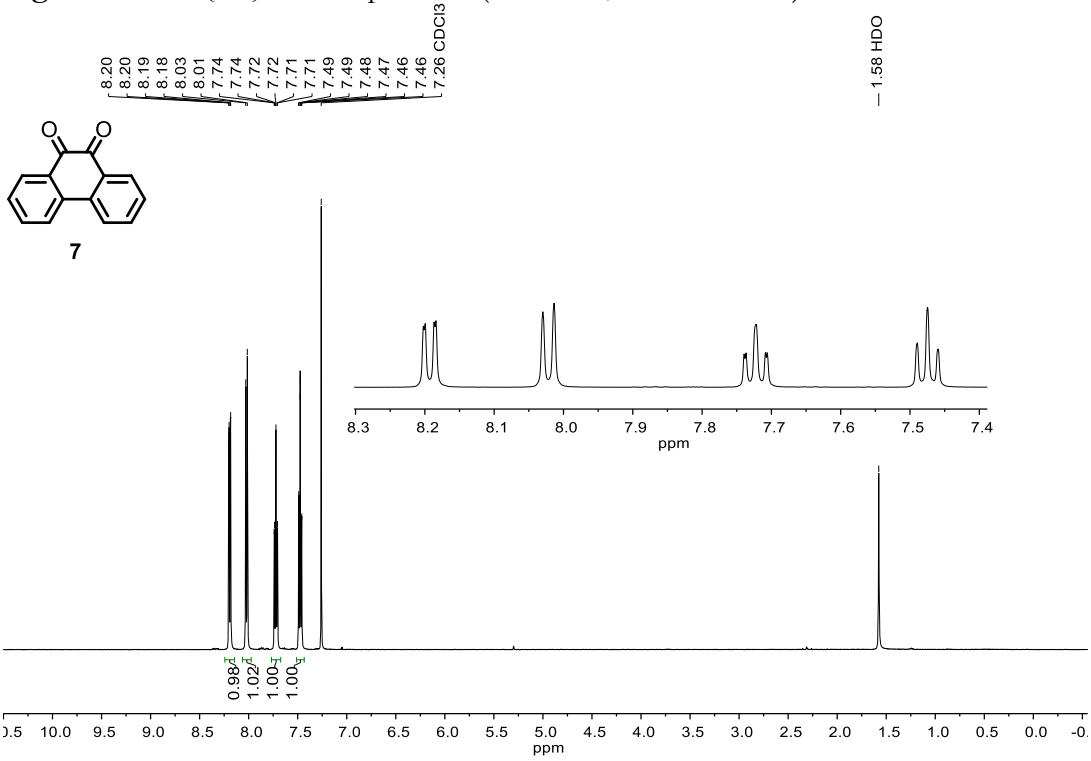

Figure S30. ^{1}H NMR Spectrum (500 MHz, Chloroform-*d*) of **7**.

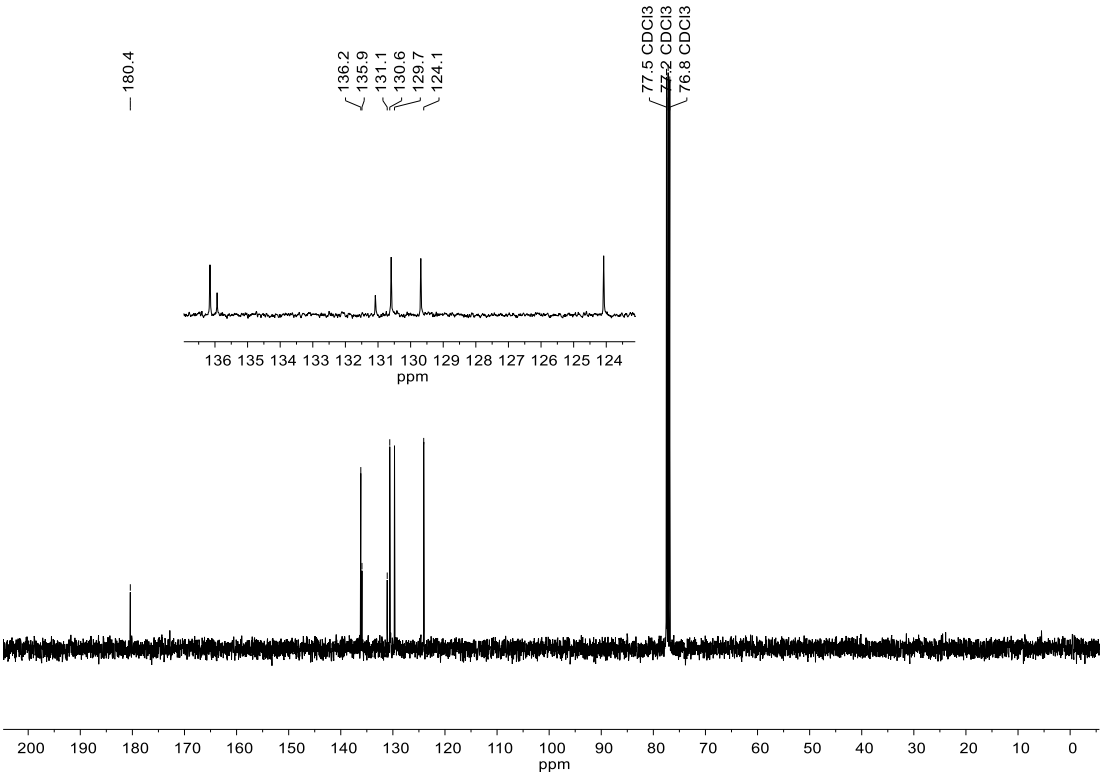

Figure S31. $^{13}C\{^{1}H\}$ NMR Spectrum (151 MHz, Chloroform-*d*) of **7**.

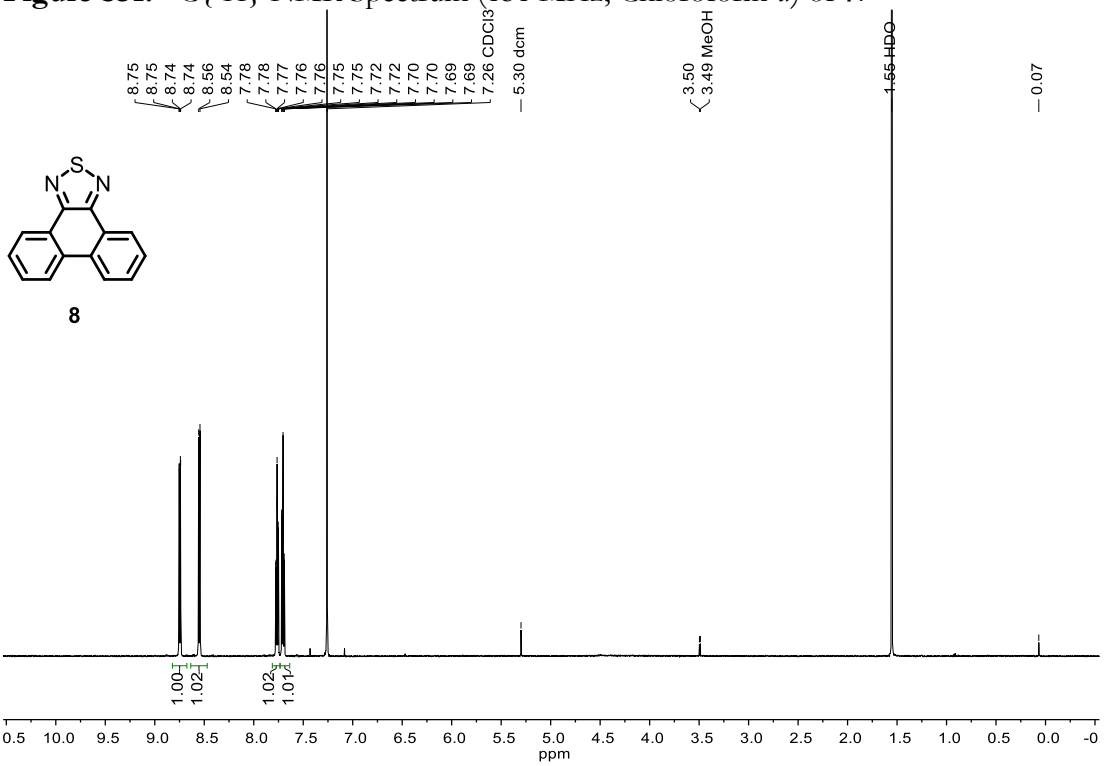

Figure S32. ^{1}H NMR Spectrum (600 MHz, Chloroform-*d*) of **8**.

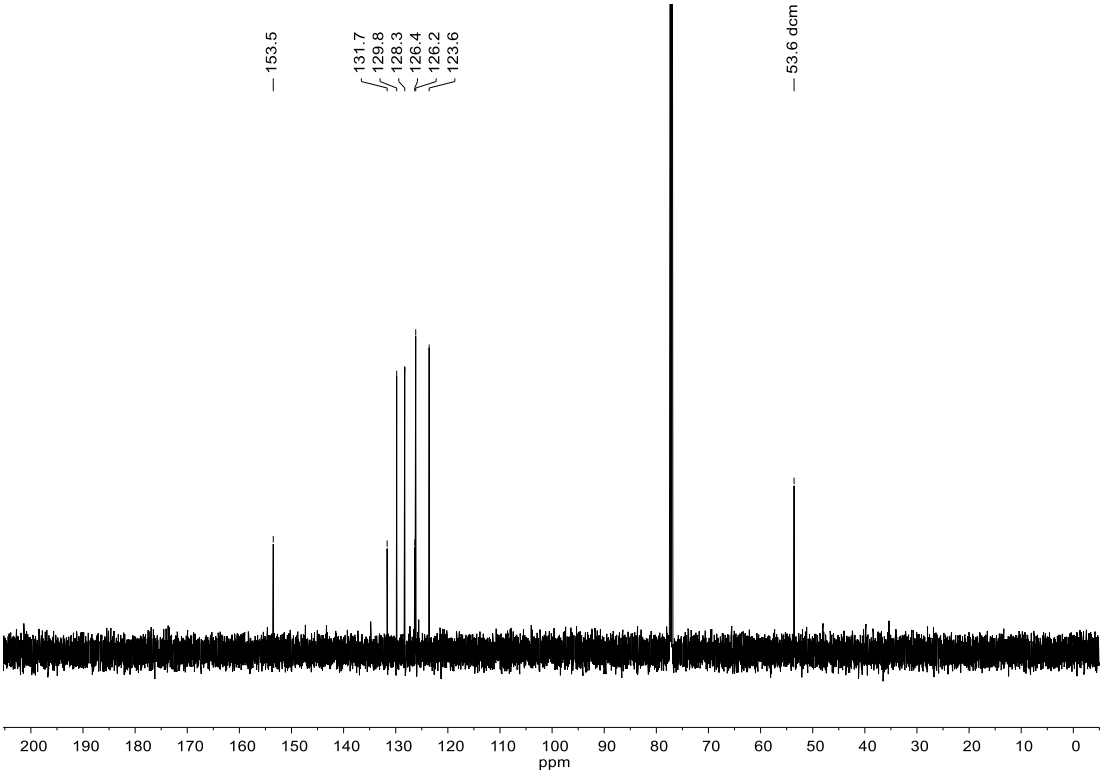

Figure S33. $^{13}C\{^{1}H\}$ NMR Spectrum (151 MHz, Chloroform-*d*) of **8**.

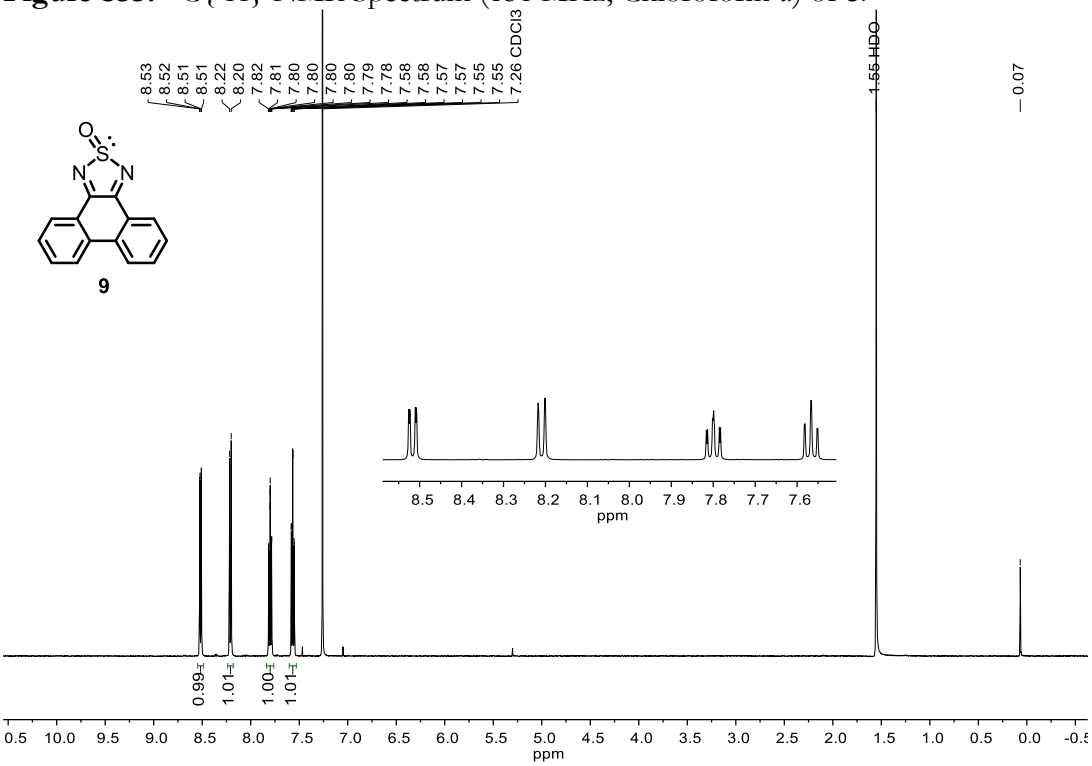

Figure S34. ^{1}H NMR Spectrum (500 MHz, Chloroform-*d*) of **9**.

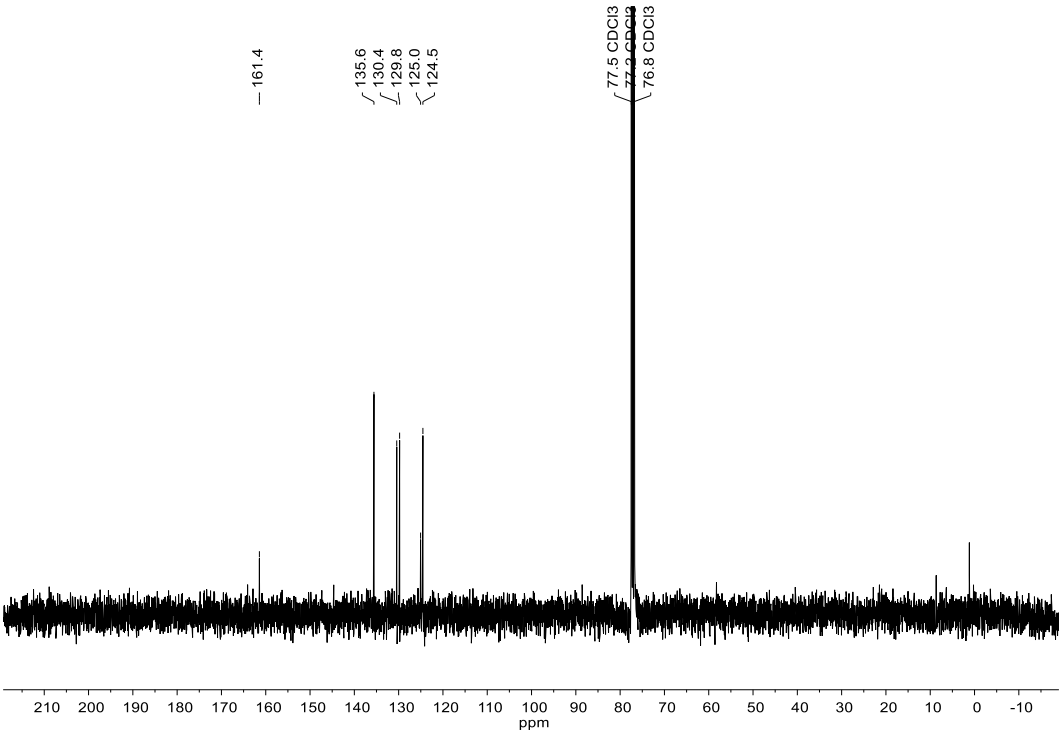

Figure S35. $^{13}C\{^{1}H\}$ NMR Spectrum (101 MHz, Chloroform-*d*) of **9**.

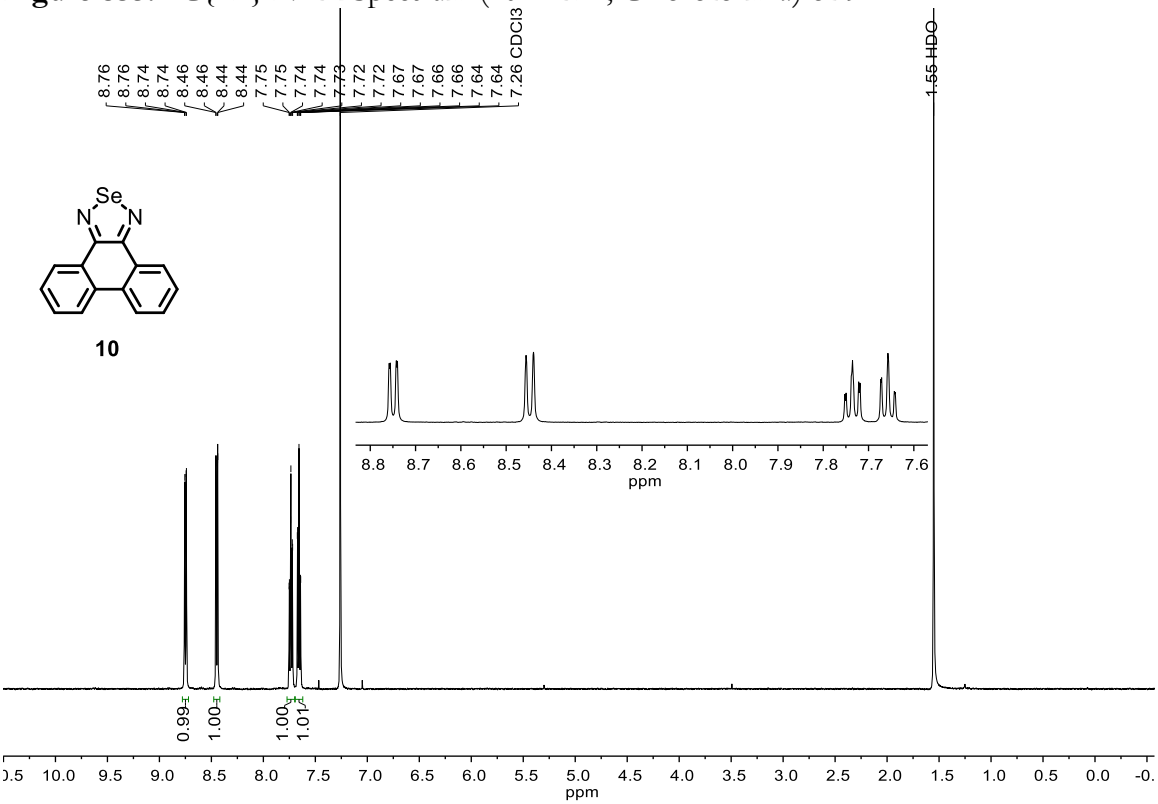

Figure S36. ^{1}H NMR Spectrum (500 MHz, Chloroform-*d*) of **10**.

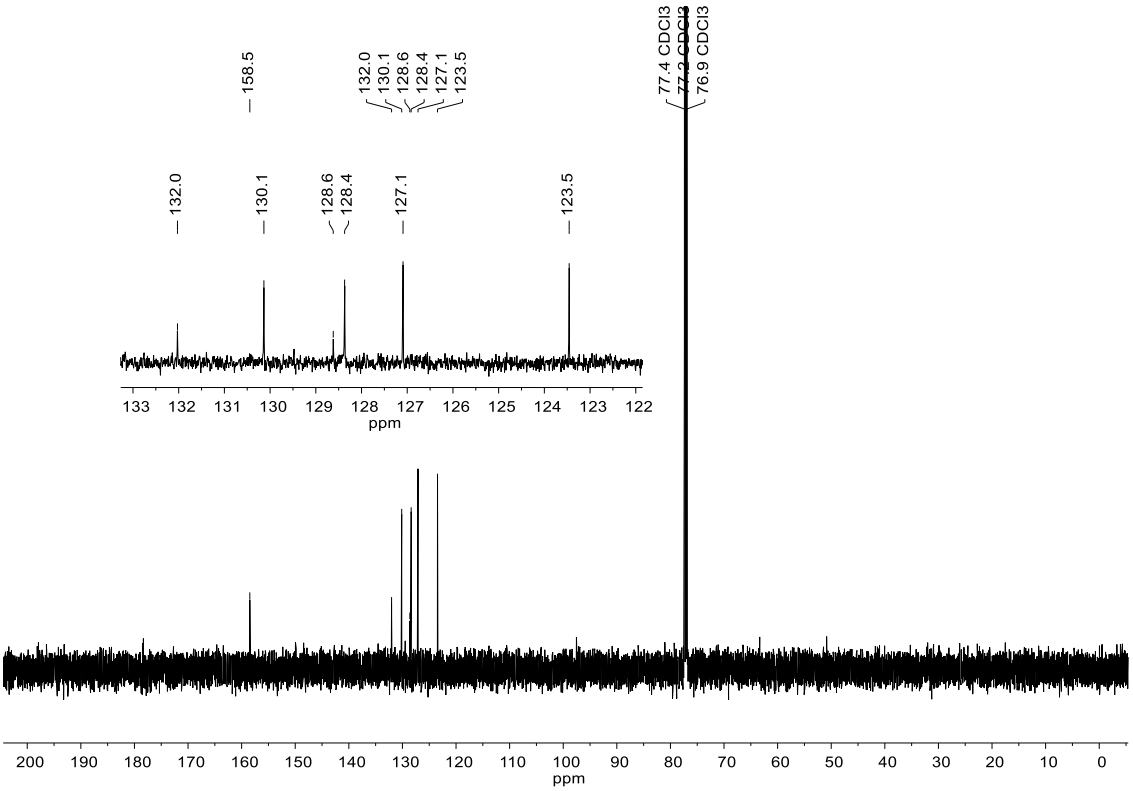

Figure S37. $^{13}C\{^{1}H\}$ NMR Spectrum (151 MHz, Chloroform-*d*) of **10**.

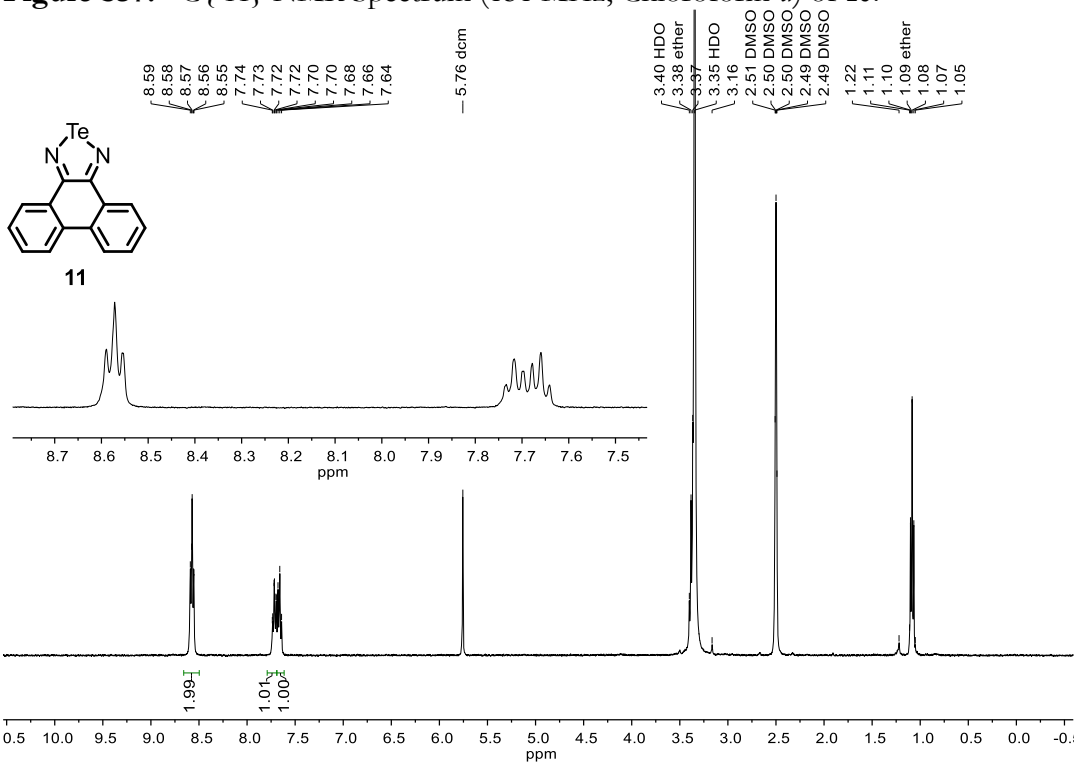

Figure S38. ^{1}H NMR Spectrum (400 MHz, dimethyl sulfoxide-d_6) of **11**.

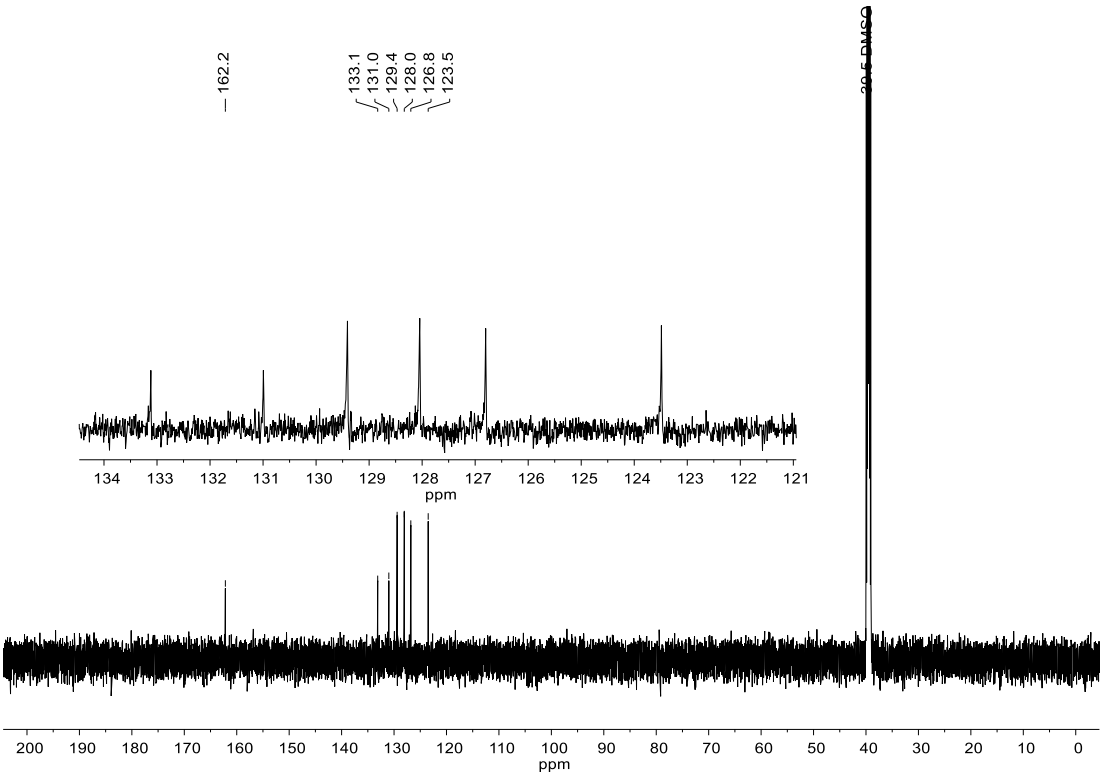

Figure S39. $^{13}C\{^{1}H\}$ NMR Spectrum (151MHz, dimethyl sulfoxide-d_6) of **11**.

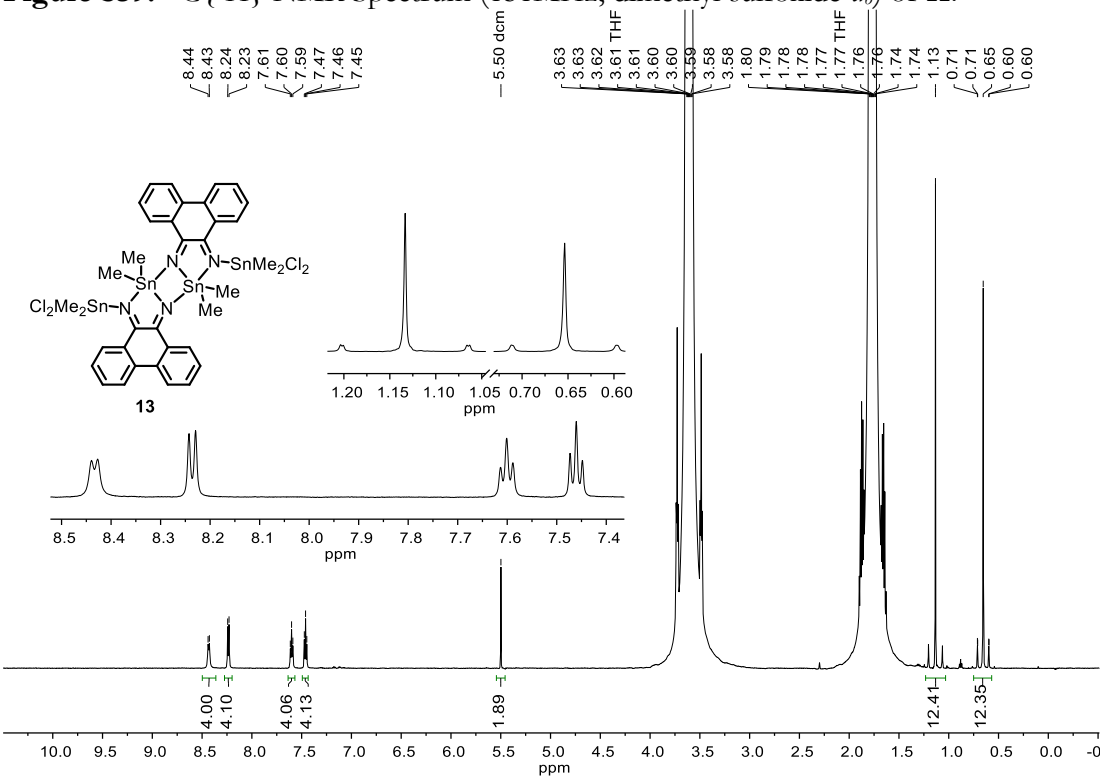

Figure S40. ^{1}H NMR Spectrum (600 MHz, tetrahydrofuran) of **13**.

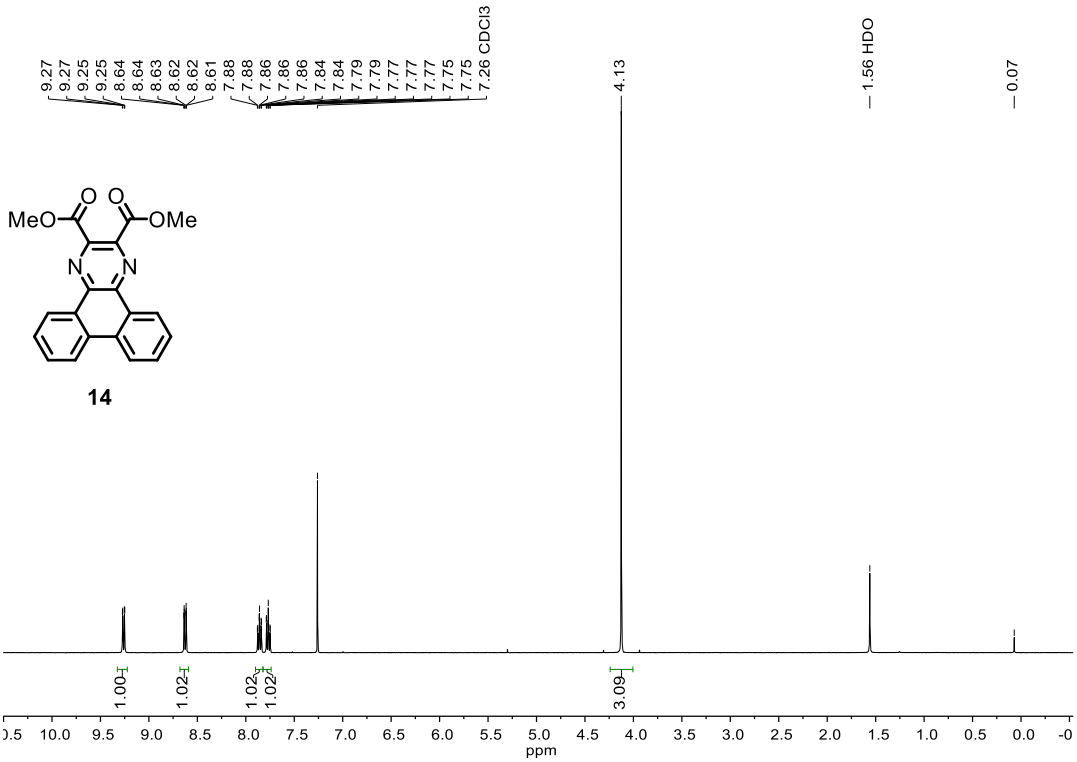

Figure S41. ^{1}H NMR Spectrum (400 MHz, Chloroform-*d*) of **14**.

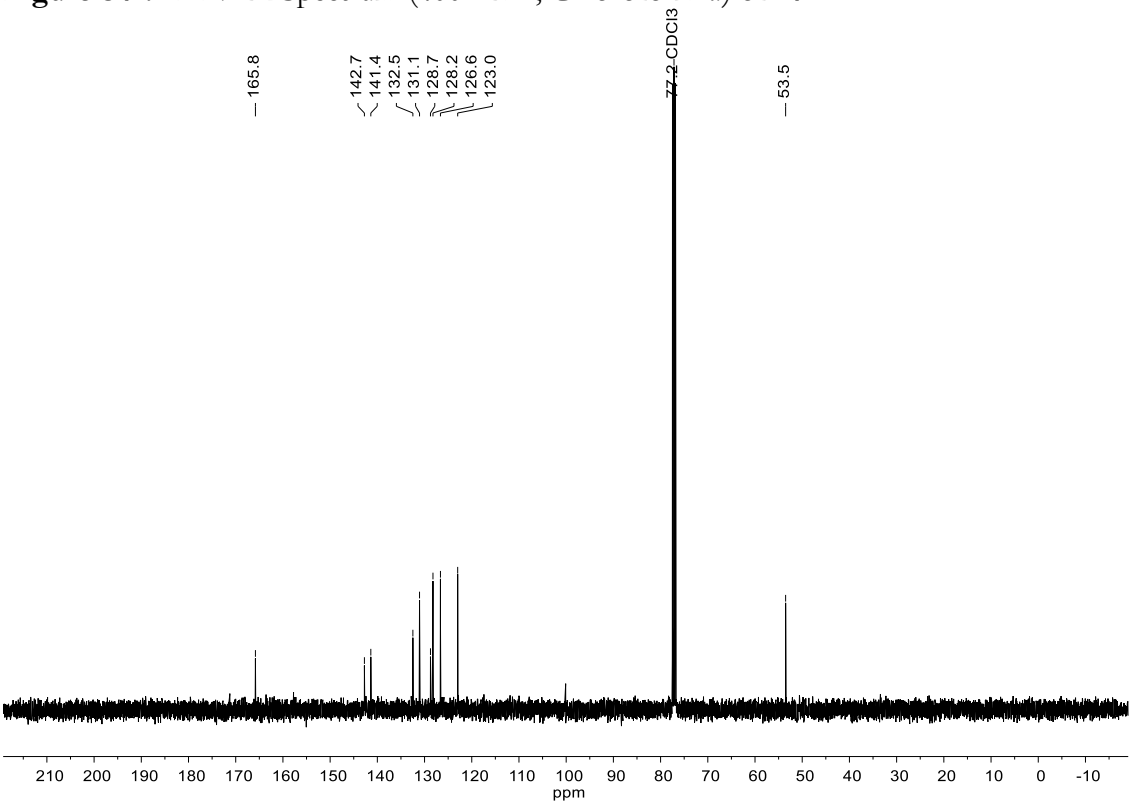

Figure S42. ^{13}C{^{1}H} NMR Spectrum (101 MHz, Chloroform-*d*) of **14**.

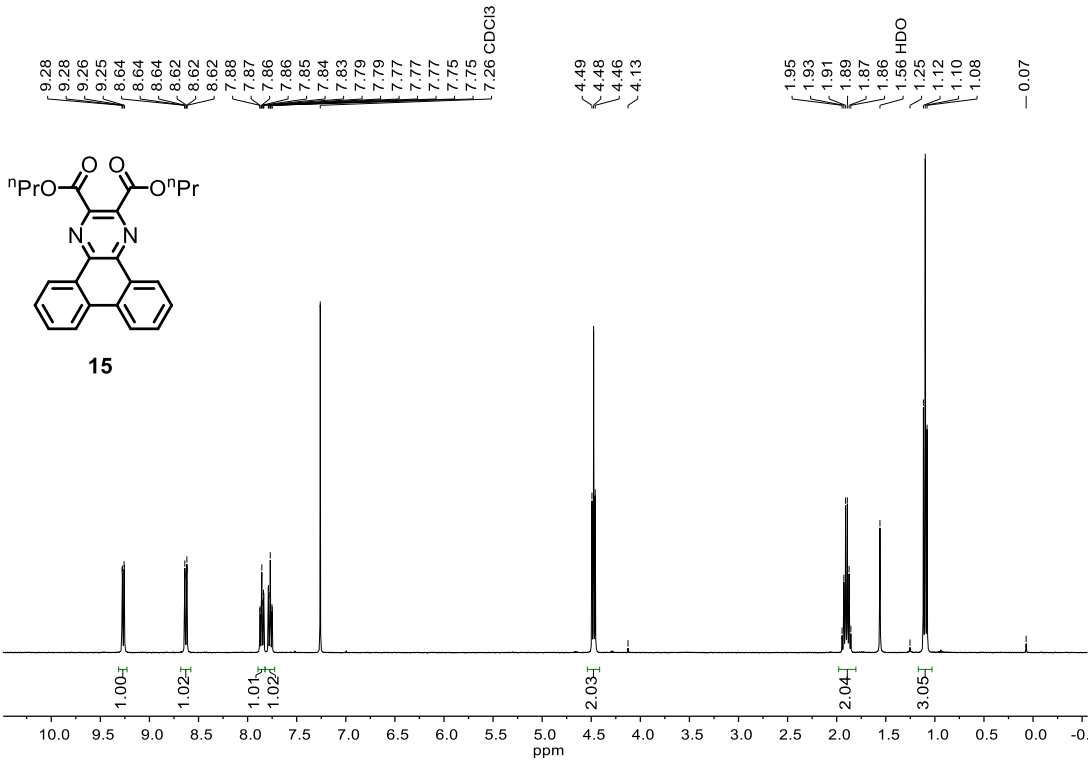

Figure S43. ^{1}H NMR Spectrum (400 MHz, Chloroform-*d*) of **15**.

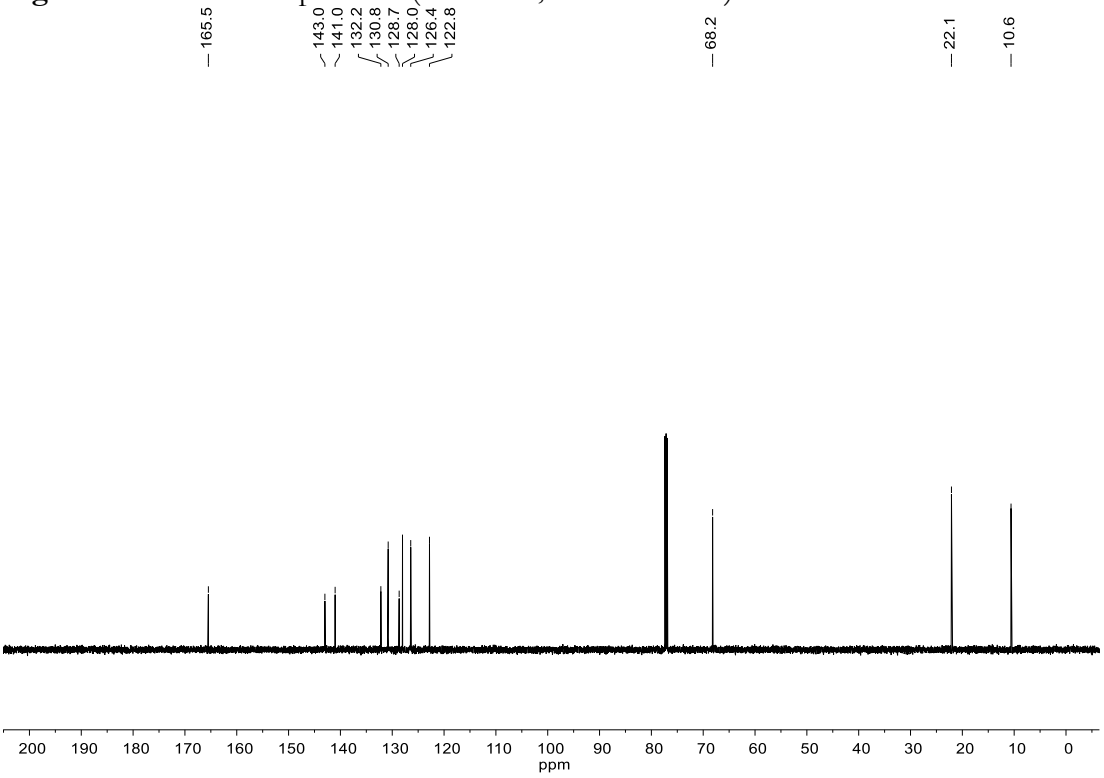

Figure S44. ^{13}C{^{1}H} NMR Spectrum (151 MHz, Chloroform-*d*) of **15**.

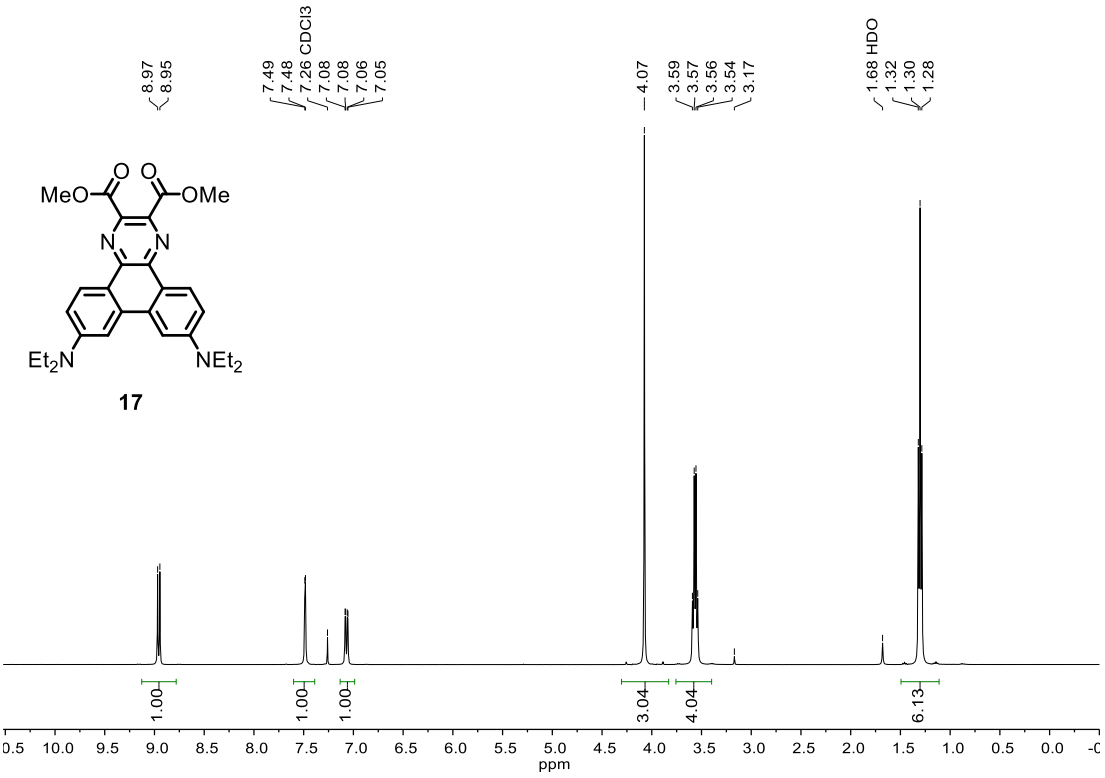

Figure S45. ^{1}H NMR Spectrum (400 MHz, Chloroform-*d*) of **17**.

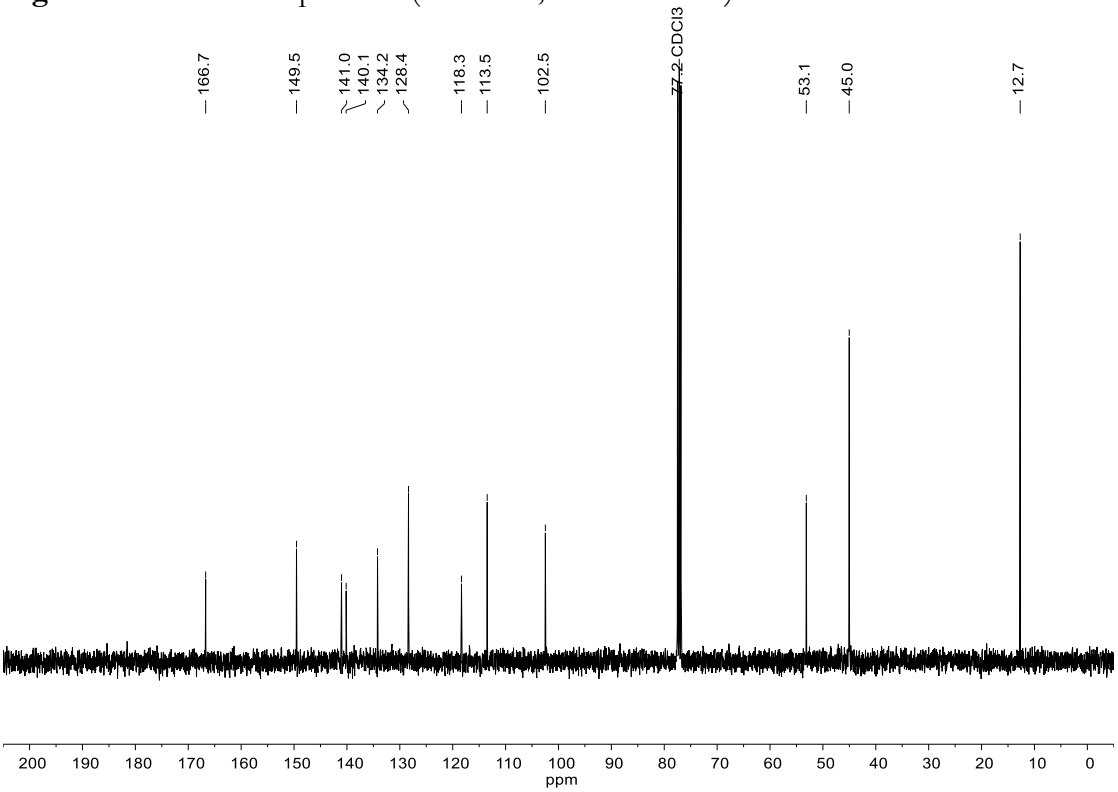

Figure S46. ^{13}C{^{1}H} NMR Spectrum (101 MHz, Chloroform-*d*) of **17**.

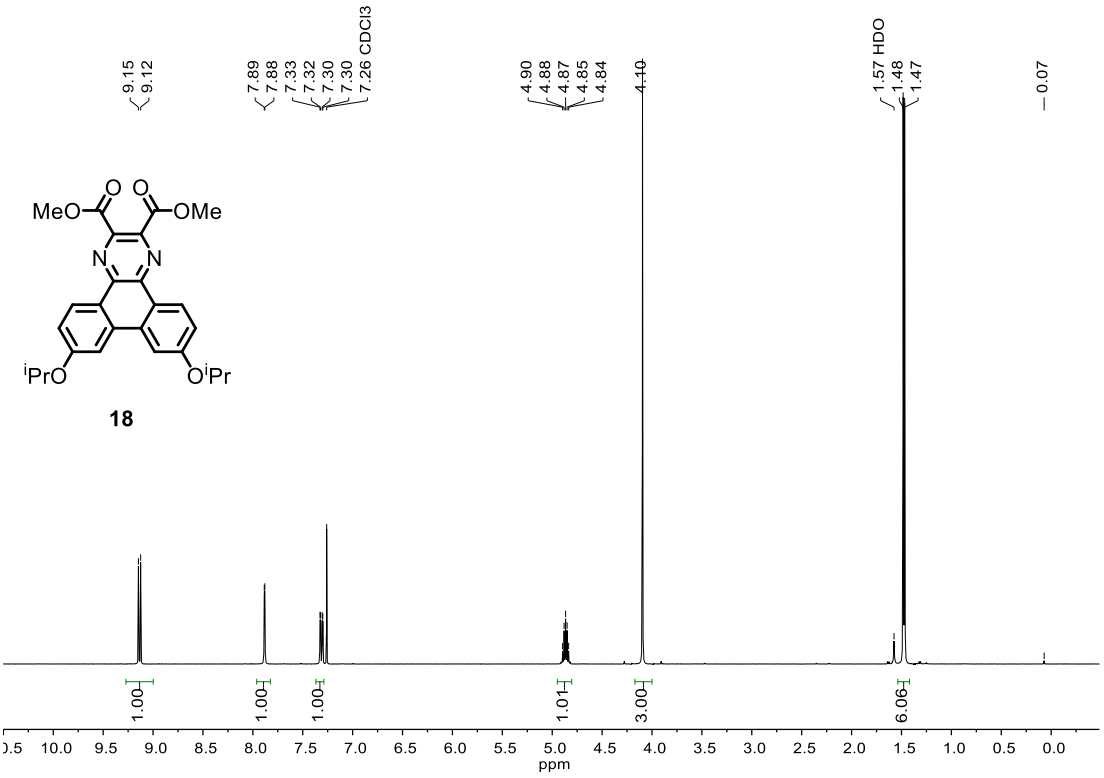

Figure S47. ^{1}H NMR Spectrum (400 MHz, Chloroform-*d*) of **18**.

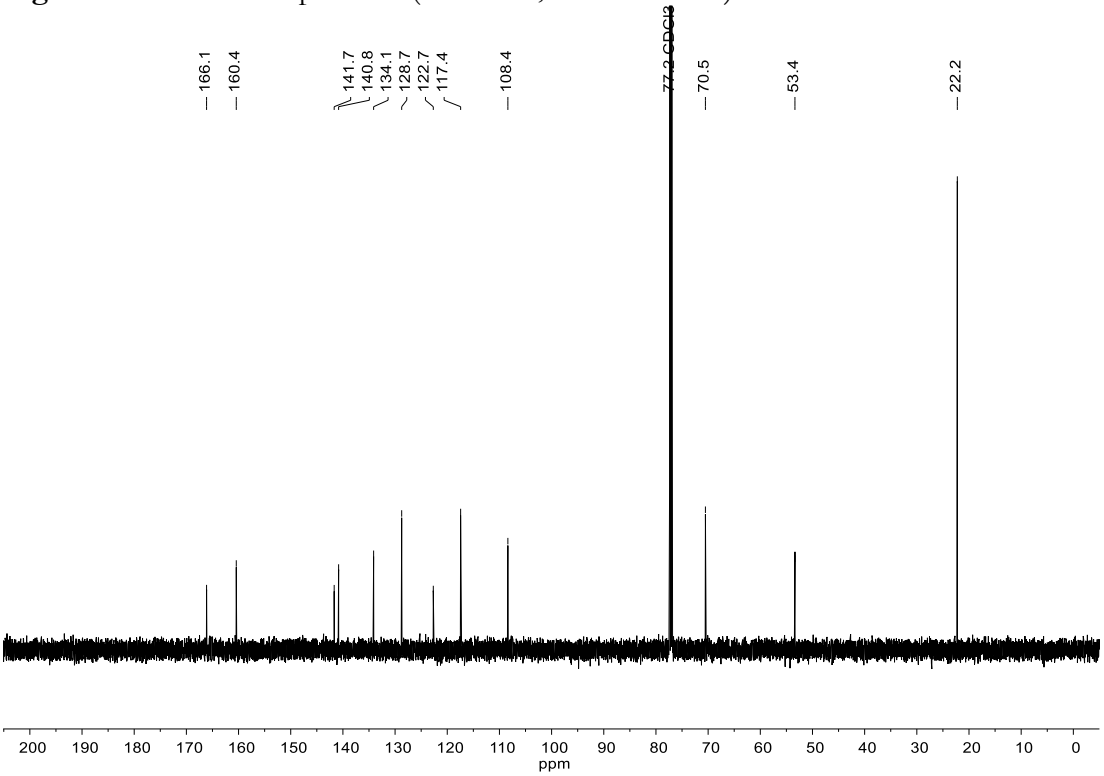

Figure S48. ^{13}C{^{1}H} NMR Spectrum (151 MHz, Chloroform-*d*) of **18**.

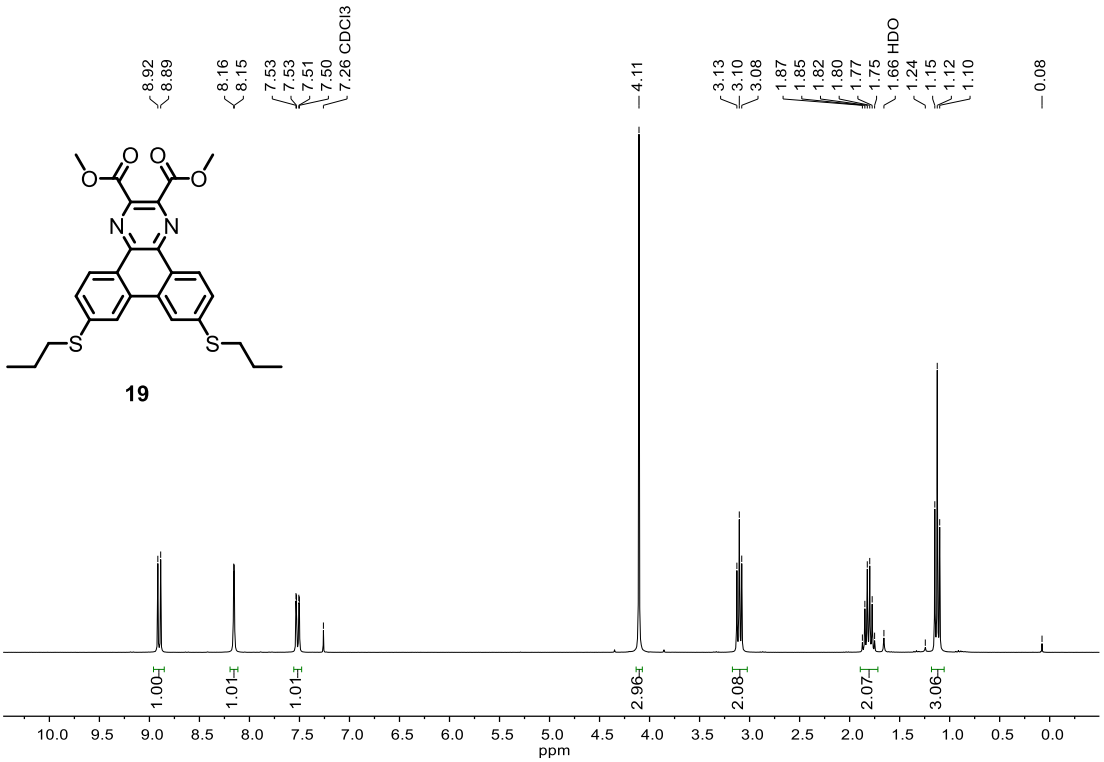

Figure S49. ^{1}H NMR Spectrum (300 MHz, Chloroform-*d*) of **19**.

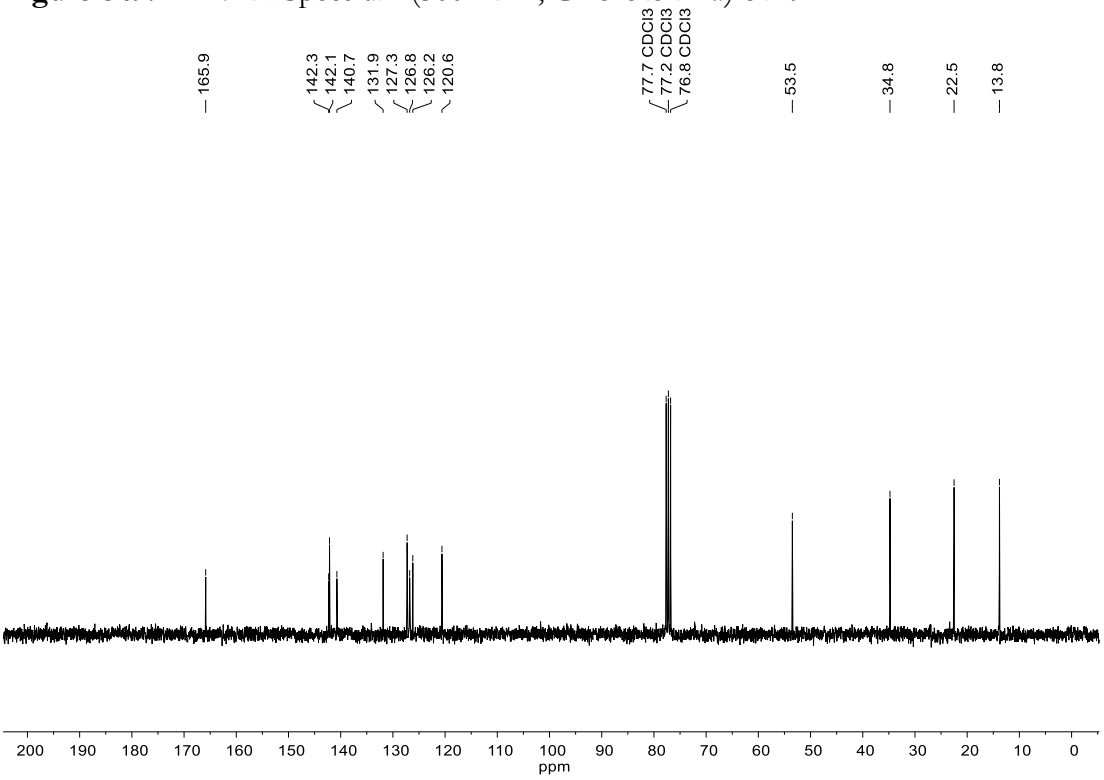

Figure S50. ^{13}C{^{1}H} NMR Spectrum (75 MHz, Chloroform-*d*) of **19**.

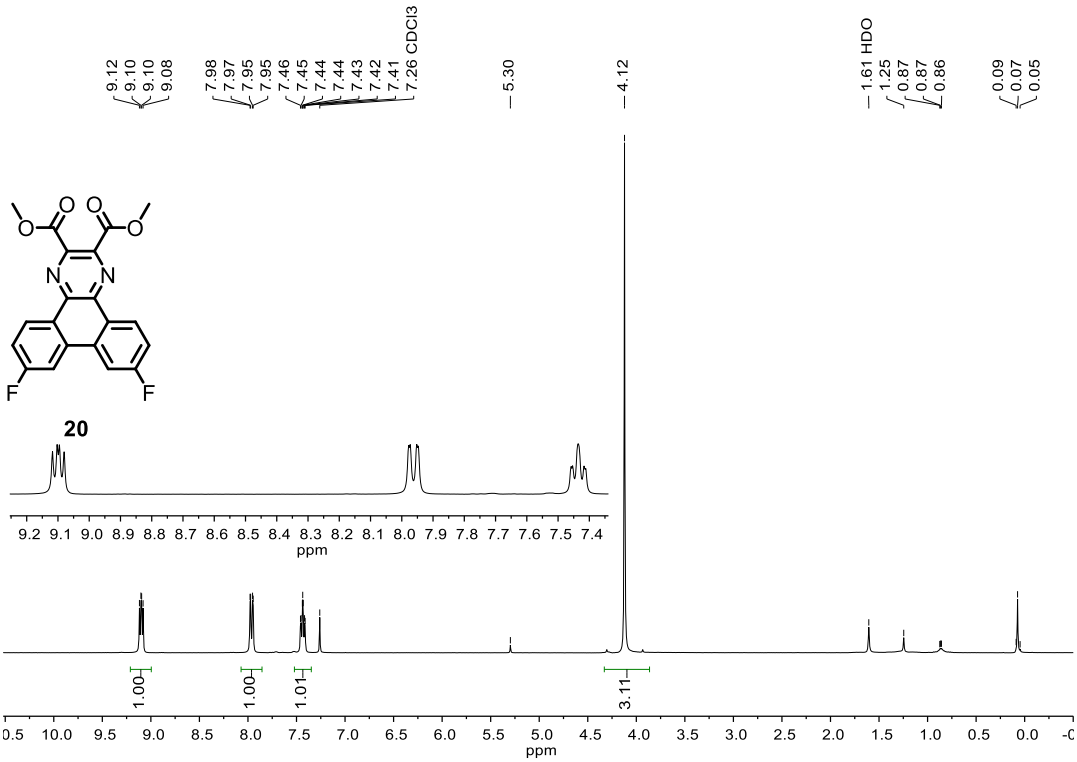

Figure S51. ^{1}H NMR Spectrum (400 MHz, Chloroform-*d*) of **20**.

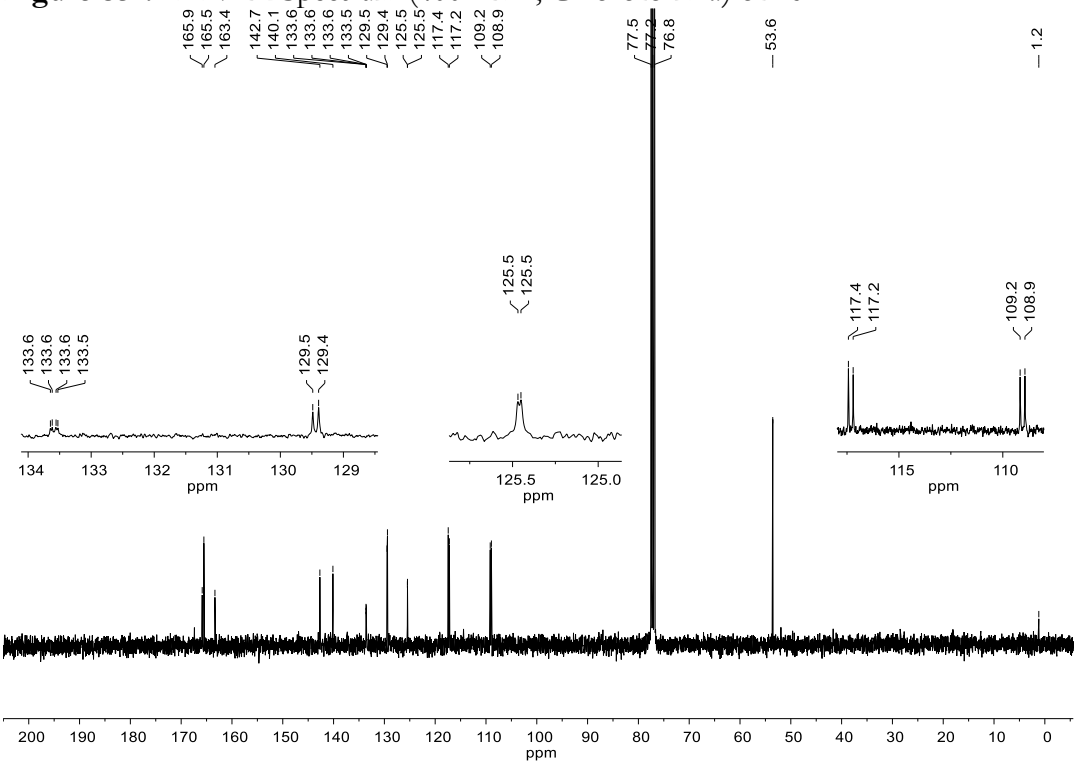

Figure S52. ^{13}C{^{1}H} NMR Spectrum (101 MHz, Chloroform-*d*) of **20**.

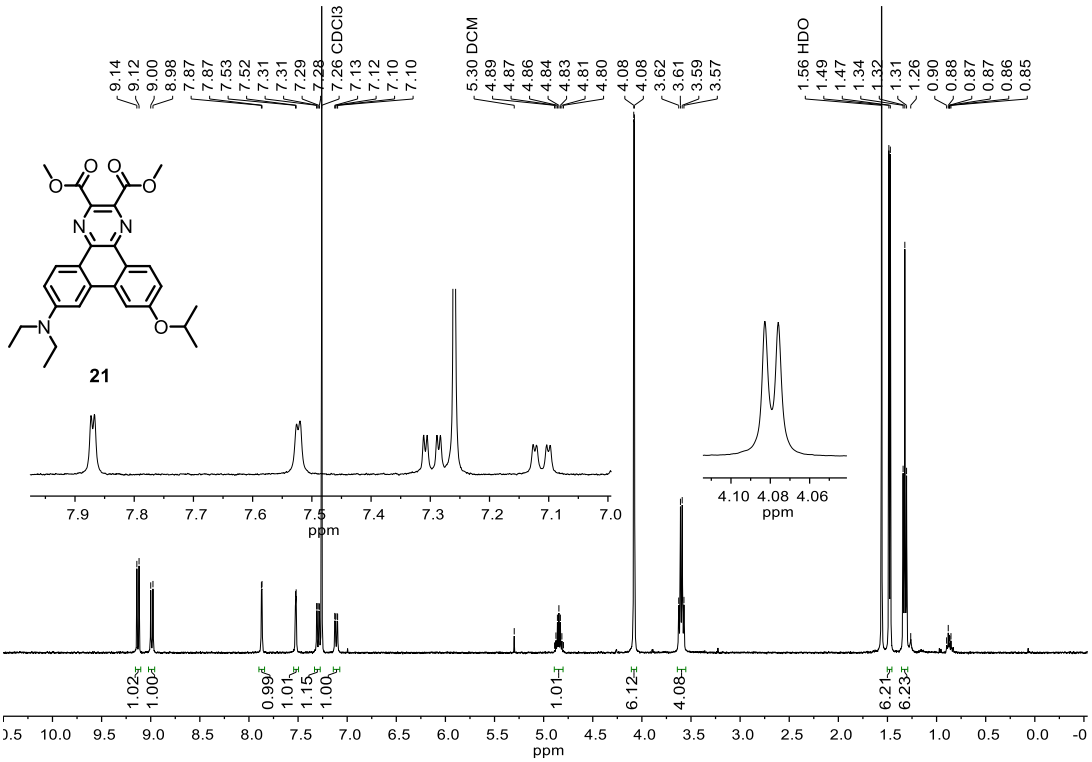

Figure S53. ^{1}H NMR Spectrum (400 MHz, Chloroform-*d*) of **21**.

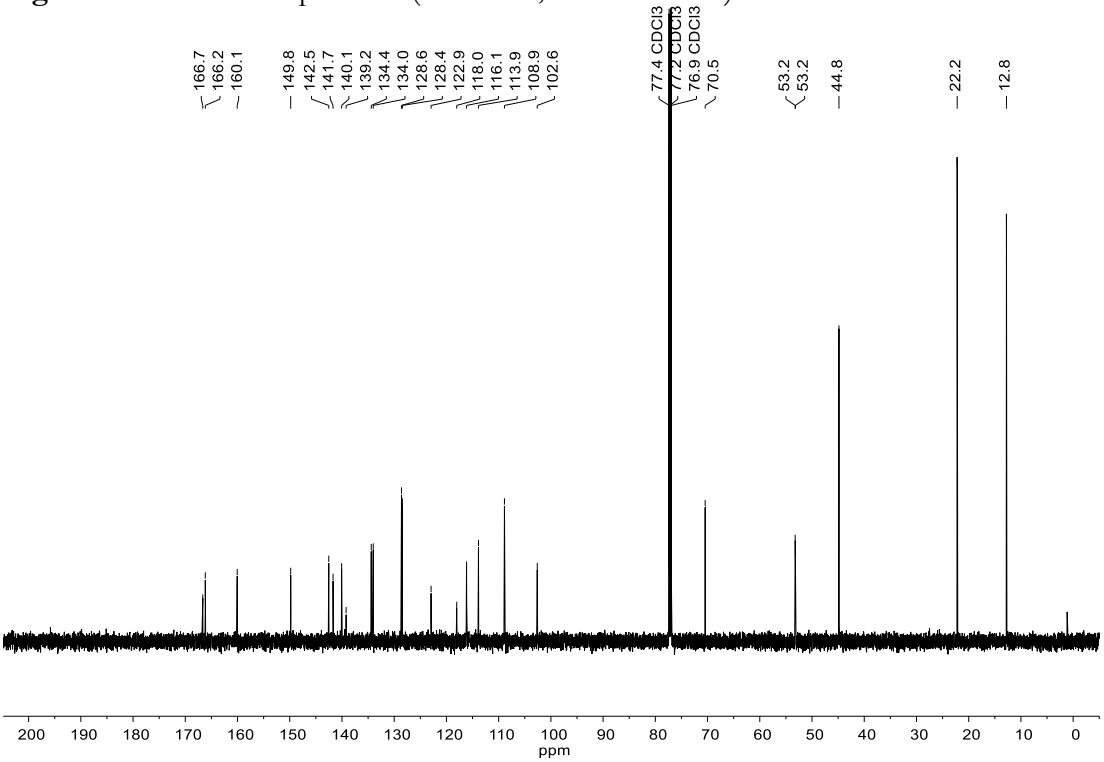

Figure S54. ^{13}C{^{1}H} NMR Spectrum (151 MHz, Chloroform-*d*) of **21**.

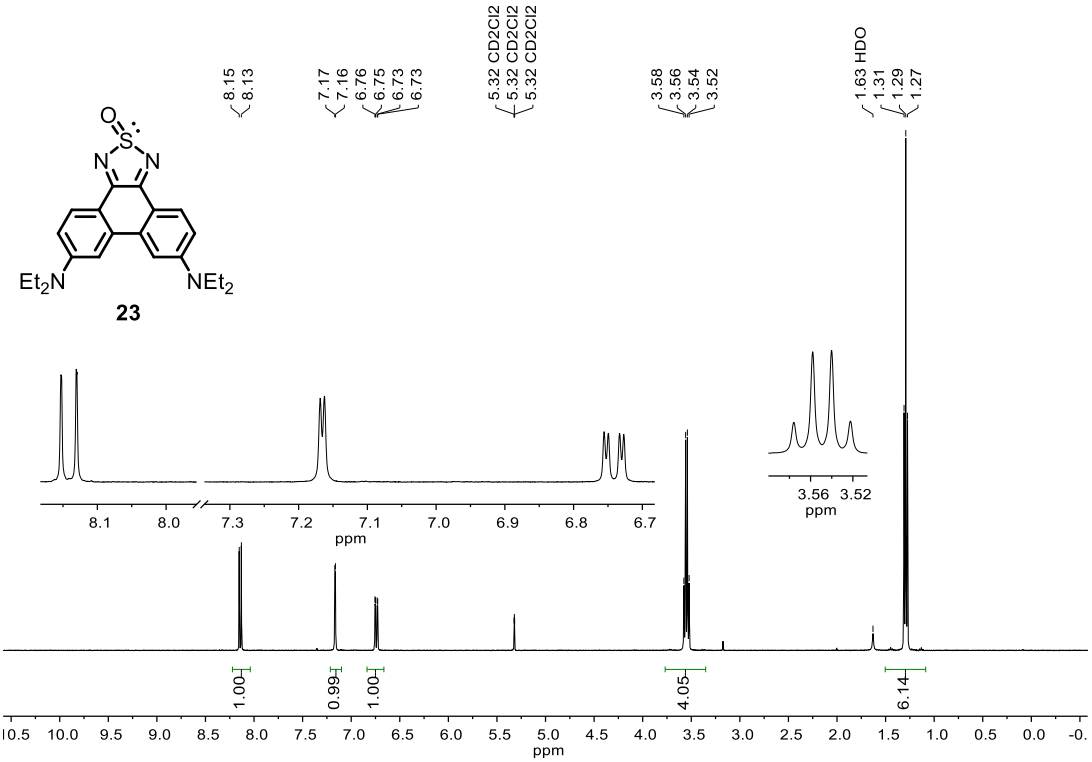

Figure S55. ^{1}H NMR Spectrum (400 MHz, dichloromethane-d_2) of **23**.

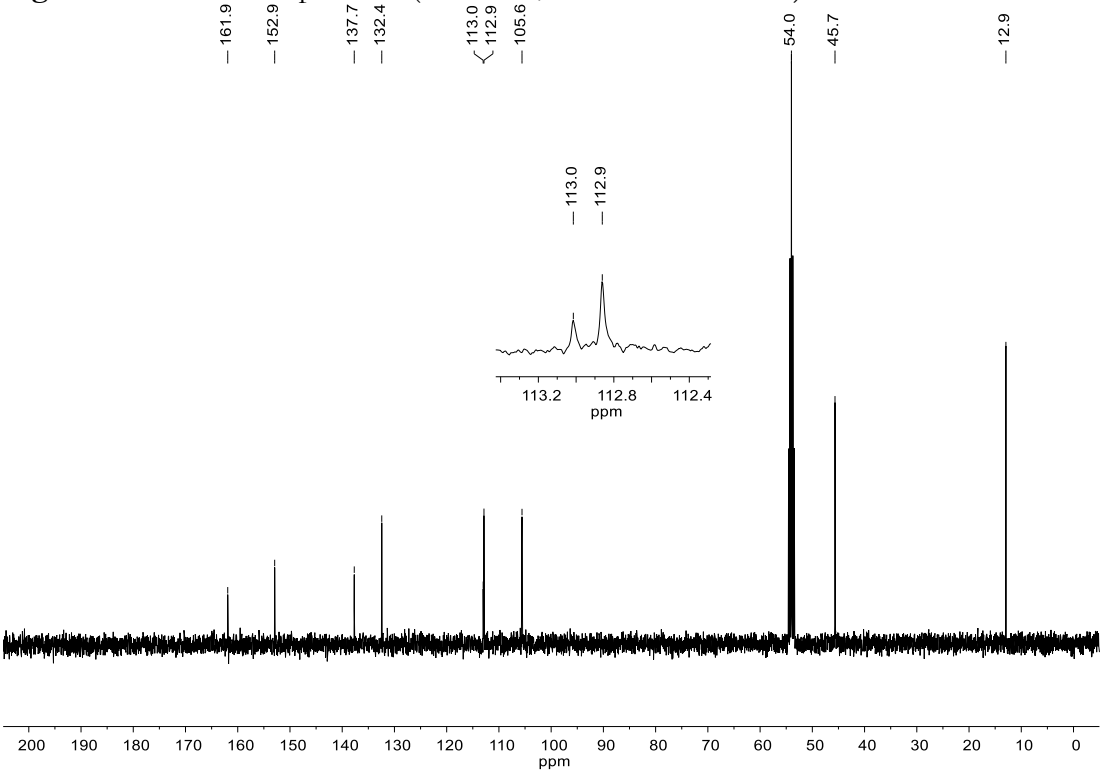

Figure S56. ^{13}C{^{1}H} NMR Spectrum (101 MHz, dichloromethane-d_2) of **23**.

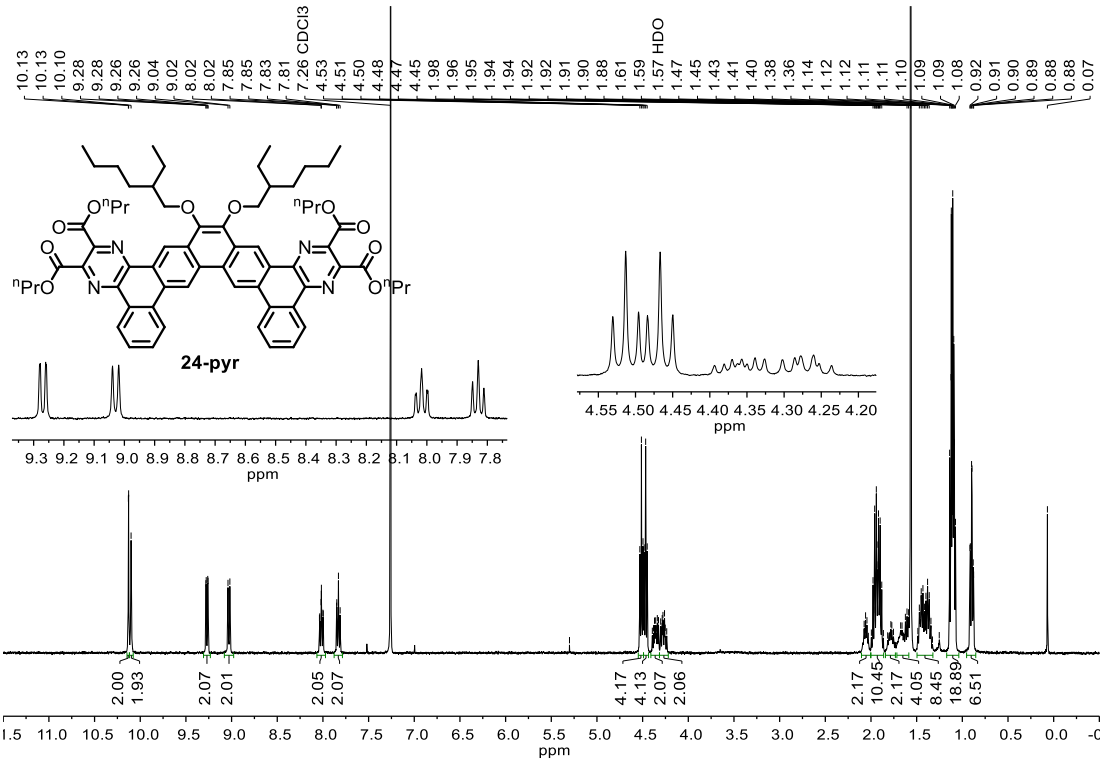

Figure S57. ^{1}H NMR Spectrum (400 MHz, Chloroform-*d*) of **24-pyr**.

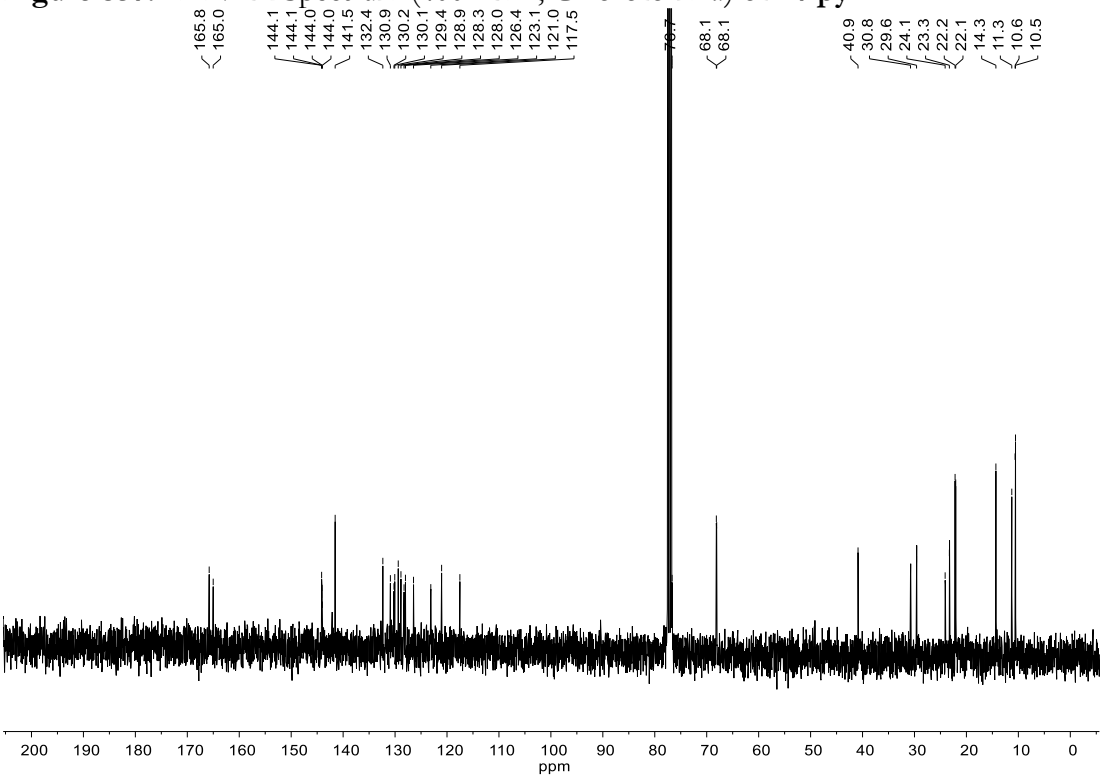

Figure S58. ^{13}C{^{1}H} NMR Spectrum (101 MHz, Chloroform-*d*) of **24-pyr**.

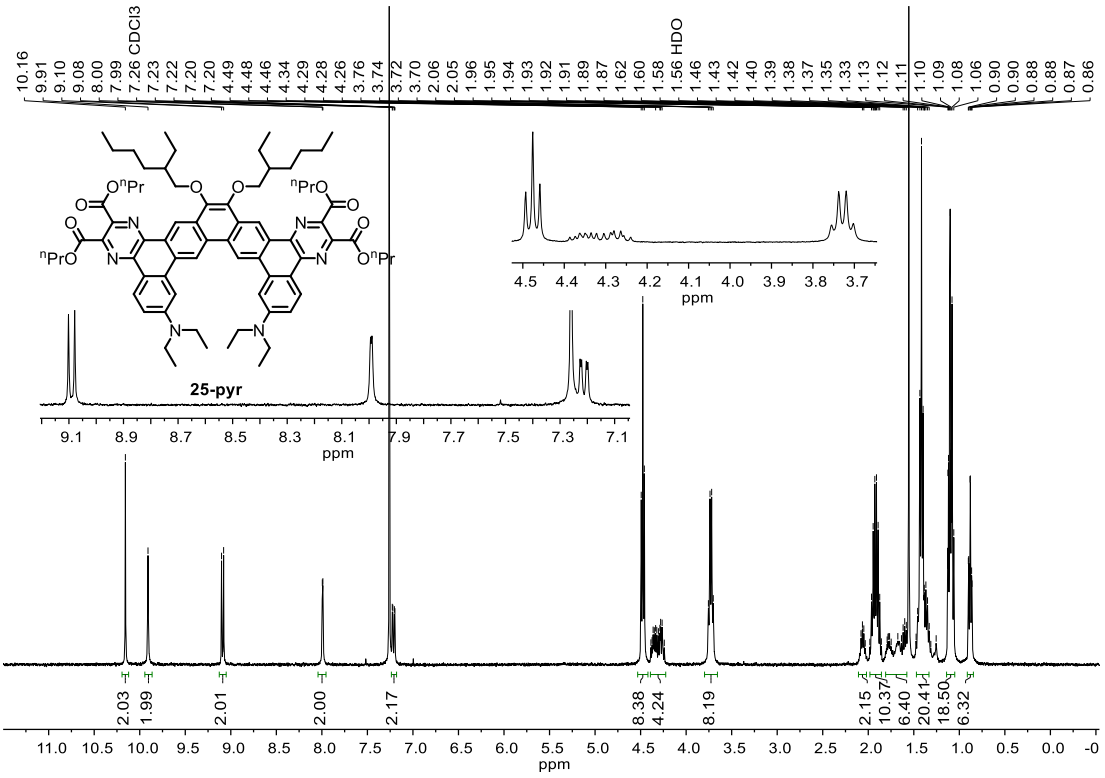

Figure S59. ^{1}H NMR Spectrum (400 MHz, Chloroform-*d*) of **25-pyr**.

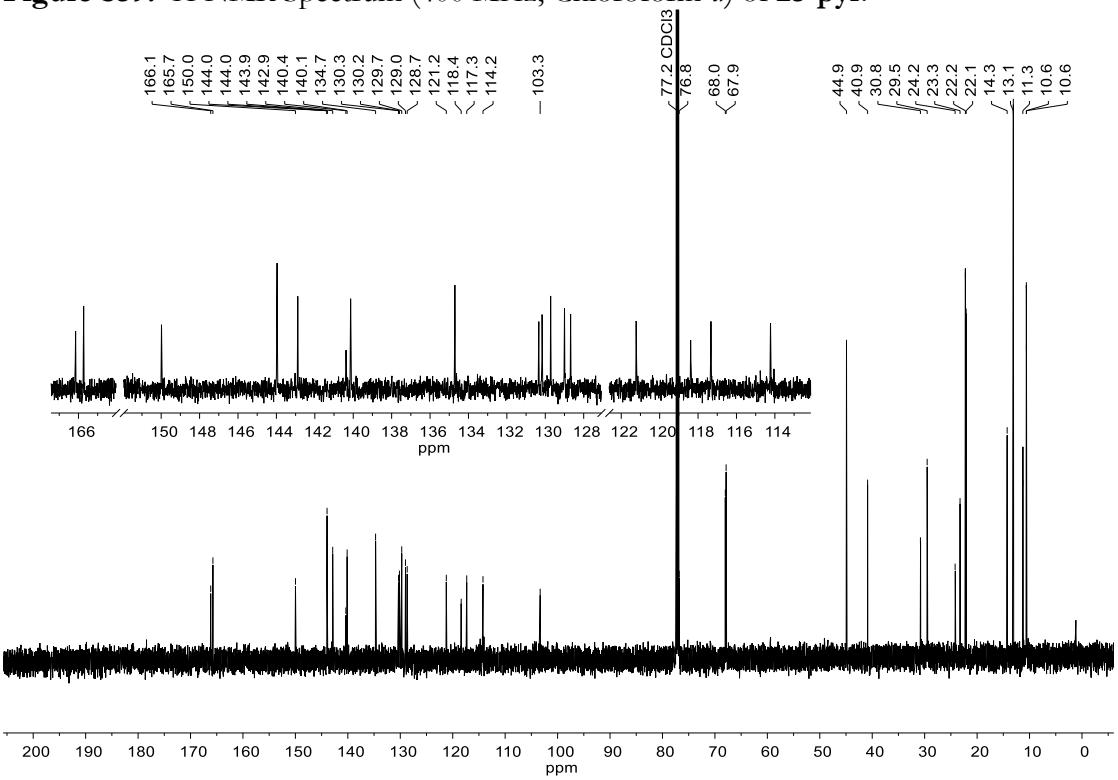

Figure S60. ^{13}C{^{1}H} NMR Spectrum (151 MHz, Chloroform-*d*) of **25-pyr**.

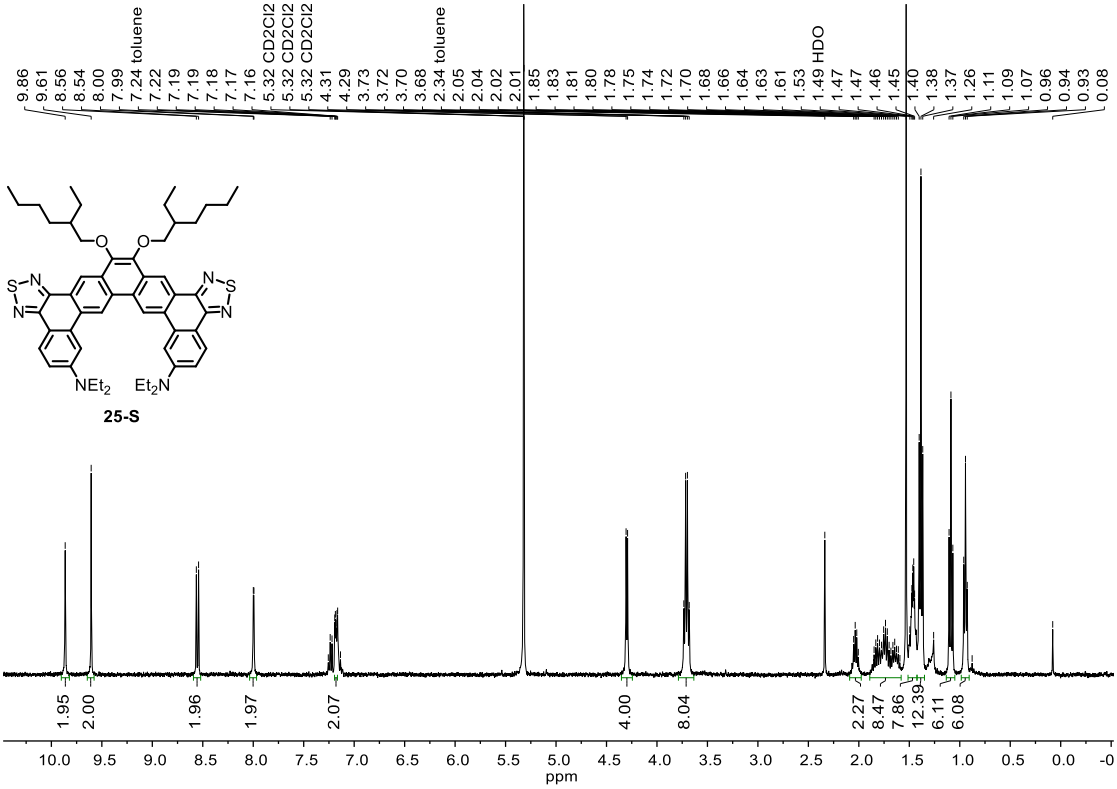

Figure S61. ^{1}H NMR Spectrum (400 MHz, dichloromethane-d_2) of **25-S**.

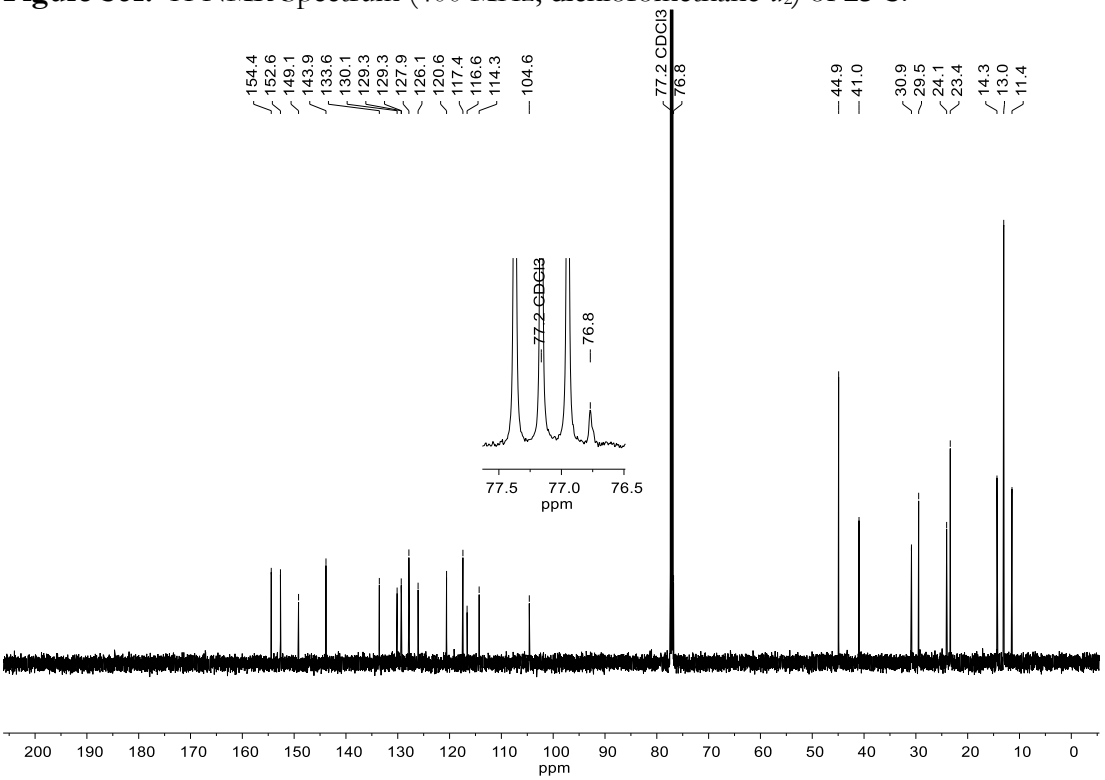

Figure S62. ^{13}C{^{1}H} NMR Spectrum (151 MHz, Chloroform-*d*) of **25-S**.

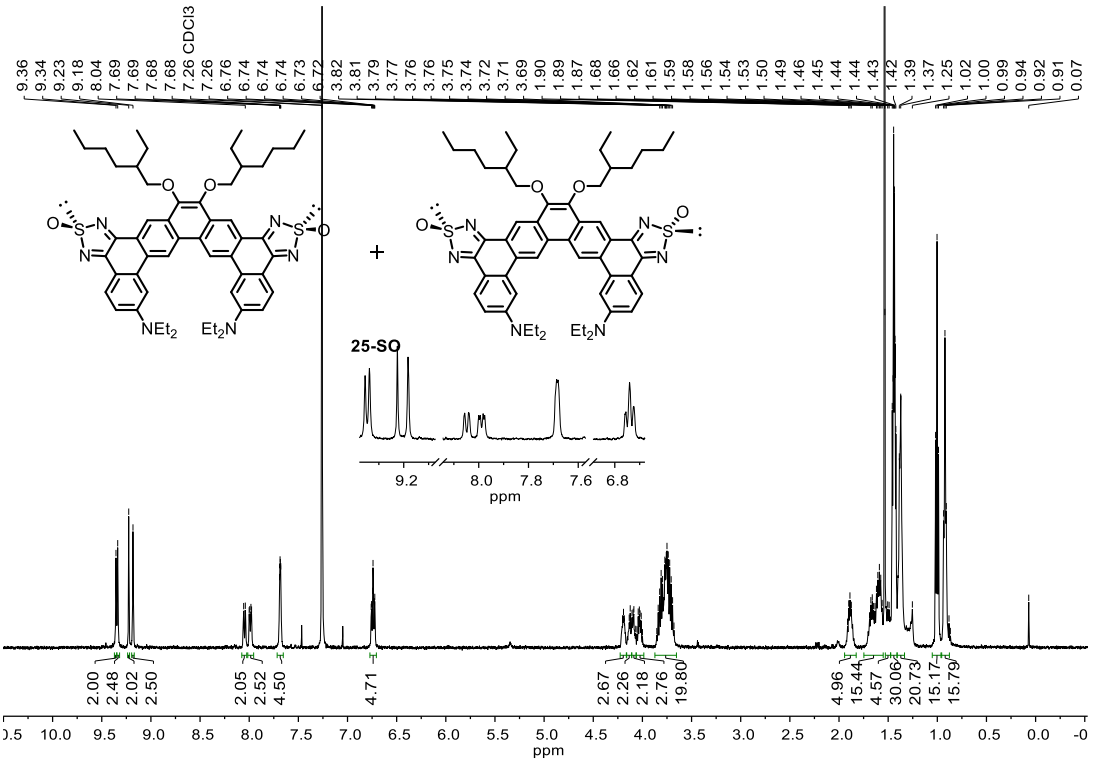

Figure S63. ^{1}H NMR Spectrum (500 MHz, Chloroform-*d*) of **25-SO**.

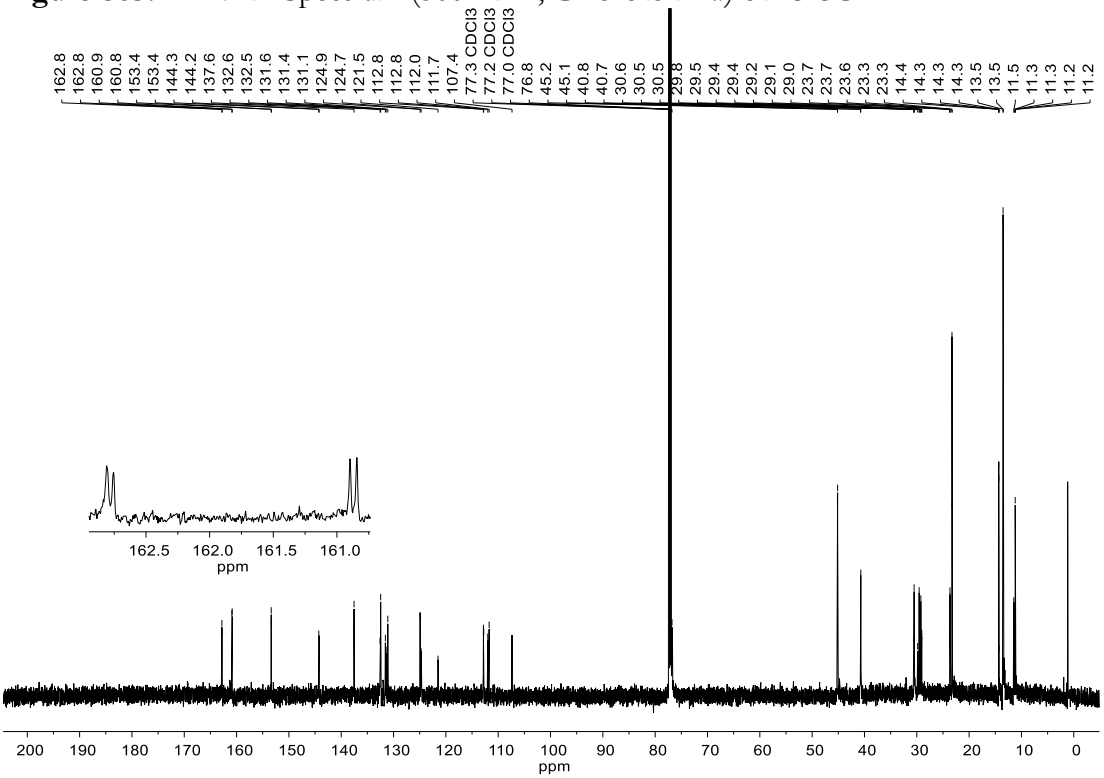

Figure S64. ^{13}C{^{1}H} NMR Spectrum (176 MHz, Chloroform-*d*) of **25-SO**.

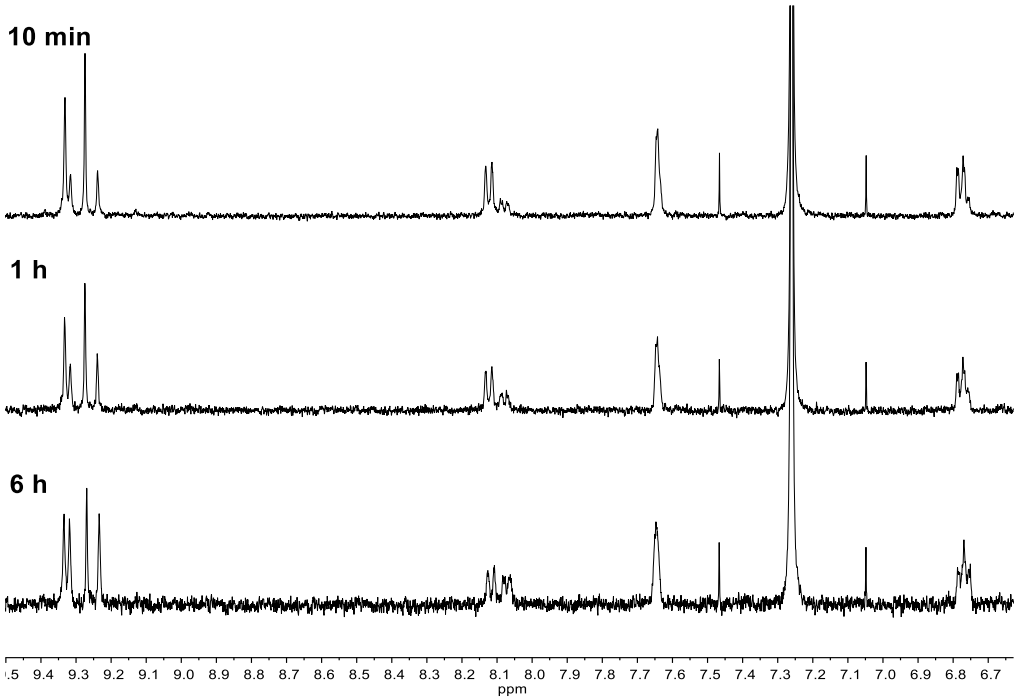

Figure S65. Partial ^{13}H NMR Spectra (500 MHz, Chloroform-*d*) of a diastereotopically enriched sample of **25-SO**. See the procedure for **25-SO** for description of sample prep. Times refer to the time elapsed after sample prep.

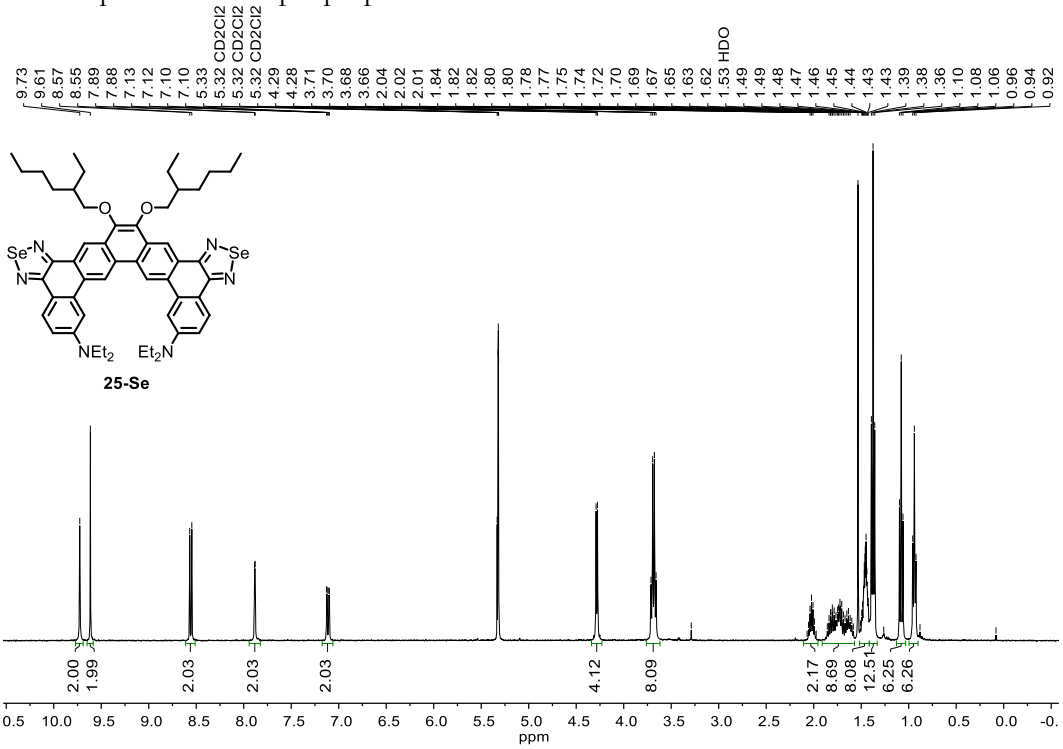

Figure S66. ^{1}H NMR Spectrum (400 MHz, Chloroform-*d*) of **25-Se**.

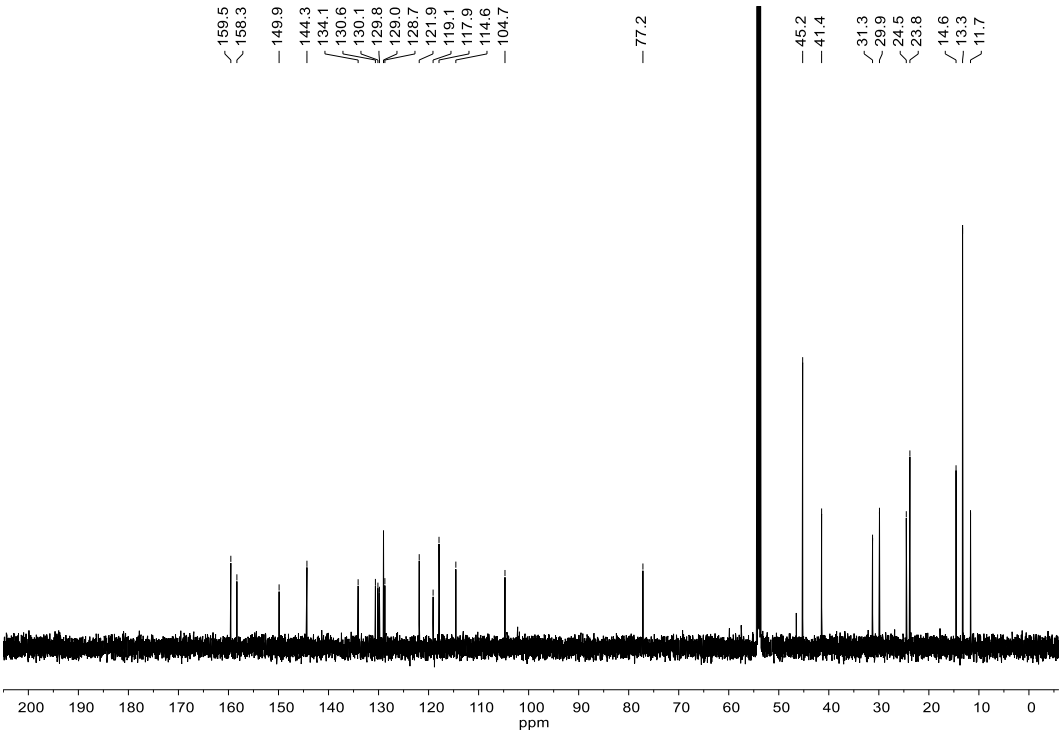

Figure S67. $^{13}C\{^{1}H\}$ NMR Spectrum (151 MHz, Chloroform-*d*) of **25-Se**.

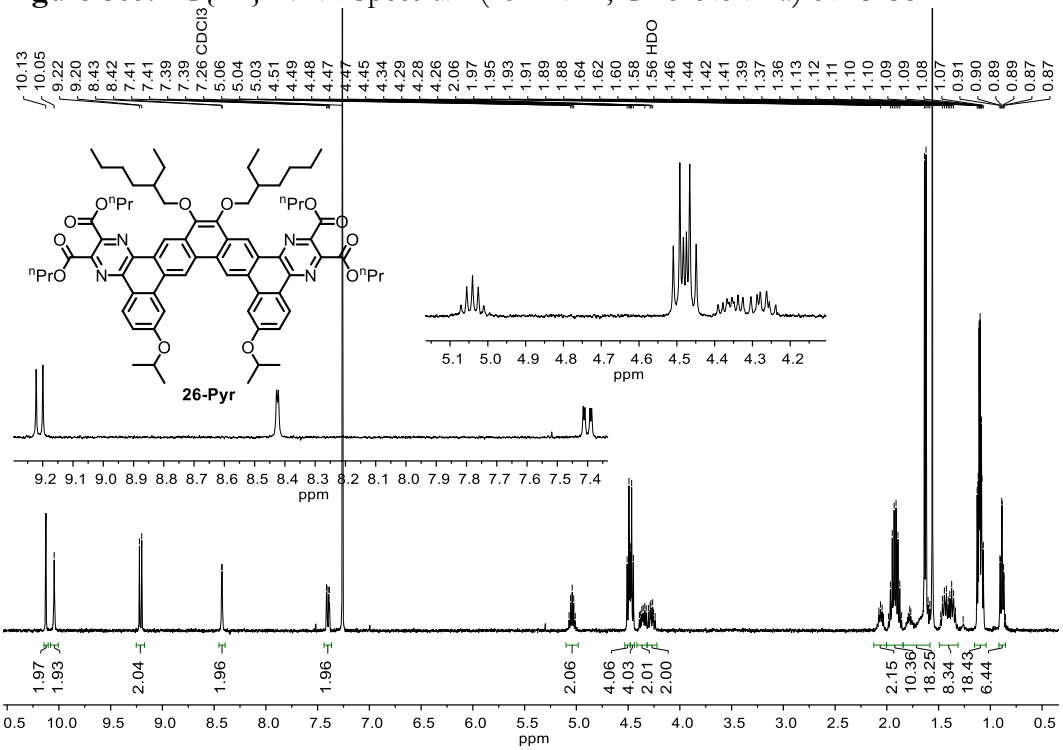

Figure S68. ^{1}H NMR Spectrum (400 MHz, Chloroform-*d*) of **26-pyr**.

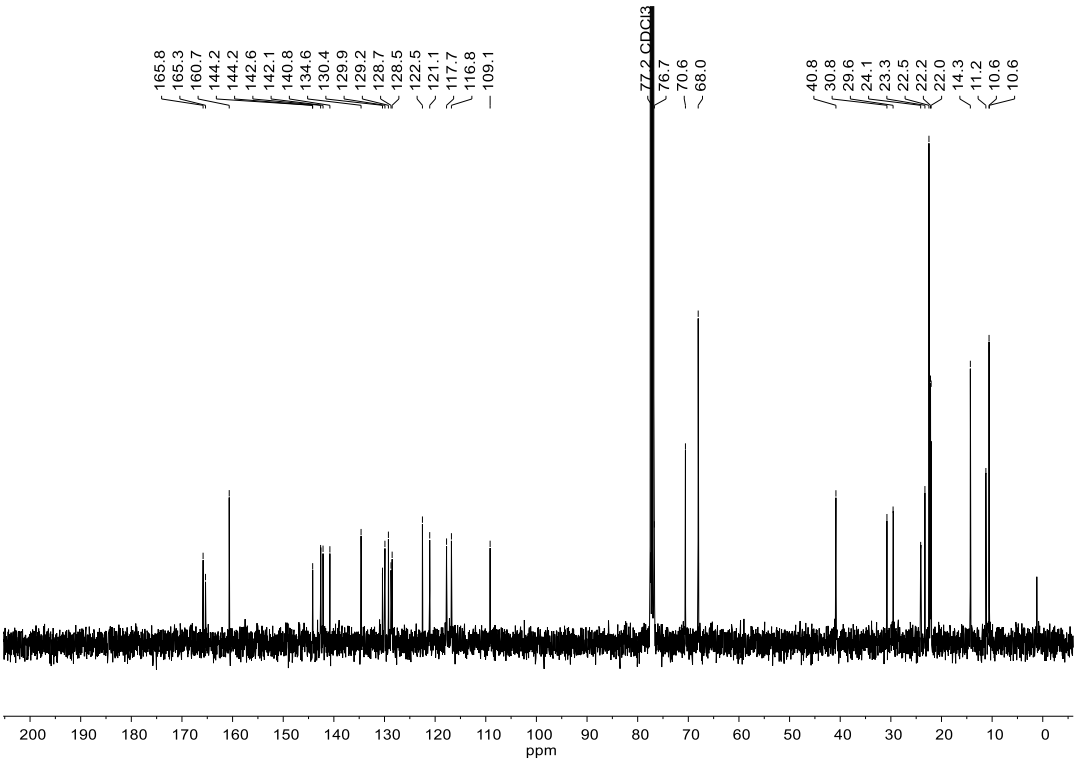

Figure S69. $^{13}C\{^{1}H\}$ NMR Spectrum (101 MHz, Chloroform-*d*) of **26-pyr**.

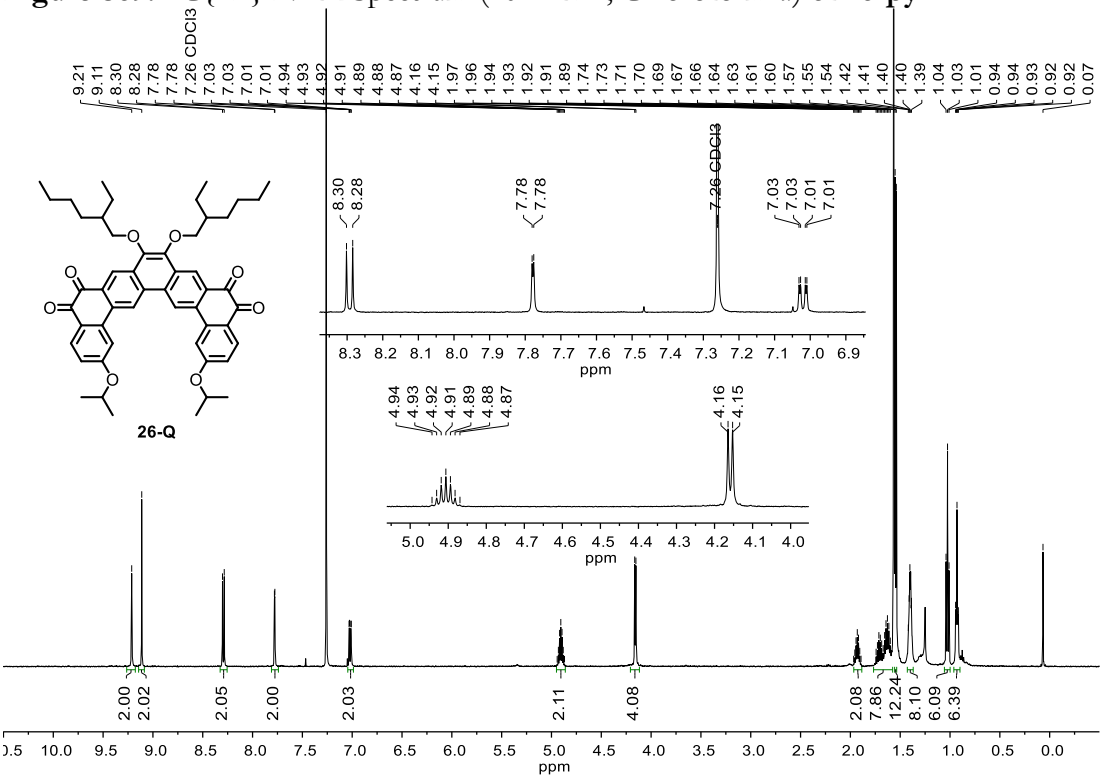

Figure S70. ^{1}H NMR Spectrum (500 MHz, Chloroform-*d*) of **26-Q**.

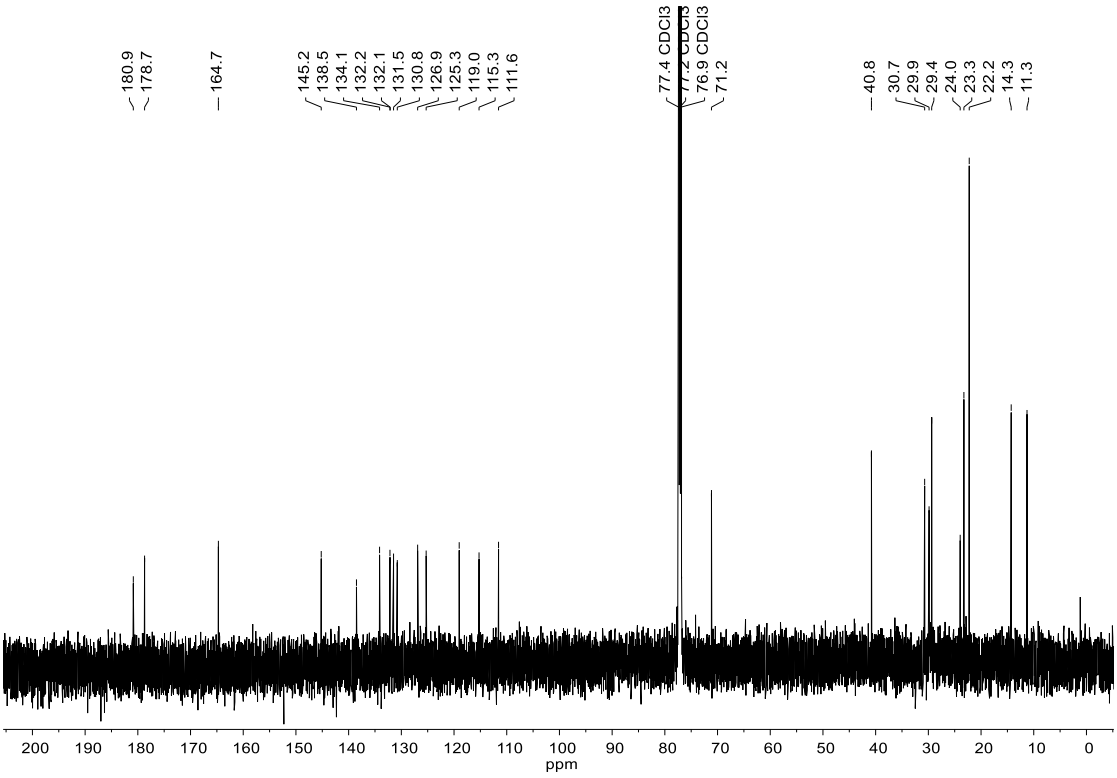

Figure S71. $^{13}C\{^{1}H\}$ NMR Spectrum (151 MHz, Chloroform-*d*) of **26-Q**.

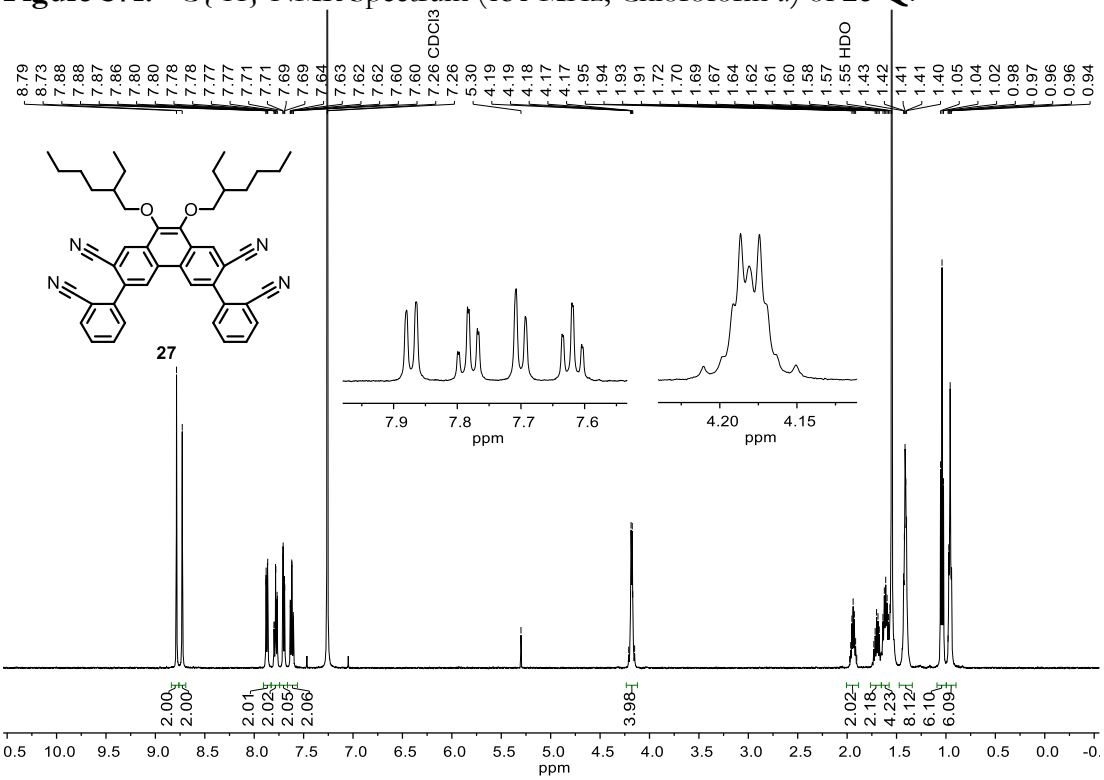

Figure S72. ^{1}H NMR Spectrum (500 MHz, Chloroform-*d*) of **27**.

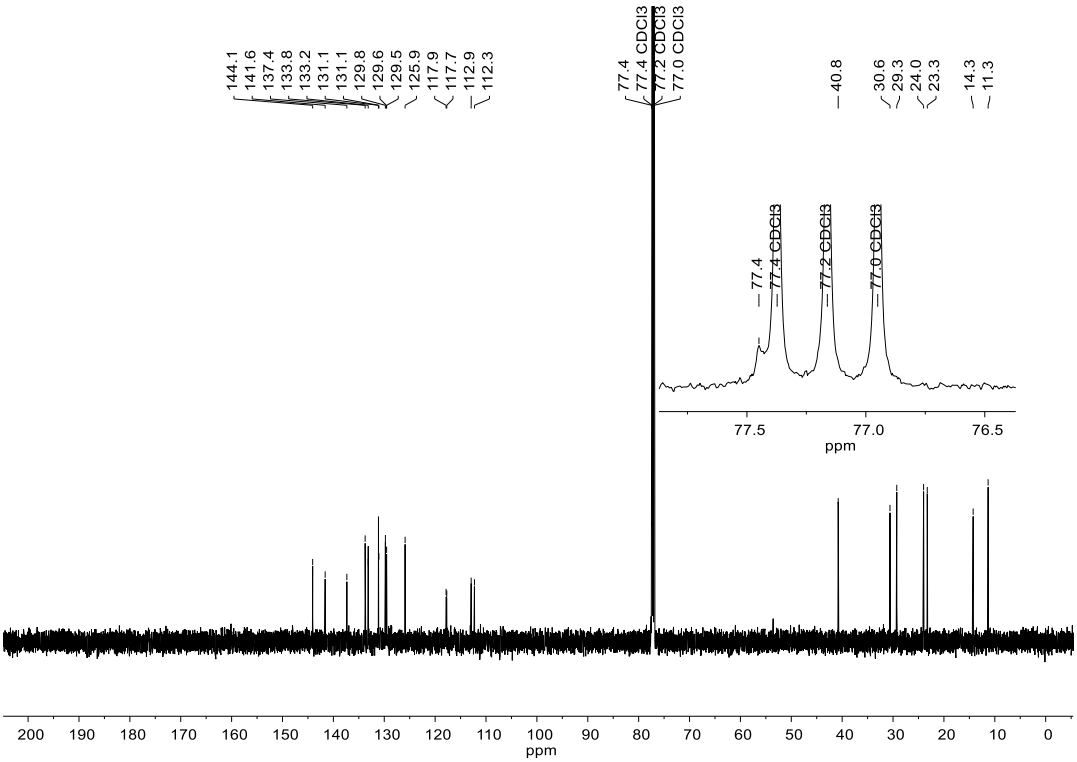

Figure S73. $^{13}C\{^{1}H\}$ NMR Spectrum (151 MHz, Chloroform-*d*) of **27**.

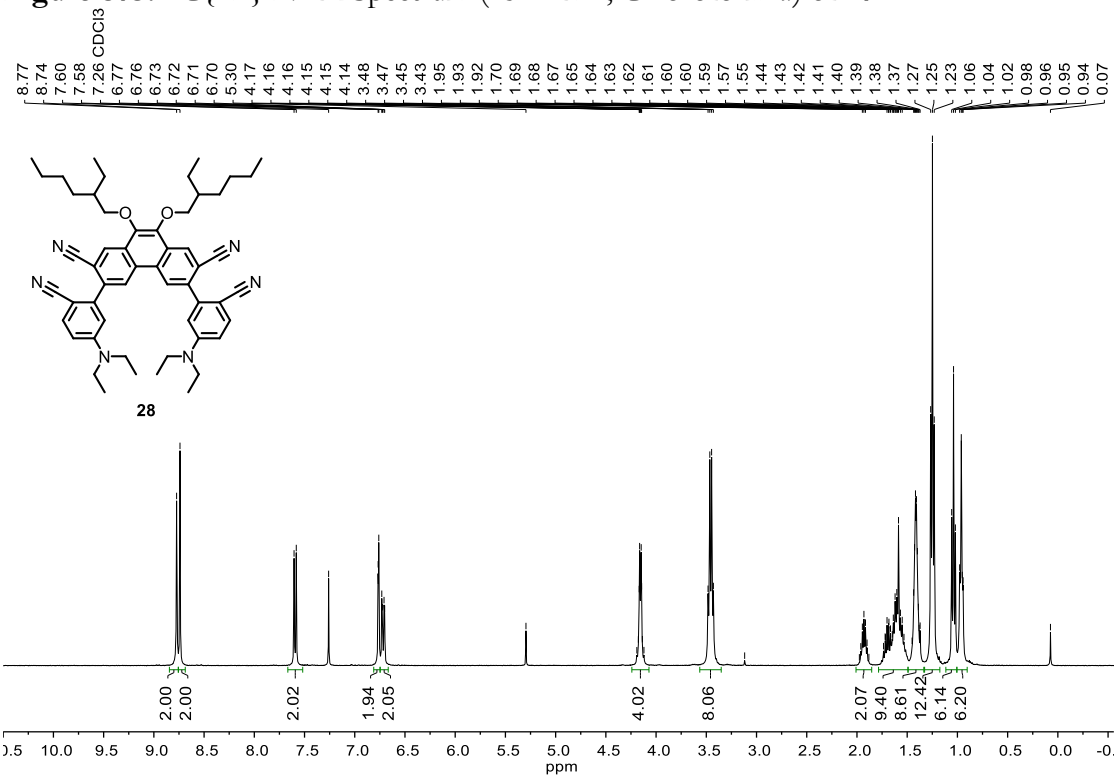

Figure S74. ^{1}H NMR Spectrum (400 MHz, Chloroform-*d*) of **28**.

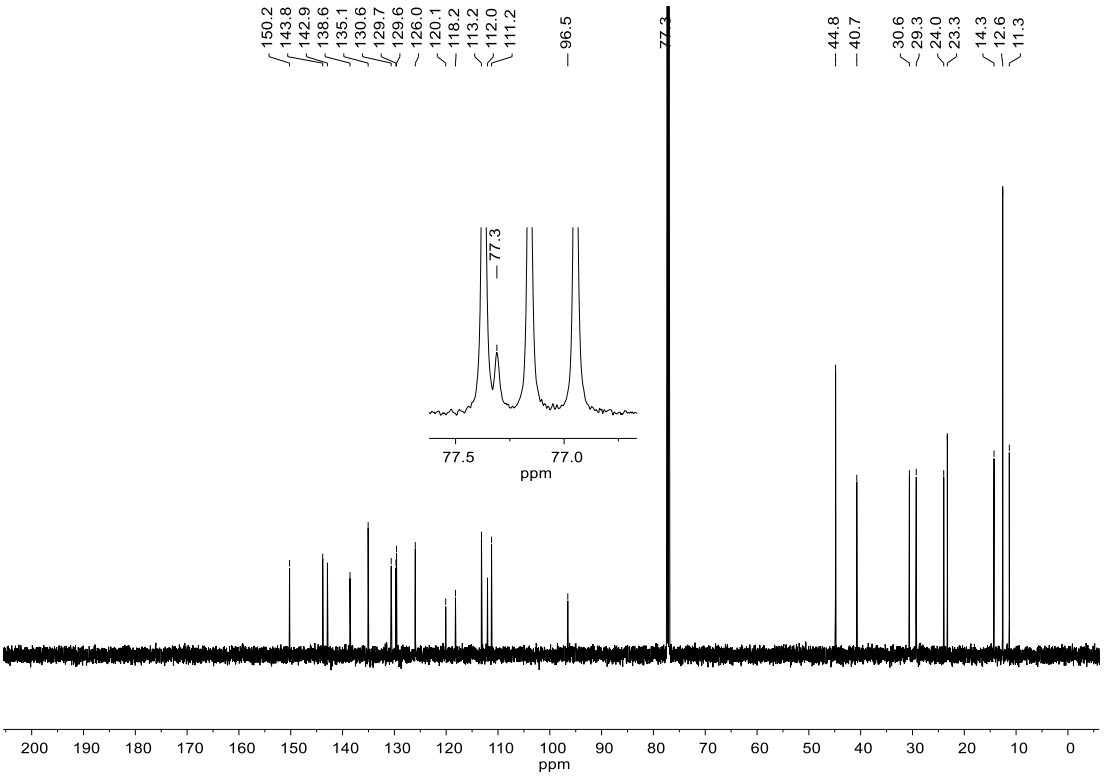

Figure S75. $^{13}C\{^{1}H\}$ NMR Spectrum (151 MHz, Chloroform-*d*) of **28**.

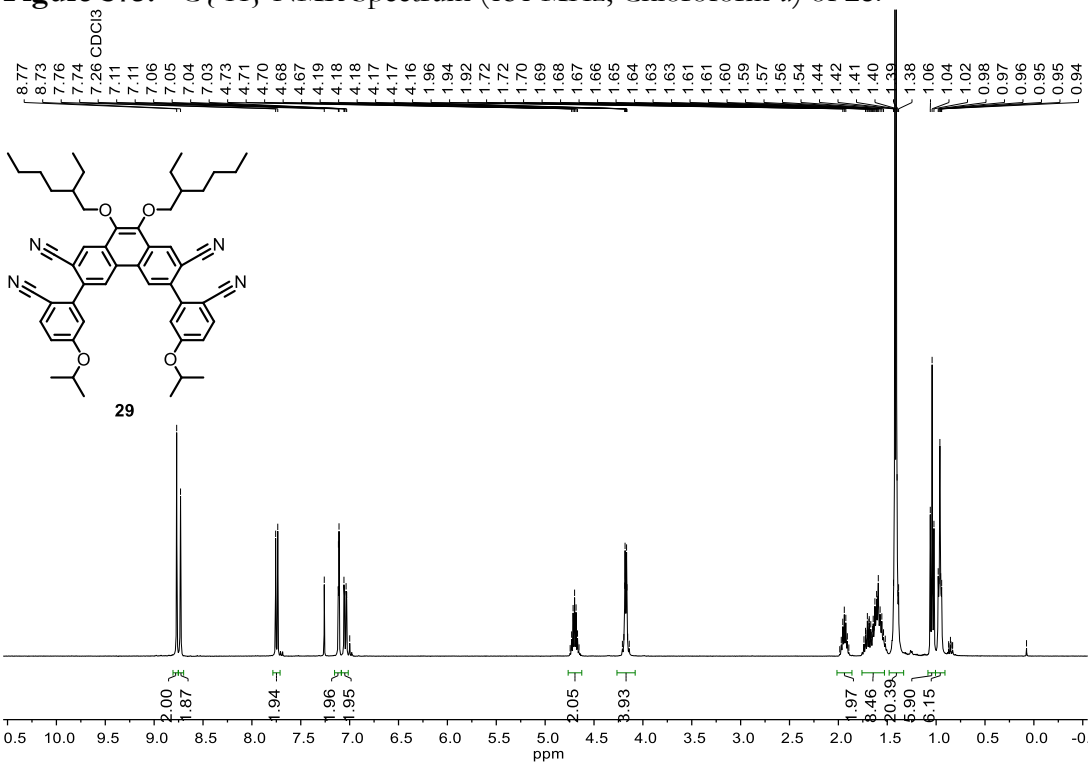

Figure S76. ^{1}H NMR Spectrum (400 MHz, Chloroform-*d*) of **29**.

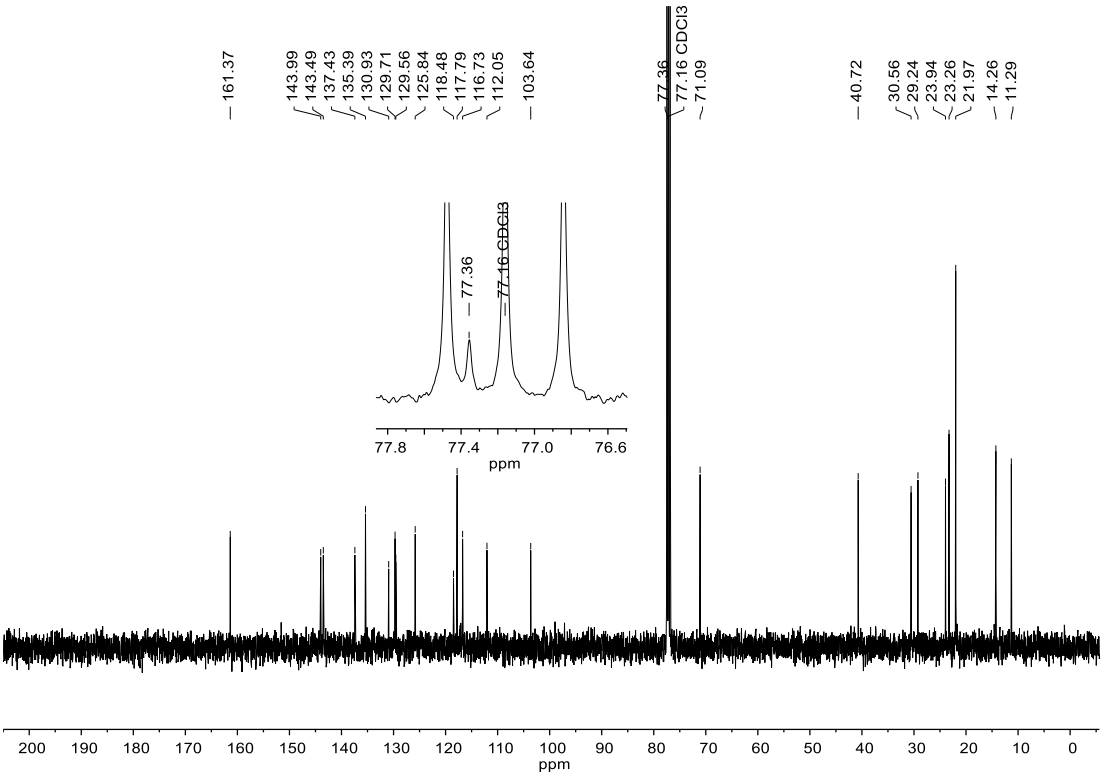

Figure S77. $^{13}C\{^{1}H\}$ NMR Spectrum (101 MHz, Chloroform-*d*) of **29**.

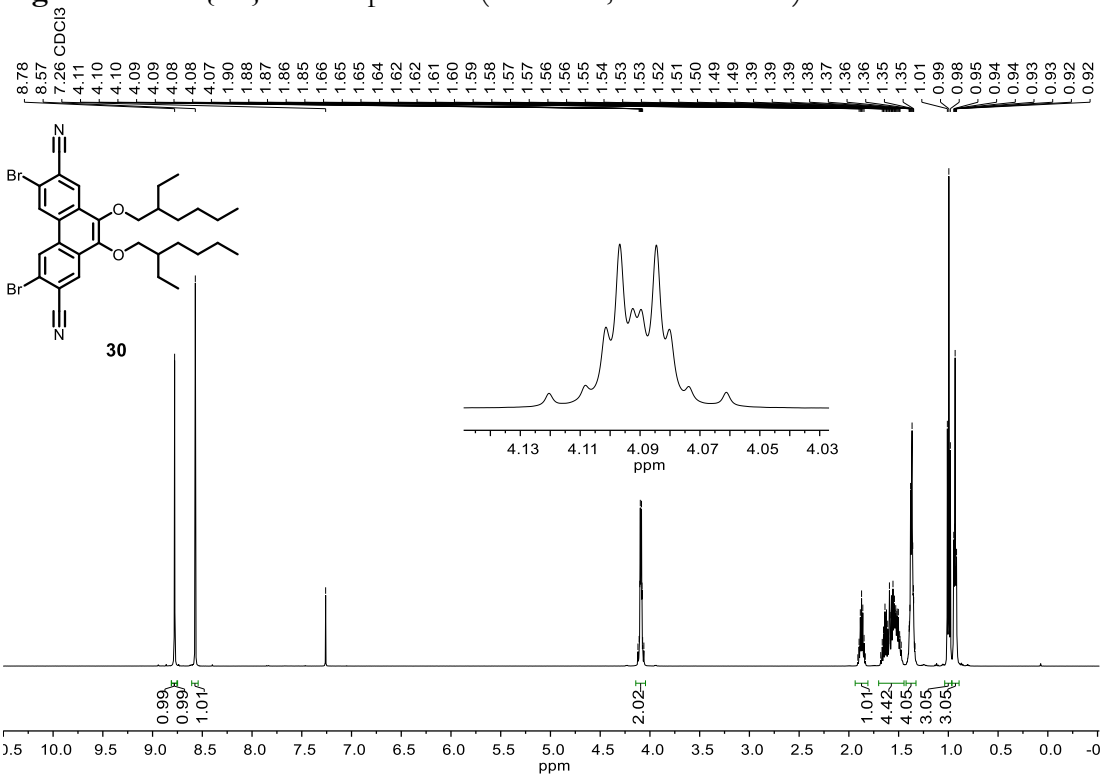

Figure S78. ^{1}H NMR Spectrum (500 MHz, Chloroform-*d*) of **30**.

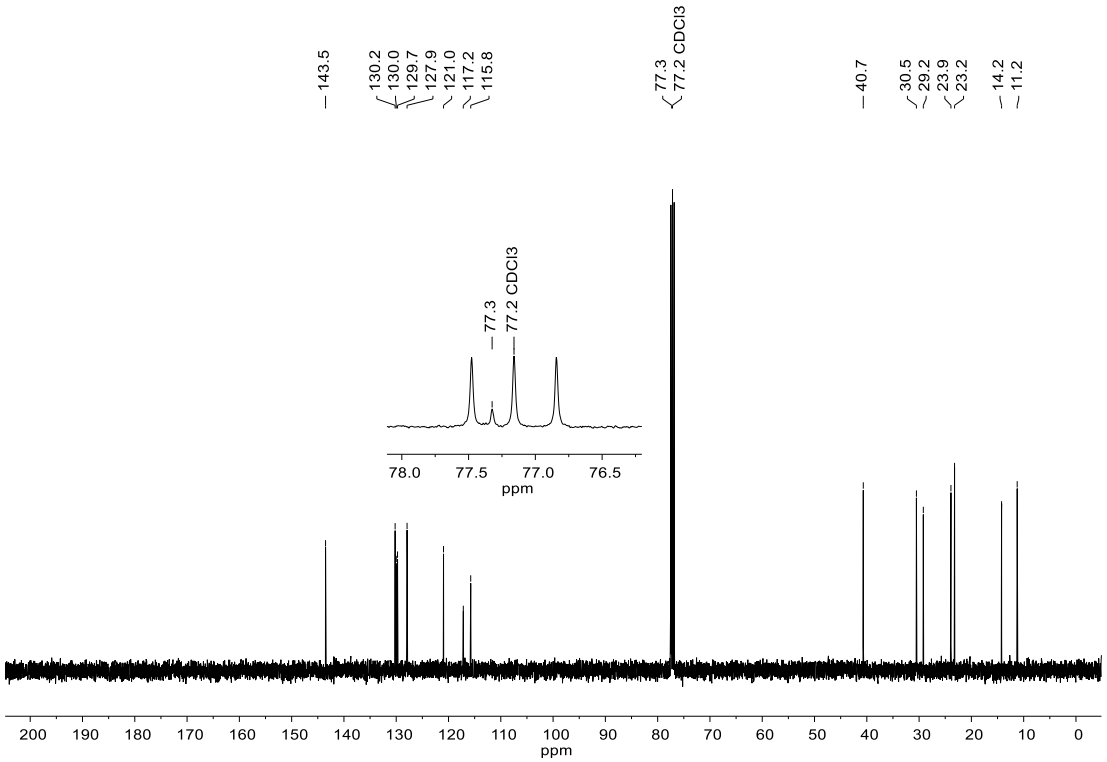

Figure S79. $^{13}C\{^{1}H\}$ NMR Spectrum (101 MHz, Chloroform-*d*) of **30**.

Photophysical Characterization

UV/Vis spectra were obtained on a Shimadzu UV-2450 UV-Visible spectrophotometer. Emission spectra were recorded on a Varian Cary Eclipse Spectrometer. All compounds were recrystallized from CH_2Cl_2 or CH_2Cl_2/hexanes to ensure high purity for analysis. All spectra are presented in the manuscript.

Compound	Absorption onset, λ_{onset} (nm)[a,b]	Emission λ_{max} (nm)[a,c]	Photophysical E_g (eV)[d]
14	393	445	3.16
17	517	556	2.40
18	429	452	2.89
19	442	479	2.81
20	388	398	3.20
21	502	580	2.47
23	601	647	2.06
24-pyr	510	562	2.43
25-pyr	537	593	2.31
25-S	469	507	2.64
25-SO	632	662	1.96
25-Se	495	557	2.51
26-pyr	506	558	2.45
26-Q	588	N/A[e]	2.11

Table S1. Summary of relevant photophysical properties. (a) Solvent = CH_2Cl_2; (b) Defined as $\varepsilon = 1.0 \times 10^3$; (c) Excited at longest wavelength absorption maximum; (d) Estimated from the absorption onset (λ_{onset}): $E_g = 1240/\lambda_{onset}$; (e) non-fluorescent

Electrochemical Characterization

Cyclic and square wave voltammetry were performed on a BASi EC Epsilon potentiostat/galvanostat and a PWR-3 Power Module using dry, oxygen-free solvents, a glassy carbon working electrode, Pt counter electrode, and Ag/Ag^+ reference electrode.

Compound	$E_{1/2}^{red}$ vs. Fc/Fc^+ (V)[a]	$E_{1/2}^{ox}$ vs. Fc/Fc^+ (V)[a]	Electrochemical E_g (eV)[b]	LUMO (eV)[c]	HOMO (eV)[d]
14	–1.73	N/A	N/A	–3.07	–6.23
17	–1.96	0.46, 0.70	2.42	–2.84	–5.26
18	–1.86	1.18	3.04	–2.94	–5.98
19	–1.73	1.00	2.73	–3.07	–5.80
20	–1.71	N/A	N/A	–3.09	–6.29
21	–1.92	0.58	2.50	–2.88	–5.38
23	–1.41	0.7	2.1	–3.39	–5.5
26-Q	–1.16, –1.32, –1.91, –3.01	N/A	N/A	–3.64	–5.75

Table S2. Summary of relevant electrochemical properties. (a) Where reversible waves were available, $E_{1/2}$ was measured using cyclic voltammetry in CH_2Cl_2 with 0.1 M $[^nBu_4N][PF_6]$ as supporting electrolyte (except for compound **26**-**Q**, where THF was used). Where only an irreversible wave was observed, $E_{1/2}$ was measured using square wave voltammetry under the same conditions. Oxidation events were not observed within the solvent window for compounds **14**, **20**, and **26**-**Q**; (b) $E_g = E_{1/2}^{ox} - E_{1/2}^{red}$; (c) Estimated from the first reduction: $-(E_{1/2}^{red} + 4.80)$; (d) Estimated from the first oxidation: $-(E_{1/2}^{ox} + 4.80)$. Where $E_{1/2}^{ox}$ was not available, HOMO = LUMO – photophysical E_g.

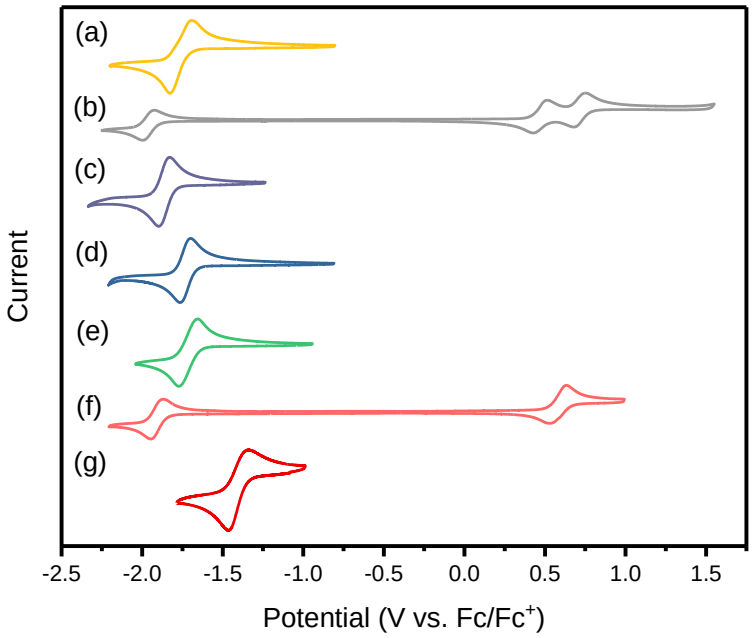

Figure S80. Cyclic voltammograms of solutions (~0.5 mM) of compounds (a) **14**, (b) **17**, (c) **18**, (d) **19**, (e) **20**, (f) **21**, and (g) **23** in CH_2Cl_2 with 0.1 M [^{n}Bu$_4$N][PF_6] as supporting electrolyte. Scan rate: 100 mV/s. Only reversible or quasi-reversible waves are shown.

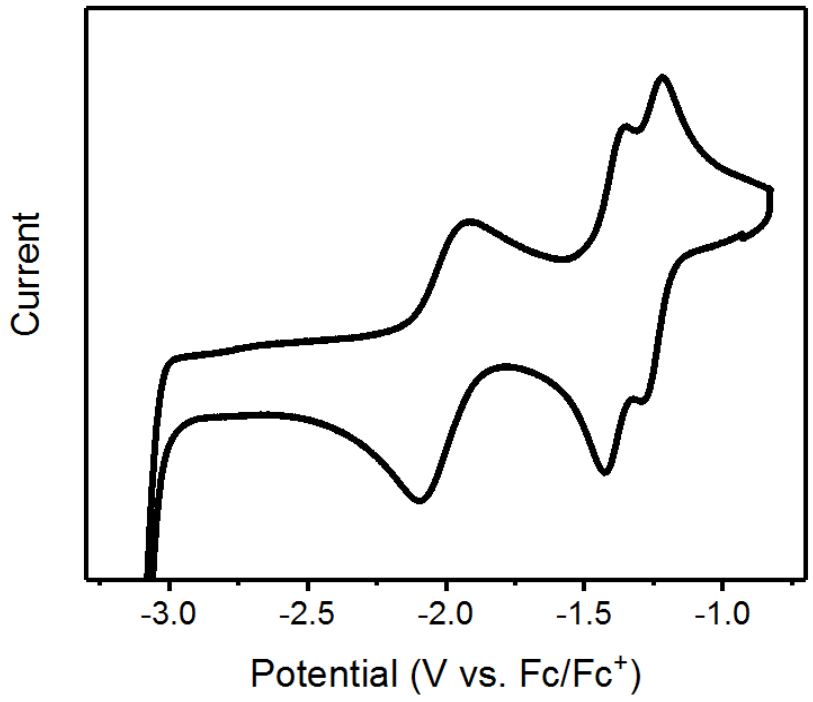

Figure S81. Cyclic voltammogram of a solution (0.2 mM) of compound **26-Q** in THF with 0.1 M [^{n}Bu$_4$N][PF_6] as supporting electrolyte. Scan rate: 100 mV/s.

X-Ray Crystallography

X-ray diffraction data for **6** was collected at beamline 11.3.1 of the Advanced Light Source at Lawrence Berkeley National Laboratory. Frames were collected on a PHOTON100 CMOS running shutterless using radiation with a wavelength of 0.7749 Å selected by a Si(111) monochromator and focused to 200 μm^2 with a toroidal mirror. Crystal was kept at 100(2) K throughout collection. Data collection, integration, scaling, and space group determination were performed with Bruker APEX3 (v. 2016.5-0) software. Structure was solved by SHELXT-2014 and refined with SHELXL-2014, with refinement of F^2 on all data by full-matrix least squares.[16–19] The 3D molecular structure figures were visualized with Mercury 3.7.[20] See the synthetic procedure for compound **6** (above) for details on crystal growth. X-ray diffraction data for compound **13** was collected using a Bruker AXS diffractometer with a Kappa geometry goniostat coupled to an APEX-II CCD detector with Mo Kα (λ = 0.71073 Å) radiation generated by a microfocus sealed tube and monochromated by a system of QUAZAR multilayer mirrors. Crystal was kept at 100(2) K throughout collection. Data collection strategy determination, integration, scaling, and space group determination were performed with APEX3 (v. 2016.5-0) software. Structure was solved by SHELXT-2014 and refined with SHELXL-2014, with refinement of F^2 on all data by full-matrix least squares.[16–19] The 3D molecular structure figures were visualized with Mercury 3.7.[20]

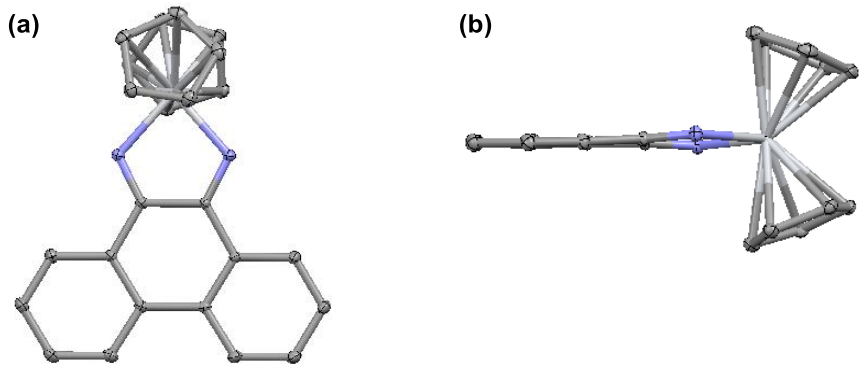

Figure S82. Solid state structure of **6** as determined by single-crystal X-ray diffraction: (a) top view; (b) side view. Thermal ellipsoids set at 50% probability.

Formula weight	382.30	
Temperature	100.05 K	
Crystal system	monoclinic	
Space group	$P2_1/n$	
Unit cell dimensions	a = 12.8931(5) Å	α = 90°
	b = 8.3339(3) Å	β = 94.691(2)°
	c = 16.0672(7) Å	γ = 90°
Volume	1720.63(12) $Å^3$	
Z	4	
Density (calculated)	1.476 g/cm^3	
μ	0.643 mm^{-1}	
F(000)	792.0	

Crystal size	0.181 × 0.108 × 0.072 mm^3
Radiation	Synchrotron (λ = 0.7749)
2Θ range for data collection	4.25 to 87.668°
Index ranges	-21 ≤ h ≤ 23, -14 ≤ k ≤ 14, -28 ≤ l ≤ 28
Reflections collected	36472
Independent reflections	10239 [R_{int} = 0.0356, R_{sigma} = 0.0363]
Data/restraints/parameters	10239/0/244
Goodness-of-fit on F^2	1.030
Final R indexes [I>=2σ (I)]	R_1 = 0.0338, wR_2 = 0.0882
Final R indexes [all data]	R_1 = 0.0446, wR_2 = 0.0936
Largest diff. peak/hole	0.68/-0.53 e $Å^{-3}$

Table S3. Crystal data and structure refinement for **6**.

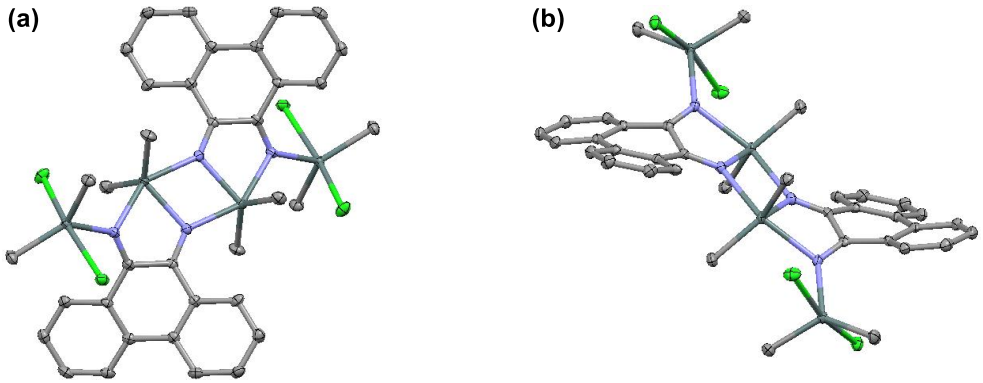

Figure S83. Solid state structure of **13** as determined by single-crystal X-ray diffraction: (a) top view; (b) side view. Thermal ellipsoids set at 50% probability.

Empirical formula	$C_{19}H_{22}Cl_4N_2Sn_2$	
Formula weight	657.56	
Temperature	100(2) K	
Wavelength	0.71073 Å	
Crystal system	Triclinic	
Space group	P -1	
Unit cell dimensions	a = 7.2579(3) Å	α = 77.066(2)°
	b = 8.3339(3) Å	β = 78.635(2)°
	c = 12.8986(5) Å	γ = 84.963(2)°
Volume	1123.94(8) $Å^3$	
Z	2	
Density (calculated)	1.943 g/cm^3	
Absorption coefficient	2.705 mm^{-1}	
F(000)	636	
Crystal size	0.060 x 0.050 x 0.020 mm^3	

Theta range for data collection	1.648 to 25.557°
Index ranges	$-8 \leq h \leq 8, -15 \leq k \leq 15, -15 \leq l \leq 15$
Reflections collected	25445
Independent reflections	4181 [R(int) = 0.0326]
Completeness to theta = 25.000°	99.9 %
Absorption correction	Semi-empirical from equivalents
Max. and min. transmission	0.4403 and 0.3698
Refinement method	Full-matrix least-squares on F^2
Data/restraints/parameters	4181 / 0 / 248
Goodness-of-fit on F^2	1.098
Final R indexes [I>=2σ (I)]	R1 = 0.0299, wR2 = 0.0692
Final R indexes [all data]	R1 = 0.0363, wR2 = 0.0722
Extinction coefficient	N/A
Largest diff. peak/hole	1.646 and -0.631 e $Å^{-3}$

Table S4. Crystal data and structure refinement for **13**.

DFT Calculations

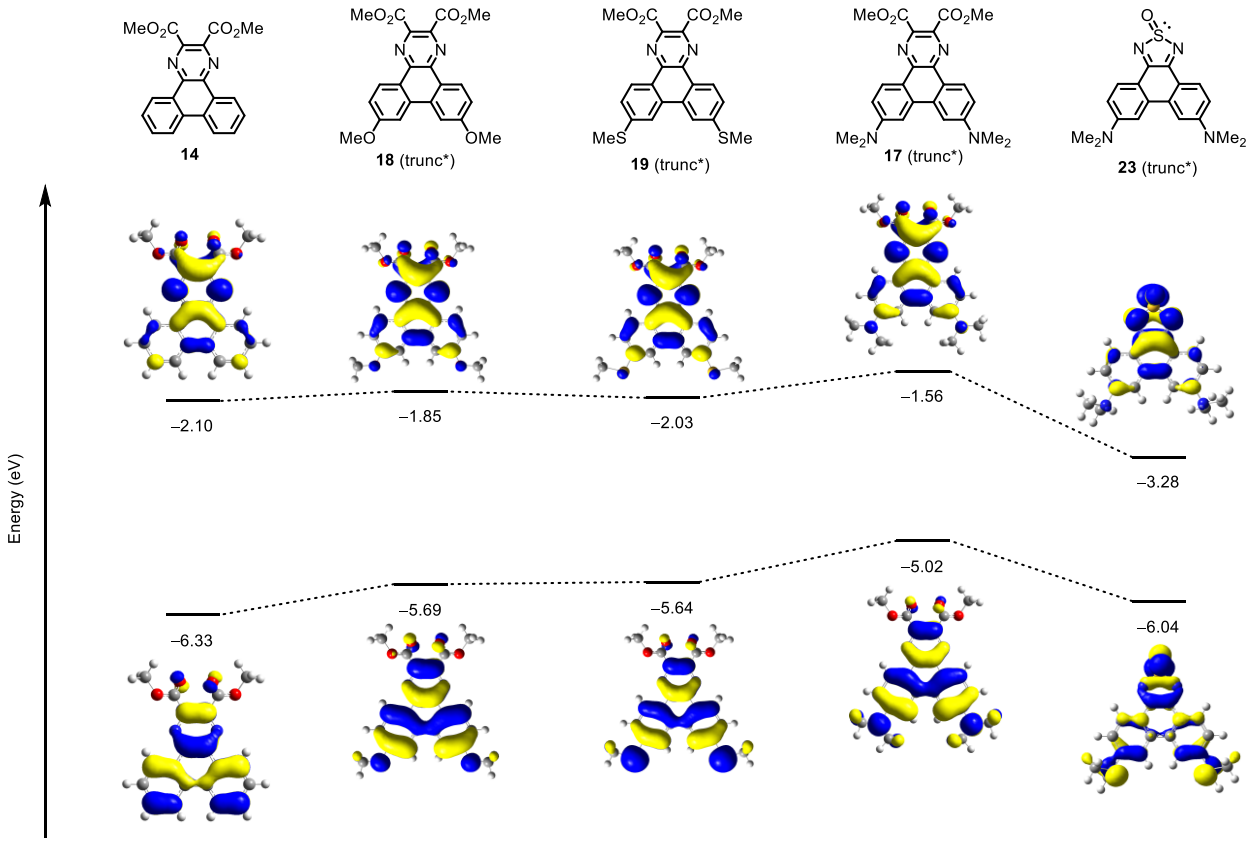

Figure S84. DFT-calculated HOMO and LUMO energy levels for compounds **14**, **17**–**19** (truncated*), and **23** (truncated*) at the B3LYP/6-31G(p,d) level of theory. Calculations were carried out using the Gaussian '09 software package. *All alkyl groups were truncated to methyl groups to save computational time.

References for Supporting Information of Chapter 6

(1) Binger, P.; Müller, P.; Langhauser, F.; Sandmeyer, F.; Philipps, P.; Gabor, B.; Mynott, R. *Chem. Ber.* **1993**, *126*, 1541.
(2) Dutton, J. L.; Farrar, G. J.; Sgro, M. J.; Battista, T. L.; Ragogna, P. J. *Chem. Eur. J.* **2009**, *15*, 10263.
(3) Shirai, Y.; Osgood, A. J.; Zhao, Y.; Yao, Y.; Saudan, L.; Yang, H.; Yu-Hung, C.; Alemany, L. B.; Sasaki, T.; Morin, J.-F.; Guerrero, J. M.; Kelly, K. F.; Tour, J. M. *J. Am. Chem. Soc.* **2006**, *128*, 4854.
(4) Servalli, M.; Gyr, L.; Sakamoto, J.; Schlüter, A. D. *Eur. J. Org. Chem.* **2015**, *2015*, 4519.
(5) Krasovskiy, A.; Knochel, P. *Angew. Chem. Int. Ed.* **2004**, *43*, 3333.
(6) Krasovskiy, A.; Tishkov, A.; del Amo, V.; Mayr, H.; Knochel, P. *Angew. Chem. Int. Ed.* **2006**, *45*, 5010.
(7) Hoye, T. R.; Eklov, B. M.; Voloshin, M. *Org. Lett.* **2004**, *6*, 2567.
(8) Mangas-Sánchez, J.; Busto, E.; Gotor-Fernández, V.; Gotor, V. *Catal. Sci. Technol.* **2012**, *2*, 1590.
(9) Urawa, Y.; Naka, H.; Miyazawa, M.; Souda, S.; Ogura, K. *J. Organomet. Chem.* **2002**, *653*, 269.
(10) Hitosugi, S.; Tanimoto, D.; Nakanishi, W.; Isobe, H. *Chem. Lett.* **2012**, *41*, 972.
(11) Cahiez, G.; Chaboche, C.; Mahuteau-Betzer, F.; Ahr, M. *Org. Lett.* **2005**, *7*, 1943.
(12) Linder, T.; Badiola, E.; Baumgartner, T.; Sutherland, T. C. *Org. Lett.* **2010**, *12*, 4520.
(13) Neidlein, R.; Knecht, D. *Helv. Chim. Acta* **1987**, *70*, 1076.
(14) Neidlein, R.; Knecht, D.; Endres, H. *Z. f. Naturforsch.* **1987**, *42*, 84.
(15) Linder, T.; Sutherland, T. C.; Baumgartner, T. *Chem. Eur. J.* **2010**, *16*, 7101.
(16) Sheldrick, G. M. *Acta Crystallogr. A* **2008**, *64*, 112.
(17) Sheldrick, G. M. *Acta Crystallogr. Sect. Found. Adv.* **2015**, *71*, 3.
(18) Palatinus, L.; Chapuis, G. *J. Appl. Crystallogr.* **2007**, *40*, 786.
(19) Sheldrick, G. M. *Acta Crystallogr. Sect. C Struct. Chem.* **2015**, *71*, 3.
(20) Macrae, C. F.; Edgington, P. R.; McCabe, P.; Pidcock, E.; Shields, G. P.; Taylor, R.; Towler, M.; Streek, J. van de. *J. Appl. Crystallogr.* **2006**, *39*, 453.

Chapter 7: Future Directions as Illustrated by Two Preliminary Results

The synthetic platform developed in Chapters 2–6 will allow in-depth studies of the nanocarbons presented in those chapters via the construction of highly functionalized analogues. More importantly, it is applicable to other nanocarbons. This chapter presents two preliminary results along these lines. The first result demonstrates how this strategy is currently being applied to a synthetically challenging and highly-sought-after class of macrocyclic nanocarbons, the cycloarenes. The second is the isolation of a *configurationally stable* expanded 23-helicene, which is 7 rings longer than any known carbohelicene. Importantly, both demonstrate the sequential application of [2+2+n] reactions to rapidly build up complexity. This is enabled in part by the site-selectivity of the [2+2+2] reaction (developed in Chapter 4), which furnishes alkynylated PAHs that are poised for further [2+2+n] reactions. Since these stories are a work-in-progress and are being completed during my last few months at Berkeley, only some highlights are presented.

Extending and Expanding Kekulene: A Modular and Divergent [2+2+n] Approach to Cycloarenes

In the 1970s, there was tremendous interest in kekulene (**1**, Figure 1), the prototypical cycloarene, due the hypothesized "superaromaticity" (i.e. stabilization that might arise from its macrocyclic structure.) Although some debate continued thereafter,[1,2] the issue was effectively settled in 1978 by Staab and Diedrich with their landmark synthesis and characterization of Kekulene.[3] They defined cycloarenes as "PAHs in which, by a combination of angular and linear annellations of benzene units, fully annellated macrocyclic systems are present enclosing a cavity into which carbon-hydrogen bonds point."[4] Even if their definition is generalized to include any aromatic ring, only five other cycloarenes have been reported (**2**–**6**).[5–10] Recent years have also witnessed the synthesis of a few remarkable cycloarene-like compounds that exhibit highly delocalized and/or polyradicaloid character.[11–14] Since these macrocyclic, fully-ladderized and -conjugated compounds are structurally analogous to cycloarenes, these compounds are included in the definition of "cycloarene" for the brief discussion below.

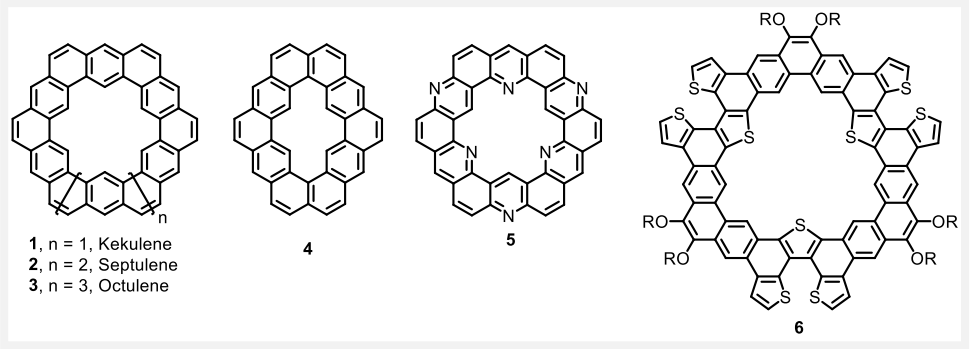

Figure 1. Known cycloarenes.

Although many important fundamental insights have been gleaned from the known cycloarenes, applications have not been explored due to synthetic difficulties. These difficulties arise from a combination of two challenging steps: macrocyclization and regioselective ring-fusion. Reported syntheses invariably involve a low yielding macrocyclization step that severely limits scalability and makes rational structural modifications difficult, but such modifications are essential for solubility and manipulation of properties.

As shown in Scheme 1, these synthetic challenges were simultaneously addressed by use of two sequential [2+2+n] reactions. First, a site-selective [2+2+2] cycloaddition gave alkynyl-terminated helicene **7** (a dibrominated version of that presented in Chapter 5), which then underwent a Cu-mediated macrocyclization to give **8** on *gram scale*. A final-step [2+2+n] cycloaddition then enabled the synthesis of a range of derivatives, including benzannulated **9** and **10** (which differ in R-group), selenophene-annulated **11**, and naphthalene-annulated **12**. This synthetic sequence is scalable and offers three potential points for diversification: 1) the modular assembly of starting hexaynes **13** (via Pd-catalyzed cross-coupling); 2) the site-selective [2+2+2] reaction to give **7** (the R-group can be varied and, in principle, other [2+2+n] reactions can be used); 3) the divergent [2+2+n] reaction.

An analogous approach is currently being employed in pursuit of "expanded kekulene" **14** (Figure 2) and related cycloarenes with expanded cavities. Investigations of the supramolecular, solid-state, photophysical, and electrochemical properties of these and related compounds are currently underway.

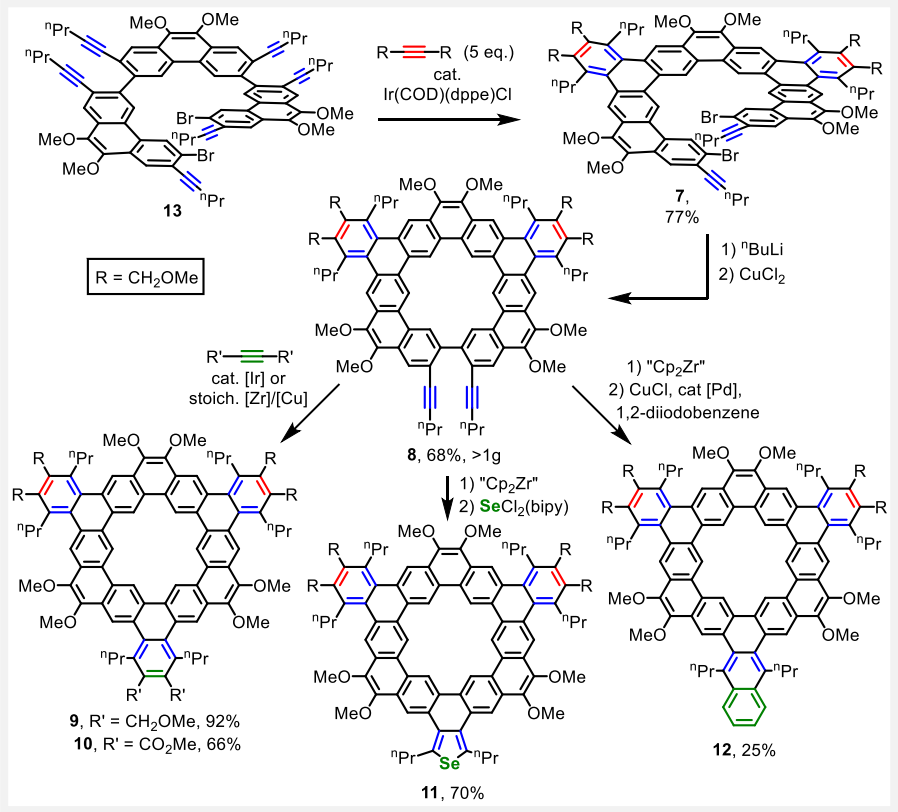

Scheme 1. Divergent synthesis of annulated kekulenes.

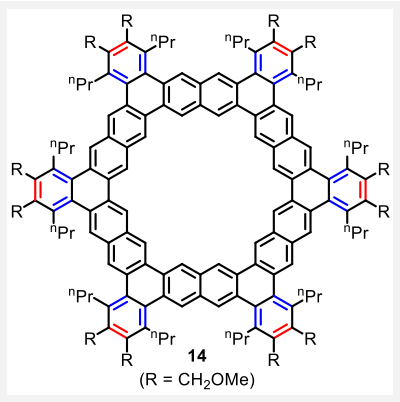

Figure 2. An "expanded kekulene" target.

A Configurationally Stable Expanded Helicene with 23 Rings on the Inner Helical Circuit

The flexibility and resulting dynamic chirality of expanded helicenes (see Chapters 3 and 5) has exciting implications for their supramolecular and solid-state chemistry, but many applications require configurational stability. The most obvious way to achieve this might be to lengthen the helicene backbone, but this presents a significant synthetic challenge. In this project, the syntheses of expanded helicenes containing 15, 19, and 23 rings (on the inner helical circuit) have been accomplished. The synthesis of the expanded 23-helicene (**15**, Figure 3) is discussed as a representative example. This compound contains nearly two helical turns and is 7 rings longer than any known carbohelicene (i.e. Fujita's 16-helicene, **16**)[15] and 6 rings longer than Vollhardt's 9-heliphene (**17**).[16]

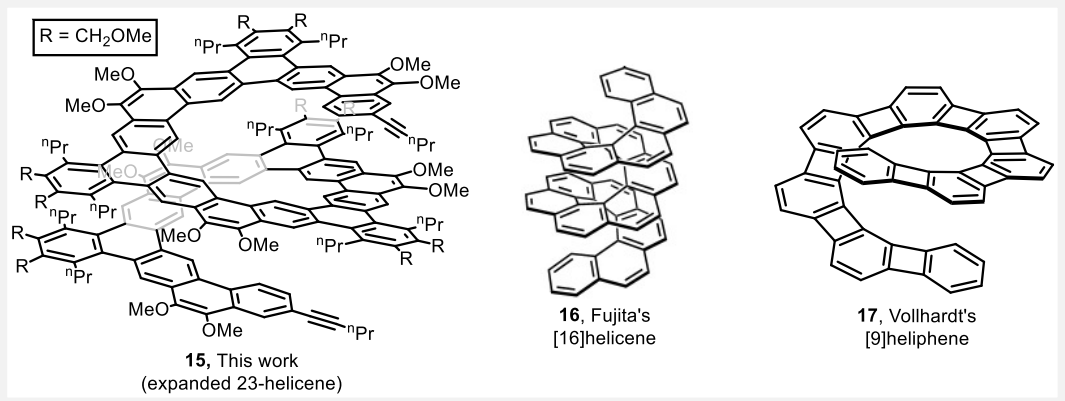

Figure 3. Longest known carbohelicenes and all-carbon, helicene-like compounds.

The synthesis of **15** is another illustration of the sequential application of two [2+2+2] reactions. The first step (Scheme 2) was developed in Chapter 4, wherein 3.4 grams of building block **18** was produced. This scalability was critical for its subsequent transformation into the two cross-coupling partners **19** and **20**. Synthesis of **19** was accomplished in high yield via lithium-bromine exchange followed by I_2 quench. The desymmetrization of **18** (to form **20**) required an unconventional approach

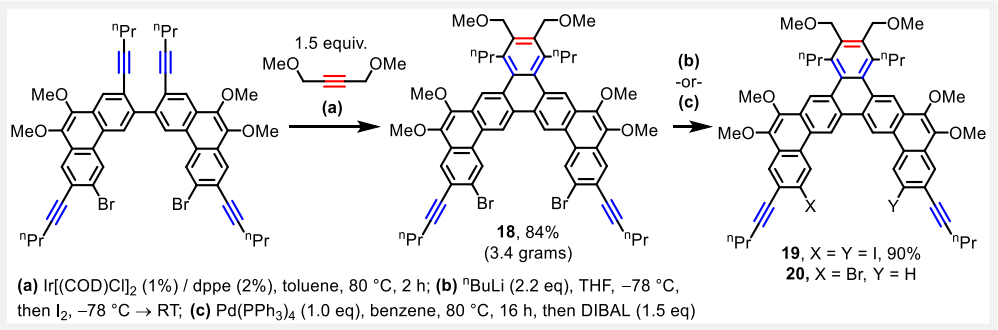

Scheme 2. Synthesis of large building block **18** and its derivatization to form cross-coupling partners **19** and **20**.

since the lithium-bromine exchange / protic workup sequence that was employed heavily in the preceding pages gave a statistical mixture of products. The successful desymmetrization strategy took advantage of the spatial proximity of the two bromide atoms in **18**. In particular, the oxidative addition of 1 equiv of the $Pd(PPh_3)_2$ fragment, followed by hydridodemetallation with DIBAL (1.5 equiv), gave **20** with acceptable selectivity.

With the two cross-coupling partners **19** and **20** in hand, the synthesis helicene **15** (Scheme 3) was accomplished in an application of the two-step cross-coupling / [2+2+2] sequence that was developed throughout this thesis.

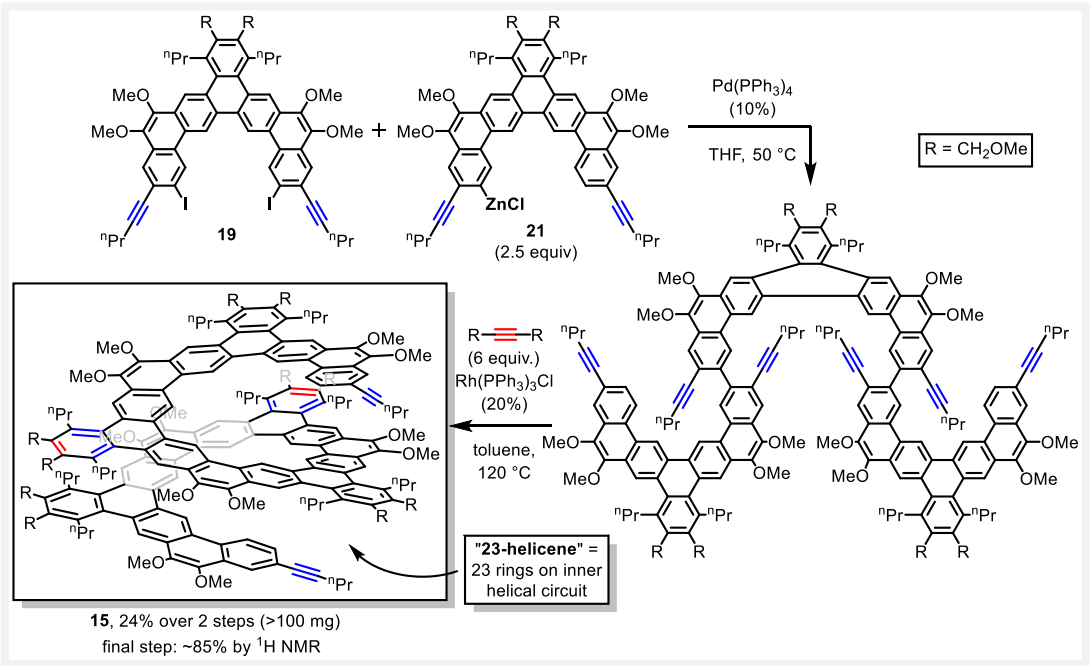

Scheme 3. Synthesis of an expanded 23-helicene

References for Chapter 7

(1) Cioslowski, J.; O'Connor, P. B.; Fleischmann, E. D. *J. Am. Chem. Soc.* **1991**, *113* (4), 1086–1089.
(2) Jiao, H.; Schleyer, P. von R. *Angew. Chem. Int. Ed. Engl.* **1996**, *35* (20), 2383–2386.
(3) Diederich, F.; Staab, H. A. *Angew. Chem. Int. Ed. Engl.* **1978**, *17* (5), 372–374.
(4) Staab, H. A.; Diederich, F. *Chem. Ber.* **1983**, *116* (10), 3487–3503.
(5) Buttrick, J. C.; King, B. T. *Chem. Soc. Rev.* **2017**, *46*, 7–20.
(6) Funhoff, D. J. H.; Staab, H. A. *Angew. Chem. Int. Ed. Engl.* **1986**, *25* (8), 742–744.
(7) Kumar, B.; Viboh, R. L.; Bonifacio, M. C.; Thompson, W. B.; Buttrick, J. C.; Westlake, B. C.; Kim, M.-S.; Zoellner, R. W.; Varganov, S. A.; Mörschel, P.; Teteruk, J.; Schmidt, M. U.; King, B. T. *Angew. Chem. Int. Ed.* **2012**, *51* (51), 12795–12800.
(8) Majewski, M. A.; Hong, Y.; Lis, T.; Gregoliński, J.; Chmielewski, P. J.; Cybińska, J.; Kim, D.; Stępień, M. *Angew. Chem. Int. Ed.* **2016**, 55 (45), 14072-14076.
(9) Yang, Y.; Chu, M.; Miao, Q. *Org. Lett.* **2018**, *20* (14), 4259–4262.
(10) Tatibouet, A.; Hancock, R.; Demeunynck, M.; Lhomme, J. *Angew. Chem. Int. Ed.* **1997**, *36* (11), 1190–1191.
(11) Miyoshi, H.; Nobusue, S.; Shimizu, A.; Tobe, Y. *Chem. Soc. Rev.* **2015**, *44*, 6560–6577.
(12) Liu, C.; Ni, Y.; Lu, X.; Li, G.; Wu, J. *Acc. Chem. Res.* **2019**, In Press; DOI: https://doi.org/10.1021/acs.accounts.9b00257.
(13) Liu, C.; Sandoval-Salinas, M. E.; Hong, Y.; Gopalakrishna, T. Y.; Phan, H.; Aratani, N.; Herng, T. S.; Ding, J.; Yamada, H.; Kim, D.; Casanova, D.; Wu, J. *Chem* **2018**, *4* (7), 1586–1595.
(14) Gregolińska, H.; Majewski, M.; Chmielewski, P. J.; Gregoliński, J.; Chien, A.; Zhou, J.; Wu, Y.-L.; Bae, Y. J.; Wasielewski, M. R.; Zimmerman, P. M.; Stępień, M. *J. Am. Chem. Soc.* **2018**, *140* (43), 14474–14480.
(15) Mori, K.; Murase, T.; Fujita, M. *Angew. Chem. Int. Ed.* **2015**, *54* (23), 6847–6851.
(16) Han, S.; Anderson, D. R.; Bond, A. D.; Chu, H. V.; Disch, R. L.; Holmes, D.; Schulman, J. M.; Teat, S. J.; Vollhardt, K. P. C.; Whitener, G. D. *Angew. Chem. Int. Ed.* **2002**, *41* (17), 3227–3230.